Reproductive Cycle of the House Gecko, *Hemidactylus flaviviridis*, in Oman in Relation to Morphological and Ultrastructural Changes and Plasma Steroid Concentrations with Reference to Localisation of Progesterone Receptors

Issa Sulaiman Said Al-Amri

The thesis is submitted in partial fulfilment of the requirements for the award of degree of Doctor of Philosophy at the University of Portsmouth.

March 2012

Dedication

I dedicate this dissertation to my beloved mother Shaikha Mohammed Said Al-Amri and late father Sulaiman Said Nasser Al-Amri, to my brothers; Dawood, Yousif, Yahya, Khalid, Majid, Moosa, and my sisters; Azza, Khalsa, Nadia, Sumaya, and to my son Aseel and daughter Asala and their mother Liqaa Saif Al-Mawali.

ABSTRACT

In Oman, a comprehensive study of the annual reproductive cycles of male and female house geckos, *Hemidactylus flaviviridis* was conducted. Circulating testosterone (T), oestradiol (E_2) and progesterone (P) concentrations were measured using a sensitive HPLC-MS/MS detection technique. Data were collected from a natural population over two consecutive seasons. The annual patterns of circulating concentrations of T, E_2 and P were measured for both sexes. In males, peak plasma T, E_2 and P concentrations occurred in the active phase, coinciding with the stages of spermatogenesis, courtship and mating, but gradually declined in the second half of the mating period with a significant drop in the quiescent phase, coinciding with testicular regression. In females, elevated plasma E_2 and T concentrations in the active phase were associated with vitellogenesis and mating. Plasma E_2 concentrations decreased significantly during the quiescent phase, coinciding with follicular regression. Plasma P concentrations were elevated during gravidity but fell significantly prior to oviposition.

The plasma steroid concentrations were related to the steroidogenic ultrastructural features and expression of progesterone receptors (PR) throughout the reproductive cycle. The steroidogenic ultrastructural features were characterized by the presence of smooth endoplasmic reticulum (SER) in the form of cisternal whorls and tubular cisternae, presence of swollen vesiculated mitochondria and association between SER, mitochondria, and lipid droplets. In the male, the rise in the three plasma steroid concentrations during the active phase was closely associated with the development of the ultrastructural features and strong PR expression in Leydig and Sertoli cells. During the quiescent phase, there was a significant decline in plasma steroid concentrations, undeveloped steroidogenic features and weakly expressed PR. In the female, the appearance of the steroidogenic ultrastructural features in the preovulatory and lutein granulosa cells was correlated with the significant rise in the three steroid concentrations and the strong expression of PR. As the steroid concentrations declined, the granulosa cells underwent general degeneration and disruption of the ultrastructural steroidogenic features. These detailed findings are the first to be reported for this species in the Arabian Peninsula.

Based on histological and gross morphological observations, the house gecko ovulates two eggs at a time, one from each ovary. This is followed by a second two egg clutch, suggesting that this species lays two clutches of eggs annually, each clutch containing two eggs.

The comprehensive data obtained from this study may be of some value for comparison with reproductive cycles of other closely related species in this region. In addition, conservation awareness for the protection of this widely distributed species may be beneficial for the protection of other wildlife.

Table of Contents

Declaration

Whilst registered as a candidate for the degree of Doctor of Philosophy, I have not registered for any other research award. The results and conclusions embodied in this thesis are the work of the named candidate and have not been submitted for any other academic award.

Issa Sulaiman Said Al-Amri

Acknowledgments

My greatest gratitude goes to Almighty Allah for the wisdom and perseverance that he has bestowed upon me during this study, and indeed, throughout my life. With His word: **"And mankind have not been given of knowledge except a little" (Qur'an 17:85)**. Indeed we are only touching the surfaces of life sciences.

Completing a PhD would not have been possible without the aid and support of many people over the past three years of my study. It is a pleasure to convey my gratitude to them all in my humble acknowledgment.

I must first express my deep and sincere gratitude towards my principal supervisor Dr. Colin P. Waring for being an outstanding advisor and excellent professor, and for being extremely helpful and offered invaluable assistance, support and guidance throughout the duration of this study. For his supervision and crucial contribution which made him a backbone of this research and so to this thesis. For his academic advice, constant encouragement and invaluable suggestions which made this work successful.

My deep and sincere gratitude is also due to the members of the supervisory committee, Professor Ibrahim Y. Mahmoud for being an outstanding advisor and excellent professor, and for his generous and enormous help in experimental work of this study in Oman and for his supervision, guidance and academic advice. With his enthusiasm, his inspiration, and his great efforts to explain things clearly and simply, he helped to make reproductive physiology and endocrinology extremely interesting for me. Throughout my study period, he provided encouragement, sound advice, excellent teaching, skill training in anatomy and physiology, and an abundance of great ideas. I would have been lost without him. Professor Abdulaziz Y. Alkindi for being an outstanding advisor and excellent professor, and for his guidance, academic advice, constant encouragement, and generous support during the experimental phase of my work in Oman. I am deeply grateful to his extraordinary efforts during the registration process, and to his valuable guidance and directives.

I deeply appreciate all my supervisor's vast knowledge and skill in the areas related to this study and their attention to detail, hard work, assistance in writing manuscripts, reports and this thesis, and for their efforts in reading and providing me with valuable suggestions and criticisms on earlier versions of this thesis. My supervisors truly made a difference in my life and I regard them as mentors and friends. Simply, I am ever indebted to their believing in me and constantly pushing me to give the best of myself.

I gratefully acknowledge Dr. Tabisam Khan from Daris Research and Development Centre, University of Nizwa for his technical assistance with HPLC/MS-MS. I am much indebted to him for his time, effort and help in identifying steroids. Many thanks also go to Dr. Charles Bakheit from Department of Mathematics and Statistics, Sultan Qaboos University for his help with the statistics and being patient with me during the study.

I convey a very special thanks to Abdulrahamn Al-Nabhani from Daris Research and Development Centre, University of Nizwa and Aisha Ambu Ali from Department of Marine Sciences and Fisheries, Sultan Qaboos University for their valuable technical assistance with sample preparation during my study period. I am indebted to Abdulrahman Al-Nabhani for his valuable assistance and his patient with me.

Many thanks also go to Kamla Al-Mawali, Mohamed Al-Kindi and Samira Al Rawahi from Department of Pathology, Sultan Qaboos University, and Khamis Al-Riyami from Daris Research and Development Centre, University of Nizwa for their valuable technical assistance and cooperation and who have been very generous to me. I would also like to thank Seyad Farook from Animal House, Sultan Qaboos University and the farm workers in Barka for helping me with sample collection.

I am very grateful to Mrs Laurice Mahmoud for her valuable effort in reading my thesis and providing valuable feedback. Special thanks also goes to Professor Anand Date for his support during my career and to his wife Dr. Sally Date for reading the manuscript and providing valuable feedback. I am very thankful as well, to Sultan Qaboos University for allowing me to use equipment and various facilities. Many thanks also to Dr. Mansoor Al-Jahdhami and the Directorate General of Civil Aviation and Meteorology, Ministry of Transport and Communications, for providing

meteorological data. Thank you also goes to my friend Zul Jiwani for helping with word document. Very special thanks to my cousin Jaifer Al-Mawali and for his help in printing this thesis. Thank you to Chris Eades for his help during my stay in Portsmouth. It is a pleasure also to express my gratitude to my friend Hamdy Elakkad for his continuous support in electron microscopy. Special thanks also go to my friends Hilal Al-Kindi and Mahmood Al-Riyami for their technical support in electron microscopy.

Finally, I would like to express my love and gratitude to my beloved family for all their love and encouragement. To my beloved mother and late father, who reared me, supported me, taught me, and loved me. To my brothers and sisters and their families, and not least, to my son and daughter for the love and support they are providing in my life.

List of Abbreviations

A	Acrosomal vesicle
AB-NF	Alcian blue with nuclear fast red
AB-PAS	Periodic acid-Schiff with Alcian blue
AC	Acrosomal complex
AG	Anterior region of epididymis
AI	Anterior infundibulum
AN	Annulus
AR	Androgen receptors
AT	Atretic follicle
AVT	Arginine vasotocin
AX	Axoneme
B	Bleb cells
BA	Basal cell
BL	Basal lamina
BV	Blood vessels
C	Corticosterone
CA	Cavity
CF	Central microtubules
CG	Cortical granules
CI	Ciliated cells
CL	Corpora lutea
CM	Columnar cells
CN	Centrioles

CR	Cortex
CT	Intertubular connective tissue
CU	Cuboidal cells
CV	Condensing vacuoles
CZ	Subacrosomal clear zone
DAB	Diaminobenzidine
DB	Dense bodies
DC	Distal centriole
DE	Ductuli epididymis
DG	Dense granule
DHT	Dihydrotestosterone
DI	Diplotene
DL	Dense layer
DP	Ductus epididymis
DR	Dense core
DS	Desmosomes
E	Epinuclear electron-lucent region
E_1	Oestrone
E_2	Oestradiol
ED	Endpiece of spermatozoon flagellum
EF	Efferent duct
EP	Luminal epithelial layer
EPH	Seminiferous epithelial height
ES	Epididymis
ER	Oestrogen receptors
EST	Early spermatids
EX	Sertoli extensions
F	Flagella

FB	Fibres
FL	Fibroblasts
FO	Nuclear fossa
FS	Fibrous sheath
FSH	Follicle-stimulating hormone
G	Endometrial gland
GB	Germinal bed
GC	Granulosa cells
GL	Golgi complex
GLC	Granulosa lutein cells
GnRH	Gonadotropin-releasing hormone
GR	Germ cells
GSI	Gonadosomatic index
GTHs	Gonadotropins
H&E	Haematoxylin and eosin stain
HB	Hyaline band
HP	Hepatic cells
HPG	Hypothalamus–pituitary–gonadal axis
HPLC-MS/MS	High performance liquid chromatography coupled with a tandom quadropole mass spectrometer
HSD	Hydroxysteroid dehydrogenase
HSI	Hepatosomatic index
IC	Intermediate cells
IF	Infundibulum
IG	Interstitial gland cells
IP	Intercellular bridge
IS	Isthmus

IT	Interstitial tissue
IK	Intercellular canaliculus
K	Kidney
L	Lumen
LA	Lamina propria
LC	Lymphatic cells
LD	Leydig cells
LFD	Diameter of largest follicles
LH	Luteinizing hormone
LP	Lipid droplets
LS	Lysosomes
LST	Late spermatids
LT	Leptonene cells
LY	Large yolk platelets
M	Mitochondria
M1	Metaphase-1 meiosis
M2	Metaphase-2 meiosis
MA	Medulla
MD	Midpiece of spermatozoon flagellum
ME	Muscularis externa
MG	Macrophages
MH	Manchette
ML	Mucosal layer
MR	Middle region of epididymis
MRM	Multiple reaction monitoring experiment
MT	Masson trichrome stain
MU	Mucoid secretory vacuoles

MV	Microvilli
MY	Medium yolk platelets
N	Nucleus
NC	Nonciliated cells
ND	Nuclear depression
NG	Newly formed secretory granules
NF	Normal follicle
NS	Nuclear shoulders
NU	Nucleolus
OC	Outer collar
ODW	Oviduct weight
OF	Oviductal eggs
OG	Oogonia
OL	Oolemma
OP	Ooplasm
OV	Ovary
P	Progesterone
PA	Pro-acrosomal vesicle
PAS-Haem	Periodic acid-Schiff with haematoxylin
PAS-FG	Periodic acid-Schiff with fast green
PB	Principal cells
PC	Proximal centriole
PCL	Pericentriolar layer
PCV	Packed cell volume
PD	Stage-III previtellogenesis
PE	Perforatorium
PF	Peripheral fibres
PG	Primary oocytes

PI	Posterior infundibulum
PL	Pre-leptotene cells
PM	Plasma membrane
PMSG	Pregnant mare's serum gonadotropin
PN	Pachytene cells
PO	Preovulatory follicle
PP	Principal piece
PR	Progesterone receptors
PRA	Progesterone receptors A
PRB	Progesterone receptors B
PS	Pseudo-stratified cells
PT	Posterior region of epididymis
PY	Pyriform cells
PV	Previtellogenic follicles
R	Nuclear rostrum
RBC	Red blood cells
RER	Rough endoplasmic reticulum
dRER	Distended RER
vRER	Vesicular RER
RNS	Renal normal segment
RSS	Renal sexual segment
RT	Radial trabeculae
S	Sperm
S1 – S7	Spermatids
SB	Sudan black-B
SE	Spermatocytes
SEM	Scanning electron micrograph
SER	Smooth endoplasmic reticulum

cSER	Cisternal SER
dSEM	Distended SER
vSER	Vesicular SER
SG	Secretory granules
SL	Smooth muscle
SM	Serosal membrane
SO	Stage-II previtellogenesis
SP	Spermatogonia
SPA	Spermatogonia A
SPB	Spermatogonia B
SQ	Squamous cells
SR	Sertoli cells
SS	Secondary spermatocytes
ST	Seminiferous tubules
STD	Seminiferous tubule diameter
SU	Subacrosomal cone
SVL	Snout–vent length
SY	Small yolk platelets
SZ	Spermatozoa
T	Testosterone
TA	Tunica albuginea
TAR	Thermoactivity range
TB	Toluidine blue stain
TC	Theca interna cells
TE	Theca externa layer
TEM	Transmission electron micrograph

TH	Thecal layer
TI	Theca interna layer
TJ	Tight junction
TLC	Theca lutein cells
TP	Tunica propria
TS	Testis
U	Uterus
UT	Uterine tube
V	Vacuoles
VE	Granular vesicles
VG	Vagina
VS	Vas deferens
Y	Yolk bodies
YP	Yolk platelets
ZP	Zona pellucida
ZR	Zona radiata
ZY	Zygotene

List of Tables

List of Figures

Chapter One:

General Introduction

1.1 Introduction: mating and reproductive cycles in reptiles/lizards

The class Reptilia includes the orders Crocodilia, Sphenodontia, Squamata, and Testudinea (Muller and Reisz, 2006) that originated around 300 million years ago (Lovern, 2011). Lizards and snakes (which arose within the lizard lineage) comprise the order Squamata. At present there are 8883 extant squamate species recognised, including 5537 species of lizards (JCVI/TIGR Reptile Database, 2011). Lizards are recognised as the suborder Sauria and are divided into two clades based on foraging mode and associated tongue morphology and function: (1) the Iguania are 'fleshy-tongued' lizards that use the tongue for feeding and (2) the Scleroglossa are 'hard-tongued' lizards that use their jaws for feeding and tongues primarily for chemoreception (Pianka and Vitt, 2003; Pough *et al.*, 2004). However, their phylogenetic relationships are still debatable (Townsend *et al.*, 2004; Vidal and Hedges, 2005; 2009). Within Sauria there are four recognised infraorders, including Gekkota. Gekkota occur in the suborder of Scleroglossa and are divided into seven families, including the family Gekkonidae (Han *et al.*, 2004). Recent estimates of Gekkotan diversity recognise approximately 1110 species in 116 genera (Kluge, 2001; Bauer, 2002) and many new taxa are described each year. According to recent molecular phylogeny studies of lizards, the Gekkonidae are thought to have originated around 100 million years ago (Figure 1.1) (Vidal, and Hedges, 2009). Lizards inhabit all continents except Antarctica, in habitats ranging from desert to rainforest, and exhibit arboreal, terrestrial, fossorial, and even semi-aquatic lifestyles (Pough *et al.*, 2004).

This high species diversity and widespread geographic distribution is reflected in the variety of their reproductive biology and associated life histories. For example, although most lizard species are oviparous, approximately 20% are viviparous (Blackburn, 1982). Also, typical clutch sizes can vary greatly in the oviparous lizards. Some species exhibit one egg [e.g., *Anolis* (Smith *et al.*, 1973)] or two-egg clutches [e.g., many geckos including *Eublepharis* (LaDage *et al.*, 2008)], whereas other species produce 20–30 eggs clutches per breeding season [e.g., *Phrynosoma* (Endriss, *et al.*, 2007)].

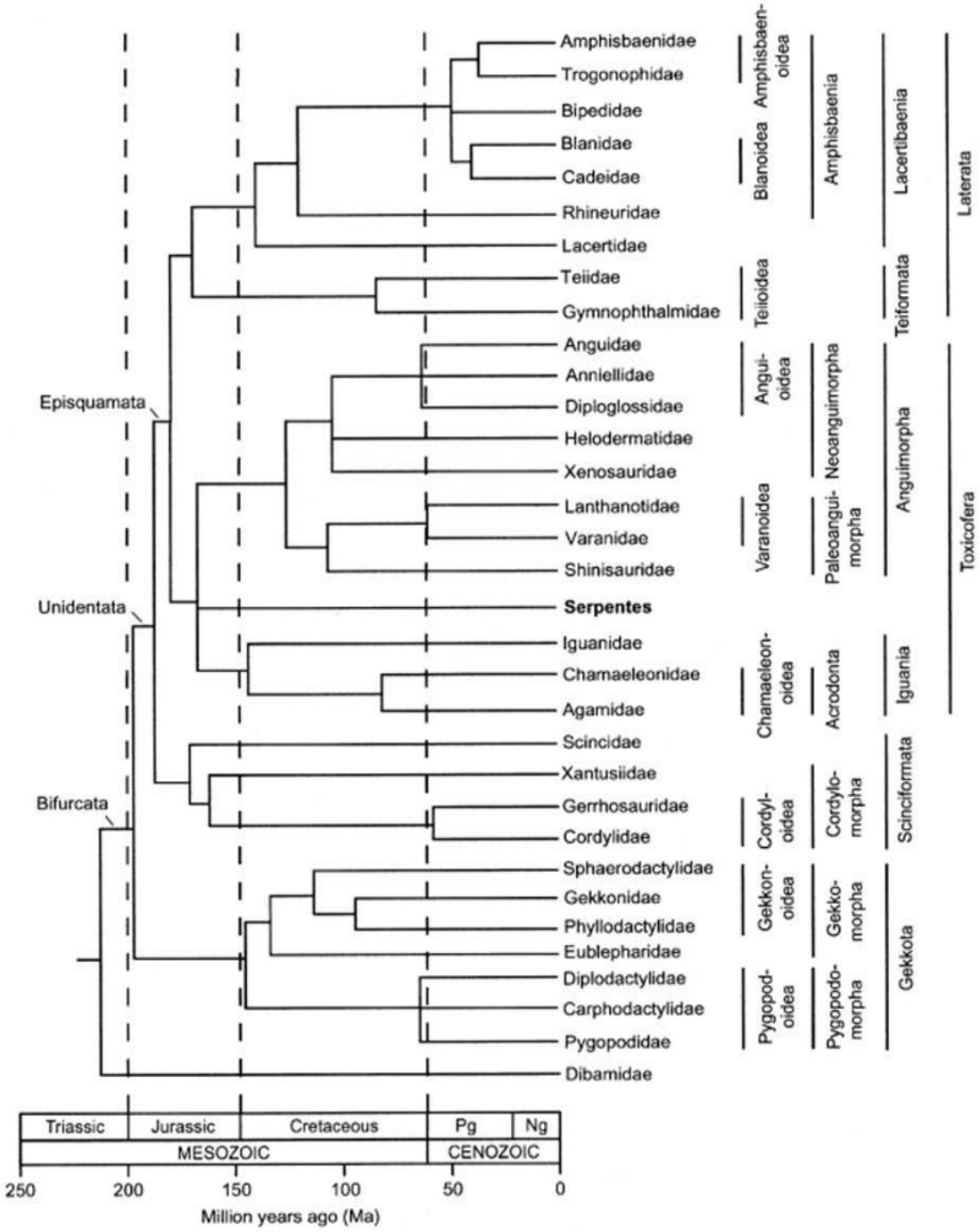

Figure 1.1. Molecular phylogeny of lizard families and associated divergence time estimates (Vidal and Hedges, 2009).

However, evidence is reported that many reptile populations, including lizards, are declining (Pianka and Vitt, 2003). Numerous factors are involved such as habitat alteration, human population growth, release of pollutants and agrichemicals into the environment, disease, parasitism (Pianka and Vitt, 2003), and global warming (e.g.,

Huey, *et al.*, 2009; Kearney, *et al.*, 2009). Monitoring these species may allow using them as indicators of environmental stability. Therefore, the study of reproductive cycles and their endocrine regulation is important as many lizards are particularly sensitive to environmental cues, such as temperature, for determining the onset of breeding (Lovern, 2011).

Reproductive studies of lizards have dealt with three distinctive aspects of reproduction. First, the reproductive period has been investigated to determine whether a species reproduces continuously or discontinuously throughout the year, and whether the level of reproductive activity is constant or temporal; secondly, which environmental factors can be correlated with reproduction and may dictate the timing of these activities; and third, which evolutionarily important selective pressures can be linked with successful reproduction in the various periods of the year. While some authors have focused on a single aspect of lizard reproduction, most studies have examined all three (Sherbrooke, 1975).

1.1.1 Types of reproductive cycles

Detailed knowledge of reproductive cycles and their endocrine mediation, although increasing, is available for only a small percentage of these species and even less when both males and females are considered (Lovern, 2011). In lizards, the reproductive cycles have been characterized based on relationships between mating behaviour, sex steroid production, and gametogenesis (Licht, 1984). Three general types of reproductive cycles are recognised: prenuptial (or associated), postnuptial (or disassociated) (Crews, 1984; Lance (1998)) and constant (or continuous) cycles (Pough *et al.*, 2004). Prenuptial reproductive cycles are those in which gonadal recrudescence, sex steroid production, and gametogenesis occur in advance of mating, whereas in postnuptial cycles they occur following mating. In the constant reproductive cycle, gonadal activity is maintained at nearly maximum level almost year round.

Associated and dissociated reproductive cycles are characterized by the presence of a discontinuous mating season. Associated reproductive cycle is common in species that live in a predictable environment in the temperate (James and Shine, 1985; Castilla and Bauwenes, 1990; Vitt, 1992; Diaz *et al.*, 1994; Shanbhag, 2003; Ikeuchi, 2004)

and the tropical and subtropical regions (Varma and Guraya, 1975; Vitt and Blackburn, 1991; Shanbhag and Prasad, 1993: Censky, 1995; Huang, 1997). Among geckonids, *Hemidactylus frenatus* breeds seasonally on Islands of the Ryukyu Archipelago and in Taiwan (Ota, 1994). The Indian house gecko *Hemidactylus flaviviridis* is known to breed between mid-March and mid-May in northwestern India (Varma and Guraya, 1975). A dissociated cycle is typically observed in species that live in temperate habitats and have brief mating seasons (Méndez de la Cruz *et al.*, 1988; van Wyk, 1995). Several species of tropical lizards exhibit a constant reproductive cycle (Somma and Brooks, 1976; Jenssen and Nunez, 1994).

Seasonal reproduction is common in lizard species (Licht, 1984; Pianka and Vitt, 2003) in which the climate produces well-defined seasons and lizards typically mate in the spring with the offspring hatching in the summer. This coordinates reproduction with the time of year providing the necessary sunlight, heat, moisture, and availability of food necessary for offspring production and survival (Duvall *et al.*, 1982; Whittier and Crews, 1987; Rubenstein and Wikelski, 2003). The relationships between reproductive cycles and climate suggest that reproduction in lizards is affected by environmental variables such as ambient temperature (Marion, 1982), precipitation (Guillette and Casas-Andreu, 1987), and photoperiod (Licht, 1967). Phylogenetic constraints may also play a major role in shaping the reproductive characteristics of lizards (Dunham and Miles, 1985). If so, it can be beneficial to study the reproductive cycles of species within a single diverse and wide-ranging lineage (Ikeuchi, 2004).

1.1.2 Mating

During the mating season the male lizard usually locates a female for mating by following her scent trail, tongue-flicking at airborne signals or searching familiar sites (Bull *et al.*, 1993). Male courtship behaviour has been described in many lizard species (e.g., Brandt and Allen, 2004; Ruiz *et al.*, 2008). Males assess whether unfamiliar females are receptive through visual (LeBas and Marshall, 2000) and chemical means (Cooper and Perez-Mellado, 2002). In many species, males prefer new females to those they may have already mated with (Tokarz, 2006). In the lizard *Sceloporus graciosus*, male courtship display was positively correlated with female latency to lay eggs, with males displaying more often toward females with eggs that

had not yet been fertilized. Courtship behaviour was not well predicted by the number of eggs laid or by female width, both measures of female quality. Thus, it appears male alter courtship intensity more in response to signals of female reproductive state than in response to variation in potential female fitness (Ruiz *et al.*, 2008).

A mating attempt by a male (e.g., *H. flaviviridis*) begins by him approaching a female from the side and grasping the resisting female from her neck with his mouth (Figure 1.2). Once in position, the male curls his body around the female, positioning his cloaca alongside hers. A receptive female usually responds by raising her tail and gaping her cloaca and allowing the male to intromit a hemipenis (Edwards and Jones, 2003). The duration of copulation is highly variable in lizards. Edwards and Jones (2003) reported that in the lizard *Tiliqua nigrolutea*, the male grasps a female for approximately six hours, with intromission only occurring towards the end of that time, while in another male it lasted only about 30 minutes. Females underwent several rhythmic contractions from posterior to anterior immediately after copulation, before the male's bite hold was released. This may be the occurrence of ovulation, or to help the sperm move into the reproductive tract (Edwards and Jones, 2003).

Figure 1.2. Mating positions of house gecko *H. flaviviridis* (Panchbudhe, 2011).

1.2 Endocrine regulation of reproductive cycles in reptiles, including effects of stress

The hypothalamus–pituitary–gonadal (HPG) axis is the main regulatory pathway for reproduction in male and female vertebrates, including reptiles (Godwin and Crews, 2002). Gonadotropin-releasing hormone (GnRH) from the hypothalamus stimulates the release of gonadotropins (GTHs) from the anterior pituitary (adenohypophysis). In mammals, these GTHs are follicle-stimulating hormone (FSH), which primarily influences gamete development, and luteinising hormone (LH), which primarily influences sex steroid production and gamete release (Norris, 2007) (Figure 1.3).

Studies to elucidate the role of GTHs in the regulation of spermatogenesis and Leydig cell function in lizards are inconsistent and confusing. Hypophysectomy caused regression of testes during the recrudescence phase in both *H. flaviviridis* (Reddy and Prasad; 1970a) and *C. versicolor* (Gaitonde and Gouder, 1981). A decrease in 3β-HSD and 17β-HSD activities in the Leydig cells, regression of the epididymis and RSS in the hypophysectomised lizards also implies lower output of androgens (Gaitonde and Gouder, 1981). The mammalian FSH could stimulate spermatogenesis in hypophysectomised as well as intact *H. flaviviridis* during the regression phase (Reddy and Prasad; 1970a; Rai and Haider; 1986), while LH and T failed to stimulate the testes. Stimulation of the RSS following FSH treatment in *H. flaviviridis* suggests that a mammalian FSH-like hormone functions as a gametogenic as well as a steroidogenic hormone. In contrast, both ovine FSH and LH stimulated spermatogenesis as well as Leydig cell activity in *C. versicolor* (Gaitonde and Gouder, 1985) during both the quiescent and recrudescent phases. Experimental studies demonstrated that exogenously administered T inhibited spermatogenesis, whereas administration of FSH alone regulates meiotic divisions, spermatogenesis and also Leydig cell activity in *H. flaviviridis* (Rai and Haider; 1991; 1995).

The work on endocrine regulation of ovarian functions is mostly confined to reptiles of temperate zones (Shanbhag, 2002). In the quiescent phase, mammalian FSH, and not LH, induced ovarian growth in *H. flaviviridis* (Rai and Haider, 1989). The treatment with FSH for a week caused an increase in the number of oocytes, primordial and previtellogenic follicles; continuation of treatment for 21 days induced

even vitellogenesis. Furthermore, in FSH-treated lizards, no atretic follicles were found. Similarly, in *M. carinata* administration of bovine FSH in the postbreeding quiescent phase caused an increase in the number of oogonia, oocytes and induced vitellogenesis, and elevated plasma E_2 concentrations (Nijagal and Yajurvedi, 1999). These studies suggest that in lizards mammalian FSH-like hormone performs the functions attributed to FSH and LH in higher vertebrates.

Studies on the ovarian cycle of *C. versicolor* suggest that pituitary GTHs are needed for the oogonial proliferation and oogonesis. An increase in the number of oogonia and primary oocytes in the germinal bed coincides with preparatory and early breeding phases in lizards (Shanbhag and Prasad, 1993). Variation in the response of the ovary to unilateral ovariectomy in the two different phases of the reproductive cycle is attributed to expected differences in the levels of GTHs prevailing in the particular season, i.e., low concentrations during postbreeding phase and high during prebreeding and breeding phase.

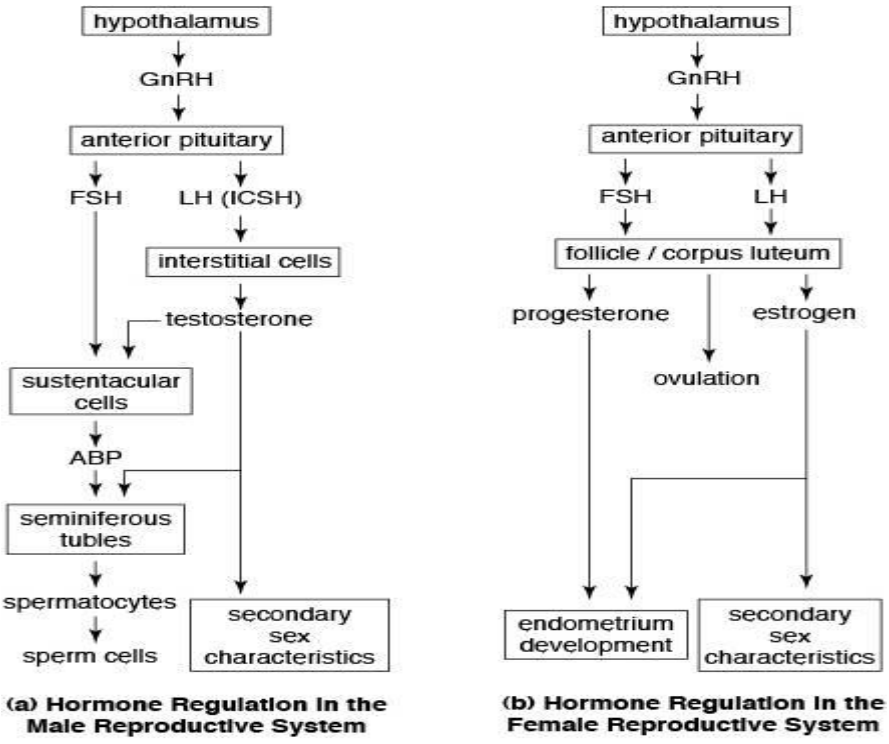

Figure 1.3. Concentrations of sex hormones in male (a) and female (b) reproductive systems are regulated by a negative-feedback mechanism with the hypothalamus. When the hypothalamus detects excessive amounts of sex hormones in the blood, it reduces its secretion of GnRH. In response, the anterior pituitary reduces its production of LH and FSH, which results in a decrease in the production of the sex hormones by the gonads (Cliffsnotes.com, 2012).

1.2.1 Effects of stress on reproduction

Inhibitory effect of stress on reproduction has been observed in different groups of vertebrates (Greenberg and Wingfield, 1987; Guillette *et al.*, 1995; Herbert, 1995; Nijagal and Yajurvedi, 1999; Tilbrook *et al.*, 2000; Yajurved and Menon, 2005; Tokarz and Summers, 2011). Although, several studies reported a decrease in sex steroid secretion due to stress, the impact on gametogenesis has not been thoroughly investigated. So far, only a few studies have been reported in reptiles (Summers, 1988; Cree *et al.*, 1990a,b; Moore *et al*.,1991; Summers *et al.*, 1995; Mahmoud and Licht, 1997; Amey and Whittier, 2000; Ganesh and Yajurvedi, 2002; Yajurved and Menon, 2005; Wack *et al.*, 2008; Lind *et al.*, 2010; Klukowski, 2011). In male reptiles stress induces alteration in spermatogenesis, whereas in females stress interferes with vitellogenic growth of ovarian follicles.

A classic marker of the stress response is an increase in plasma glucocorticoids due to the increase in secretion of the adrenal gland. The magnitude of the glucocorticoid response to stress is highly context-dependent and can be modulated by season, gender, time of day, social status, and other environmental conditions (Greenberg *et al.*, 1984; Sapolsky, 1992; Astheimer *et al.*, 1994; Dunlap and Wingfield, 1995; O'Reilly and Wingfield, 2001; Romero and Remage-Healey, 2000; Tokarz and Summers, 2011). One factor that has not received much attention is how reproductive status affects the glucocorticoid response to stress. In many species of reptiles, baseline levels of glucocorticoids differ between females of different reproductive status and it is possible that the glucocorticoid stress response might also differ among females of different reproductive status (Woodley and Moore, 2002).

Lizards are excellent model systems for studies on stress because of the ease of short-term capture in the field (e.g. Moore, 1987; Moore *et al*., 1991), and thus the effects of long-term captivity on plasma glucocorticoids can be avoided. In lizards, baseline levels of corticosterone (C), which is the primary glucocorticoid in reptiles, vary depending on reproductive status, although there is wide species variation. The magnitude of the C stress response and how it varies with reproductive status has only been studied in one species of geckos, *Hoplodactylus maculatus* (Girling and Cree, 1995; Cree *et al.*, 2003; Preest *et al.*, 2005). Girling and Cree (1995) reported that

pregnant and spent (females that had just given birth) females showed no increase in plasma C concentration after 2.5 h of capture and handling stress.

In addition to oestradiol ($E_{2)}$, testosterone (T), and progesterone (P), C may also play important roles in vertebrate reproductive cycles. Elevated plasma C concentrations have been reported during reproductive events in several reptile species in order to mobilize energy stores when resources are limited (Romero, 2002; Moore and Jessop, 2003), so species that experience strong energy limitations during reproduction may have elevated plasma C concentrations associated with reproductive events.

1.3 Mechanisms of action of sex steroids: production through to intracellular actions

Steroids are lipoidal compounds derived from cholesterol, sharing a basic four-ring structure known as the steroid nucleus (Kime, 1987; Norris, 2007). The gonadal steroids are traditionally classified as androgens, oestrogens and progestogens, according to the primary physiological processes they mediate (Norris, 2007). In some vertebrate groups these are converted to more biologically active derivatives in either the gonads or the peripheral tissue (Klicka and Mahmoud, 1977; Kime, 1987) (Figure 1.4).

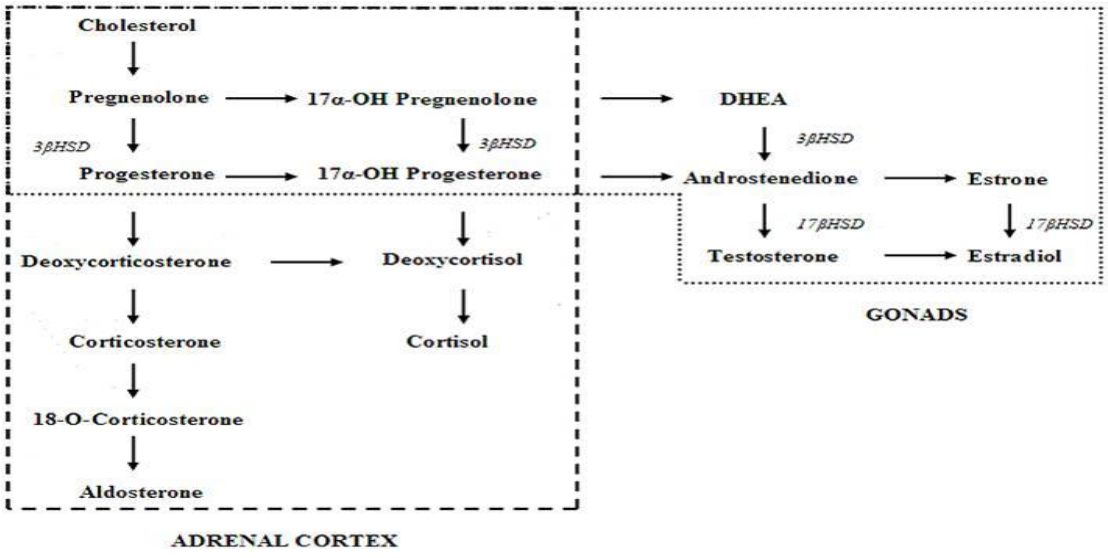

Figure 1.4. Steroid hormone synthesis pathways. All steroid hormones are synthesised from cholesterol and the end products can be classified according to their principal effects; mineralocorticoids (aldosterone), glucocorticoids, progestins, androgens and oestrogens (Herkules.oulu.fi, 2012).

1.3.1 Steroid production in reptiles

Different cell populations in the gonads are responsible for different aspects of reproductive function and steroid production. In the reptilian testis, Sertoli cells play a major role in spermatogenesis whereas Leydig cells mainly are responsible for androgen production (Gist, 1998; Norris, 2007). However, in some reptiles it is likely both Leydig and Sertoli cells are capable of significant androgen production and one or the other may be the primary source of androgen, depending on the time of year (e.g., Lofts, 1987; Mesner *et al.*, 1993; Gist, 1998). T production in some species is maximal when the testes are regressed and spermatogenically inactive. The Sertoli cells may produce sufficient androgens, along with up-regulation of ARs and production of androgen-binding proteins, to maintain spermatogenesis when the testes are spermatogenetically active, whereas during testicular regression Leydig cells produce androgens that result in a rise in plasma androgen concentrations associated with reproductive behaviour (Gist, 1998; Benner and Woodley, 2007).

In the mammalian ovary, granulosa cells of the follicular wall are responsible for egg maturation, whereas thecal cells, more exterior in the follicular wall, are responsible for the initiation of sex steroid production (Norris, 2007). Thecal cells primarily synthesise androgens, most of which are then converted to oestrogens by the granulosa cells. Granulosa cells also form the bulk of the CL following ovulation which produces P (Norris, 2007). The reptilian ovary functions very similarly to that which was described above for mammals, although squamate reptiles possess multiple granulosa cell types, one of which is unique to the group: pyriform cells, which form cytoplasmic connections to the egg in previtellogenic follicles that degenerate once follicular development (vitellogenesis) begins (Motta *et al.*, 1995; Lance, 1998; Norris, 2007).

1.3.2 Mechanisms of action of sex steroids

The effects of sex steroids are mediated through receptor proteins, which, by and large, discriminate between progesterone, oestrogen and androgen signalling and are distributed in a sex-specific pattern among female and male target organs, respectively. Binding of the steroids to their respective receptors leads to

conformational changes of the protein that allow it to interact with the transcriptional machinery directly, or indirectly via protein- protein interactions with other transcription factors (Kousteni *et al.*, 2001).These steroid hormones may act in a paracrine manner or circulate to act at target tissues in an endocrine fashion (Wierman, 2007).

In mammals, two nuclear estrogen receptors (ERα and ERβ), one androgen receptor (AR), and two forms of progesterone receptors (PR-A and PR-B, which are encoded on the same gene locus) have been identified (Ellmann *et al.*, 2009). Nuclear ER, AR, and PR also have been characterized in amphibians, reptiles, and birds (Katsu *et al.*, 2008; 2010).

Steroids circulate in the bloodstream in free and carrier protein-bound forms. At their target tissues, steroids pass through the cell membrane by passive diffusion or facilitated transport. Once in the cytosol, the steroids bind to specific receptors that are complexed with heat-shock protein. Upon binding of a steroid to its receptor, the complex changes conformation, the heat-shock protein dissociates, and two steroid-receptor complexes dimerize. The steroid-receptor dimers pass into the nucleus, where they interact with specific portions of the DNA termed 'hormone response elements' and trigger the transcription of the corresponding DNA sequence. Transcription results in increased production of mRNA and ultimately gene product proteins, which contribute to the familiar long-term effects of steroids (Figure 1.5A). This widely known mechanism is often called the 'genomic' mechanism of steroid action (Craig *et al.*, 2005).

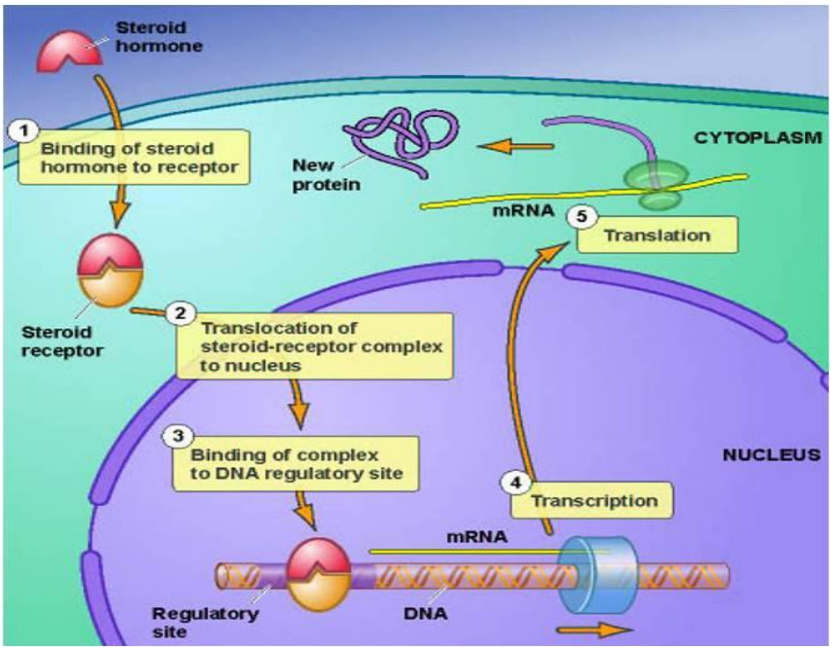

Figure 1.5A. Steroid binds to its receptor in the cytoplasm and the complex moves into the nucleus where it interacts with DNA to initiate protein synthesis (http://www.thepepproject.net).

This unified concept applies to all classes of steroid hormones except androgens. T, the principal circulating androgen, is converted intracellularly by a 5α reductase enzyme to an active metabolite, dihydrotestosterone (DHT), before receptor binding (Hughes, 1984).

The reduction of T to DHT is necessary for the androgenic actions of T in androgen target tissues such as the testis; the oxidation of T by the enzyme aromatase produces estrogens which is necessary for E_2 action in target tissues such as the ovary. The androgenic actions of T are due to the binding of DHT to its nuclear receptor, followed by dimerization of the receptor complex and binding to a specific DNA sequence. This binding of the homodimer to the androgen response element leads to gene expression, stimulation of the synthesis of new mRNA, and subsequent protein biosynthesis (Figure 1.5B) (Brueggemeier, 2005).

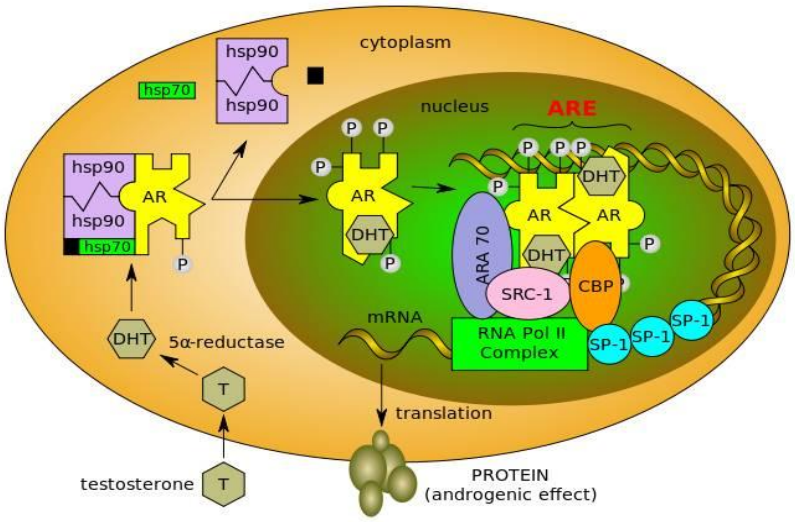

Figure 1.5B. Function of the androgen receptor. T enters the cell and, if 5-alpha-reductase is present, is converted into DHT. Upon steroid binding, the androgen receptor (AR) undergoes a conformational change and releases heat-shock proteins (hsps). Phosphorylation (P) occurs before or after steroid binding. The AR translocates to the nucleus where dimerization, DNA binding, and the recruitment of coactivators occur. Target genes are transcribed (mRNA) and translated into proteins (Meehan and Sadar, 2003).

As a member of the nuclear receptor family, PR contains three functional domains including the N-terminus, a centrally located DNA binding domain (DBD), and C-terminal ligand binding domain (LBD) (Figure 1.5C). The N-domain is functionally important, as it is required for full transcriptional activity of steroid hormone receptors and for many cell- and target gene-specific responses. In addition to binding steroid hormone, the LBD contains determinants for dimerization (DI) in the absence of DNA, binding of heat shock proteins (hsps) and for nuclear localization sequence (NLS). The DBD contains a second NLS and dimerization domain that is dependent on DNA binding. Steroid receptors contain at least two transcription activation domains (AFs), AF-1 in the N-terminal domain and highly conserved AF-2 in the C-terminal LBD. These are autonomous transferable domains required for the DNA bound receptor to transmit a transcriptional activation response and they function as specific binding sites for coactivators. AF-2 located in the LBD is hormone-dependent and becomes activated as a result of the steroid hormone inducing a conformational change that creates a hydrophobic binding pocket for members of the p160 family of steroid receptor coactivators (Leonhardt *et al*., 2003).

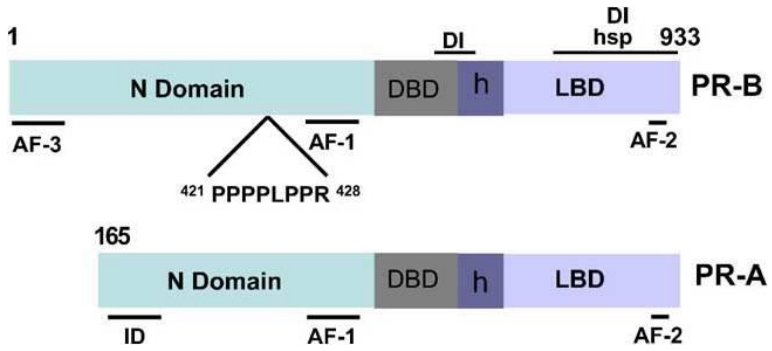

Figure 1.5C. Domain organization of the human PR-A and -B isoforms. N-domain, N-terminus; DBD, DNA binding domain; h, hinge; LBD, ligand binding domain. Transcription activation domains; AF-1, AF-2, and AF-3; dimerization domain, DI; inhibitor domain, ID; hsp, heat shock protein binding region; PXXPXR, class II consensus peptide ligand for Src kinase like SH3 homology domains (Leonhardt *et al.*, 2003).

The general pathway of progesterone (P) inducible PR-mediated gene transcription has been well characterized. P binding induces a conformational change(s) in PR that promote dissociation from a multi-protein chaperone complex, homodimerization and binding to specific progesterone response elements (PREs) within the promoter of target genes (Tsai and O'Malley, 1996; Cheung and Smith, 2000). DNA bound receptors increase or decrease rates of gene transcription by influencing recruitment of RNA polymerase II to the initiation site. Through protein–protein interaction, hormone activated PR recruits coactivators that serve as essential intermediates for transmitting signals from the receptor to the transcription initiation complex. Coactivators facilitate transcription initiation through protein interactions with components of the general transcription machinery and by promoting local remodeling of chromatin at specific promoters (Figure 1.5D).

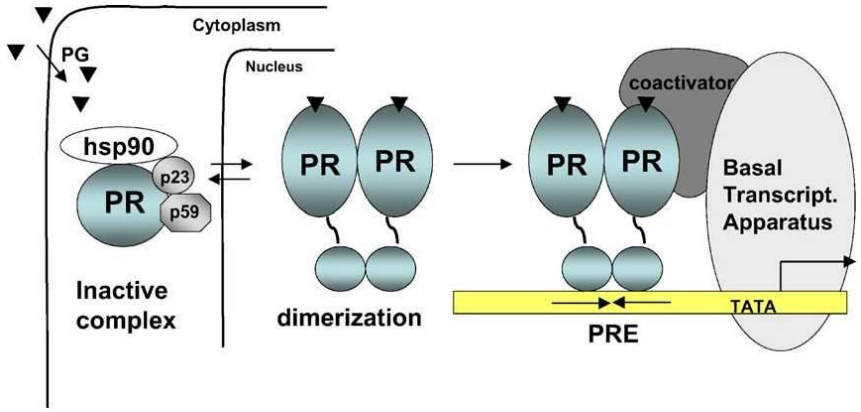

Figure 1.5D. Progesterone (PG) activation of progesterone receptor (PR). Binding of PG to the inactive receptor complex induces a conformation change which leads to immunophilin and heat shock protein (hsp) dissociation, receptor dimerization, DNA binding, and recruitment of coactivators to facilitate communication with the basal transcription apparatus. PRE, progesterone response element (Leonhardt *et al.*, 2003).

1.3.3 Progestrone receptors in reptiles

Using either binding studies or Western blot analysis, progesterone receptors (PR) have been identified in several species of reptiles (*Trachemys scripta*, Tokarz *et al.*, 1981; Selcer and Leavitt, 1991, *Nerodia*, Kleis-San Francisco and Callard, 1986; *Chelydra serpentina*, Mahmoud *et al.*, 1986; *C. picta*, Riley *et al.*, 1988; *Cnemidophorus inornatus* and *Cnemidophorus uniparens*, Young *et al.*, 1994) and the hypothalamus (Godwin *et al.*, 1996) implying that these are target tissues for this steroid. The receptors involved in ovarian function are PRA and PRB (Custodia-Lora and Callard, 2002a). A recent study by Hammouche *et al*. (2007) on the ovary of the lizard *Uromastyx acanthinura* showed that during vitellogenesis PRs were weakly detected in the nucleus of some follicular cells and well expressed in the TI cells. In previtellogenic follicles PRs were strongly expressed in the follicular cells and the signal was localised in the nucleus. In the post-reproductive period, PRs were expressed in both the nucleus and cytoplasm of follicular cells and thecal cells. During sexual quiescence, the previtellogenic follicles were all negative for PR immune-expression.

Steroid binding affinities for the two binding sites of P are also similar for the oviduct and liver of *C. picta* (Giannoukos *et al.*, 1995). P was the most effective competitor

for both sites, affinity for androgens was low, and E_2 and corticosterone (C) were weak competitors for the high-affinity site. Immunohistochemical studies of turtle oviduct and liver demonstrated a nuclear localisation for PRs in both tissues. In the oviduct PRs were seen in epithelial, glandular and smooth muscle components (Giannoukos *et al.*, 1995; Giannoukos and Callard, 1996).

1.4 Action of sex steroids (E_2, T and P) in lizards

1.4.1 Androgens

Androgens are the major male sex steroids and stimulate both the development of male physiological and secondary sexual characteristics (Norris, 2007) and male aggressive and sexual behaviours (Kime, 1987). Androgen receptors (AR) have been identified in a number of reptilian tissues, indicating that, among others, the testis (Cardone *et al.*, 1998) and oviduct (Smith *et al.*, 1995) are potential target tissues for androgens. The most biologically active androgen is T which is synthesised in the testes and adrenal glands of male vertebrates, and in the ovaries and adrenal glands of females (Kime, 1987, Mesner *et al.*, 1993).

In males, seasonal changes in plasma T concentrations are well correlated with reproductive events. Usually, both plasma T concentration and testis mass increase during spermatogenesis and peak in the final stages of gamete maturation, coinciding with mating, and falling rapidly thereafter (Bona-Gallo *et al*., 1980; McKinney and Marion, 1985; Mahmoud *et al.*, 1985a; Ando *et al*., 1992; Bonnet and Naulleau, 1996; Radder *et al.*, 2001; Kumar *et al.*, 2011). However, recent studies reported no correlation between plasma T concentration and testes morphology (Johnson *et al.*, 2011).

Androgens are sometimes considered in the context of the reproductive cycle in female squamates. In squamates plasma T concentrations can be variously elevated during late vitellogenesis and ovulation (Whittier and Crews, 1987), until oviposition (Bona-Gallo *et al*., 1980; Edwards and Jones, 2001a), only during gravidity (Arslan *et al*., 1978a) or may be low to undetectable throughout the cycle (Moore *et al*., 1985). Elevated plasma T concentrations may also be involved in the hypertrophy of the oviduct (Mahmoud and Licht, 1997; AlKindi *et al.*, 2006) and may initiate breeding

behaviour in females (Licht *et al.*, 1979). In addition, T is known to work synergistically with P to inhibit E_2-induced vitellogenesis in reptiles (Ho, 1987; Ho *et al.*, 1982; Jones, 2011).

1.4.2 Oestrogens

Oestrogens are produced from androgens, primarily in the vertebrate ovary (Norris, 2007). They are responsible for the development of female sexual characteristics in many vertebrates, and the induction of vitellogenesis in reptiles (Ho *et al.*, 1982; Ho, 1987). Additionally, oestrogens play a vital part in the sexual differentiation of the vertebrate brain (Kime, 1987). The most active naturally occurring oestrogen in reptiles is E_2. Oestrogen receptors (ER) have been identified in reptilian oestrogen target tissues including the gonad (Bergeron *et al.*, 1998), the oviduct (Paolucci and Di Fiore, 1994; Vonier *et al.*, 1997), the liver (Riley and Callard, 1988; Yu and Ho, 1989) and the hypothalamus (Godwin *et al.*, 1996).

Elevated plasma E_2 concentrations in female squamates generally correlate very well with vitellogenesis and follicular development, dropping rapidly at ovulation (Klicka and Mahmoud, 1977; Lewis *et al.*, 1979; Bona-Gallo *et al*., 1980; Kleis-San Francisco and Callard, 1986; Bonnet and Naulleau, 1994; Diaz *et al*., 1994; Jones and Swain, 1996; Jones *et al*., 1997; Amey and Whittier, 2000; Radder *et al.*, 2001; Jones, 2011). Elevated plasma E_2 has also been correlated with the hypertrophy of the female genital tract (Jones and Guillette, 1982; Gavaud, 1986) and mating (Joss, 1985; Saint Girons *et al*., 1993). Mating can also be temporally dissociated from peak plasma E_2 concentrations (Jones and Swain, 1996; Jones *et al*., 1997). A second oestrogen, oestrone (E_1), has been identified in ovarian extracts of the lizard *Lacerta sicula* (Lupo Di Prisco *et al*., 1968) and Joss (1985) proposes a role for E_1 during mating in females of the lizard, *Lampropholis guichenoti*. Moreover, the ovary is not always the major source of circulating E_2. In the viper, *Trimeresurus flavoviridis*, the adrenal gland is credited with the majority of E_2 production (Yokoyama and Yoshida, 1994).

1.4.3 Progestogens

Progestogens maintain pregnancy in mammals (Kime, 1987) and plays an important role in the maintenance of gravidity in lizards (Moore *et al.*, 1985; Fox and Guillette,

1987). They also have the ability to delay ovulation (Frieden and Lippner, 1971). The most common progestogen is progesterone (P) (Norris, 2007) which is also an active androgen antagonist in mammals, competing for androgen binding sites (Rhoades and Pflanzer, 1992). Progestogens are secreted by the CL in the ovary following ovulation, as well as by the testes and adrenal glands in both males and females (Klicka and Mahmoud, 1977; Kime, 1987). While many are biologically active themselves, progestogens such as P and pregnenolone also act as intermediates in the formation of most other steroids and are, consequently, synthesised in all steroidogenically hyper-active tissues of the body (Frieden and Lippner, 1971). Studies in reptiles have suggested that P is an important inhibitory regulator during seasonally cyclic decreases in vitellogenic synthesis (Custodia-Lora and Callard, 2002a).

Variation in patterns of P production has been documented in female reptiles during reproduction. Ovulation typically results in increased P in the ovary and plasma of oviparous reptile species (Yaron, 1972). In oviparous squamates, plasma P concentrations often becomes elevated during follicular development, peaking after ovulation during the gravid period, then falling to basal concentrations at oviposition (Arslan *et al*., 1978a; Bona-Gallo *et al*., 1980; Joss, 1985; Diaz *et al*., 1994). Postovulatory plasma P concentrations are also usually elevated, but the timing of the P peak varies. P is described as having an important role in ovulation (Chieffi and Pierantoni, 1987), and as an anti-oestrogen or inhibitor of vitellogenesis during pregnancy and gravidity (Ho *et al*., 1982; Callard and Ho, 1987; Radder *et al.*, 2001; Jones, 2011), probably by acting directly on the liver (Callard *et al.*, 1972a; Callard *et al.*, 1990). It is assumed that the CL is the source of P during gravidity (Fox and Guillette, 1987; Diaz *et al.*, 1994; Radder *et al.*, 2001; Shanbhag *et al.*, 2001).

1.4.4 Action of E_2 and P in male reptiles

Other than T, data on plasma steroids in male reptiles are few. In those species in which plasma P or E_2 have been examined, little attempt has been made to find causal relationships between temporally coincidental reproduction and steroid physiology. Saint Girons *et al*. (1993) provided one of the few published studies in which the timing of reproduction was correlated with changes in concentrations of all three

primary gonadal steroids in the plasma of a male squamate. While plasma P concentrations were highly variable, sexually inactive male *Vipera aspis* exhibited elevated plasma E_2 and low plasma androgens concentrations, and in breeding-males the situation was reversed. However, in male *Podarcis sicula sicula*, plasma E_2 concentrations increase post-reproductively (Ando *et al.*, 1992). Recent studies reported that high oestrogen concentrations have an inhibitory effect on spermatogenesis and epididymal development (Cardone *et al.*, 2002).

1.5 Reproductive anatomy in lizards: male and female

1.5.1 Male reproductive anatomy

1.5.1.1 The testes

All male reptiles possess a pair of compact testes in the abdominal cavity (Shanbhag, 2002) (Figure 1.6). The testis consists of convoluted seminiferous tubules containing permanent germinal epithelia and Sertoli cells (Figure 1.7). Leydig cells are found in the interstitium between seminiferous tubules surrounded by connective tissue, blood and lymph spaces (Al-Hajj *et al.*, 1987; Dehlawi and Ismail, 1990; Al-Dokhi, 1996; Shanghag *et al.*, 2000b; Vieira *et al.*, 2001; Ferreira *et al.*, 2002; Röll and van Düring, 2008; Ferreira *et al.*, 2009; Rheubert *et al.*, 2009; Rheubert *et al.*, 2011a).

The morphological characteristics of lizard testes typically vary with the stage of the annual reproductive cycle (Ferreira *et al.*, 2002). There are also changes in the developmental stages of germ cells, and in the quantity and metabolic activity of interstitial tissue (Wilhoft, 1963; Wilhoft and Quay, 1961). Changes in the Leydig cells apparently vary inversely with the periods of germ cell production (Goldberg and Lowe, 1966).

Studies on testicular cycles of lizard species indicated that spermatogenic patterns are specific to each species. Many male lizards exhibit a prenuptial spermatogenic cycle with variations in the testicular or seminiferous tubule size (Fitch, 1970; Sarkar and Shivanandappa, 1989; Shanbhag *et al.*, 2000b; Noriega *et al.*, 2002; Ferreira *et al.*, 2009). In recent years, a new temporal germ cell development strategy during spermatogenesis has been described in all major taxa within Reptilia [Sauria (Gribbins

and Gist, 2003; Rheubert *et al.*, 2009); Chelonia (Gribbins *et al.*, 2003); Serpentes (Gribbins *et al.*, 2005; 2008); Crocodylia (Gribbins *et al.*, 2006)]. This strategy follows a prenuptial pattern of spermatogenesis, in which germ cells enter the spermatogenic cycle with a number of predictable cytological changes during their development in association with Sertoli cells, leading to a single spermiation event at the end of the cycle (Gribbins and Gist, 2003).

However, recent histological evaluations of testicular structure and germ cell development strategies within reptiles have been restricted to temperate species only. Spermatogenesis in these species is typically limited to warmer months, due to the lack of resources, which are presumably used to facilitate metabolically demanding processes such as spermatogenesis (Olsson *et al.*, 1997) in colder periods of the year.

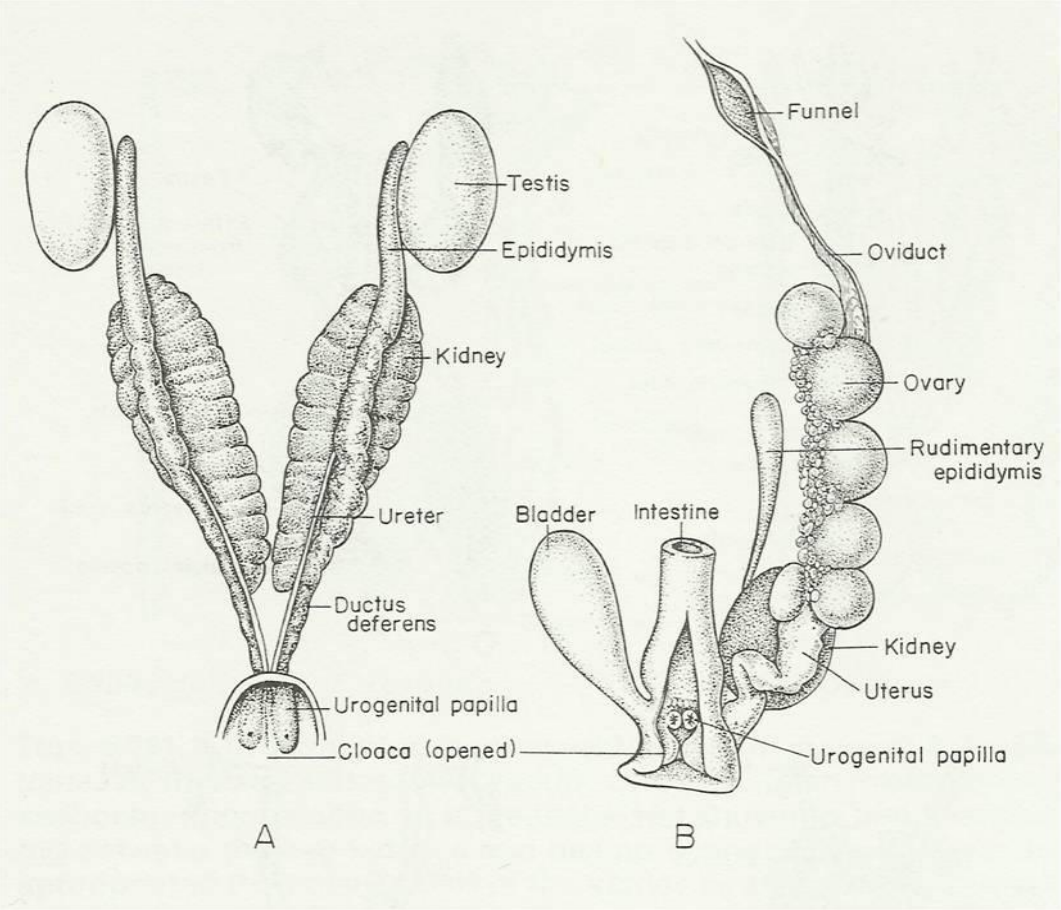

Figure 1.6. Urogenital organs in lizards. (A) Male organs of *Varanus*. (B) Female organs of *Sphendon* (Romer and Parsons, 1978).

Ultrastructural studies detailing the morphology of mature spermatozoa, which describe the steps of spermiogenesis, have been reported for many lizard species (e.g. Jamieson *et al.*, 1996; Giugliano *et al.*, 2002; Teixeira *et al.*, 2002; Ferreira and Dolder, 2003b; Vieira *et al.*, 2004; Röll and von Düring, 2008; Rheubert *et al.*, 2011a) (Figure 1.8). Spermiogenesis is the step-wise development of spermatids into mature spermatozoa, and many of the characteristics observed in mature spermatozoa are seen throughout this developmental process. Some studies have used ultrastructure of the mature spermatozoa in phylogenetic analyses (Newton and Trauth, 1992; Jamieson, 1995, 1999; Jamieson *et al.*, 1996; Vieira *et al.*, 2005; Colli *et al.*, 2007). Recent ultrastructural analyses that infer evolutionary trends among reptiles have shown that some spermatozoa morphological characteristics may be synapomorphic (shared trait among two or more taxa) in squamates. For example, Jamieson (1995) found that a single perforatorium may be a synapomorphy for squamates in their study of Iguania, and Jamieson (1999), Vieira *et al*. (2004), and Rheubert *et al.* (2010a) corroborated these data in their analysis within the Squamata. In addition, the peripheral fibers associated with microtubule doublets 3 and 8 are grossly enlarged in squamates (Jamieson, 1995, 1999; Cunha *et al.*, 2008), whereas in *Sphenodon* they are not (Healy and Jamieson, 1992). Few studies have been reported on the mature spermatozoa of geckos (Furieri, 1970; Jamieson *et al.*, 1996; Röll and von Düring, 2008); however, only one study highlights the ultrastructure of spermiogenesis within the Gekkonidae (Rheubert *et al.*, 2011a).

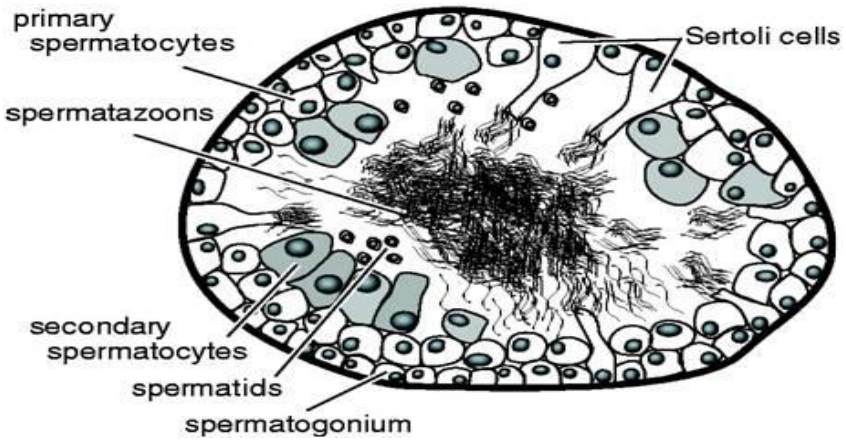

Figure 1.7. Spermatogenesis. Diagrammatic representation of a cross section through a seminiferous tubule in a reptile testis (Zug *et al.*, 2001; Elsevierdirect.com, 2012).

In the reptilian testis, the steroidogenic activity has been characterized by histochemical and ultrastructural studies, mainly detecting the presence of 3β-hydroxysteroid dehydrogenase (3β-HSD), and occasionally 17β-HSD. The secretion of hormones is associated with the development of steroidogenic ultrastructural features in Leydig and Sertoli cells such as smooth endoplasmic reticulum (SER), the presence of mitochondria with tubular cristae associated with lipids droplets, and a reduction of cytoplasmic lipid droplets (Mori, 1984; Mahmoud *et al.*, 1985a; Dubois *et al.*, 1988; Mesner *et al.*, 1993; Mahmoud and Licht, 1997; Ferreira and Dolder, 2003a). The presence of lipids in Leydig and Sertoli cells is an indication of steroidogenic activity. The lipid droplets usually become abundant in both cells during spermatogenic inactivity but decline during the active period (Callard *et al.*, 1976; Lofts and Tsui, 1977; Mahmoud *et al.*, 1985a; Dubois *et al.*, 1988). In Sertoli cells, the presence of 3β-HSD varied seasonally in turtles (Callard and Ho, 1980; Dubois *et al.*, 1988) and the presence of ultrastructural features related to steroidogenic activity in Sertoli cells has been documented in the lizard *Liolaemus darwini* (Gutierrez and Yapur, 1983) and in the snake *Eryx jayakari* (Al-Dokhi *et al.*, 2004).

Recently, the ultrastructural features of steroid activity in Leydig and Sertoli cells, and serum testosterone (T) concentrations have been reported in the lizard *Phymaturus antofagastensis* (Boretto *et al.*, 2010). Leydig and Sertoli cells presented ultrastructural features characteristic of steroid synthesis during spermatogenesis. Leydig cell steroidogenic activity is synchronized with proliferation and differentiation of germ cells (Licht, 1984), indicating the important role of androgens in spermatogenesis. The Sertoli cells function in support and nutrition of the germ cells (Röll and von Düring, 2008). They have also been reported to play a major role in Leydig cell proliferation and steroidogenesis (e.g., Skinner *et al.*, 1991; Bardin *et al.*, 1994; Lejeune *et al.*, 1996).

1.5.1.2 The epididymis

The Wolffian duct in reptiles gives rise to vas deferens. The genital region of the Wolffian duct differentiates into the epididymis (Figure 1.6). The vas deferens is a

simple structure composed of a convoluted tubule of varying diameter along its length, lined by a layer of epithelial cells in lizards (Shanbhage, 2002). The epididymal structure has been described in detail in many lizard species (e.g., Haider and Rai, 1987; Mesure *et al.*, 1991; Averal *et al.*, 1992; Jones, 2002; Akbarsha *et al.*, 2006, 2007; Rheubert *et al.*, 2010b).

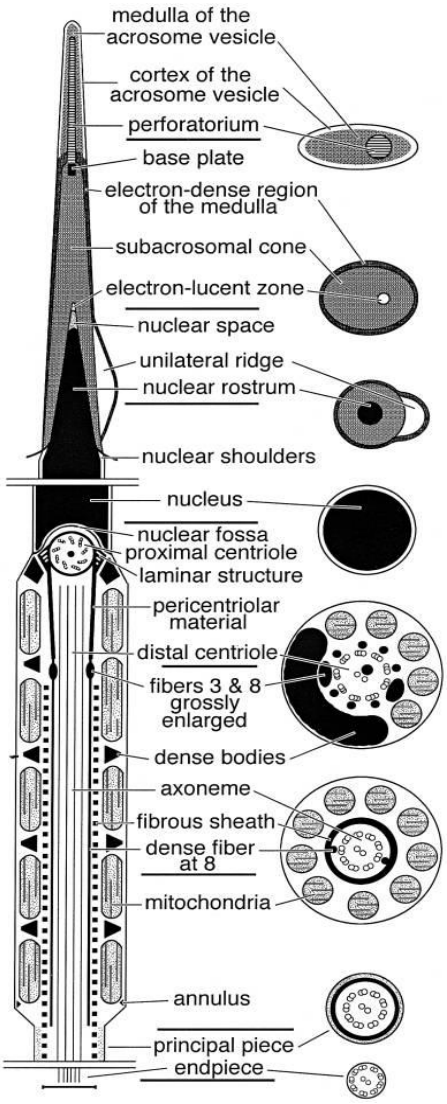

Figure 1.8. Drawing of spermatozoon in longitudinal and corresponding transverse sections from the lizard *Ameiva ameiva*. The drawing was produced from several TEM micrographs (Giugliano *et al.*, 2002).

The epididymis can be morphologically divided into several regions, depending on the species, with considerable variation in epithelial cell height and luminal diameter along its length. The ductus epididymis of *H. flavivridis* consists of a small ductuli

epididymis, and a large ductus epididymis. The ductus epididymis increases markedly in diameter posteriorly and ends in a vas deferens (Haider and Rai, 1987).

Recent studies reported that ducts in lizards and snakes are differentiated into: rete testis tubules, ductuli efferentes, ductus epididymis, ductus deferens, and ampulla ductus deferentis (Akbarsha *et al.*, 2006, 2007; Rheubert *et al.*, 2010b; Sever, 2010) (Figure 1.9). Rheubert *et al.*, (2010b) reported that in the gecko, *Hemidactylus turcicus*, the seminiferous tubules unite into a single rete testis tubule, where the rete testis divides into 3–4 ductuli efferentes which drain into the cranial portion of the ductus epididymis.

In reptiles, the epididymis is involved in sperm maturation. The spermatozoa become motile and are then capable of fertilizing the eggs during their transit through the epididymis. The lizard epididymis is a conspicuous secretory organ controlled by steroid hormones (Depeiges and Dufaure, 1981; Dufaure and Saint-Girons, 1984). It produces large secretory granules that mix with the spermatozoa in the epididymal fluid. The secretory granules contain specific proteins that are able to bind to the heads of the spermatozoa (Depeiges and Dufaure, 1983).

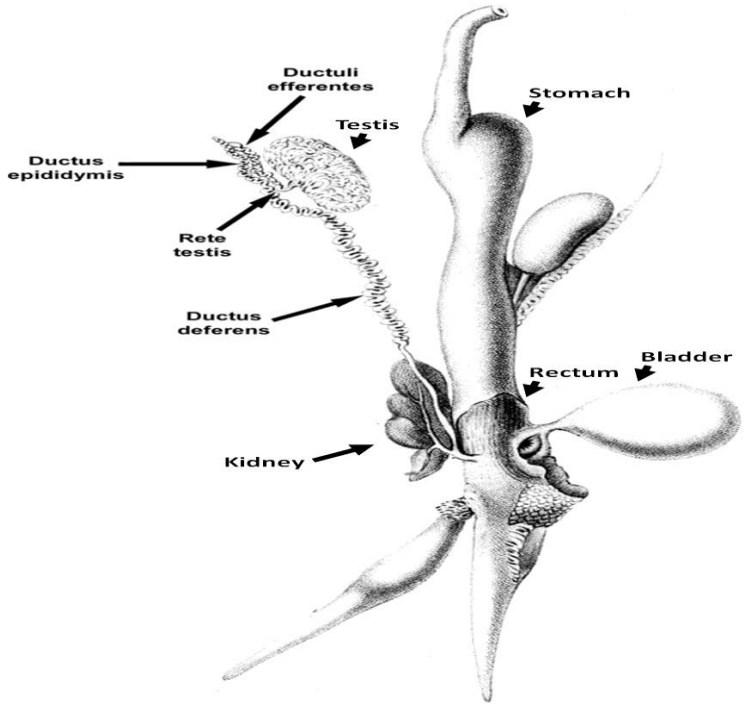

Figure 1.9. Schematic drawing of the urogenital system in the lizard *Lacerta vivipara* showing the rete testis, ductuli efferentes, ductus epididymis, and ductus deferens (Martin Saint Ange, 1854).

During the annual reproductive cycle, the epididymal cells undergo drastic morphological, physiological and biochemical modifications (Depeiges *et al.*, 1988) corresponding to successive and well characterized quiescent, maturation (recrudescent), active and degenerative (regression) phases (Haider and Rai, 1987; Mesure *et al.*, 1991). These modifications are probably correlated with the steroidogenic Leydig cells activity. During the quiescent phase, the epithelial cells appear small and cuboidal with hyperchromatic nuclei. Experimental studies involving castration and androgen replacement therapy have shown androgen dependency of the epididymis in lizards (Sarkar and Shivanandappa, 1984; Haider; 1985a; Shivanandappa and Sarkar, 1987). Treatment with anti-androgens such as cyproterone acetate and flutamide caused epididymal regression in *P. dorsalis* (Shivakumar and Sarkar, 1980) and *H. flaviviridis* (Haider and Rai, 1986). This indicates that androgens are needed for normal epididymal growth and activity in lizards (Shanbhage, 2002).

The vas deferens in lizards is a simple convoluted tube carrying the sperm from the epididymis. The anatomy of the vas deferens is described for *Calotes versicolor* (Akabarsha and Meeran, 1995). During the breeding season, the terminal part of the vas deferens appears swollen and is comparable to the ampulla of mammalian vas deferens. During the quiescent phase, the vas deferens cannot be distinguished as a duct and ampulla. However, after administration of androgens during the quiescent phase, the ampullary region becomes distinct and glandular, suggesting its androgen dependency (Akabarsha and Meeran, 1995).

1.5.1.3 Renal sexual segment

In the male gecko *Hemidactylus turcicus,* the nephrons are composed of five distinct regions: 1) a renal corpuscle and glomerulus, 2) a proximal convoluted tubule, 3) an intermediate segment, 4) a distal convoluted tubule, and 5) the sexual segment of the kidney/collecting duct (Rheubert *et al.*, 2011b). In most lizards, the renal sexual segment (RSS) mostly includes distal convoluted tubules and in some, the collecting tubules form its main part (Fox, 1977; Gabri 1983; Sarkar and Shivanandappa, 1989; Sever Hopkins, 2005) (Figure 1.6). Kidneys of female *Hemidactylus turcicus*, however, are similar to that of the male but lack the sexual segment (Rheubert *et al.*,

2011b). Sever and Hopkins (2005) studied seasonal variation of the RSS in the ground skink, *Scincella lateralis* (Scincidae) with light and electron microscopy. They reported data from lizards collected throughout the entire year and found that, like most snakes, the RSS of *S. lateralis* is discernible from other nephridic tubules during the inactive season, which differs from that of other lizards (Sever *et al.*, 2002). Although histological studies on the RSS of geckos have been reported (Misra *et al.*, 1965; Sanyal and Prasad, 1966; Saint Girons, 1972), only one ultrastructural study (Rheubert *et al.*, 2011b) has been reported so far. In recent years, the seasonal ultrastructure of the RSS in lizards has been under study to better understand the evolution of the RSS in order to establish phylogenetic relationship between squamates.

Seasonal variation in the RSS has shown strong correlation with spermatogenic activity, mating, and increased androgen concentrations (Bishop, 1959; Misra *et al.*, 1965; Prasad and Sanyal, 1969; Krohmer, 1986).

1.5.2 Female reproductive anatomy

1.5.2.1 The ovaries

The ovaries of oviparous lizards are a pair of oval sacs attached to the dorsal wall of the abdominal cavity by a mesovarium (Figures 1.6 & 1.10) (Uribe *et al.*, 1996). The ovary is covered by a simple cuboidal epithelium with a basement membrane separating the surface epithelium from the underlying stroma. The ovarian stroma mainly consists of fibrous connective tissue, degenerating corpora lutea (CL) and atretic follicles, lymphatics, blood vessels, nerves and interstitial gland cells (Shanbhag *et al.*, 1998). The amount of interstitial gland cells varies depending upon the phase of the ovarian cycle. The interstitial gland cells in the ovary of *C. versicolor*, *H. flaviviridis*, and *C. calcaratus* (Gouder and Nadkarni, 1976) exhibit 3β-HSD activity. The oogonia and oocytes are restricted to one or more isolated small regions in the ovary known as germinal beds (GBs) (Jones *et al.*, 1982; Shanbhag *et al*,, 1998). The number of GBs varies between species. In the monoautochronic lizards such as *H. flaviviridis* (Guraya and Verma, 1976) and *H. brooki* (Shanbhag *et al*,, 1998) each ovary contains one GB. The polyautochronic lizard *C. versicolor* has two GBs in each ovary (Jones *et al.*, 1982; Shanbhag and Prasad, 1993). Although

many lizard species produce a clutch size of two, the number of ovulations at one time can be as low as one or as high as 50 or more (Fitch, 1970; Ballinger, 1978). Thus, in different species a single ovary can ovulate one to several eggs during each ovulatory period. It is believed that the number of GBs may have a role in controlling the clutch size in reptiles (Jones *et al.*, 1982).

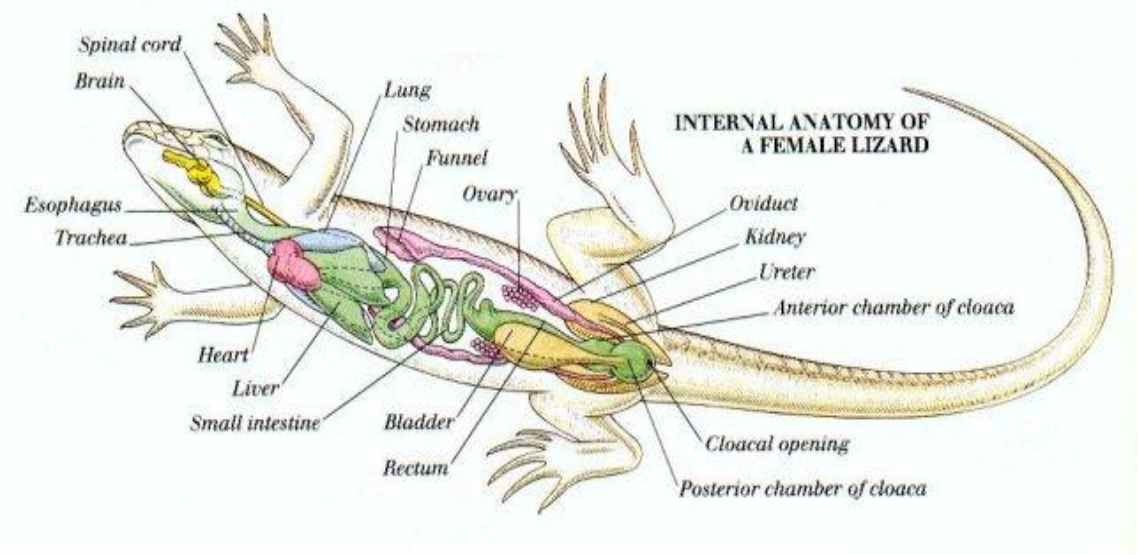

Figure 1.10. Position of the ovaries and oviducts of female lizard (Universe-review.ca, 2012).

The ovaries of reptiles exhibit various developmental and degenerative processes depending on the stage of development and/or the phase of the ovarian cycle. These include the processes of oogonial proliferation, oogenesis, follicular growth, vitellogenesis, ovulation, luteogenesis, luteolysis and follicular degeneration. In most reptiles, oogonial proliferation and oogenesis occur throughout life (Shanbhag, 2002). Lizard follicular growth not only involves the growth and maturation of the oocyte, but also requires the storage of large quantities of yolk in the ooplasm (Guraya, 1989). Although the general sequence of folliculogenesis has been described in a number of reptiles, some variation between species has been reported (e.g., Klosterman, 1987; Uribe *et al.*, 1996; 2000; Gómez and Ramírez-Pinilla, 2004; Vieira *et al.*, 2010). In particular, there is still a need for information on the cytoplasmic changes occurring during oocyte growth and vitellogenesis in most reptiles.

The ovarian follicle is composed of a central oocyte surrounded by a bi-layered, acellular membrane, the zona pellucida, which is bound by a follicular epithelium. In lizards, the follicular epithelium, the granulosa, is a highly dynamic structure that significantly changes in morphology and function in relation to oocyte growth. During early follicular growth, the primary follicles are composed of a single layer of small stem cells. In mid-previtellogenesis, some small cells differentiate into pyriform cells via intermediate cells, and the epithelium becomes multi-layered (Andreuccetti 1992). As follicular development progresses, the zona pellucida is clearly subdivided into two distinct regions: an outer homogeneous layer adjacent to the granulosa and an inner, thicker striated layer (zona radiata) lying against the oolemma. During late previtellogenesis pyriform cells regress via apoptosis (Motta *et al.*, 1996) and the follicular epithelium gradually reorganize and re-establishes a monomorphic monolayered condition in which the small cells persist as a unique component of the epithelium until ovulation (Filosa *et al.*, 1979). Surrounding the ovarian follicle are the thecal layers, the theca interna (TI) and theca externa (TE), composed of connective tissue, blood vessels, and secretory cells.

The ovary produces a variety of steroids (Di Prisco *et al.*, 1968; Chieffi and Botte 1970), which contribute to plasma sex hormone concentrations (Ciarcia *et al.*, 1986). Typically, high oestrogen (E_2) concentrations are present in the blood during oocyte growth, whereas progesterone (P) concentrations are higher during ovulation and postovulation and remain high as long as eggs are in the oviducts (Ciarcia *et al.*, 1986). Histochemical distribution of steroid dehydrogenases in gonadal tissues identifies several putative sites of steroidogenesis, i.e., follicular walls (thecal and granulosa layers), peripheral ooplasma of young oocytes, postovulatory CL, and atretic follicles (Botte and Delrio 1964). These steroidogenic sites are indicative of the ovarian steroid synthesis which regulates vitellogenin synthesis (Ho, 1987) and regulate oviductal activity (Botte et *al.*, 1976; Botte and Granata 1977). In all vertebrates, including reptiles, the ovarian sex steroid production is linked to the hypothalamus–hypophysis axis through gonadotropin-releasing hormone (GnRH) and is under its control with positive and/or negative feedback (Everett, 1988; Sherwood *et al.*, 1993). Several ultrastructural studies in reptiles reported that GnRH induces ultrastructural steroidogenic changes characteristic of active ovarian tissue which lead

to an increase in the secretion of sex hormones (Lewis *et al.*, 1979, Mahmoud *et al.*, 1985b, 1986; Mahmoud and Licht, 1997; Al-Kindi *et al.*, 2001; Mahmoud *et al.*, 2006).

Many species of oviparous snakes and lizards retain their eggs for at least half of the period of embryonic development (Shine, 1983; Andrews and Mathies, 2000) with the majority of taxa ovipositing at stages 26–33 (according to the staging system of Dufaure and Hubert, 1961). The endocrine basis for such egg retention appears to be the ability of the postovulatory follicles to secrete P (Rothchild, 1981). Plasma P concentrations generally rise in the postovulatory period, falling shortly thereafter, and there is a strong correlation between the duration of egg retention and the period of activity of the CL (Jones and Guillette, 1982; Mahmoud and Licht, 1997).

Among squamates, the pattern of plasma P concentrations and particularly the timing and duration of the peak during gestation or gravidity varies markedly between species (Xavier, 1987). For example, in the snake *Thamnophis elegans* (Highfill and Mead, 1975), and the lizard *Tiliqua rugosa* (Bourne *et al.*, 1986a), plasma P concentrations are highest during the second trimester of pregnancy, falling during the third trimester; but in the snake *Natrix taxispilota* the peak occurs during early pregnancy (Chan *et al.*, 1973). The physiological basis for such variations in plasma P profiles among squamates remains obscure, but may reflect species differences in the degree of embryonic dependence upon yolk nutrition vs. maternal transfer during gravidity or gestation (Jones *et al.*, 1997).

1.5.2.2 The oviducts

The reptilian oviduct includes all structures of the female reproductive tract derived from the embryonic Müllerian duct (Wake, 1985). In general, the oviducts of lizards are paired, thin-walled tubes that extend length wise along the body cavity on either side of the midline (Figures 1.6 & 1.10) (Blackburn, 1998), and supported by dorsal mesenteries that are continuous with the peritoneum (Corso *et al.*, 2000). The paired ovaries, suspended from the dorsal midline via their mesovaria, lie medial to the oviducts and caudal to their infundibular ostia (Blackburn, 1998). The position of the ovary relative to the oviductal ostium varies considerably among species. In some

species, the ovaries are adjacent to the ostia, whereas in others they lay considerably caudal to the oviductal opening (Blackburn, 1998). The oviducts may be of different lengths on each side of the body (Perkins and Palmer, 1996), presumably to make efficient use of body space during gravidity (Girling, 2002) (Figure 1.11).

In the majority of reptiles, the oviduct can be subdivided into five regions. The infundibulum, which receives the oocyte, the uterine tube, where albumen production and sperm storage occur, the isthmus, followed by the uterus, which is responsible for the eggshell production, and the vagina that leads to the cloaca. (e.g., Palmer and Guillette, 1988; 1990; Guillette *et al.*, 1989; Aldridge, 1992; Palmer *et al.*, 1993; Sarker *et al.*, 1995; 2003; Perkins and Palmer, 1996; Girling *et al.*, 1997; 1998; 2000; Blackburn, 1998; Girling, 2002; Adams *et al.*, 2004; Sever and Hopkins, 2004; AlKindi *et al.*, 2006; Siegel and Sever, 2008). However, the five oviductal regions are not recognised in every reptilian species, and additional regions may also be present in some species (Girling, 2002; Nogueira *et al.*, 2011) (Figure 1.11).

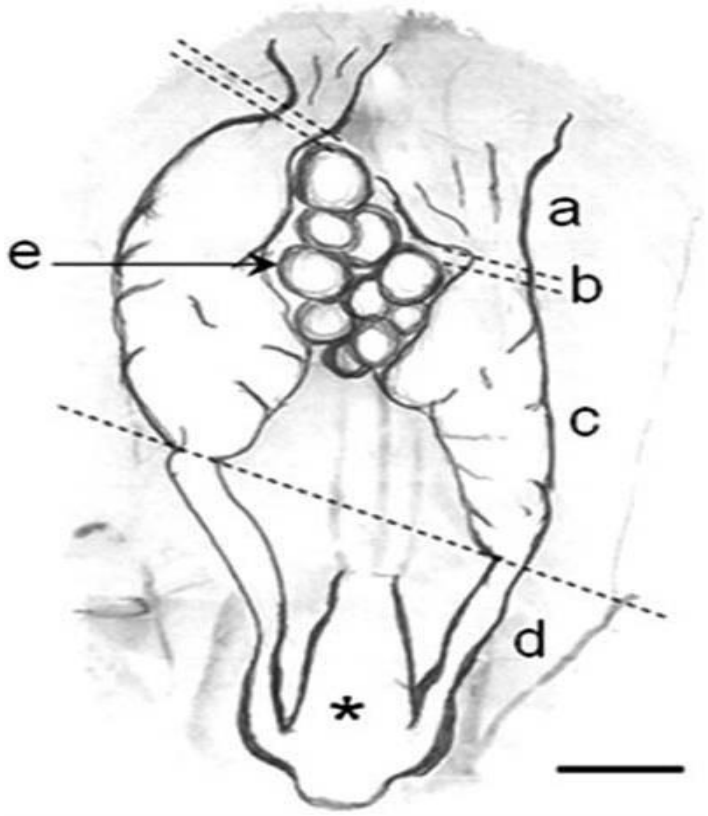

Figure 1.11. Schematic diagram of the female reproductive tract and cloaca of the lizard *H. mabouia*. Infundibulum (a), uterine tube (b), uterus (c), vagina (d), ovaries (e). Cloaca (*). Bar: 2 mm (Nogueira *et al.*, 2011).

The site of fertilization in reptilian species has yet to be determined (Blackburn, 1998; Girling, 2002). Presumably, fertilization occurs before albumen or shell membranes cover the ovulated oocyte. Eggs are coated with oviductal secretions after they enter the infundibular ostium (Palmer *et al.*, 1993) (Figure 1.12). Fertilization, therefore, occurs either in the infundibulum or in the uterine tube, where sperm is stored in these regions. For instance, in a gecko *Heteronotia binoei* the sperm were observed in the oviductal wall of the infundibulum that surrounded the unshelled ovum (Whittier *et al.*, 1994). This suggests that fertilization occurs in the infundibulum of this species.

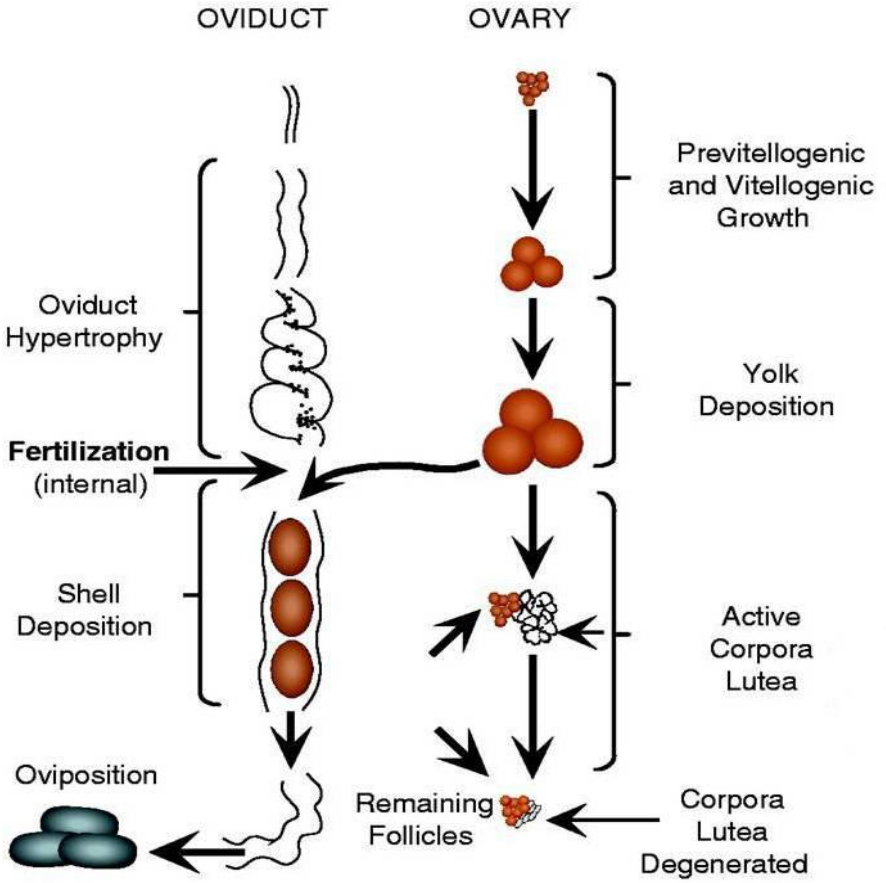

Figure 1.12. Development of eggs in reptiles. Fertilization occurs after eggs are ovulated into the oviducts (Zug *et al.*, 2001; Elsevierdirect.com, 2012).

During the active phase of the reproductive cycle, the luminal epithelium shows secretory activity throughout the oviduct which includes albumen, eggshell membrane and eggshell formation components and sperm storage (Blackburn, 1998; Girling,

2002) (Figure 1.12). Three cell types are found in the luminal epithelium: ciliated, microvillous nonciliated, and bleb-like nonciliated cells. The function of ciliated cells is presumably for movement of mucus and cellular debris down the oviduct (Palmer and Guillette, 1988). The cilia may also aid in the movement of sperm, and the ovulated egg. Apical protrusions and blebbing of the ciliated cells have also been reported, suggesting that ciliated cells may also have some secretory function (Girling *et al.*, 1997). Microvillous nonciliated cells are presumably mucus-producing, which is necessary to keep the lumen of the oviduct moist and clear of debris (Leese, 1988). The oviductal lumen is continuous with the exterior (via the urogenital sinus) and so is vulnerable to contamination. Bleb-like nonciliated cells have been identified in some reptilian species (Palmer and Guillette, 1988; Girling *et al.*, 1997; 1998; AlKindi *et al.*, 2006), and their function is still unknown.

The lizard oviduct is a dynamic organ that undergoes major structural changes associated with hormonal stimulation as a function of the cyclic reproductive activity. During the vitellogenic period E_2 is responsible for cell hypertrophy, glandular development and secretory activity (Abrams Motz and Callard, 1991; Girling *et al.*, 2000; AlKindi *et al.*, 2006). P has been implicated in the regulation of oviductal function in oviparous reptiles (Klicka and Mahmoud, 1977; Jones and Guillette, 1982; Paolucci and Di Fiore, 1994; Shanbhag *et al.*, 2001; AlKindi *et al.*, 2006) and egg-shelling (Cuellar, 1979; Radder *et al.*, 2001; AlKindi, 2006).

The thick muscular coat of the vagina is well designed for movement of eggs (Blackburn, 1998). The hormones involved in rhythmic contraction of the oviduct include; arginine vasotocin (AVT) and prostaglandins, as well as neural factors (Guillette *et al.*, 1991), but AVT appears to play a major role in the process of oviposition.

1.6 Model organism

1.6.1 The family *Gekkonidae*

Gekkonidae are a cosmopolitan family and one of the largest primitive families with over 1000 species of lizards (Han *et al.*, 2004). The family gekkonidae are distributed throughout the tropics, subtropics and warm temperate regions, including; Central and

South America, Africa, Madagascar, Southern Europe, Asia, Indo-Australian Archipelago, New Guinea, Australia and Oceania (Cogger, 2003). There are about 85 genera and more than 1000 species of this family (Ananjeva *et al.*, 2004). Many have distinctive adhesive climbing pads on their toes, formed by modified scales which allow them to climb on smooth vertical surfaces. Most are nocturnal and oviparous, but some are both diurnal and viviparous. All lack movable eyelids and many are known to use their fleshy tongues to lick their eye-spectacle clean. Many geckos also communicate by vocalization, uttering species-specific yaps, chirps and coughing sounds. Most are small to medium sized (50-400 mm total length) (Cogger, 2003).

1.6.2 The genus *Hemidactylus*

The genus *Hemidactylus* belongs to the subfamily Gekkoninae which is the largest and most widely distributed subfamily containing 670 species in 72 genera worldwide (Mattison, 2004). With more than 80 species inhabiting all warm continental land masses and hundreds of intervening continental and oceanic islands, *Hemidactylus* geckos are one of the most species-rich and widely distributed of all reptile genera (Carranza *et al.*, 2006) and newly described species are discovered every few years. The genus was named by Gray (Gray, 1825) and referred to as house geckos.

Lizards belonging to the genus *Hemidactylus* are medium-sized, nocturnal and oviparous (egg-laying), brown to pinkish in colour, with a scattering of tubercular scales among their granular ones, and with well developed toe-pads (Mattison, 2004). Each finger or toe has a slender distal-clawed joint, angularly bent and rising from within the extremity of the dilated portion (Boulenger, 1890). The fingers and toes are free, and more or less webbed and dilated; underneath they bear two rows of lamellae in a pattern resembling a paripinnate compound leaf (Boulenger, 1890). This leads to their other and more ambiguous common name, "leaf-toed geckos", used mainly for species from South Asia and its surroundings to prevent confusion with the many "leaf-toed" Gekkota not in *Hemidactylus*. The dorsal lepidosis is either uniform or heterogeneous. The pupil of the eye is vertical. Males have pre-anal or femoral pores. Apart from houses, *Hemidactylus* live in a variety of habitats, including rocks, dry-stone walls and trees (Mattison, 2004).

1.6.3 The investigated animal, the house gecko *Hemidactylus flaviviridis*

The animal used in this study is the common house gecko *H. flaviviridis*, which was named by Rüppell (Rüppell, 1835), an abundant, relatively small lizard common in many places in open or in wooded habitats. While quite cryptic and secretive, it is extremely easy to catch.

Many studies on this species in relation to its geographic distribution, natural history, ecology, life history, diet, home range and activity patterns have been documented (e.g., Ibrahim, 2000; Henkel, 2003; Carranza *et al.*, 2006; Sivaperuman *et al.*, 2008; Baig *et al.*, 2008). The reproductive biology of this species has also been studied (Sanyal and Prasad, 1967; Prasad and Sanyal, 1969; Reddy and Prasad, 1970a,b; Reddy *et al*., 1972; Varma and Guraya, 1975; Gouder and Nadkarni, 1976; Guraya and Varma; 1976; Duda, 1980; Duda and Annalakshmi, 1982; Rai and Haider, 1986; 1991; 1995; Haider and Rai, 1987; Shanbhag, 2002; Rai and Nirmal, 2003; Khan and Rai, 2004; 2005). The reproductive cycles of this species have also been studied in detail in relation to the timing of reproductive events, as well as the endocrine and paracrine controls (Sanyal and Prasad, 1967; Duda, 1980; Haider and Rai, 1987; Rai and Haider, 1986; 1989; 1991; 1995; Khan and Rai, 2004; 2005; 2008; Bharti *et al.*, 2011).

To date, there are no available data about the reproductive cycle of this species in Oman and the neighbouring countries in the Gulf Region and the Arabian Peninsula.

1.6.3.1 Geographical distribution

The gecko *H. flaviviridis* is mainly found in the warm temperate and subtropical regions, and has been reperoted in the studied areas including; Egypt (Ismailia, Sinai), Kuwait, Saudi Arabia, United Arab Emirates, Oman, Iraq, Iran, Afghanistan, Nepal, Pakistan, India (Andhra Pradesh, Assam, West Bengal, Bihar, Uttar Pradesh, Delhi, Punjab, Maharashtra, Gujarat, Rajasthan, Madhya Pradesh, Haryana, Orissa), Socotra Island (Yemen), Somalia, Sudan, Ethiopia, and Eritrea (Figure 1. 13) (JCVI/TIGR Reptile Database, 2011).

1.6.3.2 Habitat of *H. flaviviridis* in Oman

The house gecko *H. flaviviridis*, inhabiting Oman (in the subtropical zone), lives in a variety of habitats including deserts, human houses, walls of buildings close to light, ceilings, wooden beams, kitchen walls and behind doors or on window frames. Sometimes they also climb in trees close to buildings. They can also be seen in crevices, cracks in walls, between plywood, behind goods in store rooms, inside pipes, behind curtains, and behind cupboards in houses.

Figure 1.13. Studied geographical distribution of *H. flaviviridis* in Asia and Africa. (JCVI/TIGR Reptile Database, 2011).

1.7 Aims and objectives

The general aims of this study is to analyse the reproductive cycle of the house gecko, *Hemidactylus flaviviridis*, and to provide a comprehensive understanding of the role of reproductive steroids (T, E_2 and P) and PR expression in relation to histological and steroidogenic ultrastructural changes. Males and females were studied throughout their reproductive cycles. Specific aims are as follows:

1. To describe the reproductive cycles in both sexes, by monitoring the changes in plasma T, E_2 and P concentrations, gonadal histology and ultrastructure.

2. To investigate the relationship between the steroidogenic ultrastructural features, steroid hormone concentrations and the expression of PRs in reproductive tissues of both sexes.

3. To investigate the seasonal changes in seminiferous tubules, epididymis and renal sexual segments in relation to histological, histochemical and ultrastructural changes.

4. To study the role of Leydig and Sertoli cells steroidogenic activity in relation to the development and maturation of spermatozoa.

5. To investigate the seasonal changes in the oviducts and ovaries, such as vitellogenesis, ovulation and CL formation.

6. To analyse the steroidogenic activity in the granulosa lutein cells in reference to the histological, histochemical and ultrastuctural changes of ovaries and oviducts.

7. To examine the effect of stress (plasma C concentrations) on plasma steroid hormones in response to handling stress in natural populations of *H. flaviviridis* during the different reproductive phases.

This is the first comprehensive study of these reproductive features in both male and female *H. flaviviridis* from one geographical location.

Chapter Two:

Materials and Methods

2.1 Introduction

The materials and methods and other information relevant to this study are included in this chapter. The practical component of this study was carried out at Sultan Qaboos University, Muscat, Oman.

2.2 Study Area

This study was conducted in the northern part of Oman. The study area is located in Barka ($23^{o}39'42.31''$N, $57^{o}52'00.92''$E) (Figures 2.1A & 2.1B), Al-Batinah region. It is a wooded area at sea level and consists mainly of palm trees with some mango and lime trees and scattered farm houses. Annual rainfall averages 30–100 mm, with temperature ranging between 13^{o}C – 47^{o}C. The rainy season occurs between December and April.

2.3 Animals

The house gecko *H. flaviviridis* is a common species found throughout Oman with distinct physical characteristics that cannot be confused with other species (Figure 2.2). The house gecko has a stout, flattened, body with soft gray-brown skin, yellow-bellies, and weak limbs with five adhesive digit toes. The body scales are small, smooth and homogenous with a large head, unmovable eyelids, and a long depressed tail.

The house geckos are nocturnal and sometimes territorial. They stay close to lights attractive to insects. Sometime they may be seen outside on cloudy days. During the day they typically hide under tree bark or in tree hollows. In the early evening they come out to feed and sometimes for courtship and mating. Their diet is mostly insects, such as mosquitoes, ants, flies, and cockroaches.

Ninety-Eight adult male house geckos [snout–vent length (SVL) < 7.5 cm] were captured by hand at night from the study area during 2008–2010, in which 22 were sacrificed during the postbreeding (quiescent) phase (June–August), 24 during the prebreeding (recrudescent) phase (September–October) and 52 during the breeding (active) phase (November–May). Animals' were tentatively sexed by visual

examination of the cloacal opening for the presence or absence of male hemipenis musculature (Figure 2.3).

One hundred and twenty-nine adult female house geckos [snout–vent length (SVL) < 8cm] were captured from the study area during 2008–2010, in which 28 were sacrificed during the postbreeding (quiescent) phase (June–August), 50 during the prebreeding (recrudescent) phase (September–December) and 51 during the breeding (active) phase (January–May).

2.4 Environmental effects on testicular and ovarian cycles

Observations on feeding, mating, and movements on active males and females suggest that the geckos had limited activity during the cold nights (quasidormecy) (December–January) where temperature dropped below 15^{o}C. During courtship and mating (March–April) the temperature ranged between 25–35°C, and generally, the lizards were active during this period. Photoperiod during the study period 2008–2010: quiescent phase (June–August: 13 hours), recrudescent phase (September–February: 12 hours), active phase (March–May: 13 hours).

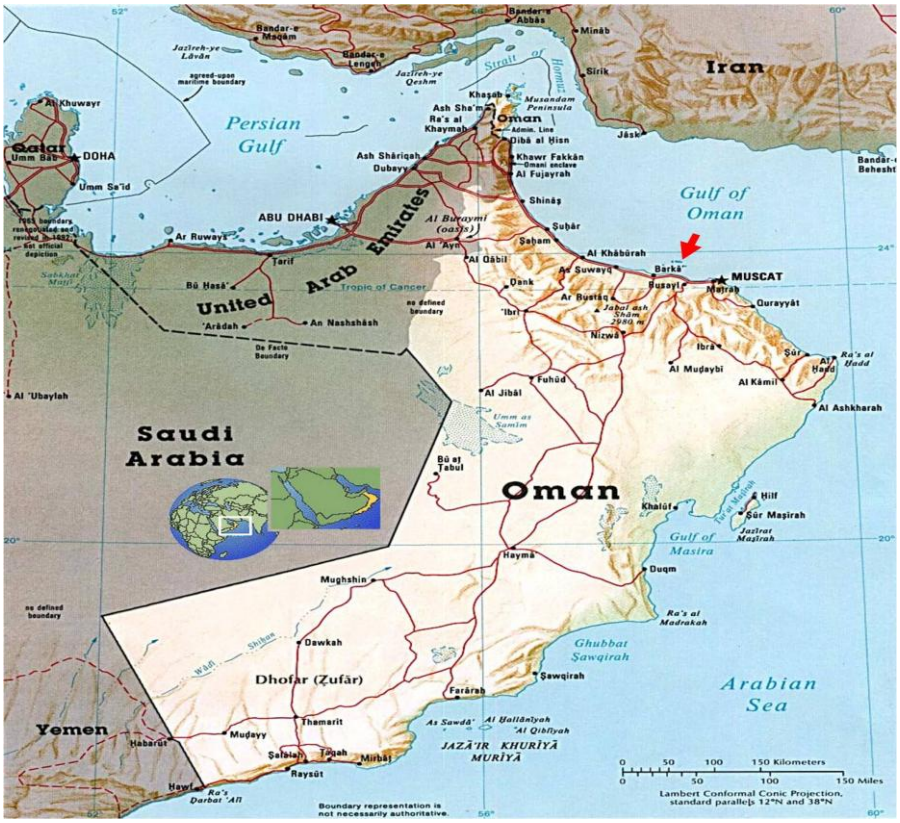

Figure 2.1A. Study area in Barka (red arrow), Oman (Haimenoonline.com, 2012).

Figure 2.1B. Specimen collection site of the house gecko *H. flaviviridis* in Barka (white circle) (Googleearth.com, 2012).

Figure 2.2. Common house gecko *H. flaviviridis.* It appears flattened and yellow to brown in colour, eyes with vertical pupils, five digits toe-pads, and a long compressed tail (Photographed by the auther).

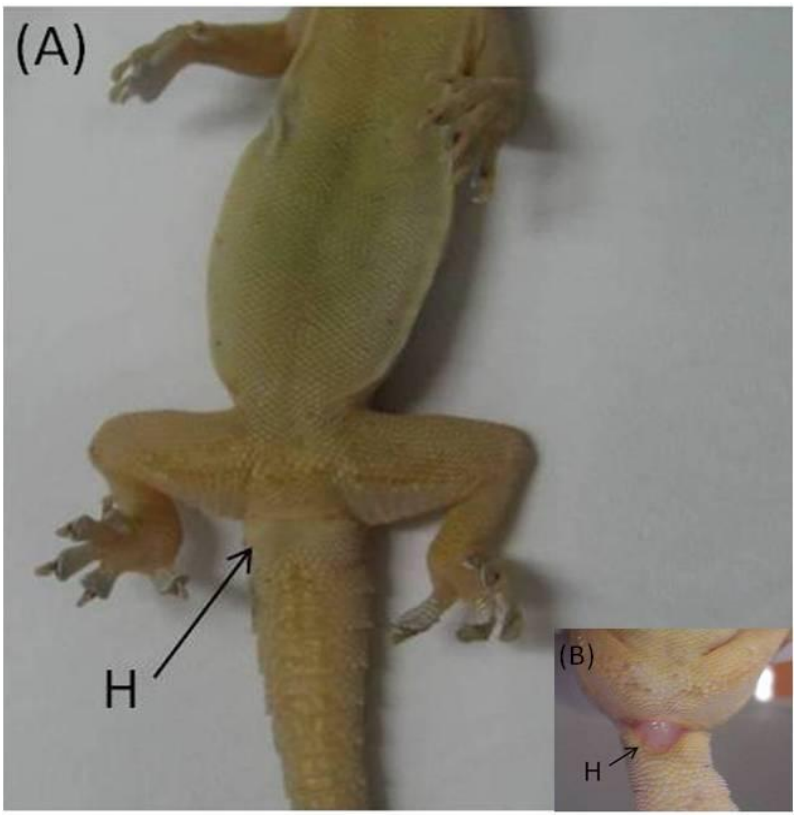

Figure 2.3. (A) Male house gecko copulatory organ, a pair of hemipenis seen as two bulges behind the cloaca at the base of the tail (H). (B) Eversion of a hemipenis musculature (H) during the mating period (Photographed by the auther).

2.5 Sacrifice of animals

The animals were caught by hand and were sacrificed immediately after capture to minimise stress which might affect hormonal concentrations (Owens and Ruiz, 1980). The animals were handled with care before they were sacrificed. This project was conducted with the approval of Sultan Qaboos University animal ethics committee under ethics permit number SQU/AEC/2008-09/4.

2.6 Blood collection and extraction of plasma

Immediately after measurements were made, the animal was sacrificed and blood was collected from the carotid vessels in EDTA tubes and then centrifuged for 10 minutes at a speed of 3000 rpm. The plasma was then dispensed into 1.5 ml microcentrifuge tubes and the samples stored at -70^{o}C until analysis.

2.7 Measurement of Haematocrit or Packed Cell Volume (PCV)

Haematocrit was determined using micro-tubes and centrifuged for 5 minutes in a Hawksley (UK) Micro-Haematocrit Centrifuge. PCV was determined by calculating the percentage of the red blood cells in the total blood volume.

2.8 Tissue dissection

Female ovaries (follicles, corpus luteum), oviducts and liver were removed with the aid of a Leica S6E dissection stereomicroscope and each was weighed separately using a sensitive digital balance (Figure 2.4A, 2.4B, 2.5A & 2.5B). Male testes, epididymis, vas deferens and kidneys were dissected and their weights were recorded (Figure 2.6A & 2.6B).

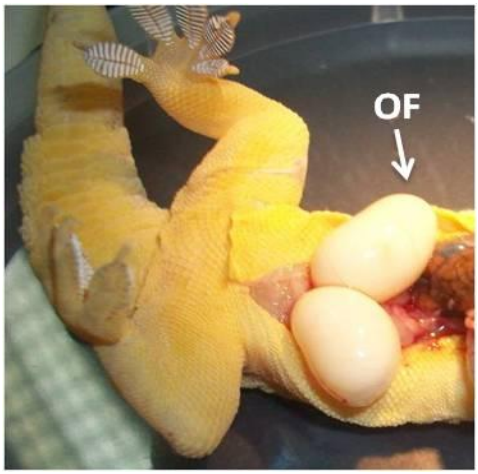

Figure 2.4A

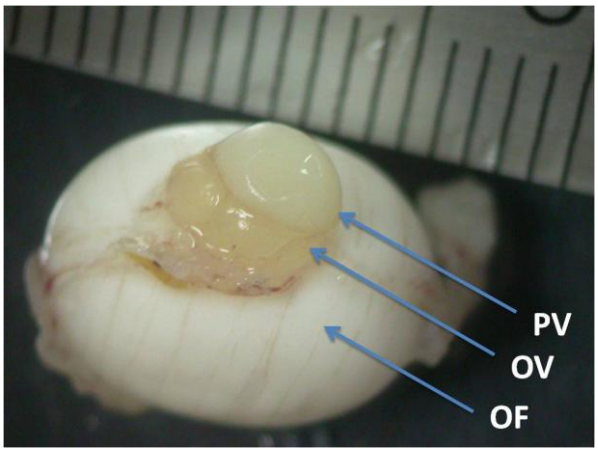

Figure 2.4B

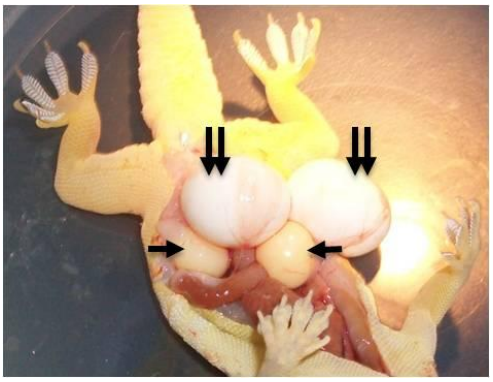

Figure 2.5A

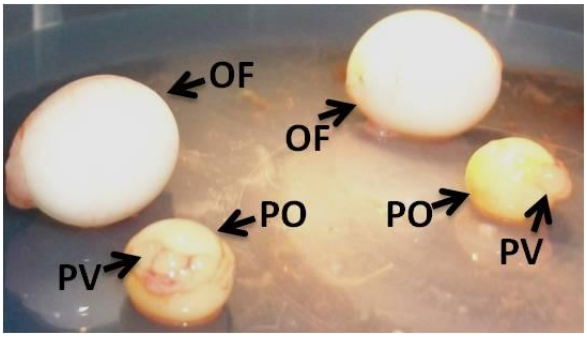

Figure 2.5B

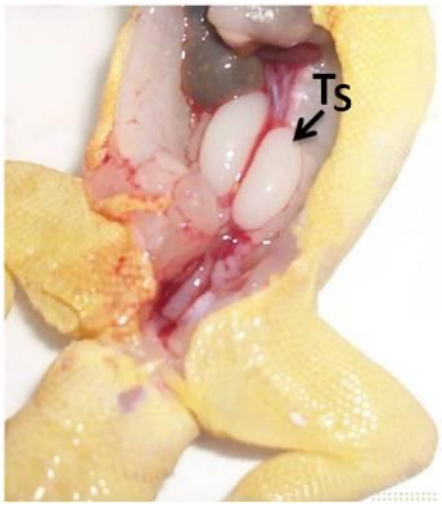

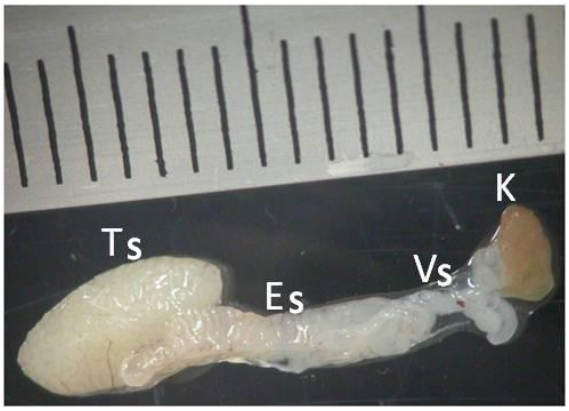

Figure 2.6A

Figure 2.6B

Figure 2.4A Midlateral cut of a gravid female abdominal cavity from the breeding season showing two oviductal eggs (OF).

Figure 2.4B Dissected oviduct from a gravid female during the breeding season with oviductal egg (OF) and ovary (OV) attached to the oviduct with small growing previtellogenic follicles and large developing previtellogenic follicle (PV).

Figure 2.5A Midlateral cut of a gravid female abdominal cavity during the breeding season showing two oviductal eggs (double arrow) and two preovulatory follicles (PO).

Figure 2.5B Dissected oviductal eggs (OF) and preovulatory follicles (PF) from the same gravid female in Figure 2.5A. Note the small developing previtellogenic follicles (PV) attached to the preovulatory follicles (OF).

Figure 2.6A Midlateral cut of a male abdominal cavity from the breeding season showing two enlarged testes (TS).

Figure 2.6B Dissected male testis (TS) from the breeding season with epididymis, (ES), vas deferens (VS), and kidney (K).

2.9 Analysis of sex and stress hormones by HPLC-MS/MS

Plasma concentrations of E_2, P, T and C were measured with the highly specific and sensitive method of high performance liquid chromatography coupled with a tandom quadropole mass spectrometer (HPLC-MS/MS). Initial separation of the steroids from the biological media was performed using an HPLC separation column and individual components were quantified by the mass spectrometer.

The samples were prepared by protein precipitation; a 500 µL aliquot of acetonitrile was added to 500 µL of plasma (1:1 ratio by volume). The sample was vortex mixed for 5min and then centrifuged at 3,000 rpm for 10 min in an Eppendorf (Hamburg, Germany) microcentrifuge. The precipitated plasma protein was discarded and the top layer containing the extract was analyzed by injecting a sample of 10 µL into the HPLC-MS/MS. A 1pg/µL standard solution of E_2, P, T and C (Sigma Aldrich, UK) was used to tune the mass spectrometer for optimum sensitivity. A tandem quadrupole mass spectrometer (Quattro Ultima Pt, Waters Corp., MA) was used in this analytical procedure. The cone voltage was set to 60V, 54V, 70V and 50V (for each of the precursor ions) and the collision energy was set to 18eV, 12eV, 23eV and 203eV (for collision induced fragmentation of the product ions) respectively. The resolution settings were tuned to 0.7Da at half height with ion energies set to 1.0 V. The precursor ion for E_2, P, T, and C were set to 271.3m/z, 429.2m/z, 289.2m/z and 347.2m/z with the fragmented product ion set at 145.2m/z, 313.1m/z, 97.0m/z and 329.2m/z respectively.

Consequently, a multiple reaction monitoring (MRM) experiment was run with Argon collision gas set at 4.21 x 10^{-3} m Bar pressure. The E_2, P, T and C were run in negative ion Electrospray which generates $[M-H]^-$. E_2, P, T and C was separated using an HPLC system (Agilent 1100, Palo Alto, CA) with an Xterra C18, 2.1 x 100mm, 3.5 µm column (Waters Corp., MA). Acetonitrile/ water (45/55, v/v) was used as mobile phase (Sigma Aldrich, UK), at a flow rate of 0.3µL/min. Validation of the extraction procedure and HPLC-MS/MS method was achieved by comparing extraction recoveries. The peak area in the chromatogram of a 10 pg/mL standards E_2, P, T and C solution in water/acetonitrile was compared with standards, at the same concentration, and spiked lizard serum that had been through the protein precipitation extraction procedure. A blank plasma sample was run and subtracted from the spiked sample.

E_2, P, T and C levels in the blank were below the limit of quantification for the method and this was used to back-calculate the concentrations in the calibration curve standards and subsequent samples. The efficiency of recovery was 98%. The back-calculated concentration from the protein precipitation extraction method was used to evaluate the steroid concentrations in actual lizard plasma samples. Calibration curves

were constructed in acetonitrile/water, first for validation only and then for the actual samples. The calibration lines were constructed using plasma that was spiked and extracted in the same way as the samples (Figures 2.7, 2.8, 2.9, 2.10). Back-calculated concentrations were obtained using a calibration curve over the concentration range 0.1–10,000 pg/mL with a correlation coefficient greater than 0.999. This gave an accurate indication of the actual steroid concentration in plasma. The sensitivity of the lowest level concentration was evaluated at 0.1pg/ µL using a signal: noise ratio of 8:1 for all components.

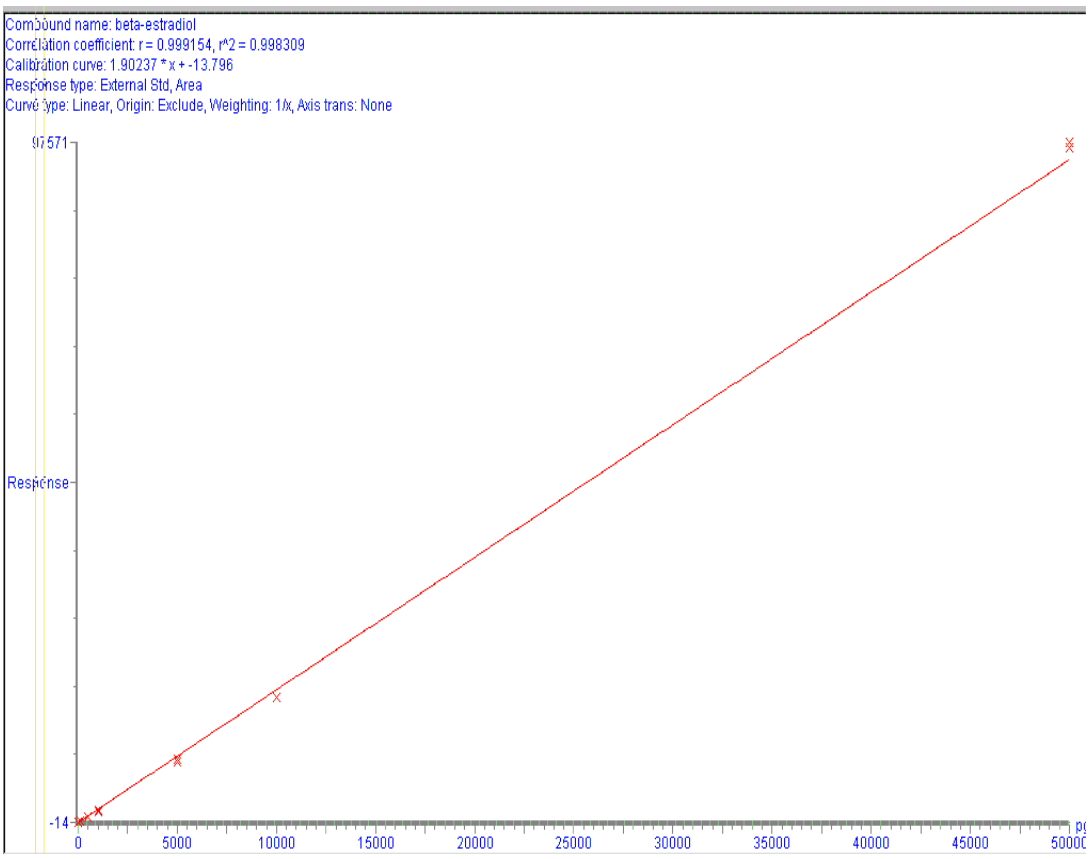

Figure 2.7. Calibration curve for determining oestradiol concentrations.

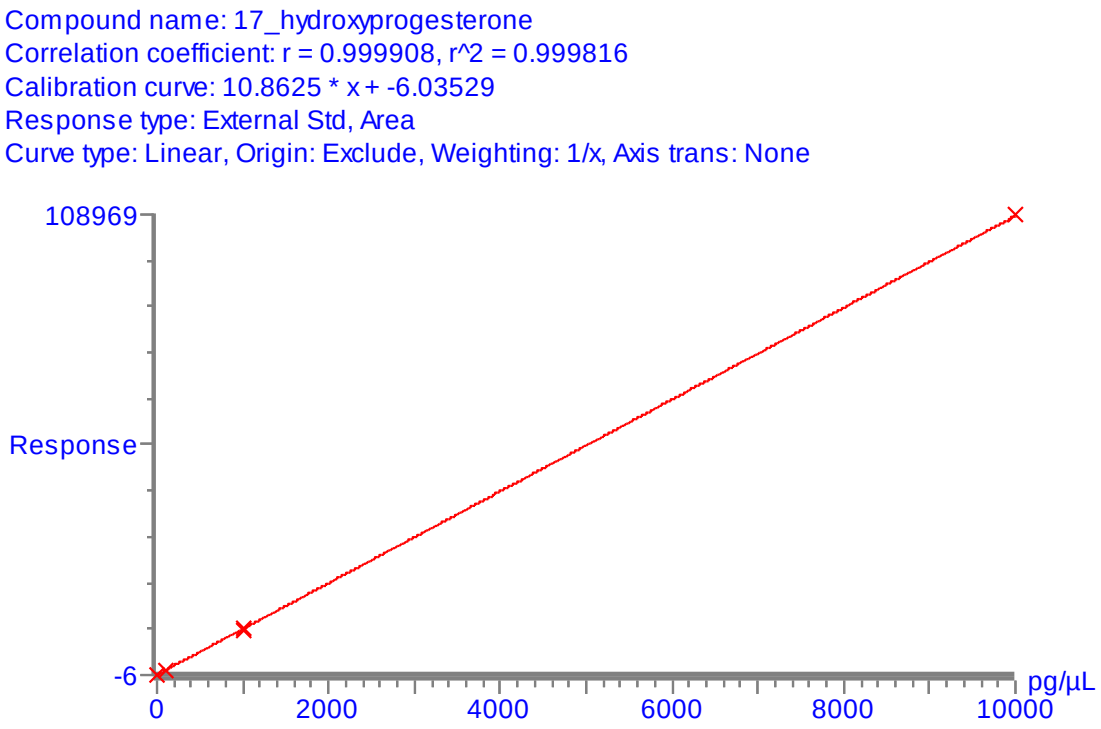

Figure 2.8. Calibration curve for determining progesterone concentrations.

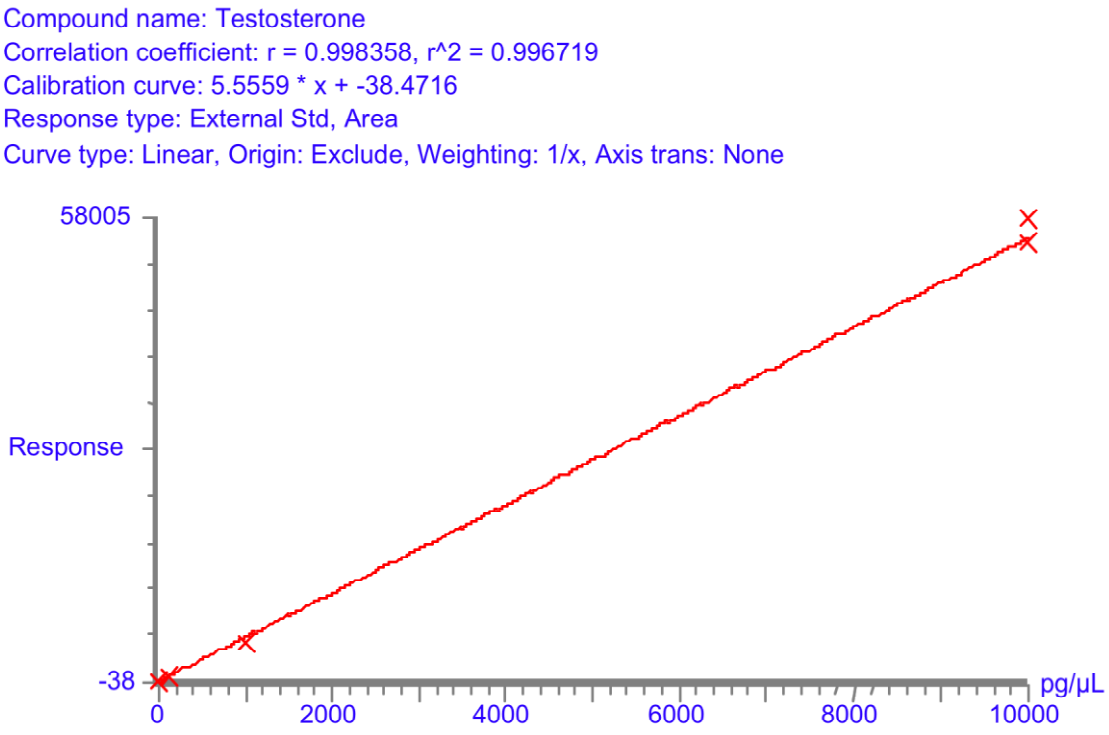

Figure 2.9. Calibration curve for determining testosterone concentrations.

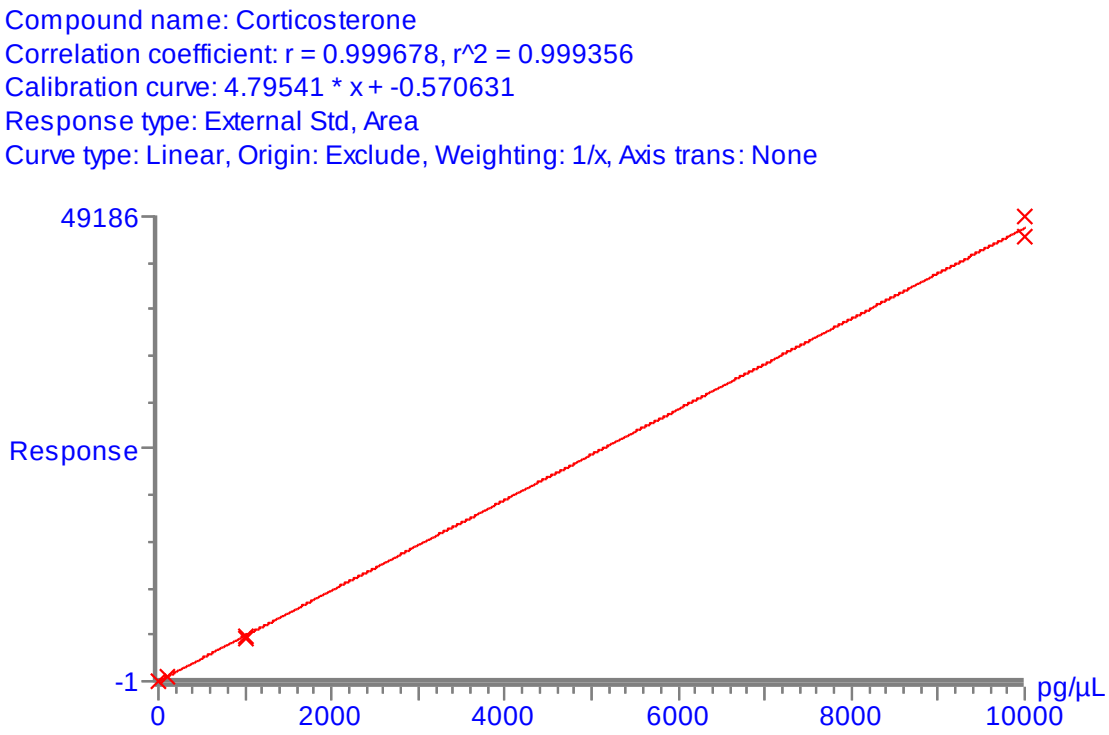

Figure 2.10. Calibration curve for determining corticosterone concentrations.

2.10 Light microscopy

2.10.1 Histology

Tissue specimens collected from the female (ovary, oviduct, and liver) and male (testis, epididymis, vas deferens, and kidney) house gecko were fixed in fresh 10% Bouin's formalin fluid and cut into small blocks 4mm thick and then placed in fresh formalin for 48 hour. Tissue blocks were dehydrated in a graded concentration of alcohol (70%, 95% & 100%) followed by four changes of absolute alcohol for 1 hour in each change. Samples were then placed in three changes of xylene for 1 hour in each change followed by two changes of paraffin wax for two hours in each change at 60^{o}C. Tissue blocks then were oriented in cassettes and embedded in fresh paraffin wax. Thin paraffin sections of 3–5 µm were produced using a Leica rotary microtome and stained with haematoxylin and eosin (see Appendix 1) for general histology. Stained sections were then examined for general histology and photographed using an Olympus photomicroscope. Measurements' of the various regions in the tissues e.g. cell height and lumen diameter were performed using an Olympus DP50 digital camera and Olysia Imaging System attached to the Olympus photomicroscope.

2.10.2 Histochemistry

Paraffin sections (3 µm) from the male and female tissues, processed as above, were stained with: (1) periodic acid-Schiff (PAS) counterstained with fast green (PAS-FG) for a variety of carbohydrates, carbohydrate–protein substances and mucopolysaccharides; (2) Masson trichrome (MT) for general histology and connective tissue; (3) PAS-haematoxylin (PAS-Haem) for nuclear demonstration (4) Alcian blue-PAS (AB-PAS) for carboxylated and sulphated acidic mucosubstances, including mucopolysaccaharides and mucoproteins; (5) Sudan black-B (SB) for demonstration of lipids and secretory granules; (6) Alcian blue pH 2.5 counterstained with nuclear fast red (AB-NF) for glandular tissue. The staining protocols are detailed in Appendix 1.

2.10.3 Plastic sectioning for toluidine blue stain

Plastic sections (0.5–1 µm) from the male and female tissues, processed for transmission electron microscopy, were stained with a toluidine blue stain (see Appendix 1) and examined under light microscope for histological description.

2.11 Immunohistochemistry

Thin paraffin sections (3 µm) from male and female house gecko reproductive organs were placed on polysin slides. Sections were then heated in citrate buffer (pH 9) using a microwave for 25 minutes. The slides were left to cool for 15 minutes and then placed in Tris buffer saline/tween 20 for 5 minutes. Slides were then placed in a fresh buffer bath. Excess buffer was taped off. Peroxidase block was then applied on the section and incubated for 5 minutes. Excess block was rinsed off gently with distilled water and section slides were then placed in fresh buffer bath.

Peptide antibodies supplied by DAKO were used. PR primary antibodies were mouse monoclonal antibodies; they were used at a dilution of 1:50. The antibody anti-P, Clone 1A6, reacts with PRA and PRB forms. Sections were incubated in primary antibody for 30 minutes and then placed in a fresh buffer bath to remove excess antibody. PR antibodies reacted with the reproductive organ tissues. Peroxidase labelled polymer (secondary antibody) was applied on the sections and reacted with the primary PR antibodies. The sections were incubated for 30 minutes. To visualize

the sites of peroxidase activity, the sections were then incubated in substrate chromogen with 3,3'-diaminobenzidine (DAB+) for 10 minutes. The chromogen produced a brown colour as an indicator of PR localization. Sections were then counter-stained with Mayer's Haematoxylin (see Appendix 1).

Negative controls were prepared without primary antibody, and showed no PR reaction. These controls were used to test the specificity of the procedure.

2.12 Transmission electron microscopy

2.12.1 Tissue processing

Tissue specimens collected from the female (ovary and oviduct) and male (testis, epididymis, vas deferens, and kidney) house geckos were placed in fresh Karnovesky's (2.5% gluteraldehyde and 4% paraformaldehyde containing 1M cacodylate buffer adjusted to pH 7.2) EM fixative and fragmented under a Leica dissection stereomicroscope into small pieces of about $1mm^3$ using a razor blade and placed in a second change of fresh Karnovesky's fixative for 3 hours at 4^oC. The following procedure was carried using a Leica EM automatic tissue processor. After fixation the tissue fragments were washed in three 10 minute changes of 1M cacodylate buffer. Secondary fixation was carried out in 1% aqueous osmium tetroxide for 1 hour. A further three changes of 10 minutes washes in distilled water were carried out to wash off excess osmium tetroxide. The specimens were then dehydrated in a graded concentration of acetone (25%, 50%, 75% and 95%) followed by four changes of absolute acetone for 15 minutes in each change to ensure complete removal of water. The tissue fragments were then infiltrated with graded acetone/Araldite CY212 epoxy plastic resin with dilutions of 3:1, 1:1, 1:3 and then into pure Araldite resin for 1 hour in each change. A further two changes in fresh pure Araldite resin were carried out for 1 hour in each change. Tissue fragments were then manually embedded in labelled BEEM capsules containing fresh resin and then polymerized in an oven set at 60^oC for 18 hours.

2.12.2 Ultramicrotomy, staining and screening

Semithin sections of 0.5 µm were produced from the resin plastic blocks using glass knives and a Richert-Jung ultramicrotome and placed on glass slides. Sections were

then stained with toludine blue for examination and area selection under light microscopy. Ultrathin sections of 60-90 nm of tissues from the selected area were microtomed using a diamond knife and a Leica ultracult E ultramicrotome. The thin sections were collected from water on to 3.05mm copper grids and stained with uranyl acetate and lead citrate (see Appendix 1). The stained sections were examined using a JEOL JEM-1230 transmission electron microscope operated at 80kV and TEM images were recorded with a Gatan Bioscan 792 CCD camera.

2.13 Scanning electron microscopy

2.13.1 Tissue processing

Tissue specimens collected from the female (ovary and oviduct) and male (testis) house gecko were placed in fresh Karnovesky's EM fixative and dissected under a Leica dissection stereomicroscope, using a razor blade to reveal areas of interest, and then placed in a second change of fresh Karnovesky's fixative for 3 hours at 4^{o}C. After fixation the tissue specimens were washed in three 10 minute changes of 1M cacodylate buffer. Secondary fixation was carried out in 1% aqueous osmium tetroxide in distilled water for 60 minutes at room temperature. A further three changes of 10 minute washes in distilled water were carried out to wash off excess osmium tetroxide. The specimens were then dehydrated in a graded concentration of ethanol (25%, 50%, 75% and 95%) followed by four changes of absolute ethanol for 15 minutes in each change to ensure complete removal of water.

2.13.2 Critical point drying, sputter coating and screening

Dehydrated tissue specimens were then critically point dried with CO_2 using a Tousimis Autosamdri-815 critical point drier and oriented and mounted on aluminium stubs using double sided carbon discs with the aid of a dissection stereomicroscope. Mounted tissue specimens were then sputter coated with gold particles for 180 seconds using a Bio-Rad SEM Coating System operated at 1.4 kV and SEM images were recorded with JEOL JSM-5600LV scanning electron microscope operated at 10 kV.

2.14 Statistical analysis

Results are reported as means ± standard error of the mean (SEM). Tests for normality and homoscedasticity were carried using Kolmogorov-Smirnov method. In addition, one-way ANOVA was performed on log transformed data followed by Duncan's multiple-comparisons test to detect any statistical differences in measurements of various parameters among reproductive and non-reproductive phases. A *P*- value of less than 0.05 was considered significant. All statistical analyses and graphs were performed using SPSS statistical package for windows (version 18.0).

Gonadosomatic Index (GSI) was calculated by dividing total gonadal mass (g) by the total body mass (g) multiplied by 100.

Hepatosomatic index (HSI) was calculated by dividing total liver mass (g) by the total body mass (g) multiplied by 100.

ANOVA was performed on log transformed data of female plasma steroid concentrations, ovary, oviduct, and liver weights, with body mass as a variate and month as the class interval to examine monthly changes in organ weights in relation to body mass, and to monitor changes in hormonal concentrations during the reproductive and non-reproductive phases. ANOVA was performed on somatic weights and diameter of the largest follicle with month as the class interval.

ANOVA was also performed on log transformed data of male plasma steroid concentrations and testes weight, with body mass as a variate and month as the class interval to examine monthly changes in organ weights in relation to body mass, and to monitor changes in hormonal concentrations during the reproductive and non-reproductive phases. ANOVA was performed on somatic weights with month as the class interval.

Pearson's correlation coefficient between plasma C and haematocrit concentrations was calculated using the following formula for sample correlation coefficient, r:

$$r = \frac{\sum(x_i-\bar{x})(y_i-\bar{y})}{\sqrt{\sum(x_i-\bar{x})^2\sum(y_i-\bar{y})^2}} \qquad \text{where } \bar{x} = 1/n\sum x_i \text{ and } \bar{y} = 1/n\sum y_i$$

Chapter Three:

The reproductive cycle of the male house gecko, *Hemidactylus flaviviridis* (Gekkonidae)

3.1 Introduction

Male lizards exhibit three general types of reproductive cycles: constant, associated and dissociated, (Pough *et al.*, 2004). These cycles are based on gonadal activity, specifically, maturation and shedding of gametes or secretion of sexual steroid hormones, or both. The large majority of lizard species studied to date exhibit an associated or prenuptial reproductive pattern, as the available data support a positive relationship between peak gametogenesis, sex steroid production, and mating behaviour for both males and females (Loverrn, 2011). In temperate and subtropical zone lizards with associated reproductive cycles, the male testicular cycle is divided into two well-defined phases: (a) the regenerative phase, that occurs in the spring and is characterized by sustained sperm production, and (b) the degenerative phase, that begins in summer, where a break in spermatogenesis is observed (Fitch, 1970; Lofts, 1987; Castilla and Bauwens, 1990). Likewise, tropical species in seasonal habitats also display a regenerative phase during the cold (reproductive) season and a degenerative phase during the warm (non-reproductive) season (Wilhoft and Reiter, 1965; Marion and Sexton, 1971).

The discontinuity of the reproductive cycle in lizards is characterized by distinct periods of reproductive quiescence, reproductive recrudescence and reproductive activity. This phenomenon is often referred to as annual cyclicity in reproductive activity. Reproductive cycles have been described for numerous lizard species. Most studies have attempted to demonstrate specific relationships between the male annual cycle of hypertrophy and regression of reproductive organs (Sanyal and Prasad, 1967; Nilson, 1980; Flemming, 1993; Aldridge and Brown, 1995; Ramírez-Bautista *et al.*, 1996; Vieira *et al.*, 2001; Hernández-Gallegos *et al.*, 2002; Ferreira *et al.*, 2002; Röll and van Düring, 2008; Ferreira *et al.*, 2009; Rheubert *et al.*, 2009; Rheubert *et al.*, 2011a), or have combined such information with descriptions of cycles of plasma androgen concentrations only (Arslan *et al.*, 1978b; Courty and Dufaure, 1979; 1980; Kuchling *et al.*, 1981; Johnson *et al.*, 1982; McKinney and Marion, 1985; Bourne *et al.*, 1986b; Moore, 1986; Ando *et al.*, 1990, 1992; Flemming, 1993; Swain and Jones, 1994; Schuett *et al.*, 1997 Jones *et al.*, 1997; Tokarz *et al.*, 1998; Phillips and Millar, 1998; Amey and Whittier, 2000; Radder *et al.*, 2001, Kumar *et al.*, 2011), except in few studies such as the male blue-tongued skinks (Edwards and Jones, 2001b). Thus,

in many cases, supposition about the roles of these gonadal steroids in the regulation of reptilian reproduction is based on analogy with mammals rather than evidence obtained from natural populations (Wiebe, 1985).

Elevated plasma T concentrations have been shown to be correlated with reproduction and mating in many squamates (Lance, 1984). Seasonal changes in plasma T concentrations are well correlated with reproductive events. Usually, both plasma T concentration and testis mass increase during spermatogenesis to peak in the final stages of gamete maturation, coincident with mating, and falling rapidly thereafter (Bona-Gallo *et al*., 1980; McKinney and Marion, 1985; Mahmoud *et al.*, 1985a; Ando *et al*., 1992; Bonnet and Naulleau, 1996; Radder *et al.*, 2001; Kumar *et al.*, 2011). However, the annual changes in plasma concentrations of E_2 or P in male reptiles have only been documented in a few species. Few published studies have correlated the timing of behaviours and mating associated with reproduction with changes in concentrations of all three primary gonadal steroids in the plasma of a male squamate reptile. Saint Girons *et al*. (1993) reported that sexually active male *Vipera aspis* exhibited elevated plasma androgen and E_2 concentrations, while non-breeding males in autumn had low circulating androgen concentrations and significantly higher plasma E_2 concentrations. Plasma P concentrations were highest during the spring and autumn mating periods. Edwards and Jones (2001b) reported that sexually active male blue-tongued skinks (*Tiliqua nigrolutea*) exhibited elevated plasma E_2 and P concentrations during the mating period which then declined during the non-mating period.

The role of testicular oestrogens is not clear, but both peripheral (hypothalamus, pituitary) as well as local (spermatogenesis) actions have been suggested (Gist *et al.*, 2007). Another target for oestrogen action in the male is the excurrent canal system. These canals (rete testis, efferent ductules, epididymis, and vas deferens) are used for the transport, maturation, and storage of sperm, and their presence is restricted to those vertebrates employing internal fertilizsation (Gist *et al.*, 2007). Several studies reported that in male reptiles, oestrogens may influence reproductive behaviour through aromatisation of androgens in the brain. Aromatase activity has been detected in the brains of the turtle *Chrysemys picta* (Callard *et al.*, 1977) and males of the lizard *Podarcis sicula sicula* (Gobbetti *et al.*, 1994). Other studies reported that the

vertebrate testis may be both a source and a target for oestrogen hormones. In vertebrates ranging from sharks to mammals, testicular tissues have been shown to contain aromatase, the rate-limiting enzyme for oestrogen formation (Carreau *et al.*, 1999). Gist *et al.* (2007) reported in the male turtle (*Trachemys scripta*) that aromatase was found in the Leydig cells surrounding the seminiferous tubules as well as in the epithelial cells of the excurrent canals at different concentrations during the spermatogenic cycle, being highest in the quiescent testis and lowest during germ cell meiosis. Cardone *et al.* (2002) reported that in *Podarcis sicula* high oestrogen concentrations have an inhibitory effect on spermatogenesis and epididymal development.

An increasing number of studies suggest that P may also be important in stimulating reproductive behaviour in some male squamates (Lindzey and Crews, 1988; 1992; Young *et al.*, 1991; Witt *et al.*, 1994). Exogenous P has been shown to stimulate sexual behaviours in males of the lizard *Cnemidophorus inornatus* (Lindzey and Crews, 1986). This finding is contrary to the usual pattern in male vertebrates where typically P inhibits male sexual behaviours (Moore and Lindzey, 1992). However, experiments with lizards, and more recently with rats, have challenged this paradigm. For example, exogenous P induces mating behaviour in some, but not all, castrated male whiptail lizards (*Cnemidophorus inornatus*), but failed to elicit sexual activity in castrated, P-insensitive males (Crews *et al.*, 1996). Individual variation in P sensitivity serves as the substrate for the evolution of P-activation of male-like pseudosexual behaviour in the descendant unisexual species (Crews and Sakata, 2000). Moreover, restoration of sexual behaviour in P-sensitive males by synthetic progestin agonists indicates that it is P, and not a metabolite of P, that produces this behavioural effect (Lindzey and Crews, 1988), and further, binding studies suggest that PRs mediates this response (Lindzey and Crews, 1993). Recent reports suggested that in mammalian males, P influences spermiogenesis, sperm capacitation, and P biosynthesis in Leydig cells (Andersen and Tufik, 2006).

Given these often conflicting reports, it is surprising that annual changes in plasma concentrations of E_2 or P in male reptiles have not been documented in more species; such information is vital for us to better understand the hormonal control of reproduction in reptiles.

The relationship between P and its receptors has been established in some reptiles. PRs have been characterized in snakes (Custodia-Lora and Callard, 2002a) and lizards (Paolucci and Di Fiori, 1994). There are at least two PR isoforms found in reptiles, PRA and PRB (Custodia-Lora and Callard, 2002a).

The effect of stress on the circulating gonadal steroids, gonadotropins and corticosteroids, has been documented in several species of reptiles (Licht, 1984; Greenburg and Wingfield, 1987; Moberg, 1985; Mahmoud and Licht, 1997; Tokarz and Summers, 2011). In several studies of reptiles, captured male tuataras, *Sphenodon punctatus*, showed a significant rise in plasma P and T concentrations (Cree *et al.*, 1990a). Plasma T concentrations declined by 50% within 4 hr of captivity in male alligators, *Alligator mississippiensis* (Lance and Elsey, 1986). In the lizard *Phrynosoma cornutum* plasma C concentrations were marginally higher in breeding than in non-breeding males (Wack *et al.*, 2008). A recent study by Klukowski (2011) on the lizard, *Sceloporus undulatus* reported that plasma C concentrations in response to confinement were significantly lower in the breeding than the postbreeding season. Further, the effect of T on the stress response was experimentally tested. Males with elevated T concentrations exhibited significantly weaker plasma C responses to 1hour of confinement than sham-implanted or gonadectomized males. These results suggest that stress of capture and/or serial bleeding enhances radical changes in circulating hormones and may suppress gonadal development.

Temperature is an important factor in the timing of the testicular phases in reptiles. In general, temperature may alter the response of gonads to circulating gonadotropins (Duvall *et al.*, 1982; Licht *et al.*, 1985; Bourne *et al.*, 1986b) and elevated temperature is a major influence on gonadal growth and development in natural populations (Licht, 1984). However, a study of the lizard *Calotes versicolor* showed that during the resting phase, high temperature does not stimulate testicular recrudescence, whereas injections of 0.5µg/kg GnRH does so. Also, the findings suggest that either higher brain centres regulating the hypothalamus or the hypothalamus itself becomes dormant, causing testicular inactivity (inactivation of hypophysial-testicular axis) during the postbreeding resting phase (Shanbhag *et al.*, 2000a). Elevated temperature, therefore, might not be the major factor stimulating testicular growth, maintaining spermatogenesis and androgen production.

Various studies on testicular cycles of lizard species indicate that spermatogenic patterns are peculiar to each species. Many male lizard species exhibit a prenuptial (discontinuous) spermatogenic cycle with variations in the testicular or seminiferous tubule size (Fitch, 1970; Sarkar and Shivanandappa, 1989; Shanbhag *et al.*, 2000b; Noriega *et al.*, 2002; Ferreira *et al.*, 2009). Spermiogenesis is a complex phenomenon (Courtens and Depeiges, 1985; Saita *et al.*, 1988; Carcupino *et al.*, 1989). Structural changes in the germinative epithelium during the testicular cycle may be related to changes in environmental conditions, such as temperature and photoperiod (Mendonça and Licht, 1986; Cree *et al.*, 1992), precipitation (Guillette and Casas-Andreu, 1987) or food availability and lipid reserves (Diaz *et al.*, 1994) or direct hypothalamic control (Shanbhag *et al.*, 2000a). These changes in the germinative epithelium may also be associated with reproductive patterns and variations in the activity of interstitial cells (van Wyk, 1995; Colli and Pinho, 1997). In *H. flaviviridis*, spermatogenesis is of a prenuptial type where Leydig cell steroidogenic activity is synchronized to proliferation and differentiation of germ cells (Licht, 1984), indicating the important role of androgens in spermatogenesis. In addition to their role in support and nutrition of the germ cells (Röll and von Düring, 2008), Sertoli cells have also been reported to play a major role in Leydig cell proliferation and steroidogenesis (Saez *et al.*, 1987; Skinner *et al.*, 1991; Bardin *et al.*, 1994; Lejeune *et al.*, 1996; Khan and Rai, 2005).

In the reptilian testis, steroidogenic ultrastructural features are correlated with plasma sex hormone concentrations and spermatogenesis. Specifically, Leydig and Sertoli cells are associated with the production of steroids such as T, E_2 and P, which are associated with an increase in smooth endoplasmic reticulum (SER), free ribosomes, mitochondria with swollen cristae and the presence of SER in the form of cisternal whorls with lipids droplets and mitochondria (Licht *et al.*, 1985; Mesner *et al.*, 1993; Mahmoud and Licht, 1997; Ferreira and Dolder, 2003a).

The developmental strategy of spermatogenesis has been explained using various stages (I-VIII), which describe the presence or absence of groups of cells within the seminiferous epithelium, presence/absence of the lumen of the seminiferous tubule, and spermatozoa in the epididymis in reptiles (Tienhoven, 1968). Furthermore,

ultrastructural studies of the mature spermatozoon have been reported for many lizards, such as in Chamaleonidae (Jamieson, 1995; Oliver *et al.*, 1996); Polychrotidae (Teixeira *et al.*, 1999a; Scheltinga *et al*., 2001); Phrynosomatidae (Scheltinga *et al*., 2000); Gymnophthalmidae (Teixeira *et al*., 1999b); Tropiduridae (Teixeira *et al*., 1999a; Ferreira and Dolder 2003b); Teiid lizards (Teixeira *et al*., 2002); Gekkonidae (Mubarak, 2004; Röll and von Düring, 2008; Rheubert *et al.*, 2011a) and also Iguanidae (Vieira *et al.*, 2004). Some descriptions focus on phylogenetic relationships. Spermiogenesis is described for some Chamaleonidae lizards (Al-Hajj *et al.*, 1987; Dehlawi and Ismail, 1990; Dehlawi *et al.*, 1992; 1993) and a few representatives of Iguanidae (Saita *et al*., 1988; Ferreira *et al.*, 2002; Vieira *et al.*, 2005; 2007). The possibility of contributing to the studies of phylogenetic relationships justifies detailed comparisons between lizard families. Data on spermatogenesis is sparse for the majority of vertebrates, and almost non-existent for lizards (Ferreira and Dolder 2003b).

The structure, function and regulation of the epididymis in reptiles have been studied (Fox, 1977; Haider and Rai, 1987; Mesure *et al*., 1991; Averal *et al*. 1992; Jones, 1998, 2002; Akbarsha and Manimekalai 1999; Desantis *et al*. 2002; Guerrero *et al*. 2004; Akbarsha *et al*. 2005, 2006; Ferreira *et al.*, 2009; Rheubert *et al.*, 2010b). However, the fact remains that the reptilian epididymis, in respect to histological variation along the length and ultrastructural organization of the epithelial lining, has only been reported in a few studies. The reptilian ductus epididymis is lined by a pseudostratified epithelium consisting of principal cells and basal cells, and probably intraepithelial lymphocytes (Jones, 1998; 2002). A light microscopic study by Haider and Rai (1987) on the lizard, *H. flaviviridis*, reported that the reptilian epididymis has three structurally distinct regions. The epididymis of this species consists of numerous, small, convoluted, ductuli epididymis which unite to form a larger ductus epididymis. The ductus epididymis is divided into anterior, middle, and posterior regions. According to Jones (1998; 2002) there is no definite evidence for the presence of an initial segment in the ductus epididymis of reptiles, as in the case of the mammalian epididymis (Hermo and Robaire 2002). However, recent study by Akbarsha *et al*. (2006) reported that the ductus epididymidis of the fan-throated lizard

Sitana ponticeriana is differentiated along its length into four histologically distinct zones, initial segment, caput, corpus and cauda.

The RSS is a hypertrophied region of the distal urinary ducts of male snakes and lizards (Sanyal and Prasad, 1966; Prasad and Reddy, 1972; Fox, 1977; Gabri, 1983; Sarkar and Shivanandappa, 1989; Sever *et al.*, 2002; Krohmer, 2004; Sever and Hopkins, 2005; Siegel *et al.*, 2009a,b; Rheubert *et al.*, 2011b). In lizards and some snakes the RSS can include the terminal segment of the distal convoluted tubules, post-terminal segment, collecting ducts, and/or portions of the ureter (Saint Girons, 1972; Fox, 1977). Studies on lizards to date have reported that the RSS is hypertrophied only during periods of sexual activity and cannot be distinguished from adjacent tubular regions during sexual quiescence (Fox, 1977; Gabri, 1983). The function of the RSS is not clearly understood but its secretions may sustain and activate sperm (Cuellar, 1966), provide courtship pheromones (Volsøe, 1944), form copulatory plugs (Devine, 1975), and/or have other purposes generally associated with seminal fluid (Prasad and Reddy, 1972). Weil (1984) suggested that the RSS secretions of the snake *Nerodia sipedon* has dual functions, one of sperm transport and capacitation in the female reproductive tract in autumn, and another related to sexual behaviour in the spring. Numerous histological studies on the RSS of squamates have been reported. However, only eleven ultrastructural studies on the RSS have been reported in snakes and lizards (Rheubert *et al*., 2011b).

The lizard, *H. flaviviridis*, is a common house gecko found throughout Oman. Information concerning the annual reproductive cycle of male *H. flaviviridis* has not been carried out before in the Gulf Region and the Arabian Peninsula but only in neighbouring countries such as India. Presented here for the first time is a comprehensive examination of annual cycles of plasma T, E_2, P and C concentrations in male *H. flaviviridis*, and detailed description of structural and ultrastructural changes during the testicular cycle, and epididymal and RSS development.

3.2 Materials and Methods

Please refer to Chapter Two: Materials and Methods.

3.3 Results

3.3.1 Environmental effects on testicular cycle

Observations on feeding, mating, and movements suggested that the geckos had limited activity during quasidormacy (December–February) with temperature ranging between 20–23°C in daytime and dropping below 15°C in cold nights (Figure 3.1A). During courtship and mating (March–April) the temperature ranged between 25–35°C (Figure 3.1A), which is the thermoactivity range (TAR). The lizards were very active during this period.

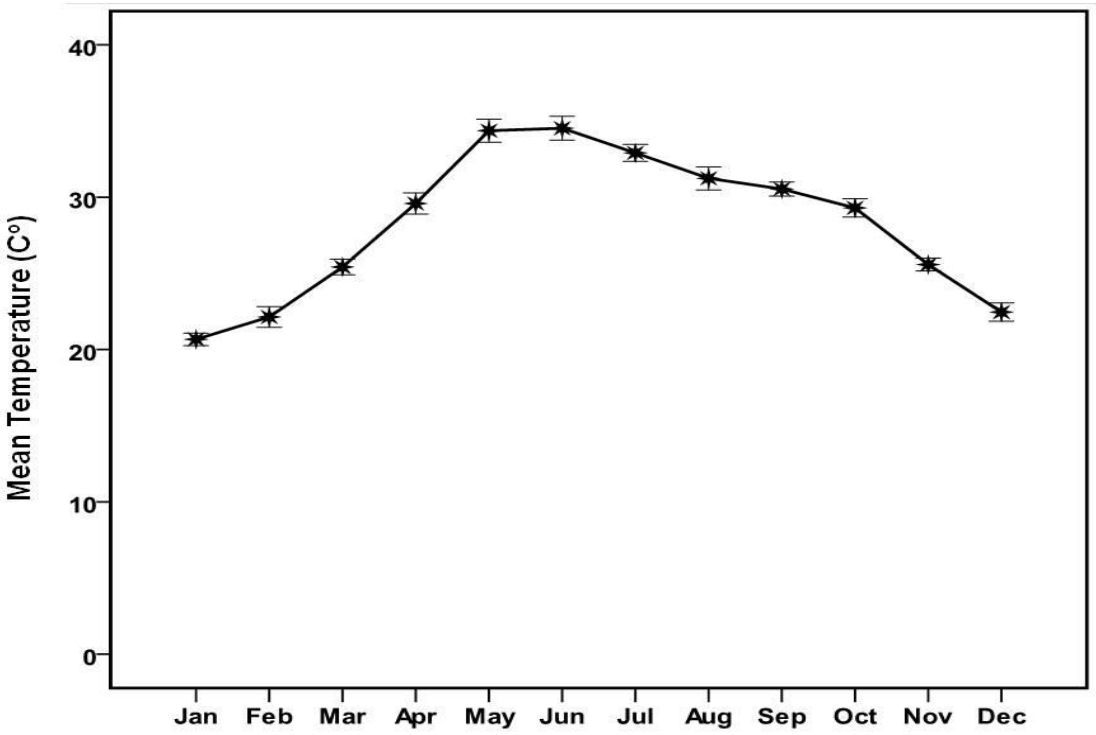

Figure 3.1A. Monthly mean (±S.E.M.) temperature.

Other environmental factors such as photoperiod (12 hours during the breeding period and 13 hours during the nonbreeding period), humidity (Figure 3.1B) and rainfall (Figure 3.1C) showed no relationship with the timing of reproductive events.

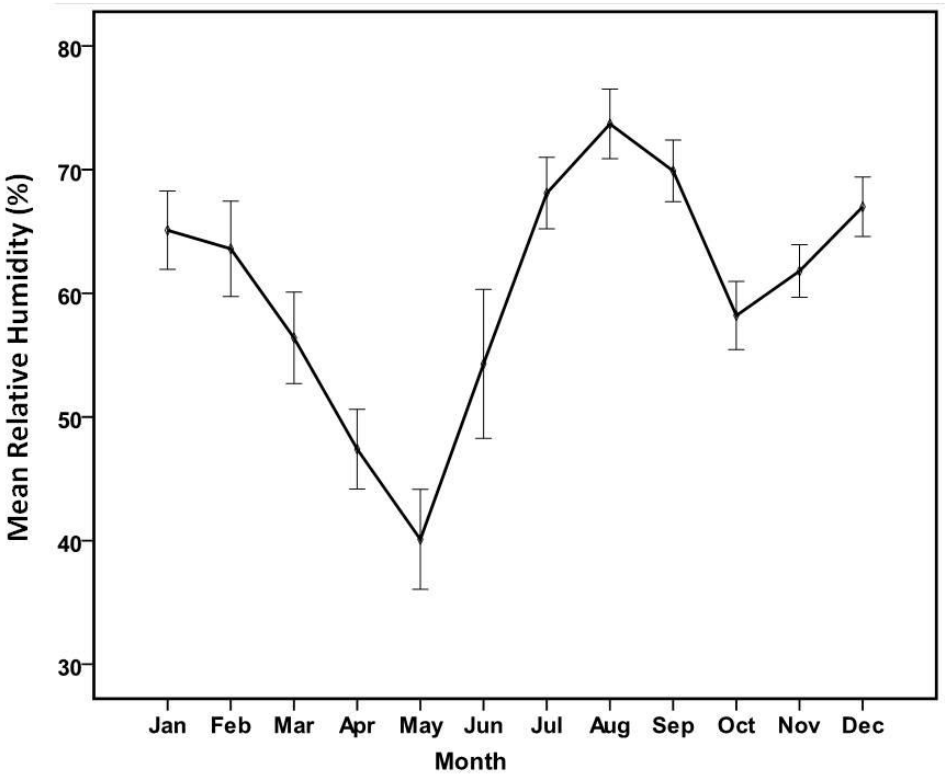

Figure 3.1B. Monthly mean (±S.E.M.) humidity.

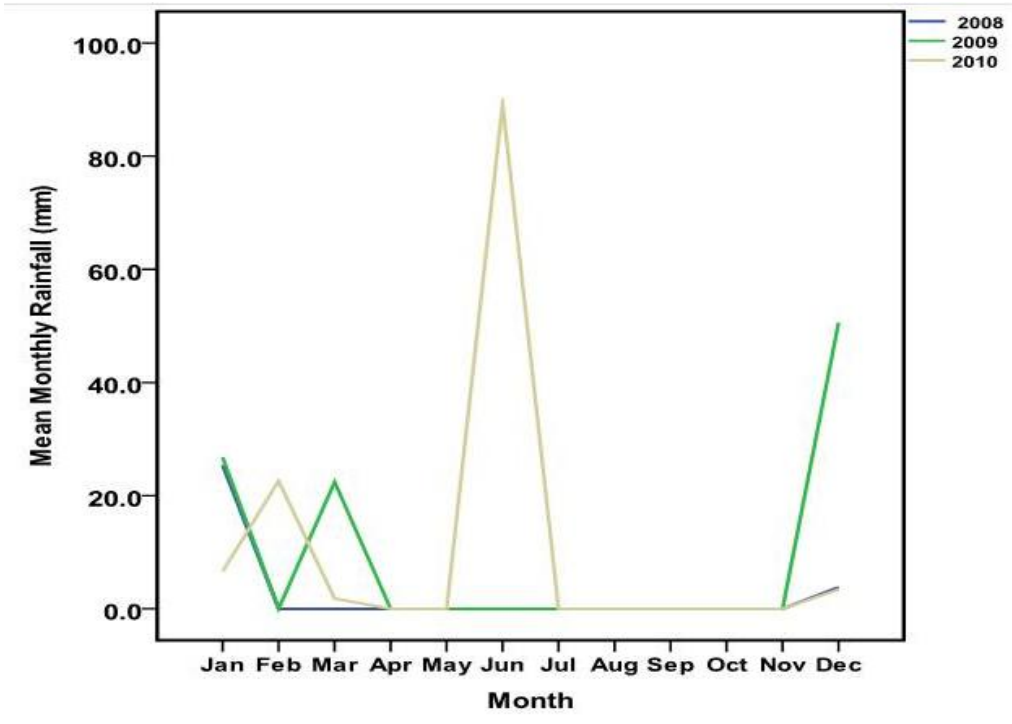

Figure 3.1C. Monthly mean (±S.E.M.) rainfall.

3.3.2 Morphometry of the reproductive organs

Changes in the testicular weight, SVL, body mass and seminiferous tubules during the reproductive cycle of *H. flaviviridis* are summarised in Table 3.1A. There are no significant variations in data of each month collected between year one and year two.

Table 3.1A. Changes (Mean ± S.E.M) in body length and body wt, testis wt, seminiferous tubule diameter (STD) and seminiferous epithelial height (EPH) in *H. flaviviridis* during year 1 reproductive cycle (N = Individual geckos).

Month / Year	N	SVL (cm)	Body wt (g)	Testis wt (g)	STD (µm)	EPH (µm)
Jan 1	3	6.767 ± 0.415^{a}	9.167 ± 1.644^{a}	0.095 ±0.012^{def}	291.111 ±8.380^{a}	64.444 ±2.825^{f}
2	3	6.833 ±0.415^{b}	10.767 ±1.644^{ab}	0.104 ±0.009^{cd}	289.091 ±7.580^{f}	65.909 ±2.556^{f}
Feb 1	3	7.667 ±0.415^{b}	12.767 ±1.644^{a}	0.124 ±0.012^{f}	362.500 ±6.719^{a}	85.000 ±2.265^{g}
2	4	7.675 ±0.359^{ab}	14.575 ±1.424^{bc}	0.113 ±0.008^{d}	347.857 ±6.719^{g}	80.769 ±2.265^{f}
March 1	5	7.940 ±0.322^{ab}	11.120 ±1.274^{a}	0. 115 ±0.009^{ef}	350.000 ±6.972^{a}	80.769 ±2.351^{g}
2	5	7.600 ±0.322^{ab}	11.120 ±1.274^{abc}	0.120 ±0.007^{d}	345.385 ±6.972^{g}	82.308 ±2.351^{f}
April 1	5	7.100 ±0.322^{b}	10.420 ±1.274^{a}	0.073 ±0.009^{cd}	222.727 ±7.580^{f}	46.818 ±2.556^{e}
2	5	7.640 ±0.322^{b}	11.320 ±1.274^{abc}	0. 086 ±0.007^{c}	205.000 ±7.950^{e}	45.500 ±2.680^{d}
May 1	4	7.325 ±0.359^{b}	10.250 ±1.424^{a}	0.019 ±0.010^{ab}	172.000 ±7.950^{d}	25.500 ±2.680^{bc}
2	4	7.325 ±0.359^{b}	9.125 ±1.424^{a}	0. 021 ±0.008^{a}	165.000 ±7.950^{c}	30.500 ±2.680^{c}
June 1	7	7.457 ±0.272^{b}	11.643 ±1.077^{a}	0. 014 ±0.008^{a}	91.000 ±7.950^{a}	16.800 ±2.680^{a}
2	9	7.444 ±0.240^{b}	9.333 ±0.949^{a}	0. 014 ±0.005^{a}	92.273 ±7.580^{a}	16.636 ±2.556^{a}

Table 3.1A. Conituned. Changes (Mean ± S.E.M) in body length and body wt, testis wt, seminiferous tubule diameter (STD) and seminiferous epithelial height (EPH) in *H. flaviviridis* during year 2 reproductive cycle (N = Individual geckos).

Month / Year		N	SVL (cm)	Body wt (g)	Testis wt (g)	STD (µm)	EPH (µm)
July	**1**	3	7.933 ± 0.415^{a}	11.533 ± 1.644^{a}	0.018 ±0.012^{a}	114.200 ±7.950^{b}	17.900 ±2.680^{ab}
	2	3	7.333 ±0.415^{b}	10.600 ±1.644^{ab}	0.017 ±0.009^{a}	114.400 ±7.950^{b}	20.000 ±2.680^{ab}
Aug	**1**	3	7.900 ±0.19^{b}	12.267 ±1.644^{a}	0.023 ±0.012^{ab}	120.091 ±7.580^{bc}	21.182 ±2.556^{abc}
	2	3	7.767 ±0.415^{ab}	13.000 ±1.644^{abc}	0.028 ±0.009^{a}	123.273 ±7.580^{b}	22.000 ±2.556^{ab}
Sept	**1**	2	7.750 ±0.508^{ab}	8.850 ±2.014^{a}	0.033 ±0.014^{ab}	140.500 ±7.950^{c}	24.200 ±2.680^{abc}
	2	3	7.667 ±0.415^{ab}	10.800 ±1.644^{ab}	0.033 ±0.009^{ab}	135.455 ±7.580^{b}	27.455 ±2.556^{bc}
Oct	**1**	6	7.750 ±0.293^{b}	11.833 ±1.163^{a}	0.053 ±0.008^{bc}	173.500 ±7.950^{d}	28.500 ±2.680^{c}
	2	7	7.929 ±0.272^{b}	15.071 ±1.077^{c}	0.054 ±0.006^{b}	174.000 ±7.950^{c}	31.100 ±2.680^{c}
Nov	**1**	3	8.167 ±0.415^{b}	12.267 ±1.644^{a}	0.081 ±0.012^{cde}	208.000 ±7.950^{e}	37.000 ±2.680^{d}
	2	3	8.000 ±0.415^{b}	10.167 ±1.644^{a}	0.054 ±0.009^{b}	199.000 ±7.950^{d}	32.500 ±2.680^{c}
Dec	**1**	2	7.750 ±0.508^{b}	10.750 ±2.014^{a}	0.082 ±0.014^{cde}	245.000 ±7.257^{f}	45.833 ±2.447^{e}
	2	3	8.267 ±0.415^{b}	15.067 ±1.644^{c}	0.082 ±0.009^{c}	247.000 ±7.950^{f}	45.000 ±2.680^{d}
F(11,34) **F(11,46)**	**1** **2**		1.154 0.865	4.755 3.557	15.038 30.482	F(11,118) 136.1 F(11,119) 163.1	101.265 91.513
P-value	**1** **2**		0.066 0.058	0.002 0.002	< 0.001 < 0.001	< 0.001 < 0.001	< 0.001 < 0.001

Statistical differences between groups obtained by Duncan's multiple-comparisons test within each year. Months with significantly different values (mean ± S.E.M) in vertical column were assigned different letters. Months with the same letter shows statistically no significant difference between them at the 0.05 level of significance.

There are no significant variations in data of each month collected between year one and year two (Table 3.1A). The body weight and SVL of male *H. flaviviridis* ranged from 6.91 – 13.80 g and 6.80 – 8.08 cm respectively. There was no significant variation in SVL in relation to body mass during the 24 month study period (Table 3.1A). The weight of the testis ($P < 0.001$) varied significantly in relation to body weight during the different months of the year (Table 3.1A). The testes regressed in the quiescent phase (June–August) but began to increase gradually in the recrudescent

phase (September–October) and continued to increase significantly ($P < 0.001$) in the active phase (November–May) coinciding with the onset of spermiogenesis (see gonadosomatic index).

3.3.3 Gonadosomatic index

The monthly variation in the gonadosomatic index (GSI) is shown in Figure 3.2A. Gonadosomatic index was calculated as (testis mass (g) / body mass (g)) x 100.

The testes regressed between June and August (quiescent phase) but began to increase gradually in September through to October (recrudescent phase) and continued to increase significantly ($P < 0.001$) in November through to May (active phase) coinciding with the onset of spermiogenesis (Figure 3.2B). During March and April (breeding phase) GSI was the highest (F (11, 86) = 13.753, $P < 0.001$). In May, the testes began to regress and by June a complete regression took place as the GSI dropped significantly ($P < 0.01$).

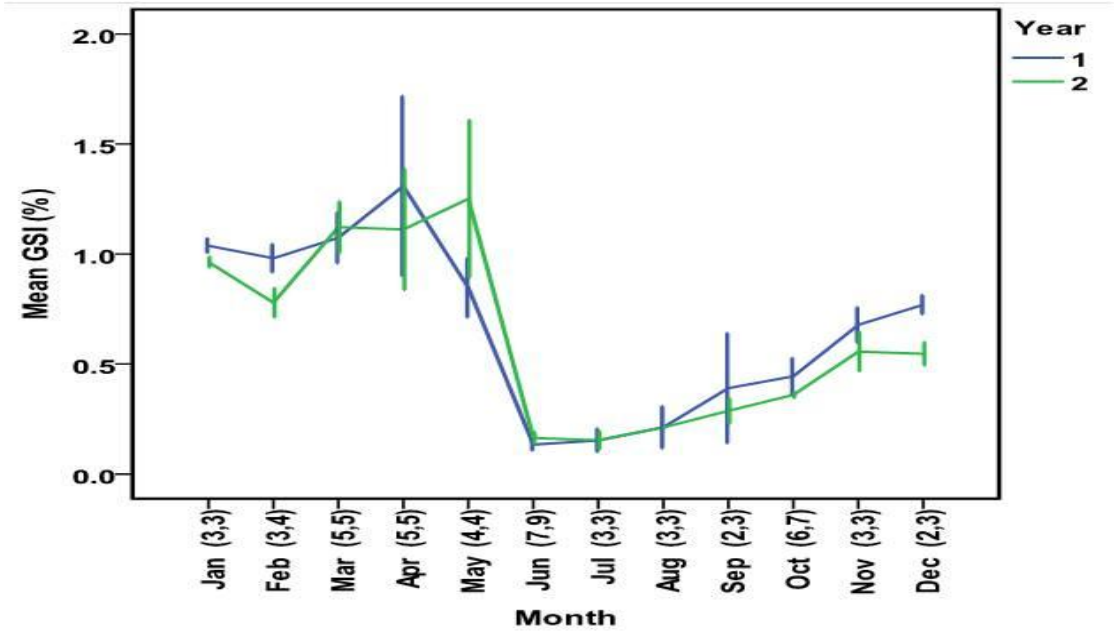

Figure 3.2A. Monthly mean (±S.E.M.) GSI during the two reproductive cycles of *H. flaviviridis*. There are no significant variations in data of each month collected between year one and year two. The active phase commenced in November, reached a peak in April, decreased significantly in June and stayed low until October. Numbers below each histogram represents sample size. Months with significantly different GSI were assigned different letters. Months with the same letter shows statistically no significant difference between them at the 0.05 level of significance. Statistical differences between groups obtained by Duncan's multiple-comparisons test within each.

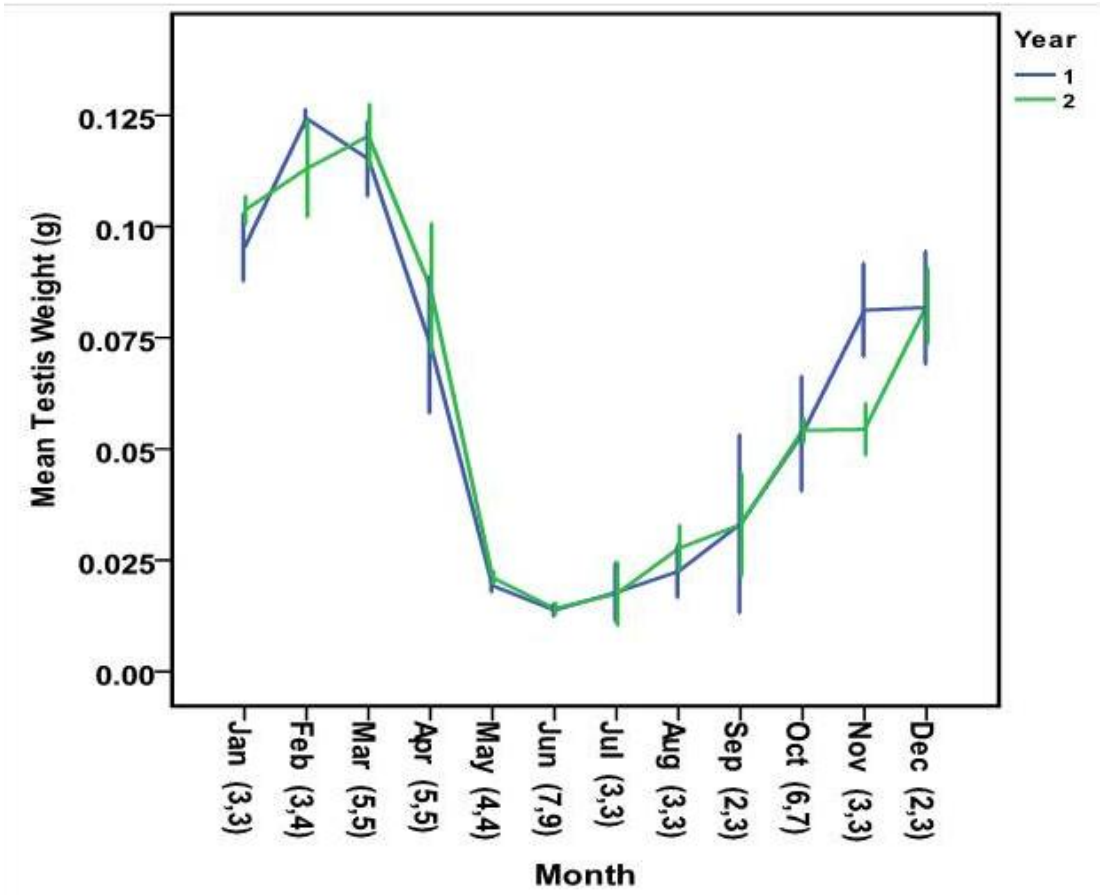

Figure 3.2B. Monthly mean (±S.E.M) testis weight (g) during the two annual testicular cycles of *H. flaviviridis*. There are no significant variations in data of each month collected between year one and year two. Numbers below each histogram represents sample size. Months with significantly different testis were assigned different letters. Months with the same letter shows statistically no significant difference between them at the 0.05 level of significance. Statistical differences between groups obtained by Duncan's multiple-comparisons test within each year.

3.3.4 Gross morphology of reproductive organs

3.3.4.1 Testes

Adult male *H. flaviviridis* had well developed abdominal oval testes with convoluted seminiferous tubules. The testes were surrounded by tunica albuginea (Figure 3.3A). The seminiferous tubules were ensheathed by tunica propria and were interspersed with interstitial tissue, blood and lymphatic vessels (Figure 3.3B). Superficially, the seminiferous epithelia had all the main spermatogenic cell types found in sexually active males. In paraffin sections, spermatogonia, spermatocytes, early spermatids,

late spermatids and luminal spermatozoa were recognised (Figure 3.3C). The cell types were arranged in successive layers from the basement membrane towards the lumen, where the tails of mature spermatids were oriented towards the lumen.

The seminiferous tubules were lined by a complex epithelium containing a non-proliferating population of supporting cells or Sertoli cells and a proliferative population of germ cells. The nuclei of Sertoli cells (Figure 3.3D) can be recognised near the basal lamina of the seminiferous epithelium. The nuclei were irregularly shaped and possessed darkly stained nucleoli. The Sertoli cells extended from the base of the seminiferous epithelium to the lumen providing lateral processes around the spermatocytes and spermatids. Apical processes of the Sertoli cells enclosed mature spermatids.

Leydig cells could be recognised in the interstitial tissue between the seminiferous tubules (Figure 3.3D). The density of the Leydig cells appeared to be similar in all preparations. They occurred singly or in groups of 2–3 cells near the blood vessels.

3.3.4.2 Epididymis

The epididymis was composed of numerous small, convoluted tubules known as ductuli epididymis (Figure 3.3E), and a larger contorted tubule called the ductus epididymis (Figure 3.3F). The convoluted tubules of the ductus had lumena of different diameters and along their length were lined by a layer of epithelial cells. The epithelial layer contained two types of cells, principal secretory and basal cells. The principal secretory cells underwent an annual cycle. In its most active state, the epithelium formed the major part of the organ volume. The principal secretory cells were tall and columnar with basal nuclei and a supranuclear cytoplasm occupied by numerous large secretory granules.

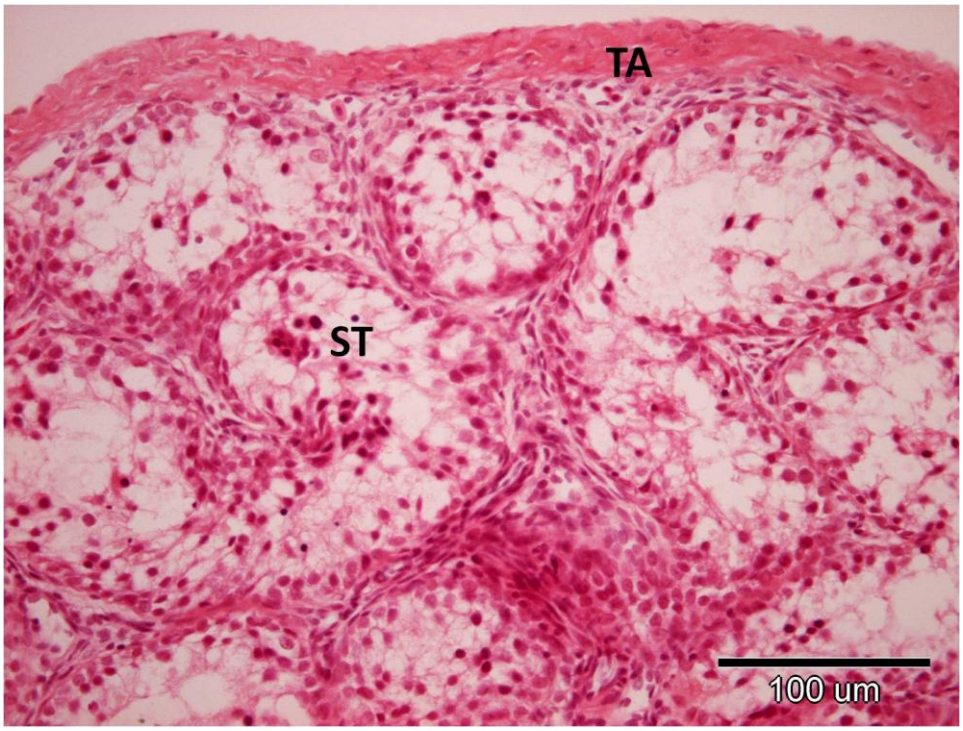

Figure 3.3A. H&E section of a testis from the quiescent phase showing tunica albuginea (TA) and seminiferous tubules (ST).

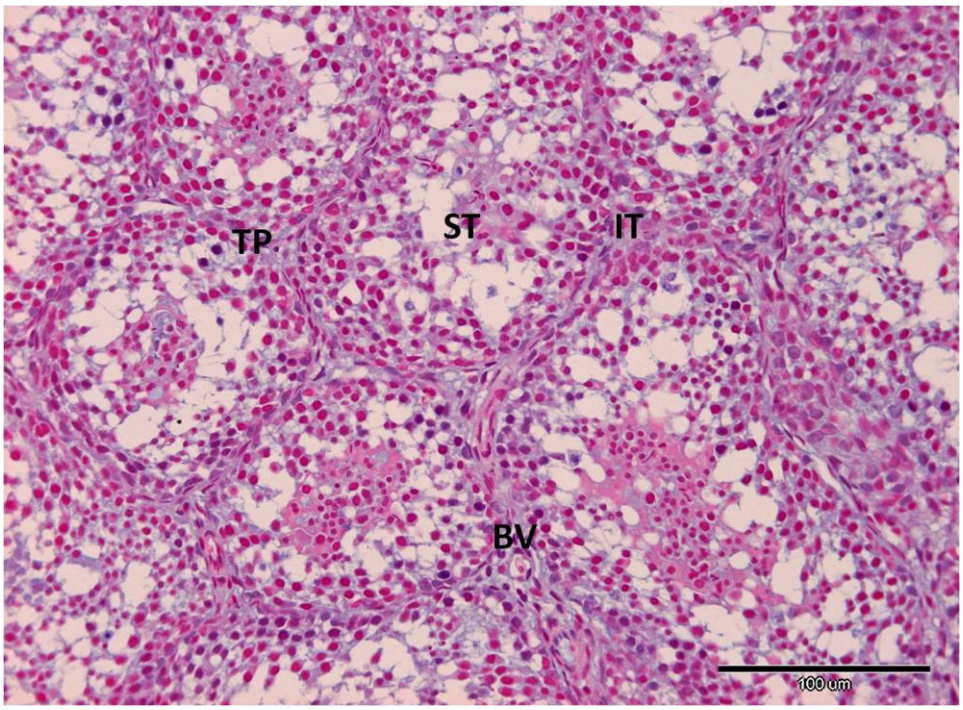

Figure 3.3B. AB-NF section of seminiferous tubules (ST) from the recrudescent phase. Tunica propria (TP) interspersed by interstitial tissue (IT) and blood vessels (BV).

Figure 3.3C. H&E section of seminiferous tubules from the active phase showing spermatogenic cells; spermatogonia (SP), spermatocytes (SE), early spermatids (Est), late spermatids with tails (Lst) and luminal spermatozoa (SZ).

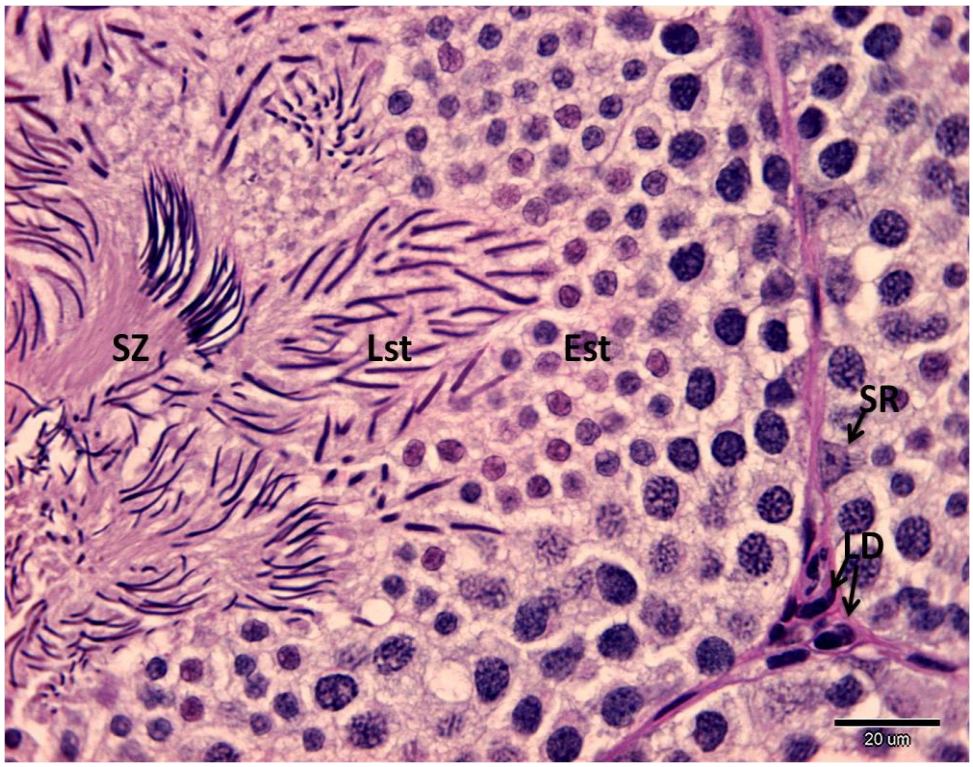

Figure 3.3D. AB-PAS section of seminiferous tubules from the active phase showing Sertoli cells (SR) near the basal lamina of the epithelium. Leydig (LD) cells in the interstitial tissue near blood vessels. Early spermatids (Est), late spermatids (Lst), spermatozoa (SZ).

Figure 3.3E. H&E section of the epididymis from the active phase showing ductuli epididymis lined by nonciliated low cuboidal epithelial cells (Cu). The lumen of some ductuli contains spermatozoa (SZ).

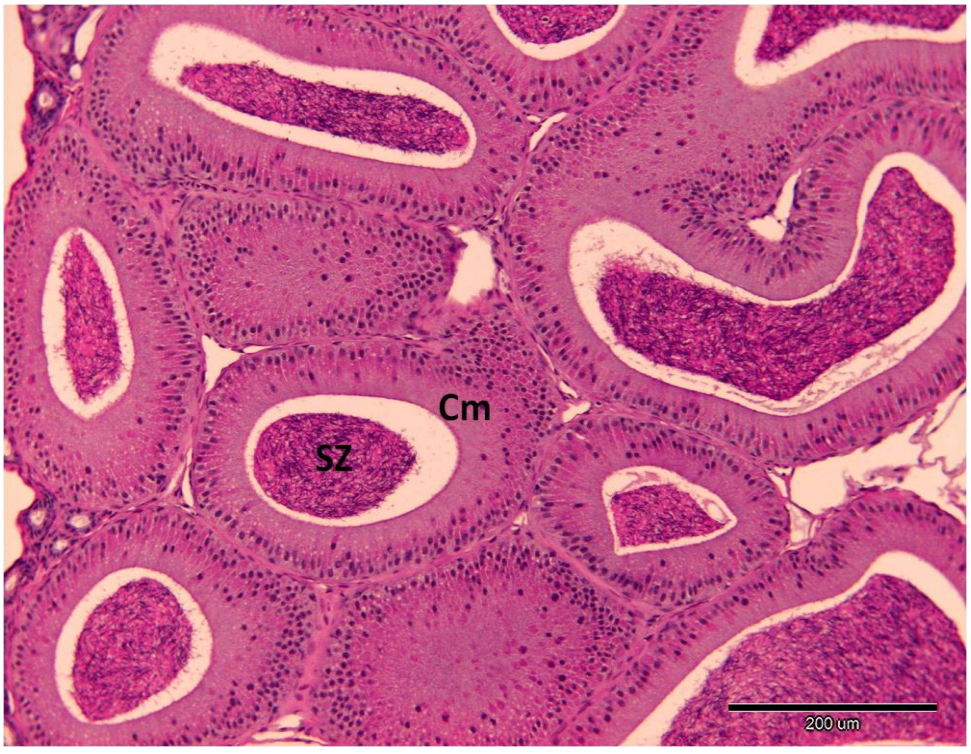

Figure 3.3F. AB-PAS section of the epididymis from the active phase. Ductus epididymis lined by a layer of tall columnar epithelial cells (Cm). The lumen is filled with spermatozoa (SZ).

3.3.4.3 Vas deferens

The vas deferens was a convoluted tube carrying the sperm from the epididymis into the hemipenis. It was composed of an outer layer of smooth muscle and luminar trabeculae with a pseudo-stratified epithelium (Figure 3.3G).

3.3.4.4 Kidneys

In kidneys from the active phase, there was a normally developed segment and a sexual segment. The normal renal segment consisted of uriniferous tubules possessing cylindrical cells with central nuclei. In contrast, the RSS had larger tubules which were characterized by hypertrophied columnar cells with basal nuclei and numerous granules (Figure 3.3H). It consisted mainly of the terminal portion of the collecting ducts lying in the renal medulla.

Figure 3.3G. H&E section of vas deferens from the active phase. Convoluted tube filled with sperm (S). The vas deferens composed of smooth muscle (SL) and luminar trabeculae with pseudo-stratified epithelial cells (PS).

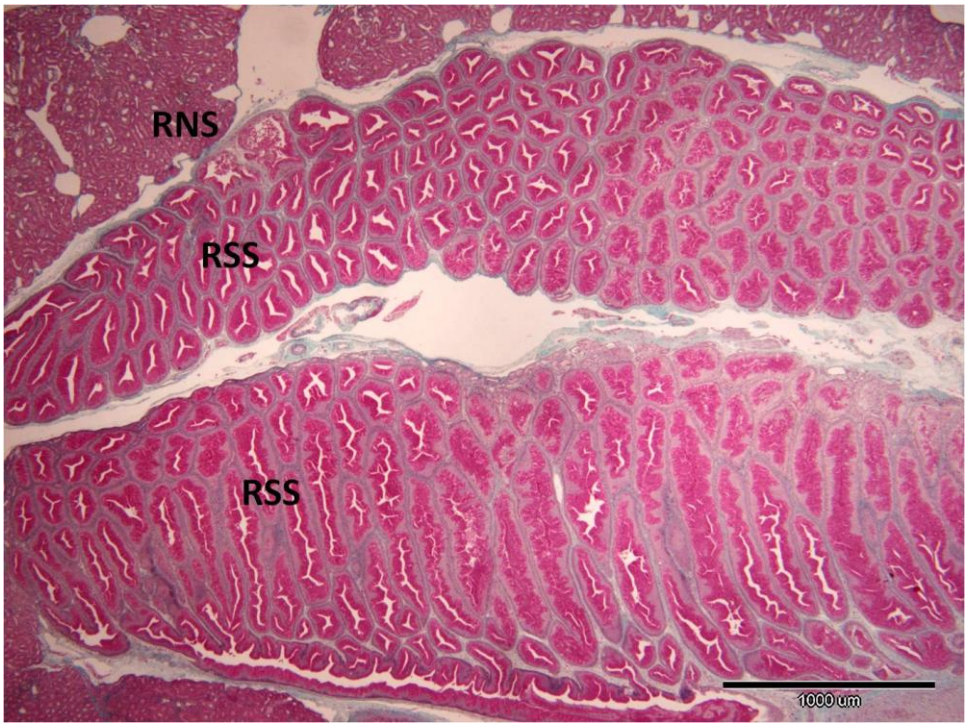

Figure 3.3H. MT section of the kidney from the active phase showing normal developed segment (RNS) and sexual segment (RSS). RNS consists of uriniferous tubules. RSS has larger tubules characterized by hypertrophied columnar cells and numerous granules.

3.3.5 Plasma steroids concentrations

3.3.5.1 Testosterone

Mean monthly plasma T concentrations are shown in Figure 3.4A. The monthly pattern of plasma T concentrations varied significantly throughout the reproductive cycle (F (11, 86) = 53.124, $P < 0.001$). Plasma T concentrations increased gradually during the recrudescent phase (September–October) with a peak between January and March in the active phase. Plasma T concentrations began to decline in April and May and reached its lowest concentrations in June ($P < 0.001$)

3.3.5.2 Oestradiol

Mean monthly plasma E_2 concentrations are shown in Figure 3.4B. The monthly pattern of plasma E_2 concentrations varied significantly throughout the reproductive cycle (F (11, 86) = 6.56, $P < 0.001$). Mean plasma E_2 concentrations was lowest in the quiescent phase during summer (June–August) and gradually increased during the

recrudescent phase in late summer (October), but began to increase steadily from November through April, then drastically decreased in May and reached its lowest concentrations in June ($P < 0.001$).

3.3.5.3 Progesterone

Mean monthly plasma P concentrations varied significantly throughout the reproductive cycle (Figure 3.4C) ($P < 0.001$). Plasma P concentrations began to rise significantly in November (F (11, 86) = 2.836, $P < 0.03$) and continued to rise through February. Plasma P concentrations peaked significantly ($P < 0.01$) in March and April but declined significantly ($P < 0.01$) in June and July.

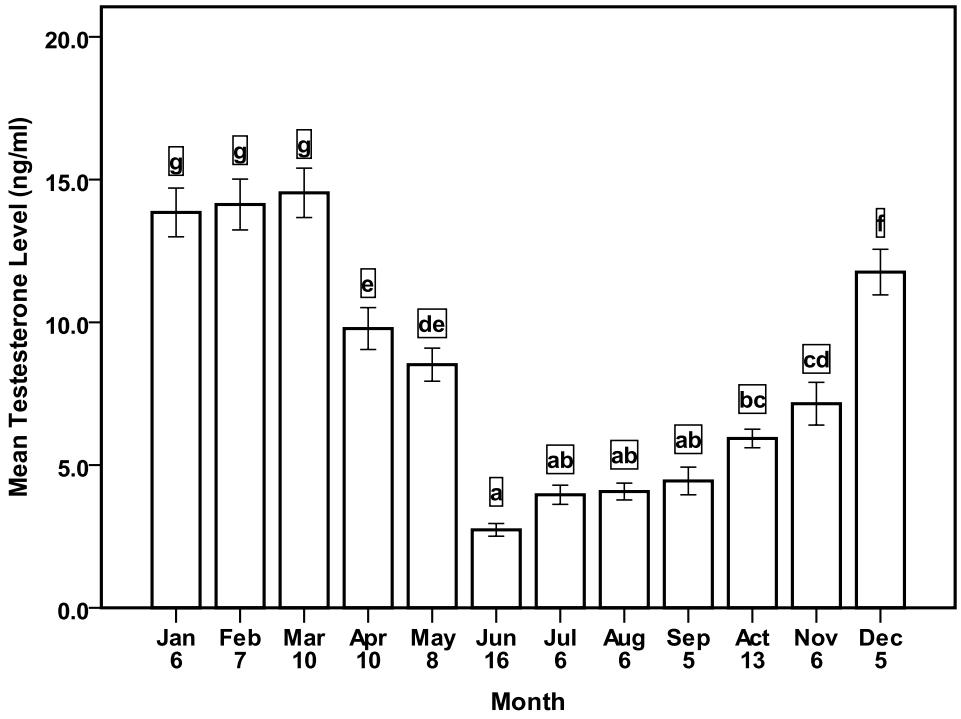

Figure 3.4A. Monthly mean (±S.E.M.) plasma T concentrations during the reproductive cycle. Plasma T concentrations increased in December through April, coinciding with spermatogenesis, spermiogenesis, courtship and mating. Numbers below each histogram represents sample size. Months with significantly different T concentrations were assigned different letters. Months with the same letter shows statistically no significant difference between them at the 0.05 level of significance. Statistical differences between groups obtained by Duncan's multiple-comparisons test.

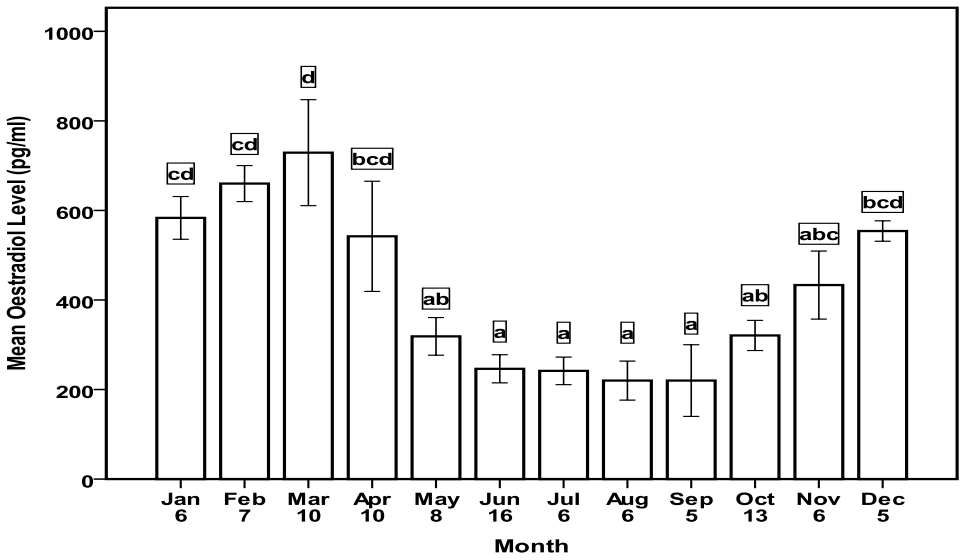

Figure 3.4B. Monthly mean (±S.E.M.) plasma E_2 concentrations. Plasma E_2 concentrations increased during the active phase with a peak in December through April. Concentrations decreased in June and then rose again in October. Numbers below each histogram represents sample size. Months with significantly different E_2 were assigned different letters. Months with the same letter shows statistically no significant difference between them at the 0.05 level of significance. Statistical differences between groups obtained by Duncan's multiple-comparisons test.

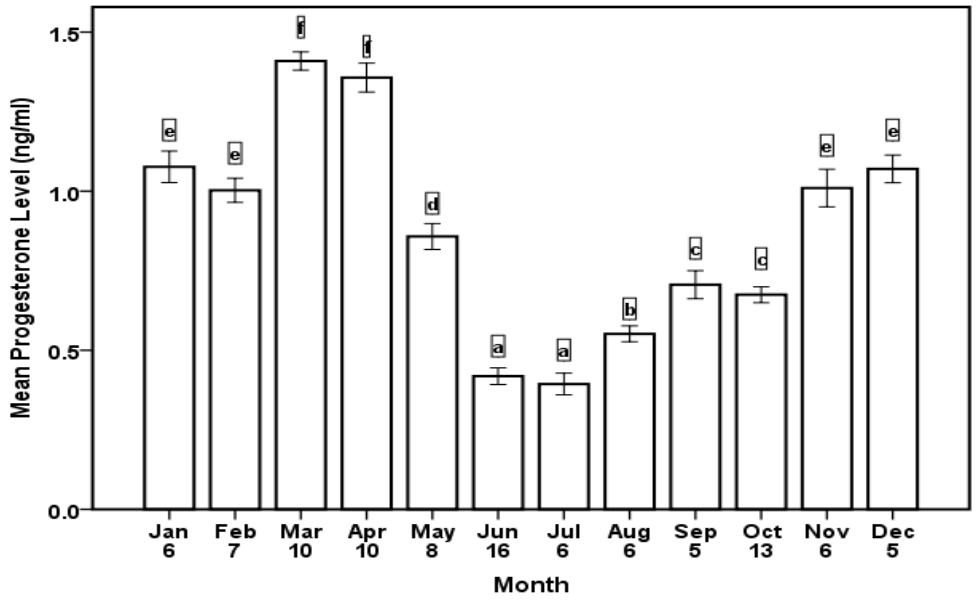

Figure 3.4C. Monthly mean (±S.E.M.) plasma P concentrations. Plasma P concentrations increased during the active phase with a peak in March and April. Concentrations decreased in June and increased again in November. Numbers below each histogram represents sample size. Months with significantly different P were assigned different letters. Months with the same letter shows statistically no significant difference between them at the 0.05 level of significance. Statistical differences between groups obtained by Duncan's multiple-comparisons test.

3.3.6 Effects of stress during the reproductive cycle

Mean monthly C concentrations are shown in Figure 3.4D. The monthly pattern of plasma C concentrations did not vary significantly throughout the reproductive cycle (F (11, 85) = 1.775, P 0.071). The relatively high plasma C concentrations were probably based on the stress caused by the capture and handling of the animals. Haematocrit concentrations stayed within the normal range (Mean PCV = 37.78±1.17%, n= 54) during the reproductive cycle. There was no significant linear correlation between plasma C concentrations and haematocrit (P 0.734).

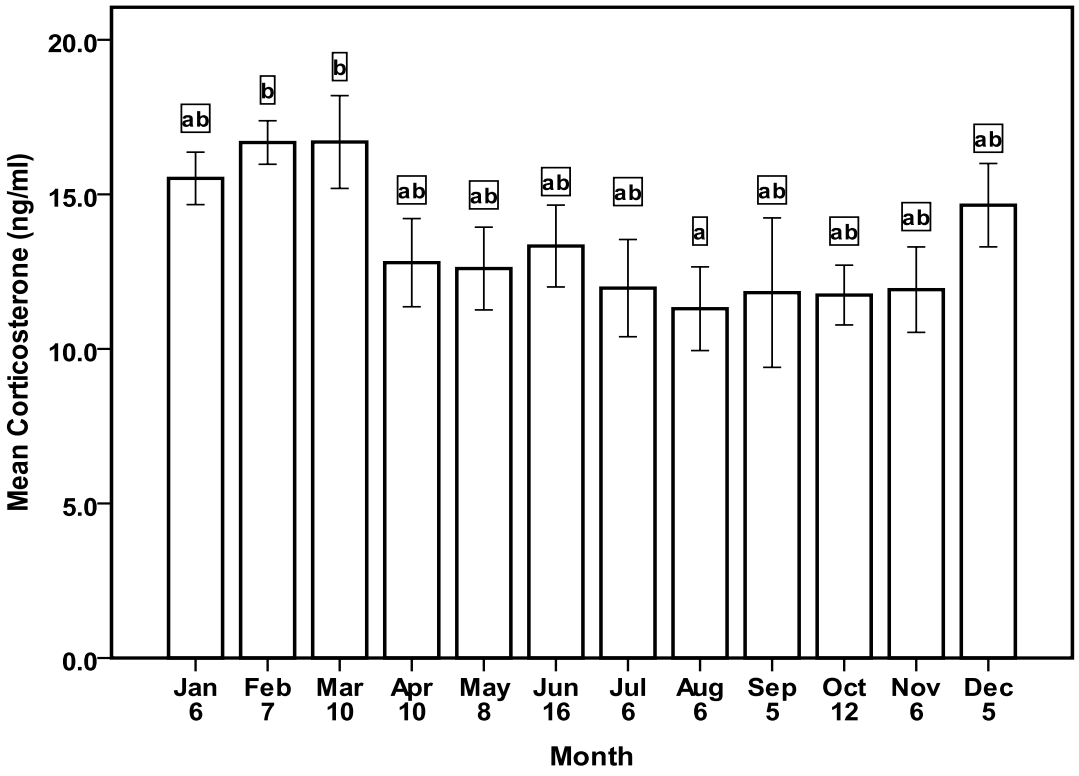

Figure 3.4D. Monthly mean (±S.E.M.) plasma C concentrations. Plasma C concentrations increased slightly during the active phase with a peak in February and March. Concentrations decreased slightly in April and increased again in December. Months with significantly different C were assigned different letters. Months with the same letter shows statistically no significant difference between them at the 0.05 level of significance. Statistical differences between groups obtained by Duncan's multiple-comparisons test.

3.3.7 Progesterone receptors

PRs were weakly expressed in the Leydig, Sertoli and germ cells in the testes during the quiescent phase (Figure 3.5A), coinciding with the low hormone concentrations: T, E_2 and P, but strongly expressed in both recrudescent and active phases coinciding with the rise in the three hormone concentrations (Figure 3.5B).

The anterior and middle segments of the epididymis showed strong expression for PR in their lumen during the active phase. The lumen of these regions contained spermatozoa and secretory granules and expressed strongly for PR. This indicated that the final maturation of the sperm took place in these segments (Figure 3.5C).

The renal sexual segments (RSS) had a highly developed section of the kidney in relation to testicular development during spermatogenesis. In this study, there was no PR expression in RSS during the active phase.

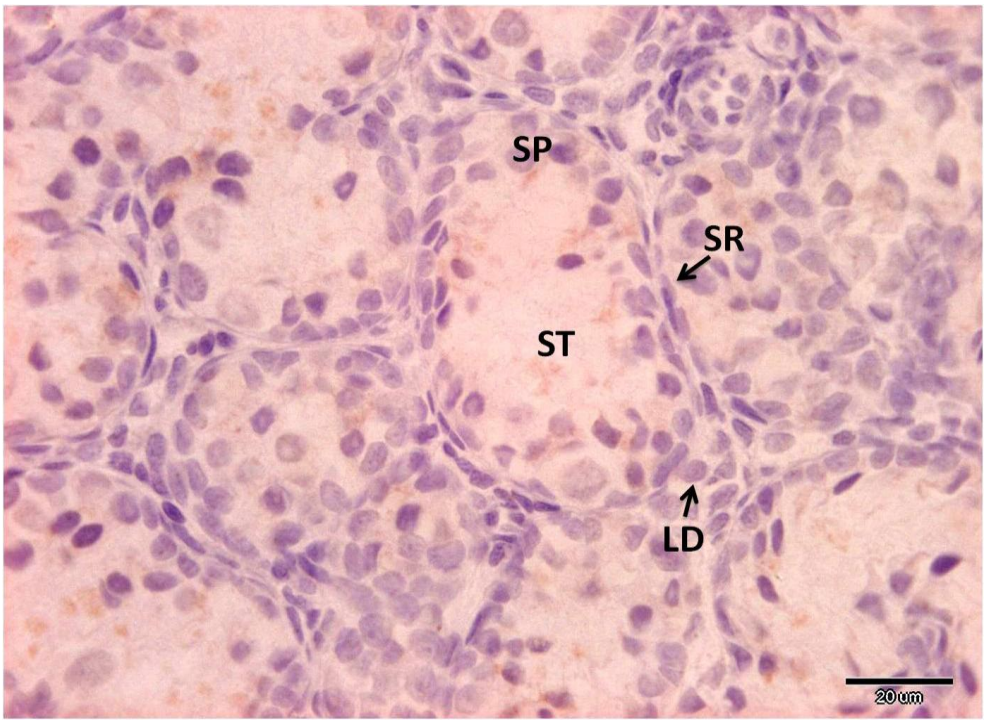

Figure 3.5A. Immunolocalisation of testis progesterone receptors (PRs) during the quiescent phase. Weak positive PR expression in Leydig cells (LD), Sertoli cells (SR) and seminiferous tubules (ST). Spermatogonia (SP).

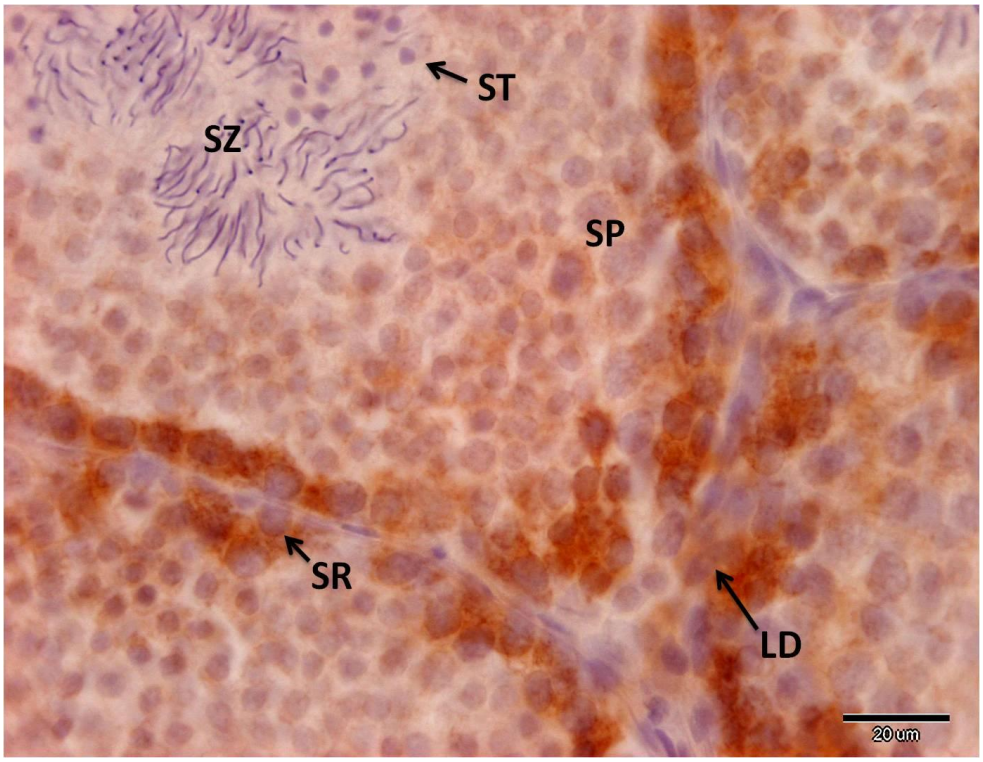

Figure 3.5B. Immunolocalisation of testis PRs during the active phase. Strong positive PR expression in Leydig cells (LD), Sertoli cells (SR) and the seminiferous tubules. Spermatogonia (SP), spermatids (ST), spermatozoa (SZ).

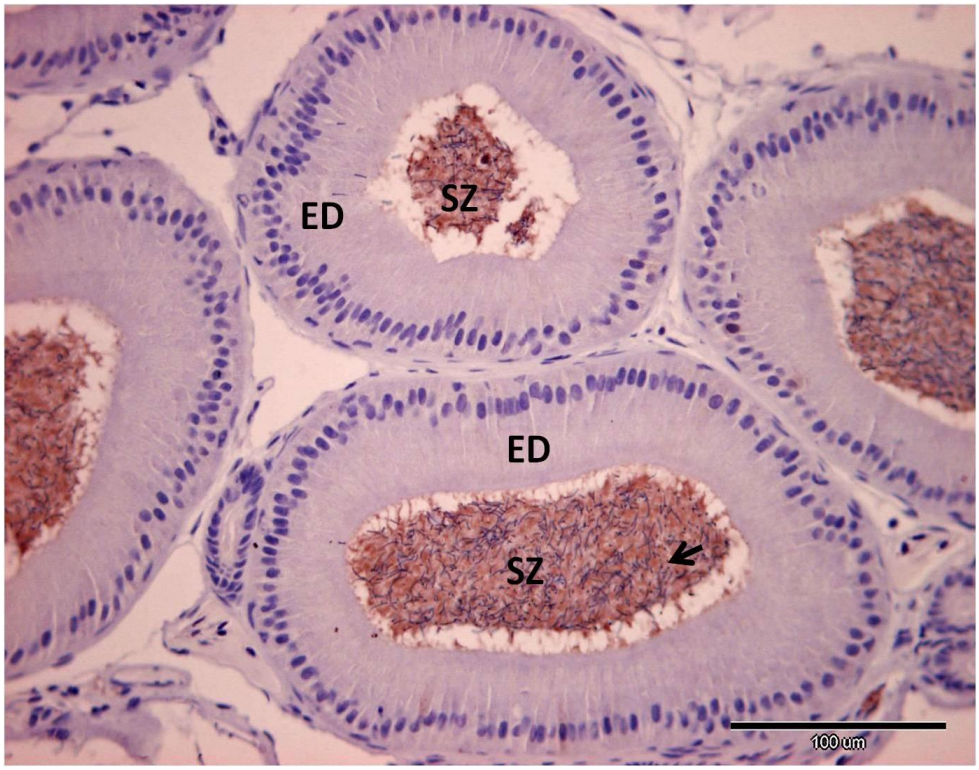

Figure 3.5C. PR immunolocalisation in the middle epididymis (ED) tubes filled with sperm (SZ) where PRs are strongly expressed (arrow) for the final maturation of sperm. Note the presence of granules amongst the sperm.

3.3.8 Testicular cycle:

Identification of cell types in the seminiferous epithelium

For identification of different cell types, especially the meiotic stages of primary spermatocytes, semithin sections of selected cell types stained with toluidine blue were used. The identification was based on reference to germ cells of the European wall lizard, *Podarcis muralis* (Gribbins and Gist, 2003) and the ground skink, *Scincella lateralis* (Rheubert *et al.*, 2009).

Description of the ultrastructure of spermatids and spermatozoa was related to neotropical lizards (Teixeira *et al.*, 1999a,b; 2002), the lizard, *Tropidurus Itambere* (Ferreira and Dolder, 2003b), and to the gecko *Hemidactylus turcicus* (Rheubert *et al*., 2011a).

3.3.8.1 Histology of spermatogenesis

During the quiescent phase (June-August), the testes were small (Figure 3.2B Table 3.1A) and regressed (mean GSI = 0.2%) (Figure 3.2A). Seminiferous tubule diameter and seminiferous epithelial height were small in size and appeared undeveloped (Figures 3.6A & 3.6B, Table 3.1A). Spermatogonia A and B were found in the basal lamina of the seminiferous epithelium. Spermatogonia A were relatively ovoid in shape with centrally located nuclei and two nucleoli. After a single mitotic division, spermatogonia A became spermatogonia B, which were slightly larger and had more spherical nuclei and 2–3 nucleoli (Figure 3.7A). These two premeiotic cells were found throughout the year and they were the source of the germ cells.

Sertoli cells surrounded the spermatogonia near the basal region of the seminiferous tubule with cellular processes absent during this phase. The Sertoli cells were irregularly spaced over the basement membrane, presenting triangular nuclei with one or two nucleoli (Figure 3.7B). These characteristics of Sertoli cells were maintained in all stages. Leydig (interstitial) cells had shrunken nuclei with esinophillous cytoplasm and were primarily restricted to the junction between three or more seminiferous tubules (Figure 3.7B). Accumulation of sudanophilic lipid droplets were observed in seminiferous tubules as well as in Leydig cells (Figure 3.7C) indicating low

steroidogenic activity in the Leydig cells. Testicular quiescence continued from June to August until the next cycle began.

During the recrudescent phase (September-October) the testes were small and ovoid (Figure 3.2B, Table 3.1A), but gradually increased in weight (mean GSI= 0.4%) (Figure 3.2A) as the diameter of the seminiferous tubules and seminiferous epithelial height increased at the onset of spermatogenesis (Figures 3.6A & 3.6B, Table 3.1A).

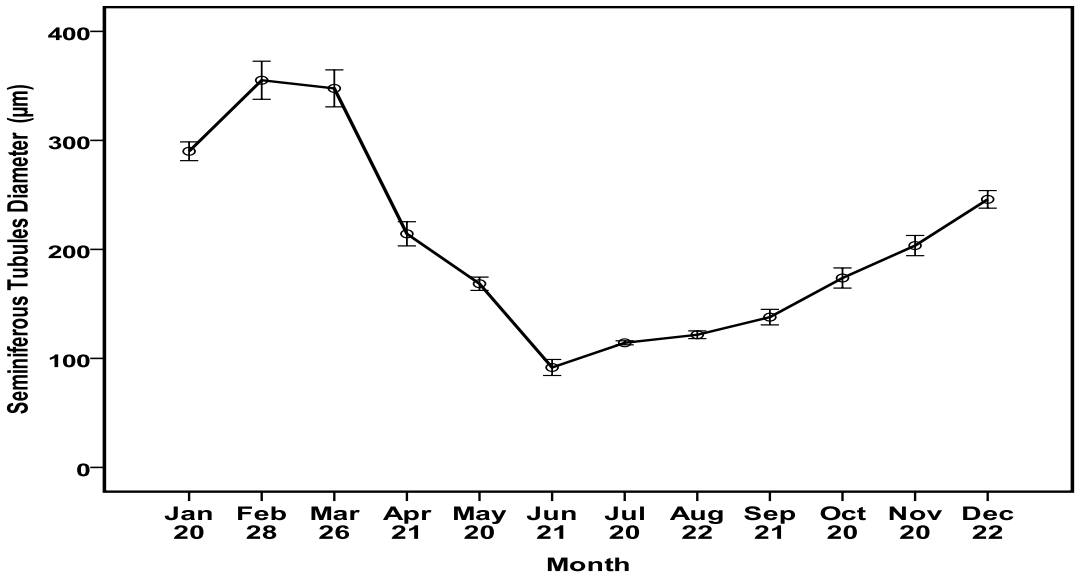

Figure 3.6A. Monthly mean (±S.E.M) seminiferous tubule diameter (µm) during the two annual testicular cycles of *H. flaviviridis.*

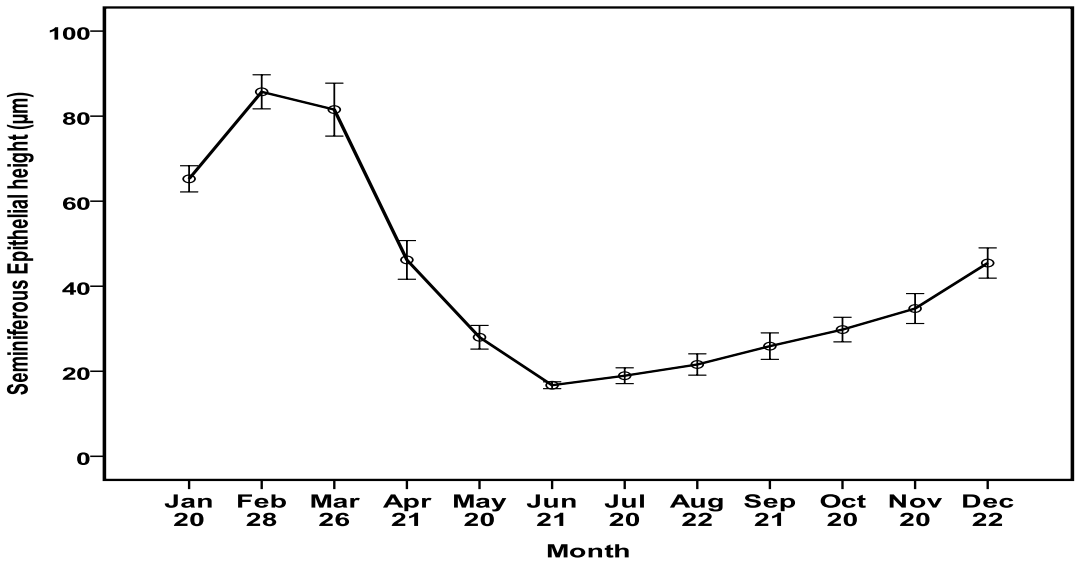

Figure 3.6B. Monthly mean (±S.E.M) seminiferous epithelial height (µm) during the two annual testicular cycles of *H. flaviviridis*.

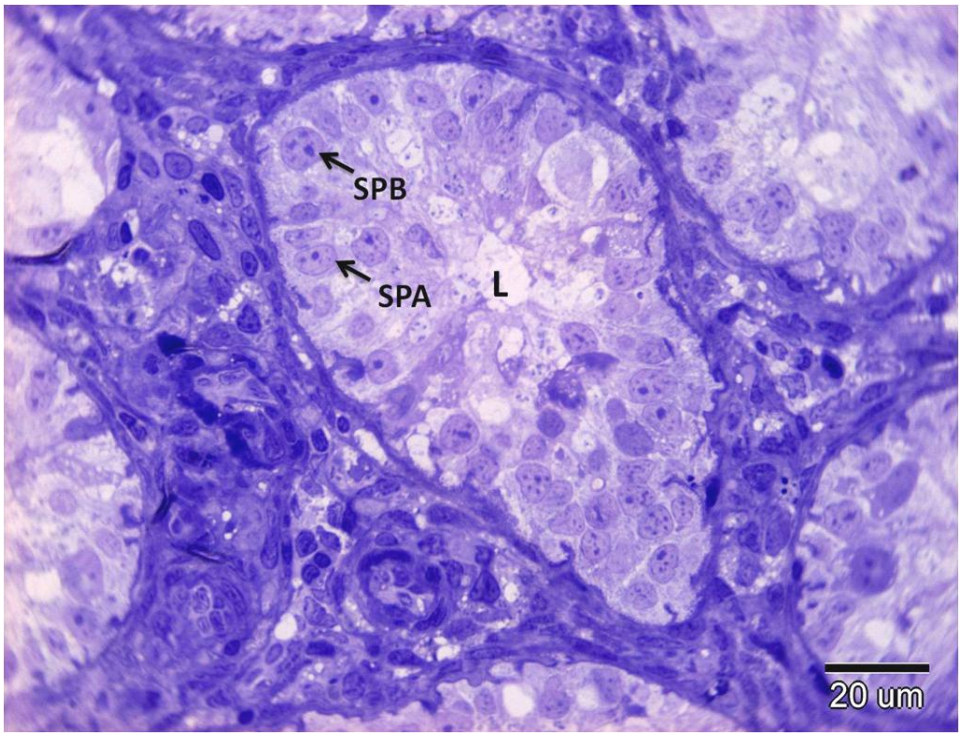

Figure 3.7A. Toluidine blue (TB) semithin section of a testis from the quiescent phase. Seminiferous tubule with spermatogonia A (SPA) and spermatogonia B (SPB) near the basement membrane of the seminiferous epithelium. Lumen (L).

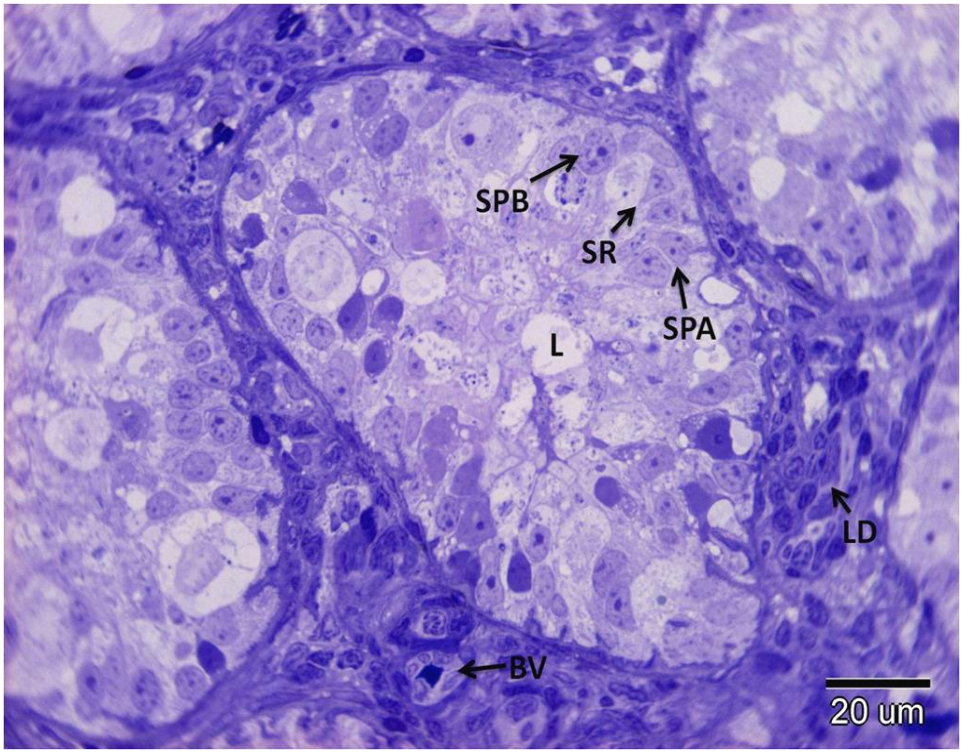

Figure 3.7B. TB section of a testis from the quiescent phase. Seminiferous tubules with Sertoli cells (SR) (triangular nuclei) irregularly spaced over the basement membrane. Leydig cells (LD) at interstitial tissue space. Spermatogonia A (SPA), spermatogonia B (SPB), Blood vessel (BV), Lumen (L).

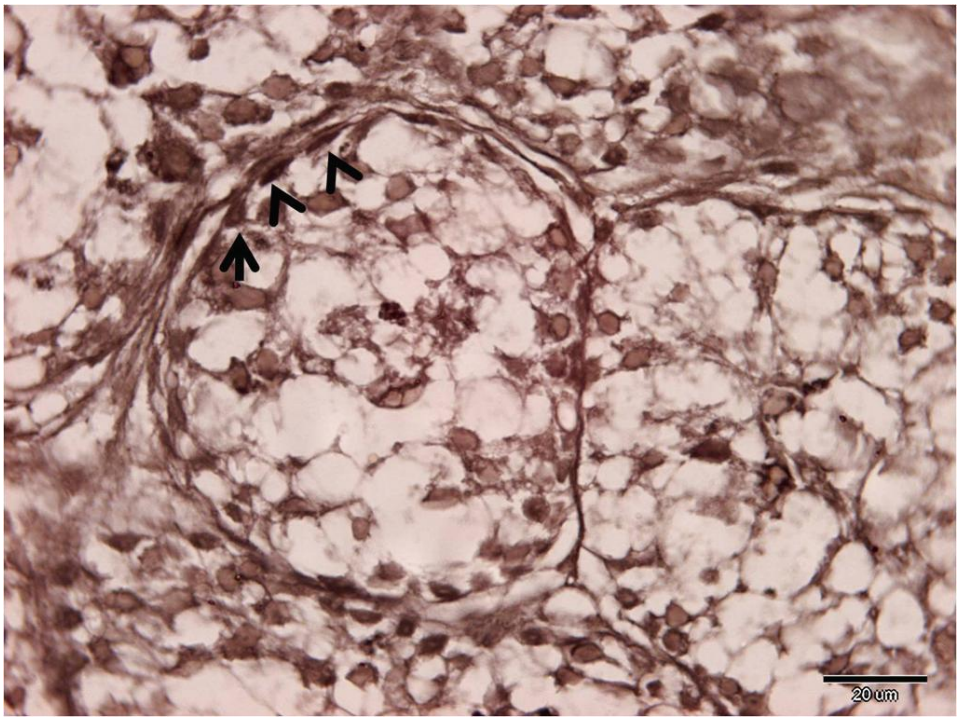

Figure 3.7C. SB section of a testis from the quiescent phase showing accumulation of sudanophilic lipids in seminiferous tubules and Leydig cells. Note Sertoli (arrow) and Leydig (arrowhead) cells intensely stained with Sudan Black B.

The lumina of the seminiferous tubules were largely occluded by the dividing spermatogonia, with a large number of meiotic primary and secondary spermatocytes and some spermatids (Figure 3.8A). The meiotic cells were characterized by a sequential increase in size of the nucleus and a condensation of chromatin into chromosomes. Spermatogonia B divide and enter prophase of meiosis I as pre-leptotene cells (Figure 3.8A). Spermatocytes appeared smaller than spermatogonia B and contained well-defined nuclear envelopes with dark staining nucleoli.

Pre-leptotene cells developed into leptotene spermatocytes which were bigger in size compared to pre-leptotene cells and were distinguished by their dense filamentous chromatin that filled the nuclei. Leptotene cells then developed into zygotene spermatocytes which were roughly the same size as leptotene cells, but had large clumps of condensed filamentous chromatin that stained more intensely than the previous stage. Zygotene cells developed into pachytene cells which were the second largest developing spermatocytes next to diplotene cells. Their larger cell size and open nucleoplasm distinguished these meiocytes from zygotene spermatocytes (Figure 3.8A).

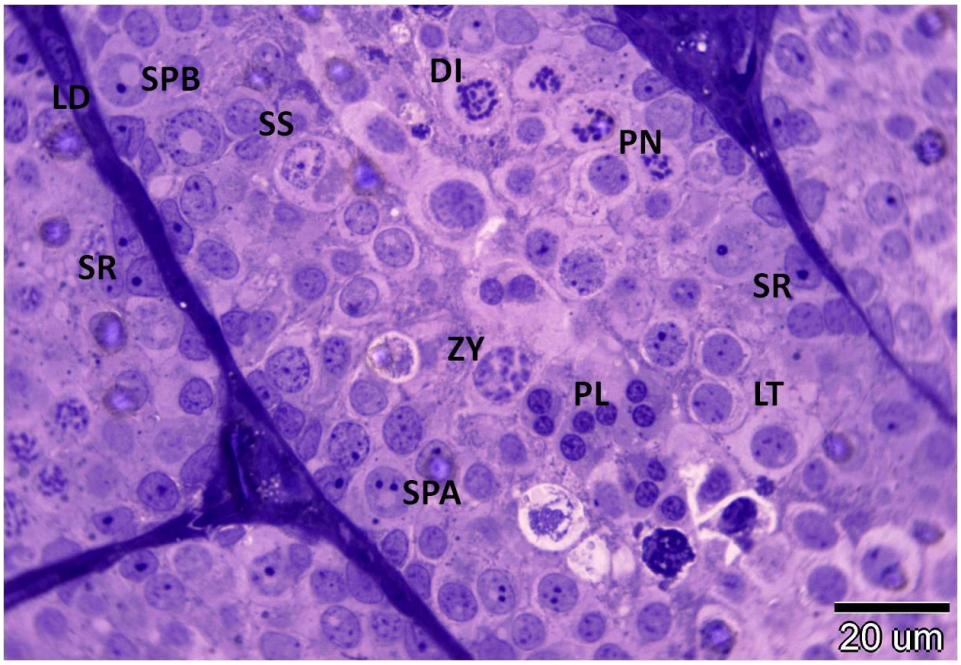

Figure 3.8A, TB section from the recrudescent phase with pre-leptotene (PL), leptotene (LT), zygotene (ZY), pachytene (PN), diplotene (DI), and secondary spermatocytes (SS). Spermatogonia A and B (SPA, SPB), Sertoli Cells (SR), Leydig cells (LD).

Diplotene spermatocytes and secondary spermatocytes were the largest in volume of the spermatocytes and were found in close association with pachytene spermatocytes. The diplotene cells had a degenerating nuclear membrane, and the chromatin fibres formed a tight circle in juxtaposition to this membrane (Figures 3.8A & 3.8B). Diplotene spermatocytes then enter metaphase 1. In metaphase 1, the cells had fully condensed chromosomes that aligned at the metaphase plate (Figures 3.8B). The results of meiosis 1 (metaphase 1) were the secondary spermatocytes (Figure 3.8A). The chromatin fibres of the secondary spermatocytes were randomly dispersed throughout their nucleoplasms. Secondary spermatocytes then enter metaphase 2. In metaphase 2, the chromosomes aligned again at the metaphase plate. The germ cell size and amount of chromatin present in metaphase 2 was approximately half that of metaphase 1 (Figure 3.8B). Metaphase 2 resulted in formation of stage 1 spermatids (Figures 3.8C & 3.8D). Stages 2–7 spermatids were found in the late recrudescent phase (Figures 3.8C & 3.8D) and during the spermatogenically active months.

During the active phase (November – mid May), all phases of spermatogenesis were completed and the germ cells were well organized, with the basally located

spermatogonia and spermatocytes occupying half of the spermatogenic epithelium. Next to the lumen a large amount of spermatids and spermatozoa were embedded in the cytoplasmic processes of the Sertoli cells. Seminiferous tubules were filled with mature spermatozoa and motile sperm. The testes were large and increased enormously in size (Figure 3.2B, Tables 3.1A & 3.1B), and were fully developed (mean GSI = 1.1%) (Figure 3.2A). The diameter of the seminiferous tubules and seminiferous epithelial height increased enormously in size (Figures 3.6A & 3.6B, Table 3.1A). Tubule lumina had highly convoluted epithelia forming convolutions in which the heads of many mature spermatozoa were embedded.

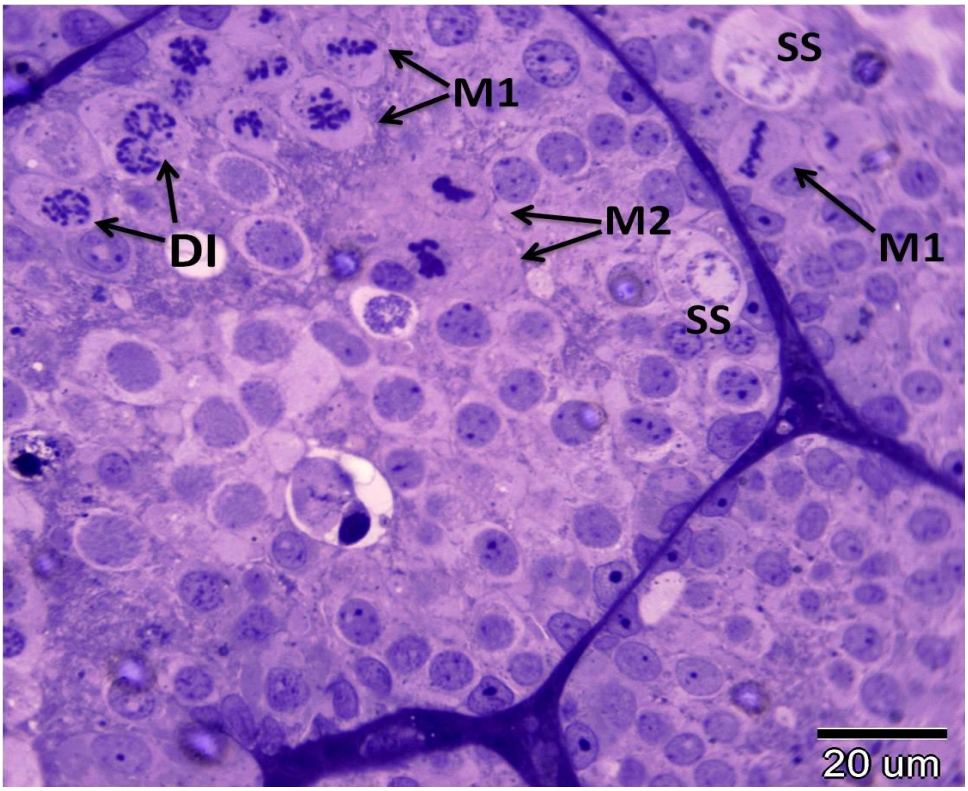

Figure 3.8B. TB section from the recrudescent phase showing Diplotene (DI), metaphase 1 meiosis (M1), secondary spermatocytes (SS) and metaphase 2 meiosis (M2).

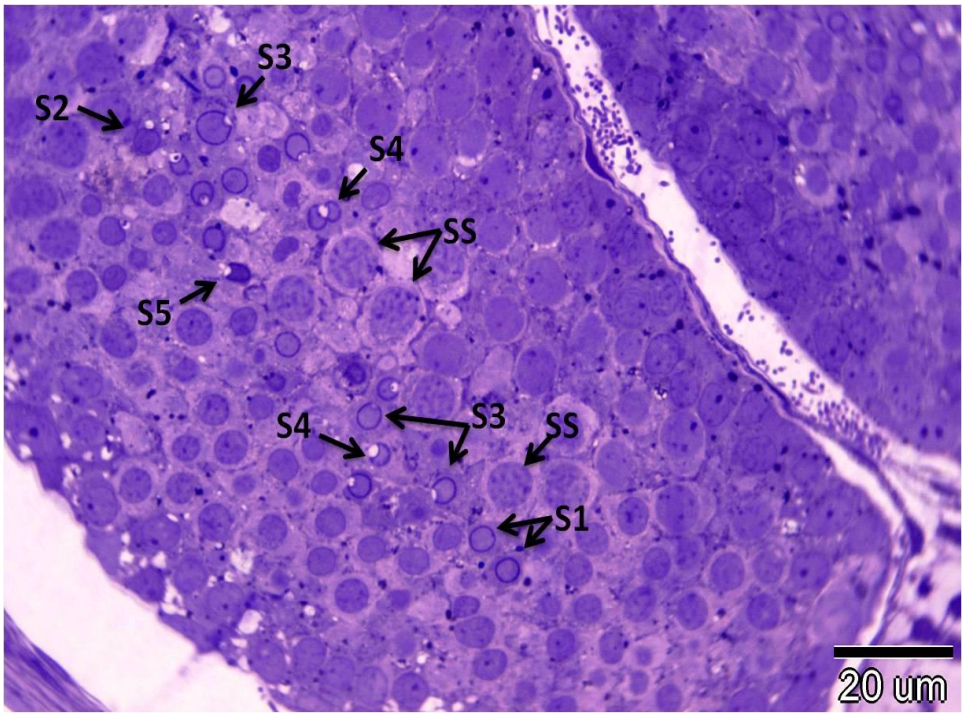

Figure 3.8C. TB section from the recrudescent phase showing secondary spermatocytes (SS) and developing stages of spermatids; S1, S2, S3, S4 and S5.

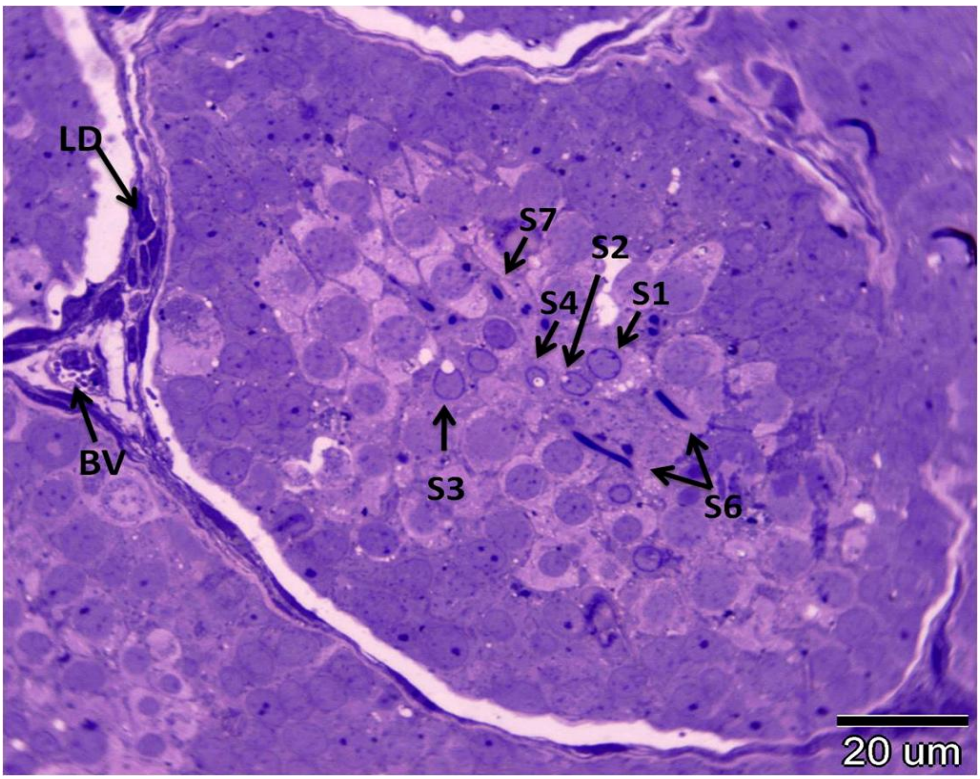

Figure 3.8D. TB section from the recrudescent phase showing developing stages of spermatids; S1, S2, S3, S4, S6 and S7. Leydig cells (LD) appear in the interstitial tissue. Blood vessel (BV).

Based on the Russell *et al.* (1990) classification, spermiogenesis was divided into seven stages. In the first stage (S1) spermatids were small in size, with well-defined nuclear membranes, and two conspicuous acrosome vesicles in contact with the apex of each nuclear membrane (Figures 3.9A, 3.9B, 3.9C & 3.9D). These two acrosome vesicles of each spermatid fused to produce a single acrosome in the second stage (S2) (Figure 3.9A). Acrosome granules were most commonly seen in the acrosome of S2. The third stage (S3) had defined acrosome vesicles which began to increase in size and envelope the nuclear heads (Figure 3.9A). As the development of the acrosomes continued, a deep depression within the apex of the nuclear head formed a feature that characterized stage four (S4) (Figure 3.9A). Nuclear elongation characterized stage five (S5) spermatids, which began opposite of the acrosome and initiated the stretching of the spermatids' dorsoventral planes (Figure 3.9A). As elongating spermatids developed, they migrated towards the apical portions of Sertoli cells, with the heads of elongates facing the basement membrane and the flagella facing the lumen. Elongation continued and condensation dominated the nuclei of stage six (S6) and seven (S7) spermatids (Figures 3.9A, 3.9B, 3.9C & 3.9D). As condensation of the chromatin material progressed, the thickness of the nuclear heads decreased, resulting in very thin and hydrodynamic nuclear heads on the mature spermatozoa (Figures 3.9A, 3.9B, 3.9C & 3.9D). Mature spermatozoa were shed to the lumina of the seminiferous tubules and a process called spermiation then takes place, which removes the remaining unnecessary cytoplasm and organelles.

The free spermatozoa collected at the efferent duct (Figure 3.9E), then entered the epididymis of *H. flaviviridis* for further maturation and storage. During copulation, mature sperm transferred from the epididymis into the hemipenis via the vas deferens.

There was a marked reduction in size of Sertoli cells due to change in the diameter of the seminiferous tubules (Figure 3.9D). The spermeogenic cells were penetrated by deep folds of the cytoplasmic elongations of the Sertoli cells. These elongations extended from the basal region to the lumen and were rich in polysaccharides, probably glycoproteins (Figures 3.9F & 3.9G). Leydig cells exhibited an increase in size by their enlarged nuclei with prominent nucleoli (Figure 3.9D). Sudanophilic lipids material was observed in tubules as well as in Leydig cells (Figures 3.9H &

3.9I). Lipid droplets were mainly confined to the basal regions of the tubules and the interstitial tissue.

Both the histologic and morphometric data closely paralleled one another during the three reproductive phases which occurred during the annual cycle within the house gecko *H. flaviviridis*.

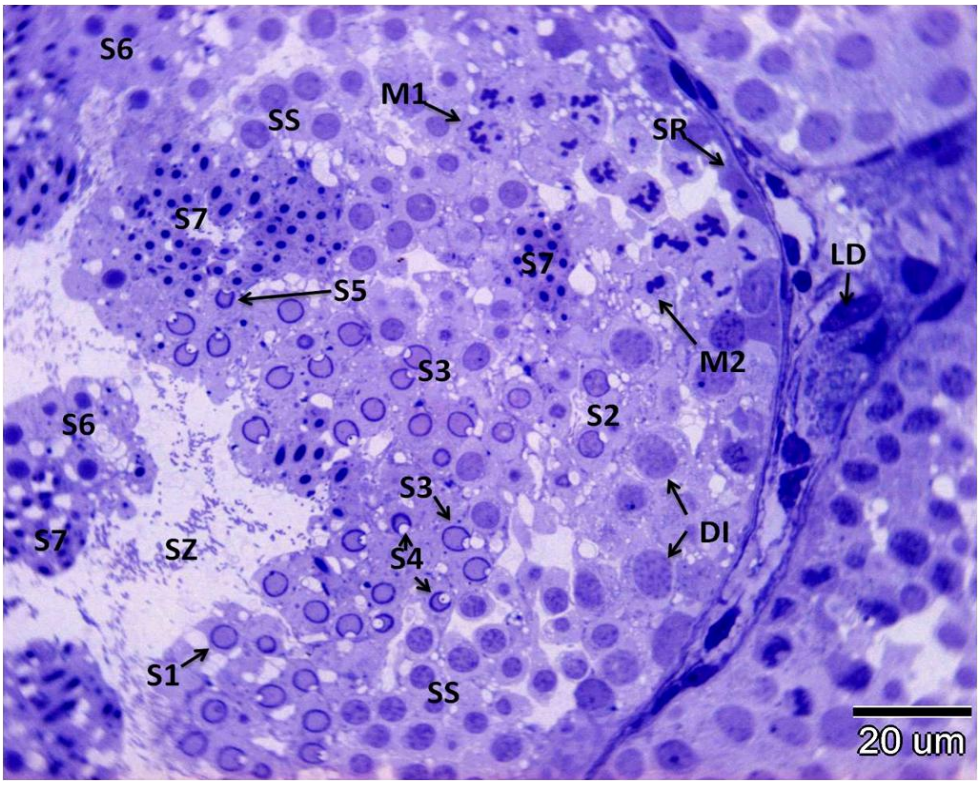

Figure 3.9A. TB section from the active phase showing developing stages of spermatids; S1, S2, S3, S4, S5, S6 and S7. Spermatozoa (SZ) released into the lumen of seminiferous tubule. Diplotene (DI), metaphase 1 meiosis (M1), secondary spermatocytes (SS) and metaphase 2 meiosis (M2), Sertoli Cells (SR), Leydig cells (LD) also seen here.

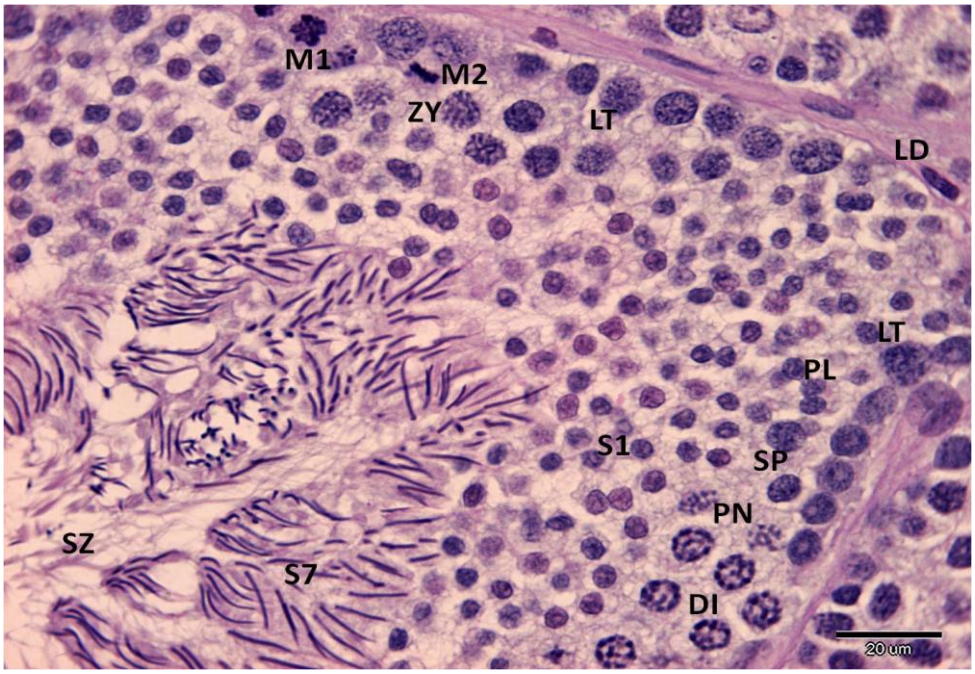

Figure 3.9B. AB-PAS section from the active phase showing developing stages of spermatids; S1 and S7. Spermatozoa (SZ) released into the lumen of seminiferous tubule. Spermatogonia (SP), pre-leptotene (PL), leptotene (LT), zygotene (ZY), pachytene (PN), diplotene (DI), metaphase 1 meiosis (M1), metaphase 2 meiosis (M2) also seen here. Leydig cells (LD) appeared squeezed in the interstitial tissue.

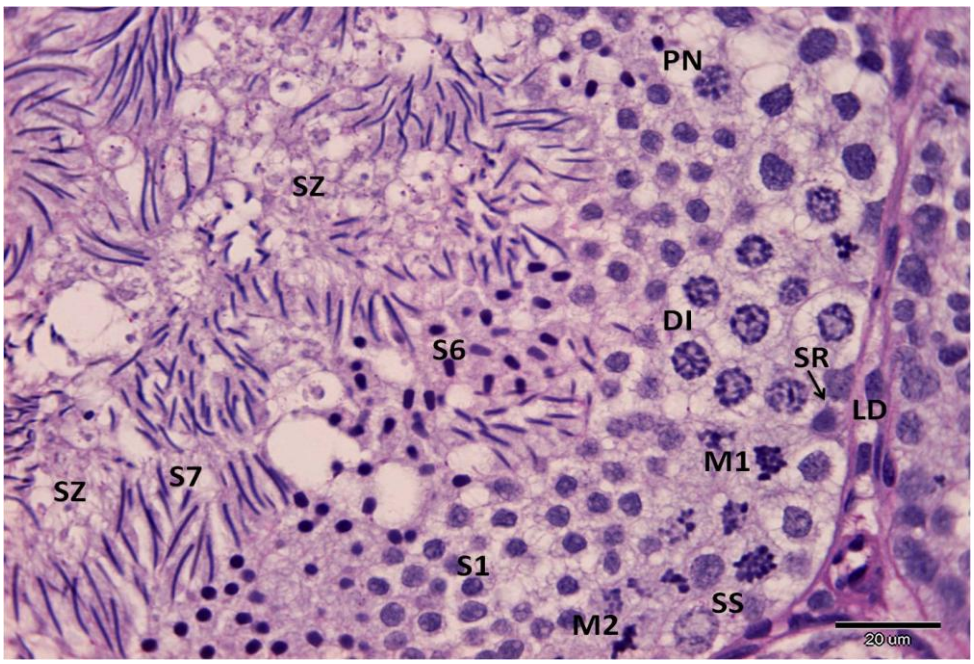

Figure 3.9C. AB-PAS section from the active phase showing developing stages of spermatids; S1, S6 and S7. Spermatozoa (SZ) released into the lumen of seminiferous tubule. pachytene (PN), diplotene (DI), metaphase 1 meiosis (M1), metaphase 2 meiosis (M2) and secondary spermatocytes (SS) also seen here. Sertoli (SR) and Leydig (LD) cells also were clearly visible.

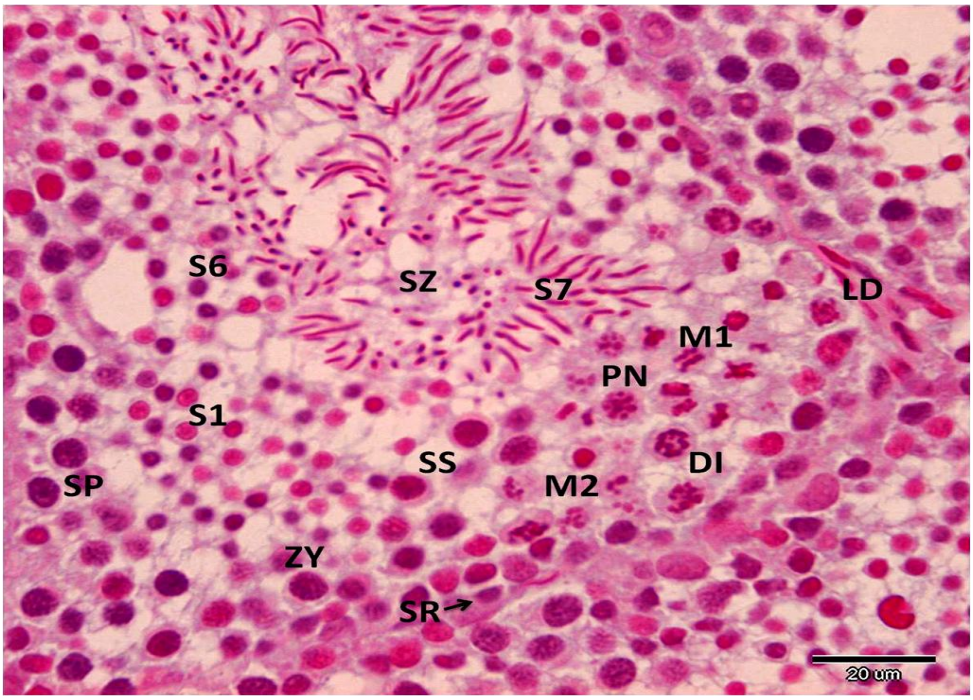

Figure 3.9D. AB-NF section from the active phase showing developing stages of spermatids; S1, S6 and S7. Spermatozoa (SZ) released into the lumen of seminiferous tubule. Spermatogonia (SP), pachytene (PN), diplotene (DI), zygotene (ZY), metaphase 1 meiosis (M1), metaphase 2 meiosis (M2) and secondary spermatocytes (SS) also seen here. Sertoli (SR) and Leydig (LD) cells also were clearly visible.

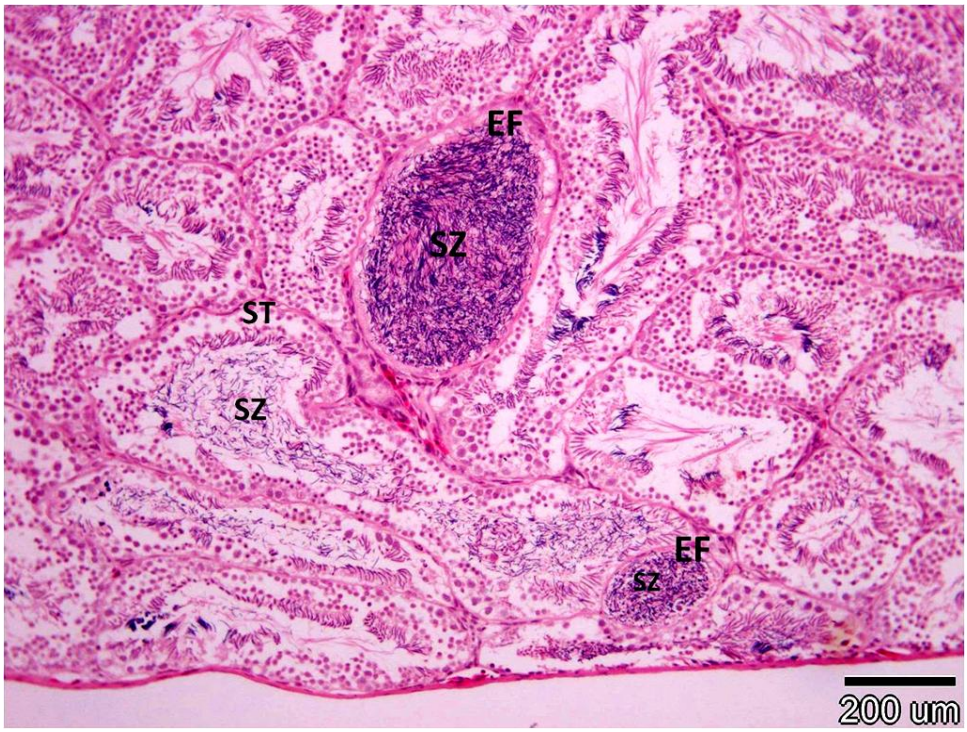

Figure 3.9E. H&E section from the active phase showing free spermatozoa (SZ) collected at the efferent duct (EF). Seminiferous tubules (ST).

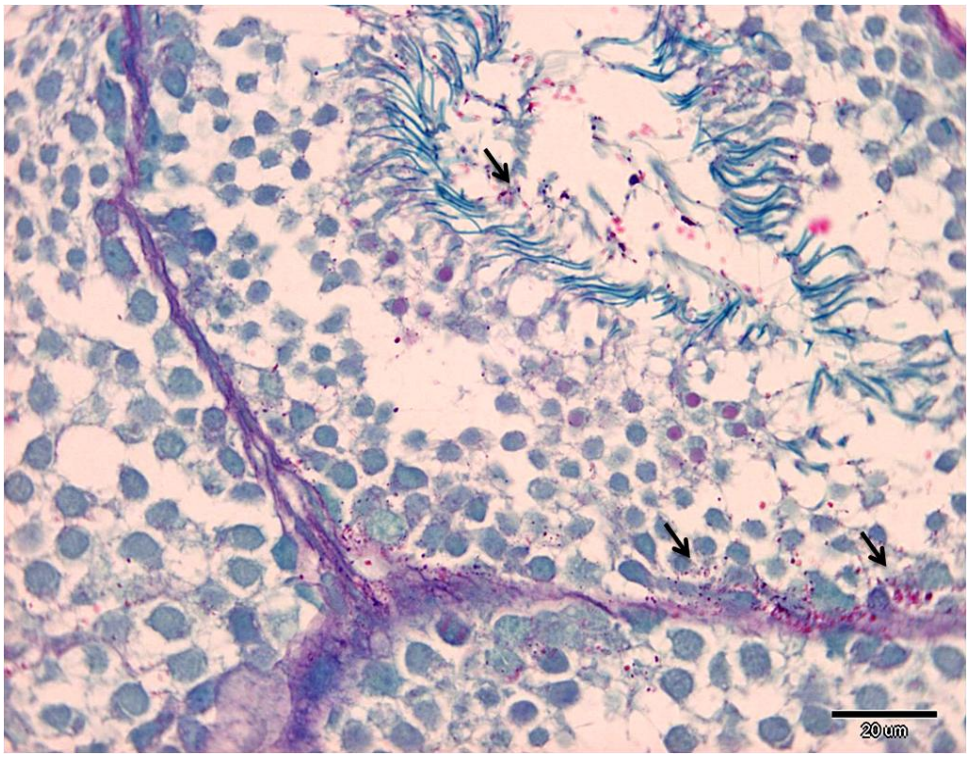

Figure 3.9F. PAS-FG section from the active phase with cytoplasmic elongations of Sertoli cells extended from the basal region to the lumen that were rich in polysaccharides (arrow).

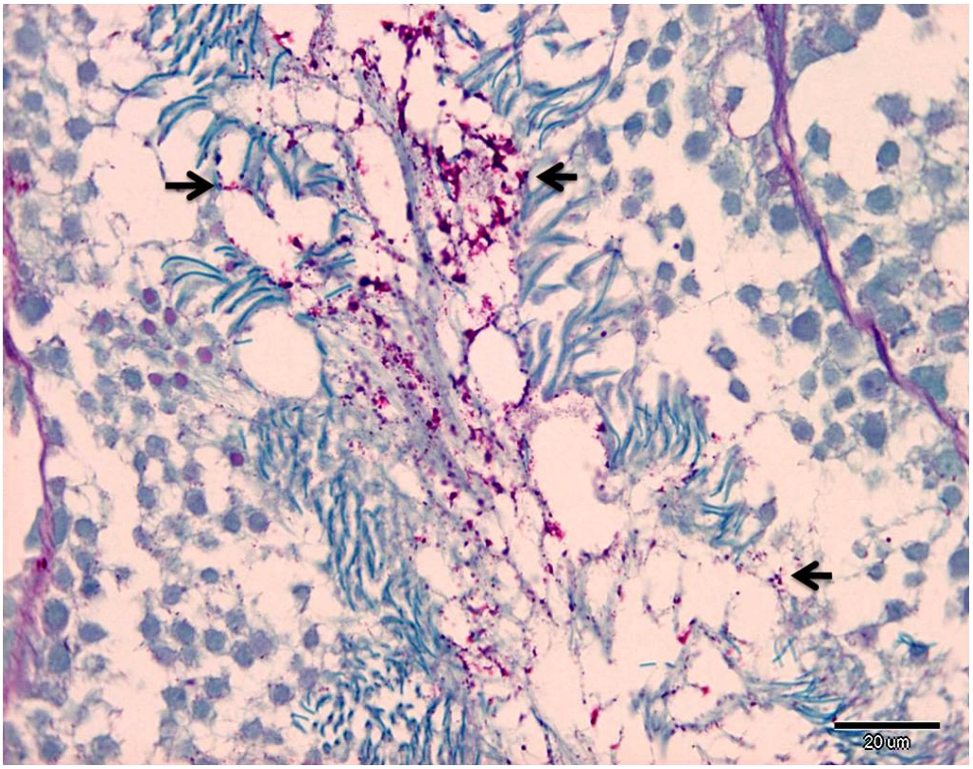

Figure 3.9G. PAS-FG section from the active phase showing cytoplasmic elongations of Sertoli cells extended from the basal region to the lumen that were rich in polysaccharides (arrow).

Figure 3.9H. SB section from the active phase showing sudanophilic lipids. Lipid material was observed in the basal regions of the tubules (Sertoli cells) as well as the interstitial tissue (Leydig cells) (arrow).

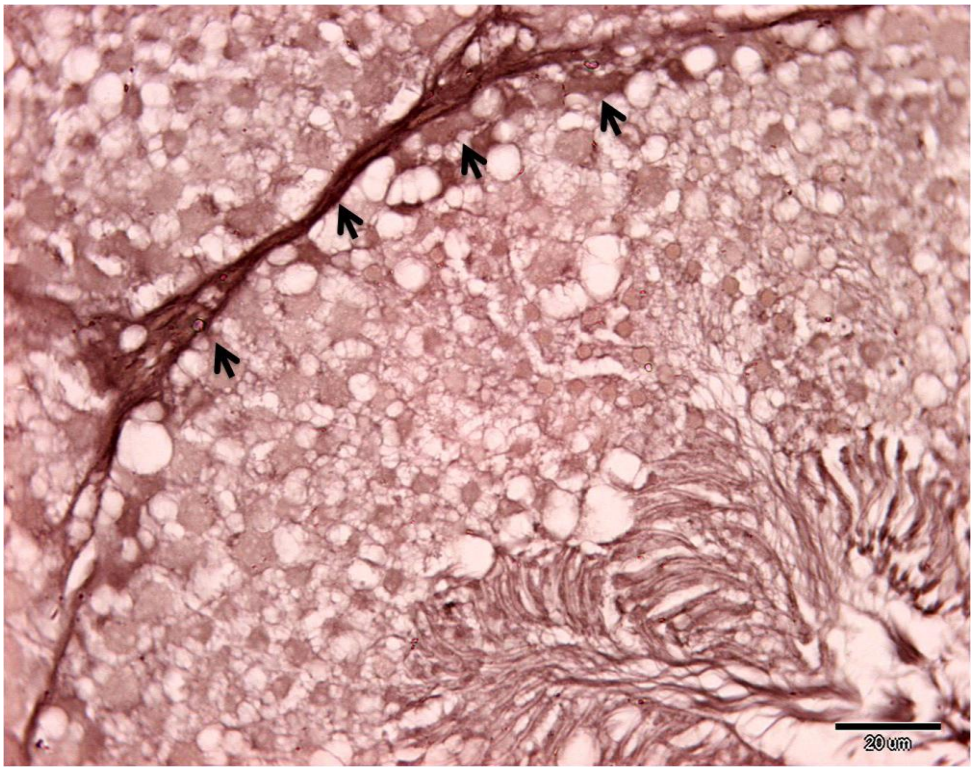

Figure 3.9I. SB higher magnification of Figure 3.9H showing clearly lipid material in the basal regions of the tubules (Sertoli cells) as well as the interstitial tissue (Leydig cells) (arrow).

3.3.8.2 Ultrastructure of spermatids and spermatozoa

The differentiation of spermatids into spermatozoa involved the events of nuclear elongation, formation of the acrosomal and axonemal complexes, and elimination of residual cytoplasm. Generally, the acrosomal region pointed towards the base of the seminiferous epithelium. The nuclei migrated from the central to the peripheral position. Furthermore, the vesicle spread and ultimately covered the entire apical nucleus. Simultaneously, the flagellum developed on the opposite pole of the acrosomal vesicle. Elongation of the nucleus and condensation of the chromatin proceed simultaneously. During the early stage, the chromatin first appeared more granular and then filamentous. With further condensation, the chromatin filaments became thicker, and at the end of the condensation process the chromatin had lost its filamentous structure. Mitochondria congregated next to the centrioles to constitute the midpiece of the tails, which were oriented towards the lumen. Chromatoid bodies were observed within the cytoplasm of late spermatids. The chromatoid bodies were cloud-like accumulations of dense fibrous material. They were irregularly shaped and were conspicuously large.

The first stage of spermiogenesis (S1) possessed a central, rounded nucleus, with granular chromatin and numerous mitochondria (Figures 3.10A & 3.10B). In addition, Golgi complexes and the endoplasmic reticulum were well developed; the endoplasmic reticulum aggregated in patches (Figure 3.10C). The second stage (S2) was characterized by the formation of the acrosomal vesicle, which grew in size and formed a nuclear depression (Figure 3.10D). The latter deepened with the growing vesicle. The acrosome complex in stage three (S3) was long and flattened apically and consisted of two caps: an external cap (the acrosome vesicle) and an internal cap (the subacrosomal cone). To constitute the acrosomal complex, numerous vesicles dispersed in the cytoplasm and accumulated beside the nucleus, and fused to form the pro-acrosomal vesicle, which lodged in a large nuclear depression (Figure 3.10E). The vesicle began to flatten, containing a loose clear material. As the pro-acrosomal vesicle developed in the fourth stage (S4), a dense granule appeared in its interior (Figure 3.10F). This granule attached to the membrane vesicle, in contact with the nucleus. Between the nucleus and the vesicle there was an electron-dense layer (Figure 3.10G). Between these layers, a clear layer was found that eventually formed

the subacrosomal clear zone. Chromatin adjacent to the vesicle became more compact than the remaining nuclear content (Figures 3.10F & 3.10G). Initial condensation and elongation of the nucleus began in the fifth stage (S5) (Figure 3.10H).

In stage six (S6), the acrosomal complex began its final structure covering the initial portion of the nucleus (Figure 3.11A). Two main compartments constituted this complex: the acrosome and the perforatorium. In the acrosome, two compartments could be further identified: an external acrosomal vesicle and an internal subacrosomal cone (Figure 3.11A). The acrosomal vesicle was made up of a clear cortex and an electron dense matrix (Figure 3.11A). The perforatorium was a short rod located between the acrosome and the nucleus partly surrounded by the subacrosomal cone (Figure 3.11B). Separating the perforatorium and the vesicular acrosome was a clear layer identified as the subacrosomal clear zone (Figures 3.11A & 3.11B).

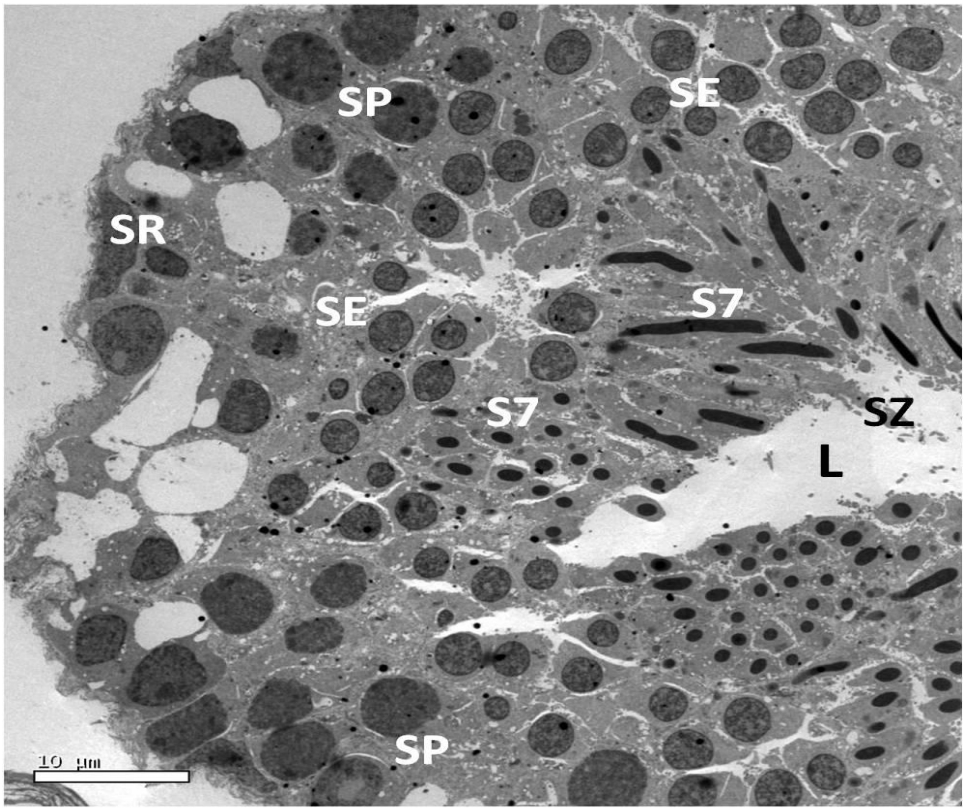

Figure 3.10A. TEM of a seminiferous tubule from the active phase showing epithelia at various stages of spermatogenesis; spermatogonia (SP), spermatocytes (SE), spermatids (S7), and spermatozoa (SZ). Sertoli (SR), lumen (L).

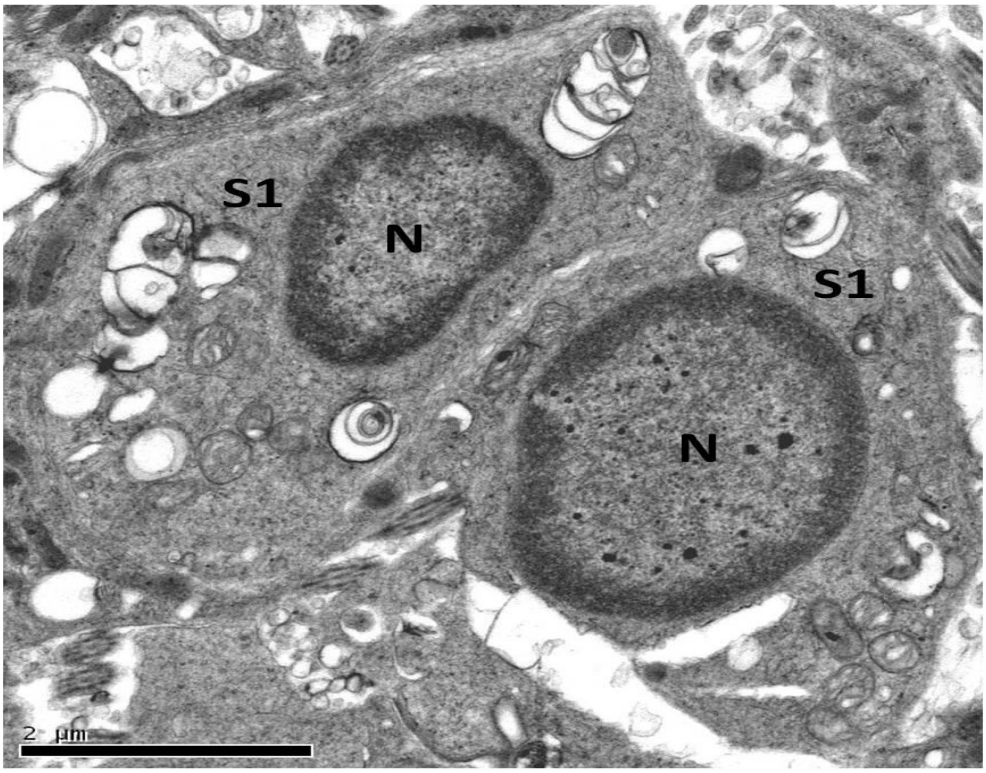

Figure 3.10B. TEM of a seminiferous tubule from the active phase showing spermatids (S1) with round central nucleus (N) and granular chromatin.

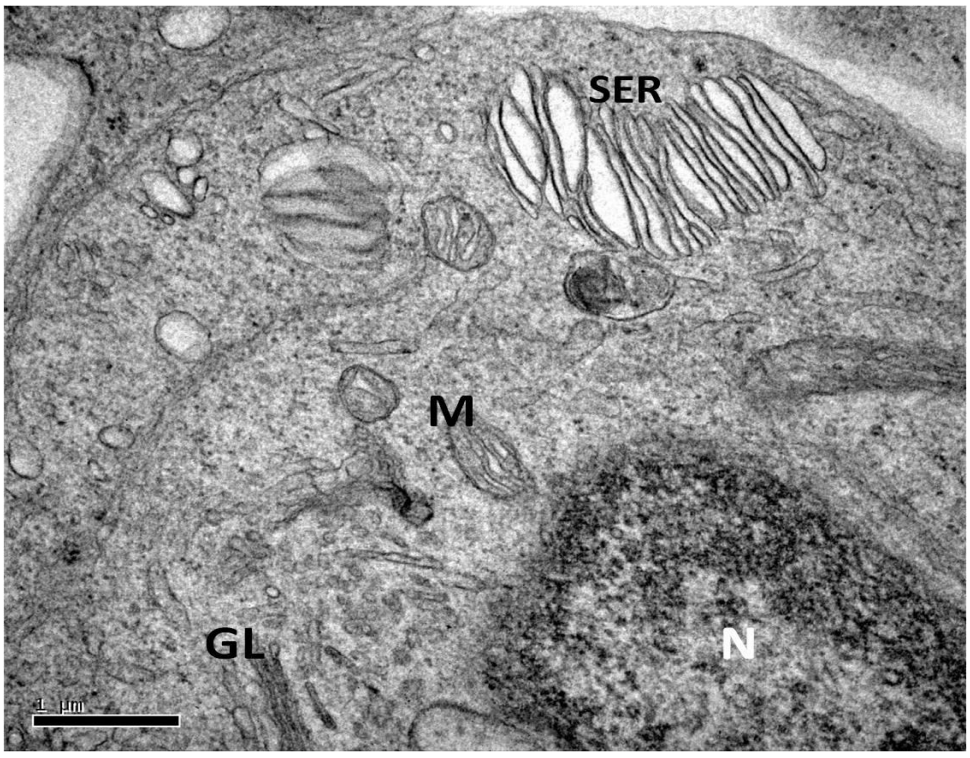

Figure 3.10C. TEM of a spermatid (S1) showing mitochondria (M) Golgi complex (GL) and SER aggregates in patches. Nucleus (N).

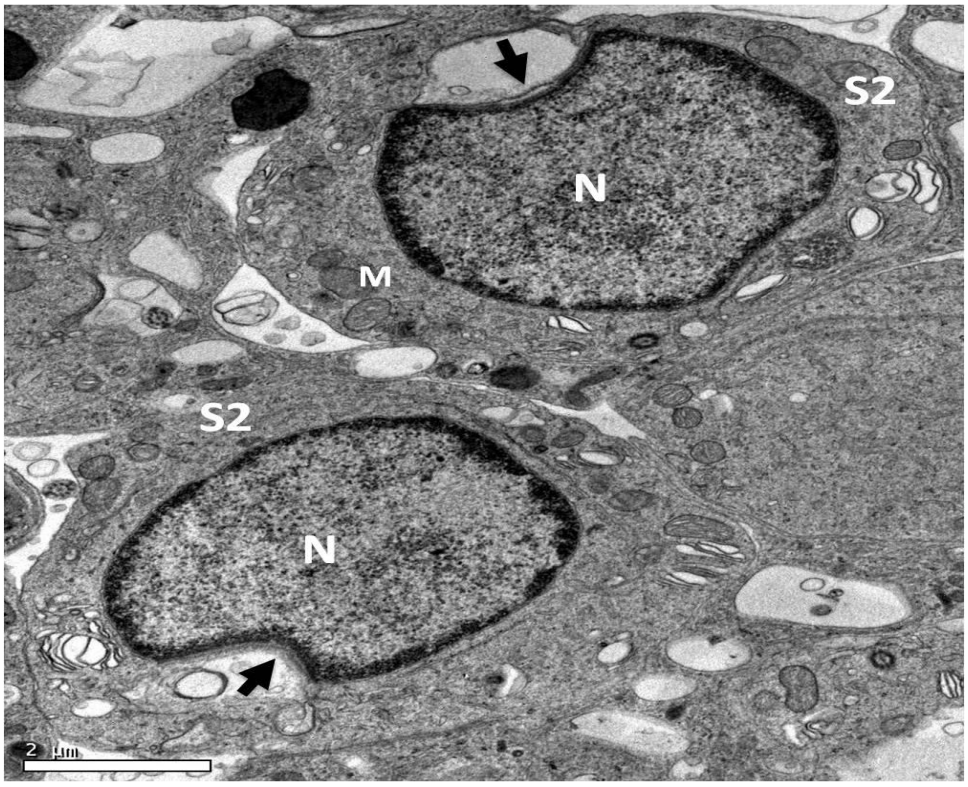

Figure 3.10D. TEM of spermatids (S2) showing a nuclear depression (arrow) that deepens as the formation of the acrosomal vesicle progresses. Nucleus (N), mitochondria (M).

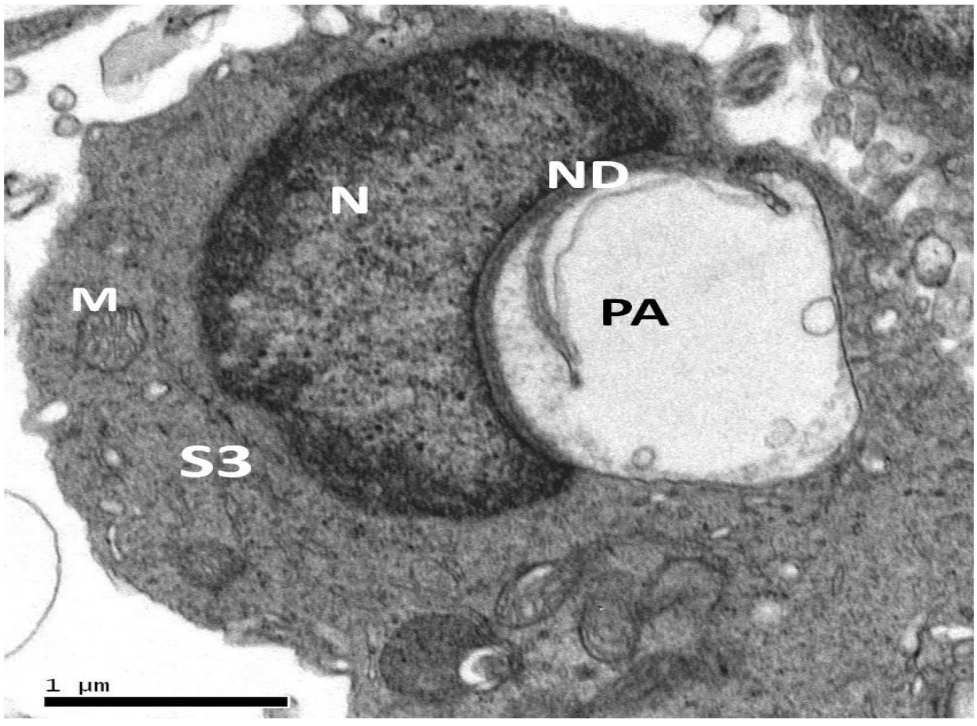

Figure 3.10E. TEM of a spermatid (S3) showing first stage in the formation of the acrosomal complex; innumerable vesicles dispersed in the cytoplasm to form the pro-acrosomal vesicle (PA), which is lodged in a large nuclear depression (ND). Nucleus (N), mitochondria (M).

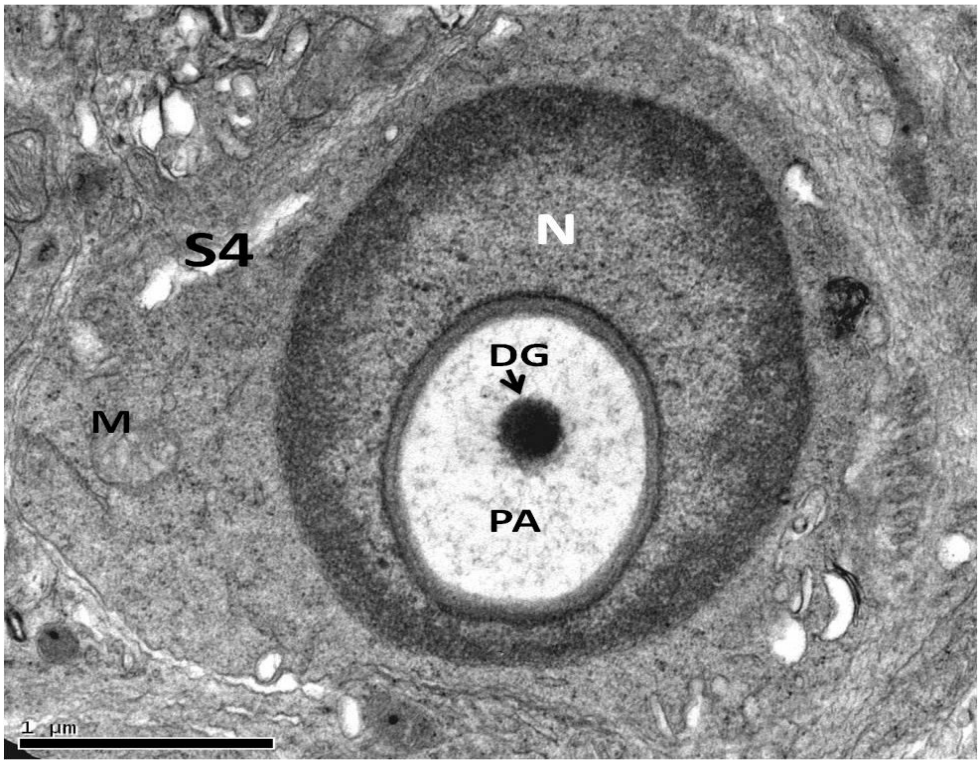

Figure 3.10F. TEM image of spermatid (S4) showing a dense granule (DG) appearing in the interior of the pro-acrosomal vesicle (PA). Nucleus (N), mitochondria (M).

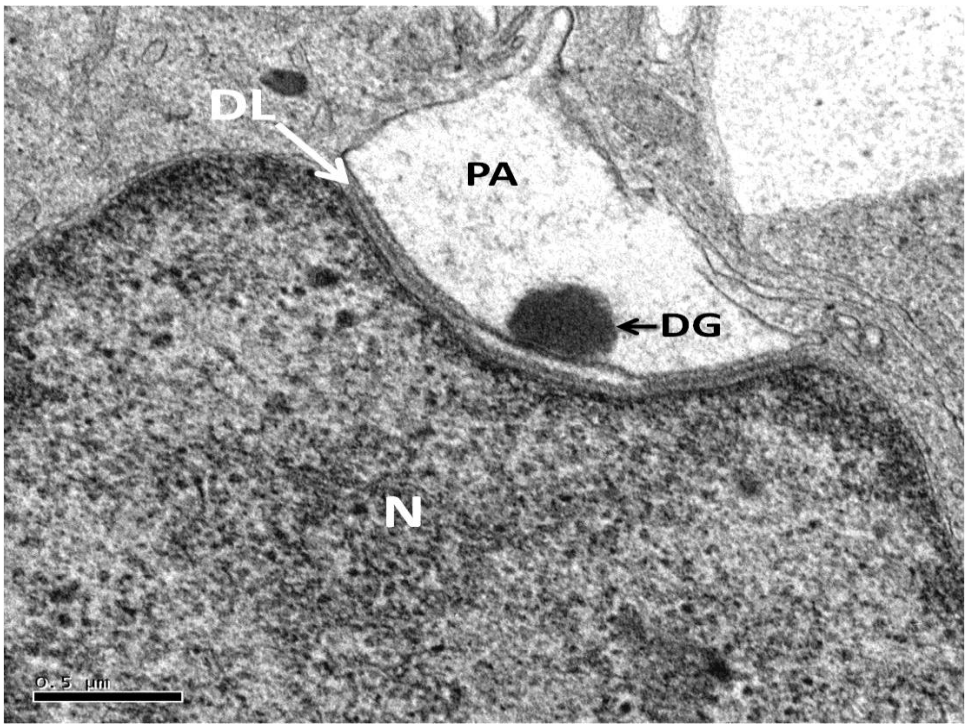

Figure 3.10G. TEM showing electron dense layer (DL) between the nucleus and vesicle. A clear layer seen between the two layers that will form the subacrosomal clear zone. Pro-acrosomal vesicle (PA), dense granule (DG), nucleus (N).

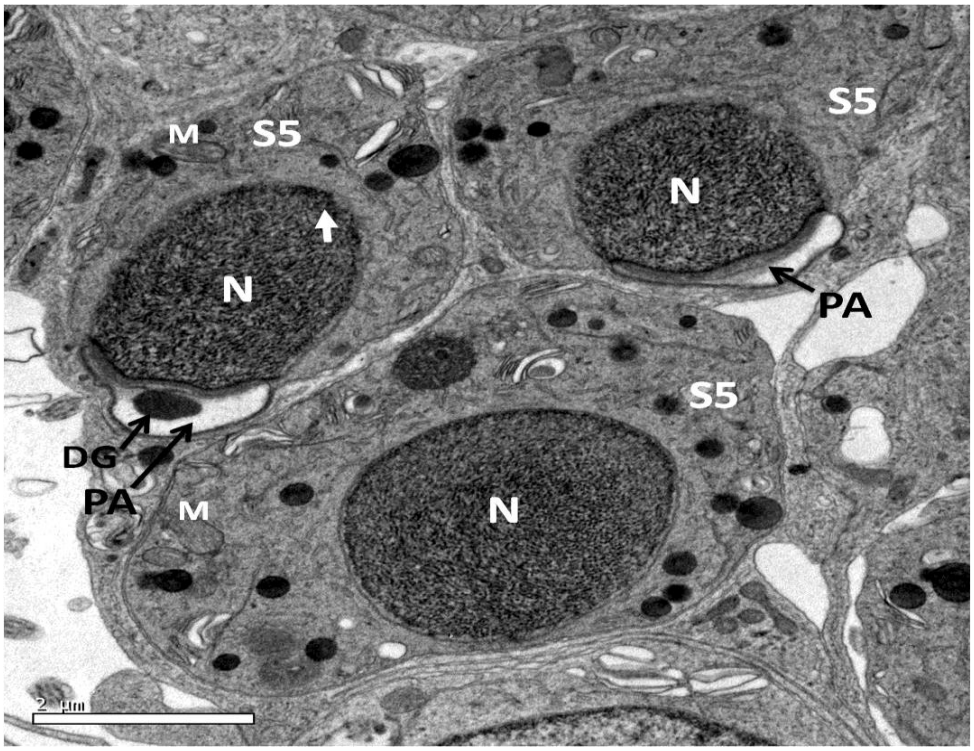

Figure 3.10H. TEM of late stage spermatids (S5) showing the initial condensation and elongation of the nucleus chromatin (arrow) and flattening of pro-acrosomal vesicle (PA). Dense granule (DG), nucleus (N), mitochondria (M).

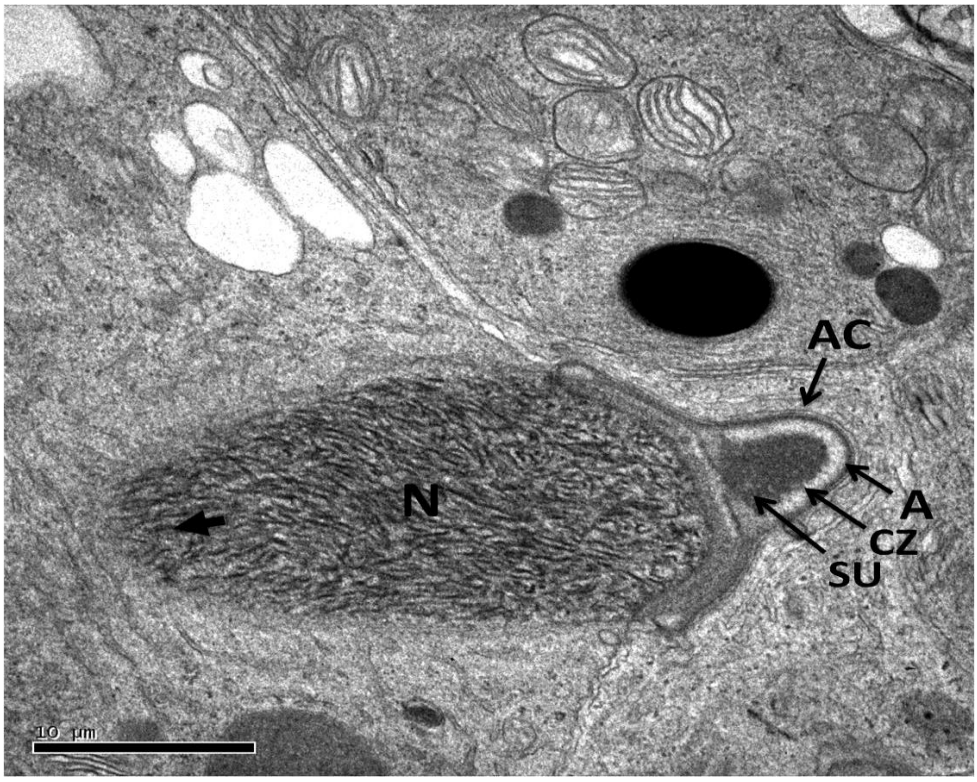

Figure 3.11A. TEM of elongating spermatid (S6) (arrow) with acrosomal complex (AC) attached to the nucleus (N). External acrosomal vesicle (A) and an internal subacrosomal cone (SU) separated by a subacrosomal clear zone (CZ).

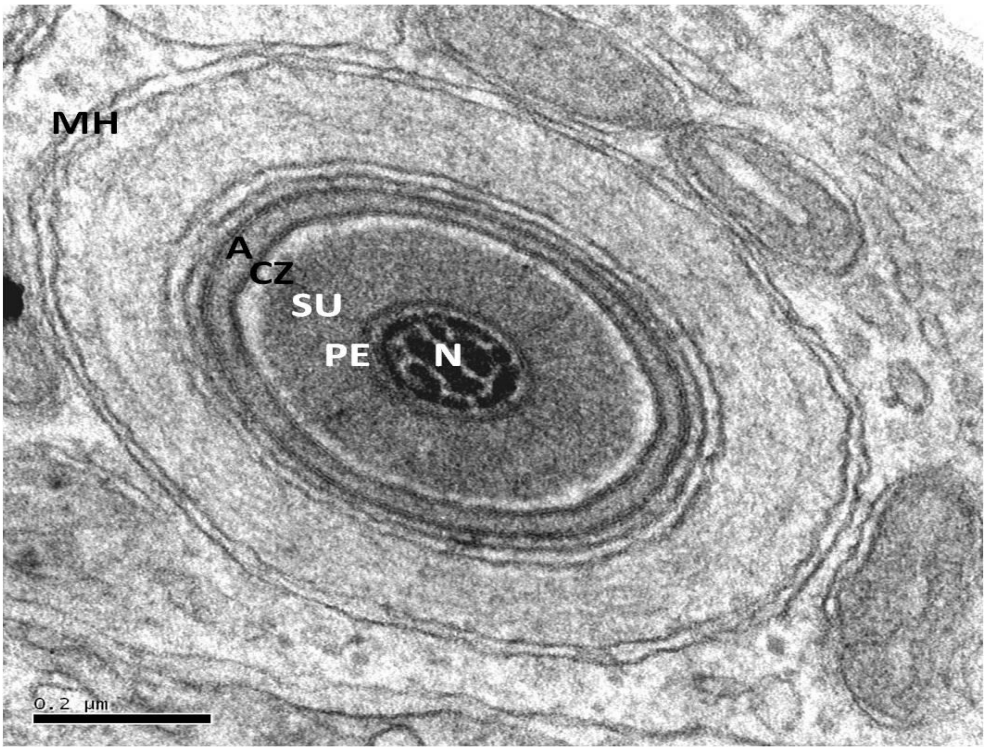

Figure 3.11B. TEM of progressive transverse section of the acrosomal complex of an S6. Acrosome (A), subacrosomal clear zone (CZ), subacrosomal cone (SU), perforatorium (PE), manchette (MH), nucleus (N).

The nuclei exhibited loose chromatin that gradually became compacted (Figure 3.11C). During chromatin condensation, thick fibres were formed and twisted in a spiral arrangement then fused into a honeycomb arrangement of lamellae (Figures 3.11C, 3.11D & 3.11E). A microtubular structure, called the manchette, wrapped helically around the nucleus in the beginning, straightening to a longitudinal arrangement with further nuclear condensation (Figures 3.11D & 3.11E). These microtubules also surrounded the acrosomal complex (Figures 3.11B & 3.11C). Completing its condensation, the nucleus became homogeneously electron-dense, arched and conical in its anterior portion, where it was inserted in the subacrosomal cone (Figures 3.11F & 3.11G). The transition between the conical and the cylindrical portion, called the nuclear shoulders, was abrupt and marked the posterior limit of the acrosome (Figure 3.11F). A layer of radial trabeculae was observed between the nucleus and the microtubules of the manchette at the nuclear shoulders (Figure 3.11H).

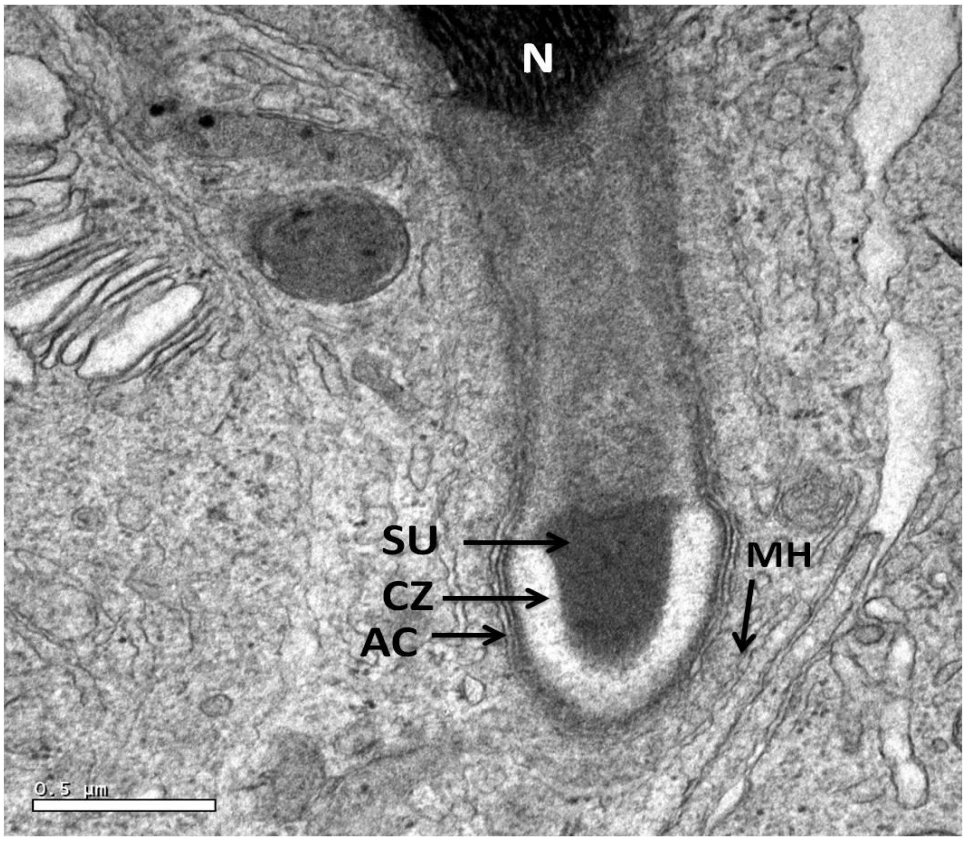

Figure 3.11C. TEM showing further development of an S6. The manchette (MH) surround the acrosomal complex (AC). Subacrosomal clear zone (CZ), subacrosomal cone (SU), nucleus (N).

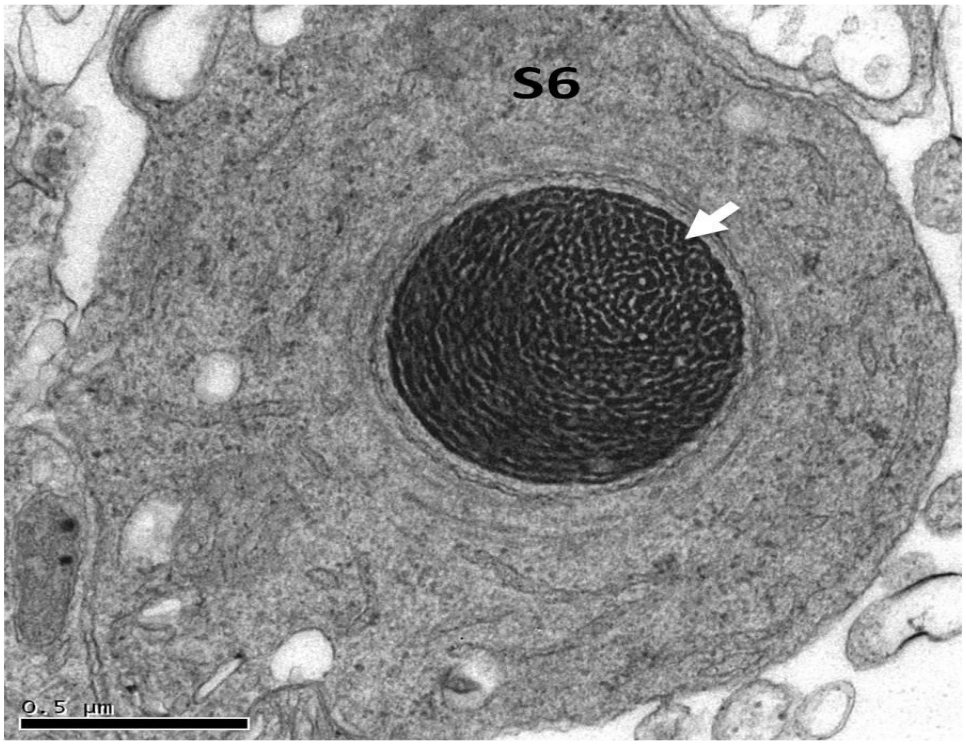

Figure 3.11D. TEM transverse section of an S6 nucleus. During chromatin condensation, thick fibres are formed and twisted in a spiral arrangement (arrow).

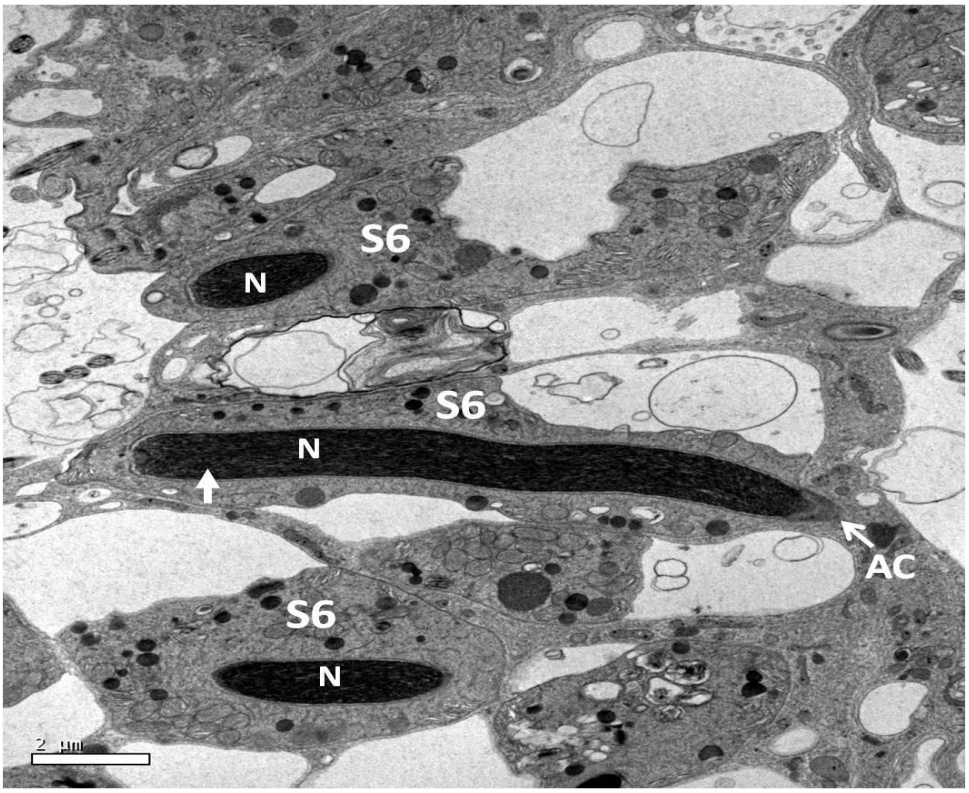

Figure 3.11E. TEM longitudinal section of an S6 nucleus (N) with longitudinal arrangement and further nuclear condensation (arrow). Acrosomal complex (AC).

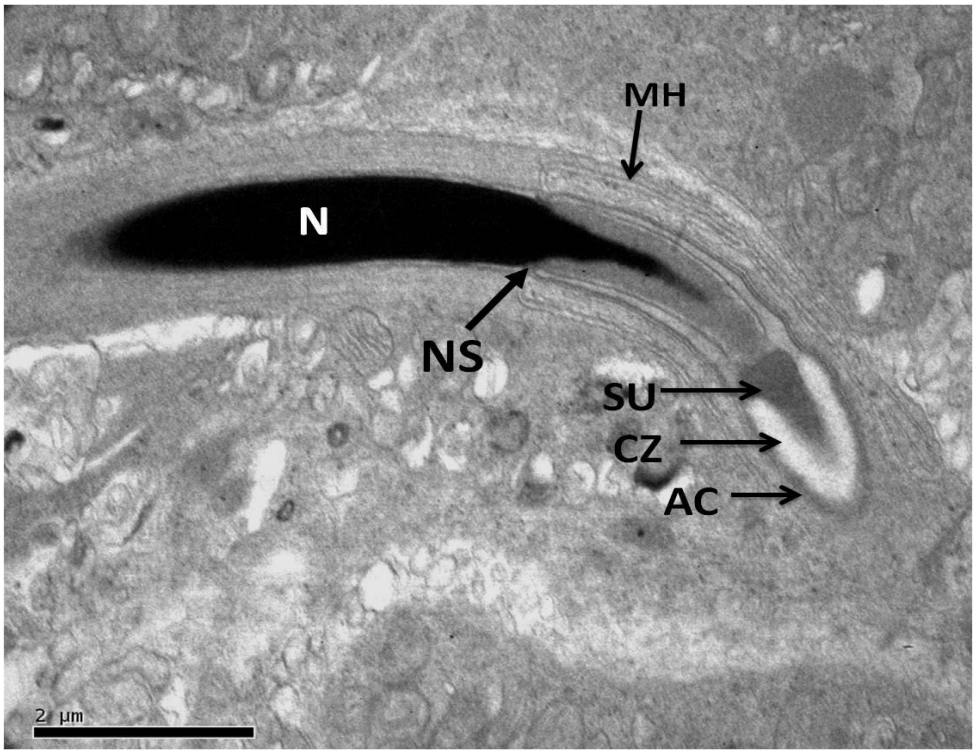

Figure 3.11F. TEM of an S6 with homogeneous electron dense nucleus, arched and conical in its anterior portion, and inserted in the subacrosomal cone. Nuclear shoulders (NS) is clearly visible. Manchette (MH), acrosomal complex (AC), subacrosomal clear zone (CZ), subacrosomal cone (SU), nucleus (N).

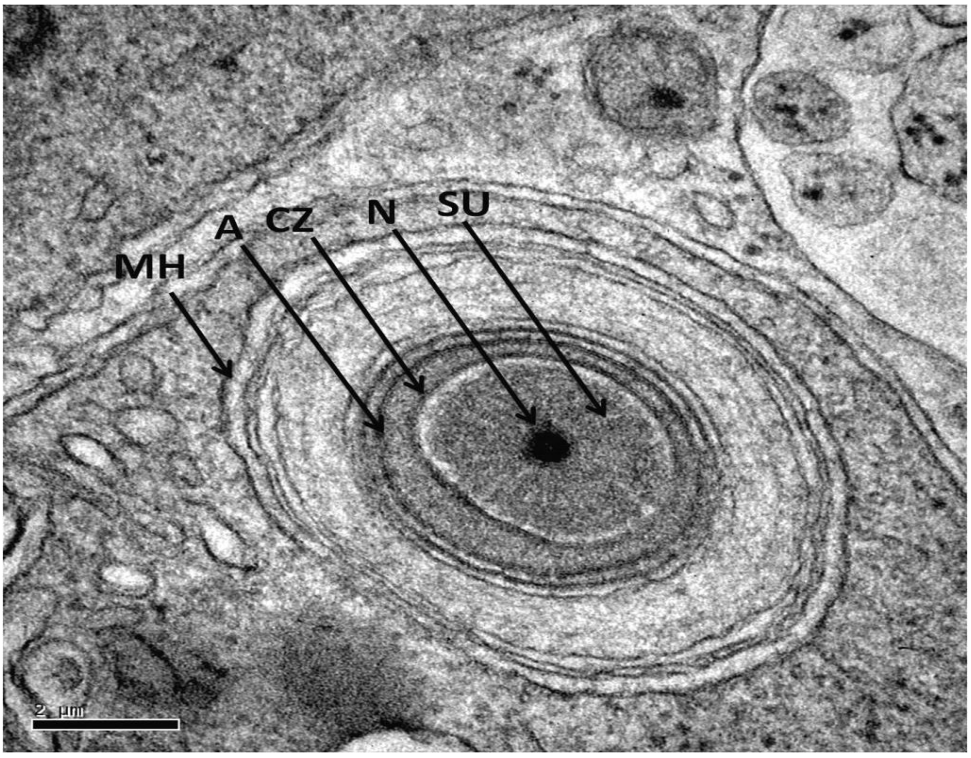

Figure 3.11G. TEM of progressive transverse section of the acrosomal complex in an S6. Manchette (MH), acrosome (A), subacrosomal clear zone (CZ), subacrosomal cone (SU), nucleus (N).

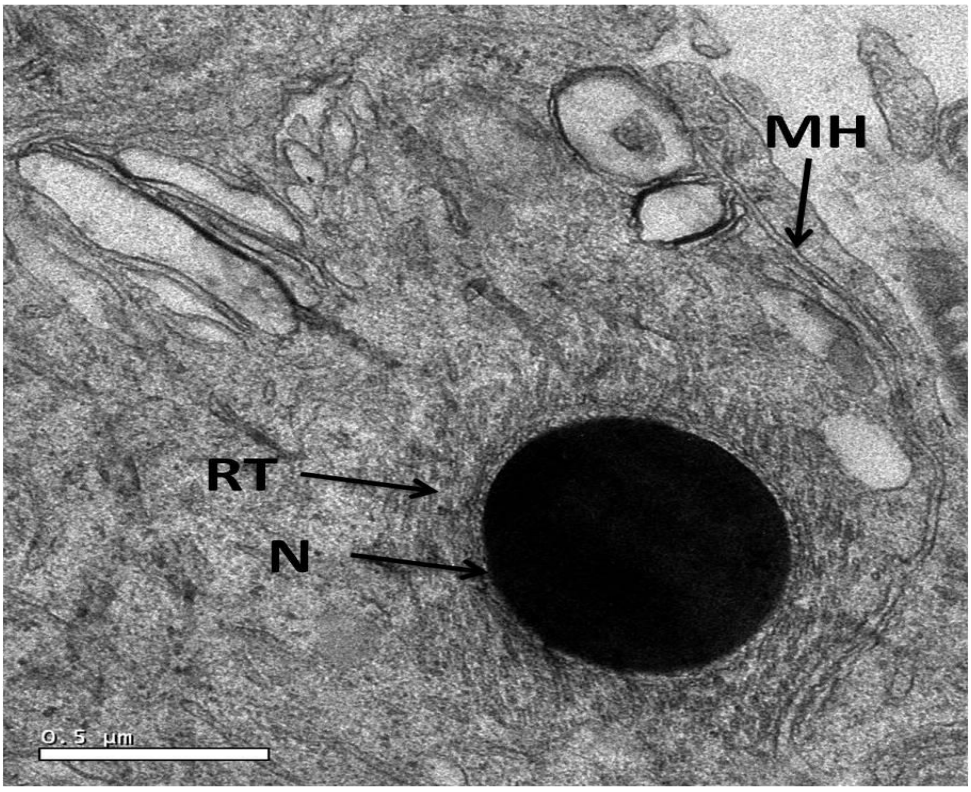

Figure 3.11H. TEM of a layer of radial trabeculae (RT) between the homogeneous electron dense nucleus (N) and the microtubules of the manchette (MH).

Accumulation of mitochondria around the nucleus, annulate lamellae and chromatoid bodies were observed within the cytoplasm of late S6 spermatids (Figure 3.11I). The chromatoid bodies were cloud-like accumulations of dense fibrous material called nuage. As spermiogenesis progressed, at the nuclear base, a deposit of electron dense material called the pericentriolar layer was found (Figure 3.11J). This region was considered the "spermatozoon neck" and consisted of two centrioles; a proximal and a distal one, wrapped in the electron dense pericentriolar material (Figures 3.11K & 3.11O). Nine triplets of microtubules constituted each centriole, associated with nine peripheral fibres and a central pair of microtubules, one of which had a dense fibre associated with it in the distal centrioles (Figure 3.11L). The distal centriole was short and maintained an intermediate position, just above the axoneme (Figures 3.11K & 3.11O). Mitochondria congregated next to the centrioles to constitute the midpieces of the tails, (Figures 3.11I, 3.11J & 3.11L). Dense bodies developed between the mitochondria in the midpiece, forming the inter-mitochondrial rings (Figure 3.11L). The midpiece of the flagellum was formed by an axoneme constituted by nine microtubule doublets, a central pair and peripheral dense fibres, associated with each of the nine pairs of microtubules (Figures 3.11M, 3.11O & 3.11P). The midpiece was limited by a dense ring called the annulus (Figure 3.11N).

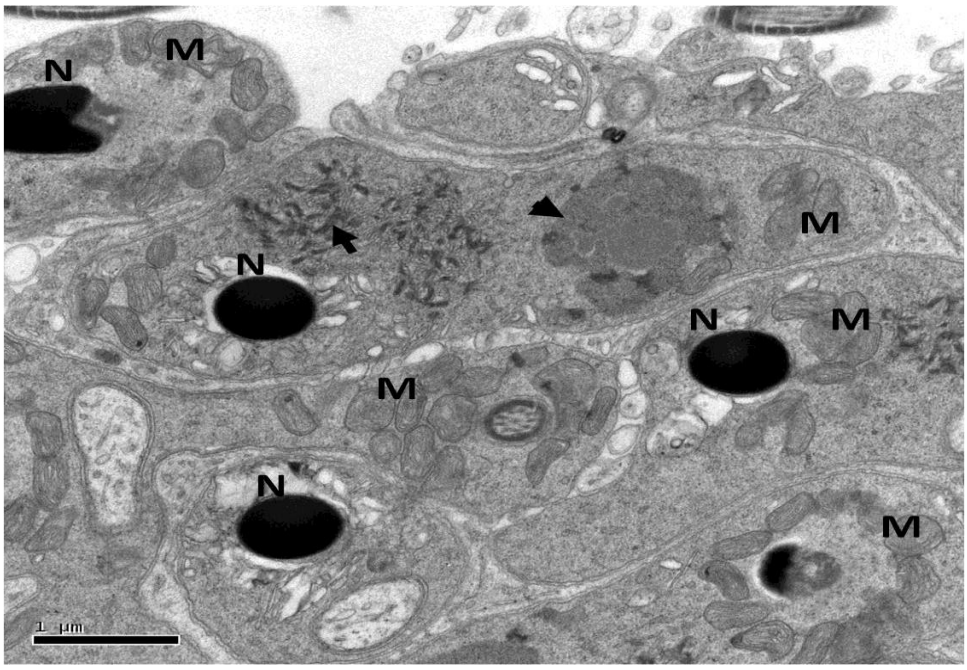

Figure 3.11I. TEM of an S6. Mitochondria (M) start to accumulate near the spermatid nucleus (N), annulate lamella (arrowhead) and chromatoid bodies (arrow) are observed within the cytoplasm.

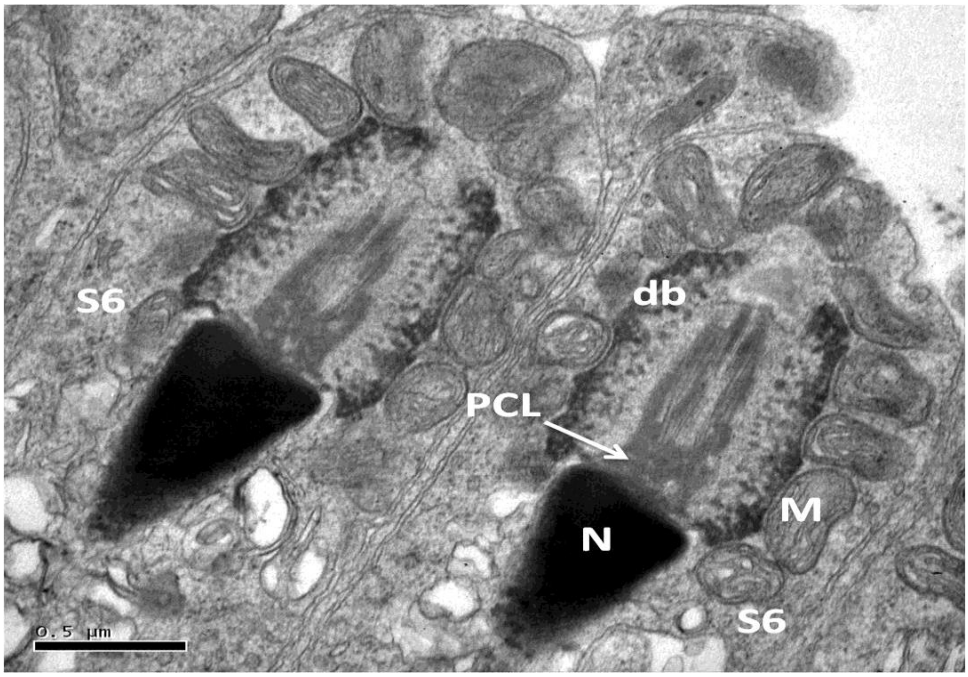

Figure 3.11J. TEM of the midpiece of an S6. Deposit of pericentriolar layer (PCL) at the nuclear base, and mitochondria (M) aggregates next to the layer. Dense bodies (db).

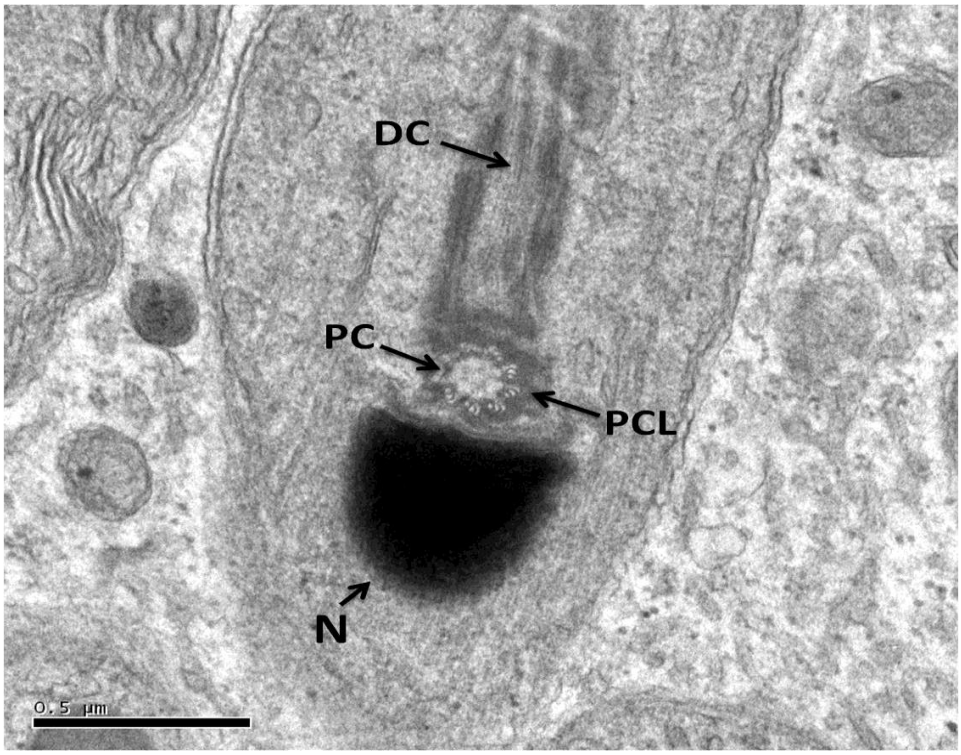

Figure 3.11K. TEM of a midpiece. Spermatozoon neck consists of two centrioles, a proximal (PC) and a distal (DC) one, wrapped in the electron-dense pericentriolar material (PCL). Nucleus (N).

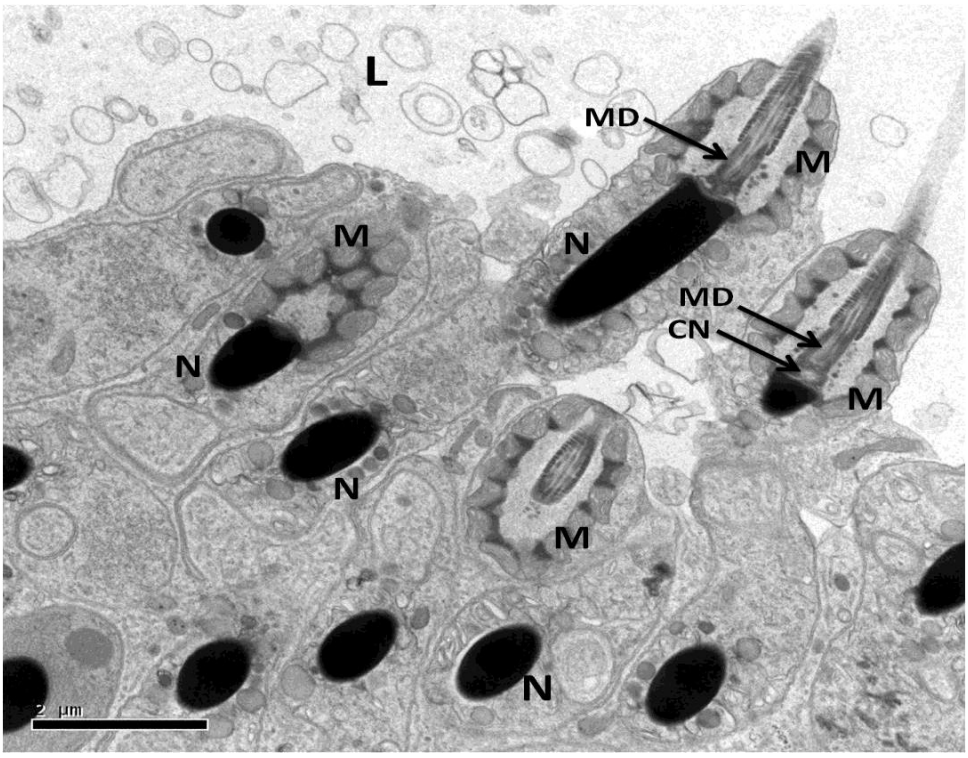

Figure 3.11L. TEM of midpieces (MD) of flagellae. Mitochondria (M) congregate next to centrioles (CN) to constitute the midpieces of the tails. Nucleus (N), lumen (L).

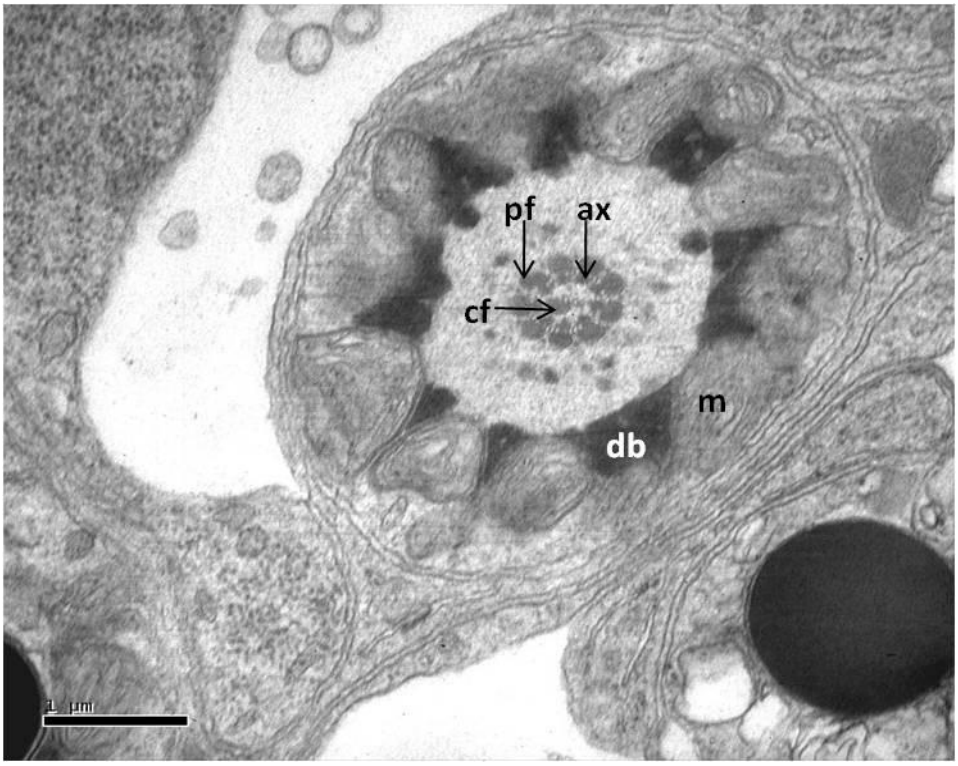

Figure 3.11M. TEM transverse section of the midpiece in the initial portion of the axoneme (ax) with peripheral fibers (pf) associated with the doublets and one of the central microtubules (cf). Dense bodies (db), mitochondria (m).

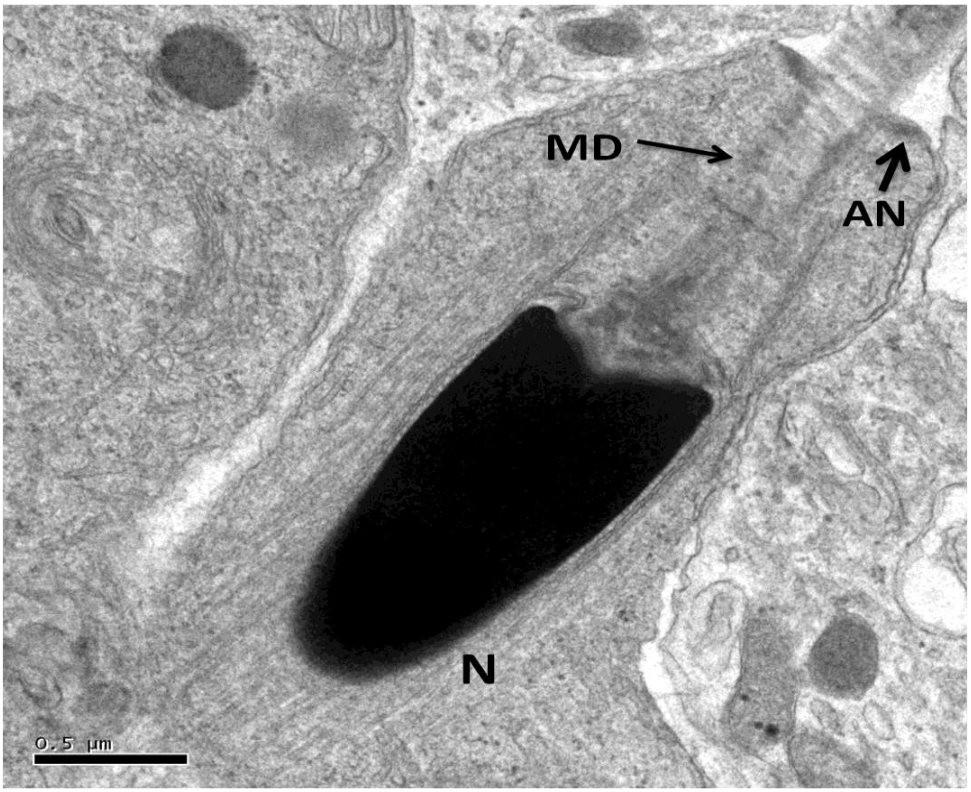

Figure 3.11N. TEM of longitudinal section of the midpiece (MD). The midpiece is limited by a dense ring called the annulus (AN). Nucleus (N).

The principal piece of the flagellum developed in the early stage seven (S7) spermatids and consisted of the axoneme (9+2), and vestigial peripheral dense fibres associated with pairs 3 and 8, all surrounded by the fibrous sheath and the plasma membrane (Figures 3.11O, 3.11P, 3.12A & 3.12F). The fibrous sheath was formed by regular individual rings observed, in longitudinal sections, in two columns (Figures 3.11P & 3.12A). The flagella were oriented towards the lumen of the seminiferous tubule and were anchored to the Sertoli cell extensions (Figures 3.12B, 3.12C & 3.12F). The end piece of the flagellum was narrower and consisted only of the axoneme; with peripheral dense fibres associated only with the 3rd and 8th pairs and covered by the plasma membrane (Figure 3.12D). The peripheral dense fibres decreased in diameter along the length of the axoneme, and remained attached only to pairs 3 and 8 of the axoneme up to the flagellar end piece. Mature spermatids (S7) (Figures 3.12E, 3.712 & 3.12H) and spermatozoa (Figures 3.12G & 3.12H) had elongated, entirely black stained nuclei with an acrosomal complex at its apical end and a flagellar tail consisting of a midpiece, principal piece and endpiece.

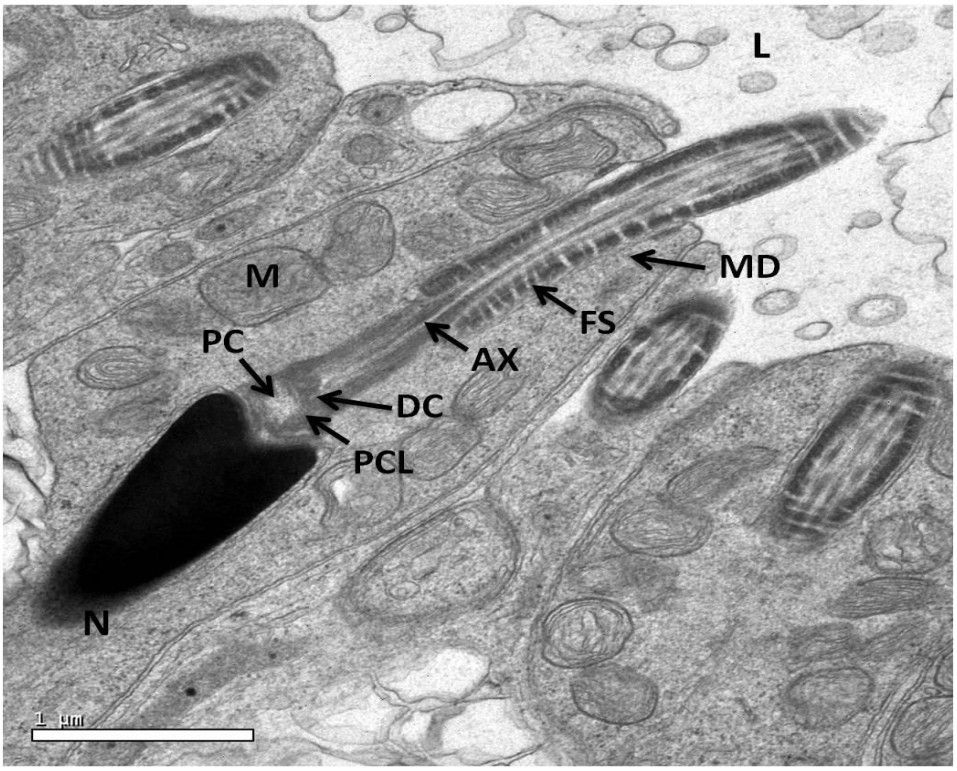

Figure 3.11O. TEM of an S7 showing longitudinal section of the midpiece (MD) of the flagellum, surrounded by the fibrous sheath (FS). Proximal (PC) and a distal (DC) centrioles, pericentriolar layer (PCL), nucleus (N), axoneme (AX), mitochondria (M), lumen (L).

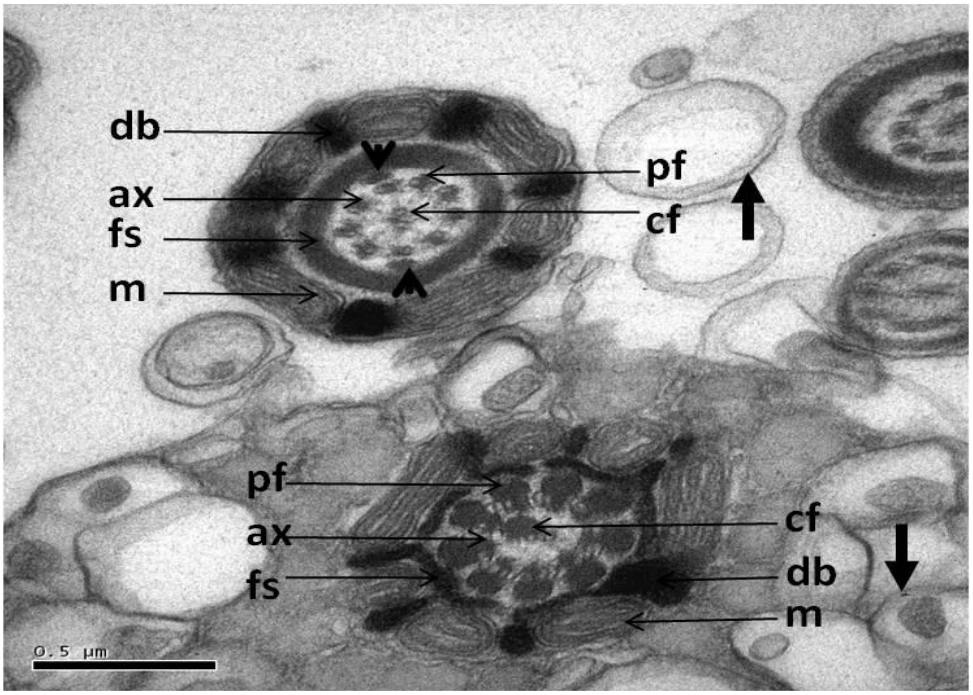

Figure 3.11P. TEM transverse section of the midpiece in a spermatozoon (up arrow) and midpiece in an S7 (down arrow). The axoneme (ax) presents vestigial peripheral fibers (pf) binding to the 3rd and 8th doublets (arrow head) and to the fibrous sheath (fs). Central microtubules (cf), dense bodies (db), mitochondria (m).

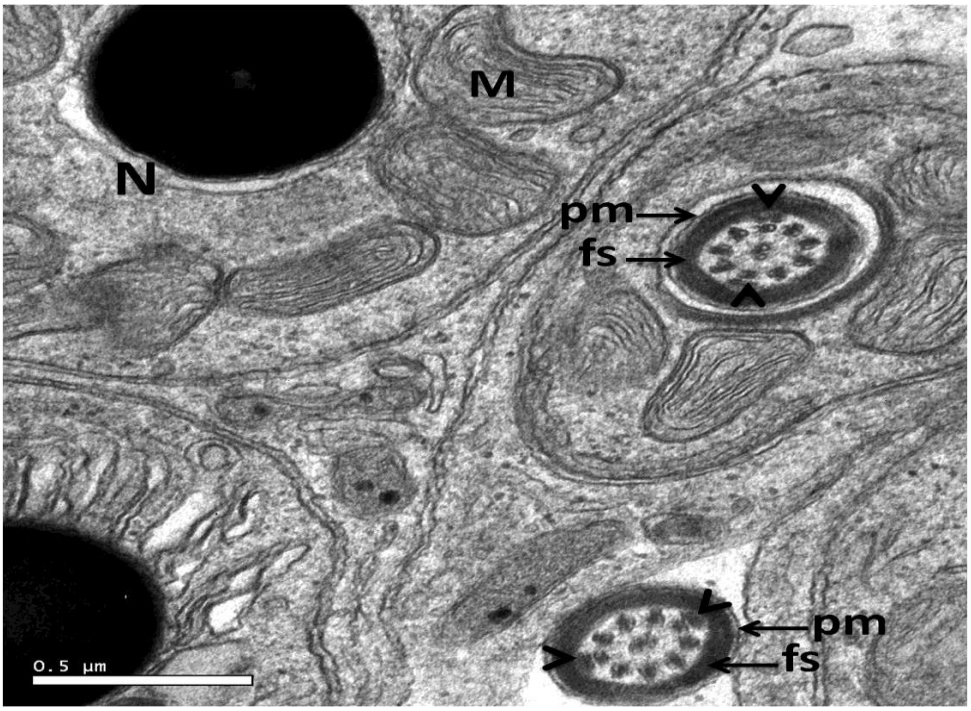

Figure 3.12A. TEM transverse sections of a flagellum, in its principal piece, formed by a 9+2 axoneme, connected to the fibrous sheath (fs) by the 3rd and 8th doublets (arrow heads) and surrounded by the plasma membrane (pm). Nucleus (N), mitochondria (M).

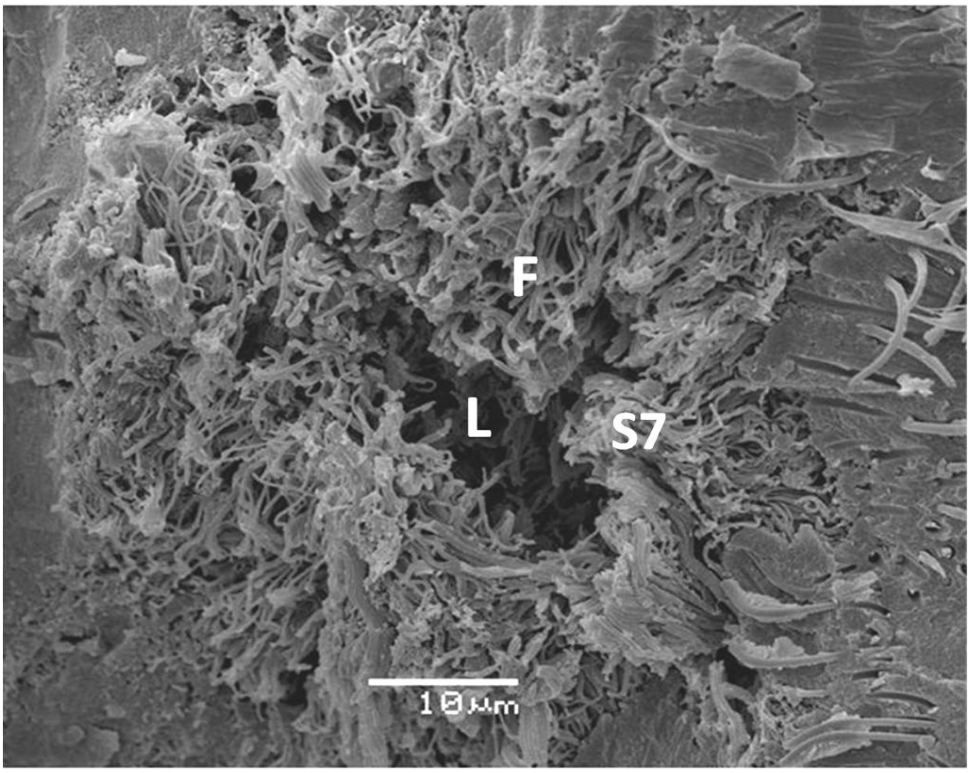

Figure 3.12B. SEM of a seminiferous tubule. Flagella (F) of late stage spermatids (S7) oriented towards the lumen (L).

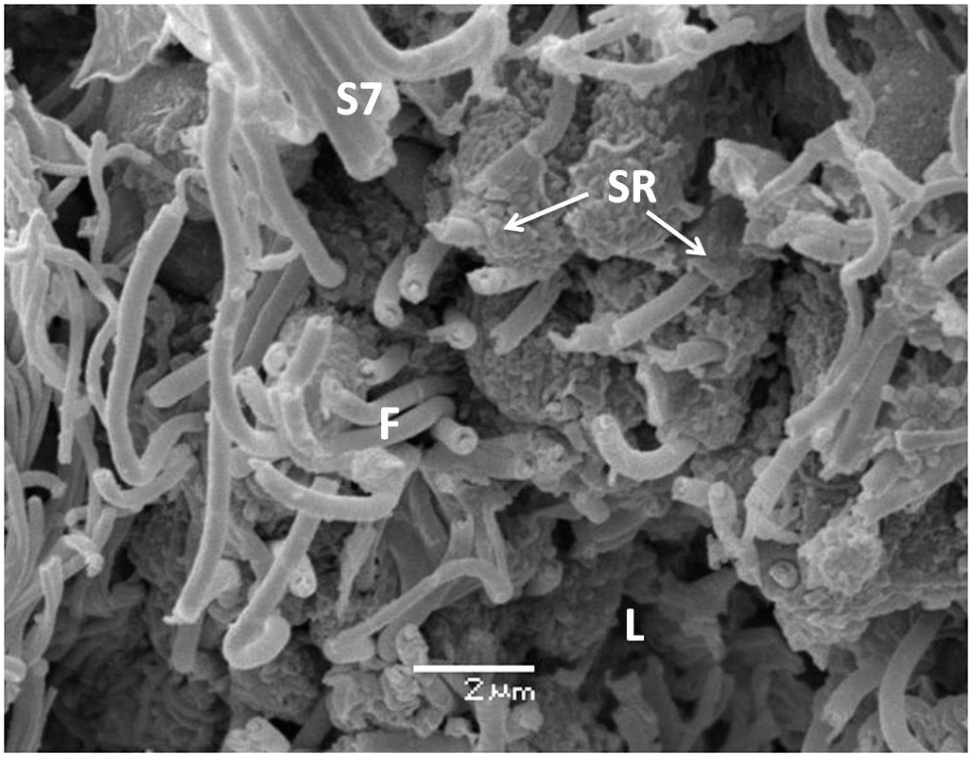

Figure 3.12C. SEM higher magnification of Figure 3.12B. Flagella (F) of an S7 oriented towards the lumen of the seminiferous tubule and enclosed in the apical processes of Sertoli cells (SR).

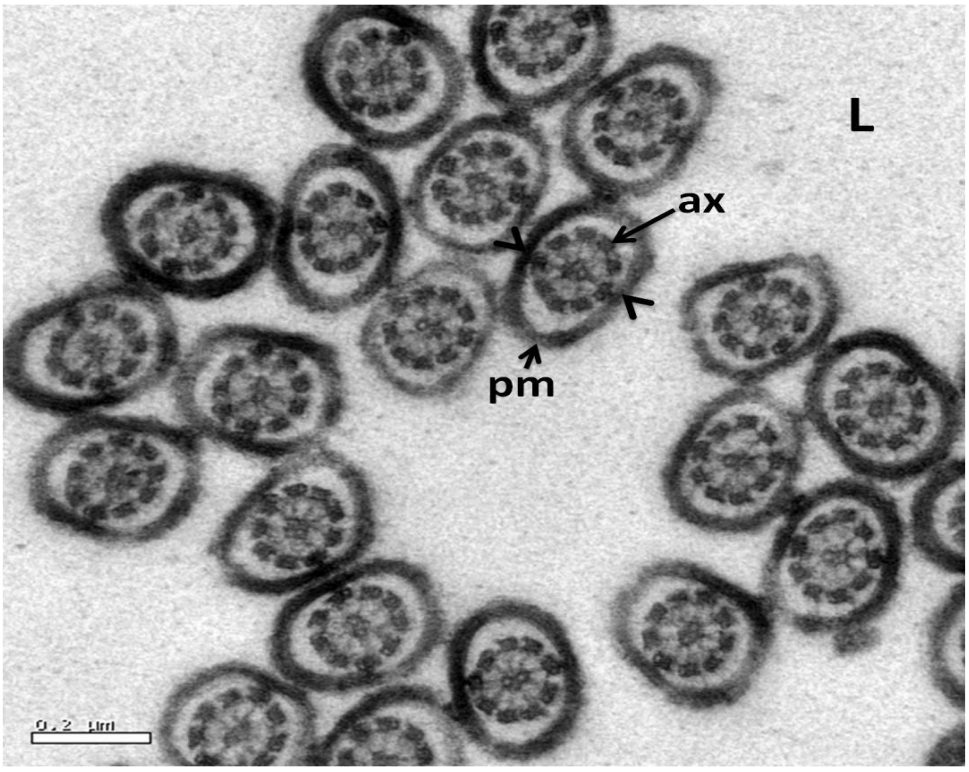

Figure 3.12D. TEM of the end piece of the flagellum consists of the axoneme (ax), with peripheral dense fibres associated to the 3rd and 8th pairs (arrowhead) and covered by the plasma membrane (pm). Lumen (L).

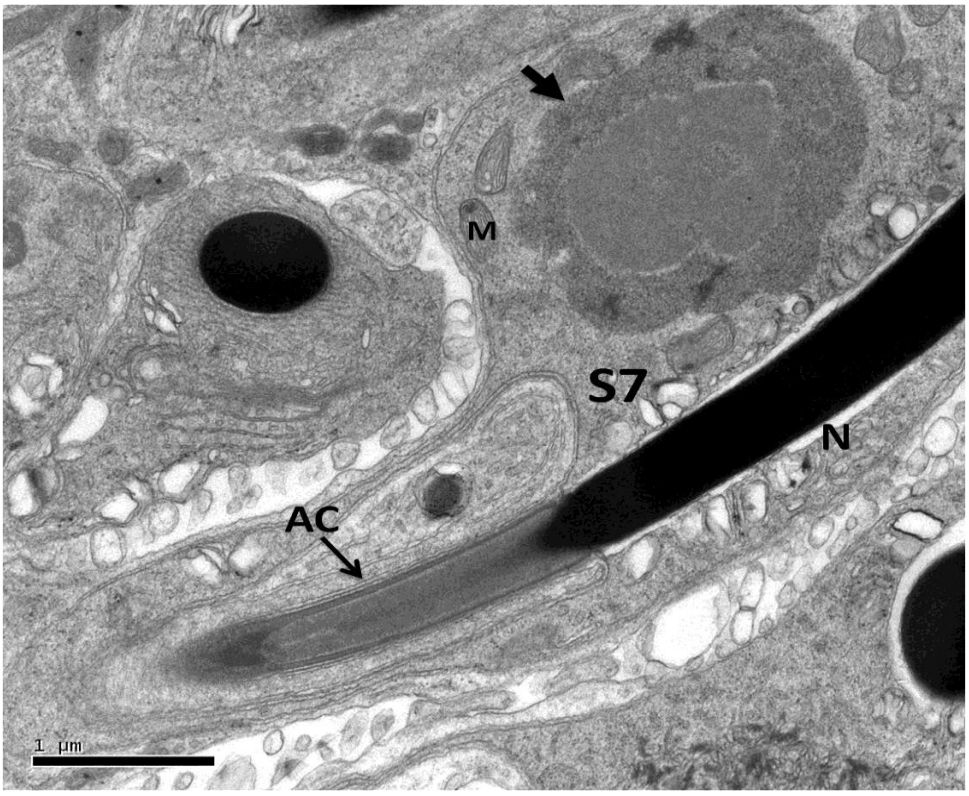

Figure 3.12E. TEM of a mature S7 spermatid showing acrosome complex (AC) and elongating electron dense nucleus (N). Chromatoid body (arrow), mitochondria (M).

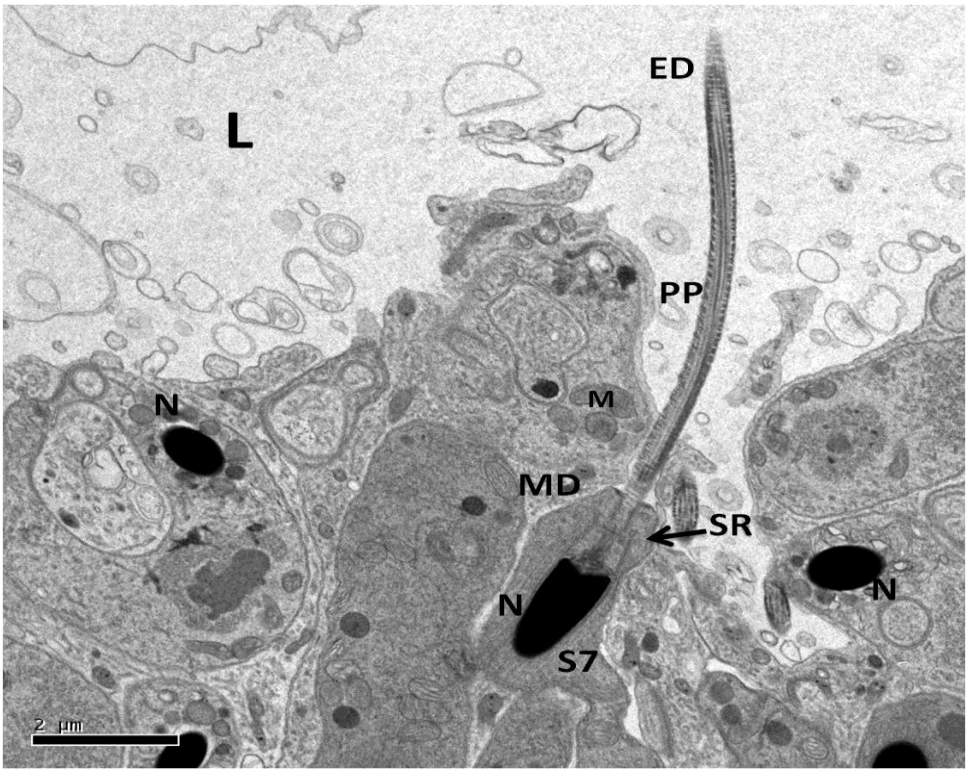

Figure 3.12F. TEM showing midpiece (MD), principal piece (PP) and endpiece (ED) of the flagellum. Flagellum is oriented towards the lumen (L) and enclosed in the apical processes of Sertoli cells (SR). Nucleus (N), mitochondria (M), lumen (L).

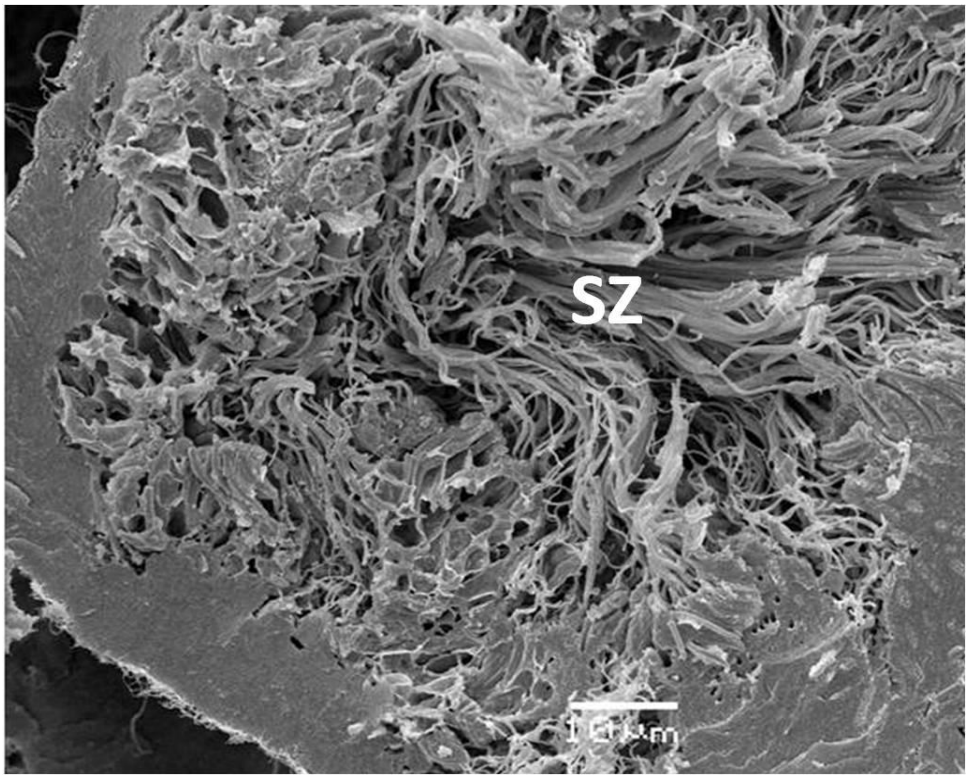

Figure 3.12G. SEM of a seminiferous tubule. The lumen is full of free spermatozoa (SZ).

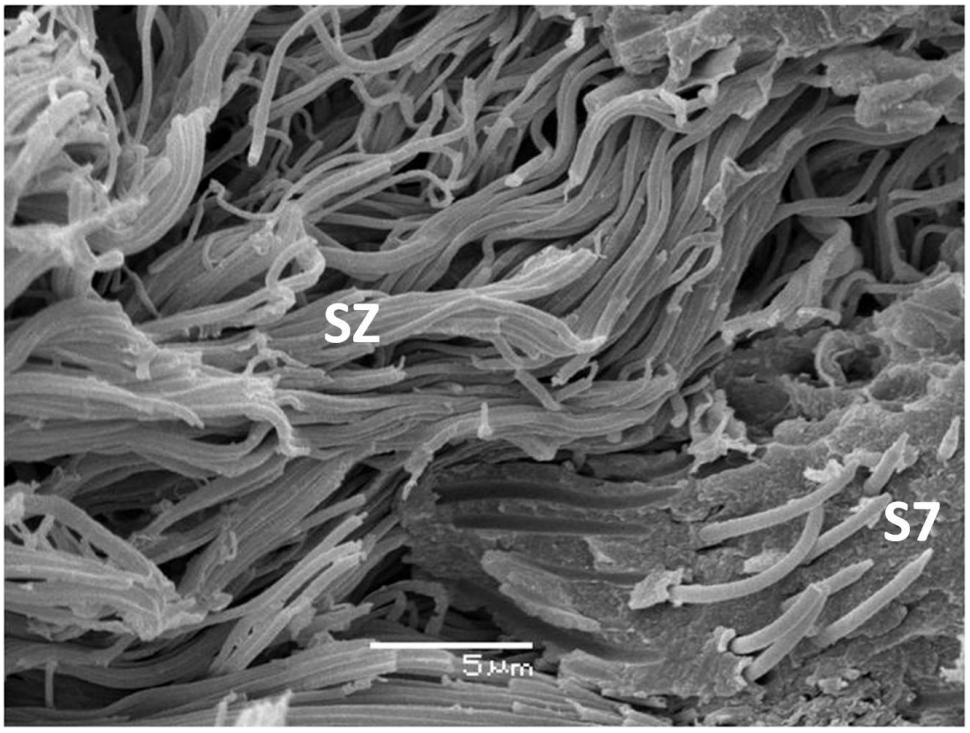

Figure 3.12H. SEM higher magnification of Figure 3.12G. The lumen is full of free spermatozoa (SZ). Mature spermatids (S7).

As in the main part of the seminiferous lumen, the lumina of the ductus epididymis (Figure 3.13A) and ductus deferens (Figure 3.3G) were full of mature spermatozoa. The acrosomal piece of mature spermatozoa consisted of an acrosome vesicle and a subacrosomal cone which surrounded the nuclear attenuation, which is also called the nuclear point (Figures 3.13B & 3.13C). In transverse section, the acrosome vesicle was depressed apically, becoming circular at its base (Figure 3.13B). The acrosome vesicle capped the subacrosomal cone and was uniformly divided into a narrow cortex and a wide medulla at its anterior portion. In longitudinal sections the cortex exhibited a tubular organization and the medulla appeared as a moderately electron-dense structure, filling the interior of the acrosome vesicle (Figures 3.13B & 3.13C). The tip of the acrosome contained the perforatorium. The single perforatorium extended from the anterior region of the subacrosomal cone into the acrosome vesicle and ended with a pointed tip (Figures 3.13B & 3.13C). The nucleus was composed of highly condensed, electron-dense chromatin. In transverse section, the nucleus was circular throughout (Figure 3.13B). The nucleus formed a point within the acrosome complex, the nuclear rostrum (Figures 3.13B & 3.13C). The transition from the nuclear rostrum to the cylindrical portion of the nucleus was abrupt and marked by rounded nuclear shoulders.

Basally the nucleus terminated with a shallow concave depression, the nuclear fossa, which housed the anterior half of the proximal centriole and dense pericentriolar material (Figure 3.13D). The proximal centriole resided in the neck region directly beneath the nucleus. The distal centriole formed the axoneme which extended through the whole tail (Figure 3.13D). Electron-dense fibres formed a fibrous sheath around the axoneme of the midpiece and the principal piece (Figures 3.13D, 3.13E & 3.13F). It appeared as a ring in cross section (Figure 3.13F). In the midpiece both the axoneme and the fibrous sheath were covered with mitochondria and dense bodies (Figure 3.13F). The endpiece of spermatozoon contained only the axoneme (Figure 3.13F).

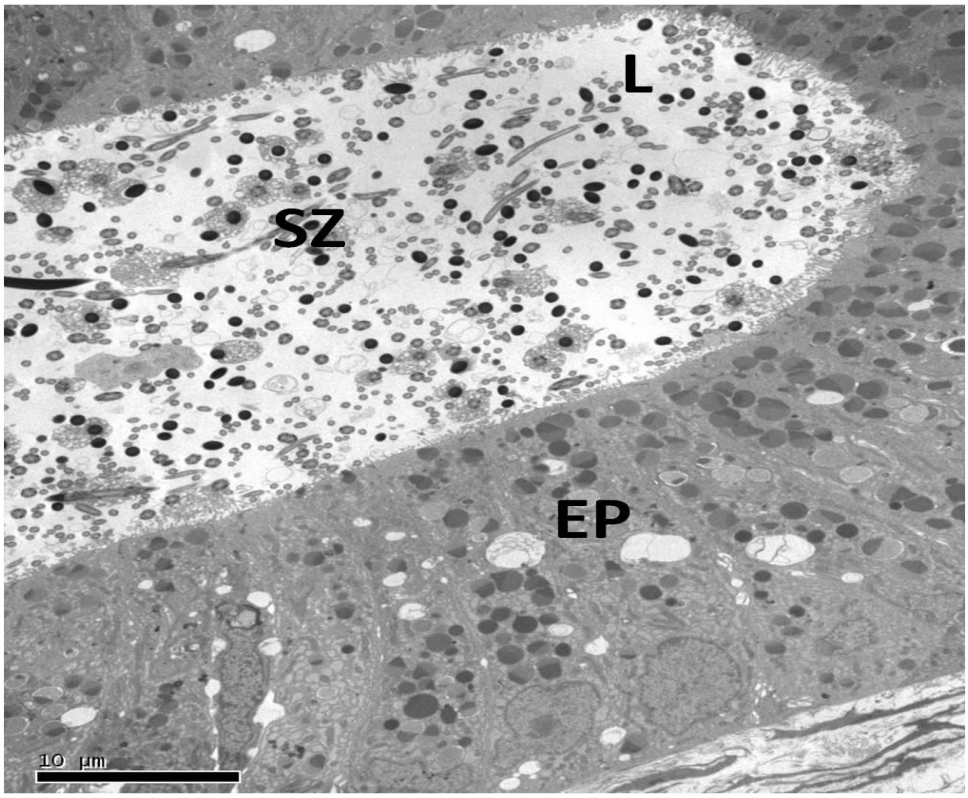

Figure 3.13A. TEM lumen (L) of the middle region of an epididymis from the active phase full of spermatozoa (SZ). Epithelial layer (EP) of epididymis.

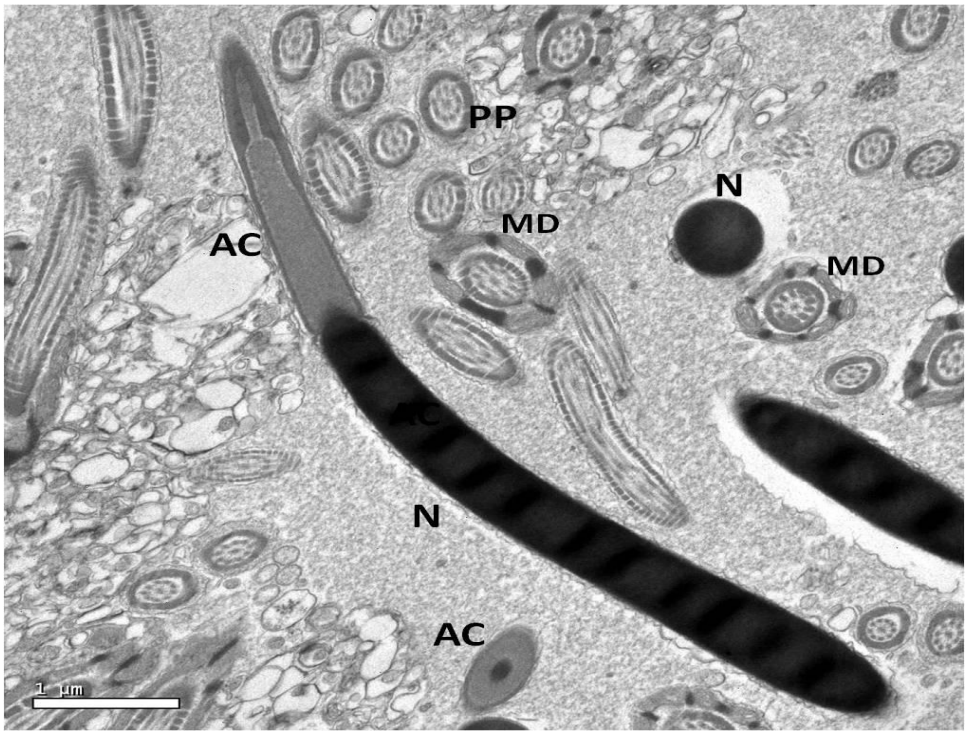

Figure 3.13B. Higher magnification of Figure 3.13A. Longitudinal section of Spermatozoon with electron-dense nucleus (N) and acrosomal complex (AC) at its apical end. Transverse section of electron-dense nucleus (N), acrosomal complex (AC), principle piece (PP) and midpiece (MD) also seen here.

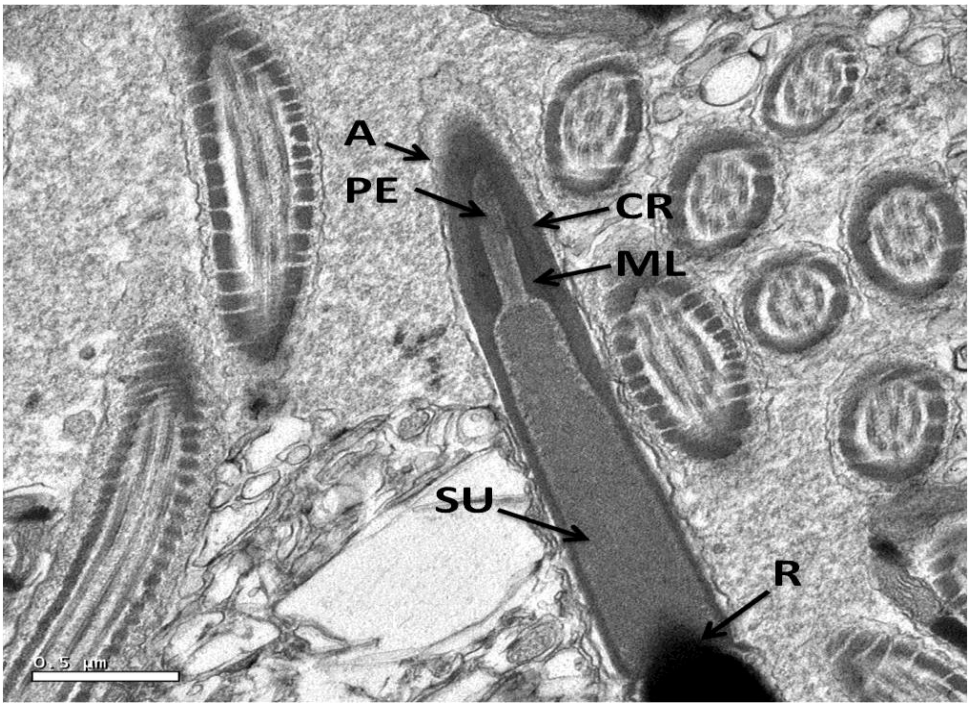

Figure 3.13C. Higher magnification of Figure 3.13B. Acrosome vesicle (A) capping the subacrosomal cone (SU) and is uniformly divided into a narrow cortex (CR) and a wide medulla (ML). The tip of the acrosome contains the perforatorium (PE). Nuclear rostrum (R).

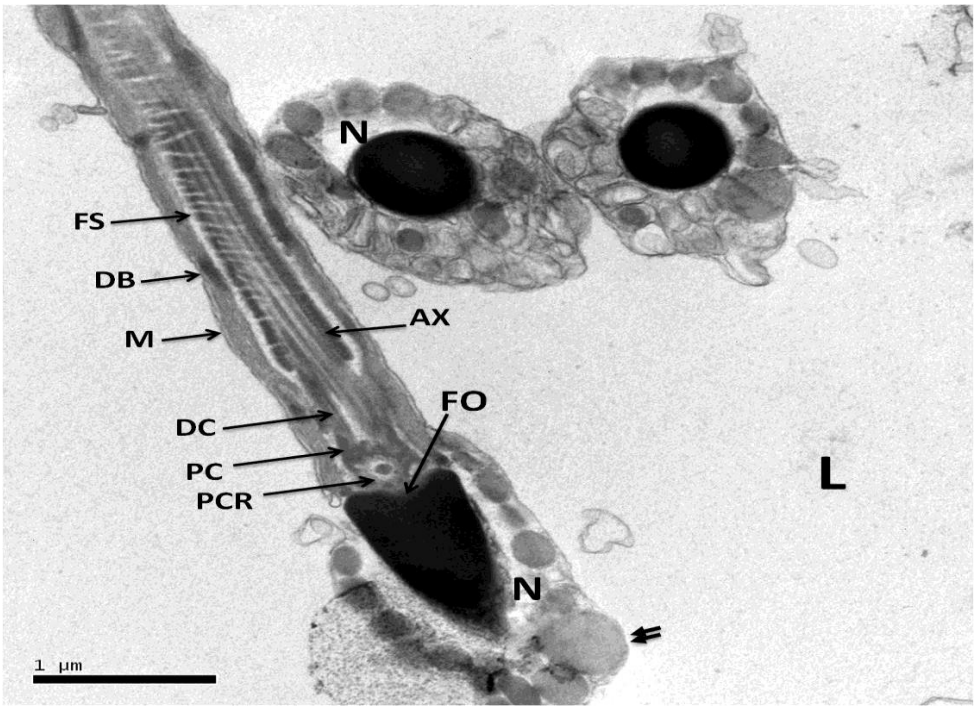

Figure 3.13D. TEM of spermatozoon. Nuclear fossa (FO) houses anterior half of proximal centriole (PC) and dense pericentriolar material (PCR). Distal centriole (DC), axoneme (AX), fibrous sheath (FS), mitochondria (M) and dense bodies (DB), lumen (L). Note the secretory granules produced by the epididymis binds to the head of spermatozoon (double arrow).

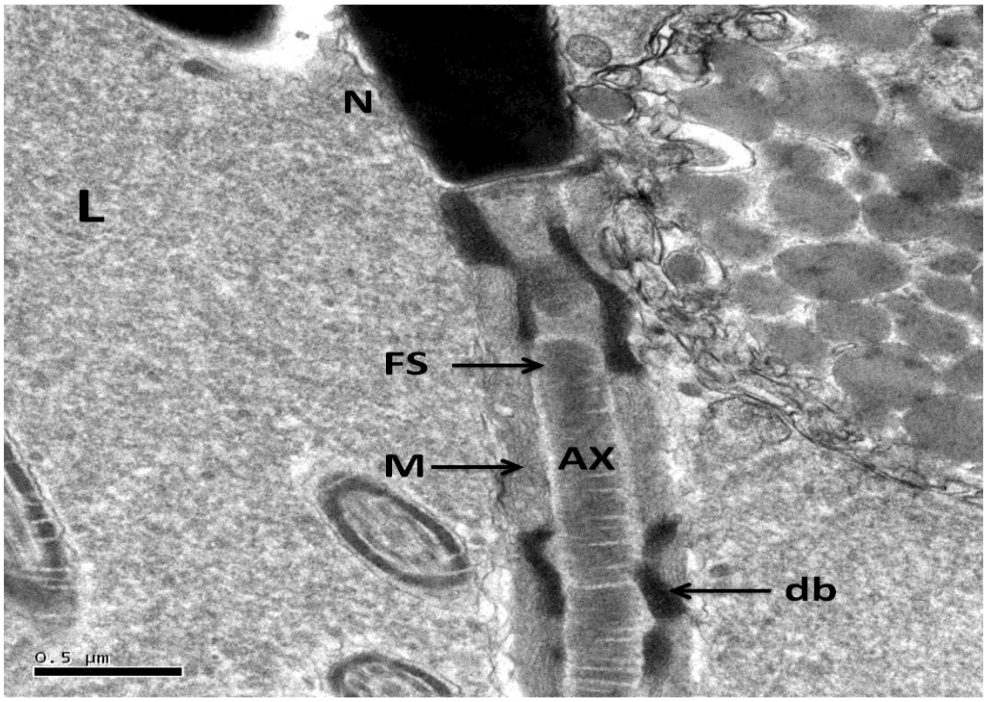

Figure 3.13E. TEM of spermatozoon. Fibrous sheath (FS) around the axoneme (AX) of the midpiece. Fibrous sheaths are surrounded by mitochondria (M) and dense bodies (db). Nucleus (N), lumen (L).

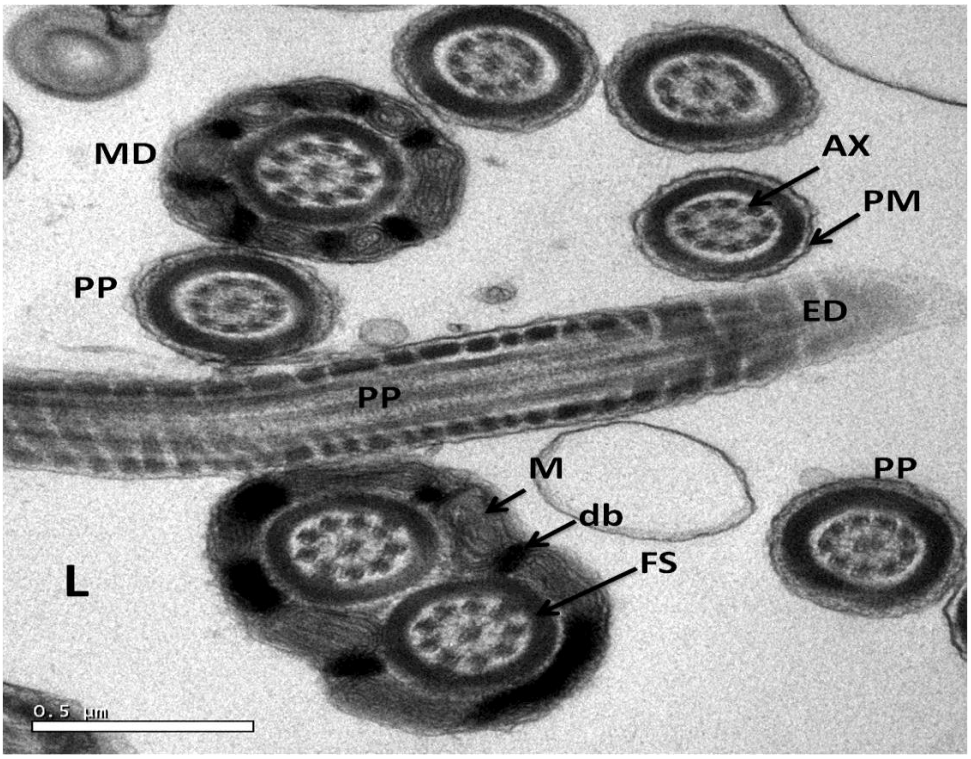

Figure 3.13F. TEM transverse section of spermatozoa. Midpiece (MD), principle piece (PP) and endpiece (ED). MD surrounded by mitochondria (M) and dense bodies (DB). Axoneme (AX), fibrous sheath (FS), plasma membrane (PM), lumen (L).

3.3.8.3 Ultrastructural changes in Sertoli and Leydig cells

3.3.8.3.1 Sertoli cells

Sertoli cells were anchored to the basal lamina throughout the year and their nuclei were different from that of nuclei of the germ cells, as they appeared triangular in shape with numerous indentations (Figures 3.14A & 3.14B).

During the recrudescent phase, the basal cytoplasm contained numerous lipid droplets, mitochondria, SER and RER (Figures 3.14A, 3.14C, 3.14D & 3.14E). Both lipids and mitochondria were aggregated in dense clusters adjacent to the basal lamina (Figures 3.14D & 3.14E). The SER was composed of cisternal and vesicular elements (Figure 3.14E). Sertoli cell extensions began to surround germ cells and became highly interdigitated and folded (Figures 3.14A, 3.14F & 3.14G).

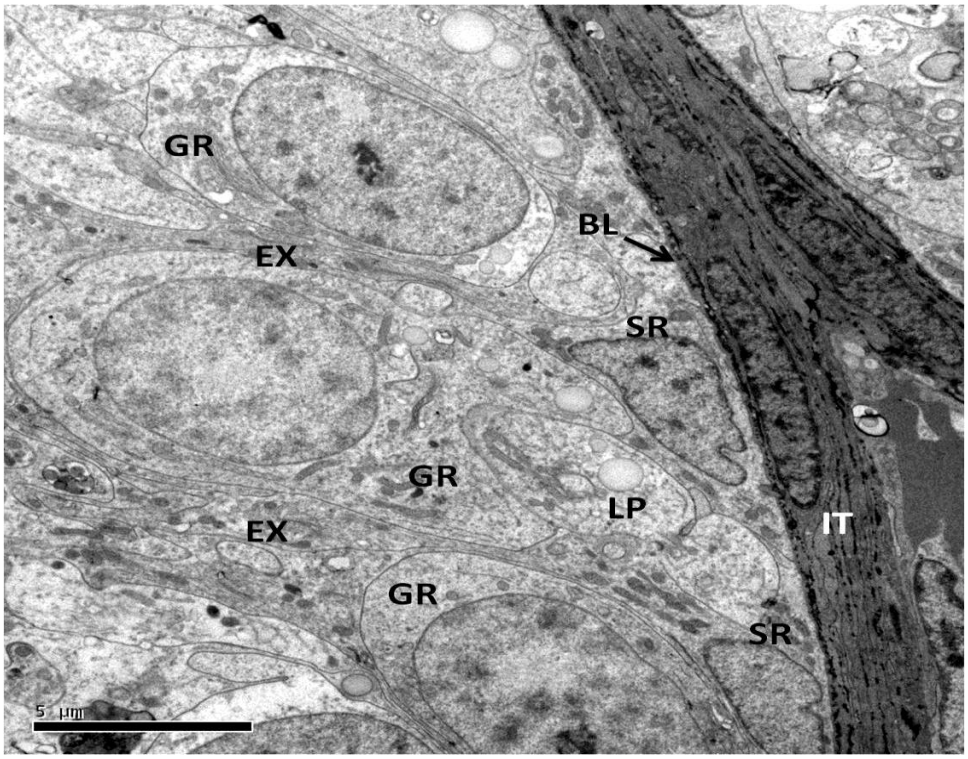

Figure 3.14A. TEM of a seminiferous tubule from the recrudescent phase showing Sertoli cell (SR) attached to the basal lamina (BL). Sertoli extensions (EX) surround germ cells (GR) at basal region. Interstitial tissue (IT). Lipid droplets (LP) appeared in both Sertoli and germ cells.

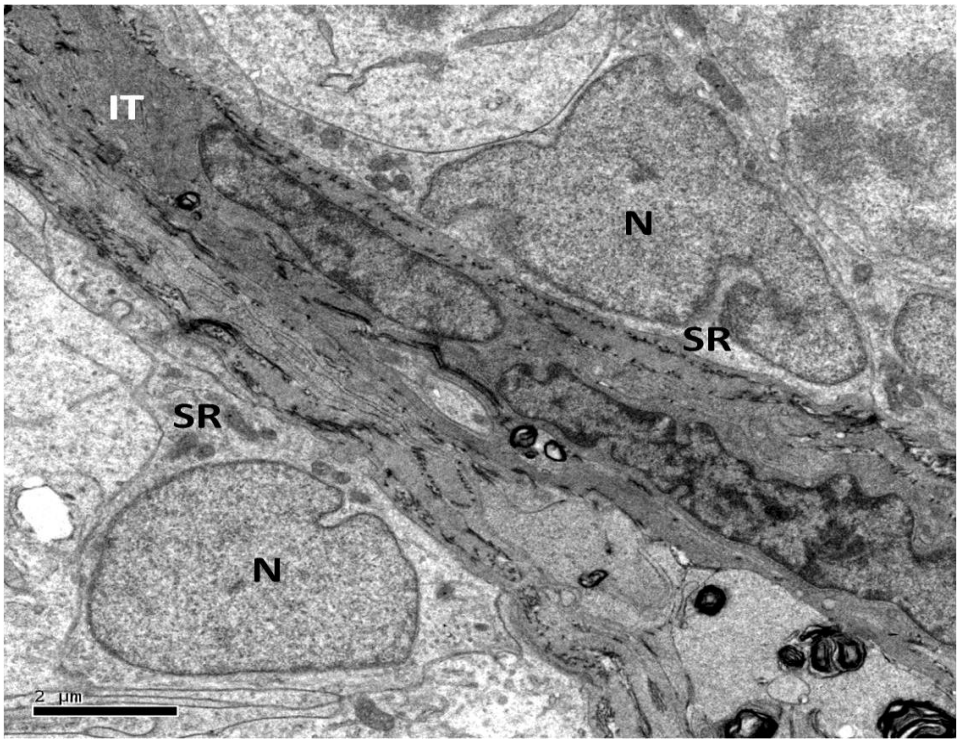

Figure 3.14B. TEM of a seminiferous tubule from the recrudescent phase showing Sertoli cell (SR) attached to the basal lamina. The nuclei (N) appeared triangular in shape with numerous indentations. Interstitial tissue (IT).

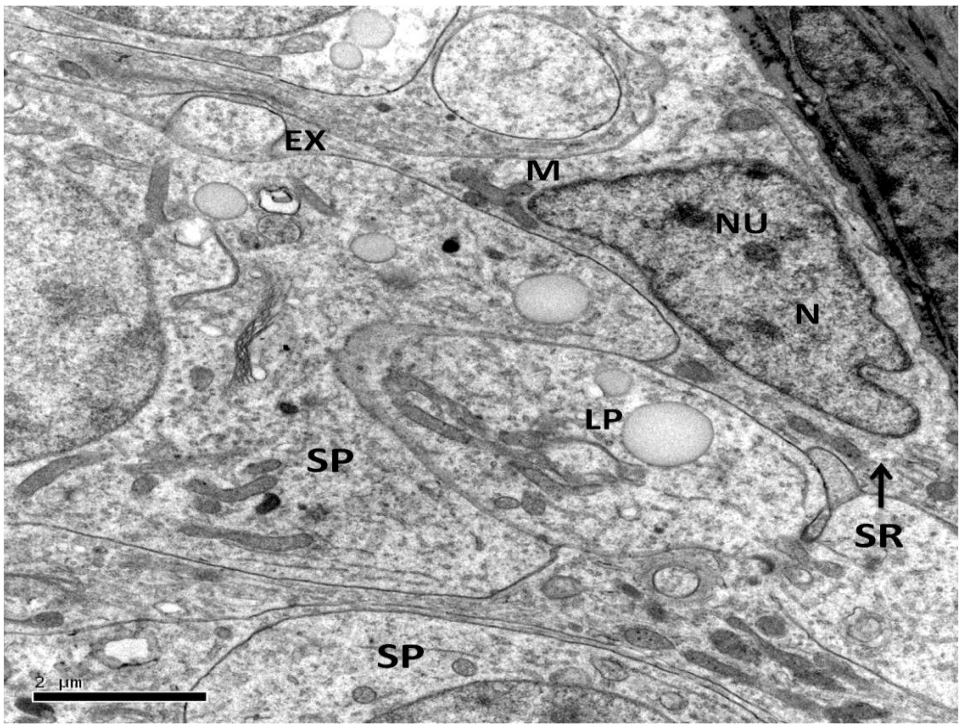

Figure 3.14C. TEM of a Sertoli cell (SR) attached to the basal lamina. The nucleus (N) appeared triangular in shape with two nucleoli (NU). Lipid droplets (LP) and mitochondria (M) are aggregated in dense clusters adjacent to the basal lamina. Spermatogonia (SP), Sertoli extensions (EX). Lipid droplets (LP) seen in both Sertoli and germ cells.

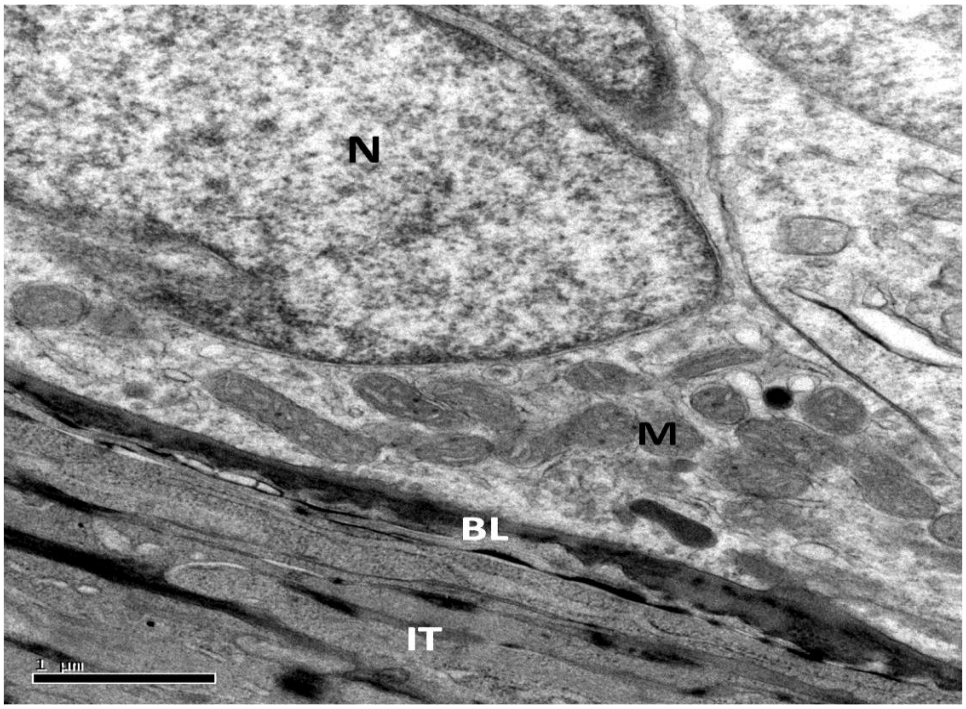

Figure 3.14D. TEM of a Sertoli cell attached to the basal lamina. Mitochondria (M) are aggregated in dense clusters adjacent to the basal lamina (BL). Nucleus (N), interstitial tissue (IT).

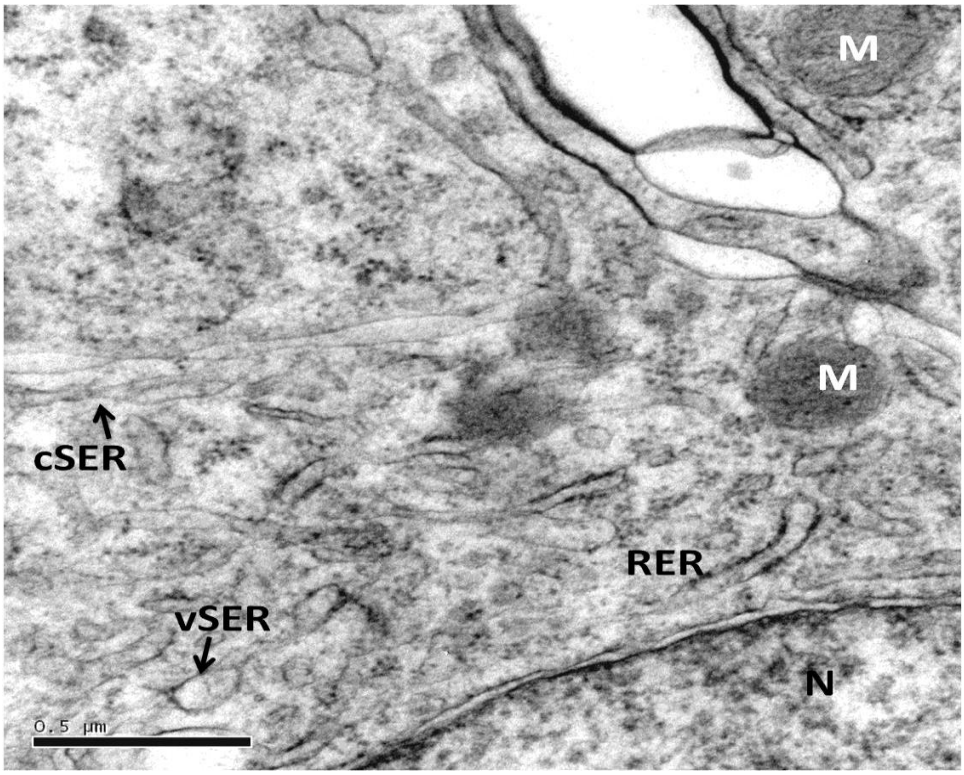

Figure 3.14E. TEM of a Sertoli cell. Smooth endoplasmic reticulum (SER) composed of cisternal (cSER) and vesicular elements (vSER). Mitochondria (M), nucleus (N), rough endoplasmic reticulum (RER).

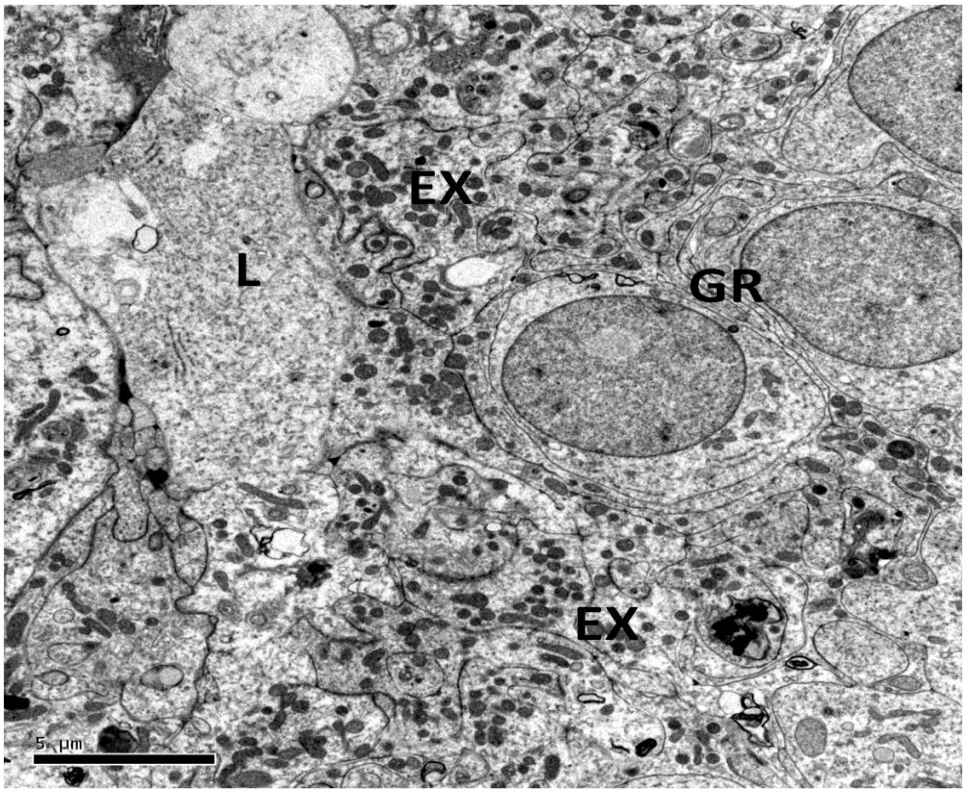

Figure 3.14F. TEM of a seminiferous tubule from the recrudescent phase showing Sertoli extensions (EX) surrounding germ cells (GR) at the apical region. Lumen (L).

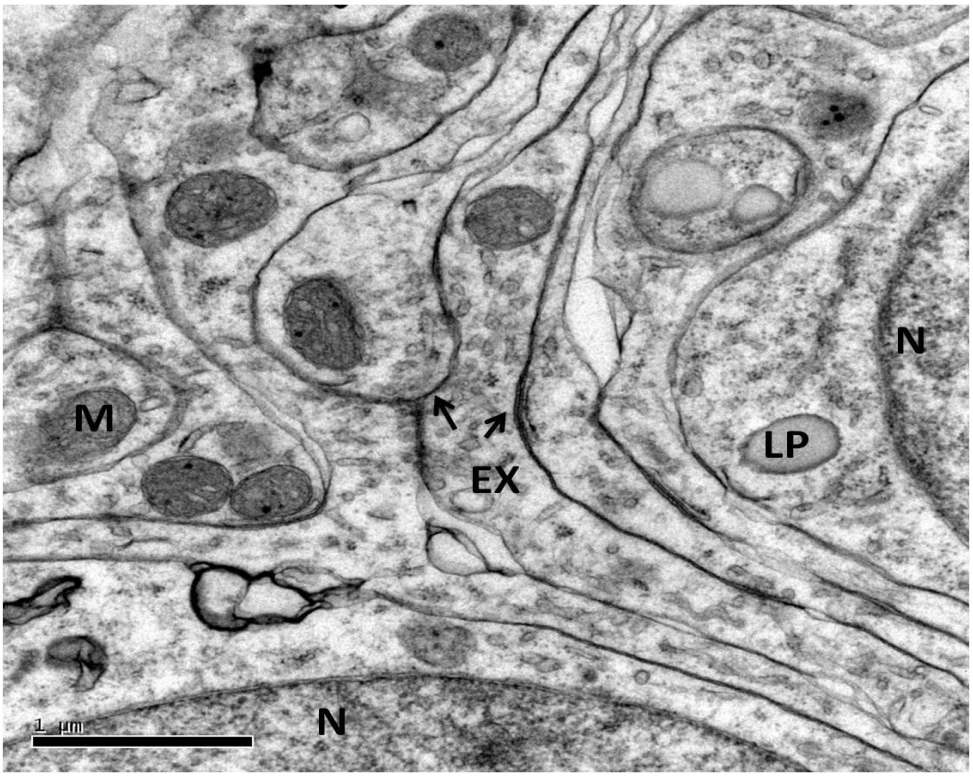

Figure 3.14G. TEM of Sertoli cell extensions (EX) during the late recrudescent phase surrounding germ cells with highly interdigitated folds. Nucleus (N), mitochondria (M), lipid droplets (LP).

During the active phase, SER were much more developed in the apex than in the base of the Sertoli cells. They were composed of extensive arrays of cisternae arranged parallel to the long axis of the extension (Figure 3.14H). Mitochondria with swollen tubular cristae were also present in the apical region but with few lipid droplets (Figure 3.14H). The Sertoli cell processes or extensions were dilated during the active phase (Figures 3.14H & 3.14I), and they appeared throughout the layer of the germinal epithelium (Figures 3.14H & 3.14I). As spermiogenesis progressed the extensions began to withdraw and the number of recesses declined as the sperm were released in the seminiferous lumen.

During the quiescent phase, the extensions were absent (Figure 3.14J). Lipid droplets were no longer confined to the basal region and there was an increase in total lipid content throughout. Mitochondria declined in number and most of the SER were converted into vesicular elements (Figure 3.14J).

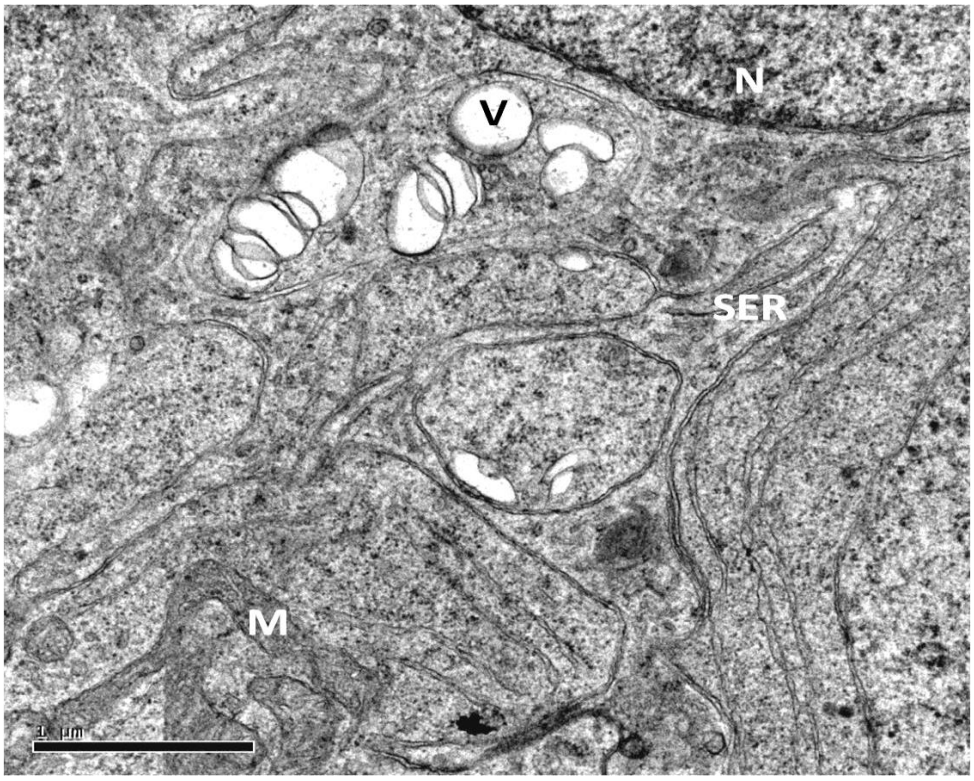

Figure 3.14H. TEM of a seminiferous tubule from the active phase showing SER arrays of cisternae parallel to the long axis of the extension. Mitochondria (M) with swollen tubular cristae. Nucleus (N), vacuoles (V).

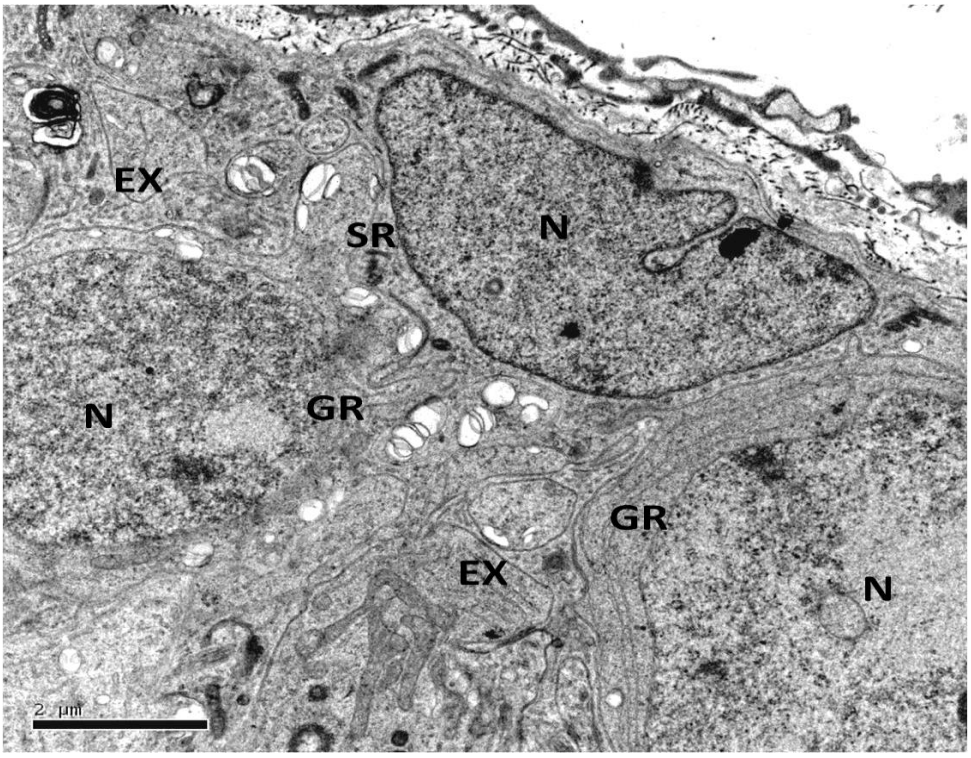

Figure 3.14I. TEM of a seminiferous tubule from the active phase showing Sertoli cell (SR) attached to the basal lamina. Sertoli extensions (EX) surround germ cells (GR) at the basal region. Nucleus (N).

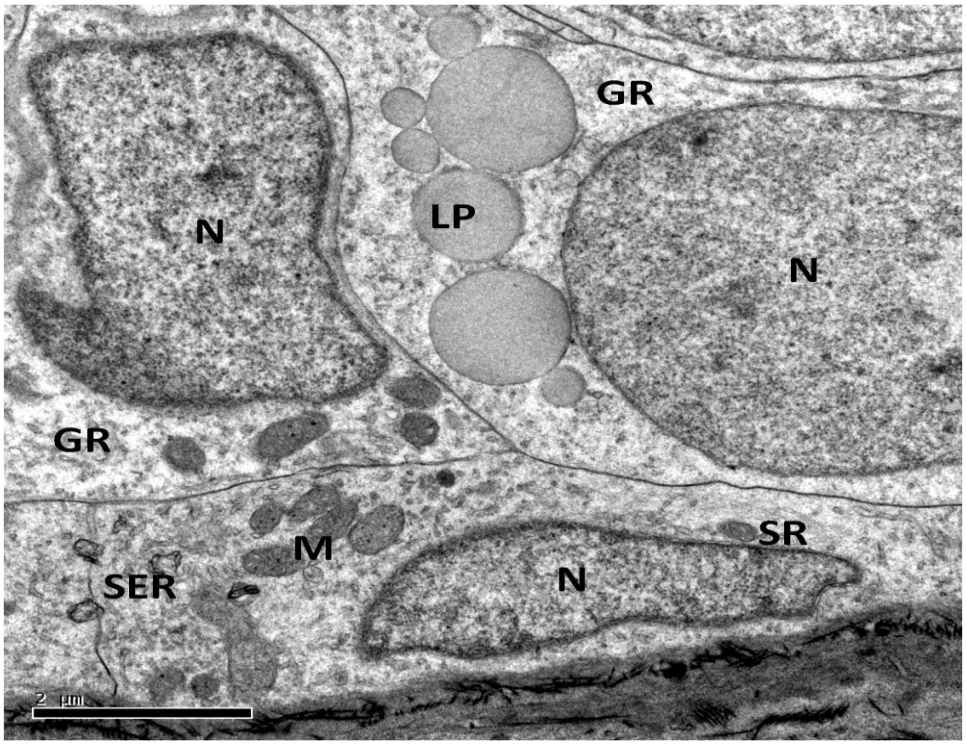

Figure 3.14J TEM of a seminiferous tubule from the quiescent phase showing Sertoli cell (SR) without cytoplasmic extensions with vesicular SER. There was a reduction in mitochondria (M) and an increased amount of lipid droplets (LP). Nucleus (N), germ cells (GR). Lipid droplets were also present in germ cells.

3.3.8.3.2 Leydig cells

Leydig cells exhibited ultrastructural steroidogenic features such as: extensively developed arrays or concentrations of SER, large mitochondria with tubular cristae, and lipid droplets. The nuclei of the Leydig were often finely granular with a clearly defined outline (Figures 3.15A, 3.15B & 3.15C). Leydig cells of sexually mature lizards generally had flattened nuclei (Figure 3.15D).

During the recrudescent phase, vesicular SER transformed into arrays of tubular and cisternal elements, (Figure 3.15C), however, during the active phase the tubular and cisternal SER were well developed with elaborate whorls and branched cisternae (Figure 3.15E). However, during the quiescent phase SER returned to a vesicular state (Figure 3.15F). There was a close association between mitochondria, SER and lipids during the recrudescent and active phases (Figures 3.15C & 3.15E).

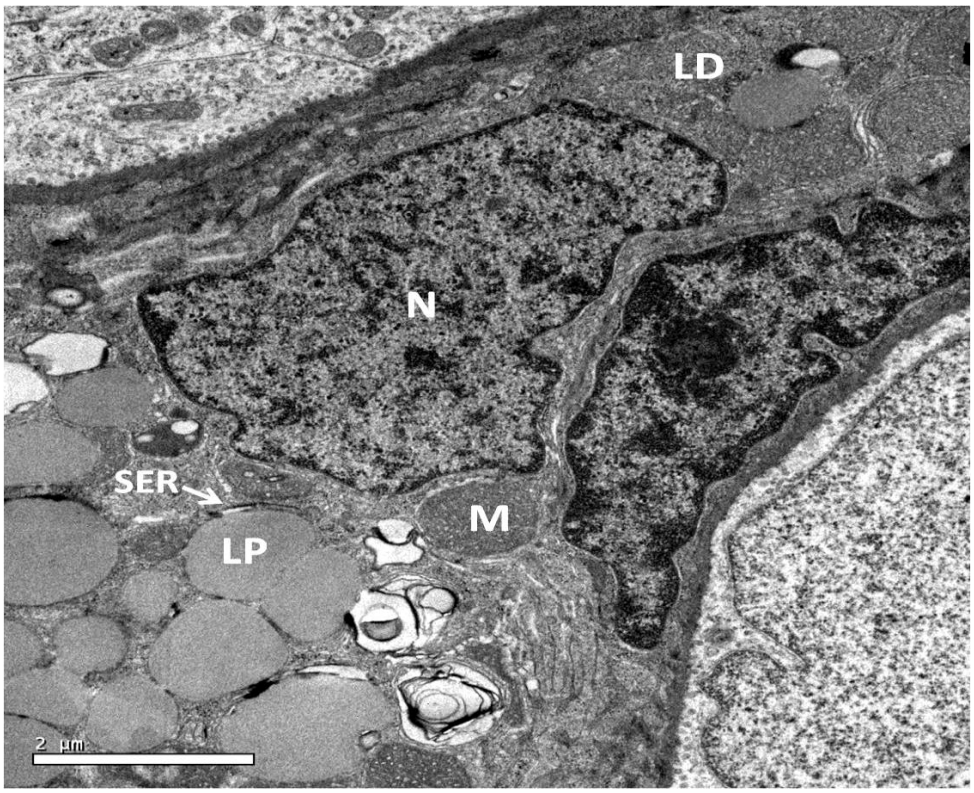

Figure 3.15A. TEM of a Leydig cell (LD) from the recrudescent phase showing finely granulated nucleus (N), mitochondria (M), and lipid droplets (LP) associated with SER.

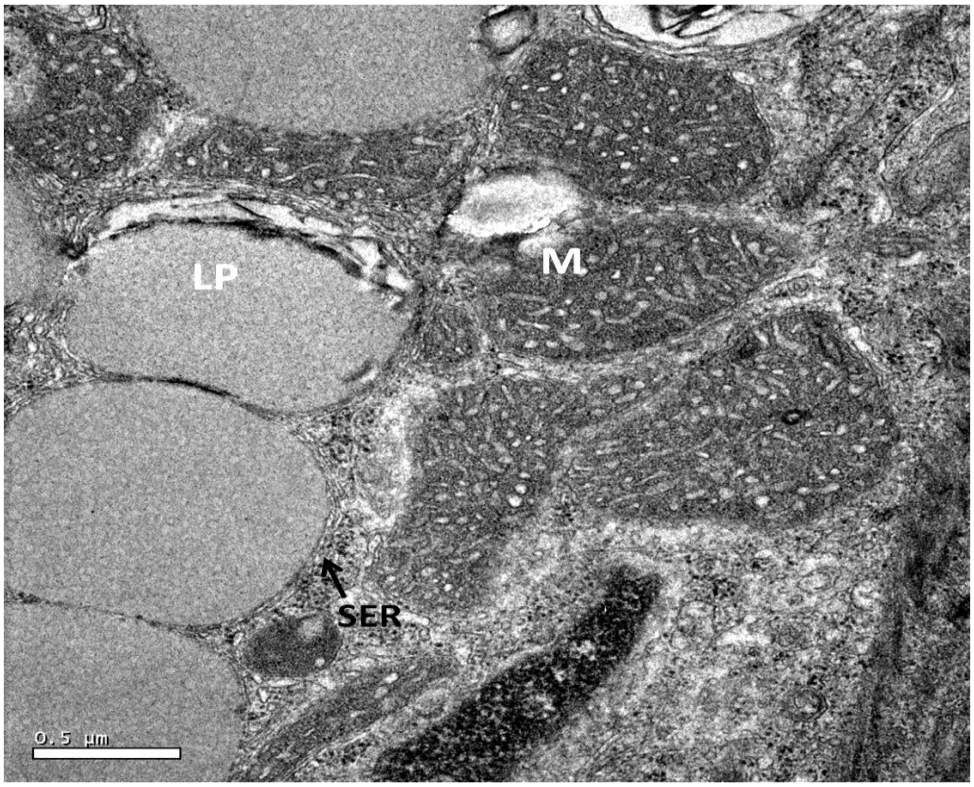

Figure 3.15B. TEM higher magnification of Figure 3.15A showing mitochondria with cisternal tubules (M), and lipid droplets (LP) associated with SER.

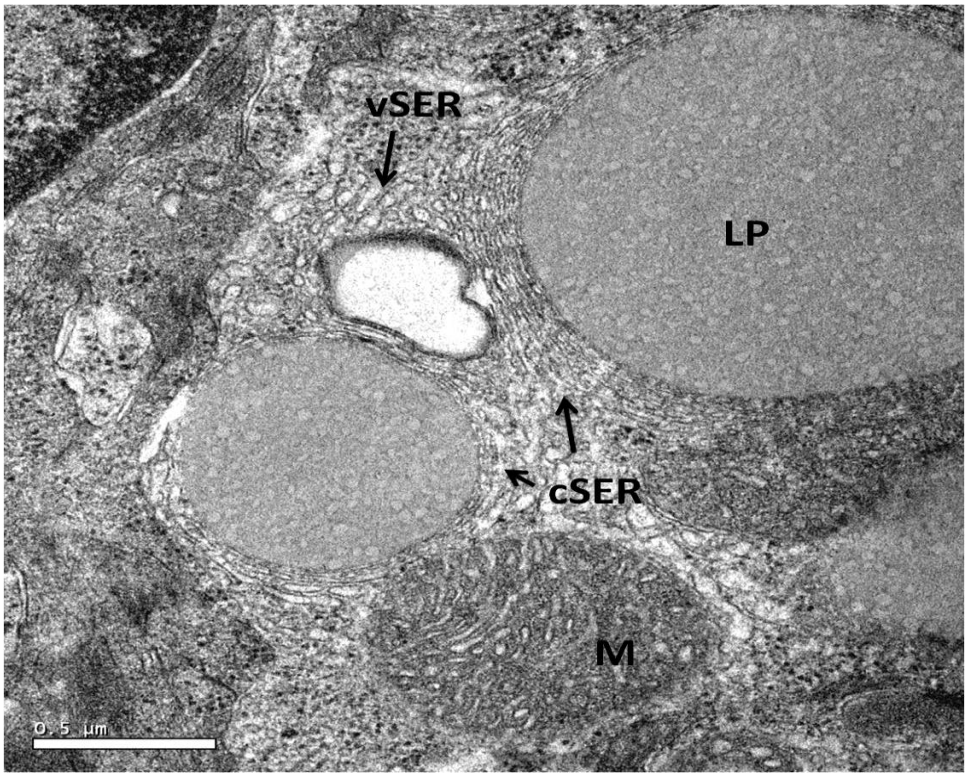

Figure 3.15C. TEM of a Leydig cell from the recrudescent phase showing vesicular (vSER) and tubular cisternal elements (cSER) associated with mitochondria (M) and lipid droplets (LP).

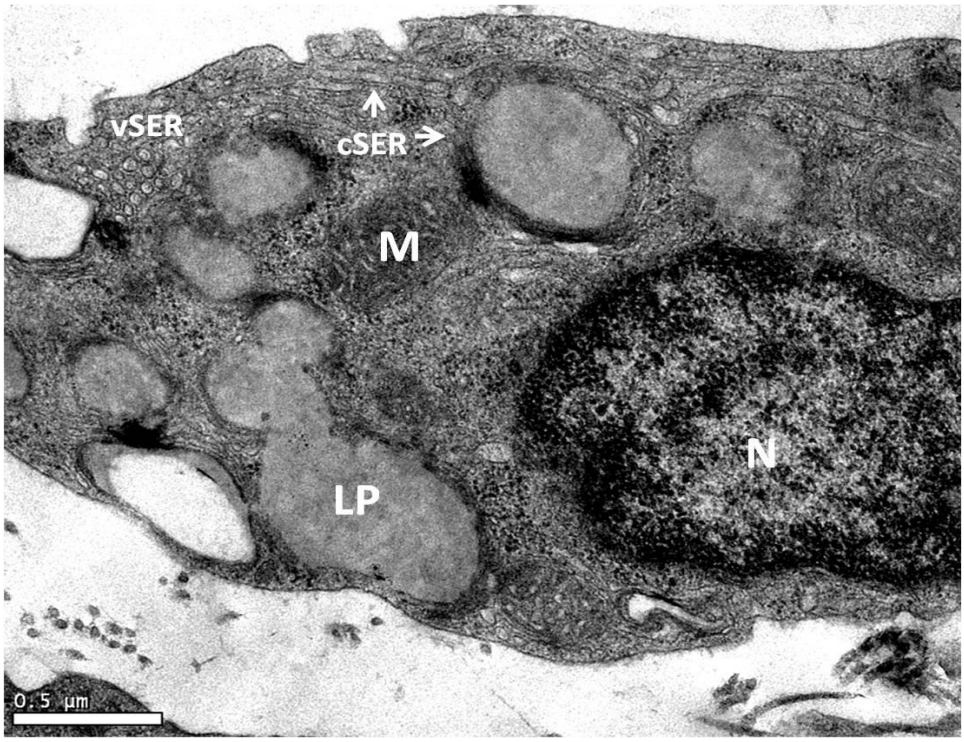

Figure 3.15D. TEM of a Leydig cell from the ctive phase showing flattened nucleus (N), mitochondria (M) and lipid droplets (LP) associated with vSER and cSER.

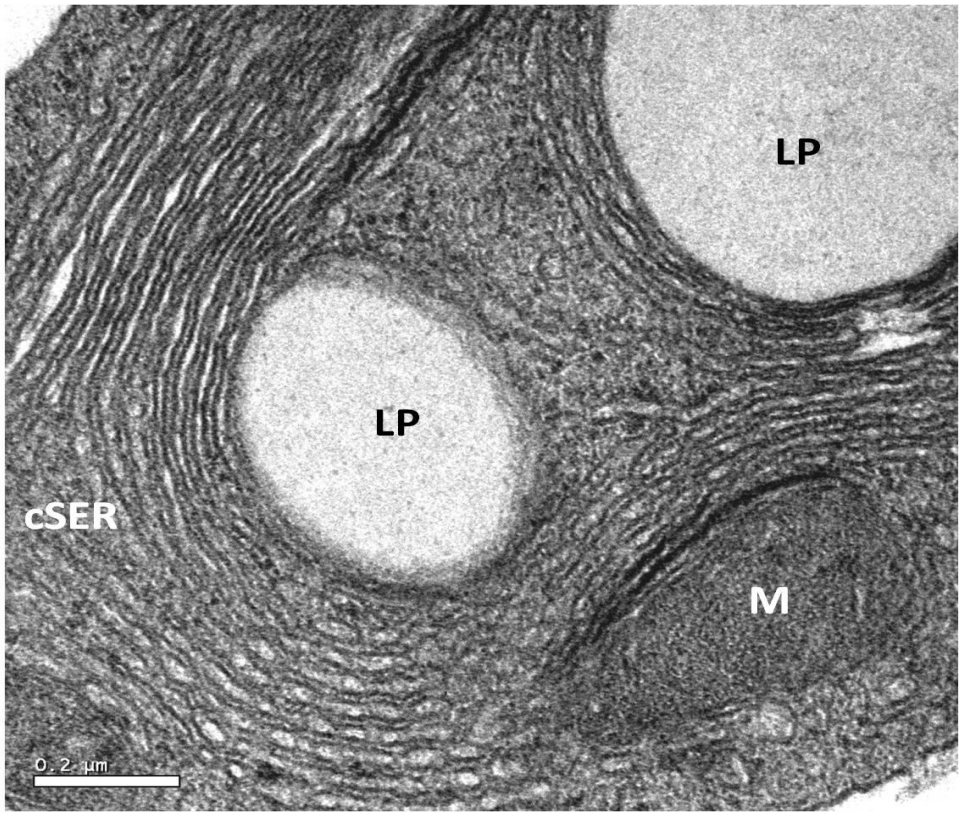

Figure 3.15E. TEM of a Leydig cell from the active phase showing well developed SER with elaborate whorls and branched cisternae (cSER) associated with mitochondria (M) and lipid droplets (LP).

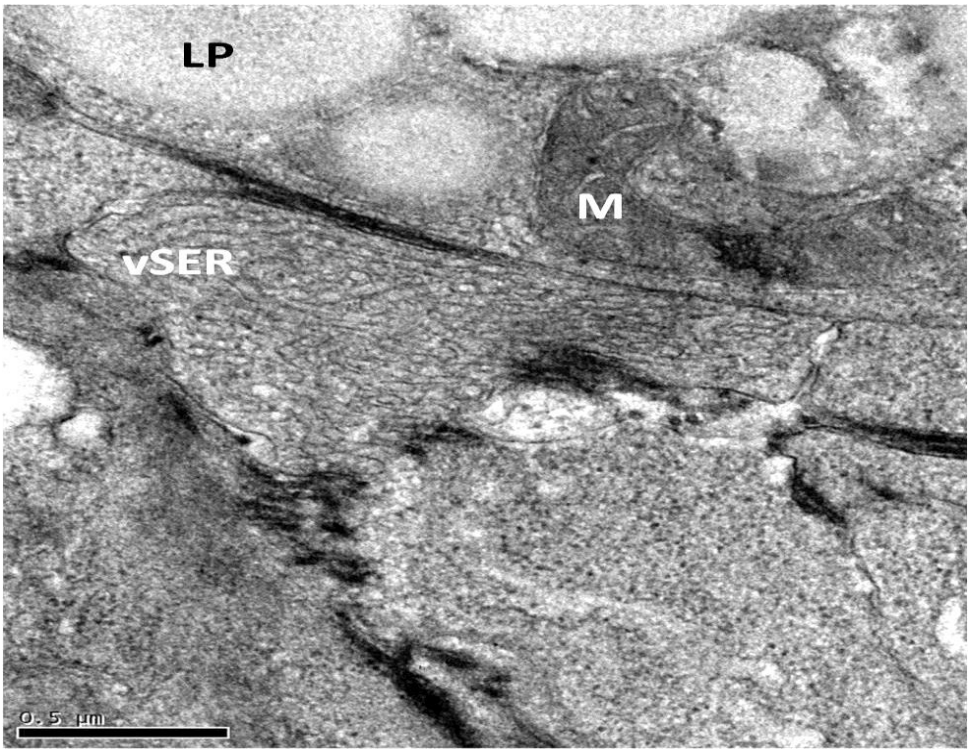

Figure 3.15F. TEM of a Leydig cell from the quiescent phase with SER returning to a vesicular state (vSER). Mitochondria (M), lipid droplets (LP).

3.3.9 Seasonal development of the epididymis

3.3.9.1 Histology of the epididymis

Changes in size of the epididymis during the reproductive cycle of *H. flaviviridis* are summarised in Table 3.2.

The size of the epididymis ($P < 0.001$) varied significantly during the different months of the year (Table 3.2). The epididymis regressed between June and August (quiescent phase) but started to increase gradually in September and October (recrudescent phase) and November through to December (early active phase) but increased significantly ($P < 0.001$) in January through to May (late active phase) coinciding with spermiogenesis. During March and April (breeding phase) epididymal size was the highest (F (4, 73) = 592.36, $P < 0.001$). In May, the epididymis began to regress and by June a complete regression took place as the size decreased significantly ($P < 0.001$).

Table 3.2. Seasonal changes (mean ± S.E.M) in the diameter of the epididymal lumen and epithelial cell height of the ductuli, anterior, middle, and posterior regions of the ductus during the reproductive cycle of *H. flaviviridis*.

Stage	Lumen Diameter (μm)				Epithelial cell height (μm)			
	Ductuli	Anterior	Middle	Posterior	Ductuli	Anterior	Middle	Posterior
Recrud-escent (Sept – Oct)	33.43 $\pm 1.38^{b}$	64.86 $\pm 2.77^{b}$	82.50 $\pm 2.15^{b}$	150.00 $\pm 2.77^{b}$	5.07 $\pm 0.27^{bc}$	12.00 $\pm 0.35^{b}$	13.71 $\pm 0.49^{b}$	8.50 $\pm 0.36^{c}$
Early Active (Nov – Dec)	41.07 $\pm 2.88^{c}$	91.29 $\pm 2.15^{c}$	121.07 $\pm 3.68^{c}$	201.43 $\pm 5.92^{c}$	5.93 $\pm 0.44^{c}$	16.00 $\pm 0.42^{c}$	18.57 $\pm 0.66^{c}$	13.86 $\pm 0.55^{d}$
Late Active (Jan – May)	60.05 $\pm 3.10^{d}$	181.89 $\pm 2.87^{d}$	221.58 $\pm 3.92^{d}$	390.53 $\pm 5.54^{d}$	8.83 $\pm 0.35^{d}$	44.39 $\pm 2.16^{d}$	55.56 $\pm 2.08^{d}$	22.67 $\pm 0.76^{e}$
Regre-ssion (Late May)	29.06 $\pm 2.43^{ab}$	65.31 $\pm 2.44^{b}$	78.44 $\pm 2.49^{b}$	111.56 $\pm 3.31^{a}$	4.38 $\pm 0.32^{b}$	11.88 $\pm 0.18^{b}$	15.31 $\pm 0.13^{bc}$	5.25 $\pm 0.39^{b}$
Quies-cent (June–Aug)	23.67 $\pm 1.86^{a}$	42.67 $\pm 2.06^{a}$	54.67 $\pm 2.56^{a}$	106.00 $\pm 6.68^{a}$	4.38 $\pm 0.47^{a}$	7.13 $\pm 0.44^{a}$	8.93 $\pm 0.71^{a}$	3.00 $\pm 0.46^{a}$
F(4,73)	35.14	523.86	490.74	592.36	29.93	179.92	280.21	221.68
P-value	< 0.001	< 0.001	< 0.001	< 0.001	< 0.001	< 0.001	< 0.001	< 0.001

Statistical differences between groups obtained by Duncan's multiple-comparisons test. Months with significantly different values (mean ± S.E.M) in vertical column were assigned different letters. Stages with the same letter shows statistically no significant difference between them at the 0.05 level of significance.

In the quiescent phase, the ductuli epididymal tubules were regressed (Table 3.2) and lined by nonciliated low cuboidal epithelial cells having shrunken (hyperchromatic) nuclei (Figure 3.16A). The epithelium showed atrophic changes and were devoid of any secretory granules. The ductus epididymal tubules were also regressed (Table 3.2) and their lumen had few secretory materials and sperm (Figure 3.16D). No histological differences were observed between the anterior and middle region of the regressed epididymis (Figure 3.16B).

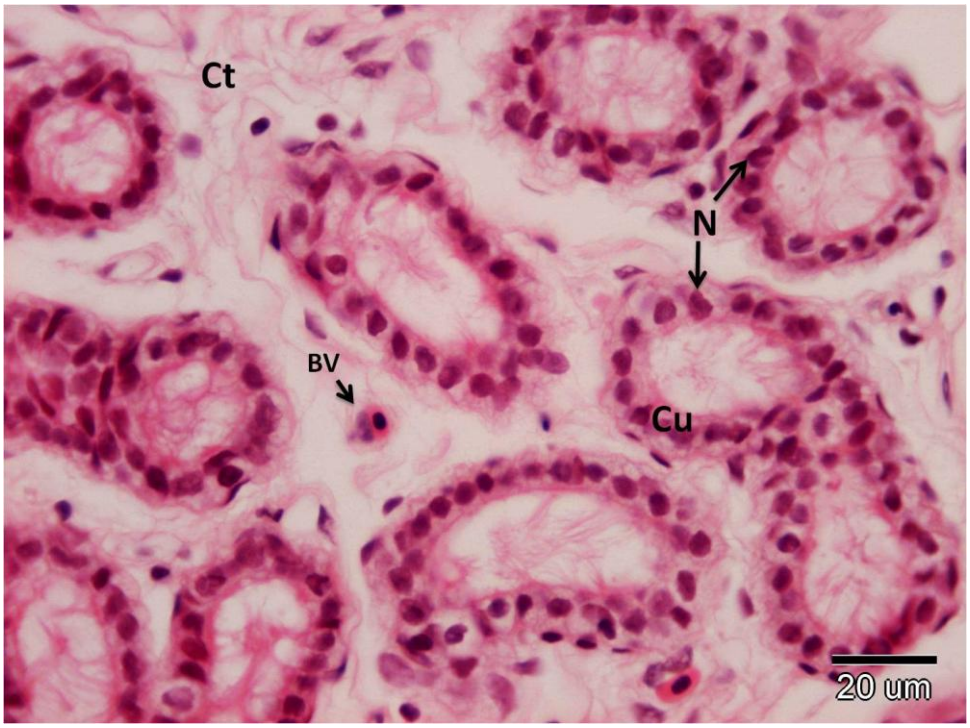

Figure 3.16A. H&E section of ductuli epididymis from the quiescent phase showing nonciliated low cuboidal epithelial cells (Cu) with shrunken nuclei (N). Intertubular connective tissue (Ct), blood vessel (BV).

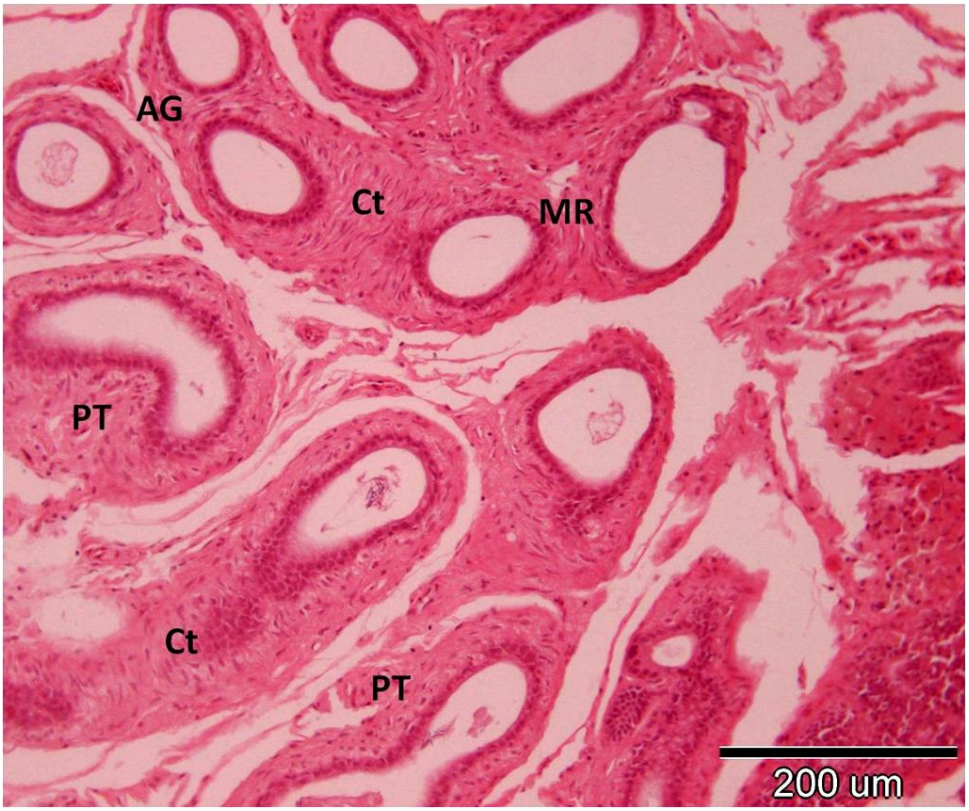

Figure 3.16B. H&E section of ductus epididymis from the quiescent phase showing the anterior (AG), middle (MR) and posterior (PT) regions. Intertubular connective tissue (Ct) present in all regions.

The tubular epithelium in these two regions was low cuboidal (Figure 3.16C). The posterior region, however, clearly differed from the other two regions; its epithelium was squamous and it had a larger lumen diameter (Figure 3.16D). The epithelium was nonciliated and devoid of secretory granules and intertubular connective tissue was extensive in all regions of the regressed ductus epididymis (Figures 3.16B & 3.16E).

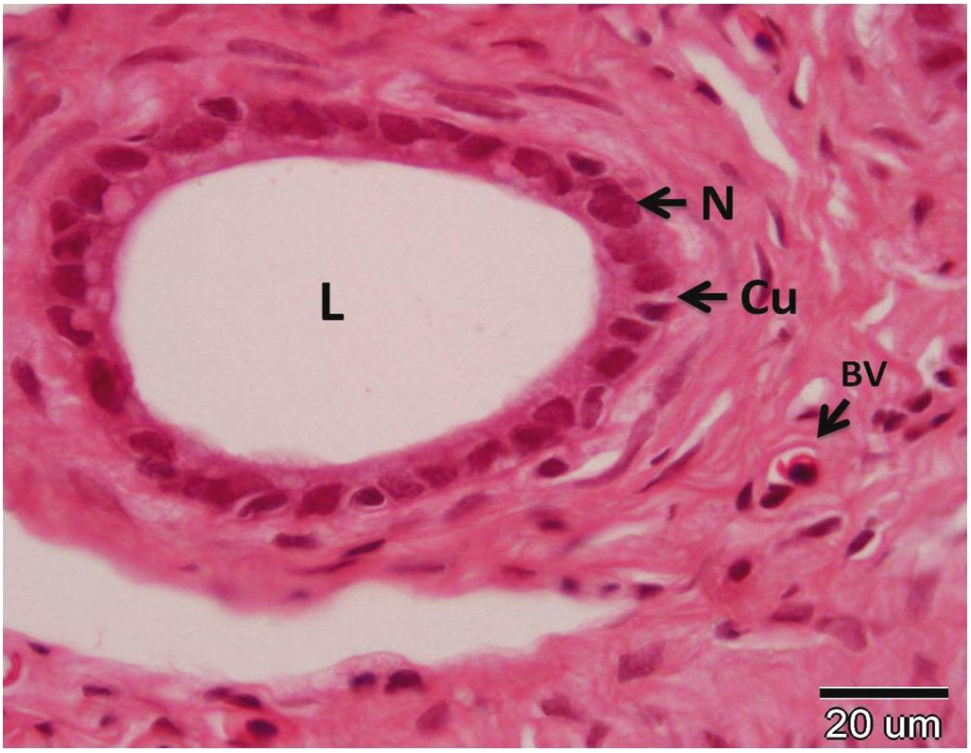

Figure 3.16C. H&E section of ductus epididymis from the quiescent phase showing cuboidal epithelial cells (Cu) of the anterior and middle regions. Nucleus (N), lumen (L), blood vessel (BV).

Figure 3.16D. H&E section of ductus epididymis from the quiescent phase showing squamous epithelial cells (SQ) of the posterior region. Few secretory materials and sperm present in the lumen (L). Nucleus (N).

Figure 3.16E. H&E section of ductuli epididymis (DE) and ductus epididymis (DP) from the quiescent phase. Extensive intertubular connective tissue (Ct) present in the ductus epididymis.

In the recrudescent phase, epithelial cell height and lumen diameter of ductuli epididymis were enlarged compared to their state in the quiescent phase (Table 3.2)

(Figure 3.17A). The ductus epididymis exhibited significant variation in epithelial cell height and lumen diameter within its anterior, middle, and posterior regions ($P < 0.001$) (Figures 3.17B, 3.17C & 3.17D). The epithelial cell height of the middle region was significantly more than that of the anterior region (Figure 3.17C), while the height of the epithelium in the posterior region was significantly lower than that of any other region (Figure 3.17D). The lumen of the ductus epididymis became wider toward the posterior end (Figure 3.17D). A significant increase in epithelial cell height and lumen diameter was recorded in all regions of the reproductively active ductus epididymis when compared to sexually regressed counterparts ($P < 0.001$).

In the active phase, the ductuli epididymis were lined by low columnar, nonciliated epithelial cells having rounded or oval nuclei with prominent nucleoli (Figures 3.18A & 3.18B). The hypertrophied epithelium of the ductuli at this time was filled with PAS-positive secretory granules (Figure 3.18C). Sperm were rarely seen in the lumen, however, probably due to rapid passage through this region (Figures 3.18A & 3.18B).

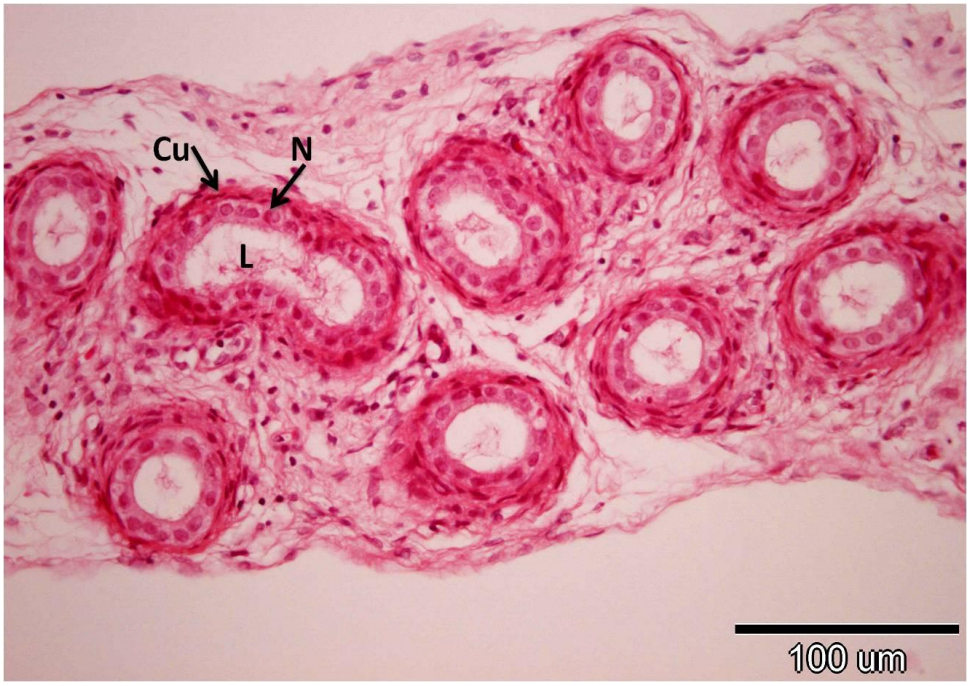

Figure 3.17A. H&E section of ductuli epididymis from the recrudescent phase showing enlarged cuboidal epithelial cell (Cu) height and lumen (L) diameter. Nucleus (N).

Figure 3.17B. H&E section of the anterior region of ductus epididymis from the recrudescent phase. An increase in cuboidal epithelial cell (Cu) height and lumen (L) diameter is clearly evident. Nucleus (N), intertubular connective tissue (Ct).

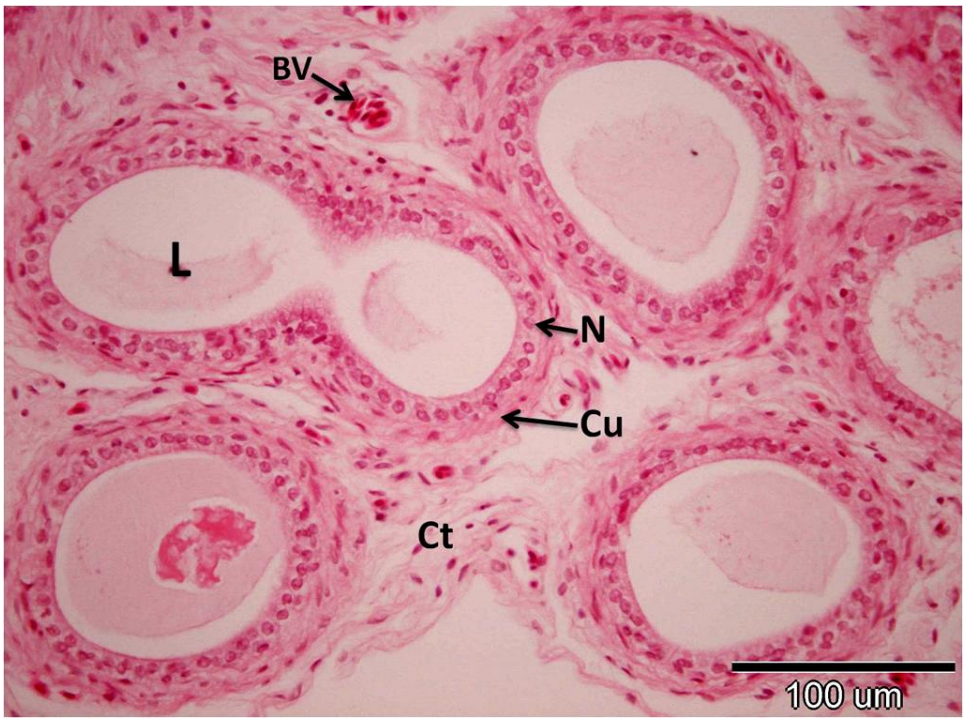

Figure 3.17C. H&E section of the middle region of ductus epididymis from the recrudescent phase. The epithelial cuboidal cell (Cu) height increased significantly over that of the anterior region. Nucleus (N), lumen (L), intertubular connective tissue (Ct), blood vessel (BV).

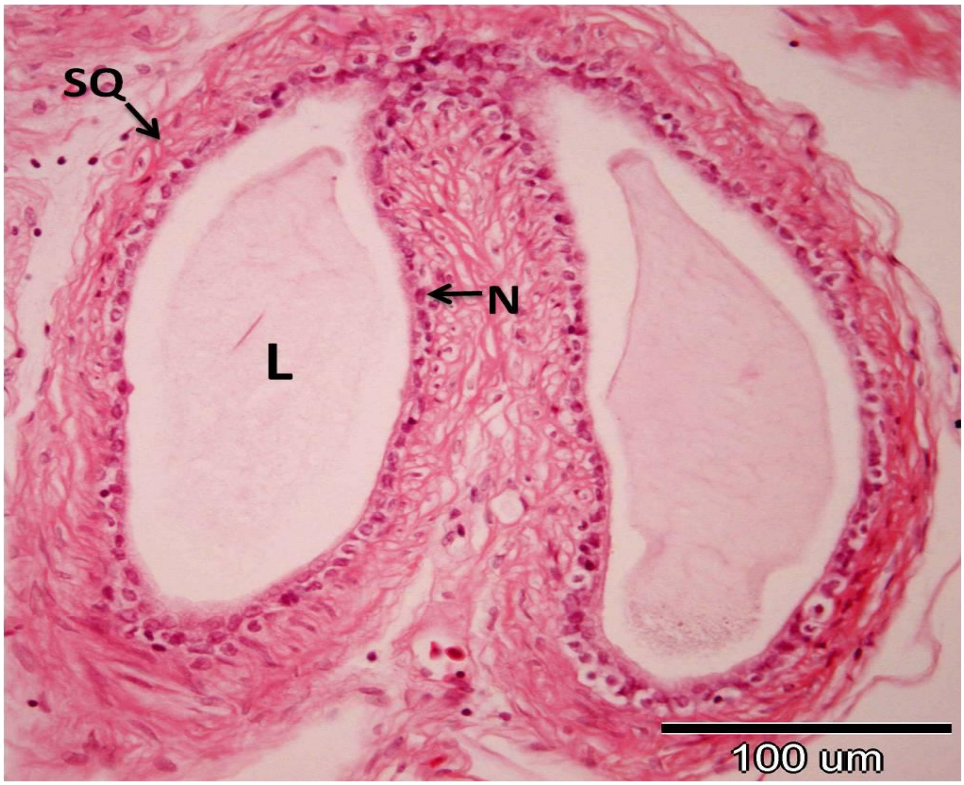

Figure 3.17D. H&E section of the posterior region of ductus epididymis from the recrudescent phase. The squamous epithelial cell (SQ) height is lower than the posterior and anterior regions. Nucleus (N), lumen (L).

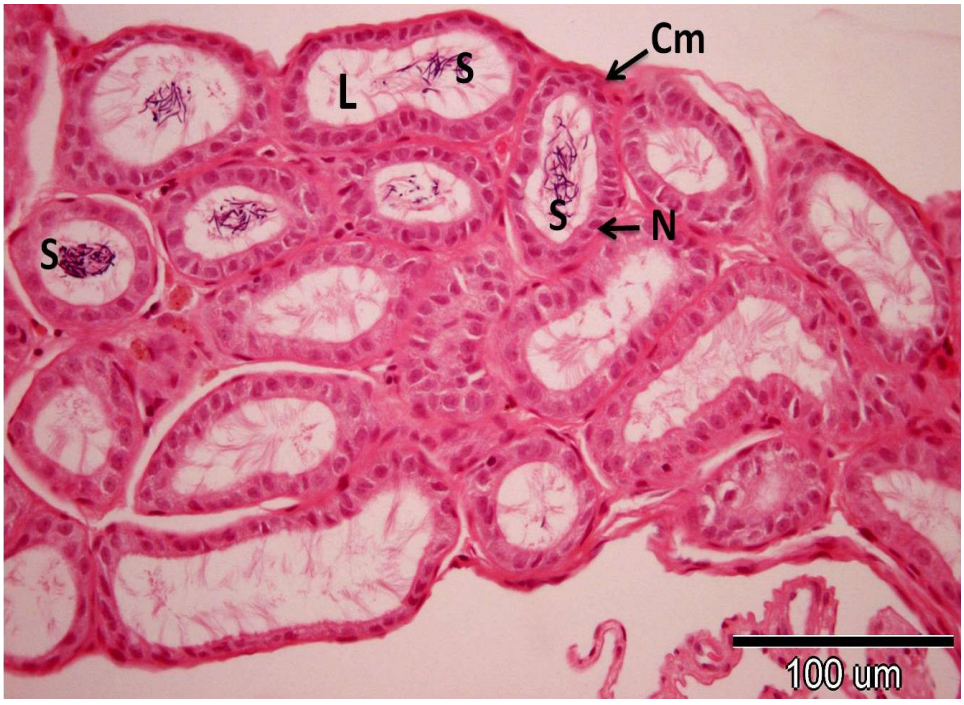

Figure 3.18A. H&E section of ductuli epididymis from the active phase. The hypertrophied low columnar epithelium (Cm) of the ductuli is filled with secretory granules. Few sperm (S) were present in the lumen (L). Nucleus (N).

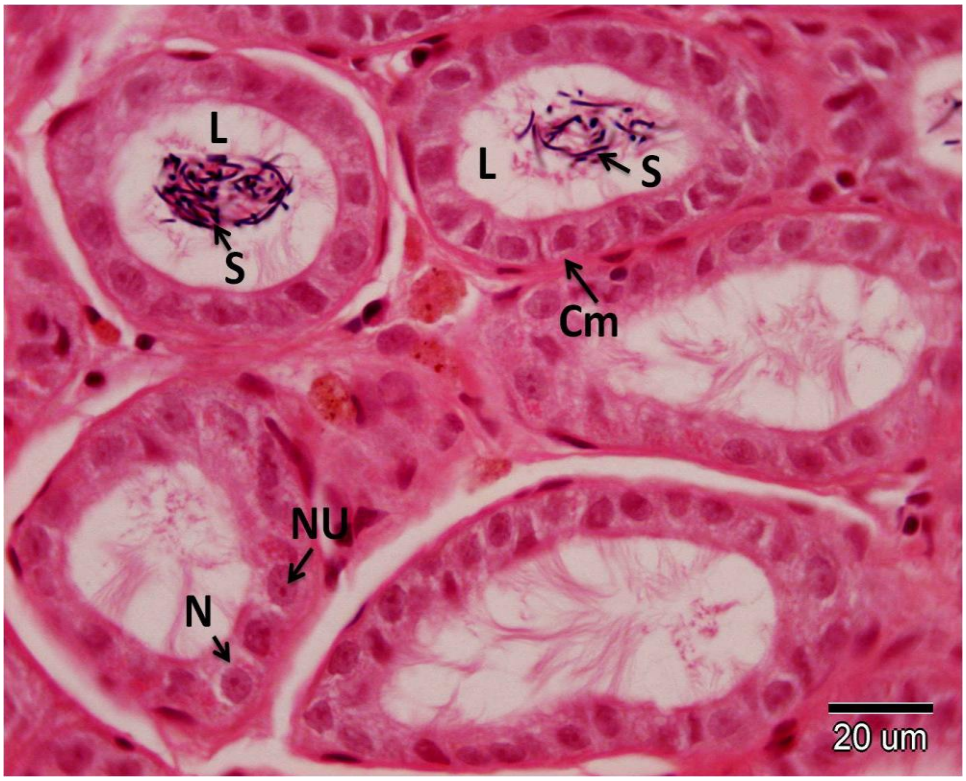

Figure 3.18B. H&E higher magnification of Figure 3.18A. The ductuli is lined by low columnar, nonciliated epithelial cells (Cm) having rounded or oval nuclei (N) with prominent nucleoli (NU). Few sperm appeared in the lumen (S).

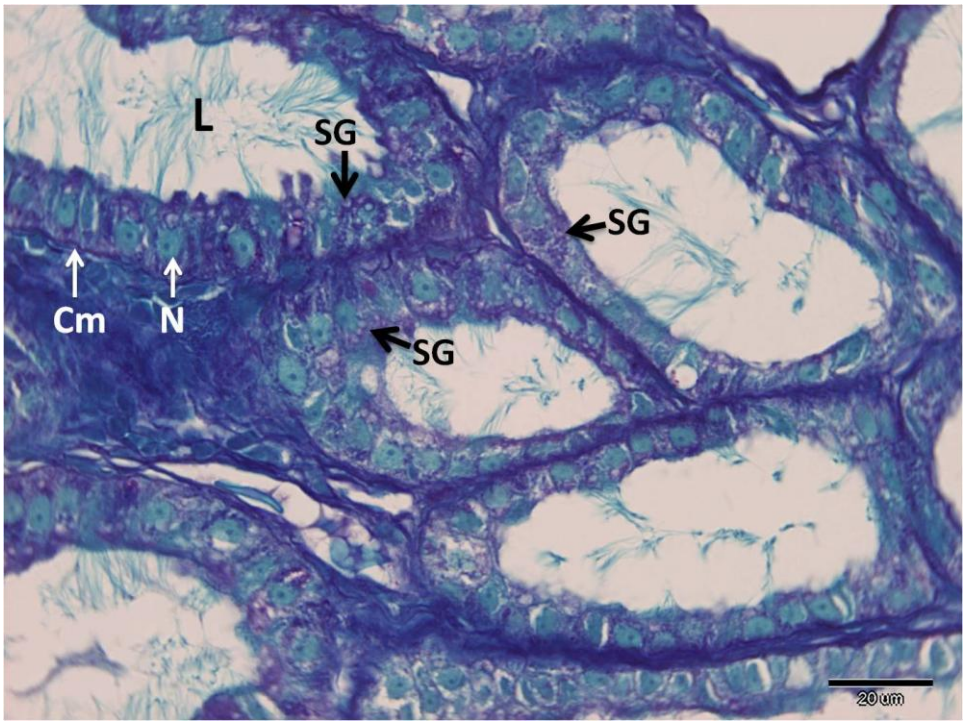

Figure 3.18C. PAS-FG section of the ductuli epididymis from the active phase. Hypertrophied low columnar epithelial cells (Cm) were filled with secretory granules (SG). Nucleus (N), lumen (L).

During this phase the epithelium of the ductus epididymis was columnar in the anterior and middle regions, and cuboidal in the posterior region (Figures 3.18D, 3.18E, 3.18F, 3.18H & 3.18I). A few cells of the epithelium were ciliated in the anterior and middle regions, while the cells in the posterior region were nonciliated (Figures 3.18D & 3.18G). The epithelia in all the regions of this duct were significantly hypertrophied, and the anterior and middle regions were filled with PAS-positive secretory granules (Table 3.2, $P < 0.001$, Figures 3.18E, 3.18G & 3.18I). The lumen diameter increased markedly and was filled with sperm from anterior to posterior regions along the ductus epididymis (Figures 3.18D, 3.18E, 3.18F, 3.18H & 3.18I). Intertubular connective tissue was poorly developed in all regions of the reproductively active ductus epididymis. During late April and early May the epididymis contained, besides sperm, cells sloughed from the seminiferous epithelium.

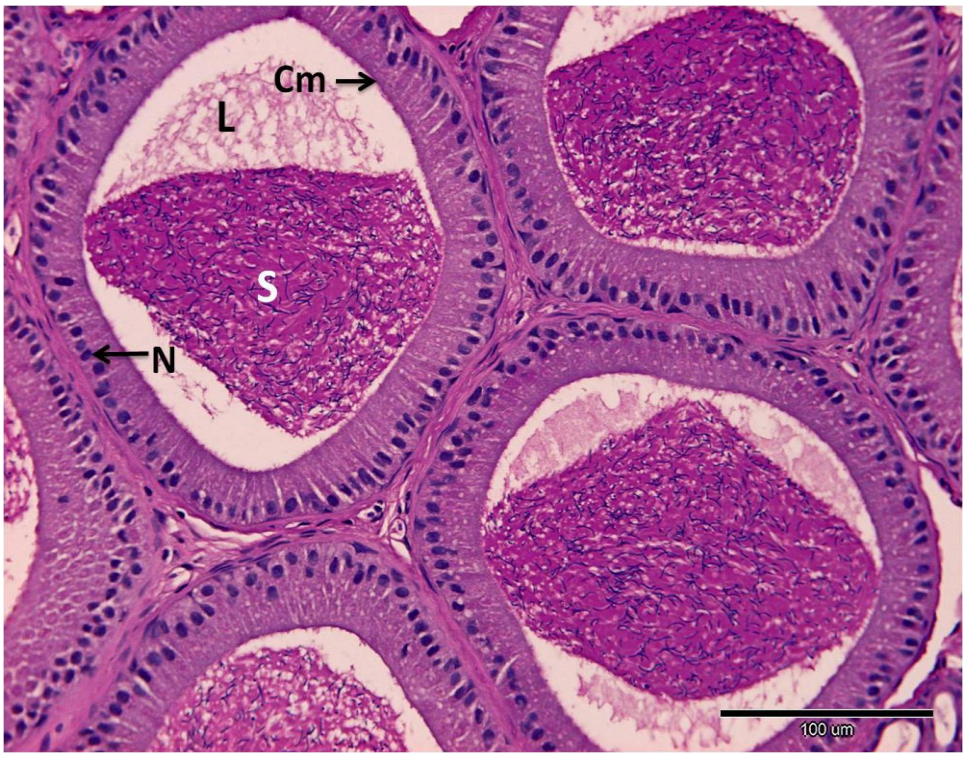

Figure 3.18D. PAS-Haem section of the anterior region of ductus epididymis from the active phase showing hypertrophied columnar epithelium (Cm). The lumen (L) diameter markedly increased and filled with sperm (S). Nucleus (N).

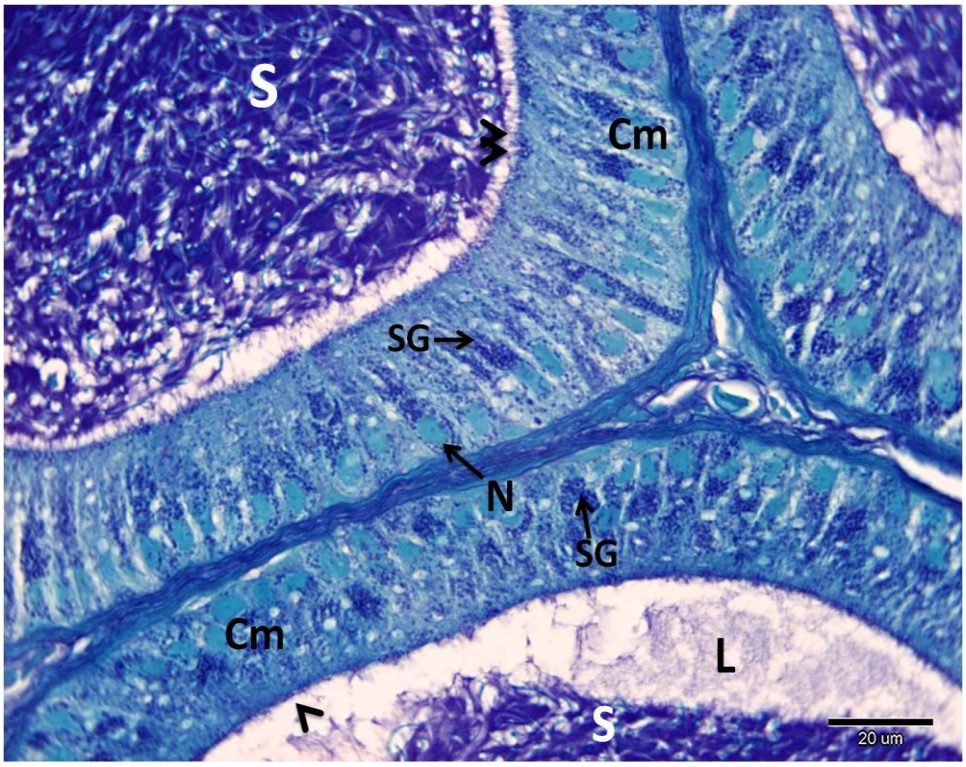

Figure 3.18E. PAS-FG epithelium of the anterior region from the active phase showing ciliated (double arrowhead) and nonciliated (arrowhead) columnar epithelial cells (Cm), and filled with secretory granules (SG). Sperm (S).

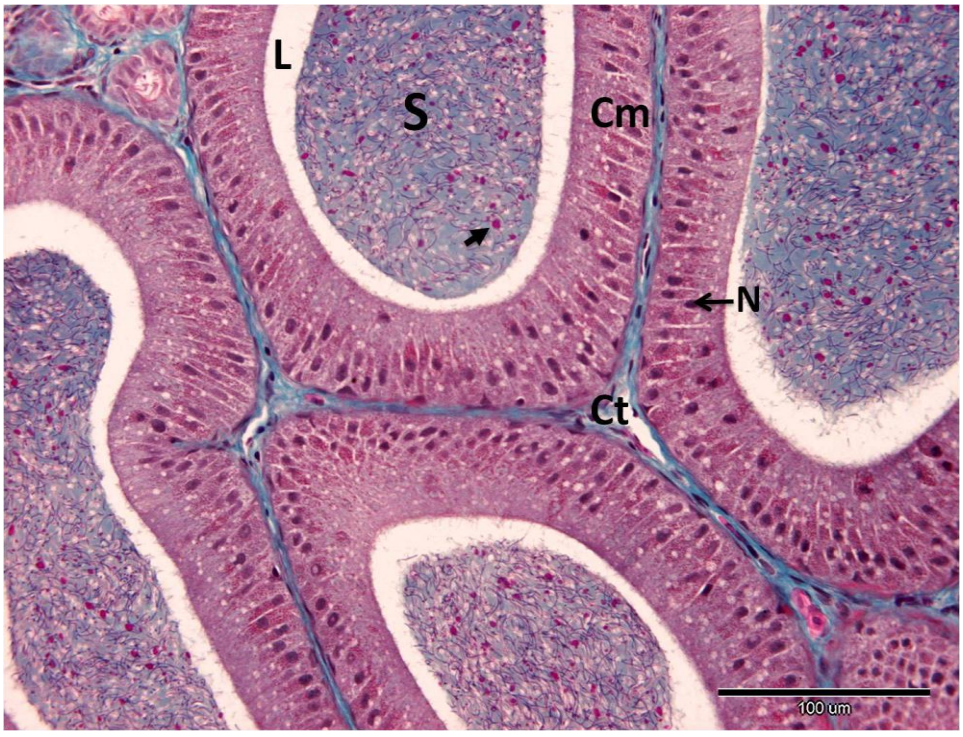

Figure 3.18F. MT section of the middle region of ductus epididymis from the active phase showing hypertrophied columnar epithelium (Cm). The lumen (L) diameter increased and filled with sperm (S) and secretory material (arrow). Intertubular connective tissue (Ct) appeared poorly developed. Nucleus (N).

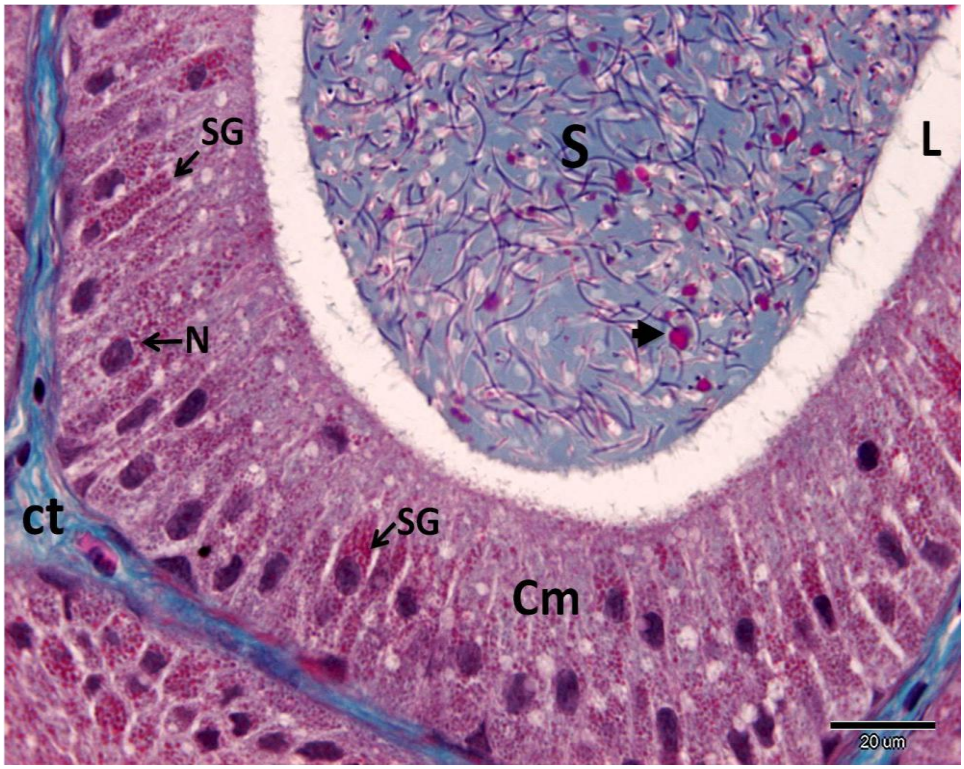

Figure 3.18G. MT higher magnification of Figure 3.18F. Columnar epithelium (Cm) filled with secretory granules (SG). The lumen (L) filled with sperm (S) and secretory materials (arrow). Nucleus (N), intertubular connective tissue (Ct).

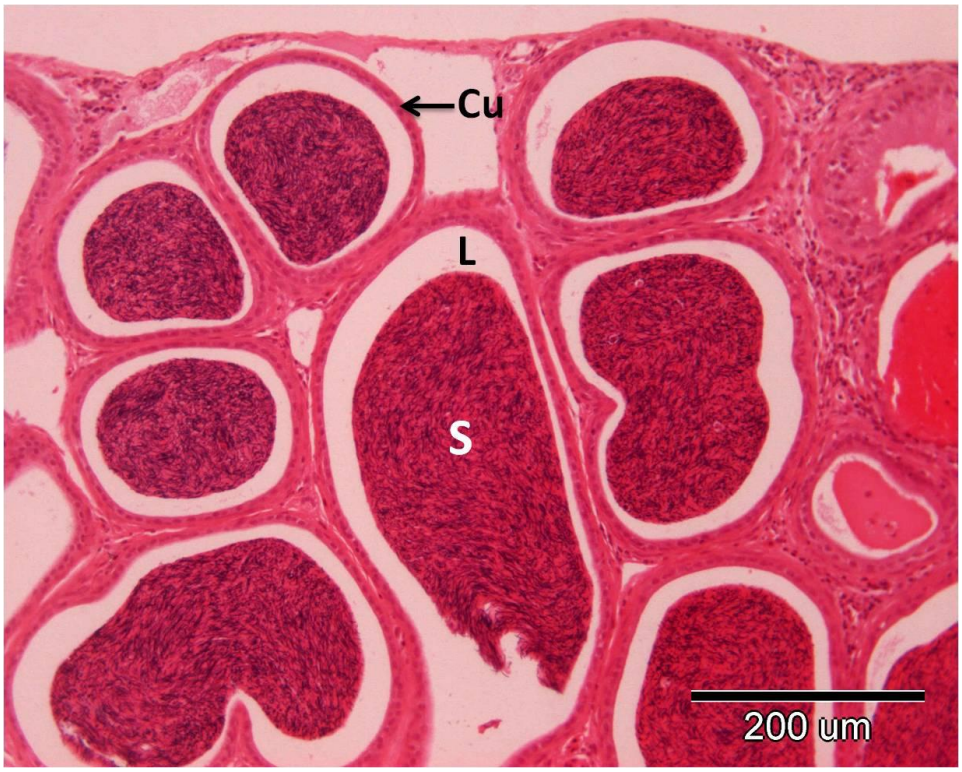

Figure 3.18H. H&E section of the posterior region of ductus epididymis from the active phase showing hypertrophied cuboidal epithelium (Cu). The lumen (L) diameter increased and filled with sperm (S).

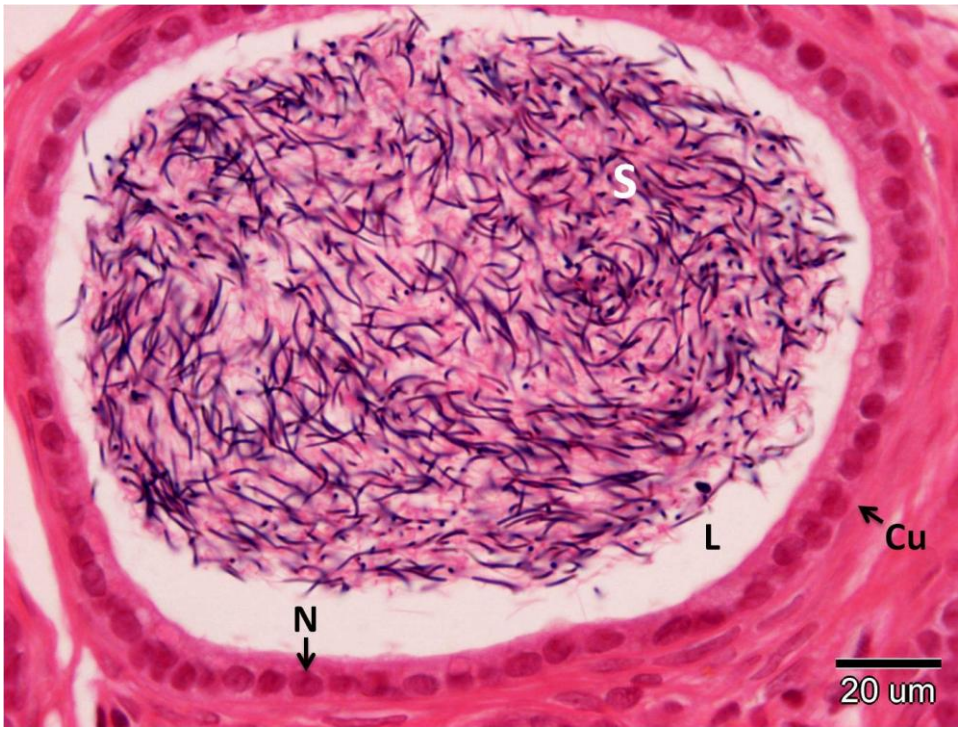

Figure 3.18I. H&E higher magnification of Figure 3.18H. The cuboidal epithelial cells (Cu) height is much lower than that of the anterior and posterior regions. Nucleus (N), lumen (L).

3.3.9.2 Ultrastructure of epididymal epithelial cells during the active phase

The principal cells were the major constituents of the epithelial lining of the anterior, middle, and posterior regions of the ductus epididymis. The basal cells and intraepithelial leucocytes were present in all regions of the ductus epididymis.

3.3.9.2.1 Principal cells

The fully developed secretory principal cells extended from the basal lamina to the lumen. They were tall and narrow at the anterior and middle regions, and short and broad at the posterior region (Figure 3.19A). Occluding junctions closer to the lumen and apical gap junctions comprising true desmosomes were present between the tall columnar cells that displayed typical specialisation for cell to cell attachment (Figure 3.19B). Microvilli projected from the apical border (Figure 3.19B). They were long in the anterior and middle regions, but reduced in height in the posterior region.

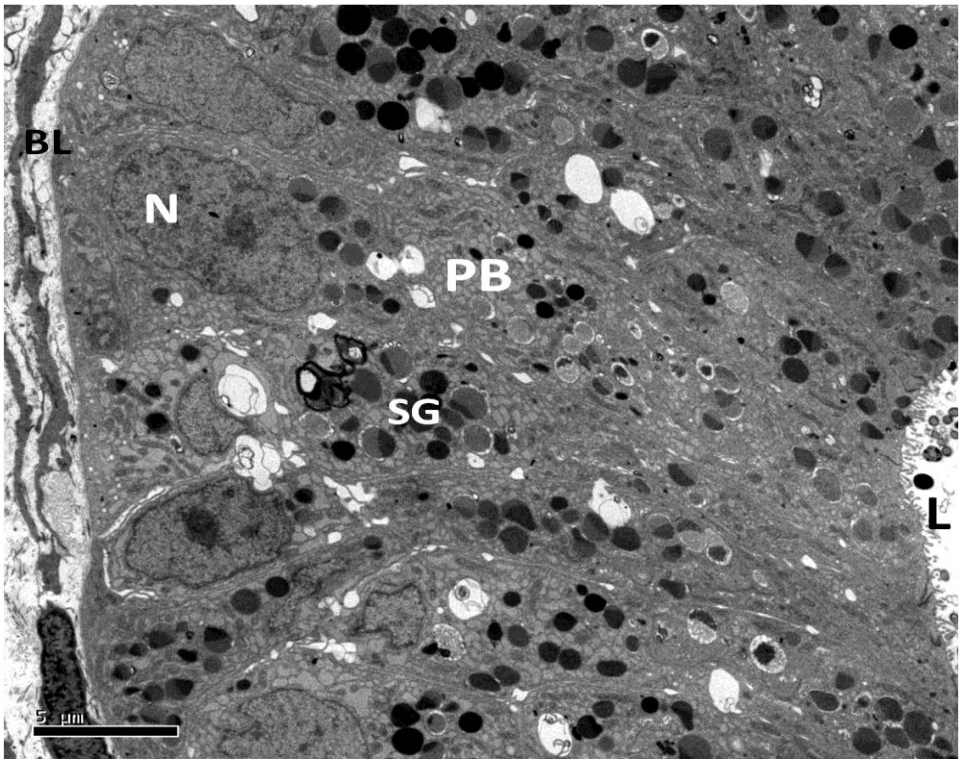

Figure 3.19A. TEM. Secretory principal cells (PB) from the anterior and middle regions of epididymis from the active phase. Tall and narrow PB extends from the basal lamina (BL) to the lumen (L). Nuclei (N) located basally. Secretory granules (SG).

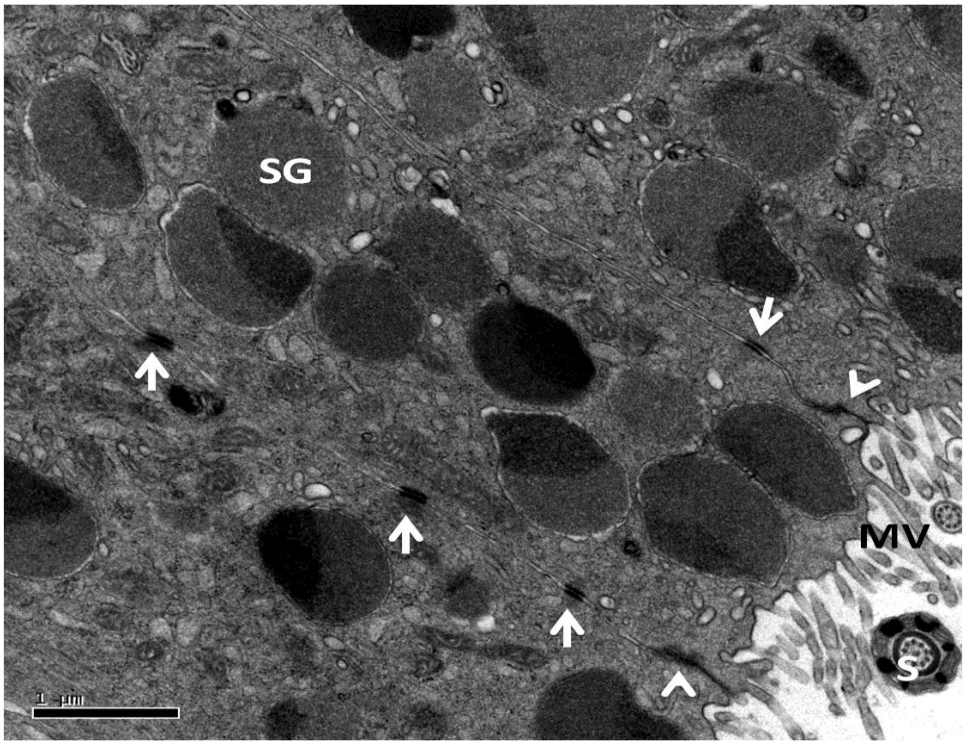

Figure 3.19B. TEM. Higher magnification of Figure 3.19A. Occluding junctions (arrowhead) close to lumen and gap junctions (arrow) at the apical regions of principal cells. Microvilli (MV), secretory granules (SG).

The nucleus was located basally and appeared oval, elliptical or elongated and it was fairly heterochromatic with a thin layer of dense chromatin underlying the nuclear envelope (Figure 3.19C). One or two prominent nucleoli were present the nucleus of the principal cell. The most prominent organelles in the cytoplasm were the endoplasmic reticulum components, particularly RER, Golgi complexes and mitochondria. The endoplasmic reticulum reflected different morphologies along the height of the cell. RER was present in the whole cytoplasm and was rather vesicular and sometimes distended. Its contents were electron-dense, indicating accumulation of secretory products (Figures 3.19D & 3.19E). The Golgi complexes occupied the supranuclear cytoplasm and consisted of several stacks of flat saccules with typical cistrans polarization surrounding groups of secretory granules (Figures 3.19F & 3.19G). Golgi networks were closely associated with the RER. The Golgi sacs were vesicular and had a smooth surface. Transition vesicles were often very numerous. Mitochondria were numerous and concentrated in the apical and basal cytoplasm. They were either round or elongated with a dense matrix and numerous vesiculated cristae (Figures 3.19H, 3.19I & 3.19J).

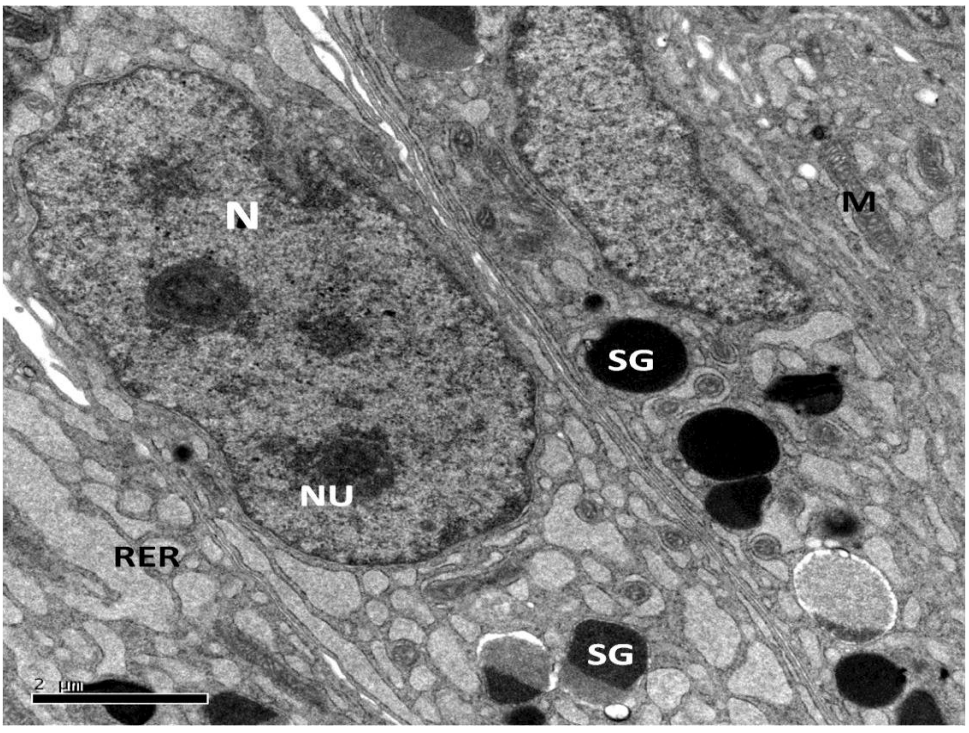

Figure 3.19C. TEM showing elliptical and elongated nuclei (N) of principal cells with a thin layer of dense chromatin underlying the nuclear envelope. Two prominent nucleoli (NU) appear in the elongated nucleus. Mitochondria (M), RER, secretory granules (SG).

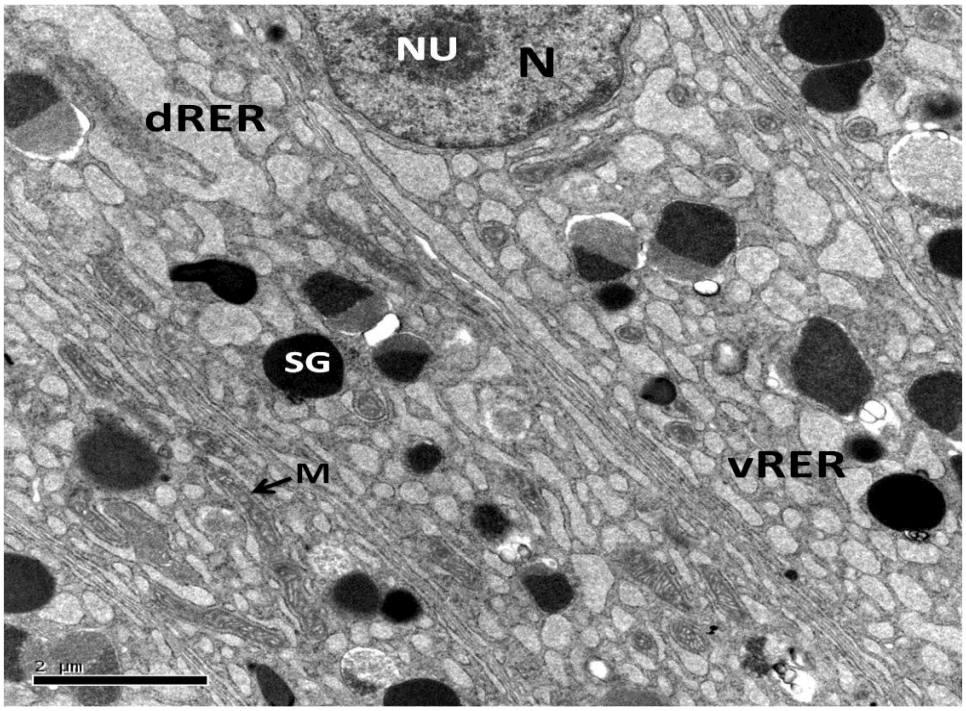

Figure 3.19D. TEM showing rough endoplasmic reticulum (RER) with vesicular (vRER) and distended (dRER) appearances. Nucleus (N), nucleolus (NU), mitochondria (M), secretory granules (SG).

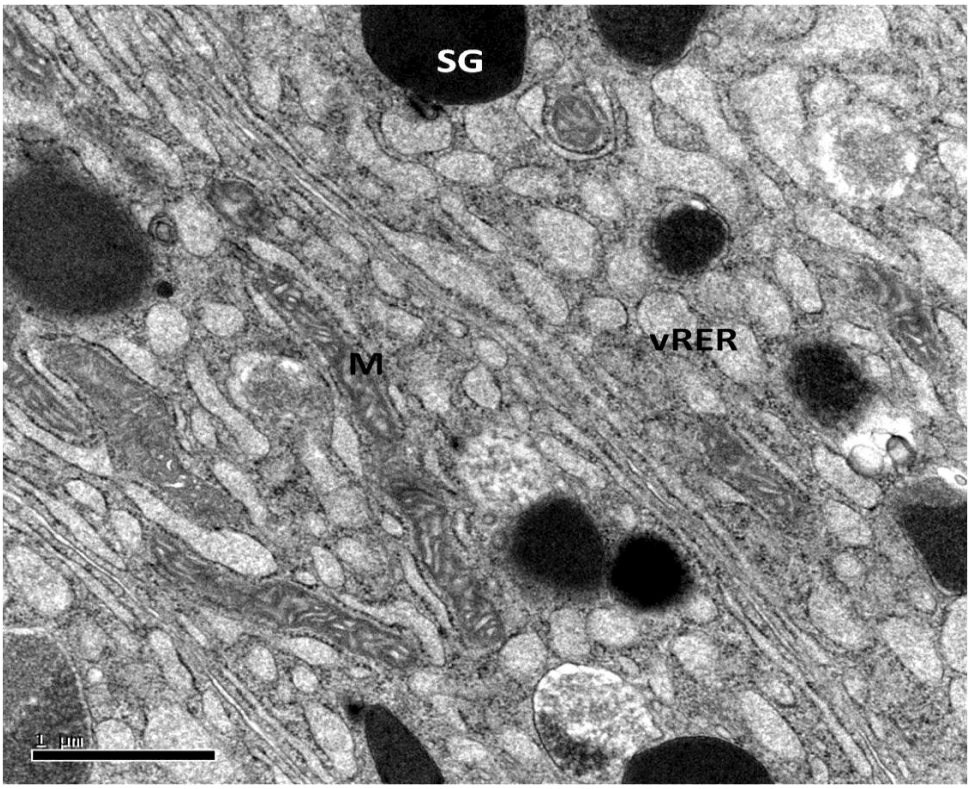

Figure 3.19E. Higher magnification of Figure 3.19D showing vesicular vRER in the cytoplasm of principal cells. Mitochondria (M), secretory granules (SG).

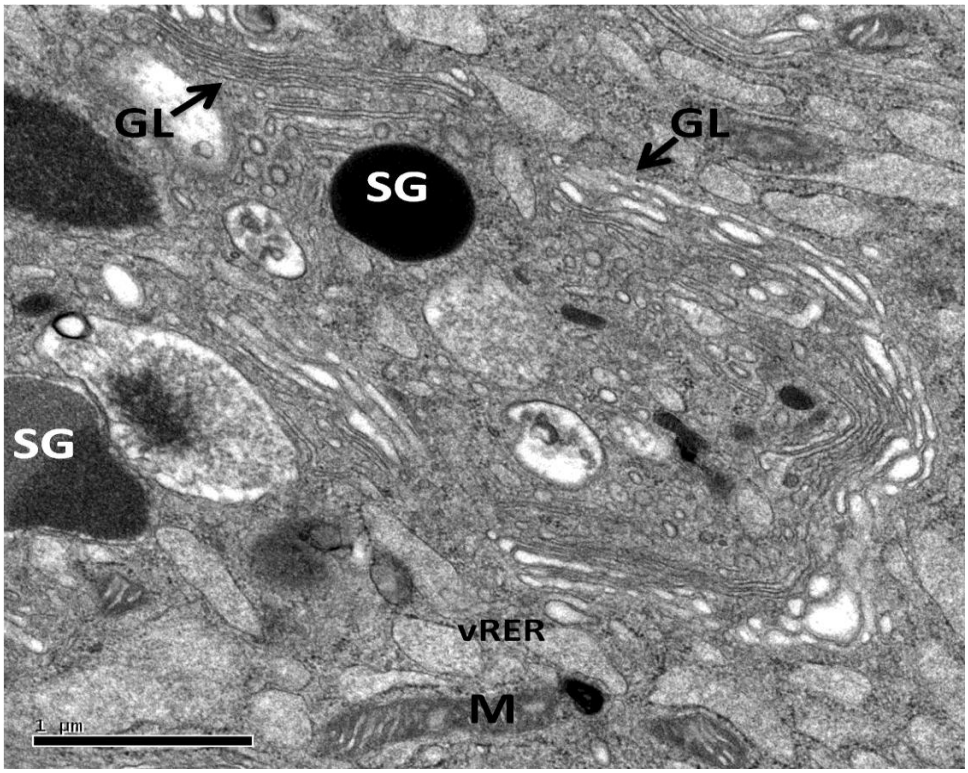

Figure 3.19F. TEM showing Golgi complexes (GL) consisting of several stacks of flat saccules with typical cistrans polarisation. Mitochondria (M), vesicular vRER, secretory granules (SG).

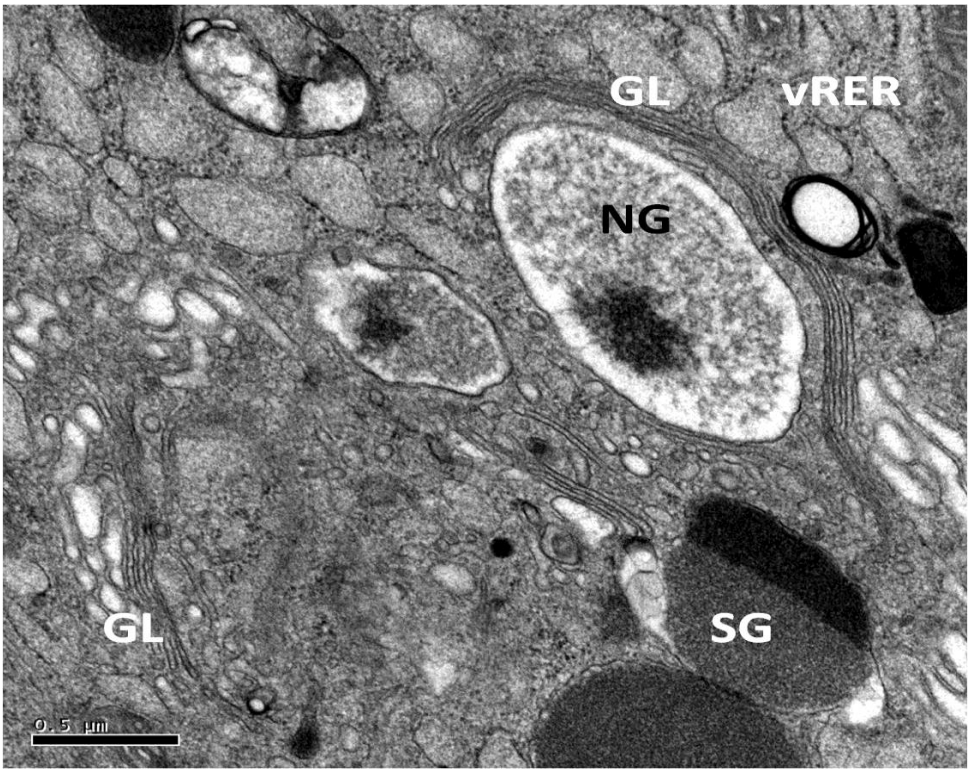

Figure 3.19G. TEM showing Golgi complexes (GL) surrounding groups of newly formed (NG) and developed secretory granules (SG) which were closely associated with the vRER.

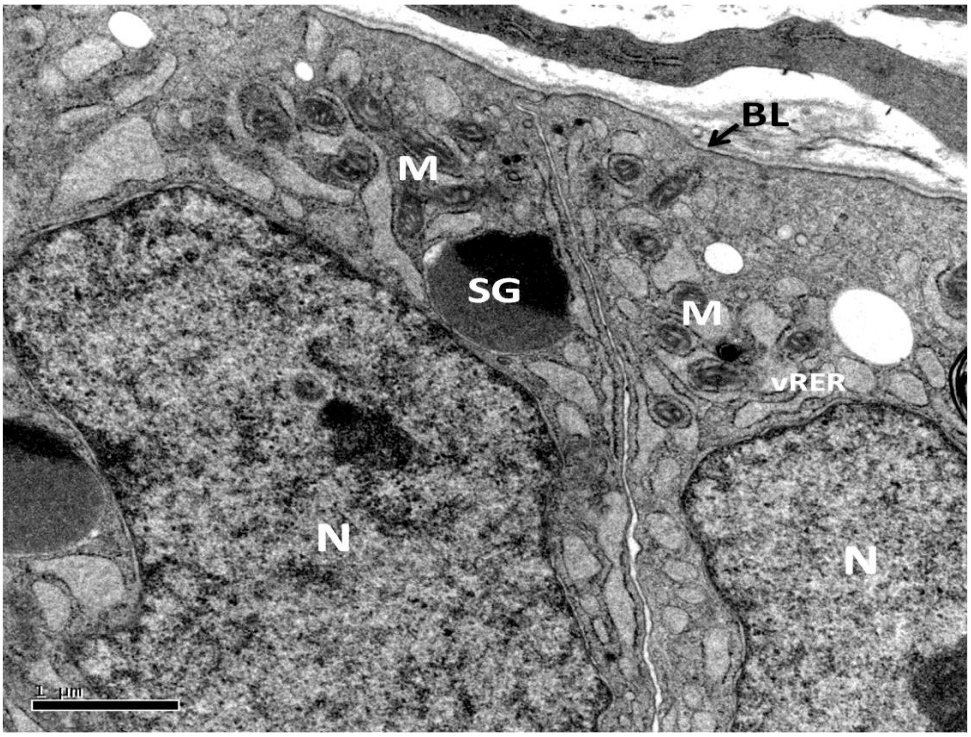

Figure 3.19H. TEM showing mitochondria (M) concentrated in the basal cytoplasm of principal cells. Nucleus (N), vRER, basal lamina (BL), secretory granules (SG).

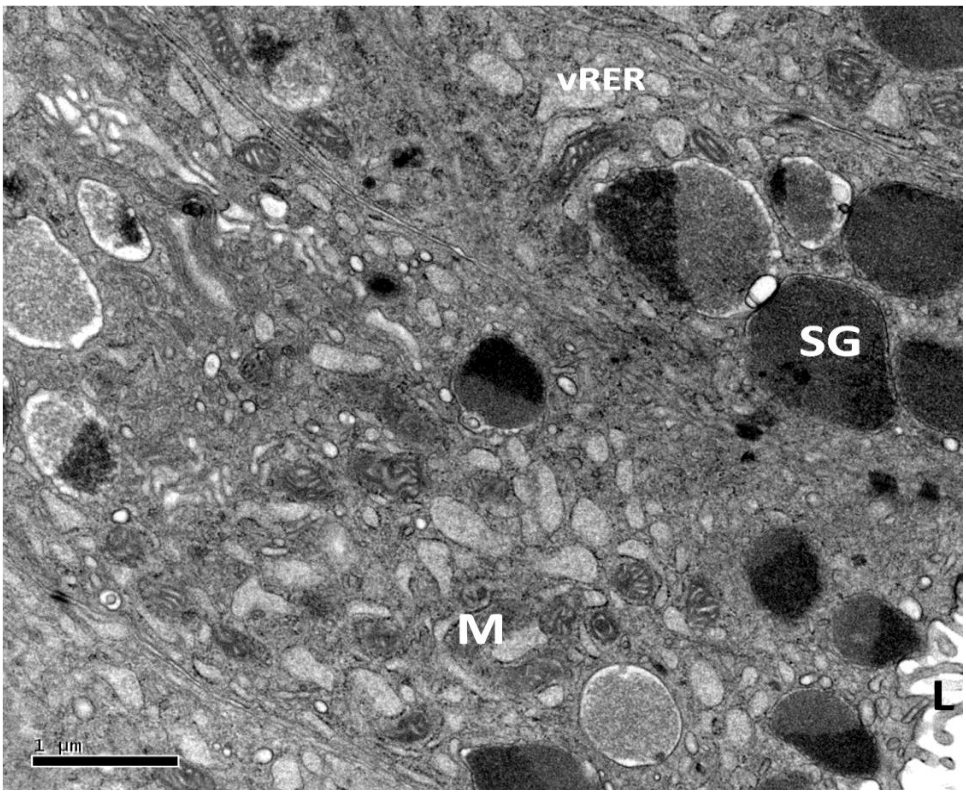

Figure 3.19I. TEM showing mitochondria (M) concentrated in the apical cytoplasm of principal cells. Secretory granules (SG), vRER, lumen (L).

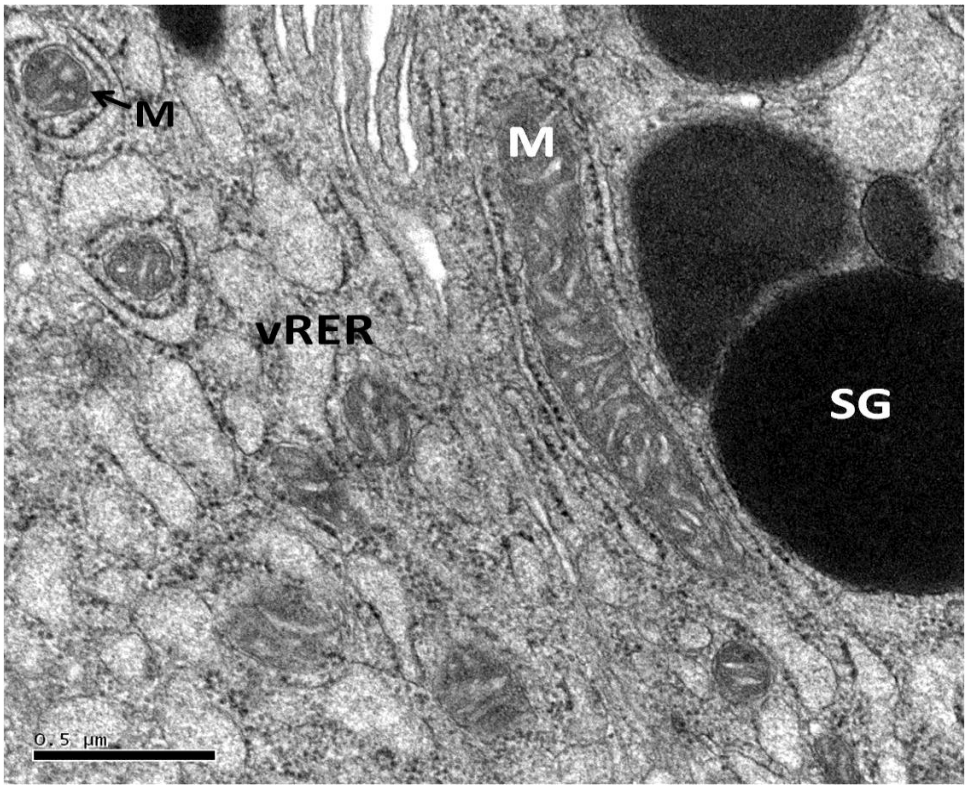

Figure 3.19J. TEM showing round and elongated mitochondria (M) in the cytoplasm of principal cells. Mitochondria were closely associated with vRER and secretory granules (SG).

Another prominent feature of the principal cells of the anterior and middle regions was the presence of characteristic granules that represent intracytoplasmic accumulations of secretory granules or their precursors (Figure 3.19K). The secretory granules were membrane-bound vesicles and were formed in the Golgi complex (Figures 3.19F & 3.19G). They increased in numbers towards the apical region (Figure 3.19A). Each granule had a dense homogeneous portion and a less dense heterogeneous portion and was PAS-positive (Figures 3.18E & 3.19G). Their release towards the lumen by exocytosis was apparent, as inferred from the occurrence of the dense sections of similar granules (Figure 3.19L). Membrane bound vesicles with fairly homogenous electron-dense material, apparently lipid inclusions, were also present in the cytoplasm of principal cells (Figure 3.19K). The principal cells of the posterior, the storage region for sperm, did not possess such granules and were therefore not secretory cells.

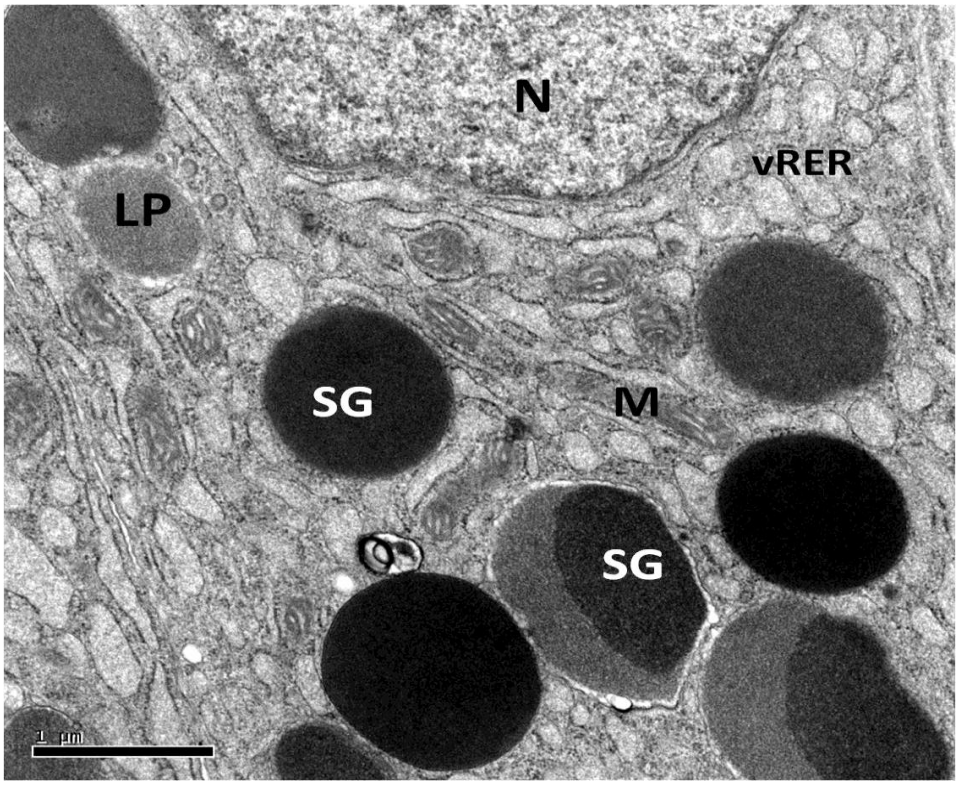

Figure 3.19K. TEM showing secretory granules (SG) which are membrane-bound vesicles. Some granules had a dense homogeneous portion and a less dense fairly heterogeneous portion, others were completely electron-dense homogeneous granules. Nucleus (N), vRER, mitochondria (M), lipid (LP).

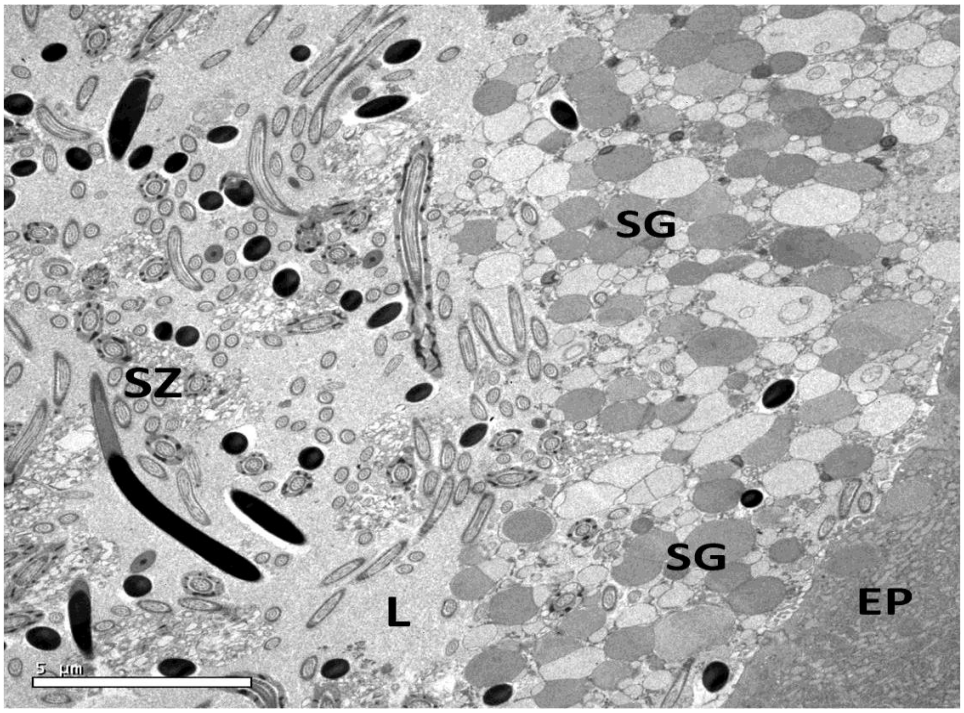

Figure 3.19L. TEM secretory granules (SG) released into the lumen of the anterior and middle regions of the epididymis by exocytosis. SG eventually bind to the heads of spermatozoa (SZ). Epithelium of epididymis (EP), lumen (L).

3.3.9.2.2 Basal cells

The basal cells were confined to the region closer to the basal lamina (Figures 3.19M & 3.19N). Their nuclei had various shapes and were heterochromatic. The nucleolus was prominent. The basal cell cytoplasm contained some organelles and a few membrane-bound vesicles with electron-dense material (Figure 3.19O).

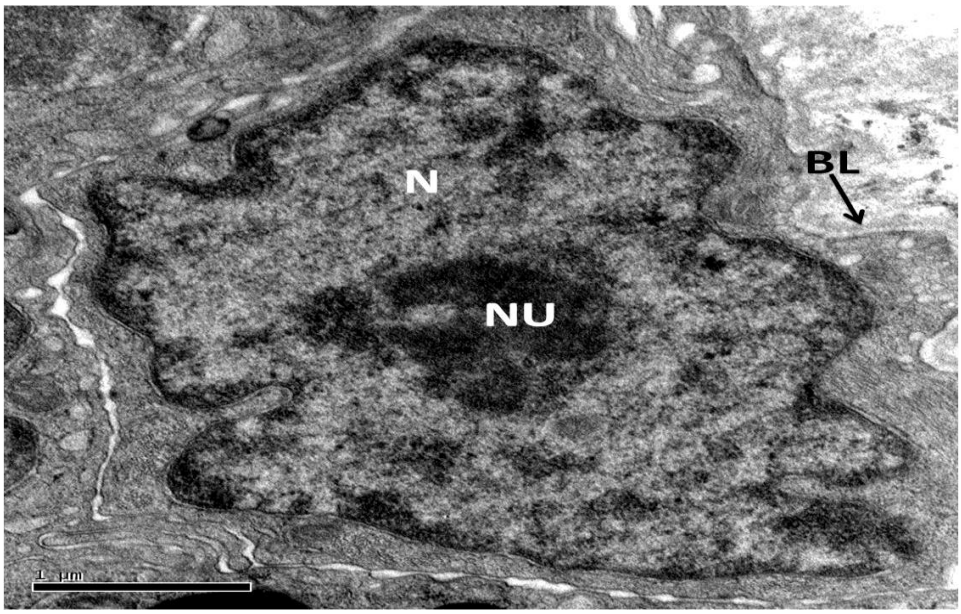

Figure 3.19M. TEM of a basal cell at the basal lamina (BL) of the middle region of epididymis with heterochromatic nucleus (N) and prominent nucleolus (NU).

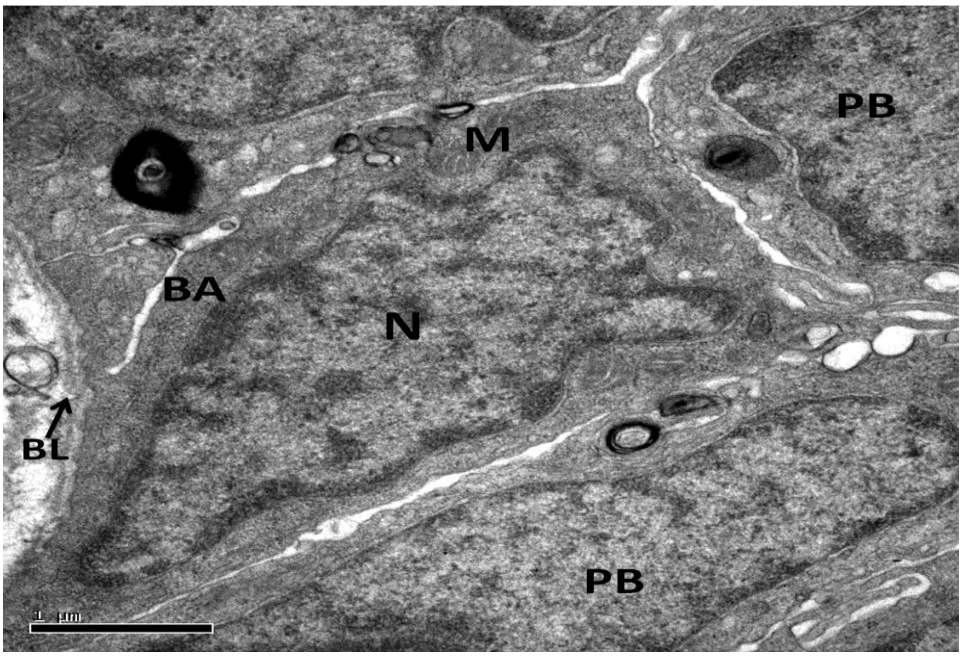

Figure 3.19N. TEM of a basal cell (BA) at the basal lamina of middle region adjacent to principal cells (PB).

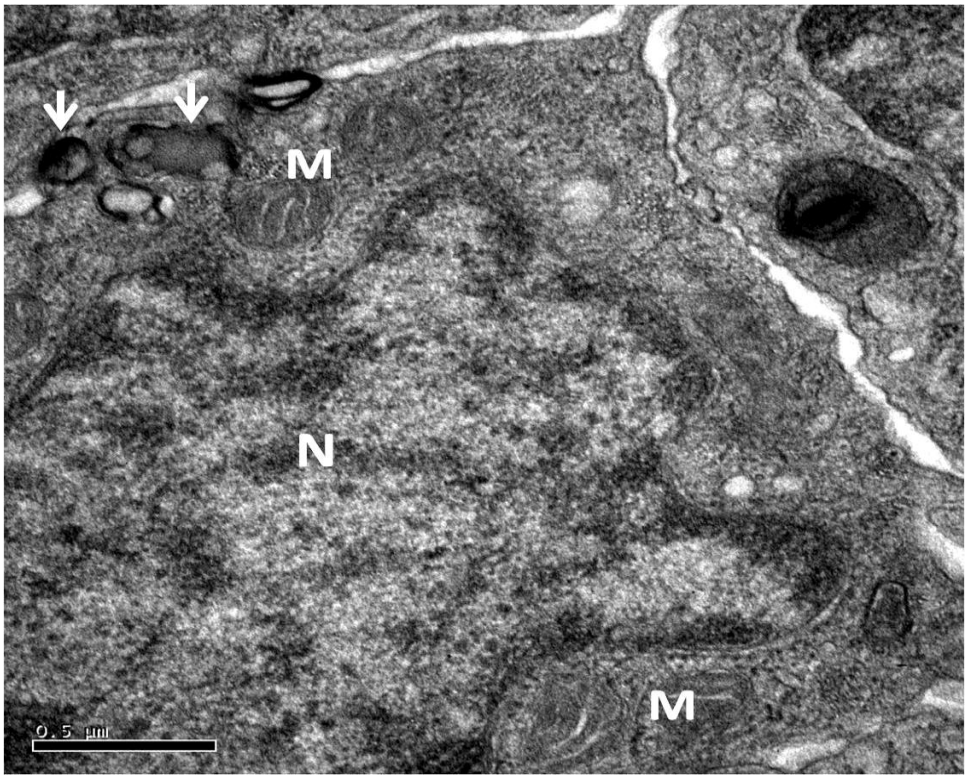

Figure 3.19O. TEM higher magnification of Figure 3.19N. Cytoplasm of the basal cell contained mitochondria (M) and membrane-bound vesicles with an electron dense material (arrow). Nucleus (N).

3.3.10 Renal sexual segment (RSS)

3.3.10.1 Histology of RSS

During the quiescent phase, the male RSS tubules were regressed and indistinguishable from the normal tubular portions of the nephron (Figure 3.20A). The RSS were lined by cuboidal epithelial cells having rounded nuclei with prominent nucleoli (Figure 3.20B). The diameter of the tubules ranged from 60–70 µm and the epithelium height was between 12 and 15 µm. The tubules were empty and surrounded by dense intertubular fibrous connective tissue.

During the recrudescent phase, the RSS epithelial cell height and lumen diameter were larger, compared to the quiescent phase (Figure 3.15C). The RSS were lined by low columnar, nonciliated epithelial cells having basal rounded or oval nuclei (Figure 3.20D). The diameter of tubules ranged between 80–110 µm and the epithelium height was between 20 and 35 µm.

During the active phase, development of the sexual segment was initiated; the RSS tubule cells were hypertrophied and became secretory (Figures 3.20E, 3.20F & 3.20G). At this phase, the RSS epithelium consisted of columnar cells with basal, euchromatic nuclei and prominent, usually eccentric nucleoli (Figures 3.20H & 3.20I). With further development, all the RSS was fully hypertrophied and became actively secretory (Figures 3.20E, 3.20F & 3.20G). The diameter of tubules ranged from 150–400 µm and the epithelium height was between 40–110 µm. The columnar epithelial cell boundaries were intact and the granules were primarily located in the apical region of the cells towards the lumen (Figures 3.20G & 3.20H). The secretory granules reacted strongly with PAS (Figures 3.20G & 3.20H). After November, the cell membrane ruptured, liberating the secretory granules into the lumen (Figures 3.20E, 3.20F, 3.20G & 3.20J). At the peak of reproductive activity the tubule lumen was filled with granules and some tubules were filled with a nongranular substance (Figure 3.20J). Regression of the sexual segment began in May as the cell height was usually low and the cytoplasm was relatively nongranular. The lumina of the sexual segment tubules and ureter were filled with secretory granules during this period.

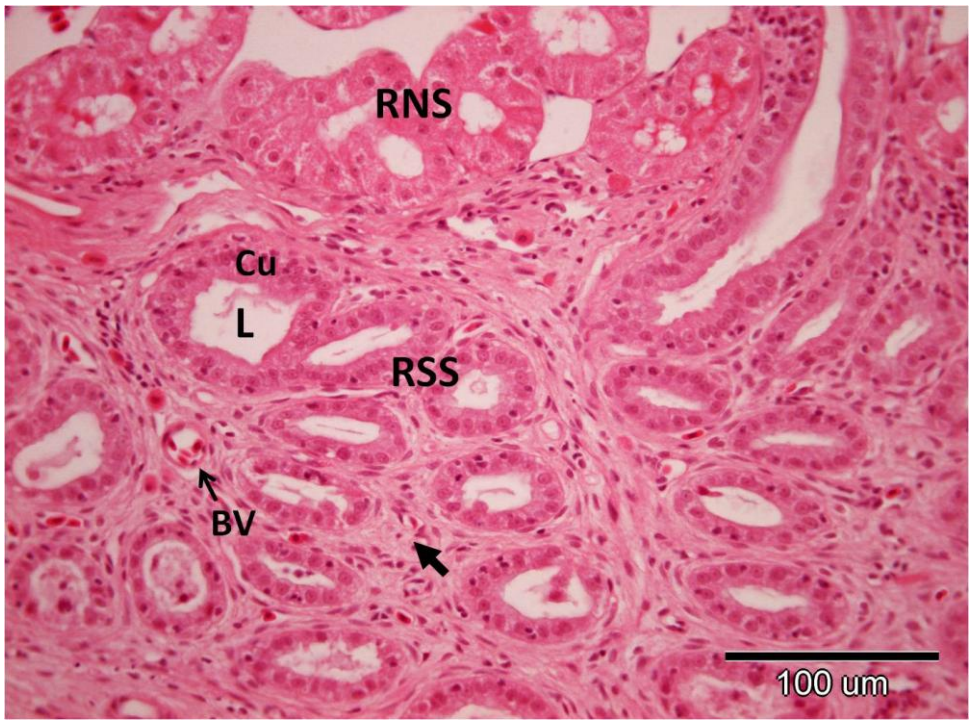

Figure 3.20A. H&E section of RSS from the quiescent phase showing tubules surrounded by cuboidal epithelial cells (Cu). Tubules lack secretory granules in their lumens (L) and were surrounded by intertubular fibrous connective tissue (arrow). Portion of normal renal segment were clearly visible (RNS). Blood vessel (BV).

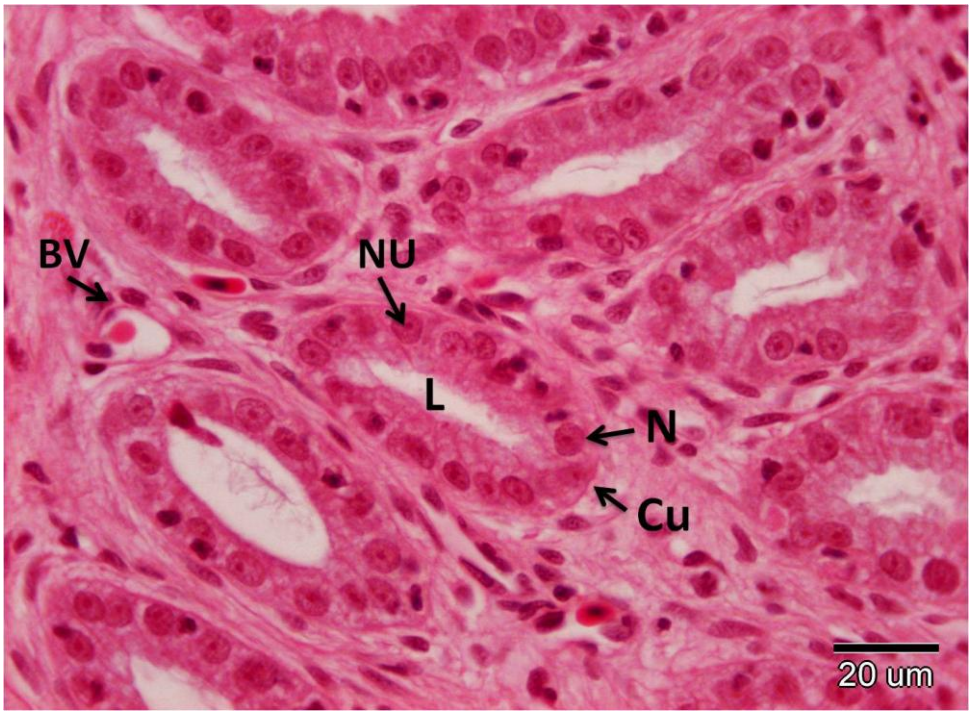

Figure 3.20B. Higher magnification of Figure 3.20A showing RSS lined by cuboidal epithelial cells (Cu) having rounded nuclei (N) with prominent nucleoli. Lumen (L), blood vessel (BV).

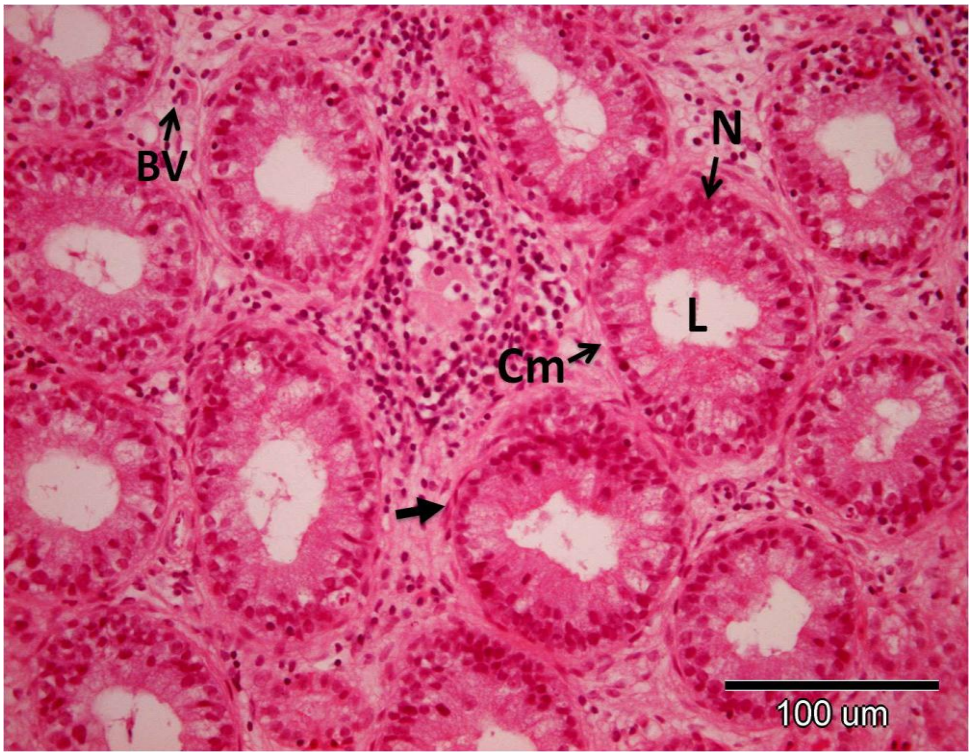

Figure 3.20C. H&E section of the RSS from the recrudescent phase showing enlarged tubules with low columnar cells (Cm). Nucleus (N), lumen (L), blood vessel (BV).

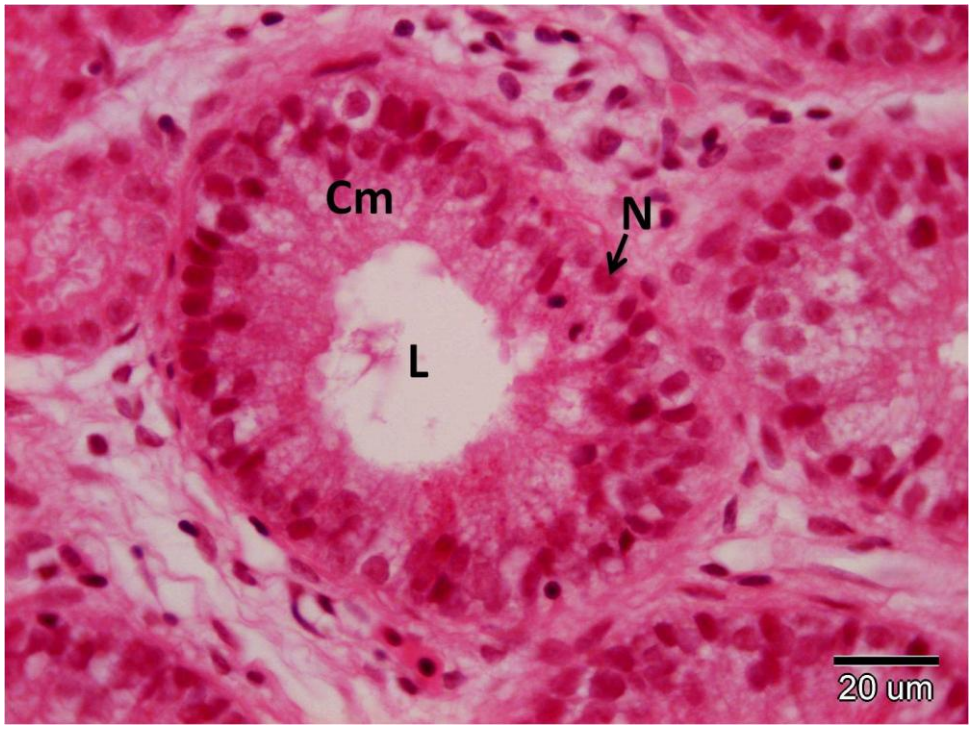

Figure 3.20D. Higher magnification of Figure 3.20C. Tubules were lined by low columnar epithelial cells (Cm) with rounded or oval nuclei (N). Lumen (L).

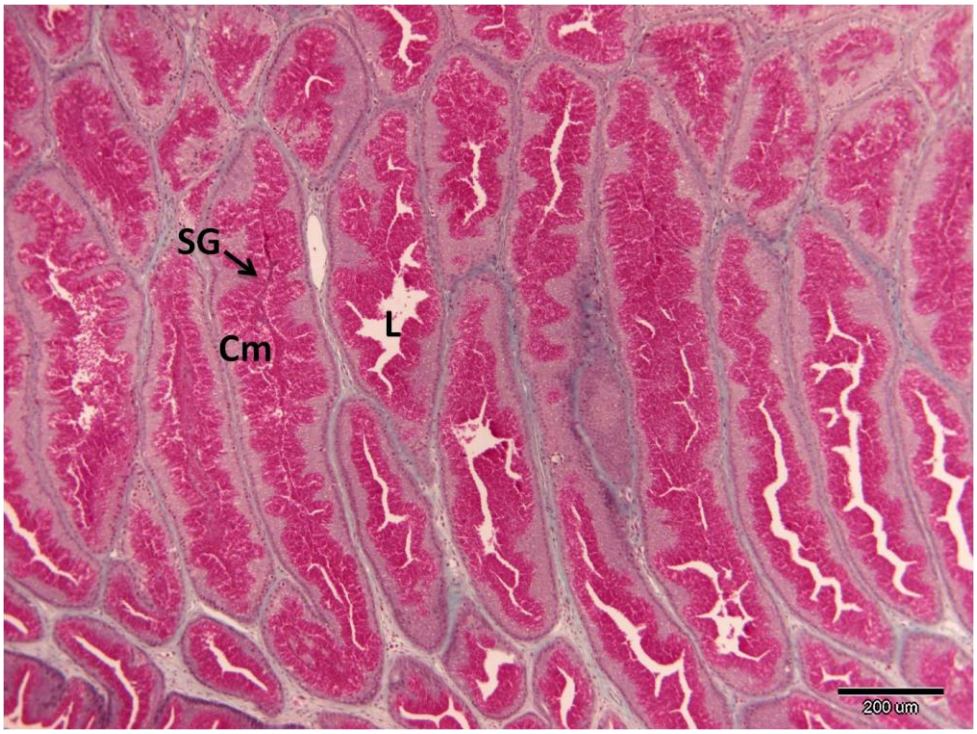

Figure 3.20E. MT longitudinal section of renal tissue from the active phase showing fully developed RSS tubules with columnar epithelium (Cm) and the lumen (L) filled with secretory granules (SG).

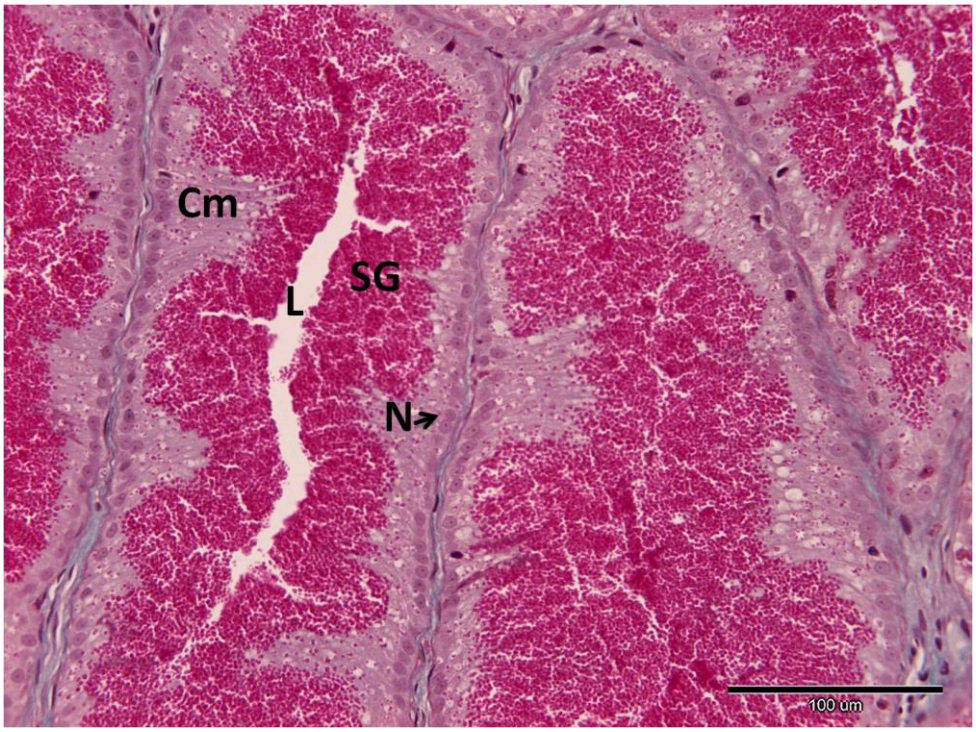

Figure 3.20F. MT Higher magnification of Figure 3.20E showing columnar epithelial cells (Cm) and the lumen (L) filled with the secretory granules (SG). Nucleus (N).

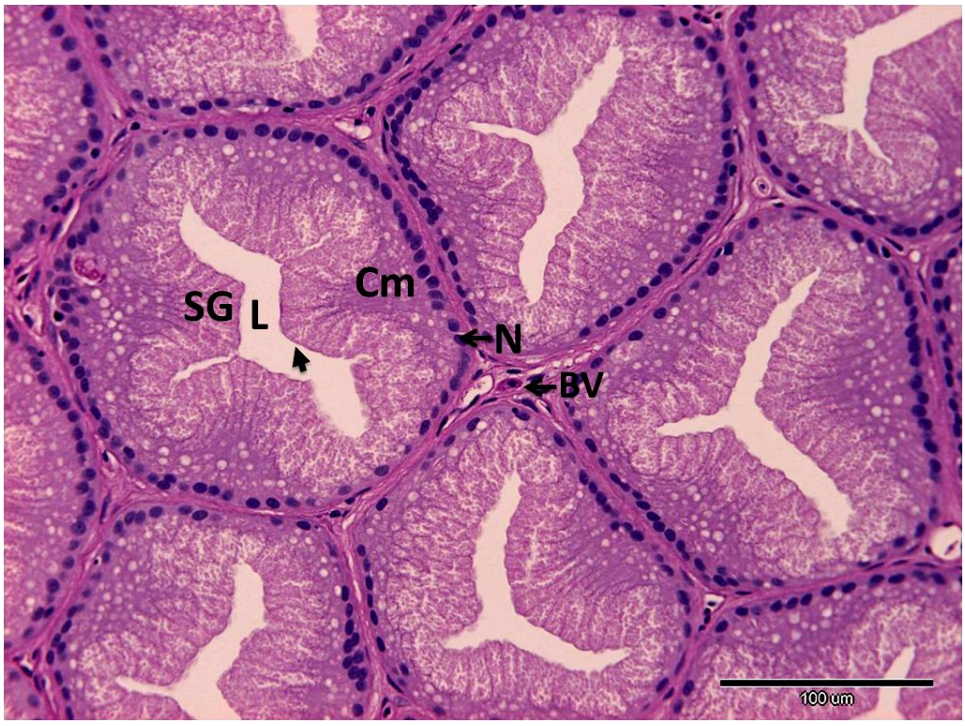

Figure 3.20G. PAS-Haem cross section of RSS showing intact columnar epithelial cell (Cm) boundaries (arrow) with the secretory granules (SG) in the apical region of the cells towards the lumen (L). Nucleus (N), blood vessel (BV).

Figure 3.20H. PAS-Haem higher magnification of Figure 3.20G of RSS showing intact columnar epithelial cell (Cm) boundaries (arrow) with the secretory granules (SG) in the apical region of the cells towards the lumen (L). Nucleus (N).

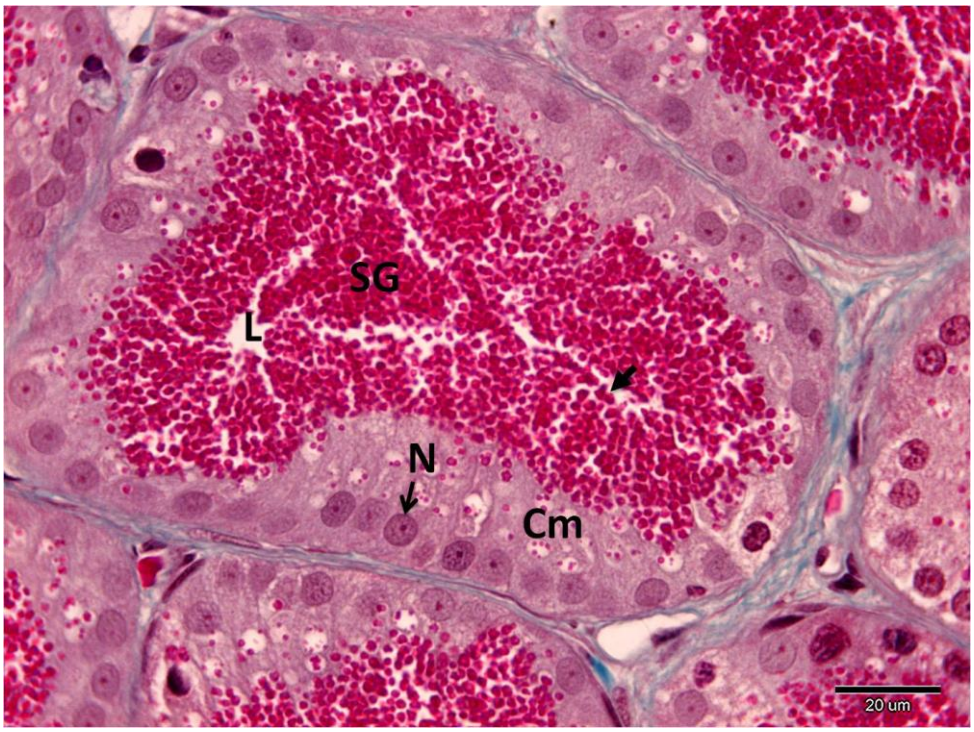

Figure 3.20I. MT section of RSS tubule from the active phase showing rupture of cell membrane (arrow) of columnar epithelial cells (Cm) liberating the secretory granules (SG) into the lumen (L) of the tubule. Nucleus (N).

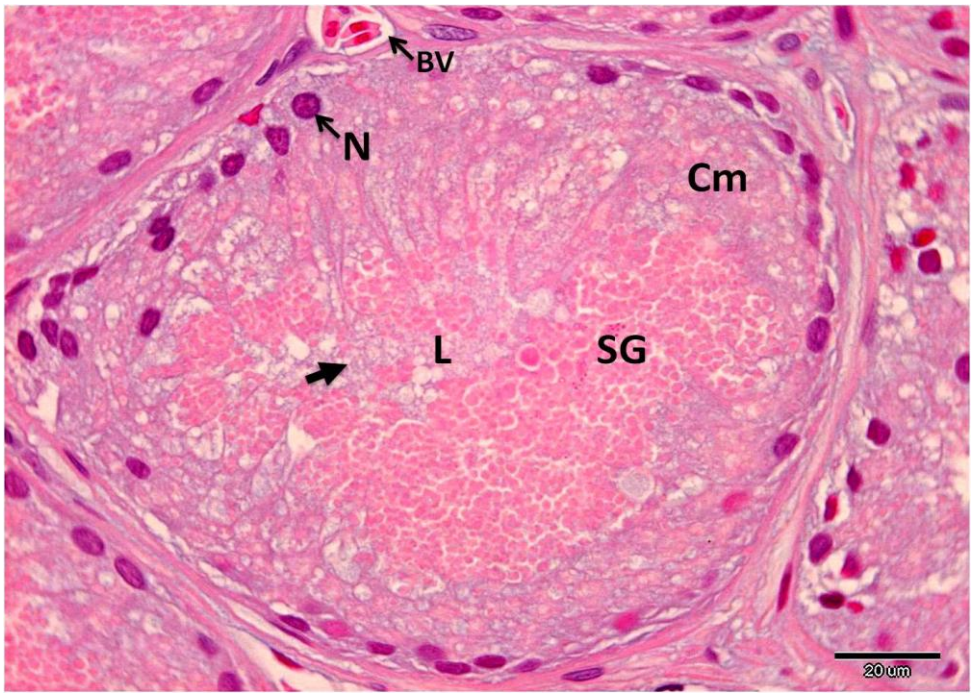

Figure 3.20J. AB-NF section of RSS tubules from the active phase showing RSS tubules with columnar epithelial cells (Cm) and lumen (L) with granules (SG) and nongranular substance (arrow). Nucleus (N), blood vessel (BV).

3.3.10.2 Ultrastructure of RSS

The hypertrophied epithelium of RSS consisted of columnar cells with basal, euchromatic nuclei and prominent eccentric nucleoli (Figures 3.21A & 3.21B). Extensive supranuclear Golgi complexes and RER were abundant throughout the cytoplasm (Figure 3.21C). Secretory granules were produced at various stages of maturity, with condensing vacuoles associated with the trans-face of the Golgi complexes (Figures 3.21C & 3.21D). Dense, spherical secretory granules were numerous in the apical cytoplasm (Figure 3.21E). Secretory granules appeared uniformly dense and most of them possessed an inner dense core, an outer irregular collar and surrounding cytoplasm. The outer collar was composed of material with less density than the dense core of the secretory granules (Figure 3.21E). Secretory granules appeared to be released independently, with some peripheral cytoplasm, into the lumen (Figure 3.21F). Thus secretion was an apocrine process. Dissolution of the secretory granules in the lumen resulted in a secretory product, in general, smaller than the central core (Figure 3.21E). Cell junctions were obscure between cells except for terminal tight junctions (Figure 3.21G). With further development of the RSS

epithelium, mature secretory granules appeared to occupy most of the cytoplasm and Golgi complexes were few (Figure 3.21H).

The regressed RSS epithelium was almost indistinguishable from the normal tubular segments of the nephron (Figures 3.22A & 3.22B). The RSS tubules appeared as inactive cords of cells (Figures 3.22A & 3.22B). The epithelial cells reduced greatly in size and became more cuboidal and the nuclei were more irregular with prominent nucleoli (Figure 3.22C). The lumen and the cytoplasm were even more reduced (Figures 3.22A & 3.22B). Mucoid secretory vacuoles clustered along the luminal border of many epithelial cells, and organelles such as Golgi complexes, RER, and mitochondria involved in product synthesis, occurred in the cytoplasm (Figures 3.22C & 3.22D).

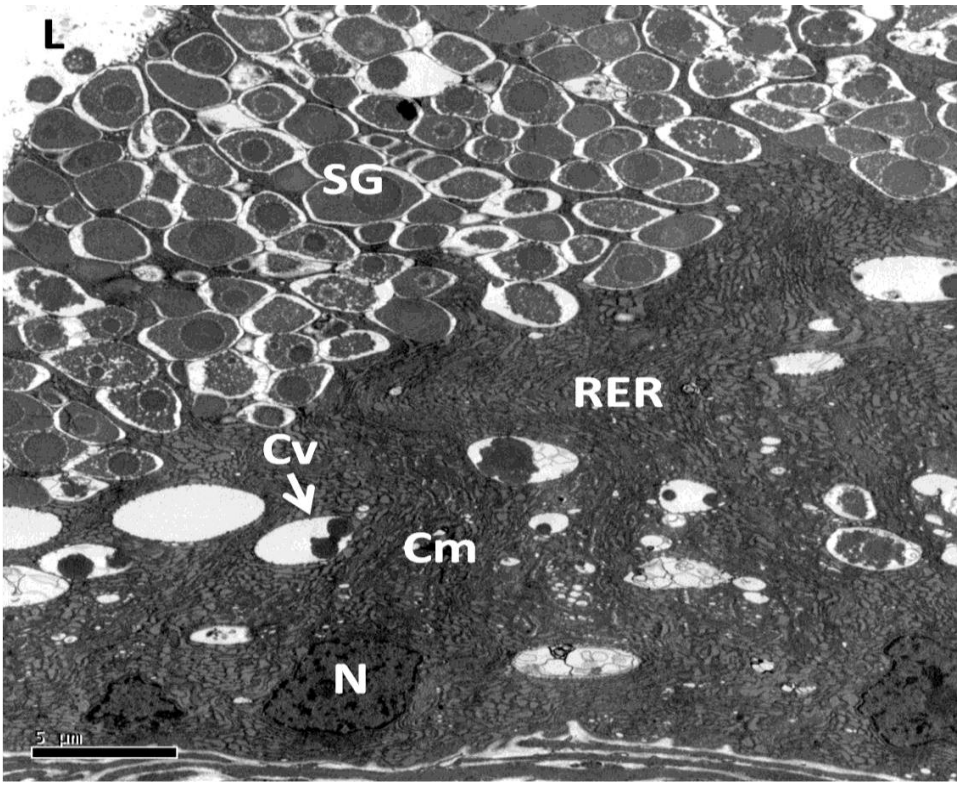

Figure 3.21A. TEM of RSS tubules from the active phase showing columnar epithelial cells (Cm) with basal, euchromatic nuclei (N). Secretory granules (SG) and condensing vacuoles (Cv) in close association with RER. Lumen (L).

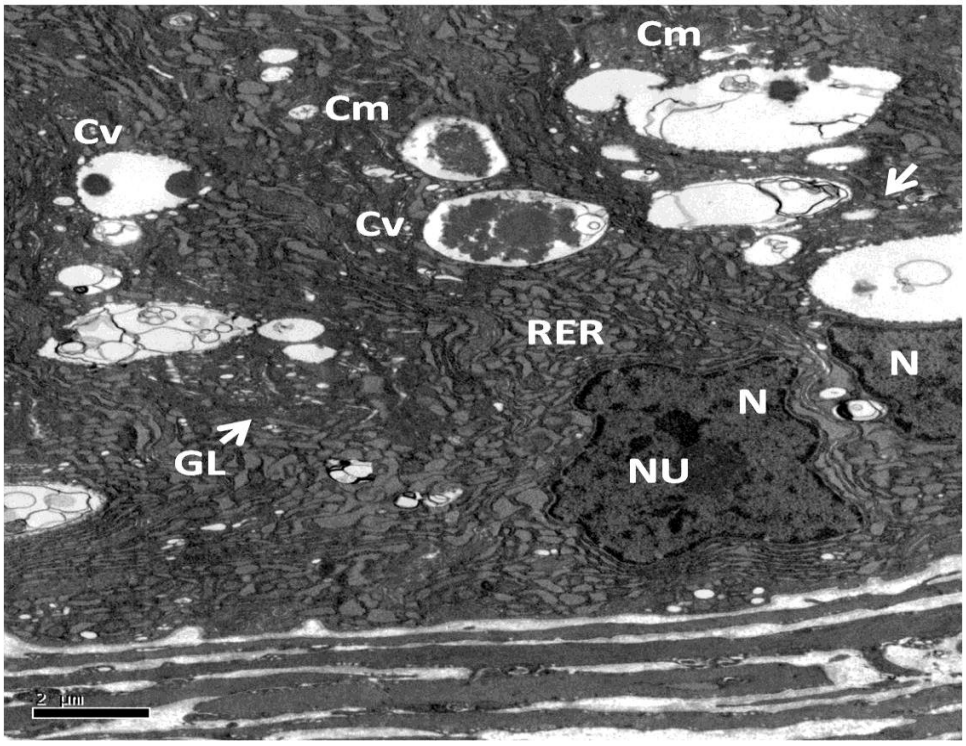

Figure 3.21B. TEM Higher magnification of Figure 3.21A showing columnar epithelial cells (Cm) with basal, euchromatic nuclei (N) prominent eccentric nucleoli (NU). Condensing vacuoles (Cv) in close association with Golgi complex (GL) and RER.

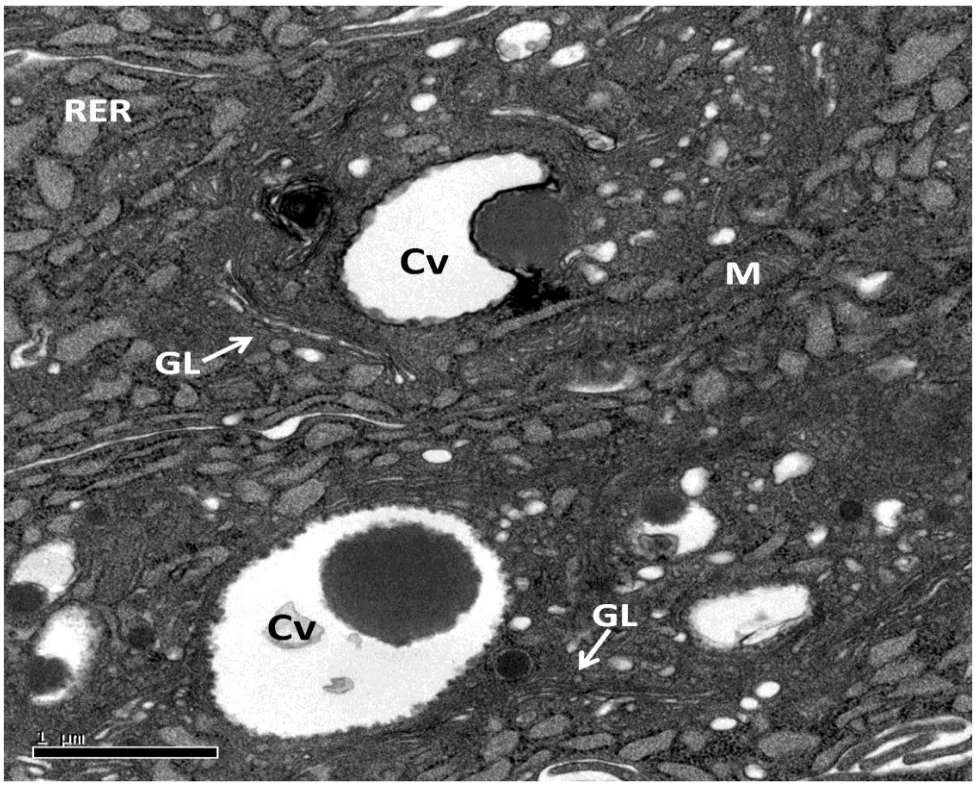

Figure 3.21C. TEM High magnification showing condensing vacuoles (Cv) in close association with Golgi complex (GL), RER and mitochondria (M).

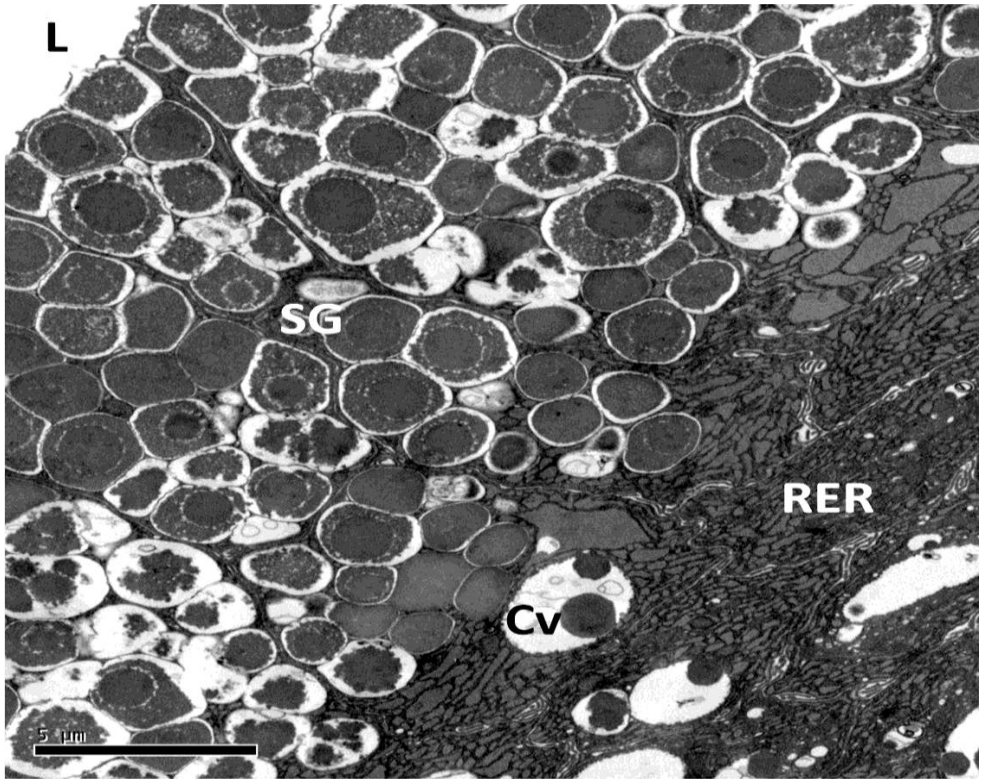

Figure 3.21D. TEM High magnification showing secretory granules (SG) in various stages of maturity. Numerous RER in close association with the condensing vacuoles (Cv). Lumen (L).

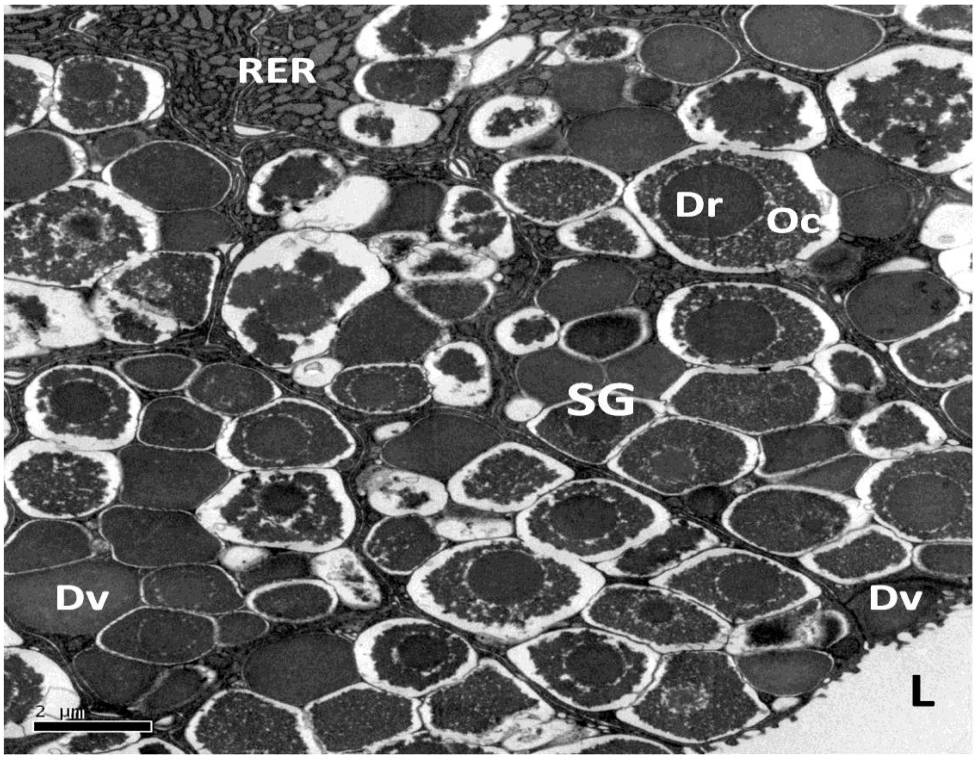

Figure 3.21E. TEM showing secretory granules (SG) at the lumenal border (L). Dense secretory granules (Dv), and secretory granules with dense core (Dr) and outer collar (Oc). RER closely associated with the secretory granules.

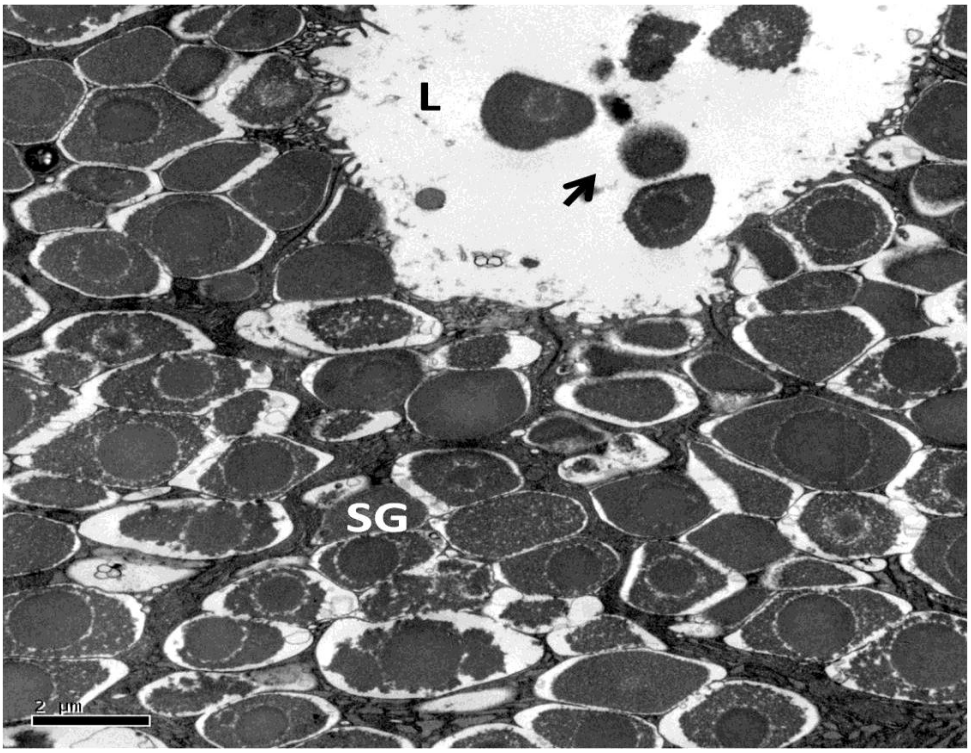

Figure 3.21F. TEM showing secretory granules (SG) at the lumenal border. Dissolution of secretory granules (arrow) which were released independently into the lumen (L).

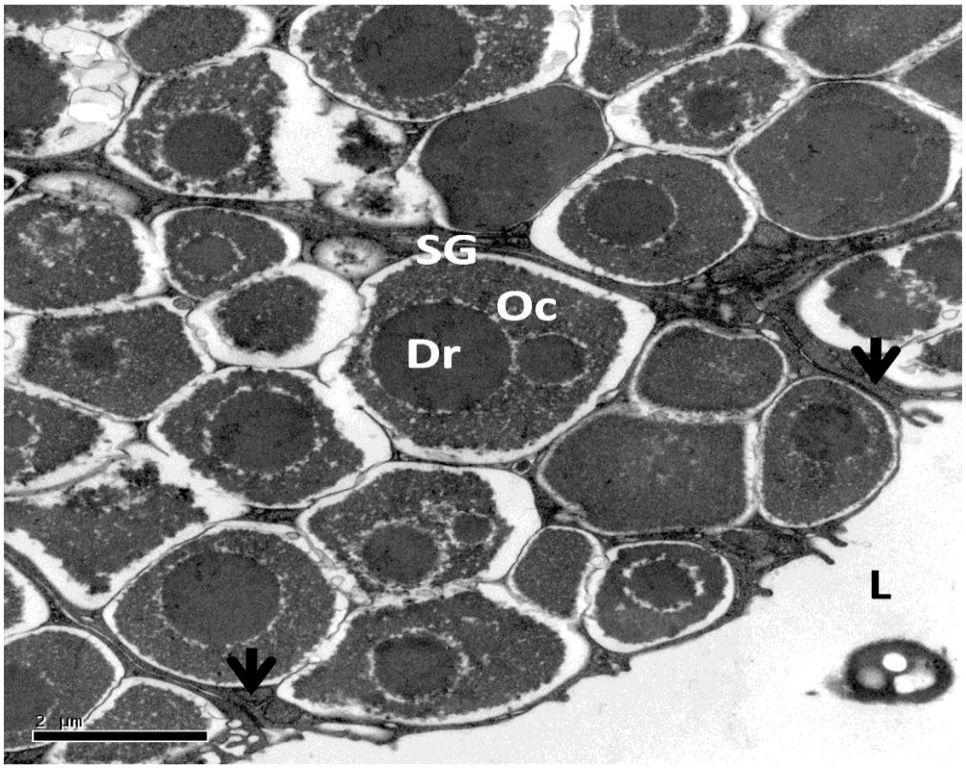

Figure 3.21G. TEM showing terminal tight junctions at apical portion of epithelial cells (arrow). Secretory granules (SG) with dense core (Dr) and outer collar (Oc) were clearly visible. Lumen (L).

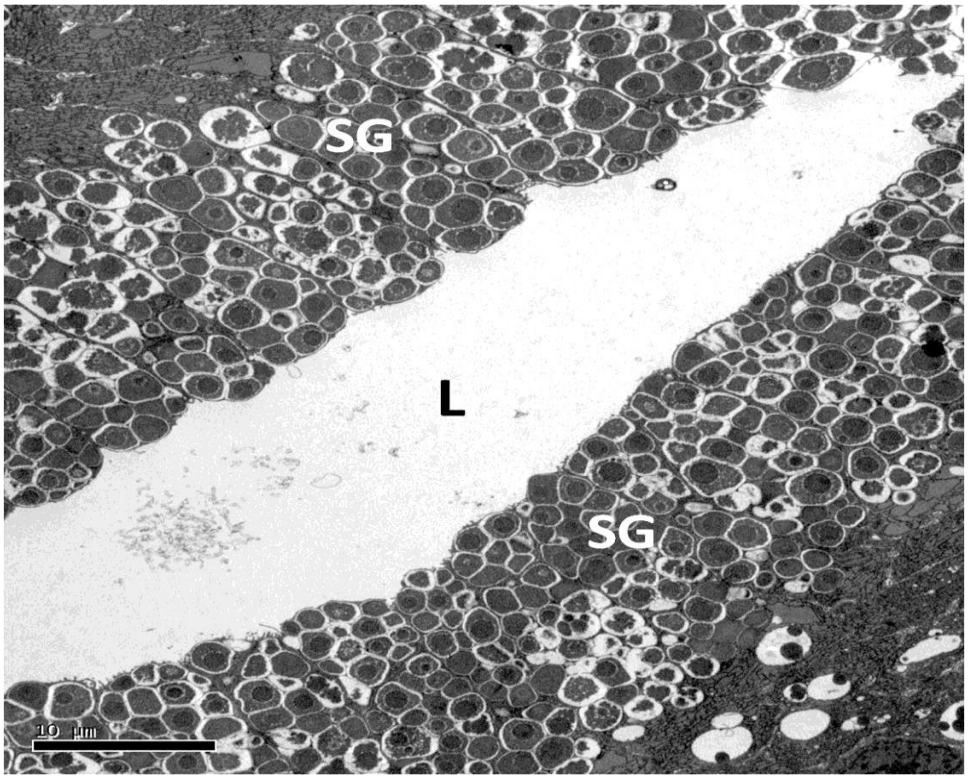

Figure 3.21H. TEM showing secretory granules (SG) occupied more of the epithelial cells cytoplasm.

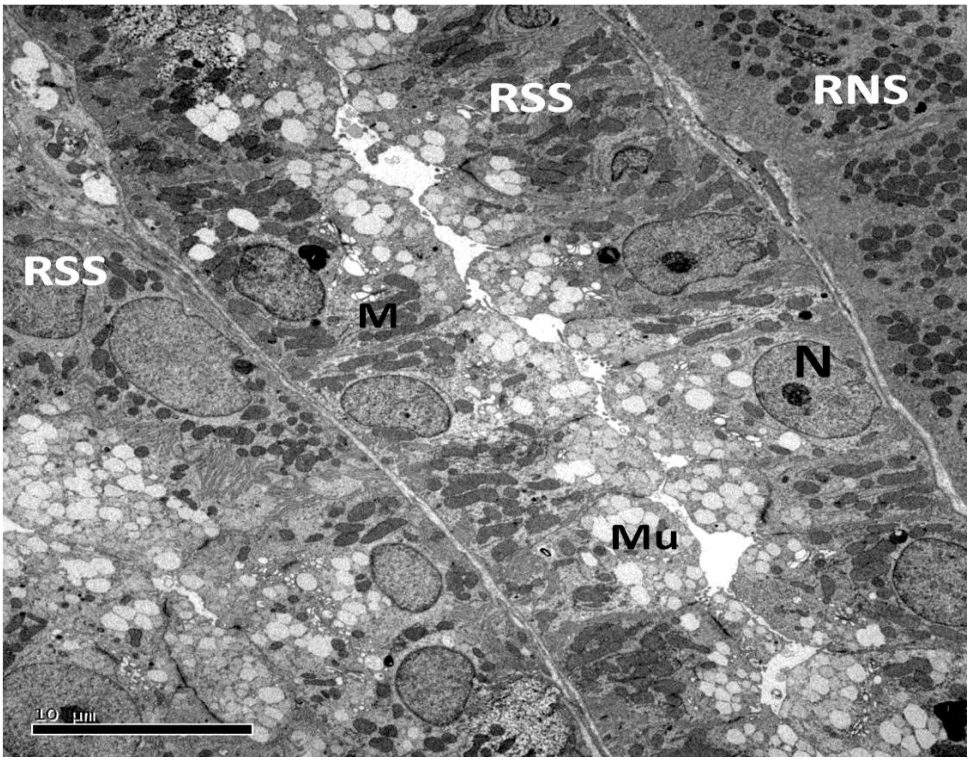

Figure 3.22A. TEM of renal section from the quiescent phase showing inactive RSS and normal tubular segment (RNS). RSS nucleui (N) appeared rounded with prominent nucleoli. The cytoplasm filled with numerous mitochondria (M) and mucoid secretory vacuoles (Mu).

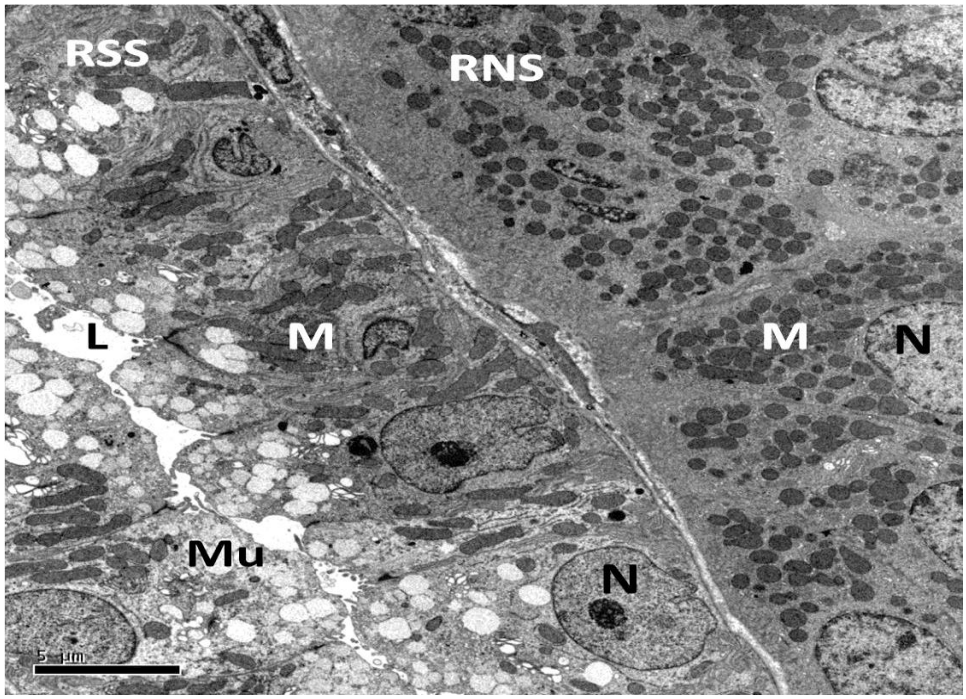

Figure 3.22B. TEM higher magnification of Figure 3.22A showing RSS and RNS. Some nuclei (N) of RSS appeared irregular. Mitochondria (M), mucoid secretory vacuoles (Mu), lumen (L).

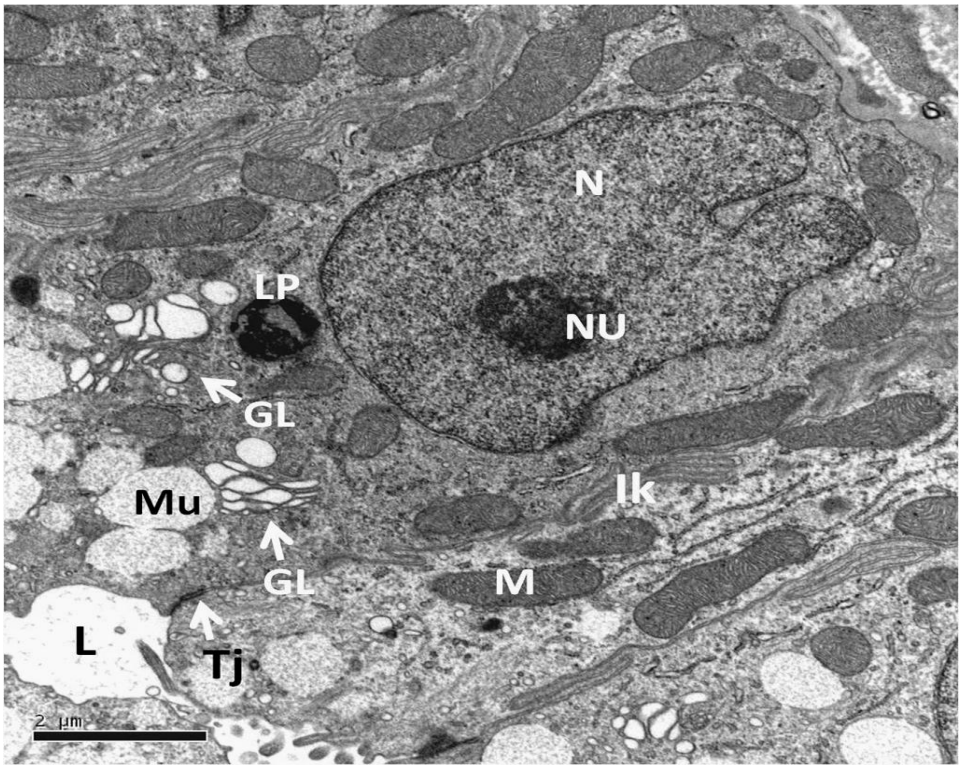

Figure 3.22C. TEM higher magnification of Figure 3.22B showing inactive RSS with irregularly shaped nucleus (N) and prominent nucleolus (NU). Mucoid secretory vacuoles (Mu) appeared in close association with Golgi complex (GL), mitochondria (M) and lipid droplets (LP). Lumen (L), tight junction (Tj), intercellular canaliculus (IK).

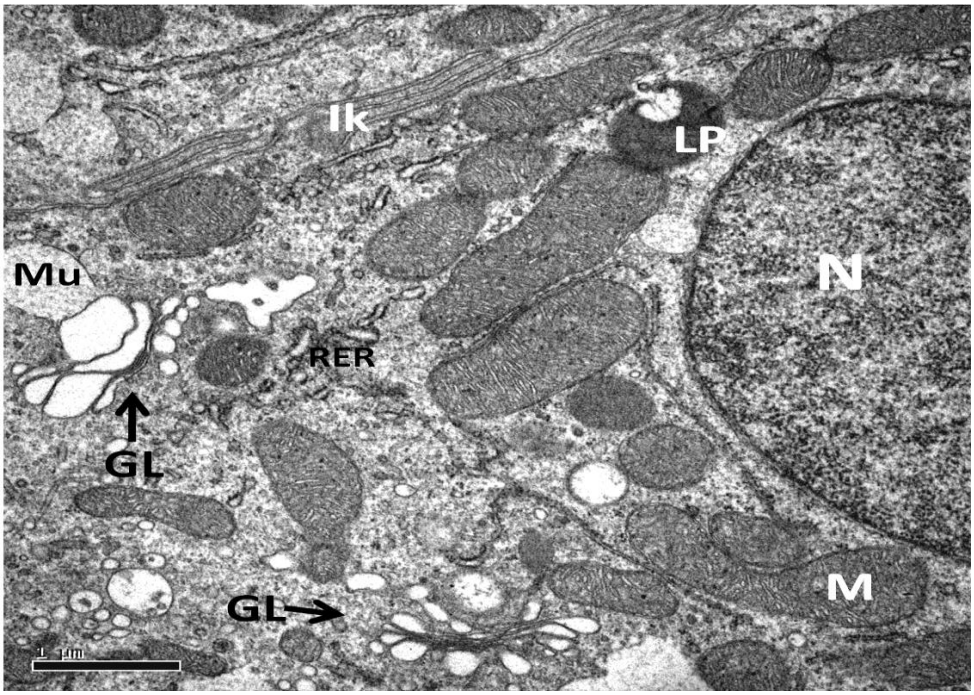

Figure 3.22D. TEM of inactive RSS epithelial cytoplasm. Mucoid secretory vacuoles (Mu) appeared in close association with Golgi complex (GL), mitochondria (M) RER, and lipid droplets (LP). Nucleus (N), intercellular canaliculus (IK).

3.4 Discussion

This investigation was based on comprehensive data obtained from the male house gecko, *H. flaviviridis*, freshly captured from natural populations throughout their reproductive cycles. The hormone levels were coincident with the gonadal growth and development. The plasma hormone concentrations were monitored immediately following capture to avoid stress and to ensure that the values are closely related to the natural condition (Owens and Ruiz, 1980).

The house gecko exhibited a peak in plasma T concentrations coincident with an increase in testicular mass, spermiogenesis and mating (March–April). Spermatogenesis is prenuptial, commencing in late summer (September) and completed the following spring. These testicular events were closely associated with a gradual rise in plasma T concentrations and PR expression. This type of reproductive cycle followed a pattern similar to that of the same species living in northern regions of India (Sanyal and Prasad, 1967).

In the house gecko spermatogenesis commenced in late summer (September), following a period of reproductive quiescence (June–August). Spermiogenesis was completed by early winter (November) but the activity slowed down during winter. However, they became active again during February. Sperm maturation was completed during the active phase and allowed mating to occur during spring (March–April).

In this study, plasma T concentrations were low during the early stages of spermatogenesis but peaked during spermiogenesis, corresponding with maximum testicular increase, as reported in other reptilian species (Lance, 1984). In addition, the house gecko exhibited a typical pattern of plasma T concentrations associated with the development of the epididymis and RSS which were androgen-linked. Plasma T concentrations were low during the quiescent phase (June–August), and the recrudescent phase (September–October) at the onset of spermatogenesis, but rose significantly during spermiogenesis in spring (March) during the active phase and declined during the second half of the mating period. This pattern resembles that reported in other species of lizards with a prenuptial type of spermatogenesis (Arslan *et al.*, 1978b; Courty and Dufaure, 1980; Bourne *et al.*, 1986b; Ando *et al.*, 1990, 1992; Phillips and Millar, 1998; Tokarz *et al.*, 1998; Radder *et al.*, 2001; Hu *et al.*, 2004; Kumar *et al.*, 2011). Association of maximum plasma T concentrations in individuals with high testicular activity suggest that high concentrations of androgens play an important role in stimulating spermatogenesis, courtship, and mating. In addition, *H. flaviviridis* exhibited a typical pattern of plasma T concentrations associated with the development of epididymis and RSS, as reported in other lizard species (e.g., Akbarsha and Balasuhramanian, 1983; Haider and Rai, 1987; Nirmal and Rai, 2000; Krohmer, 2004, Sever and Hopkins, 2005). The patterns of plasma T concentrations in *H. flavivridis* may suggest a role in spermatogenesis and the development of accessory organs in this species.

The plasma E_2 concentrations in male *H. flaviviridis* rose during the mating period (March–April) but dropped rapidly to basal levels for the rest of the season. This implied a role for E_2 in the induction of sexual behaviours and testicular growth. However, in other lizards exhibiting annual cycles of E_2 production, elevated plasma E_2 concentrations did not always coincide with mating. Saint Girons *et al*. (1993)

reported that sexually active male *Vipera aspis* had high plasma T and low E_2 during the mating period, with E_2 being elevated in non-mating males. In the male lizard *Podarcis s. sicula* plasma E_2 concentrations increased in the post-reproductive refractory period (Ando *et al.*, 1992).

The cessation of spermatogenic activity in male *H. flaviviridis* during late April–May could be related to high plasma E_2 concentrations which may suppress spermatogenesis. High E_2 concentrations are known to have a negative effect on spermatogenic activity. Recently, Bharti *et al.* (2011) reported that PMSG (pregnant mares serum gonadotropin) injected into regressed testes of *H. flaviviridis* showed stimulated spermatogenesis associated with a significant rise in plasma T concentrations. However, co-administration of PMSG with a high dose of E_2 significantly slowed down germ cell proliferation and also induced apoptosis in germ cells. It has been reported that high E_2 concentrations blocked spermatogenesis for the seasonally breeding lizard *Podarcis sicula* (Cardone *et al.*, 2002).

In this study, a significant rise in plasma E_2 concentrations during March–April may have had some effect on the gradual degeneration of spermatogenic activity and the significant decrease in plasma T concentrations.

Plasma P concentrations showed a seasonal pattern in male *H. flaviviridis* similar to T and E_2. Mean concentrations were low during the quiescent and recrudescent phases but elevated significantly during the active phase. This significant change observed in male plasma P concentrations may be related to P conversion to other steroids. P may also have a primary role in stimulating reproductive behaviours in males, as P has been shown to stimulate male reproductive behaviour in some lizards (Lindzey and Crews, 1986; 1988; 1992; Young *et al.*, 1991; Moore and Lindzey, 1992; Witt *et al.*, 1994).

In this study, PRs were strongly expressed in Leydig and Sertoli cells throughout the active phase, but was weak during the quiescent phase coinciding with plasma sex hormone concentrations. This may suggest hormonal control on the regulation of spermatogenesis in this species. Although there are only few reports on the existence of PRs in male gonads, PRs have been detected in Leydig cells, Sertoli cells, germ cells, fibroblasts, and the epithelium of excurrent ductules in sea turtles (Otsuka *et al.*,

2008). The localization of PR has been detected in testes of immature rats (Weber *et al.*, 2002), chicken (Seiki *et al.*, 1981), and spiny dogfish (Cuevas and Callard, 1992), indicating that P plays an important role in the development of the testes of immature mammals and lower vertebrates. In sperm, P was thought to induce androgen receptors (AR) expression to initiate acrosome reaction (Sirivaidyapong *et al.*, 1999), and localization of its receptor has been reported in the cell membranes of spermatocytes and spermatids in rats (Galena *et al.*, 1974) and in the sperm of dogs (Sirivaidyapong *et al.*, 1999). A recent study by Otsuka *et al.* (2008) also reported PR expression in both the testes and epididymis of the turtle *Chelonia mydas*. In these tissues, PRs were expressed in Sertoli, Leydig and germ cells, and in the epithelial cells of the excurrent ducts. In the testis, as the number of cells that contain PR increased with each successive stage, they suggested that P plays key roles in Leydig and Sertoli cells' maturation and function in the green turtles. In *H. flaviviridis*, PRs also were strongly expressed in the epididymis during the active phase, but was negatively expressed in the RSS. Expression of PRs in the epididymis of *H. flaviviridis* during the active phase may also suggest a hormonal role in sperm maturation in the epididymis. Pietrobon *et al*., (2003) reported PR expression in mouse sperm during maturation and capacitation in the epididymis. P produced by Leydig cells regulates the transportation of sperm and epithelial secretions in efferent ductules via PR (Ergün *et al.*, 1997), indicating that if the epididymis of *H. flaviviridis* have these functions, they might be regulated by P. The RSS showed no PR expression during the active phase of spermatogenesis which may indicate that P and E_2 had no stimulatory effect in the development of the RSS. Prasad and Sanyal (1969) demonstrated that anabolic and androgenic steroids stimulated the development of the RSS in male and female geckos and that E_2 and P had no stimulatory effect.

Although further studies are required for a more detailed understanding on the role of steroid hormone receptors in regulating male reproductive organs of *H. flaviviridis* during the reproductive cycle, the findings related to PR expressions in male *H. flaviviridis* are the first reported and may provide further information to understanding the role of sex steroid hormones in the control and regulation of reproductive organs in reptiles. In general, few published studies have detailed comprehensively the correlation between plasma steroid hormone concentrations and the timing of

reproductive events in male squamate reptiles. Thus the information presented in this study may be useful for future research.

In this study, seasonal variation in plasma C concentrations was not correlated with the testicular cycle and showed no significant variations throughout the reproductive cycle. Therefore, any stress caused by handling and blood sampling was unlikely to have had a significant impact on plasma steroid concentrations in this species. Tokarz *et al*. (1998) reported that plasma C concentrations of *Anolis sagrei*, measured on a monthly basis were negatively correlated with monthly changes in testes mass and positively correlated with monthly changes in abdominal fat-body mass. Kreger and Mench (1993) considered the impact of handling and restraint on *Tiliqua scincoides* and found no significant chronic effect on plasma concentrations of C. Additionally, Moore *et al*. (1991) observed that the effects of acute handling stress in the lizard *Urosaurus ornatus* were rapidly dissipated. However, other studies showed that stress caused by capture, confinement, and repeated blood sampling in male and female reptilian species triggered rapid changes in plasma sex steroids concentrations, gonadotropin, and corticosteroids in turtles (Licht *et al.*,1985; Mahmoud *et al.*, 1989; Mahmoud and Licht, 1997), alligators (Lance and Elsey, 1986), and tuatara (Cree *et al.*, 1990a,b). These studies suggested that stress can alter the hormonal concentrations from natural conditions. The mean plasma steroid concentrations reported in this study reflect those in natural conditions. Klukowski, (2011) reported that male *Sceloporus undulates* captured during the breeding and postbreeding periods demonstrated different response to stress when captured and kept for a 4-hour confinement. Post-breeding lizards had higher plasma C concentrations than breeding lizards which may indicate that breeding lizards had more tolerance to stress than post-breeding lizards.

In this study, the situation was different since the lizards were sacrificed immediately upon capture, and there was only a brief period for the lizards to react to capture and handling. Thus, there was no pattern in the plasma C concentrations except for the months of January–March when plasma C concentrations rose slightly.

In this study, there was no significant relation between the haematocrit and plasma C concentrations. Amey and Whittier (2000) reported that in the bearded dragon lizard

(*Pogona barbata*), high haematotocrit is an indicator of dehydration and it may stimulate C secretion.

Temperature is an important factor influencing reptilian reproduction. An annual spermatogenic cycle is the most common pattern, and reptiles must reproduce during the warmer months, because completion of spermatogenesis typically requires a period of eight to ten weeks with body temperatures above 20^{o}C (Saint Girons, 1985). Extrinsic factors, such as diet, relative humidity (Shanbhage, 2002), rainfall (DeWolfe and Telford, 1966) and climatic variations at different altitudes (Licht and Gorman, 1975), may affect the reproductive cycle. Some lizards, such as *L. rhomboidalis* (Wilhoft, 1963), have a slower process of spermatogenesis that extends throughout the year, with spermiation occurring only in spring. Mean annual temperature levels in Oman were above 20^{o}C throughout the reproductive cycle. In this study, temperature and other physical factors such as photoperiod (13 hours during the breeding period and 12 hours during the prebreeding period), rainfall and humidity appear not to be important factors in influencing the reproductive events in the male house gecko of Oman (Figures 3.1A, 3.1B, and 3.1C). However, between January and February there was a decrease in the daily activities when the temperature reached below 20^{o}C.

Testicular organization of the gecko was similar to other reptiles (Pudney, 1995). As germ cells developed spermatogenically, they migrated from the basal lamina of the seminiferous epithelium towards the lumina of the seminiferous tubules, which was similar to that described for other lizards such as *Podarcis muralis* (Gribbins and Gist, 2003). The largest diameters of the seminiferous tubules and the highest measurements in germinal epithelial height occurred in the spring in the house gecko and was similar to other lizards, which are known to breed or show courtship behaviour during this time (Fitch, 1970; Trauth, 1994).

The testes in *H. flaviviridis* were spermatogenically inactive during the quiescent phase (June–August). This inactivity was characterized by the presence of only spermatogonia A and B within the germinal epithelium, as well as low rates of mitotic activity. In September, spermatogenesis again had an increase in activity and mitotic divisions of spermatogonia were very common near the basement membrane of the seminiferous epithelium, consistent with recrudescence of spermatogenesis. This

increase in spermatogenic activity, seminiferous tubule diameter and epithelial height right before the winter period and a continuation of spermatogenesis in the following spring is commonly referred to as a Mixed-Type of reproductive/ spermatogenic cycle (Goldberg, 1972). The testicular organization and germ cell development strategies in squamates, however, differ greatly from that of birds and mammals (Rossen-Runge, 1977; Kumar, 1995; Foreman, 1997) in which a spatial germ cell development strategy is employed during spermatogenesis.

Spermatogenesis in *H. flaviviridis* is prenuptial, similar to that of other lizard species (Fitch, 1970; Sarkar and Shivanandappa, 1989; Shanbhag *et al.*, 2000b; Noriega *et al.*, 2002; Ferreira *et al.*, 2009). Most squamate reptiles occupying the temperate and subtropics regions have a more temporal germ cell development, where germ cell generations move and complete the stages of spermatogenesis as a single cohort during the reproductively active months (Gribbins and Gist, 2003). In, *H. flaviviridis*, spermatogonia A and B were present throughout the entire year in close association with basally located Sertoli cells. Spermatogenesis occurred once every year with similar mitotic and meiotic activity for every cycle. Spermiogenesis climaxed during the active phase and major spermiation events occurred during this phase, leading to a single burst of spermatozoa release. These observations confirmed that *H. flaviviridis* exhibit a temporal germ development strategy similar to other lizard species (Gribbins and Gist, 2003; Rheubert *et al.*, 2009).

The ultrastructure of the spermatozoa of *H. flaviviridis* corresponded well to that of other gekkonidae species and in main parts to that of other lizards (Jamieson *et al.*, 1996; Teixeira *et al.*, 1999a,b; 2002; Giugliano *et al.*, 2002; Ferreira and Dolder, 2003b; Vieira *et al.*, 2004; 2007; Colli *et al.*, 2007; Gribbins *et al.*, 2007; Rheubert *et al.*, 2010a; 2011a). The spermatozoa of *H. flaviviridis* exhibited the following ultrastructural characteristics: acrosomal complex consisting of acrosome and subacrosomal cone; acrosome vesicle divided into medulla and cortex; apical portion of acrosome was depressed; single prenuclear perforatorium positioned at the centre of the flattened acrosome; proximal centrioles, short distal centrioles; peripheral fibres of the distal centrioles and axoneme; short nuclear rostrum, nucleus narrow basally, midpiece short and fibrous sheath extending into midpiece; annulus; mitochondria columnar; dense bodies solid, in regular and complete rings, juxtaposed to the fibrous

sheath; ring structures of dense bodies separated by mitochondrial tiers; and thick zone of cytoplasm between plasma membrane; fibrous sheath in the anterior portion of principal piece; and axoneme extending throughout the flagellum.

All lizard spermatozoa are slender, as in *H. flaviviridis*, except in the lizard *Nangura spinosa* (Jamieson and Scheltinga, 1993) which possess a larger diameter. The epinuclear electron-lucent zone is usually absent in Scincidae (Jamieson and Scheltinga, 1993) and Gekkonidae (Jamieson *et al.*, 1996). Among the Squamata, the spermatozoa almost always present linear mitochondrial cristae, intermitochondrial dense bodies, a short and distal centriole, and the fibrous sheath beginning already in the midpiece. The centriole serves as a pattern for axoneme formation and this process is similar for all Squamata (Al-Hajj *et al.*, 1987; Phillips and Asa, 1993). Nine peripheral dense fibres follow parallel to the nine doublets, as well as a single dense fiber attached to one of the central pair of microtubules which is characteristic of all Squamata. Another characteristic for Squamata is the presence of a short distal centriole. It does not extend along the entire midpiece, but ends well above the annulus, within the layer of encircling mitochondria. In Sphenodontia and Chelonia the distal centriole is long (Healy and Jamieson, 1992; Jamieson and Healy, 1992; Oliver *et al.*, 1996). The annulus occurs in most reptiles and is also found in many invertebrate groups (Baccetti and Afzelius, 1976). It consists of a set of closely associated filamentous sub-units, adjoined and firmly adhering to the plasma membrane. Its function is to avoid the dislocation of mitochondria from the midpiece during flagellar movement (Fawcett, 1970).

The peripheral fibres of the distal centrioles and axoneme are characteristic for reptiles (Jamieson *et al.*, 1997). These peripheral fibres apparently lend extra motor force, contributing to bending movements (Hamilton and Fawcett, 1968). Another function attributed to these peripheral fibres is a control mechanism for sperm movement (Anderson and Personne, 1969). These peripheral fibres also stabilize, longitudinally, the rings that make up the fibrous sheath (Austin, 1965). This sheath has elastic properties that also suggest a role in spermatozoon mobility (Fawcett, 1970). The dense bodies in *H. flaviviridis* form rings that closely resemble those of other lizard species (Jamieson *et al.*, 1996; Oliver *et al.*, 1996; Teixeira *et al.*, 1999a,b; 2002; Scheltinga *et al.*, 2000; 2001; Ferreira and Dolder, 2003b; Rheubert *et*

2011a). Other Squamata present dispersed or helically arranged dense bodies (Jamieson, 1995; Oliver *et al.*, 1996). The dense bodies are considered to originate from mitochondria and are homologous to the intermitochondrial dense bodies (Carcupino *et al.*, 1989; Healy and Jamieson, 1992).

The pattern of the axoneme microtubules in the flagellar end piece of lizards varies greatly, where it may maintain the typical 9+2 arrangement (Scheltinga *et al.*, 2000; 2001) or disarrange this typical pattern, as in other Squamata (Jamieson *et al.*, 1996). The radial projections observed in the region described as the nuclear shoulders, are observed in *H. flaviviridis* and other lizard species (Al-Hajj *et al.*, 1987; Jamieson *et al.*, 1996; Vieira *et al.*, 2001; Ferreira and Dolder, 2003b).These structures most likely establish connection between the microtubules of the manchette and the nucleus as defined by Butler and Gabri (1984) and Al-Hajj *et al.* (1987). The great electron density of the nucleus, resulting from the extreme chromatin condensation, favours mobility and protects the genome against physical and chemical alterations during transport and storage (Krause, 1996). This elongated shape is established during spermiogenesis by the manchette (Soley, 1994) and by the degree of DNA and protein aggregation (Fawcett *et al.*, 1971).

Detailed ultrastructural features of spermatogenesis in *H. flaviviridis* was described for the first time in this study. This work may contribute toward the confirmation of a close phylogenetic relationship between the species of this genus. For example, Jamieson (1995) found that a single perforatorium may be a synapomorphy for squamates in their study of Iguania, and Jamieson (1999), Vieira *et al.* (2004), and Rheubert *et al.* (2010a) corroborated these data in their analysis within the Squamata. Also, the peripheral fibres associated with microtubule doublets 3 and 8 are grossly enlarged in squamates (Jamieson, 1995, 1999; Cunha *et al.*, 2008), whereas in *Sphenodon* they are not (Healy and Jamieson, 1992). Few studies have been reported on the mature spermatozoa of geckos (Furieri, 1970; Jamieson *et al.*, 1996; Röll and von Düring, 2008); however, only one study highlights the ultrastructure of spermiogenesis within the Gekkonidae (Rheubert *et al.*, 2011a).

Leydig and Sertoli cells of *H. flaviviridis* showed steroidogenic ultrastructural features characteristic of steroidogenic activity at different phases of the testicular cycle

similar to those reported in other reptiles (Callard *et al.,* 1976; Mahmoud *et al.*, 1985a; Dubois *et al.,* 1988; Mahmoud and Licht, 1997; Khan and Rai, 2004; Boretto *et al.*, 2010). Evidence of temporal separation of function in the two cells was also based on the asynchronous changes in the ultrastructure steroidogenic feature. The present study indicated that Leydig cells were active prior to spermatogenesis, associated with low plasma T concentrations and the onset of the ultrastructural steroidogenic features. Leydig cells remained active for the rest of the entire reproductive cycle. The Leydig cells began to increase their steroidogenic activities in synchrony with the increase in the ultrastructural steroidogenic features and expression for PRs. The ultrastructural steroidogenic features in Sertoli cells began to develop in October and, like the Leydig cells, they remained active for the rest of the cycle. This is consistent with the concept of a temporal separation of androgen secretion and spermatogenesis (Licht, 1982).

Sertoli cells have various functions essential for spermatogenesis, e.g. support and nutrition of the germ cells, release of mature spermatids into the lumen of the seminiferous tubule, phagocytosis both of residuals of released and degenerated spermatids, secretion of androgen-binding protein, and formation of the blood–testis barrier (Baccetti. *et al.*, 1983; Röll and van Düring, 2008). Ferreira and Dodler (2003a) reported in the lizard, *Tropidurus itambere* that glycoprotein secretions in cytoplasmic extensions of these cells are consistently present throughout the reproductive period as well as the quiescent period. During the entire reproductive cycle, Sertoli cells support all stages of germ cells throughout the active period but are disorganized during the quiescent period. Higher organization of Sertoli cells is expected during active spermatogenesis, where glycogen and glycoconjugates are associated with germ cell nutrition. Sertoli cells are the source of a large number of proteins that are secreted (Griswold, 1988). Sertoli cells also secrete macromolecules at their abluminal side. The glycogen in cytoplasmic extensions has an important function in energy supply to spermatids and spermatozoa (Dufaure, 1971). The presence of lipid droplets in germ cells during the different reproductive phase seen in this study may be an indicative of protein secretions which are presumably used to facilitate metabolically demanding processes such as spermatogenesis (Olsson *et al.*, 1997).

Khan and Rai (2004) demonstrated *in vitro* that FSH stimulates the Sertoli cell nursing function by the increase in lactate production (which is utilized by the germ cells as an energy substrate). This confirms the *in vivo* studies in several lacertilian species, including *H. flaviviridis*, in which mammalian FSH alone was capable of controlling spermatogenesis (Reddy and Prasad, 1970a,b; Licht, 1984; Rai and Haider, 1986; Callard, 1991). Also, FSH alone regulates the testicular functions, spermatogenesis, and steroidogenesis in lizards (Reddy and Prasad, 1970b; Licht, 1984; Rai and Haider, 1986, 1995).

T is reported to induce spermatogenesis and sperm production in *Uromastix hardwickii* (Ramaswami and Jacob, 1963), whereas it could neither initiate the spermatogenesis in regressed phase in *H. flaviviridis* (Rai and Haider, 1986) nor maintain the spermatogenesis in hypophysectomised wall lizards during the breeding phase (Reddy and Prasad, 1970b); rather, it caused the degeneration of germ cells and regression of Sertoli as well as Leydig cells (Rai and Haider, 1986). Bhaktaraj *et al.*, (2000) reported administration of T alone initiated mitotic proliferation of spermatogonial cells in *Calotes versicolor* during the non-breeding phase. Furthermore, T treatment in combination with GnRH resulted in the formation of spermatozoa, though exogenous GnRH alone in *in vivo* could stimulate the spermatogenesis through gonadotropin up to spermatid stage. Similarly, the synergistic effect of testosterone and FSH are also reported in mammals (Bartlett *et al.*, 1989; Huang *et al.*, 1991; Lerchl *et al.*, 1993).

The stimulatory effect of FSH alone or in combination with dihydrotestosterone (DHT) on lactate production by Sertoli cells was significantly enhanced, whereas DHT alone significantly reduced the lactate secretion by Sertoli cells (Khan and Rai, 2004). This confirms that androgens have additive effect on the nursing function of Sertoli cells only when they are in an activated state in response to gonadotropin (Khan and Rai, 2004). Therefore, synchronization of both the testicular activities in lizards, including *H. flaviviridis* (Licht, 1984; Rai and Haider, 1986; Khan and Rai, 2004), suggests the involvement of androgens, in addition to gonadotropins, in the control of spermatogenesis.

Recently, in addition to gonadotropins and androgen, increasing importance has been attached to the role of E_2 in male reproduction of mammals (Staub and De Beer, 1997), though the reports are ambiguous. E_2 *in vivo* accelerates gonadal recrudescence in photoregressed male Siberian hamsters via a mechanism independent of FSH (Pak *et al.*, 2002). On the other hand, E_2 decreases the spermatocytes number of foetal rat testis in *in vitro* culture (Lassurguere *et al.*, 2003). In reptiles, the high concentration of E_2 in autumn has been suggested as an important contribution factor in the blockage of spermatogenesis for a seasonally breeding lizard *Podarcis sicula*, (Cardone *et al.*, 2002). Khan and Rai (2004) also demonstrated the inhibitory effect of E_2 on lactate production by Sertoli cells. However, E_2-induced suppression was more pronounced than DHT possibly due to the major role of E_2 in inducing post-reproductive refractoriness, as suggested in male *Podarcis sicula sicula* (Paolucci and Di Fiore, 1992). The present investigation of normal populations of male *H. flaviviridis* reports increased plasma E_2 concentrations during the recrudescent and active phases which confirms a stimulatory effect on testicular activities. This observation provides the background for future studies to explore the role of E_2 in maintaining the testes in a regressed state during the non-breeding phase.

In many lizards, including the geckos *H. flaviviridis* and *P. dubia*, Leydig cells are most numerous in quiescent testes and sparsest in active testes (Fox, 1977). However, the low number in active testes could be due to dispersion of the interstitial cells as a result of the expansion of the seminiferous tubules. Most of the Leydig cells of the males investigated here include lipid droplets that are necessary for steroids production. During the active phase, the cytoplasm and endoplasmic reticulum are well developed with many mitochondria and lipid inclusions. Upadhyay and Guraya (1972) verified that the diffuse lipids present in these cells consist of phospholipids, triglycerides, and/or cholesterol. All agree that these lipid characteristics of Leydig cells are directly related to the production of steroids controlling spermatogenesis. In Indian population of *H. flaviviridis* maximum secretory activity of the Leydig cells was found during the breeding season and minimum activity during the sexually quiescent phase (Rai and Haider, 1986). A marked hypertrophy of the Leydig cells has been demonstrated when sexually quiescent individuals of *H. flaviviridis* were treated with FSH (Rai and Haider, 1986). An abundance of diffuse lipoproteins, as

demonstrated histochemically, may also serve as a reservoir of hormone precursors (Guraya, 1968). According to Upadhyay and Guraya (1972), the anatomical relationship between lipid inclusion bodies and cytoplasmic membranous components (or diffuse lipoproteins) favours possible interactions between these components, resulting in steroid biosynthesis. The accumulation of lipid droplets in the interstitial gland cells of the testis of lizards, which show little spermatogenetic activity, suggests that the cells may function as reservoirs for a hormone precursor that is necessary to stimulate the next reproductive stage.

Khan and Rai (2004) demonstrated *in vitro* endocrine as well as paracrine control of Leydig cell steroidogenesis and proliferation in *H. flaviviridis* during the regressed testicular phase. FSH stimulated Leydig cell proliferation which caused an increase in T production. However, LH had no effect on the testicular functions in squamates including wall lizards (Arslan *et al.*, 1981; Rai and Haider, 1986; Reddy and Prasad, 1970a,b), although Leydig cell steroidogenesis is controlled by LH in amphibians (Tanaka *et al.*, 2004), chelonians (Callard *et al.*, 1976; Licht, 1984), crocodilians (Licht, 1984) and other higher vertebrates (Haider, 2004; Williams, 1992).

In addition, Sertoli cell paracrine factors play important roles in controlling Leydig cell activities as they stimulated T production by both non-activated and FSH-preactivated Leydig cells (Khan and Rai, 2004). FSH-preactivated Sertoli cells enhanced the production of Sertoli cell-secreted steroidogenic factors that in turn increased the T production by Leydig cells. Similarly, FSH-preactivated Leydig cells increased their responsiveness to Sertoli cell-secreted paracrine factors, since FSH-preactivated Leydig cells, in response to Sertoli cell-secreted paracrine factors, produced greater amounts of T than non-activated Leydig cells. In mammals, however, contradictory results are reported. Sertoli cells stimulated both basal and LH-induced testosterone production by Leydig cells and the stimulation was more pronounced in the presence of FSH (Benahmed *et al.*, 1985; Perrard-Sapori *et al.*, 1987; Bellve and Zheng, 1989).

The free spermatozoa that emerge from the efferent duct enter the epididymis of *H. flaviviridis* for further maturation and storage prior to transportation into the hemipenis via the vas deferens. Histologically, the epididymis consists of numerous,

small, convoluted, ductuli epididymis which unite to form a larger ductus epididymis. The ductus epididymis of this species can be divided into anterior, middle, and posterior regions. During the active phase the epithelial cell height and lumen diameter of all the regions of the ductus epididymis were significantly increased and the cells of the anterior and middle regions were filled with secretory granules, which reacted strongly with PAS. This great divergence has been observed among the squamates during the annual cycle (Haider and Rai, 1987; Mesure *et al*., 1991, Desantis *et al.*, 2002; Akbarsha *et al.*, 2006). The avian ductus epididymis is not formed into segments or zones comparable to those in reptiles or eutherian mammals (Jones 1998, 2002).

Furthermore, only two types of cells, principal/secretory and basal, have been conclusively shown to line the epithelium of the ductus epididymidis of the lizards *L. vivipara* (Mesure *et al*., 1991) and *P. sicula* (Desantis *et al*., 2002), two types of tall columnar cells in the crocodile *Caiman crocodilus* (Guerrero *et al*., 2004), four types of cells, vesicular, basal, narrow and mitochondria-rich in the turtle *C. picta* (Holmes and Gist, 2004) and six types of cells, principle, narrow, apical, basal and clear cells, and intraepithelial leucocytes, have been identified in the epithelial lining of the epididymis of the fan-throated lizard *Sitana ponticeriana* (Akbarsha *et al.*, 2006). In the present study, the epithelium in the ductus epididymis of *H. flaviviridis* showed only two types of cells at the ultrastructural level; the principal/secretory and the basal cells.

In this study, the anterior and middle regions of the ductus epididymidis were involved in the maturation and preparation of spermatozoa for storage, and protein secretion as PRs were strongly expressed during the spermiation process. The posterior region of the ductus epididymis was involved in sperm storage where sperm transit was slowed by the occlusion of the end of the collapsed ductus deferens as is the case in other lizards (Haider and Rai, 1987; Akbarsha *et al.*, 2006). The anterior and middle regions secrete glycoproteins as discrete biphasic granules which contribute to the physiological maturation of spermatozoa (Depeiges *et al.*, 1988; Morel *et al.*, 1991; 1993; 2000; Nirmal and Rai, 1997; 2000).

Studies on the inhibition of growth and secretory activity of the epididymis in castrated specimens and their maintenance by exogenous T in several squamates (Depeiges and Dufaure, 1977; Akbarsha and Balasubramanian, 1983, including *H. flaviviridis*, Haider, 1985a), suggested the dependence of the epididymis on testicular androgens. It appears that secretory activity of the epididymis in *H. flaviviridis* is parallel to the functional activity of the Leydig cells. Hypophysectomy in reptiles caused regression of both the Leydig cells and accessory reproductive organs (Eyeson, 1971; Licht, 1972), but the gonadotropin responsible for this regression has not been established. In the hypophysectomised lizard, *Agarna agarna*, only mammalian LH has been reported to be capable of maintaining the activity of the Leydig cells as well as the epididymis (Eyeson, 1971). Haider and Rai (1987) suggested that the most active gonadotropin in the male *H. flaviviridis* is similar to mammalian FSH and regulates androgenic secretion.

The secretory cells of the epididymis undergo an annual cycle which has been divided into 10 stages (Mesure *et al.*, 1991). Secretory cells contained vesiculated mitochondria, RER, Golgi complex, and secretory granules at various stages of synthesis before being discharged into the lumen. Each granule is membrane-bound and contained a spherical electron-dense central core and a peripheral vacuole which varies in density. During the active phase, the height of the principal cell increased with a conspicuous increase in volume of mitochondria, RER and Golgi complex. In the post-active phase, the cell undergoes a dramatic involution. After a transient hypertrophy of the RER, numerous autophagic vacuoles invade the cytoplasm. This degeneration can lead to complete lysis of the cell and to its rebuilding after elimination of the greatest part of the cytoplasm. With antibodies raised against the protein family which constitutes the main part of the secretion (L proteins of 19 kDa), it was shown by immunohistochemistry that these proteins are concentrated into secretory granules which are discharged into the lumen to finally bind with the heads of the spermatozoa (Depeiges and Dufaure, 1983; Depeiges *et al.*, 1988).

The pattern of distribution of the different versions of endoplasmic reticulum along the height of the principal cell of *H. flaviviridis* conforms to that described for the principal cells of various mammals (Hermo and Robaire, 2002) and of the lizards, *L. vivipara*, (Mesure *et al*., 1991), *P. sicula* (Desantis *et al*., 2002) and S. *ponticeriana*

(Akbarsha *et al.*, 2006). The abundance and pattern of the Golgi complexes in the principal cells of *H. flaviviridis* epididymis are also comparable to those in mammals and the lizards *L. vivipara* and, to a certain extent, *P. sicula.* Their distribution and the relationship among these organelles suggest synthesis of glycoproteins in the rough and sparsely granulated endoplasmic reticulum which are transferred to the Golgi complexes, in which modification by glycosylation of the proteins would occur and the secretory material is then held and concentrated in the condensing vacuoles which are saccular endoplasmic reticulum cisternae. The condensed material present in these vacuoles forms into discrete granules in the supranuclear and apical cytoplasm. The epididymal secretion of proteins in the form of discrete and structured granules is already known in several species of lizards (Akbarsha and Manimekalai, 1999; Desantis *et al*., 2002; Akbarsha *et al.*, 2006). The present study confirms epididymal secretion in the form of discrete granules to those of other lizard species. The large membrane-bound vesicles containing a homogeneous electron-dense material in the basal cytoplasm of the principal cells of anterior and middle epididymidis of *H. flaviviridis* are lipid droplets, which were reported in other lizards (Akbarsha *et al.*, 2006).

Basal cells have been reported in the lizards *L. vivipara* (Mesure *et al*., 1991), *P. sicula* (Desantis *et al*., 2002), *S. ponticeriana* (Akbarsha *et al.*, 2006), and in the turtle *C. picta* (Holmes and Gist, 2004). The basal cells are confined to the basal aspect of the epithelium and never reach the lumen, although they may extend processes halfway towards the lumen (Veri *et al*., 1993) or even up to the apical part of the epithelium (Abe and Takano, 1989). They form a three-dimensional latticework underneath the tall columnar cells (Young *et al*., 1994). The basal cells in the lizard epididymis resemble those of the mammals in the clear cytoplasm and the sparse organelles (Mesure *et al*., 1991; Desantis *et al*. 2002; Akbarsha *et al.*, 2006; present study). In recent times the basal cell has been attributed with three important roles: (i) supportive role (Young *et al*., 1994), (ii) neutralizing the harmful electrophiles (Veri *et al*., 1993), and (iii) immune surveillance of sperm and other testicular antigens (Seiler *et al*., 1998). Jones (2002) and Akbarsha *et al.* (2006) speculated that the reptilian epididymal epithelium could possess intraepithelial lymphocytes.

In *H. flaviviridis*, the anterior and middle regions of the ductus epididymis are involved in the maturation and preparation of spermatozoa for storage, and secretion of considerable proteins. The posterior sperm storage region is where sperm transit is slowed by widening of the ductus epididymis and by occlusion of the end of the collapsed ductus deferens, as in mammals (Jones 1998, 2002) and other lizards (Akbarsha *et al.*, 2006). The anterior and posterior region secretes glycoproteins as discrete biphasic granules which contribute to physiological maturation of spermatozoa (Depeiges and Dufaure, 1981; 1983; Depeiges *et al*., 1988; Morel *et al*., 1991; 1993; 2000; Nirmal and Rai, 1997, 2000). Several other types of sperm physiology have been indicated in a few studies (e.g. Nirmal and Rai, 1997; Rai and Nirmal, 2003). The posterior region, with its larger diameter, shorter epithelium, highly muscular tunica and more spacious lumen, indicates a role in storage of sperm, as in mammals. The major differences between mammals and several reptiles lie in the epididymal secretion of glycoproteins as granules, with a soluble coat and a dense core (Akbarsha and Manimekalai 1999; Desantis *et al*., 2002; Akbarsha *et al*., 2005) and the highly spacious ductus deferens which, unlike in the mammals, can store sperm (Akbarsha and Meeran 1995; Gist *et al*. 2001; Sever *et al*. 2004; Akbarsha *et al*., 2005). The distal portion of the ductus epididymis and the ductus deferens of the lizard produce spermatozoa at a very slow rate (Akbarsha and Meeran 1995; Gist *et al*., 2001; Sever *et al*., 2004; Akbarsha *et al*., 2005) in order to establish a store of spermatozoa for use during the mating season (Jones, 1998).

Hypertrophy and recrudescence of the *H. flaviviridis* RSS are in synchronous with androgen secretion and spermatogenic activity, similar to those reported in other squamates (Sanyal and Prasad, 1966; Prasad and Sanyal, 1969; Weil, 1984; Krohmer, 2004, Sever and Hopkins, 2005; Rheubert *et al.*, 2011b). Prasad and Sanyal (1969) demonstrated that anabolic and androgenic steroids stimulated development of the RSS in male and female, *H. flaviviridis* and that E_2 and P had no stimulatory effect. Billy and Crews (1986) found that administration of T to the parthenogenetic (all phenotypically female) teiid lizard, *Cnemidophorous uniparens*, resulted in development of the RSS.

During spermatogenic inactivity in June–October, the RSS became indistinguishable from other nephridian tubules. Sperm were present in the posterior ductus deferens of

male *H. flaviviridis* during the active phase (November–May), in the annual spermatogenic cycle and results in the release of sperm into the hemipenis during copulation in spring, coinciding with maximum development of the RSS. In this locale, the female *H. flaviviridis* may possess stored sperm in vaginal crypts during late February–May and large oviductal eggs in March–May. This correlation between mating and RSS activity has been observed in other squamates (Sever and Hopkins, 2004; 2005). Thus, the hypertrophic RSS are often indicators of breeding as they are implicated in seminal fluid production (Prasad and Reddy, 1972) and sperm sustenance (Bishop, 1959). The PAS-positive RSS secretion that contains phospholipids, proteins and amino acids is known to be androgen dependent and they may serve as a source of energy, a substrate for survival of spermatozoa in the oviduct (Sanyal and Prasad, 1966; Reddy *et al*., 1972; Sarker and Shivanandappa, 1989). The nature of the secretion of the active RSS has been reviewed extensively in recent studies by Sever *et al.* (2002) and Krohmer (2004). The PAS reaction found in *H. flaviviridis* has also been reported for other squamates, such as the snake *Seminatrix pygaea* (Sever *et al*., 2002), and *S. laterale* (Sever and Hopkins, 2005). Other studies have indicated that granules may contain a complex of lipids, glycogen, mucopolysaccharides, mucoproteins, and phosphatases, and that the chemical composition may change during the active season (Krohmer, 2004).

This study describes in detail the seasonal ultrastructural changes in the RSS during the reproductive cycle, which have not been reported before in this species. Similar studies on ultrastructural details have also been reported in the gecko, *Hemidactylus turcicus* (Rheubert *et al.*, 2011b). The secretory granules at the ultrastructural level have invariably been described as electron-dense granules. Sever and Hopkins (2005) characterized the epididymal secretory granules of lizards as being composed of a "dense central core and a peripheral vacuole." This cytology is very similar to that of the secretory granules of the RSS of *H. flaviviridis,* in which the present study found a dense core surrounded by a more electron-lucent collar. The epididymis of squamates is the only source of seminal fluid other than the RSS. The similarity in ultrastructure between the epididymal and RSS secretory granules indicates that a similar product may be produced (Sever and Hopkins, 2005).

In conclusion, this chapter reports the histology, histochemistry, ultrastucture and hormonal control of the reproductive system in *H. flaviviridis*, the testes, epididymis, vas deferens and RSS, during the annual reproductive cycle. The epithelial organization of these organs in relation to hormonal concentrations, stress and environment reflects a role in the maintenance of the reproductive cycle. This study presents the first detailed ultrastructural description of spermatogenesis, steroidogenic ultrastructural features of Leydig and Sertoli cells, and ultrastructual description of epididymis and RSS in *H. flaviviridis*. Our understanding of the evolution of germ cell development strategy and the process of spermatogenesis, spermiogenesis, epididymal and RSS development in relation to hormonal control within vertebrates may become clearer by investigating the reproductive biology, patterns and strategies in reptilian species.

Due to a lack of published work in which data on reproductive biology and coincident steroid hormone profiles are available, further studies are required to elucidate the hormonal control of reproductive biology in male *H. flaviviridis* and other squamates.

Chapter Four:

The reproductive cycle of the female house gecko, *Hemidactylus flaviviridis* (Gekkonidae)

4.1 Introduction

Female reproductive cycles have been studied in many species of lizards (e.g. Licht, 1984; James and Shine, 1985; Whittier and Crews, 1987; Sarkar and Shivanandappa, 1989; Shanbhag and Prasad, 1993; Flemming, 1994; Ramirez-Pinilla, 1995; Huang, 1996; Shanbhag *et al*., 1998; Edwards *et al*., 2002; Ikeuchi, 2004; Menezes *et al*., 2004; Jimènez-Cruz *et al*., 2005; Holmes and Cree, 2006; Loverrn, 2011). In squamates, oviposition usually occurs at the time of year that provides optimal conditions for growth and survival of hatchlings. Lizards in the temperate and sub-tropical zones breed seasonally, usually in late spring or summer (Varma and Guraya, 1975; Licht, 1984; Vitt and Blackburn, 1991; Shanbhag and Prasad, 1993; Huang, 1996; Ikeuchi, 2004). Their gonadal development is essentially synchronous within a population, resulting in a short, well defined breeding season (Licht, 1984). The timing of ovulation and the length of gravidity are key variables determining when oviposition occurs in oviparous squamates (Heatwole and Taylor, 1987; Loverrn, 2011), and a variety of reproductive strategies have evolved to ensure that young are hatched into favourable conditions.

In the majority of lizard species studied, the most common reproductive pattern is one in which vitellogenesis, ovulation, gravidity and oviposition are all completed within one year (Guraya and Varma, 1976; Shine, 1985; Diaz *et al.*, 1994; Ota, 1994; Huang, 1997; Okada *et al.*, 2002; Shanbhag, 2002; Ikeuchi, 2004). Squamate ovarian follicles undergo a period of early growth known as previtellogenesis, in which RNA and nutrients are transferred into the follicle but no yolk is deposited (Uribe *et al*., 1995; 1996; Motta *et al.*, 1995; 2001). This is followed by more rapid growth (vitellogenesis) as yolk protein accumulates in the oocyte (Guraya and Varma, 1976; Guraya, 1989; Uribe *et al*., 1996; 2000). Two patterns of yolk deposition have been described in temperate zone squamates (Aldridge, 1979; Yokoyama and Yoshida, 1994): type I, in which vitellogenesis is initiated and completed wholly after spring emergence prior to ovulation as occurs in some snakes (Whittier *et al*., 1987; Yokoyama and Yoshida, 1994); and type II vitellogenesis, which begins in late summer or autumn following ovipostion and is completed the following spring (Yokoyama and Yoshida, 1994; Lind *et al.*, 2010). In many reptiles, ovulation usually occurs in spring (Sanyal and Prasad, 1967; Guraya and Varma, 1976; Xavier, 1982;

Shanbhag and Prasad 1993; Shine *et al*., 1996; Shanbhag, 2002; Lind *et al.*, 2010), presumably to allow oviposition to begin as early as possible once thermal conditions have become favourable in the active season. Females are usually gravid during the warmer part of the active season, as the length of gravidity is largely determined by temperature (Castilla and Swallow, 1996). The rate of embryonic development increases with rising temperature, and so gravidity length is influenced by the body temperature and thermoregulatory opportunities of the gravid female (Schwarzkopf and Shine, 1991; Shanbhag, 2002; Willson and Brooks, 2006). The timing of the mating period usually coincides with spring ovulation (Taylor, 1985; Rostal *et al.*, 1998; Shanbhag, 2002). In such species, the hormonal control of gonadal development is related to courtship and copulation (Whittier and Crews, 1987; Crews and Gans, 1992).

Ovarian morphology and follicular development are well known for several species of squamates (Guraya, 1989; Shanbhag and Prasad, 1993; Uribe *et al*., 1995; 1996; 2000; Shanbhag *et al*., 1998; Gómez and Ramírez-Pinilla, 2004; Hernández-Franyutti *et al.*, 2005; Vieira *et al.*, 2010). The general sequence of folliculogenesis has been described in a number of reptiles; some variation between species has been reported (e.g., Guraya, 1989; Uribe *et al.*, 1996; Uribe and Guillette, 2000; Gómez and Ramírez-Pinilla, 2004; Siegel *et al.*, 2009b; Vieira *et al.*, 2010). Follicular growth in the reptilian ovary is a complex process that includes physiological and morphological changes in the oocyte (nucleus, ooplasmic components, and deposition of yolk), as well as modifications in the peripheral structures such as the zona pellucida, follicular epithelium, and theca (for reviews, see Hubert, 1985; Guraya, 1989; Norris, 2007). In most species of reptiles, maturation and the majority of the growth of the preovulatory oocyte occurs during vitellogenesis, involving formation of a telolecithal egg, with large amounts of yolk (Gómez and Ramírez-Pinilla, 2004).

In reptiles, extensive evidence, both direct and indirect, demonstrates that follicle cells (granulosa) execute multiple and variable functions throughout life and at different stages of gamete and follicle development. Follicle cells have been implicated in a number of gonadotrophin-regulated processes involving oocyte growth and maturation. These include steroidogenesis (Joss, 1985; Al-Kindi *et al.*, 2001), initiation of yolk protein (vitellogenin) uptake (Ho, 1987), and other processes such as

RNA transfer (Motta *et al.*, 1995) and organelle transfer (Andreuccetti, 1992; Motta *et al.*, 1995). In reptiles, during different stages of folliculogenesis, the granulosa is first arranged as a single layer of homogeneous cells. As folliculogenesis progresses, the granulosa cells of the previtellogenic oocyte are transformed and become polymorphic and multilayered, being characterized by the presence of three distinct cells: small, intermediate and pyriform cells (Guraya, 1989; Uribe *et al.*, 1996; Uribe and Guillette, 2000).). The heterogeneity of the granulosa cell population disappears from the vitellogenic oocytes by regression of intermediate and pyriform cells via programmed cell death (apoptosis) (Motta *et al.*, 1996, 2001).

Follicular atresia, a process by which the ovarian follicles degenerate, is of wide-spread occurrence in the ovaries of all reptiles. The histological changes in the follicles undergoing atresia have been documented in many species of squametes (Hubert, 1985; Sarkar & Shivanandappa, 1989; Guraya, 1989; Uribe *et al.*, 1995; Gómez and Ramírez-Pinilla, 2004). Atretic follicle functions are poorly understood in reptiles. They may be related to clutch size regulation (Jones and Swain, 2000), and to steroid hormone production (Gouder *et al.*, 1979).

In lizards, following ovulation, secretory CL are formed from postovulatory follicles, and fertilized eggs are retained in the oviduct for a species-specific duration before oviposition (Saidapur, 1982; Xavier, 1987; Jones and Baxter, 1991; Villagrán-Santa Cruz and Méndez de la Cruz, 1999). The morphological changes during luteogenesis and luteolysis in the CL are described in many lizard species (Varma & Guraya, 1973; Guraya & Varma, 1976; Gouder and Nadkarni, 1976; Sarkar & Shivanandappa, 1989; Uribe *et al.*, 1995; Shanbhag *et al.*, 1998; Shanbhag *et al.*, 2001; Gómez and Ramírez-Pinilla, 2004). In reptiles, CL functions in the production of P and the inhibition of vitellogenesis (see further below).

In lizards, the oviducts function in egg uptake and transport, fertilization, sperm storage, albumen production, eggshell deposition, maintenance of the early embryo, and oviposition (for reviews see Blackburn 1998, Girling, 2002). The Gekkonidae family includes both viviparous and oviparous species (Girling *et al.*, 1998). In oviparous species, such as *H. flaviviridis*, a prominent function of the oviducts is eggshell production. In viviparous species, oviducts act in the formation of the

placenta (Blackburn, 1998; Girling, 2002). In addition to providing a nurturing environment for the egg, specializations of the oviduct may also contribute to variations in the reproductive cycle of geckos. Some species of the family Gekkonidae store sperm in specific oviduct regions, dissociating mating from fertilization (Nogueira *et al.*, 2011).

The structure of the reptilian oviduct has been studied in many lizard species (Haider, 1985b; Adams and Cooper, 1988; Uribe *et al.*, 1988; Guillette *et al.*, 1989; Picariello *et al.*, 1989; Girling *et al.*, 1997; 1998; Adams *et al.*, 2004; Nogueira *et al.*, 2011). The reptilian oviduct is usually divided into five regions: infundibulum, uterine tube, tubal–uterine junction (isthmus), uterus, and vagina (Girling *et al.*, 1998). At the anterior end, the infundibulum receives the ovulated egg through an ostial opening. The infundibulum leads into the uterine tube and then through the isthmus into the uterus. Most posterior is the vagina, which leads into a common urogenital sinus (cloaca, Fox, 1977). The oviduct regions differ histologically in their epithelia, glands, and myometrial layers. Seasonal cycles occur in all oviductal regions, most prominently in the uterine region, and are under hormonal control (Blackburn, 1998). All five oviductal regions are not recognised in every reptilian species examined. For instance, Kumari *et al*. (1990) considered the uterine tube to be the posterior part of the infundibulum in the agamid lizard, *Calotes versicolor*. The lizard *Sceloporus woodi* has a single uterine region, which is responsible for the secretion of both shell fibres and calcium (Palmer *et al.*, 1993).

The reptilian oviduct can be divided into three main layers, which vary in thickness and function in different regions (Blackburn, 1998; Girling, 2002). The inner layer or mucosa is subdivided into ciliated and nonciliated cells that line the lumen of the oviduct, and an underlying lamina propria, which contains connective tissue, blood vessels and any glands present. The middle layer contains smooth muscle (muscularis) that has an inner circular and/or outer longitudinal muscle layer. The outermost layer is the serosa and is continuous with the peritoneum (Blackburn, 1998; Girling, 2002).

Two major cell types are found throughout the reproductive oviduct of reptiles; microvillous nonciliated and ciliated cells (Palmer and Guillette, 1988; Sarker *et al.*,

1995, 1996; Girling *et al.*, 1997; 1998; Corso *et al.*, 2000). However, a third cell type, bleb cells, have been reported in the infundibulum of oviparous geckos *Hemidactylus turcicus* and *Saltuarius wyberba*, (Girling *et al.*, 1998) and viviparous geckos *Hoplodactylus maculates* (Girling *et al.*, 1997), *Hoplodactylus maculates* and *Hoplodactylus duvauvelii* (Girling *et al*., 1998). The function of bleb cells is unknown, but they may be involved in apocrine or merocrine secretory processes (Palmer and Guillette, 1988). Cell shape, size, definition, and other morphological characteristics, such as microvillous height and cilia number, have been assessed and related to stages of the reproductive cycle in many reptiles (Haider, 1985b; Uribe *et al.*, 1988; Guillette *et al.*, 1989; Picariello *et al.*, 1989; Girling *et al.*, 1997; 1998; Adams *et al.*, 2004; AlKindi *et al.*, 2006; Nogueira *et al.*, 2011).

Reptilian oviductal epithelia also undergo morphological changes in response to seasonal variations that correlate with seasonal hormonal cycles. In particular, E_2 during the vitellogenic period is responsible for cell hypertrophy, an increase in gland number, and in secretory activity (Mead *et al.*, 1981; Abrams Motz and Callard, 1991; Girling *et al.*, 2000; AlKindi *et al.*, 2006). P has been implicated in the regulation of oviductal function in oviparous reptiles (Klicka and Mahmoud, 1977; Paolucci and Di Fiore, 1994; Shanbhag *et al.*, 2001; AlKindi *et al.*, 2006) and egg-shelling (Cuellar, 1979; Radder *et al.*, 2001; AlKindi *et al.*, 2006).

Relationships between gonad development, steroidogenesis, and plasma sex steroid concentrations have been studied in many reptiles (Licht *et al.*, 1980; Mendonça and Licht, 1986; Diaz *et al.*, 1994; Mahmoud and Licht, 1997; Owens, 1997; Staub and De Beer, 1997; Amey and Whittier, 2000; Edwards and Jones, 2001a; Al-Kindi *et al.*, 2001; AlKindi *et al.*, 2006; Mahmoud *et al.*, 2006). In squamate females with a seasonal cycle, an annual pattern of plasma concentrations is usually evident for each of the three primary steroids E_2, P and T, suggesting a role for each steroid in the regulation of various stages of the annual reproductive cycle. In addition to the direct actions of each hormone, many aspects of reproductive physiology are known to be under multihormonal control (Guillette *et al.*, 1981; Ho *et al.*, 1982; Ho, 1987; Callard *et al.*, 1992).

In most reptiles, plasma E_2 concentrations typically rise at the onset of vitellogenesis which is essential for follicular development and maturation (Bona-Gallo *et al.*, 1980; Joss, 1985; Owens and Morris, 1985; Moore and Crews, 1986; Ho, 1987; Nagahama, 1987; Jones *et al.*, 1997; Amey and Whittier, 2000; Jones, 2011). E_2 is almost exclusively responsible for the stimulation of hepatic vitellogenesis in reptiles (Callard *et al*., 1972b; Callard and Ho, 1987; Ho, 1987; Kime, 1987; Diaz *et al.*, 1994). It may also have a role in the uptake of vitellogenin by the follicle, which is known to induce cellular endocytosis (Callard and Ho, 1987). E_2 is synthesised by the growing follicles (Etches and Petitte, 1990) and plasma E_2 concentrations fall rapidly at or around the time of ovulation (Callard *et al*., 1978; Bona-Gallo *et al*, 1980; Yokoyama and Yoshida, 1994). The annual patterns of circulating E_2 concentrations vary among oviparous squamates.

P plays an important role in the maintenance of gravidity in lizards (Moore *et al.*, 1985; Fox and Guillette, 1987; Diaz *et al.*, 1994; Radder *et al.*, 2001; Shanbhag *et al.*, 2001; Jones, 2011). This may be an indirect role through the antigonadal properties ascribed to P (Callard *et al*., 1972a). Elevated plasma P concentrations are thought to inhibit E_2-induced follicular growth during gravidity (Callard *et al*., 1972b; Guillette *et al.*, 1981; Ho, 1987), ensuring that vitellogenesis and gravidity or gestation are mutually exclusive (Callard *et al.*, 1992). Elevated plasma P concentrations are related mainly to the secretory activities of CL. Plasma P concentrations peak during the gravidity period as the eggshell and eggshell membrane are formed (Callard *et al.*, 1972a,b; Lewis *et al.*, 1979; Jones and Guillette, 1982; Moore and Crews, 1986; Fox and Guillette, 1987; Jones and Baxter, 1991; Sarkar *et al.*, 1996; Mahmoud and Licht, 1997; Edwards and Jones, 2001a; Shanbhag *et al.*, 2001). The life span of the CL has been positively correlated with P production in some species (Callard *et al*., 1972b; Bona-Gallo *et al*., 1980), but not in others (Guillette *et al.*, 1981; Guarino *et al*., 1998). As with circulating E_2 concentrations, there is a considerable variation in patterns of circulating P concentrations among squamates, especially regarding the proportion of gravidity or gestation during which P remains elevated (Xavier, 1982; Van Wyk, 1994; Jones *et al.*, 1997).

In female reptiles little is known about the function of T in reproduction beyond its importance as a precursor in the synthesis of E_2 (Staub and De Beer, 1997). In

oviparous species a cyclical pattern of plasma T concentrations is apparent (Arslan *et al*., 1978a; Callard *et al*, 1978; Bona-Gallo *et al*., 1980; Whittier and Crews, 1987; Cree *et al*., 1992; Saint Girons *et al*., 1993; Rostal *et al*., 1998; 2001). The plasma T is likely to be of both ovarian and adrenal origin (Staub and De Beer, 1997; Rostal *et al*., 2001). Elevated plasma T concentrations may be involved in the regulation of vitellogenesis and ovulation (Bona-Gallo *et al*., 1980; Edwards and Jones, 2001a; Edwards *et al.*, 2003; Jones, 2011) and in the hypertrophy of the oviduct (Mahmoud and Licht, 1997; AlKindi *et al.*, 2006) and may initiate breeding behaviour in females (Licht *et al.*, 1979). In addition, T is known to work synergistically with P to inhibit E_2-induced vitellogenesis in reptiles (Ho, 1987; Ho *et al.*, 1982). The mechanism of action of T in female reptiles is yet to be elucidated.

In squamates, plasma E_2, P, and T concentrations are usually low during the inactive (non-breeding) period but rise significantly during the active (breeding) period. This indicates that sex hormones play an important role in regulating reproductive phases such as vitellogenesis, courtship, mating, ovulation and uterine secretory activities (Callard *et al.*, 1992; Staub and De Beer, 1997; Owens, 1997; Edwards and Jones, 2001a; Taylor *et al.*, 2004; Al-Habsi *et al.*, 2006; Smith *et al.*, 2010; Lind *et al.*, 2010).

The ultrastructural changes in granulosa cells of the ovarian follicles and granulosa lutein cells in reptiles reveal several steroidogenic features correlated with endocrine function (Cyrus *et al.*, 1978; Mahmoud and Licht, 1997; Al-Kindi *et al.*, 2001; Mahmoud *et al.*, 2006). Specifically, steroidogenic ultrastructural features are in the granulosa cells of the ovarian follicle and CL. These changes in steroidogenic features are associated with production of gonadal steroids mainly E_2 and P which are related to an increase in SER, the presence of cisternal whorls, free ribosomes, and close association of lipid droplets with swollen vesiculated mitochondria and SER (Bjersing, 1967; Cyrus *et al.*, 1978; Mahmoud and Licht, 1997; Al-Kindi *et al.*, 2001; Mahmoud *et al.*, 2006).

Al-Kindi *et al.*, (2001) reported that when female painted turtles with mature preovulatory and secondary follicles were injected prior to ovulation with synthetic mammalian GnRH, the granulosa cells acquired more apparent steroidogenic

ultrastructural characteristics compared to the controls. Reproductive function is controlled by the hypothalamic release of GnRH in many vertebrates (Evertt, 1988; Sherwood *et al.*, 1993). GnRH stimulates release of gonadotropins which in turn stimulates steroid secretions which control follicular development and steriodogenesis.

It has been reported that ultrastructural changes occur in the granulosa cells under natural condition in the ovarian follicles of some reptiles (Cyrus *et al.*, 1978; Mahmoud and Licht, 1997).

Until recently, the relationship between sex hormones and their receptors has not been clearly established in reptiles. PRs have been characterized in lizards (Paolucci and Di Fiori, 1994), in snakes (Kleis-San Francisco and Callard, 1986) and in turtles (Mahmoud *et al.*, 1986; Giannoukos and Callard, 1996; Custodia-Lora and Callard, 2002a). There are two PR isoforms recognised in female reptiles, PRA and PRB with different expression profiles (Riley *et al.*, 1988; Giannoukos and Callard, 1996; Custodia-Lora and Callard, 2002a), and it has been reported that PR are down-regulated by P (Gemmell, 1995).

The aim of this study was to examine the reproductive cycle of females of the oviparous lizard, *H. flaviviridis*. The timing of reproductive events and annual cycles of plasma E_2, P and T concentrations are presented, with correlated histological, histochemical, and ultrastructural changes. In addition, the relationship between plasma sex-steroids and the development of ultrastructural steroidogenic features, and the presence of PRs during different phases of the ovarian and oviductal cycles in the house gecko, *H. flaviviridis*, are presented. This species is a widely distributed species in Oman and the rest of the Arabian Peninsula.

Until now, the ovarian and oviductal seasonal changes in this species have not been studied in this region. Moreover, for the first time this study presents information on the ultrastructural changes related to the hormonal dynamics in this oviparous species.

4.2 Materials and methods

Please refer to Chapter Two: Materials and Methods.

4.3 Results

4.3.1 Gravidity

The mating period occupied approximately six weeks during the breeding season (active phase) in spring (mid March - late April). Gravid females were recognised by the appearance and gross morphology of two large oviducal eggs (Figures 2.4A & 2.5A). Length of gravidity was not recorded due to the animals not being kept in captivity.

4.3.2 Clutch size

Examination of gravid females collected during the breeding season showed that they had two oviductal eggs (Figures 2.4A & 2.4B). However, some females showed two oviductal eggs and two preovulatory follicles (Figures 2.5A & 2.5B). The preovulatory follicles presumably started their growth later than the first clutch, suggesting that this species laid two clutches of eggs annually, each clutch containing two eggs. Moreover, histological and gross morphological examinations of the ovary during April–May showed that there were two sets of CL, a degenerated type and a freshly formed type.

4.3.3 Morphometry of the reproductive organs

Changes in the ovarian and oviductal weight, SVL, body mass and size of largest follicle during the reproductive cycle of *H. flaviviridis* are summarised in Table 4.1A. There are no significant variations in data of each month collected between year one and year two.

The body weight and SVL of female *H. flaviviridis* ranged from 9.69 – 13.43 g and 7.11 – 7.93 cm respectively. There was no significant variation in SVL in relation to body mass during the 24 month study period (Table 4.1A). The weight of the ovary ($P < 0.001$) and oviduct ($P < 0.001$) varied significantly in relation to body weight during the different months of the year (Table 4.1A).

Table 4.1A. Changes (Mean ± S.E.M) in body length (SVL) and body wt, ovary, oviduct weight (ODW), and diameter of largest follicles (LFD) in *H. flaviviridis* during two reproductive cycles (N = Individual geckos).

Month / Year		N	SVL (cm)	Body wt (g)	Ovary wt (g)	ODW (g)	LFD (cm)
Jan	**1**	4	7.200 ± 0.314^{a}	7.325 ± 1.306^{a}	0.041 ±0.091^{a}	0.448 ±0.113^{ab}	0.041 ±0.094^{a}
	2	3	7.000 ±0.362^{a}	6.367 ±1.508^{a}	0.043 ±0.105^{a}	0.440 ±0.131^{ab}	0.040 ±0.109^{a}
Feb	**1**	6	8.167 ±0.256^{abc}	17.583 ±1.066^{c}	0.156 ±0.074a^{b}	0.620 ±0.093^{abc}	0.139 ±0.077^{ab}
	2	7	7.400 ±0.237^{ab}	9.871 ±0.987^{bc}	0.124 ±0.069^{bc}	0.420 ±0.086^{ab}	0.156 ±0.071^{ab}
March	**1**	3	8.000 ±0.362^{a}	12.267 ±1.508^{b}	0.470 ±0.105^{c}	1.004 ±0.131^{d}	0.503 ±0.109^{c}
	2	4	7.875 ±0.314^{bc}	12.175 ±1.306^{c}	0.480 ±0.091^{c}	0.739 ±0.113^{c}	0.518 ±0.094^{c}
April	**1**	6	7.517 ±0.256^{a}	11.433 ±1.066^{ab}	0.529 ±0.074^{c}	0.845 ±0.093^{cd}	0.583 ±0.077^{c}
	2	7	7.543 ±0.237^{abc}	12.200 ±0.987^{c}	0.788 ±0.069^{d}	1.026 ±0.086^{d}	0.850 ±0.071^{d}
May	**1**	6	7.317 ±0.256^{a}	10.433 ±1.066^{ab}	0.302 ±0.074^{bc}	0.740 ±0.093^{bcd}	0.317 ±0.077^{bc}
	2	5	7.500 ±0.280^{abc}	10.160 ±1.168^{bc}	0.344 ±0.081^{bc}	0.699 ±0.101^{bc}	0.382 ±0.084^{bc}
June	**1**	7	7.314 ±0.237^{a}	9.571 ±0.987^{ab}	0.002 ±0.069^{a}	0.314 5±0.086^{a}	0.003 ±0.071^{a}
	2	8	7.088 ±0.222^{ab}	8.625 ±0.924^{ab}	0.002 ±0.064^{a}	0.271 ±0.080^{a}	0.004 ±0.067^{a}

Table 4.1A. Continued. Changes (Mean ± S.E.M) in body length (SVL) and body wt, ovary, oviduct weight (ODW), and diameter of largest follicles (LFD) in *H. flaviviridis* during two reproductive cycles (N = Individual geckos).

Month / Year		N	SVL (cm)	Body wt (g)	Ovary wt (g)	ODW (g)	LFD (cm)
July	**1**	3	7.700 ± 0.362^{a}	10.267 ± 1.508^{ab}	0.005 ±0.105^{a}	0.351 ±0.131^{a}	0.006 ±0.109^{a}
	2	4	7.375 ± 0.314^{abc}	9.500 ±1.306^{abc}	0.004 ±0.091^{a}	0.278 ±0.113^{a}	0.006 ±0.094^{a}
Aug	**1**	3	7.667 ±0.362^{a}	9.800 ±1.508^{ab}	0.006 ±0.105^{a}	0.319 ±0.131^{a}	0.008 ±0.109^{a}
	2	3	7.833 ±0.362^{bc}	9.333 ±1.508^{abc}	0.006 ±0.105^{a}	0.320 ±0.131^{a}	0.008 ±0.109^{a}
Sept	**1**	5	7.280 ±0.280^{a}	9.400 ±1.168^{ab}	0.010 ±0.081^{a}	0.340 ±0.101^{a}	0.012 ±0.084^{a}
	2	5	8.000 ±0.280^{c}	10.100 ±1.168^{bc}	0.010 ±0.081^{a}	0.306 ±0.101^{a}	0.012 ±0.084^{a}
Oct	**1**	5	7.660 ±0.280^{a}	8.880 ±1.168^{ab}	0.019 ±0.081^{a}	0.352 ±0.101^{a}	0.022 ±0.084^{a}
	2	6	7.200 ±0.256^{abc}	8.567 ±1.066^{ab}	0.016 ±0.074^{a}	0.348 ±0.093^{a}	0.011 ±0.077^{a}
Nov	**1**	9	7.667 ±0.209^{a}	12.722 ±0.871^{b}	0.019 ±0.061^{a}	0.427 ±0.076^{ab}	0.027 ±0.063^{a}
	2	10	7.450 ±0.198^{abc}	10.160 ±0.826^{bc}	0.017 ±0.057^{a}	0.365 ±0.072^{a}	0.018 ±0.060^{a}
Dec	**1**	5	7.800 ±0.280^{a}	11.600 ±1.168^{ab}	0.019 ±0.081^{a}	0.393 5±0.101^{ab}	0.021 ±0.084^{a}
	2	5	7.300 ±0.280^{abc}	9.440 ±1.168^{abc}	0.019 ±0.081^{a}	0.430 ±0.101^{ab}	0.028 ±0.084^{a}
F(11,50) **F(11,55)**	**1** **2**		0.894 1.529	4.147 2.233	5.355 12.408	4.256 7.042	5.740 13.562
P-value	**1** **2**		0.270 0.148	< 0.001 < 0.001	< 0.001 < 0.001	< 0.001 < 0.001	< 0.001 < 0.001

Statistical differences between groups obtained by Duncan's multiple-comparisons test within each year. Months with significantly different values (mean ± S.E.M) in vertical column were assigned different letters. Months with the same letter shows statistically no significant difference between them at the 0.05 level of significance.

The ovaries regressed in the quiescent phase (June–August) but started to increase gradually in the recrudescent phase (September–January) and increased significantly in late January, coinciding with the onset of vitellogenesis. During mating in March

and April, the ovary weight was the highest ($P < 0.001$). After ovulation in March, the ovaries began to regress during gravidity (May) (see gonadosomatic index). Preovulatory follicles increased in size between January and May, reaching full vitellogenic size during March and April. After May, the follicles began to regress. The oviduct weight coincided with the ovarian cycle. Oviduct weight increased in March during vitellogenesis and mating, peaked in April and May during gravidity, and began to regress in June and July. In August through to February the oviduct weight was lowest (see gonadosomatic index).

4.3.4 Gonadosomatic index (GSI)

The monthly variation in the GSI is shown in Figure 4.1A. Gonadosomatic index was calculated as (ovary mass (g) / body mass (g)) x 100. The ovarian weight is shown in Figure 4.1B. There are no significant variations in data of each month collected between year one and year two.

The ovaries regressed between June and August but started to increase gradually after August and increased significantly (F (11,117) = 17.73, $P < 0.001$) in January, coinciding with the onset of vitellogenesis. During mating in March and April, GSI was the highest (F (11,117) = 19.02, $P < 0.001$). After ovulation in March, the ovaries began to regress during gravidity (May) and remained inactive during the quiescent phase, June through to August, and the recrudescent phase, September through to December.

Preovulatory follicles increased in size between January and May, reaching full vitellogenic size during March and April. After May, the follicles began to regress (Figure 4.1C).

The oviduct weight coincided with the ovarian cycle (Figure 4.1D). Oviduct weight increased in March during vitellogenesis and mating, peaked in April and May during gravidity, and began to regress in June and July. In August through to February the oviduct weight was lowest.

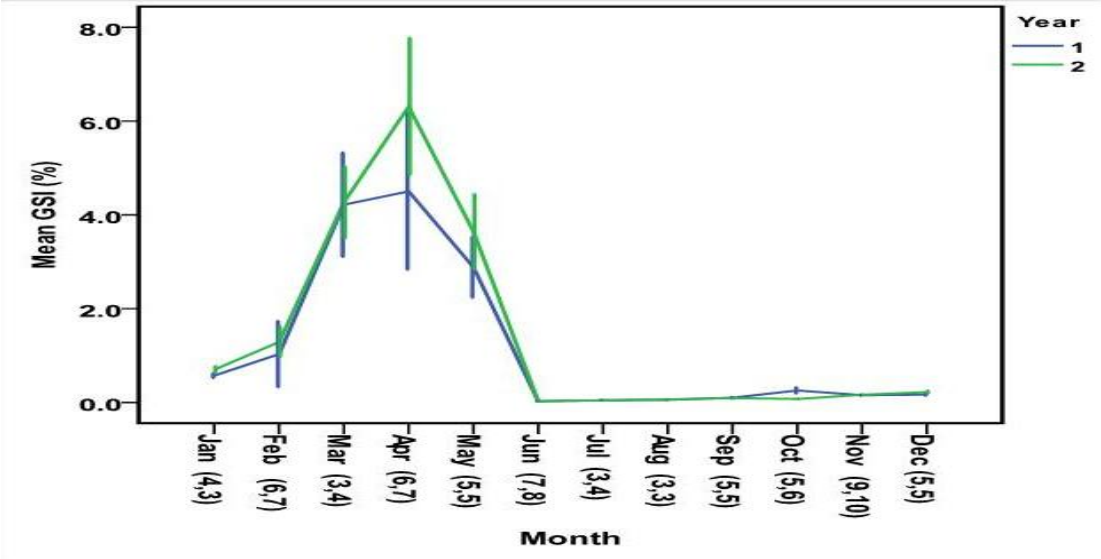

Figure 4.1A. Monthly mean (±S.E.M.) GSI during two reproductive cycles. There are no significant variations in data of each month collected between year one and year two. The active phase commenced in January, reached a peak in April, decreased significantly in June and stayed low until December. Numbers below each histogram represents sample size. Months with significantly different GSI were assigned different letters. Months with the same letter shows statistically no significant difference between them at the 0.05 level of significance. Statistical differences between groups obtained by Duncan's multiple-comparisons test within each year.

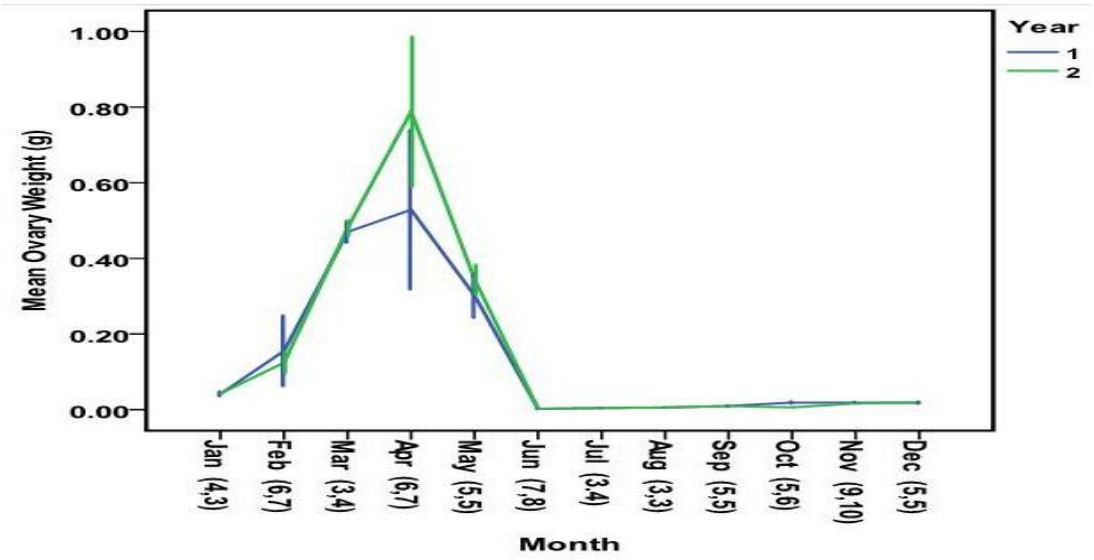

Figure 4.1B. Monthly mean (±S.E.M.) ovarian weight during two reproductive cycles. There are no significant variations in data of each month collected between year one and year two. Ovaries regressed between June–August, increased significantly in February, and reached a peak in March–May. Ovaries began to regress in May, and remained inactive during June–December. Months with significantly different ovary weight were assigned different letters. Months with the same letter shows statistically no significant difference between them at the 0.05 level of significance. Statistical differences between groups obtained by Duncan's multiple-comparisons test within each year.

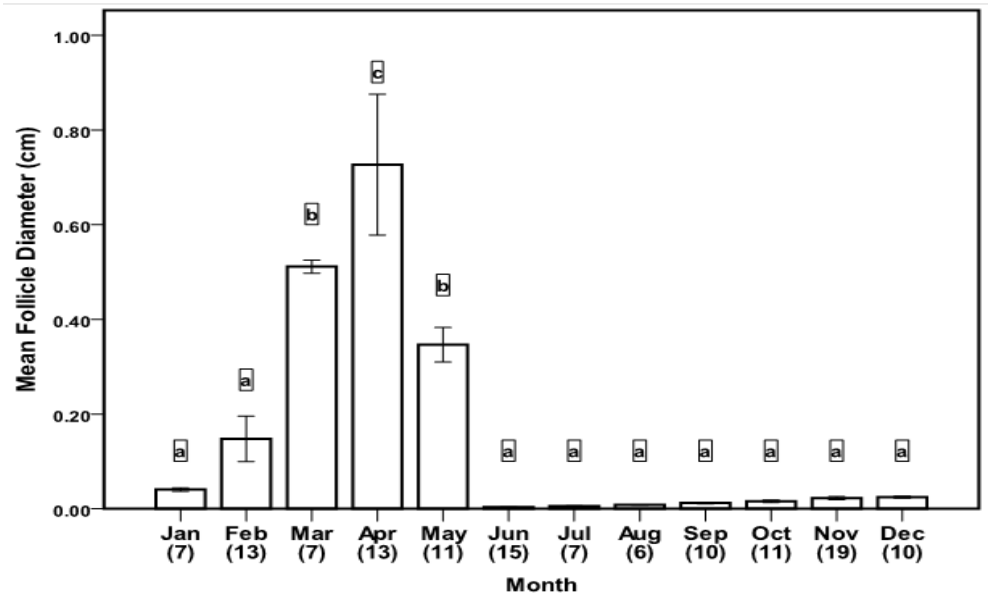

Figure 4.1C. Monthly mean (±S.E.M.) follicular diameter during a reproductive cycle. Only small immature follicles were present in the ovary during June through January. March through May, some follicles increased to preovulatory size. Numbers below each histogram represents sample size. Months with the same letter shows statistically no significant difference between them at the 0.05 level of significance. Statistical differences between groups obtained by Duncan's multiple-comparisons test.

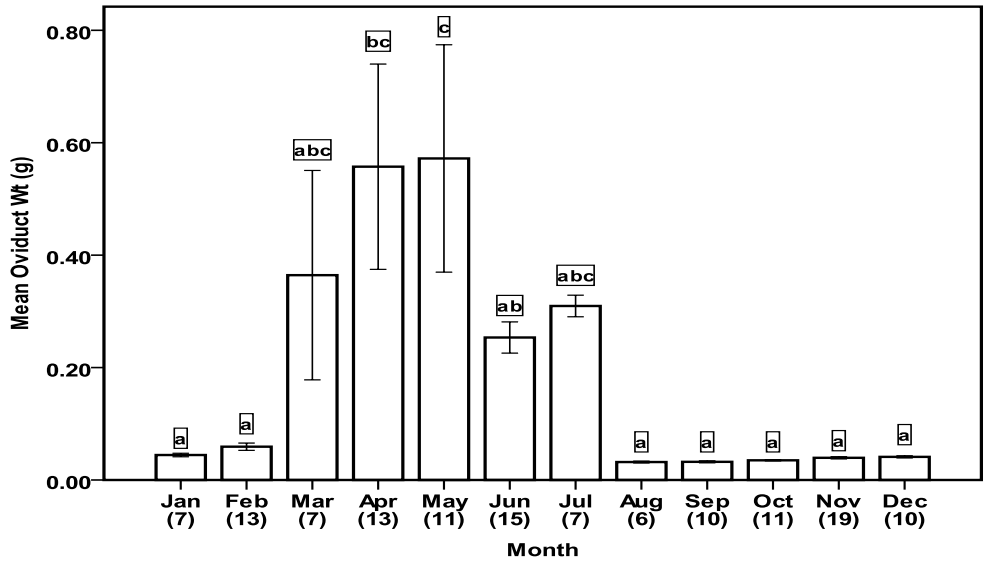

Figure 4.1D. Monthly mean (±S.E.M.) oviduct weight during a reproductive cycle. Oviduct weight increased in March, peaked in April and May, and began to regress in June and July. In August through February the oviduct weight was at the lowest. Numbers below each histogram represents sample size. Months with the same letter shows statistically no significant difference between them at the 0.05 level of significance. Statistical differences between groups obtained by Duncan's multiple-comparisons test.

4.3.5 Hepatosomatic index (HSI)

The monthly variation in the HSI is shown in Figure 4.1E. Hepatosomatic index was calculated as (liver mass (g) / body mass (g)) x 100. The liver weight showed minimal change during the reproductive cycle. Liver weight increased significantly in January (F (11,117) = 7.36, P < 0.001) coinciding with the onset of vitellogenesis, and remained unchanged for the rest of the reproductive cycle.

4.3.6 Plasma hormone concentrations

4.3.6.1 Oestradiol

The mean monthly plasma E_2 concentrations varied significantly throughout the reproductive cycle (F (11,113) = 16.19, P < 0.001) (Figure 4.2A). Plasma E_2 concentrations rose significantly between January and May with a peak in April (P < 0.05). It fell significantly in June (P < 0.001) but began to rise gradually again in July through to December. Plasma E_2 concentrations increased significantly during vitellogenesis (January–March) (P < 0.05).

4.3.6.2 Progesterone

Mean plasma P concentrations rose in March following ovulation and peaked during gravidity and luteinisation in April and May with the presence of oviductal eggs (F (11,107) = 119.11, P < 0.001) (Figure 4.2B). Mean plasma P concentrations fell significantly in June (P < 0.001) following luteolysis and remained low through to February.

4.3.6.3 Testosterone

Significant variations in mean plasma T concentrations were observed throughout the reproductive cycle (Figure 4.2C). Plasma T concentrations were elevated significantly (F (11,109) = 22.26, P < 0.001) during vitellogenesis and by May plasma T concentrations fell significantly (P < 0.001) from June to February. Plasma T concentrations began to rise again in February.

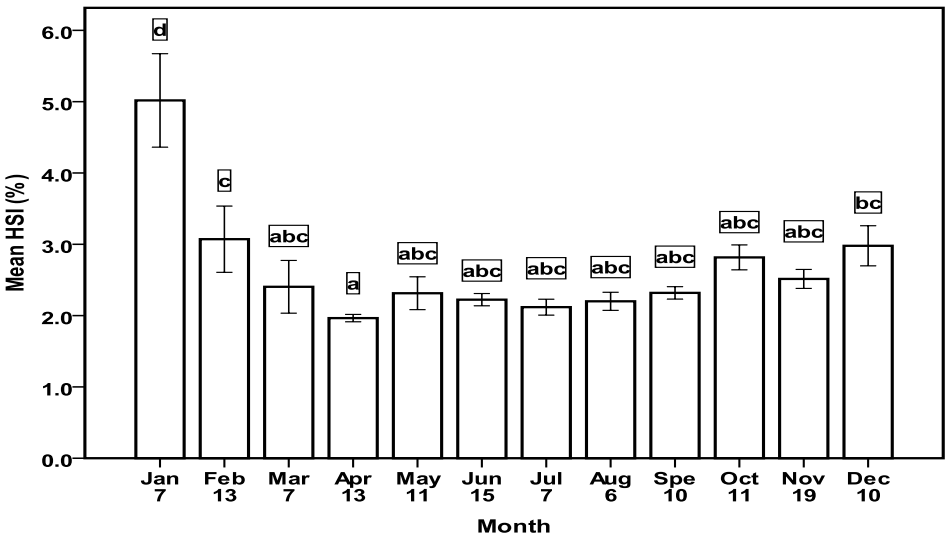

Figure 4.1E. Monthly mean (±S.E.M.) HSI during the reproductive cycle. Liver weight increased in January coinciding with the onset of vitellogenesis, and remained unchanged for the rest of the reproductive cycle. Numbers below each histogram represents sample size. Months with significantly different HSI were assigned different letters. Months with the same letter shows statistically no significant difference between them at the 0.05 level of significance. Statistical differences between groups obtained by Duncan's multiple-comparisons test.

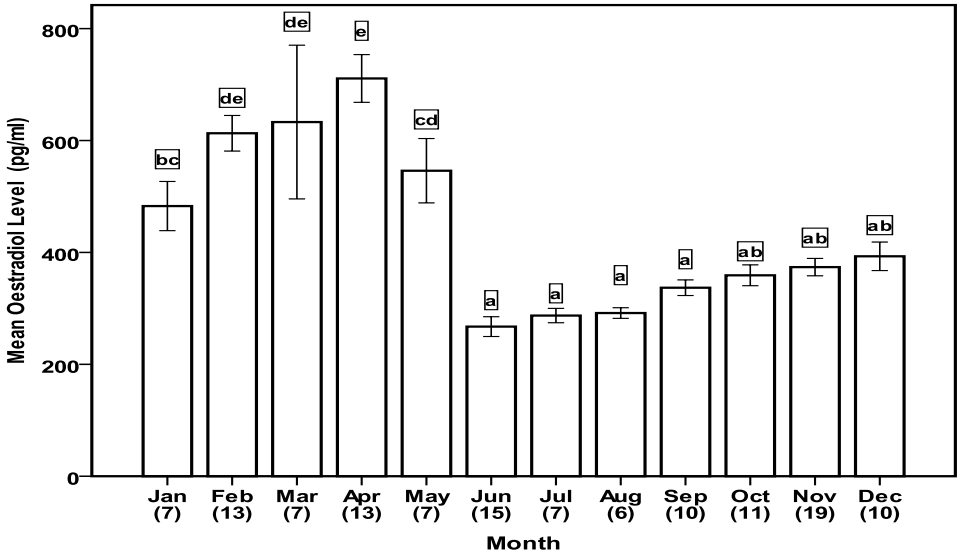

Figure 4.2A. Monthly mean (±S.E.M.) plasma E_2 concentrations. Plasma E_2 concentrations increased during the breeding phase with a peak in January through May, decreased in June and then started to rise again in July through December. Vitellogenesis and follicular growth commenced in January through April, coinciding with the E_2 rise. Numbers below each histogram represents sample size. Months with significantly different E_2 were assigned different letters. Months with the same letter shows statistically no significant difference between them at the 0.05 level of significance. Statistical differences between groups obtained by Duncan's multiple-comparisons test.

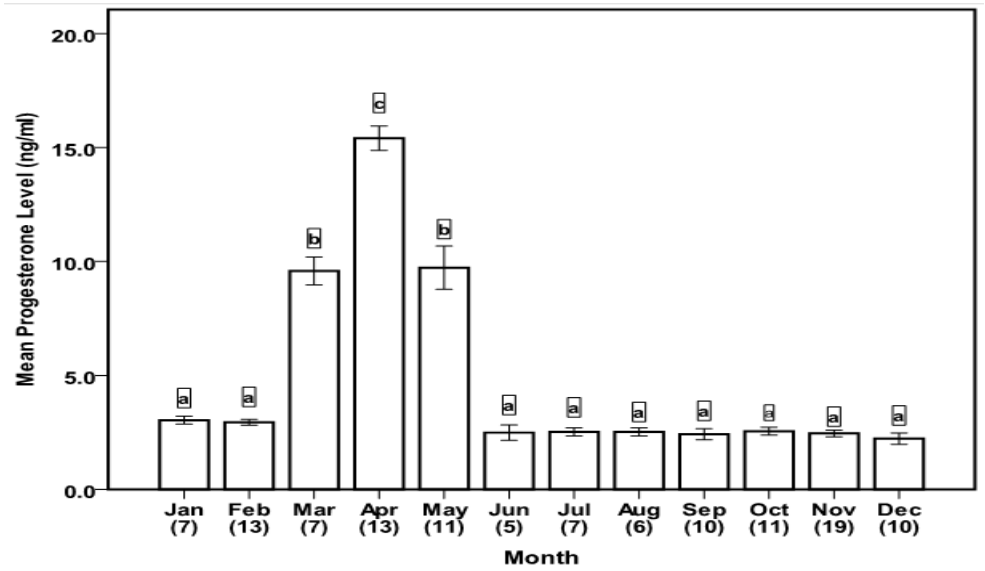

Figure 4.2B. Monthly mean (±S.E.M.) plasma P concentrations. Plasma P concentrations increased during the breeding phase (luteal phase) between March and May, with a peak in April, coinciding with the activity of corpus lutea. Luteolysis took place after May as P concentrations began to decrease significantly. Numbers below each histogram represents sample size. Months with significantly different P were assigned different letters. Months with the same letter shows statistically no significant difference between them at the 0.05 level of significance. Statistical differences between groups obtained by Duncan's multiple-comparisons test.

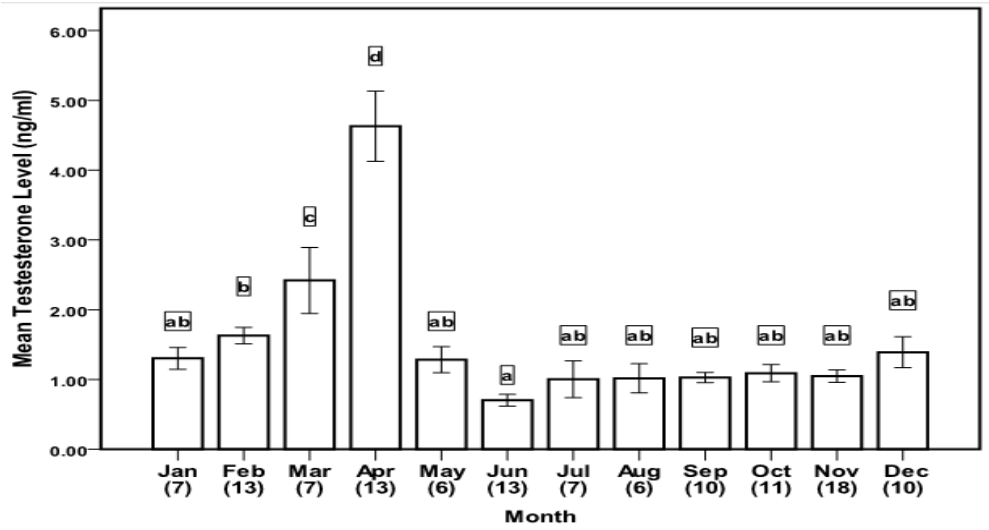

Figure 4.2C. Monthly mean (±S.E.M.) plasma T concentrations during the reproductive cycle with a rise in December through to April. Plasma T concentrations peaked in April, coinciding with vitellogenesis, follicular growth, courtship and mating. Numbers below each histogram represents sample size. Months with significantly different T concentrations were assigned different letters. Months with the same letter shows statistically no significant difference between them at the 0.05 level of significance. Statistical differences between groups obtained by Duncan's multiple-comparisons test.

4.3.7 Effects of stress during the reproductive cycle

Mean monthly C concentrations are shown in Figure 4.2D. The annual pattern of plasma C concentrations showed no significant variations throughout the reproductive cycle (F (11, 107) = 2.721, P 0.064). The relatively high mean plasma C concentrations were probably based on the stress caused by the capture and handling of the animals. Haematocrit concentrations stayed within the normal range (Mean PCV = 38.6 $\pm$ 1.3%, n= 56) during the reproductive cycle. There was no significant linear correlation between plasma C concentrations and haematocrit (P 0.50).

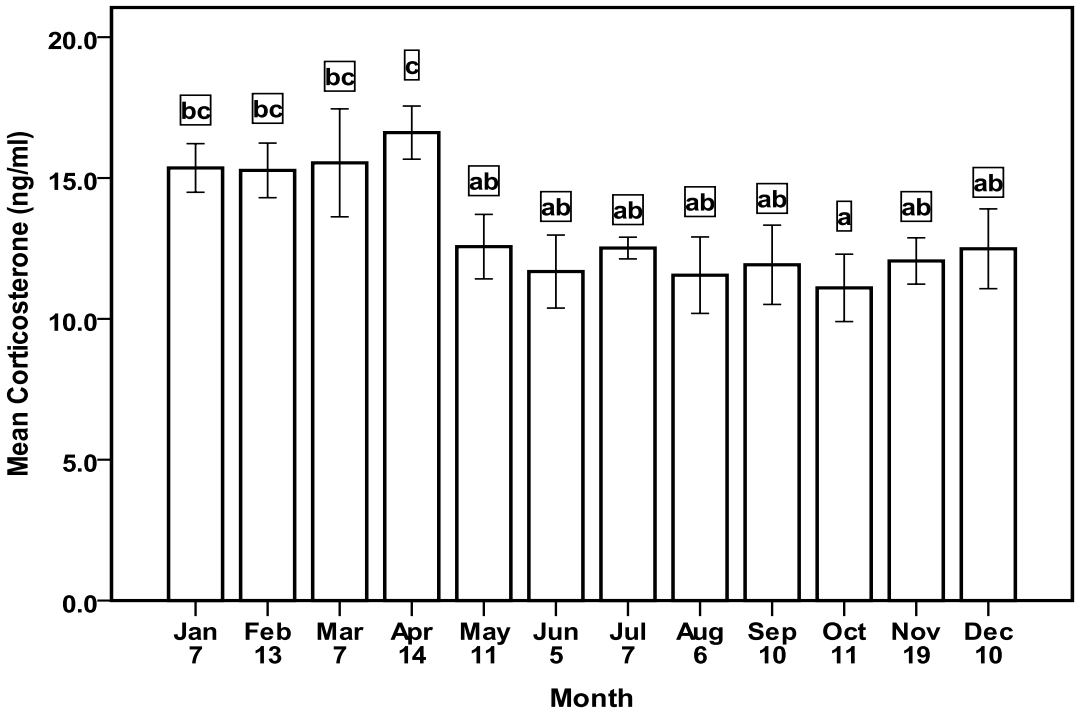

Figure 4.2D. Monthly mean (±S.E.M.) plasma C concentrations. Plasma C concentrations increased slightly during the active phase with a peak in April. Concentrations decreased slightly in May and increased again in January. Months with significantly different C were assigned different letters. Months with the same letter shows statistically no significant difference between them at the 0.05 level of significance. Statistical differences between groups obtained by Duncan's multiple-comparisons test.

4.3.8 Progesterone receptors

PRs were strongly expressed in the granulosa and theca interna cells of previtellogenic and vitellogenic follicles in both the nucleus and cytoplasm when the plasma E_2 concentrations were high (Figures 4.3A & 4.3B).

In the CL, PRs were less expressed in the cytoplasm and the nucleus of granulosa lutein cells during luteinisation when plasma P concentrations were high (Figure 4.3C). In the epithelial and glandular layers of the oviduct, during the egg shelling process, PRs were also less expressed in the nucleus and cytoplasm as the plasma P concentrations were high (Figure 4.3D). During vitellogenesis, the hepatic cells showed a strong expression for PR when the plasma E_2 concentrations were high (Figure 4.3E). However, during the non-reproductive period, the ovary, oviduct and liver were negative for PR immunoexpression (Figure 4.3F).

Overall, the rise in PR expression coincided with the presence of the ultrastructural steroidogenic features and the rise in plasma steroid concentrations.

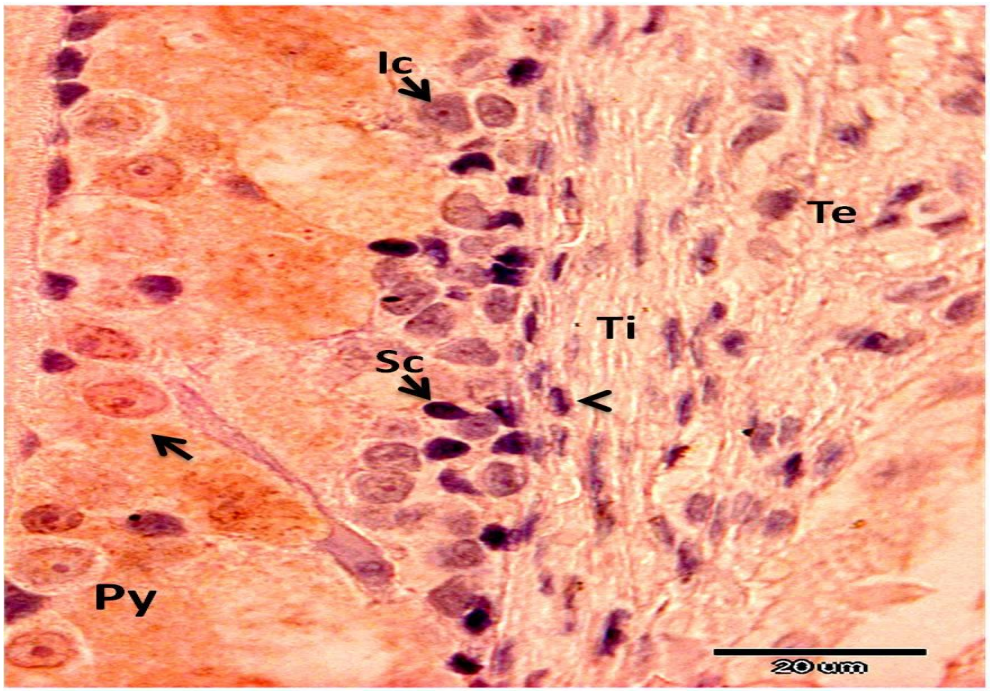

Figure 4.3A. Immunolocalisation of previtellogenic follicle PRs. All granulosa cells stained positive in nuclei and cytoplasm (arrow). Theca interna cells stained positive for PRs (arrowhead). Pyrifom cells (Py), Intermediate cells (Ic), Small cells (Sc), Theca externa (Te), Theca Interna (Ti).

Figure 4.3B. Immunolocalisation of vitellogenic follicle PRs. Granulosa small cells (Gc) stained positive in nuclei and cytoplasm (arrow). Theca interna cells (Ti) stained positive for PR (arrowhead). Theca externa (Te), Zona pellucida (Zp), lipid platelets (LP).

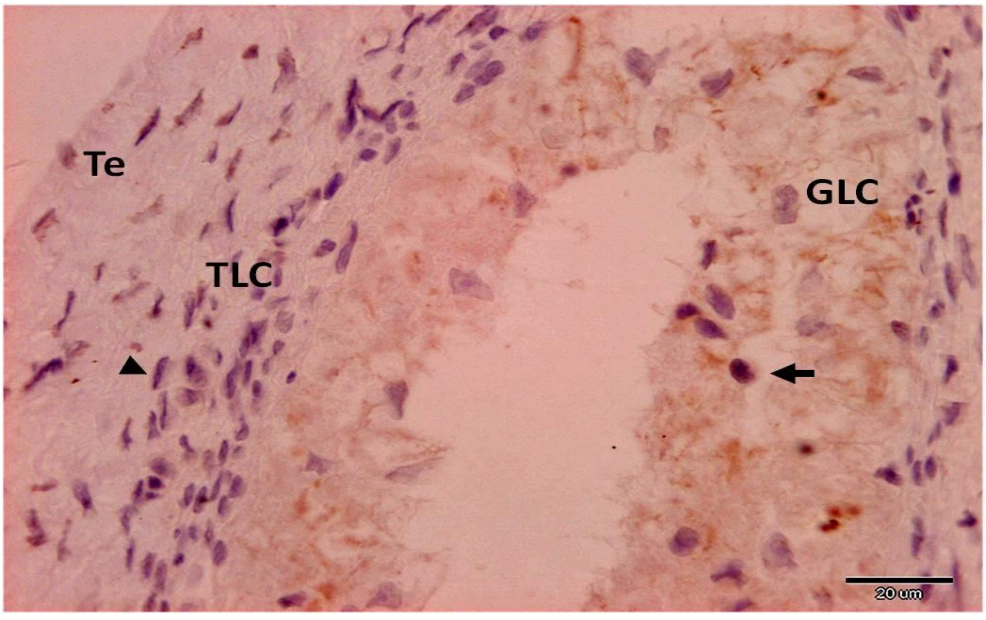

Figure 4.3C. Immunolocalisation of active corpus luteum PR. Granulosa lutein cells (GLC) stained positive in nuclei and cytoplasm (arrow). Theca lutein cells (TLC) stained negative for PRs (arrowhead). Theca externa (TE).

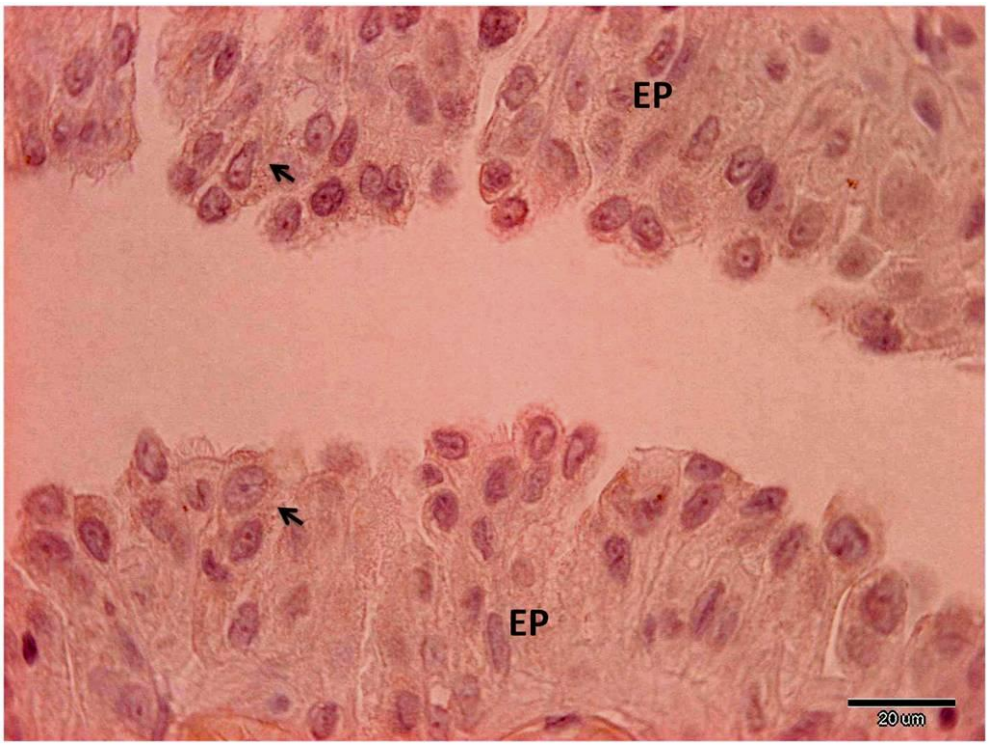

Figure 4.3D. Immunolocalisation of the uterus PRs. Epithelial cells (EP) stained positive in nuclei and cytoplasm (arrow).

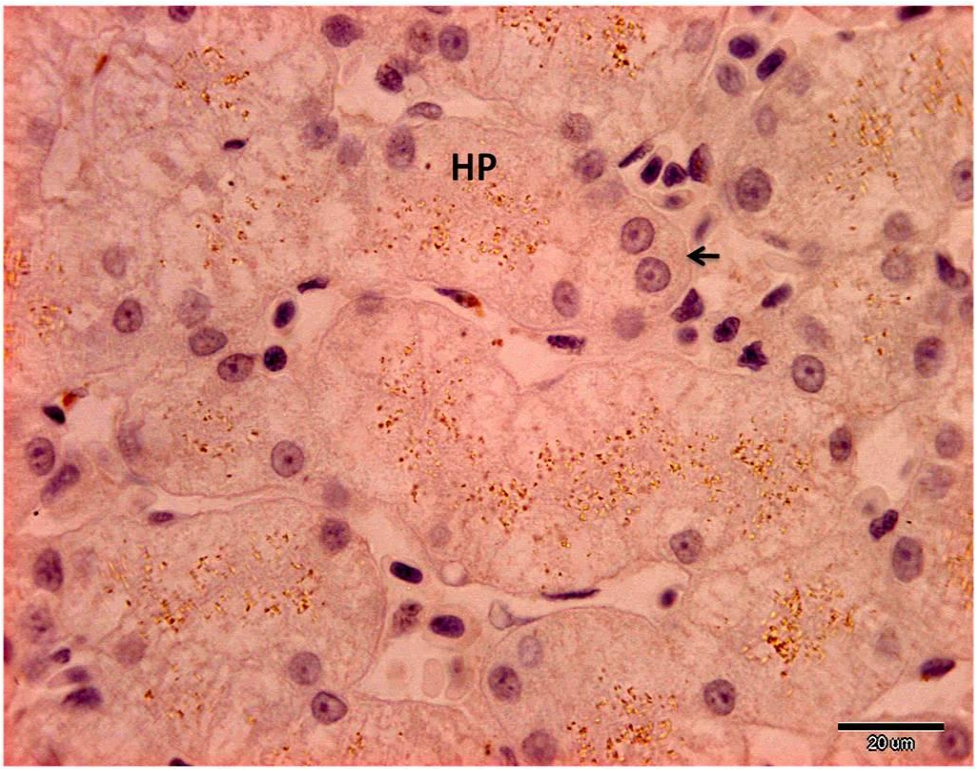

Figure 4.3E. Immunolocalisation of hepatic cells (HP) PRs during vitellogenesis. Hepatic cells stained positive (arrow) for PR.

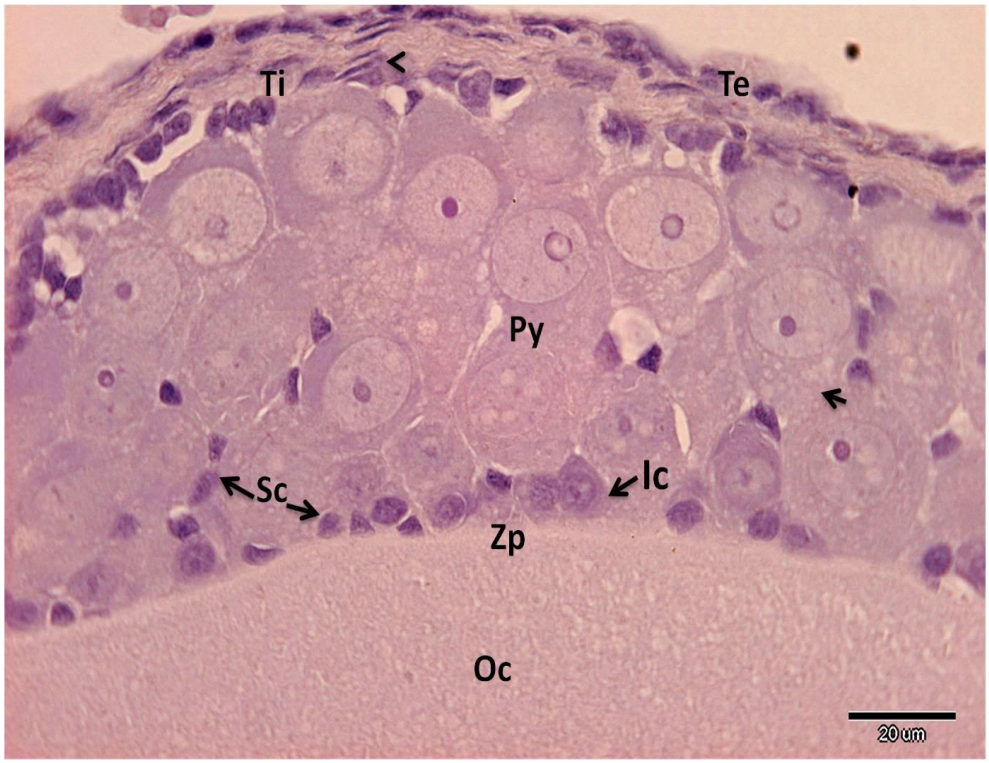

Figure 4.3F. Immunolocalisation of previtellogenic follicle (inactive phase) showing negative staining for PR. All granulosa cells stained negative for PR in nuclei and cytoplasm (arrow). Theca interna cells also stained negative for PR (arrowhead). All other tissues tested during the inactive phase also showed negative PR expression. Pyriform cells (Py), Intermediate cells (Ic), Small cells (Sc), Theca externa (Te), Theca Interna (Ti), Zona pellucida (Zp), Oocyte (Oc).

4.3.9 Ovarian cycle

Histological features observed at each stage of the ovarian cycle are summarised in Table 4.2. Throughout the ovarian cycle the thecal layer was visible as a single layer in early previtellogenic follicles and as a double layer in late previtellogenic and vitellogenic follicles. In non-reproductive females, the granulosa layer was polymorphic (pyriform, intermediate and small stem cells), and monomorphic (small stem cells only) in the reproductive and post-ovipositing females. The zona pellucida became differentiated into an outer hyaline and an inner striated zona radiata throughout the vitellogenic period. However, during this time, yolk granules were deposited in the ooplasm of the reproductive females. Vacuoles (Table 4.2) were present throughout the ooplasm during early previtellogenesis, but became localised peripherally during late previltellogenesis and were situated in the centre of the follicle during vitellogenesis and gravidity.

4.3.9.1 General observations

The ovaries of *H. flaviviridis* are paired organs attached to the dorsal body wall by a thin mesovarium. They contained small previtellogenic and atretic follicles of variable size and in different developmental stages in the non-reproductive females and were found between June and December (Figures 4.4A & 4.4B). In each ovary, one follicle was always larger than the others which contained the potential oocyte to be ovulated first by each ovary. The germinal beds were near the ovarian hilum, derived from and in contact with the ovarian epithelium (Figure 4.4B). The ovarian wall was formed by the ovarian epithelium and a very thin tunica albuginea. The surface epithelium was simple squamous and the tunica albuginea was composed of very thin fibrous connective tissue. The ovarian stroma consisted of a loose connective tissue containing, degenerating CL and atretic follicles, lymphatics, interstitial gland cells, nerves and blood vessels (Figure 4.4C).

Vitellogenic follicles appeared in late January when most of the yolk deposition started to occur. Heavy yolk deposition was seen in follicles in reproductive females between March and May, after which the ovaries were again reduced in size. Oviductal eggs were seen in gravid females between mid March and mid May. CL were observed in gravid females as flattened structures of different sizes.

At different developmental stages; degenerating atretic follicles and CL formed the ovarian cortex (stroma), whereas, the ovarian medulla formed the normal and atretic follicles of the ovary.

Table 4.2. Histological features of ovarian follicles throughout the reproductive cycle in female *H. flaviviridis.*

Season	Early Summer (June–Aug)	Late Summer (Sept–Oct)	Winter (Nov–Jan)	Late winter & Spring (Late Jan–May)
Phase	Postbreeding (Quiescent)	Prebreeding (Recrudescent)	Prebreeding (Recrudescent)	Breeding (Active)
Thecal layer	Single layer	Single layer	Differentiated Theca externa/ Theca interna	Differentiated Theca externa/ Theca interna
Granulo-sa layer	Monomorphic Small cells	Dimorphic Small / intermediate cells	Polymorphic Small/ intermediate/ Pyriform cells	Monomorphic Small dark cells
Zona pellucida layer	Homogeneous Hyaline layer	Homogeneous Hyaline layer	Differentiated Hyaline / Zona radiata	Differentiated Hyaline / Zona radiate
Ooplasm	Vacuolated throughout	Vacuolated Throughout	Vacuolated peripherally	Vacuolated centrally
Yolk granules	absent	absent	Present peripherally	Present throughout
Ovarian stage	Early previtellogenesis	Mid previtellogenesis	Late previtellogenesis	Vitellogenesis (preovulatory)

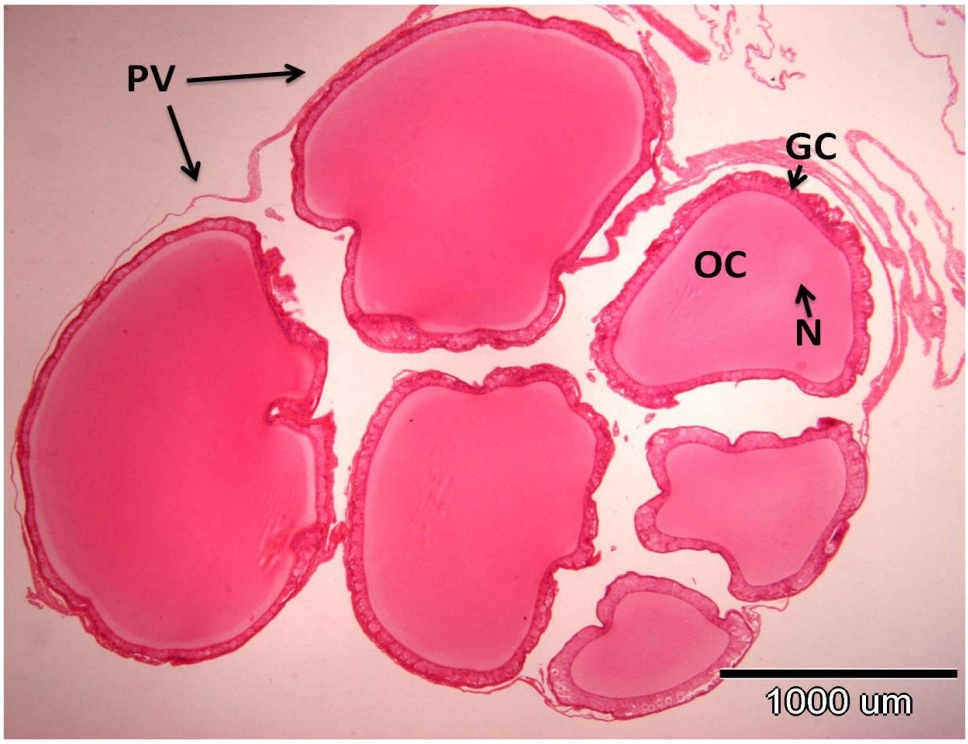

Figure 4.4A. H&E section of the ovary from the recrudescent phase showing six developing previtellogenic follicles (PV) of various sizes with the oocytes (OC), nucleus (N) and granulosa cells layer (GC) clearly visible.

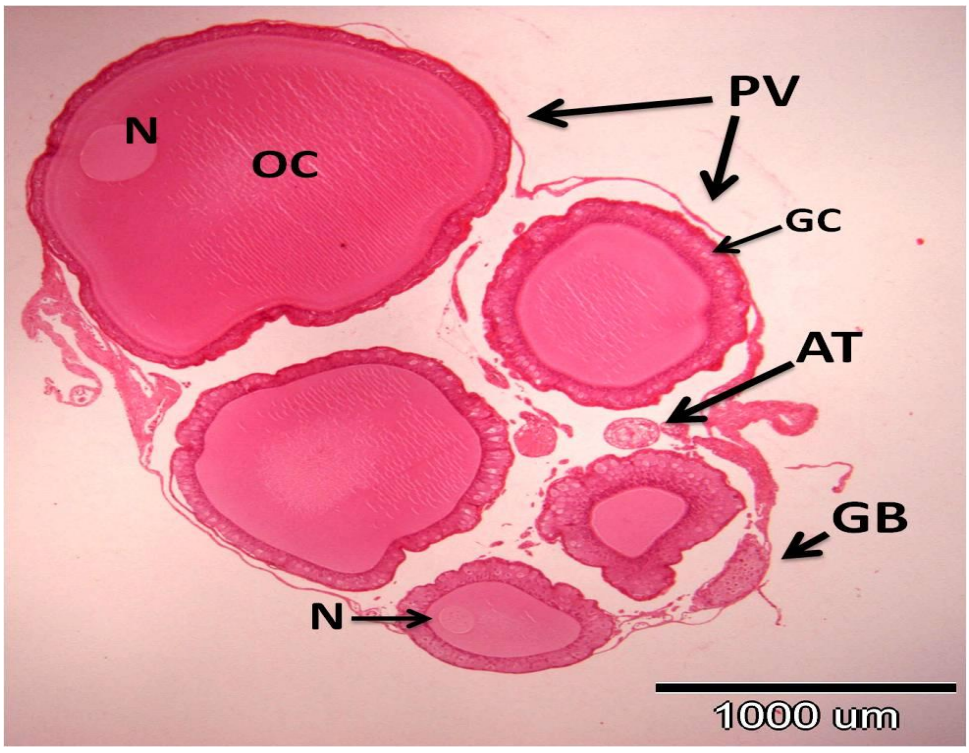

Figure 4.4B. H&E section of the ovary from the recrudescent phase showing five developing previtellogenic follicles (PV) of various sizes with the oocytes (OC), nuclei (N) and granulosa cells layer (GC) clearly visible. Atretic follicle (AT) and germinal bed (GB) were also present.

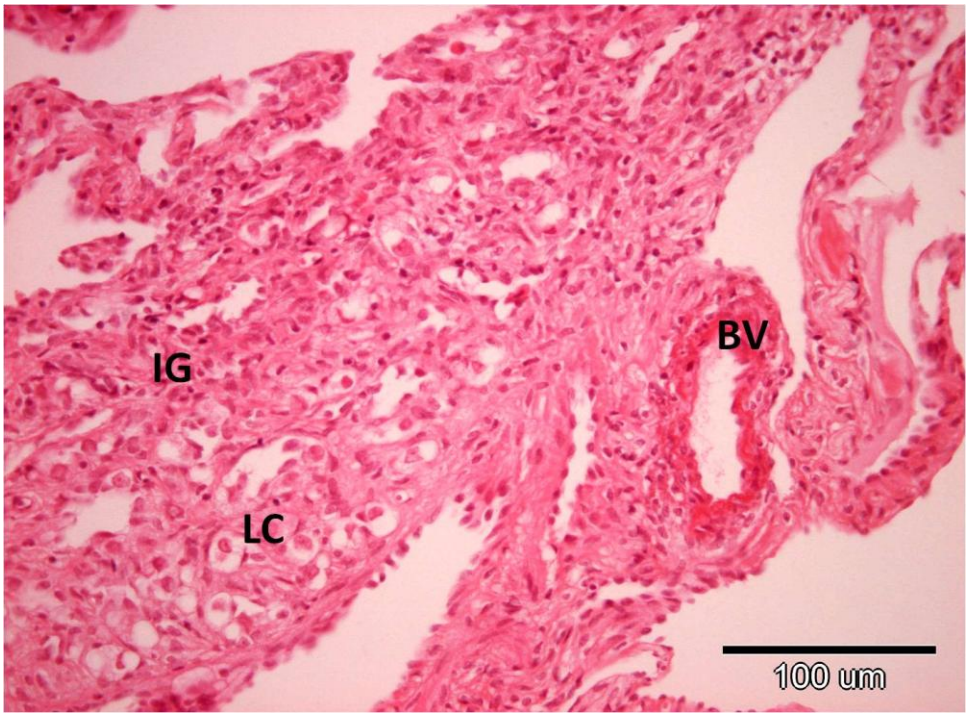

Figure 4.4C. H&E section of the ovary. Portion of the ovarian stroma with lymphatic cells (LC), interstitial gland cells (IG) and blood vessels (BV).

4.3.9.2 Germinal epithelium

Each ovary of *H. flaviviridis* showed one elongated germinal bed lying on the dorsal surface of the ovary near the ovarian hilum. The germinal bed was thinner at the periphery than in the middle (Figures 4.5A) and contained three types of cells; follicular cells, oogonia and oocytes. Oogonia were the first germinal cells observed with pale nuclei and dark cytoplasm. Primary oocytes were clearly identified by their large round dark nuclei and prominent nucleoli in meiotic prophase I (diplotene) and lightly stained cytoplasm. The follicular cells were the smallest cells partially surrounding the primary oocytes. They had a darkly stained cytoplasm and a small nucleus (Figures 4.5A & 4.5B). This latter arrangement constituted the first stage of follicular development.

Figure 4.5A. Higher magnification of Figure 4.4B. Germinal bed with oogonia (OG), primary oocytes (PG) and epithelial cells (arrow).

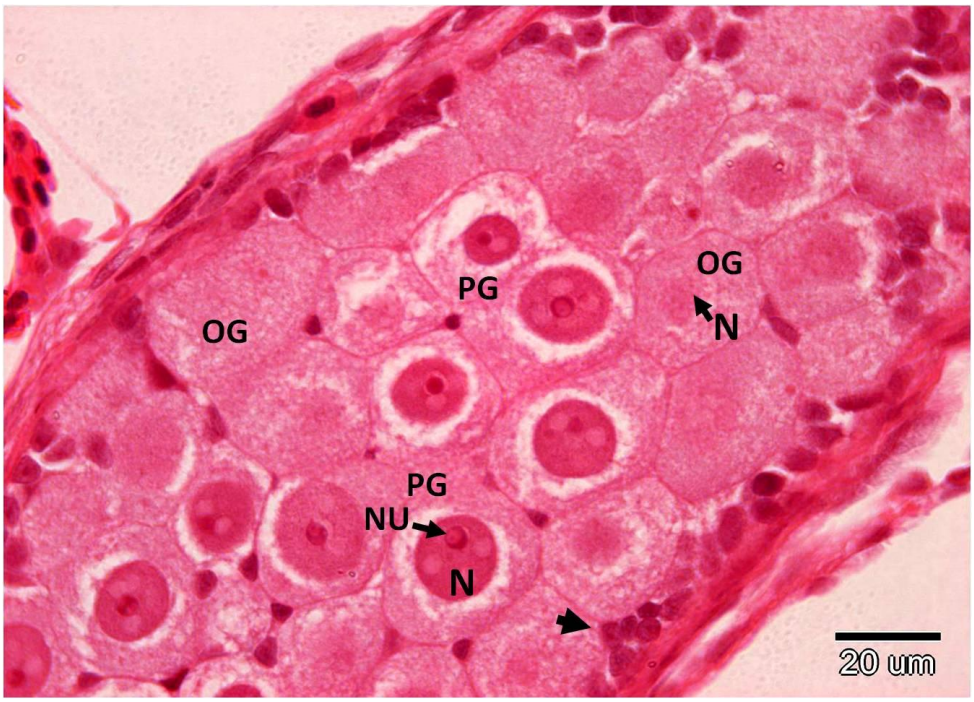

Figure 4.5B. Higher magnification of Figure 4.5A. Primary oocytes (PG) with dark nuclei (N) and prominent nucleoli (NU). Oogonia (OG) appeared with pale nuclei (N). Epithelial cells appeared flat (thick arrow).

4.3.9.3 Folliculogenesis

Changes in the size of follicular structures (follicular diameter, oocyte diameter, thickness of zona pellucida, follicular epithelium height, and thickness of thecal layer) during the reproductive cycle of *H. flaviviridis* are summarised in Table 4.3.

The size of follicular structures ($P < 0.001$) varied significantly during the different stages of folliculogenesis (Table 4.3). The size of the follicular structures increased gradually in previtellogenesis stages II–V and in vitellogenesis stages VI–VII but increased significantly ($P < 0.001$) in vitellogenesis stages VIII–IX coinciding with the completion of vitellogenesis and follicular development. Preovulatory follicles reached full vitellogenic size during the breeding season.

4.3.9.3.1 Stage-II Previtellogenesis

In the late quiescent phase, the oocyte was surrounded by a monolayered follicular epithelium or granulosa consisting of small dark flattened cells (Figure 4.6A) (average oocyte diameter 93.18±12.93 µm, average follicular diameter 102.76±13.75 µm) (Table 4.3). As folliculogenesis progressed in the early recrudescent phase, the oocyte increased in diameter with a nucleus containing pre-lampbrush chromosomes and the ooplasm exhibited large fibre aggregates which appeared as empty vacuolated spaces (Figure 4.3A). Balbiani's vitelline body (juxtanuclear aggregation of organelles) was not observed during this stage (Figure 4.6A). With further development, the follicular epithelium began to differentiate within the germinal bed and was constituted of two cellular types, small dark cells with ovoid nuclei, and large intermediate cells with spherical nuclei containing lampbrush chromosomes and a lighter cytoplasm which appeared finely granulated and vacuolated (Figure 4.6A) (average epithelial height 9.06±0.68 µm) (Table 4.3). At the end of this stage the follicle was transformed into a stage-III previtellogenic follicle.

4.3.9.3.2 Stage-III Previtellogenesis

During the recrudescent phase, the growing oocyte migrated from the germinal bed with a further increase in diameter and contained a round nucleus (average oocyte diameter 389.70±48.31 µm, average follicular diameter 472.00±53.60 µm) (Table 4.3) (Figure 4.6B). The fibres in the ooplasm were shorter and more homogeneously

distributed and appeared to be empty vacuolated spaces throughout the oocyte. As in Stage II, the granulosa was composed of small cells and intermediate cells, but the intermediate cells were greater in number and size than in Stage II (Figure 4.6B) (average epithelial height 50.00±7.64 µm) (Table 4.3). The ooplasm was separated from the granulosa layer by a noncellular layer called the zona pellucida (Figure 4.6B) (average zona pellucida thickness 3.20±0.382 µm) (Table 4.3). The zona pellucida was clearly observed as a lightly stained noncellular and homogeneous layer formed at the interface between the oolemma and the apical membranes of the follicular epithelium. The follicular epithelium rested externally upon a thin homogeneous membrana propria (basal lamina). External to the latter lay a band of stromal tissue, the vascular theca. The theca was thin, formed by fibroblasts, fibres, and blood capillaries (Figure 4.3B) (average thecal thickness 8.35±1.52 µm) (Table 4.3).

4.3.9.3.3 Stage-IV Previtellogenesis

As folliculogenesis progressed, the oocyte increased in diameter and had ovoid nucleus (larger than in the previous stage) containing lampbrush chromosomes (average oocyte diameter 1225.90±88.34 µm, average follicular diameter 1312.00±83.90 µm) (Table 4.3) (Figure 4.6C). The ooplasm contained an abundance of fibrillar cytoplasmic clumps. The granulosa differentiated and became polymorphic with three types of cells: small, intermediate, and large pyriform cells (Figure 4.6D) (average epithelial height 62.50±7.43 µm) (Table 4.3). Small cells were located in the outer and inner layers of the epithelium, and were more abundant at the apical boundary of the granulosa, closest to the oocyte. The small cells were spherical and had round nuclei with single nucleoli. Intermediate cells were oval with round nuclei, single conspicuous nucleoli, and lightly granular cytoplasm. They were located near the oocyte membrane. These cells, along with the small cells, stained negatively by PAS reaction (Figure 4.6D). Pyriform cells were flask-shaped and exhibited large nuclei and dense nucleoli with chromatin bodies. Their cytoplasm was PAS-positive and contained granules, vacuoles, and fibres (Figure 4.6D). Both the zona pellucida and the theca layer appeared thicker in this stage (Figure 4.6D) (average zona pellucida thickness 7.10±0.722 µm, and average thecal thickness 16.50±0.27 µm) (Table 4.3).

Table 4.3. Follicular morphometry of *H. flaviviridis* (N= Individual geckos, R= Range of follicle size).

Stage	N/ R	Follicular diameter (μm)	Oocyte diameter (μm)	ZP thickness (μm)	Follicular epithelial height (μm)	Theca thickness (μm)
II. Previtello-genesis (Late Aug)	17 R	102.76 ±13.75[a] 46–204	93.18 ±12.93[a] 40–188	0.39 ±0.087[a] 0.10–1.0	9.06 ±0.68[ab] 6–14	0.48 ±0.07[a] 0.20–1.0
III. Previtello-genesis (Sept-Oct)	10 R	472.00 ±53.60[a] 250–690	389.70 ±48.31[a] 232–606	3.20 ±0.382[b] 1.5–5.0	50.00 ±7.64[d] 15–80	8.35 ±1.52[b] 1.5–14
IV. Previtello-genesis (Nov)	10 R	1312.00 ±83.90[b] 790–1500	1225.90 ±88.34[b] 691–1454	7.10 ±0.722[c] 4.0–9.0	62.50 ±7.43[e] 20–90	16.50 ±.27[c] 15–17
V. Previtello-genesis (Dec)	8 R	2137.50 ±65.30[c] 2000–2500	2078.13 ±67.00[c] 1920– 445	10.63 ±0.625[d] 10–15	27.50 ±3.66[c] 20–50	23.25 ±2.75[d] 18–40
VI. Vitello-genesis (Jan-Feb)	8 R	3050.00 ±137.58[d] 2500–3600	2983.50 ±136.20[d] 2439–3528	16.50 ±0.327[e] 15–17	17.25 ±0.45[b] 15–19	32.50 ±2.99[e] 25–50
VII. Vitello-genesis (Mar-Apr)	8 R	4712.50 ±252.44[e] 4000–6000	4639.75 ±250.35[e] 3934–5915	18.13 ±0.441[f] 17–20	16.50 ±0.73[b] 15–19	38.13 ±2.82[f] 25–50
VIII. Vitello-genesis (Mar-Apr)	8 R	7850.00 ±387.30[f] 6200–9600	7754.38 ±384.18[f] 6115–9485	21.88 ±0.915[g] 20–25	13.75 ±0.82[ab] 10–15	58.13 ±1.88[g] 50–65
IX. Vitello-genesis / Pre-Ovulatory (Mar-Apr)	8 R	11500.00 ±626.78[g] 10000–15000	11169.37 ±621.20[g] 9985–14905	21.88 ±0.915[g] 20–25	10.00 ±0.00[ab] 10–10	61.88 ±.92[g] 60–65
F(8,88)		362.4	352.9	395.4	34.81	273.54
P-value		< 0.001	< 0.001	< 0.001	< 0.001	< 0.001

Statistical differences between groups obtained by Duncan's multiple-comparisons test. Months with significantly different values (mean ± S.E.M) in vertical column were assigned different letters. Stages with the same letter shows statistically no significant difference between them at the 0.05 level of significance.

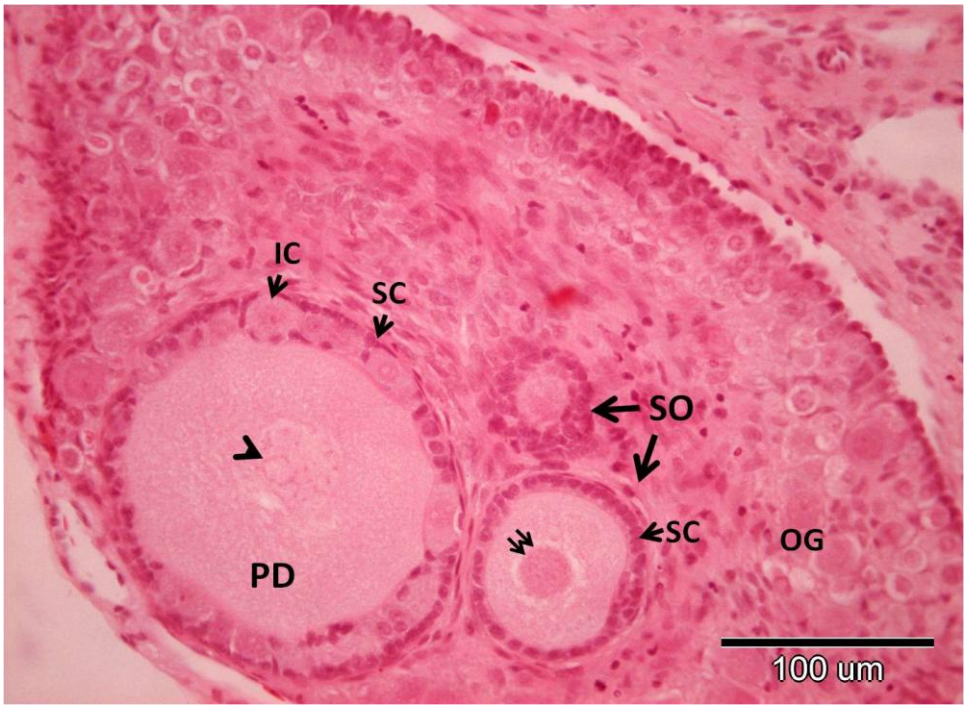

Figure 4.6A. H&E section of germinal bed (GB) with oogonia (OG) and oocytes at different developmental stages. Stage-II follicles (SO) with monolayered granulosa containing small cells (SC) with nucleus containing pre-lampbrush chromosomes (double arrow). Stage-III follicle (PD) with bilayered granulosa containing small (SC) and intermediate cells (IC) with nucleus containing lampbrush chromosomes (arrowhead).

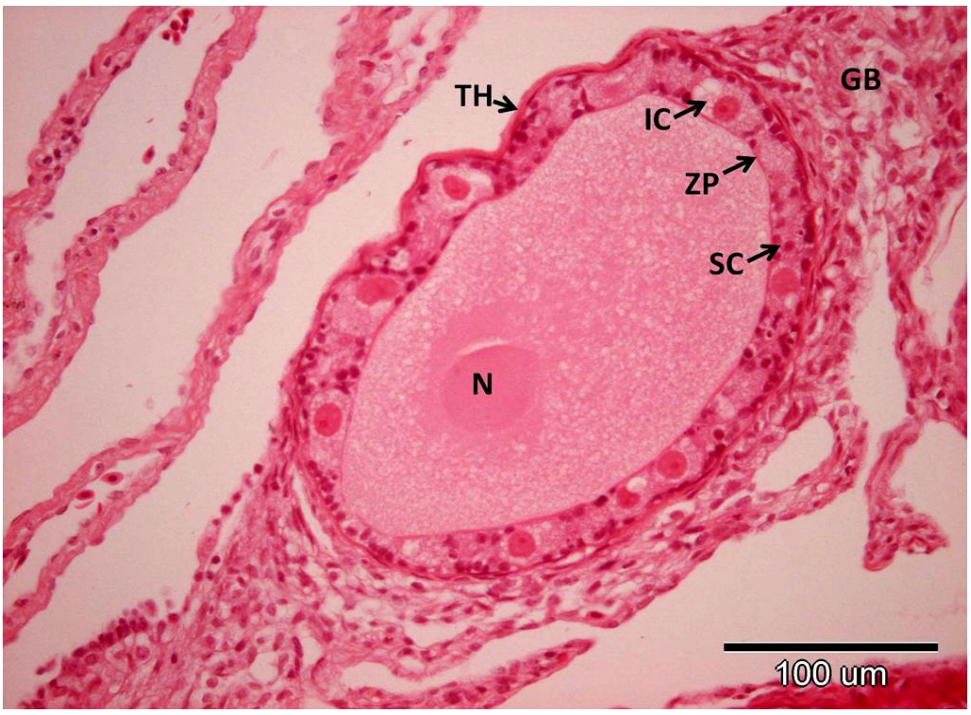

Figure 4.6B. H&E section of large stage-III follicle migrating from the germinal bed (GB) with bilayered granulosa containing small cells (SC) and intermediate cells (IC). Zona pellucida (ZP), thecal layer (TH), oocyte nucleus (N).

4.3.9.3.4 Stage-V Previtellogenesis

In the late recrudescent phase, the oocytes showed a marked increases in diameter (average oocyte diameter 2078.13±67.00 µm, average follicular diameter 2137.50±65.30 µm) (Table 4.3). The ooplasm was homogeneous and finely reticular with many vacuoles located mainly at the periphery (Figure 4.6E). Small PAS-positive granules occurred in the peripheral ooplasm and appeared similar to those in the pyriform cells (Figures 4.6F & 4.6G). The pyriform cells contained large nuclei with single nucleoli and clumps of heterochromatin (Figures 4.6E & 4.6G) (average epithelial height 27.50±3.66 µm) (Table 4.3). The PAS positive reaction in the pyriform cells exhibited varying intensities and distributions; some cells exhibited a patchy or light distribution of stain in the cytoplasm, whereas other cells stained intensely at the apical region of the cytoplasm (Figure 4.6G). The pyriform cells had narrow but long cytoplasmic digitations that extended from the cell body towards the oocyte and joined the zona pellucida (Figure 4.6G). The digitations ended in intercellular bridges. Thus, there appeared to be close communication between the ooplasm and granulosa cells in the developing previtellogenic follicle. The zona pellucida differentiated into an outer noncellular and homogenous layer (hyaline band) and an inner clear striated layer (zona radiata) (Figures 4.6F & 4.6G). The theca also differentiated into an outer theca externa and an inner theca interna. The theca interna was more cellular than the theca externa, which was more fibrous and contained blood cells (Figures 4.6F & 4.6G). (Average zona pellucida thickness 10.63±0.625 µm, and average thecal thickness 23.25±2.75 µm) (Table 4.3).

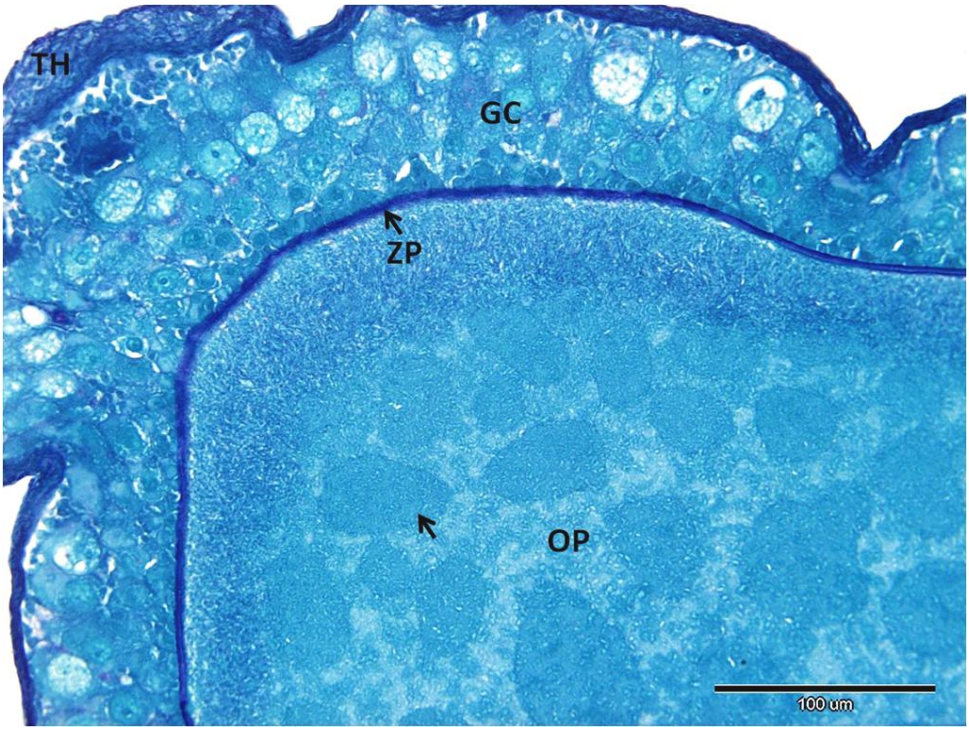

Figure 4.6C. PAS-FG. Stage-IV Previtellogenesis. Ooplasm (OP) with abundant fibrillar cytoplasmic clumps (arrow). Granulosa cells (GC), zona pellucida (ZP), thecal layer (TH).

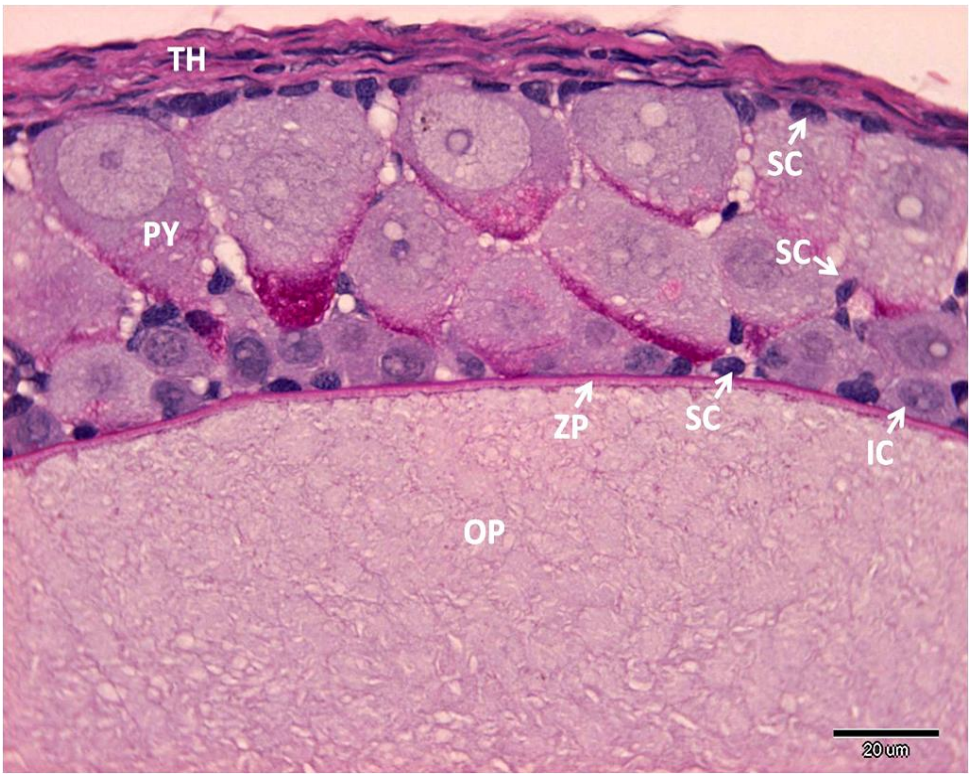

Figure 4.6D. PAS-Haem. Polymorphic granulosa with three types of cells; small (SC), intermediate (IC) and pyriform cells (PY). PAS-positive in cytoplasm of PY. Ooplasm (OP), zona pellucida (ZP), thecal layer (TH).

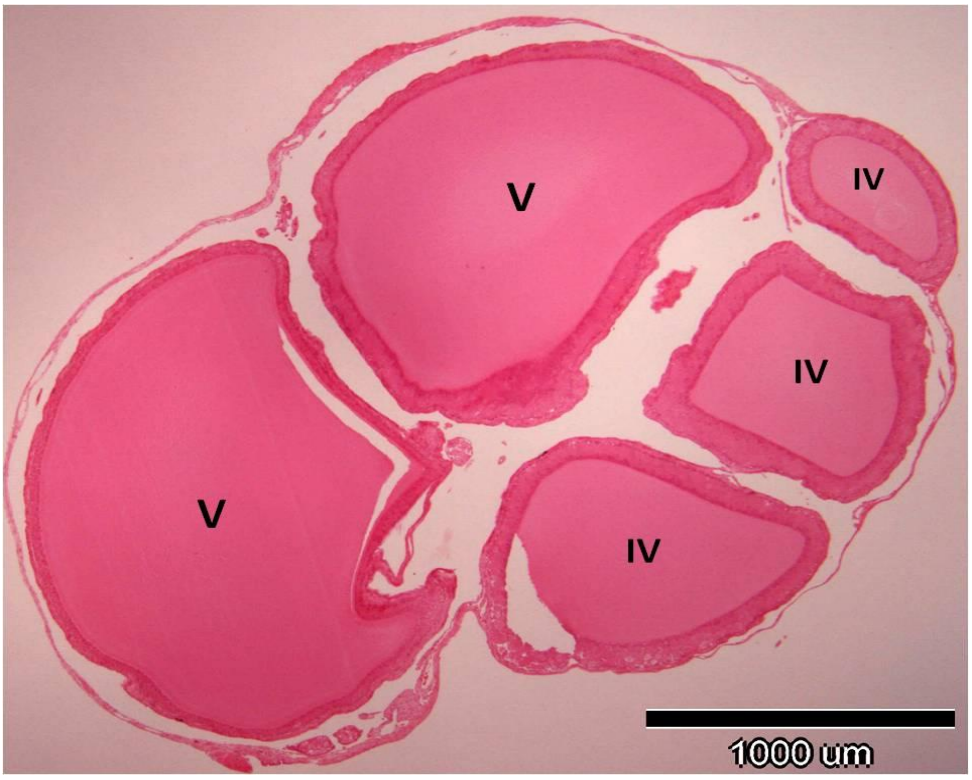

Figure 4.6E. H&E. Stage-V and stage-IV Previtellogenesis. Stage-V showed a significant increase in follicular size.

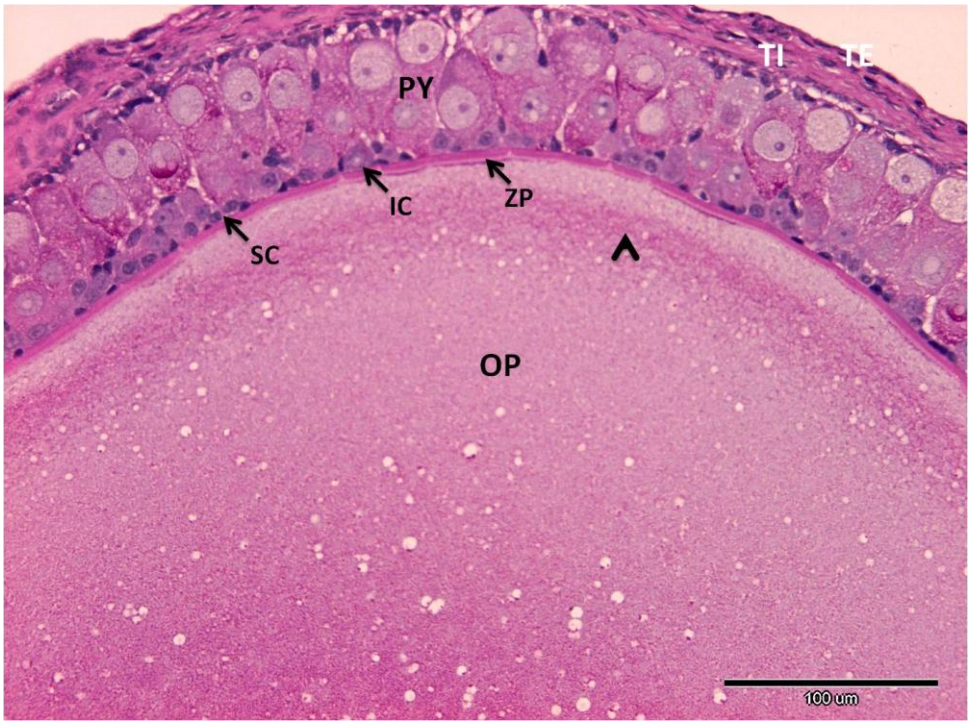

Figure 4.6F. PAS-Haem. Stage-IV Previtellogenesis. Small PAS-positive granules (arrowhead) in peripheral ooplasm similar to those in pyriform cells (PY). Zona pellucida (ZP). Thecal layers; theca externa (TE) and theca interna (TI).

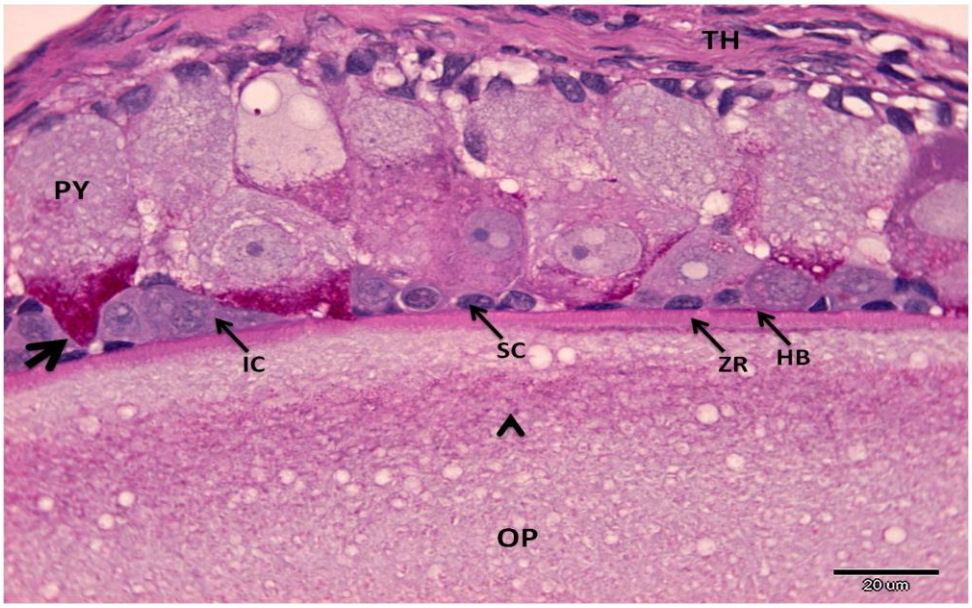

Figure 4.6G. PAS-Haem. Stage-IV Previtellogenesis. Granulosa PAS-positive. Pyriform cells with cytoplasmic extensions (arrow) stained strongly for PAS. Small granules in peripheral ooplasm (arrowhead) stained positive for PAS. Zona pellucida layers; hyaline band (HB) and zona radiata (ZR). Theca (TH).

4.3.9.3.5 Stage-VI Vitellogenesis

During the early active phase, the oocyte diameters increased greatly in size compared to those observed in previtellogenic stage-V (average oocyte diameter 2983.50±136.20 µm, average follicular diameter 3050.00±137.58 µm) (Table 4.3). In vitellogenic follicles yolk bodies started appearing among the vacuoles in the peripheral ooplasm. The yolk platelets were small, spherical, and homogeneous. The region rich in yolk bodies was separated from the oolemma and zona pellucida by a peripheral, platelet-free zone and exhibited fine fibres (Figures 4.7A, 4.7B & 4.7C). Small granular vesicles also appeared in the peripheral ooplasm between the platelet-free zone and the zona pellucida (Figure 4.7B). The granulosa diminished in width and the polymorphic nature of follicle cells disappeared as the pyriform cells became reduced in size and lost their cytoplasmic extensions (Figure 4.7B) (average epithelial height 17.25±0.45 µm) (Table 4.3). The transition from the pyriform cell granulosa to the homogenous, monolayered granulosa of vitellogenic follicles involved the degeneration of pyriform and intermediate cells, leaving only small cells. The zona pellucida continue to grow with the well developed hyaline band and zona radiata (Figure 4.7B) (average zona pellucida thickness 16.50±0.327 µm) (Table 4.3). The

theca layer also continued to grow and the theca externa and theca interna were well developed (Figure 4.7B) (average theca thickness 32.50±2.99 µm) (Table 4.3).

4.3.9.3.6 Stage-VII Vitellogenesis

With further development, the oocytes increased in diameter (average oocyte diameter 4639.75±250.35 µm, average follicular diameter 4712.50±252.44 µm) (Table 4.3). Follicles were in active vitellogenesis and were characterized by large numbers of yolk platelets in the ooplasm (Fig 4.7D). The number, size, and morphological diversity of the yolk platelets in the ooplasm continued to increase as vitellogenesis progressed. Small platelets were observed at the periphery of the oocyte and towards the centre. Yolk platelets grew larger in size. Small and medium sized yolk platelets were present in this stage (Fig 4.7D). They appeared round and homogenous in structure. The granulosa diminished further in size and became monolayered and was composed of small flat dark cells (Figure 4.7D) (average epithelial height 16.50±0.73 µm) (Table 4.3). The zona pellucida and theca appeared thicker than in previous stages with numerous blood cells (Figure 4.7D) (average zona pellucida thickness 18.13±0.441 µm, and average thecal thickness 38.13±2.82 µm).

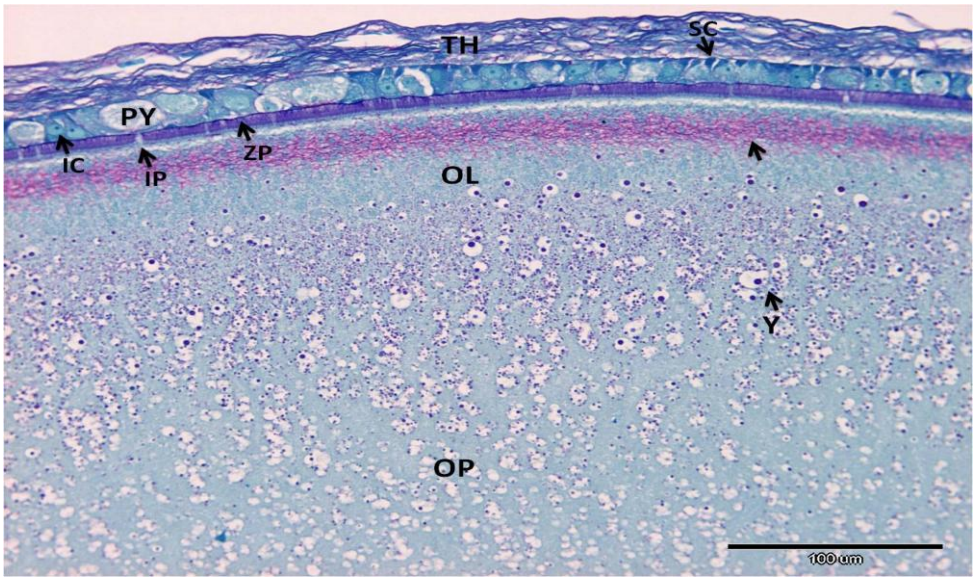

Figure 4.7A. PAS-FG. Stage-VI Vitellogenesis. Yolk bodies (Y) in the peripheral ooplasm (OP). The region is rich in yolk separated from the oolemma (OL) and zona pellucida (ZP) by a peripheral, platelet-free zone (arrow). Pyriform cells (PY) started degenerating and appeared reduced in size. Intercellular bridges (IP) connecting pyriform (PY) cells with the ooplasm (OP) through zona pellucida (ZP). Theca (TH) continued to grow during this stage.

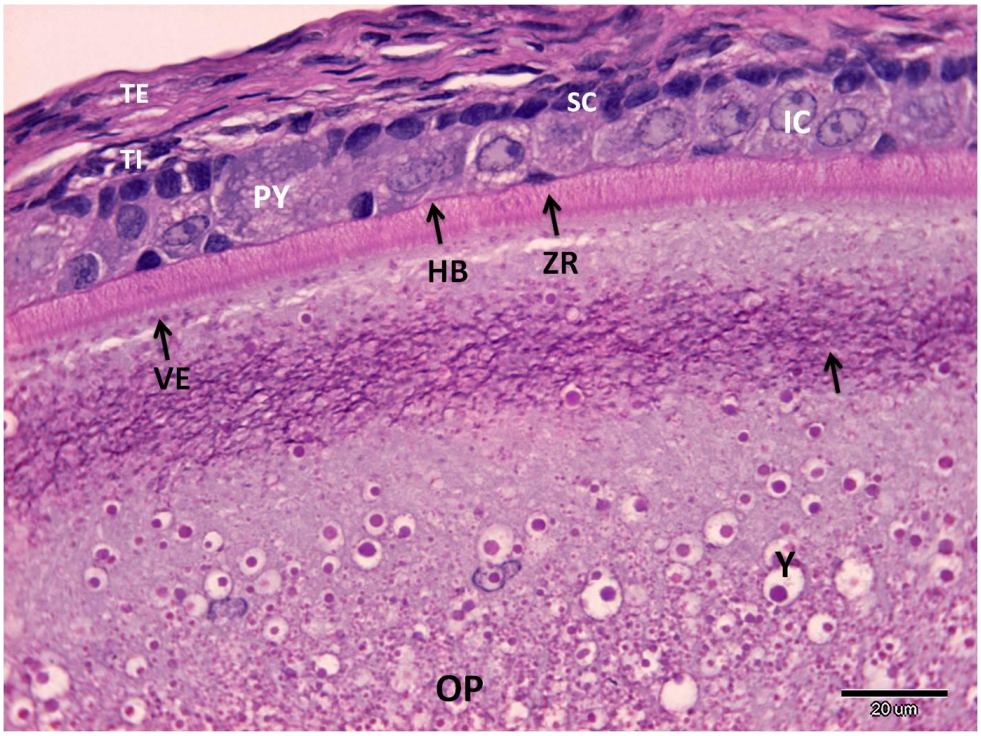

Figure 4.7B. PAS-Haem. Stage-VI Vitellogenesis. Polymorphic nature of granulosa follicle cells begins to disappear. Pyriform cells (PY) lost its nuclei and cytoplasmic contents. Zona pellucida layers; hyaline band (HB) and zona radiata (ZR). Theca layers; theca externa (TE) and theca interna (TI). Platelet-free zone with fine fibres (arrow), and granular vesicles (VE) appeared close to zona pellucida. Yolk bodies (Y) started appearing at the periphery of ooplasm (OP).

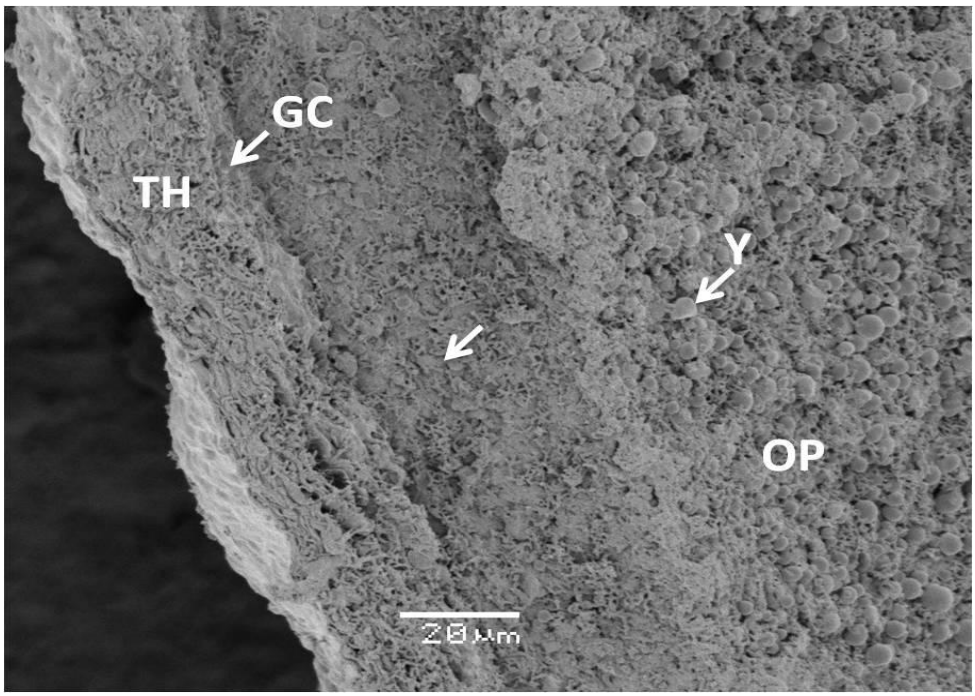

Figure 4.7C. SEM. Stage-VI Vitellogenesis. Yolk (Y) in the peripheral ooplasm (OP). Platelet-free zone with fine fibres (arrow). Granulosa layer (GC), thecal layer (TH).

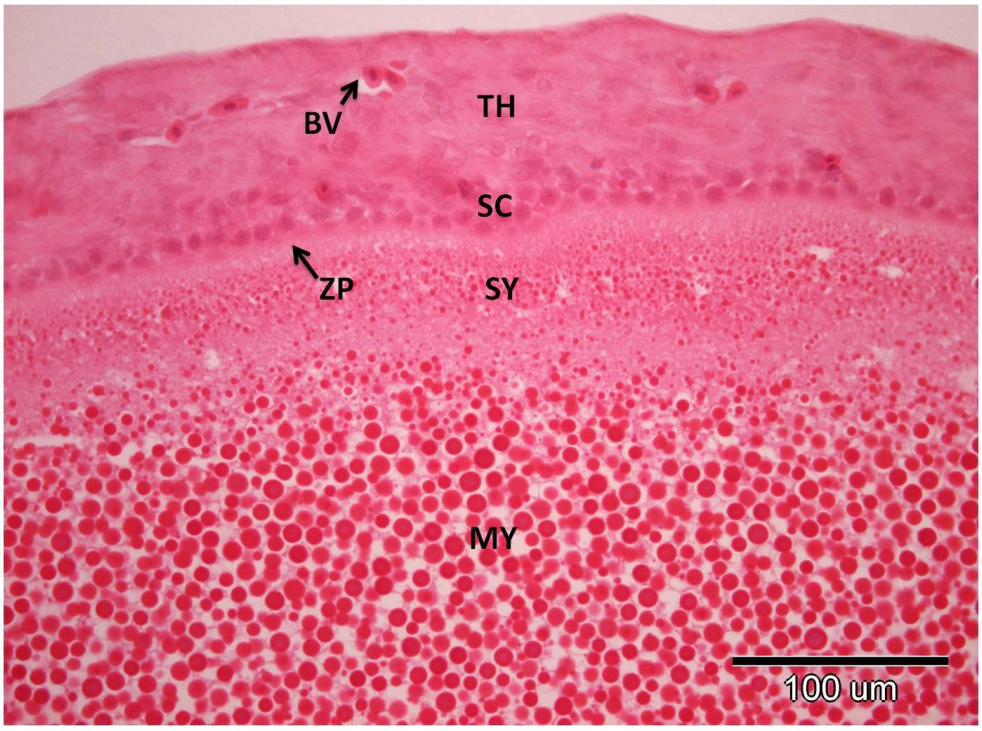

Figure 4.7D. H&E. Stage-VII Vitellogenesis. Small (SY) and medium (MY) size yolk platelets in the ooplasm. Granulosa composed of small flat dark cells (SC). Zona pellucida (ZP) and thca (TH) become thicker and numerous blood vessels (BV) present in the thecal layer.

4.3.9.3.7 Stage-VIII Vitellogenesis

As vitellogenesis progressed, the oocytes increased further in diameter (average oocyte diameter 7754.38±384.18 µm, average follicular diameter 7850.00±387.30 µm) (Table 4.3). Most of the ooplasm was full of yolk platelets. At the periphery, there was a layer with small platelets. Toward the centre of the oocyte, the yolk platelets increased in diameter with medium and large size yolk platelets that filled most of the ooplasm (Figure 4.7E). The granulosa was monolayered with small cells (Figure 4.7E) (average epithelial height 13.75±0.82 µm) (Table 4.3). Thickening of the zona pellucida and theca continued at this stage (Figure 4.7E) (average zona pellucida thickness 21.88±0.915 µm, and average thecal thickness 58.13±1.88 µm).

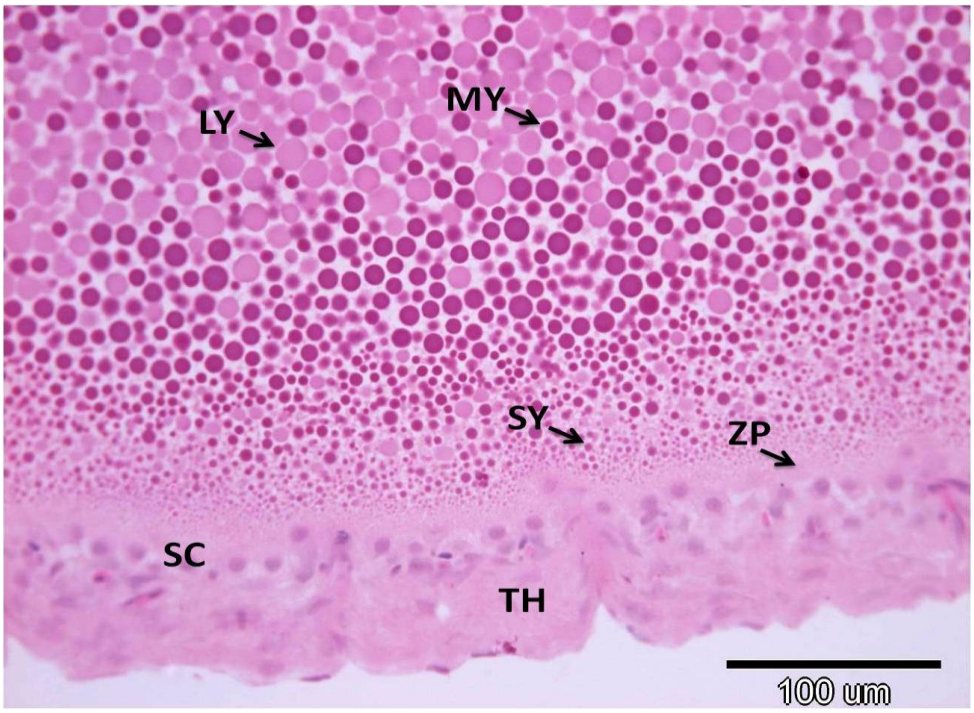

Figure 4.7E. H&E. Stage-VIII Vitellogenesis. Yolk platelets exhibiting small (SY), medium (MY) and large (LY) size which filled most of the ooplasm. The granulosa appeared monolayered with small cells (SC). Zona pellucida (ZP) and theca (TH) continued to grow during this stage.

4.3.9.3.8 Stage-IX Vitellogenesis

Oocyte growth continued as the yolk platelets filled the majority of the ooplasm (average oocyte diameter 11169.37±621.20 µm, average follicular diameter 11500.00±626.78 µm) (Table 4.3). Yolk platelets created regions with platelets of similar sizes: small platelets, medium platelets and then large size yolk platelets (Figure 4.7F). Associated with the medium and large size yolk platelets were very large vacuolated platelets (Figure 4.7G). Centrally, homogeneous platelets appeared; the size and number of platelets diminished toward the centre of the oocyte, where the ooplasm was finely reticulated but lacked yolk platelets (Figure 4.7H). The granulosa was monolayered with simple squamous small cells (Figure 4.7F).

4.3.9.3.9 Preovulatory follicles

The preovulatory follicles attained a mean diameter of 14.06±09.03 mm. The morphology of the granulosa remained unchanged as in Stage-IX. The principal difference during this stage was the great change in the oocyte diameter.

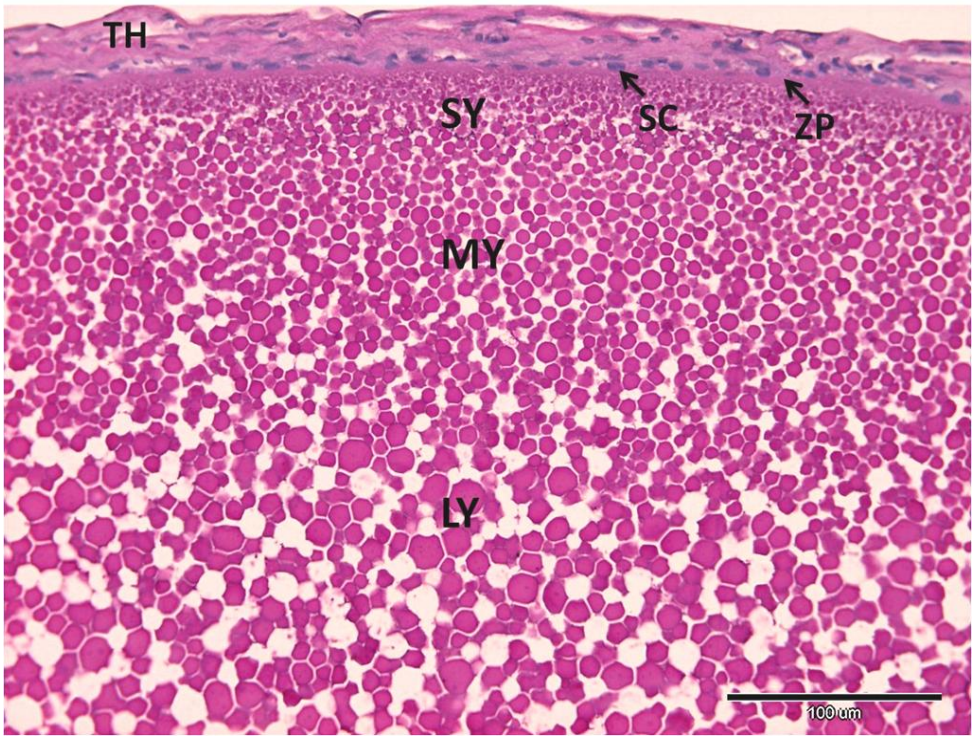

Figure 4.7F. PAS-Haem. Stage-IX Vitellogenesis. Regions of small (SY), medium (MY) and large (LY) size yolk platelets arranged towards the centre of the oocytes. The granulosa was monolayered with simple squamous small cells (SC). Zona pellucida (ZP) thickness remained unchanged whereas theca layer (TH) continued to grow during this stage.

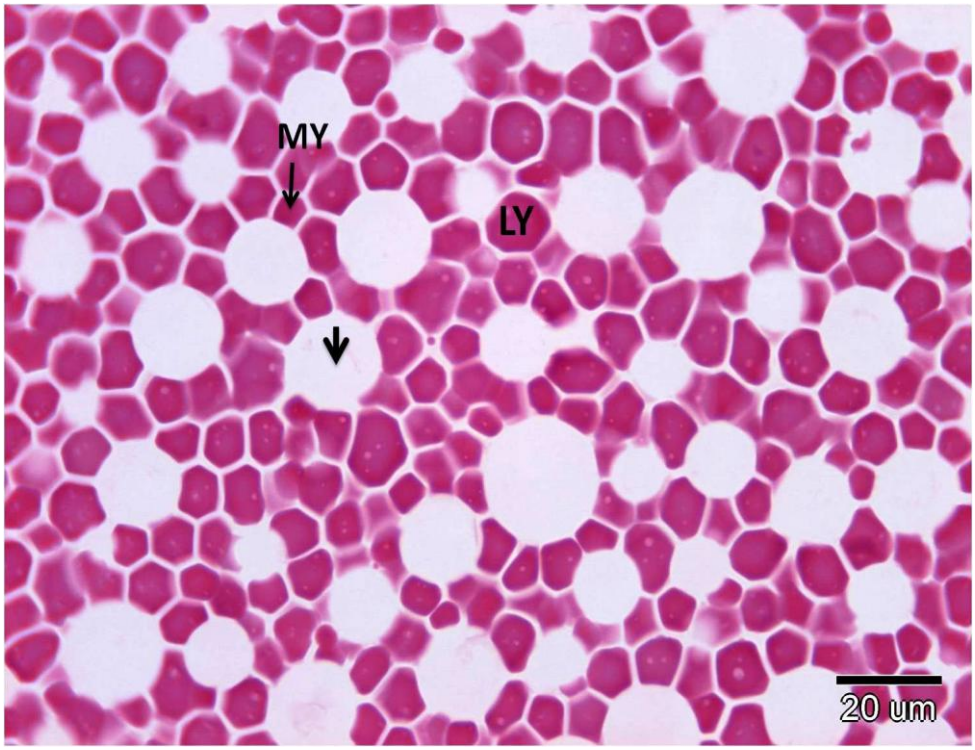

Figure 4.7G. H&E. Stage-IX Vitellogenesis. Associated with the medium (MY) and large size (LY) yolk platelets, large vacuolated platelets (arrow).

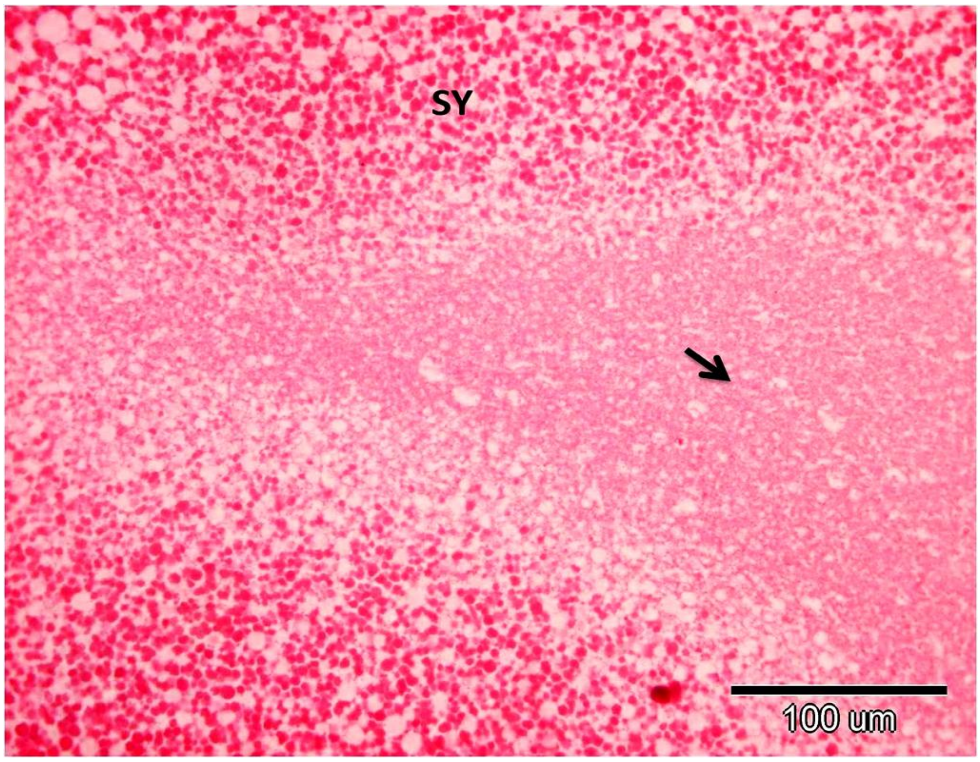

Figure 4.7H. H&E. Stage-IX Vitellogenesis. Size and number of platelets diminished toward the centre of the oocyte, where the ooplasm was finely reticulated but lacked platelets (arrow). Mainly small yolk platelets (SY) appeared near the centre of the oocyte.

4.3.9.4 Ultrastructural changes in the granulosa cells and thecal layer

The ultrastructural changes in the granulosa cells of the ovarian follicles were related to the increase in the steroidogenic activity of the ovarian follicles. These included ultrastructural steroidogenic characteristics such as an increase in SER, lipid droplets, and the presence of swollen vesiculated mitochondria with tubular cristae. Occasionally, tubular and cisternal SER organized into folded arrays and elaborate concentric whorls associated with lipid droplets or mitochondria were observed. In addition, numerous vesicles produced by the Golgi complexes were also seen.

The details of the ultrastructure of granulosa cells are presented in the following three stages of granulosa development throughout the reproductive cycle:

4.3.9.4.1 Stage-I Previtellogenic follicles with a monolayered granulosa

During the late quiescent phase (early privitellogenesis), the granulosa was monolayered and consisted of small cells only. Small granulosa cells rested against a

basal lamina that entirely separated the epithelium from the theca. Nuclei of small cells were located basally and contained one or two nucleoli and scattered clumps of heterochromatin (Figure 4.8A). The cytoplasm contained undeveloped steroidogenic features. Some RER and free ribosomes were observed, scattered singly or in clusters, but were not abundant. Mitochondria were elongated or oval without distinct tubular cristae (Figure 4.8B).

4.3.9.4.2 Stage-II Previtellogenic follicles with a polymorphic granulosa

During the recrudescent phase (previtellogenesis), the granulosa differentiated and became polymorphic with three types of cells: small, intermediate, and large pyriform cells. These cells were interconnected by desmosomes (Figure 4.8C), and thereby constituted a coherent epithelium, and occurred at the apical surface opposite the oocyte (Figure 4.8D), and the basal surface which delineated the granulosa from the theca (Figure 4.8E). Granulosa cells showed a gradual increase in steroidogenic ultrastructural features.

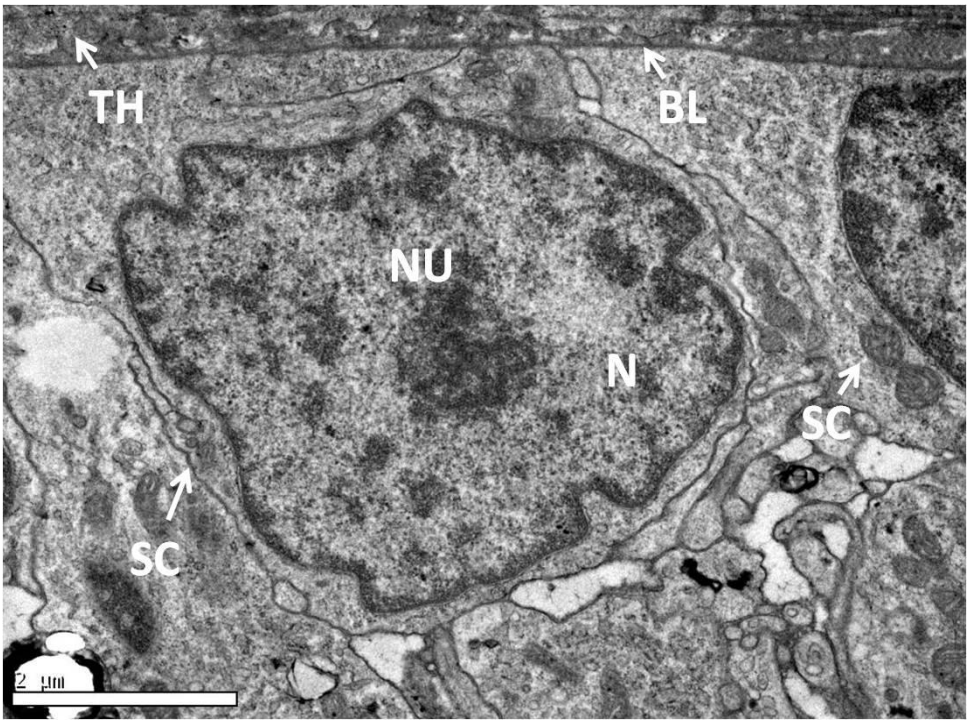

Figure 4.8A TEM. Early Previtellogenesis. Small cells (SC) rested against basal lamina (BL) separating granulosa from the theca (TH). Nucleus (N) of small cell appeared with one nucleolus (NU) and scattered clumps of heterochromatin.

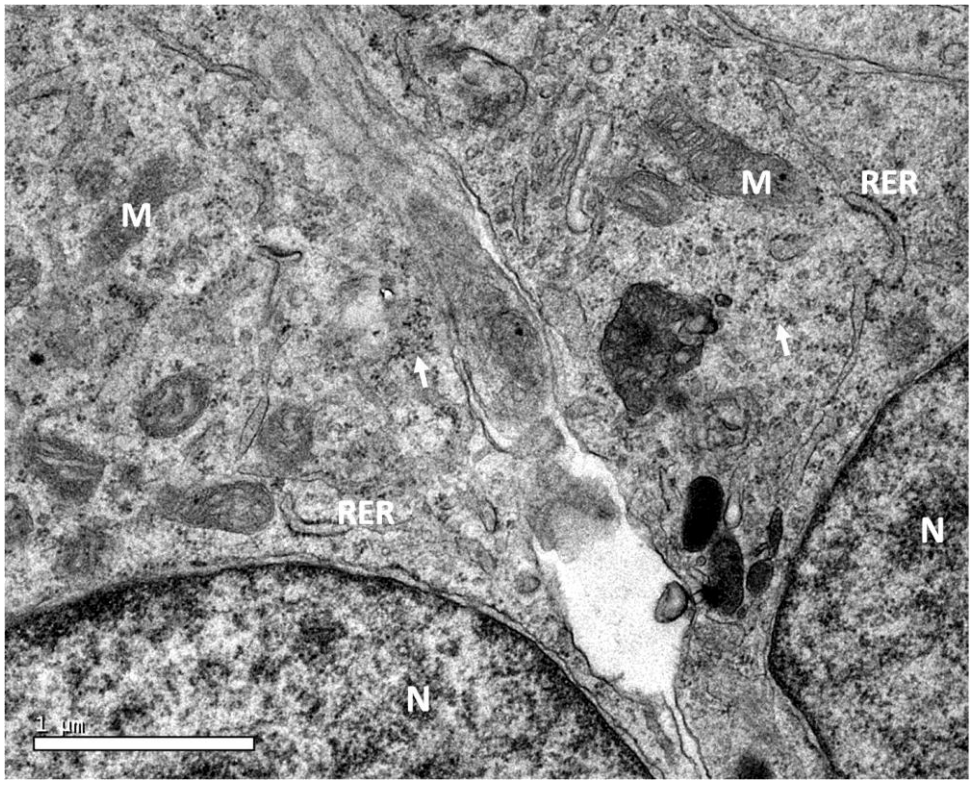

Figure 4.8B. TEM. Early previtellogenesis, the granulosa small cells contained few RER and free ribosomes (arrow) scattered singly or in clusters. Mitochondria (M) without distinct tubular cristae. Nucleus (N).

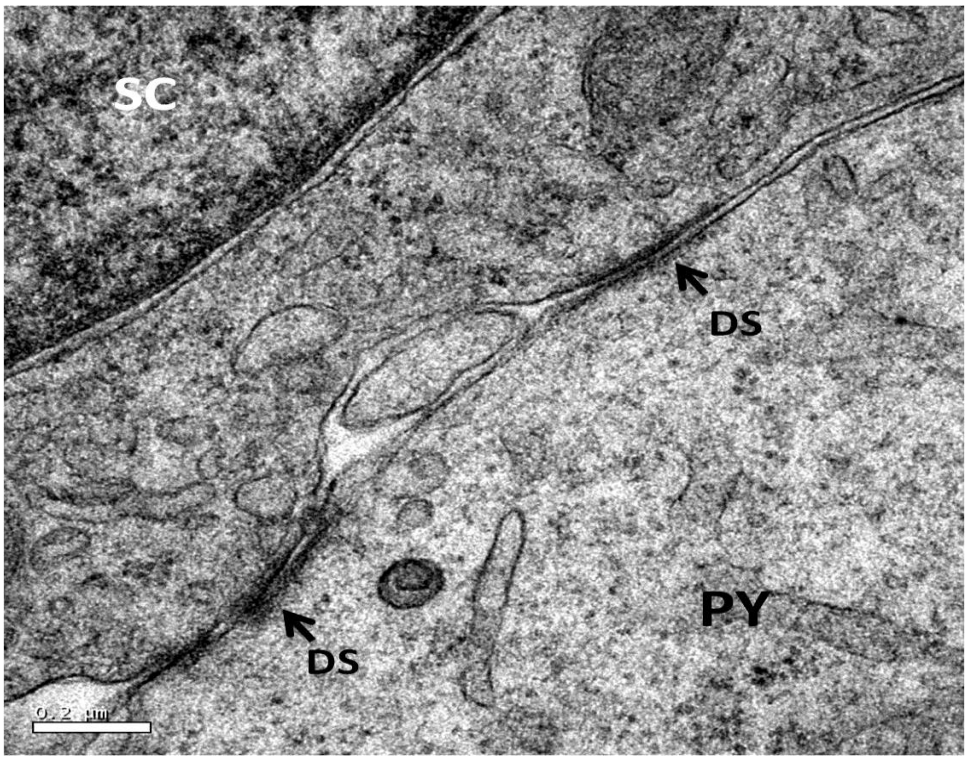

Figure 4.8C. TEM. Polymorphic granulosa. Small (SC) and pyriform (PY) cells interconnected by desmosomes (DS).

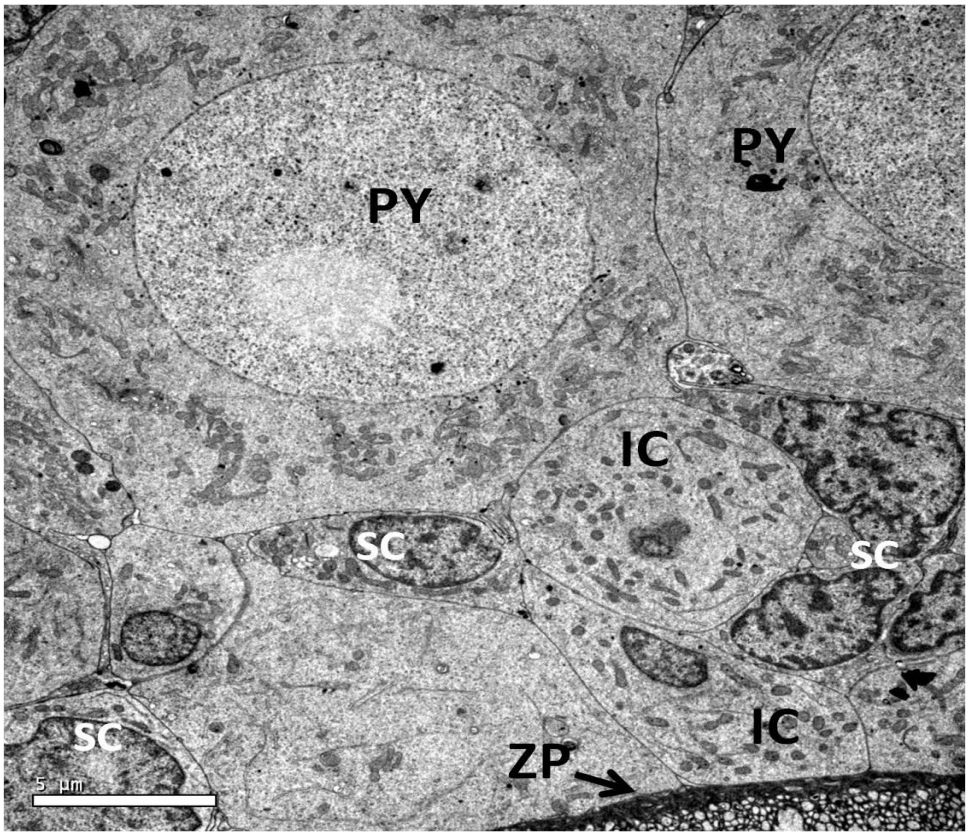

Figure 4.8D. TEM. Polymorphic granulosa. Small (SC), intermediate (IC) and pyriform (PY) cells at the apical surface opposing the oocyte. Zona pellucida (ZP).

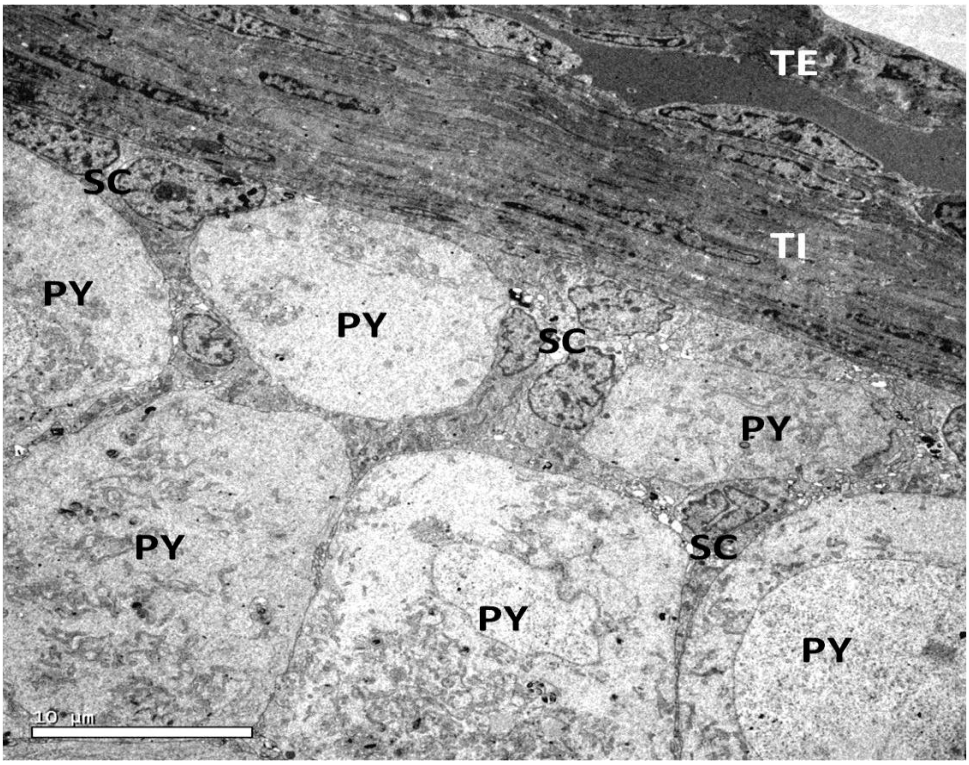

Figure 4.8E. TEM. Polymorphic granulosa. Small (SC) and pyriform (PY) cells at basal surface next to theca layers; theca externa (TE) and theca interna (TI).

4.3.9.4.2.1 Small cells

Most small cells were in contact with the basal lamina. However, several were situated adjacent to the oocyte, or interspersed between other granulosa cells (Figures 4.8D & 4.8E). Apically, small cells were separated from the oocyte by its surface microvilli (zona pellucida) (Figure 4.8F). The narrow apical region or cytoplasmic extension of apical small cells constricted and united with the oocyte through the intercellular bridge in the zona pellucida (Figure 4.8F) The nucleus was oval or polyhedral in shape and contained clumps of condensed chromatin and one or two nucleoli (Figures 4.8F & 4.8G). The cell cytoplasm contained many ribosomes, most of which were associated with RER. However, in some cells, free ribosomes were also found throughout the cytoplasm. Increased amounts of mitochondria with tubular cristae in an electron-dense matrix were dispersed throughout the cell. Golgi complexes consisted of several membrane platelets associated with rounded vesicles (Figure 4.8H). Tubular and cisternal SER were also found. The cisternae in some areas were organized into folded arrays and elaborate concentric whorls. The folded membrane arrays and cisternal whorls were often associated with lipid droplets or mitochondria (Figure 4.8H). The SER were closely associated with mitochondria and lipid droplets (Figure 4.8H). Surface contact between small cells and other granulosa cells commonly involved the elaboration of microvilli on the surfaces of pyriform and intermediate cells. (Figures 4.8G & 4.8H).

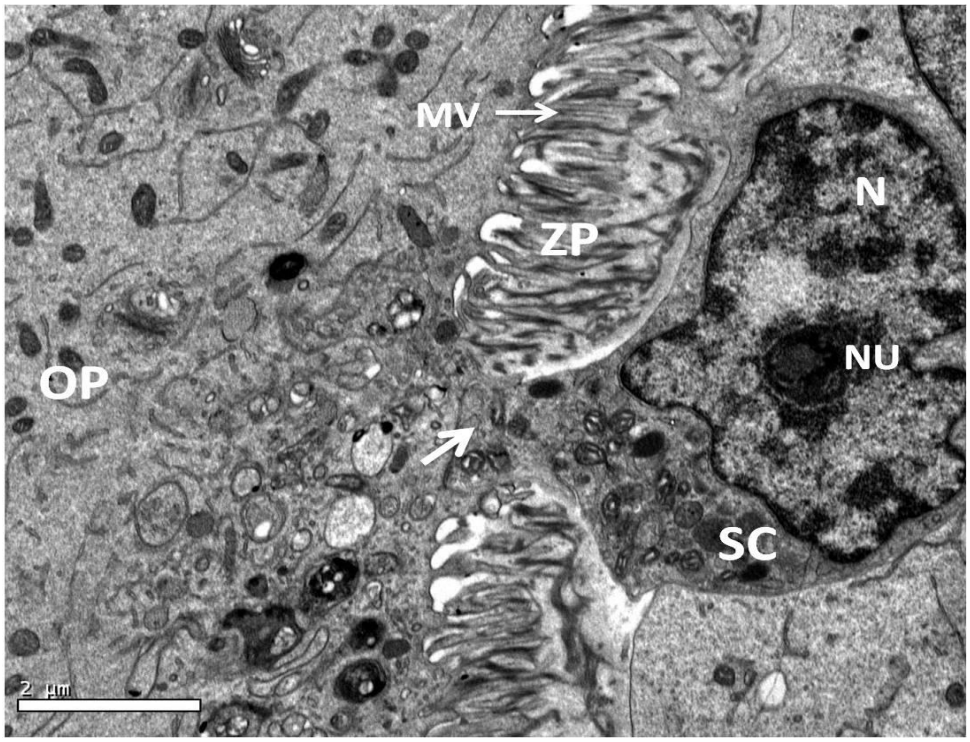

Figure 4.8F. TEM. Small cell (SC) adjacent to ooplasm (OP) of oocyte separated by microvilli (MV) of zona pellucida (ZP). Cytoplasmic extensions (arrow) of SC connect with oocyte through intercellular bridge. Nucleus (N) of small cells with prominent nucleolus (NU).

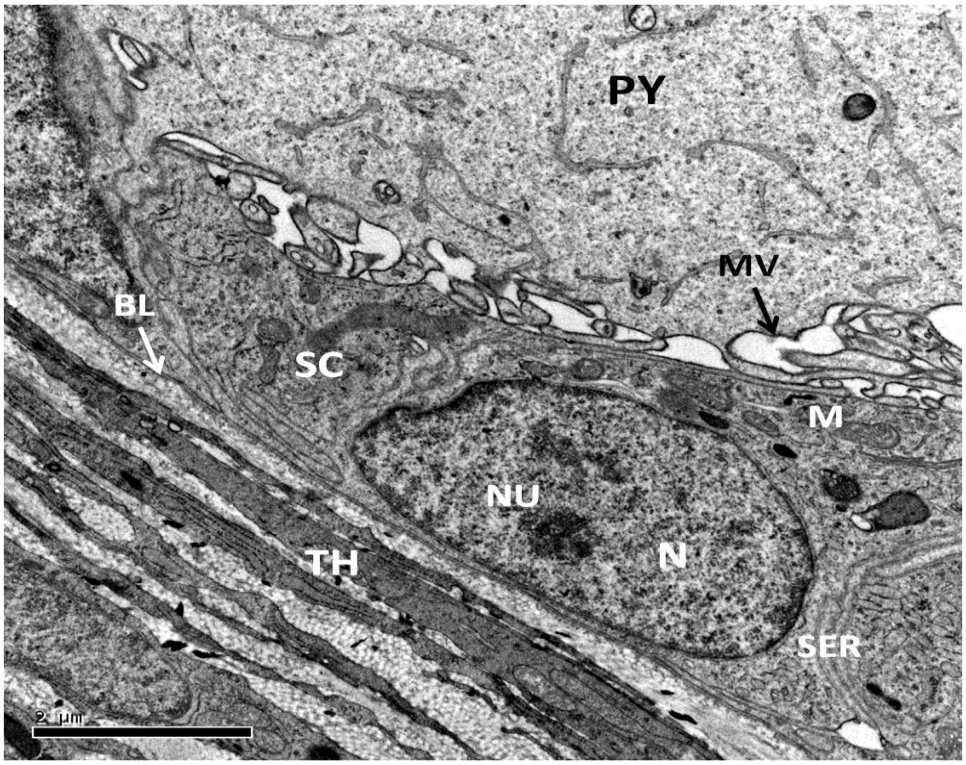

Figure 4.8G. TEM. Small cells (SC) at the basal lamina (BL) with oval nuclei (N) and nucleolus (NU). Mitochondria (M), SER, pyriform cell (PY), microvilli (MV), theca (TH).

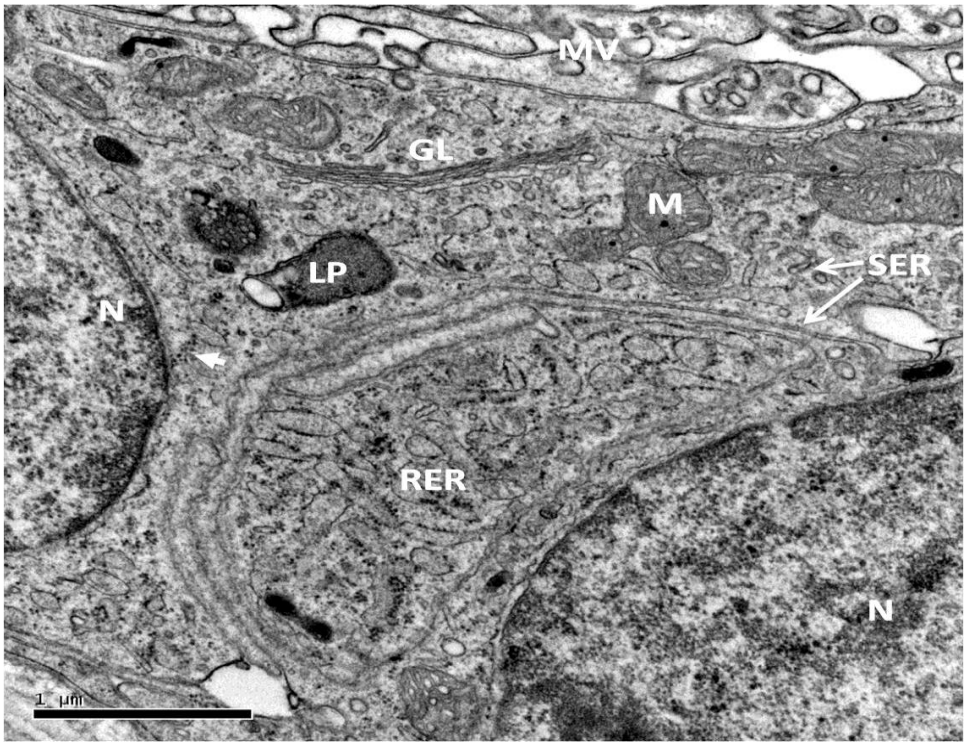

Figure 4.8H. TEM. Higher magnification of Figure 4.5G. Small cell showing cytoplasm with tubular or cisternal whorls SER, RER and free ribosomes (arrow). Numerous mitochondria (M) with tubular cristae associated with Golgi complex (GL), and lipid droplet (LP). Nucleus (N), microvilli (MV).

4.3.9.4.2.2 Intermediate cells

Intermediate cells located apically in the granulosa were separated from the oocyte by the zona pellucida (Figure 4.8I). They were connected to the oocyte via intercellular bridges. The striations of the zona radiata corresponded to microvilli that originated on the surface of the oocyte and to cytoplasmic extensions of the follicular cells (Figure 4.8J). Intermediate cells were bell-shaped with large nuclei that contained highly dispersed chromatin and prominent nucleoli. The cytoplasm contained increased amounts of mitochondria which appeared elongated with tubular cristae and were seen either scattered throughout the cell or grouped around dense granular material (Figures 4.8I, 4.8K & 4.8L). Golgi complexes, RER, SER, lipid droplets, microfilaments and microtubules were also present in these cells. Tubular and cisternal SER were frequently interconnected. Tubular SER was densely packed, whereas the cisternal SER was more loosely arranged. The cisternae in some areas were organized into folded arrays and elaborate concentric whorls. The folded

membrane arrays and cisternal whorls were often associated with lipid droplets or mitochondria (Figures 4.8K & 4.8L). A close association between SER, mitochondria and lipid droplets was clearly evident (Figure 4.8L).

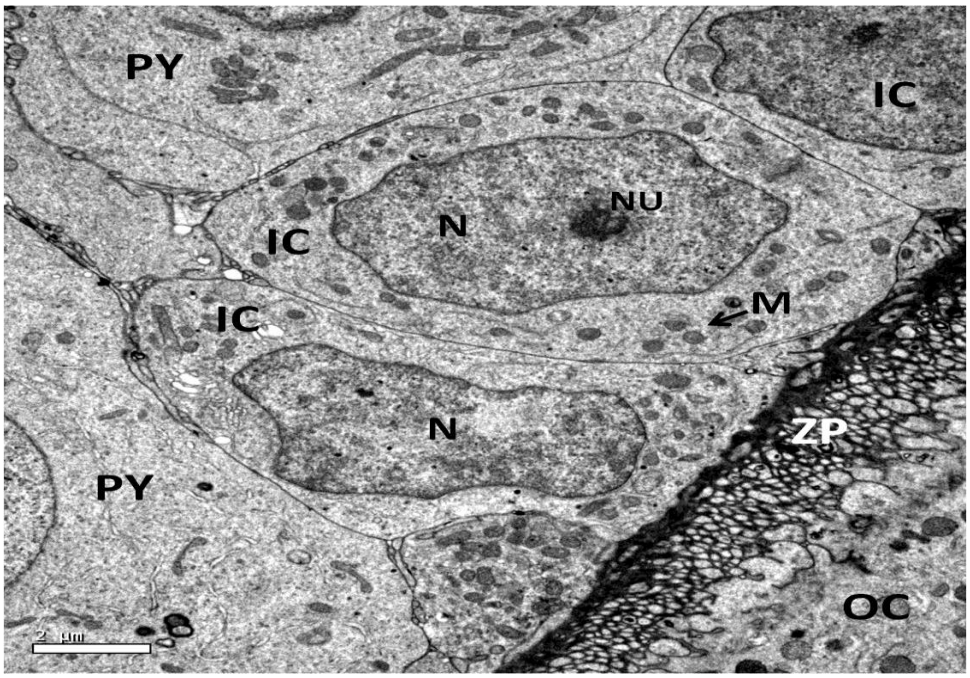

Figure 4.8I. TEM. Intermediate cells (IC) adjacent to oocyte (OC) with large nuclei (N) and nucleoli (NU). Zona pellucida (ZP), pyriform cells (PY).

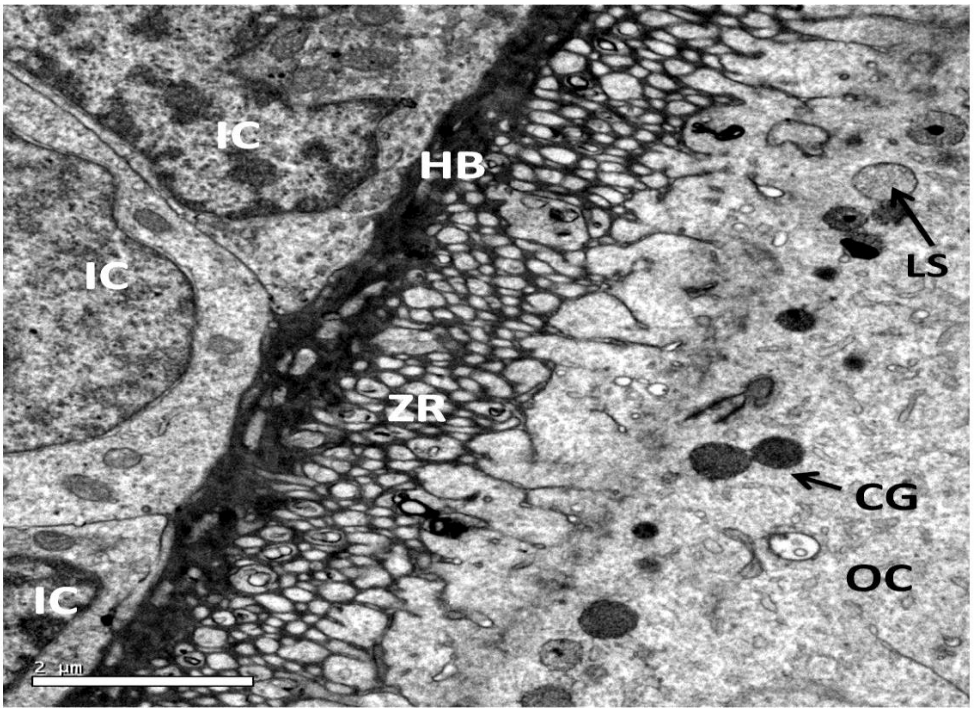

Figure 4.8J. TEM. Intermediate cells (IC) separated from the oocyte (OC) Zona pellucida. Zona pellucida consisting of striated zona radiata (ZR) and thin hyaline band (HB). Lysosomes (LS), cortical granules (CG).

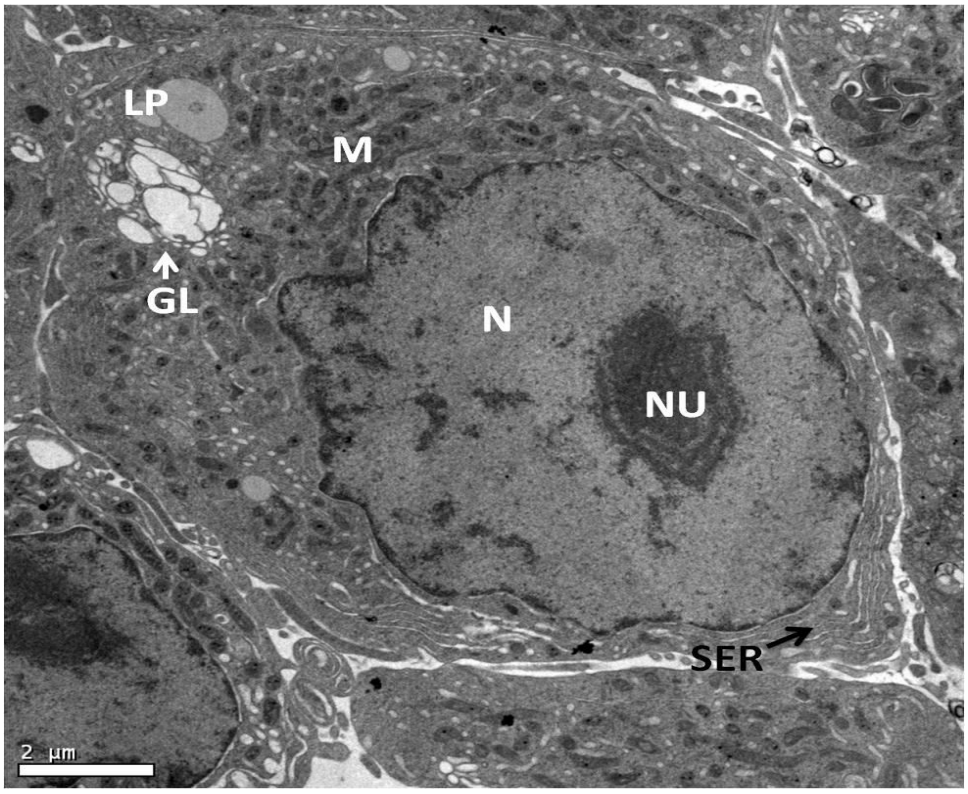

Figure 4.8K. TEM. Intermediate cell showing Golgi complex (GL), SER, lipid droplets (LP), mitochondria (M). Nucleus (N), nucleolus (NU).

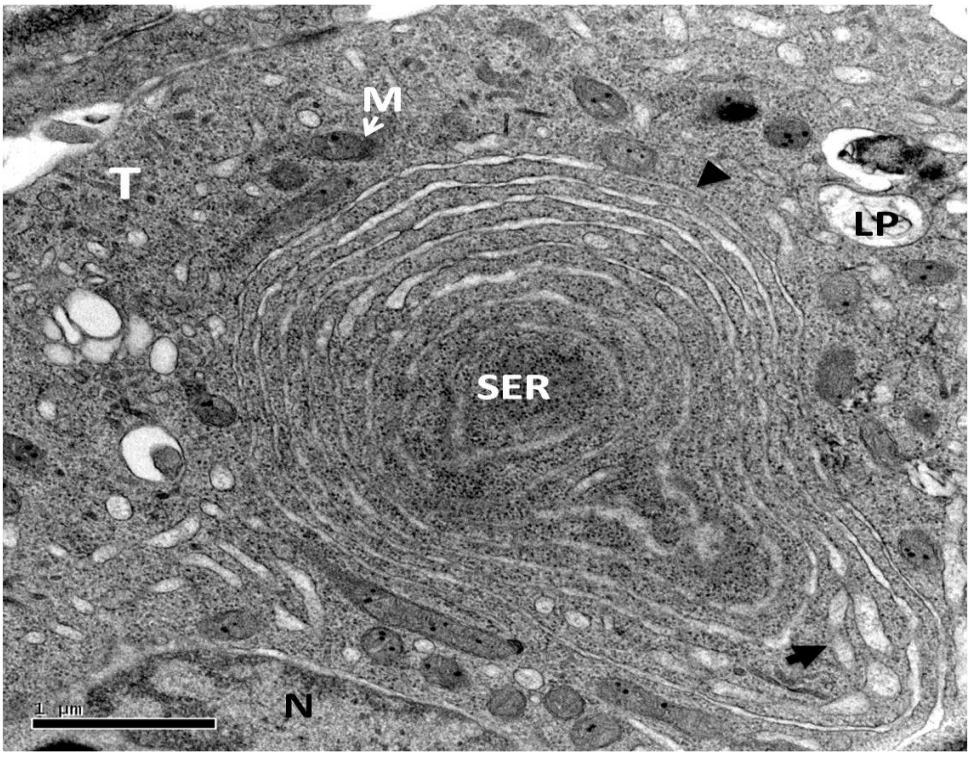

Figure 4.8L. TEM. High magnification of intermediate cell cytoplasm with interconnected tubular (arrow) and cisternal whorls SER (arrowhead). The cisternal whorls SER associated with mitochondria (M) and lipid droplets (LP). Scattered microtubules (T). Nucleus (N), vacuoles (V).

4.3.9.4.2.3 Pyriform cells

Pyriform cells extended through the full thickness of the granulosa from the basal lamina to the oocyte (Figures 4.8D & 4.8E). The nucleus was large and located basally and contained highly dispersed chromatin and a prominent nucleolus that appeared ring-shaped or vacuolated (Figure 4.8M). The cytoplasm had a large number of mitochondria, greatly extended Golgi complexes, lipid droplets, scarce RER, clusters of ribosomes, and small round vesicles with varying granular contents (Figures 4.8N & 4.8O). Tubular and cisternal SER were also present and were seen in the developed pyriform cells. Tubular SER was densely packed, whereas the cisternal SER was loosely arranged (Figure 4.8O). There was a close association between SER, mitochondria and lipid droplets (Figure 4.8O).

The pyriform cells had narrow but long cytoplasmic digitations that extended from the cell body towards the oocyte and joined the zona pellucida. The digitations ended in an intercellular bridge (Figure 4.8P). The cytoplasm of some pyriform cells contains granules and cytoplasmic contents that were similar in size, and shape to those in the peripheral ooplasm (Figure 4.8Q).

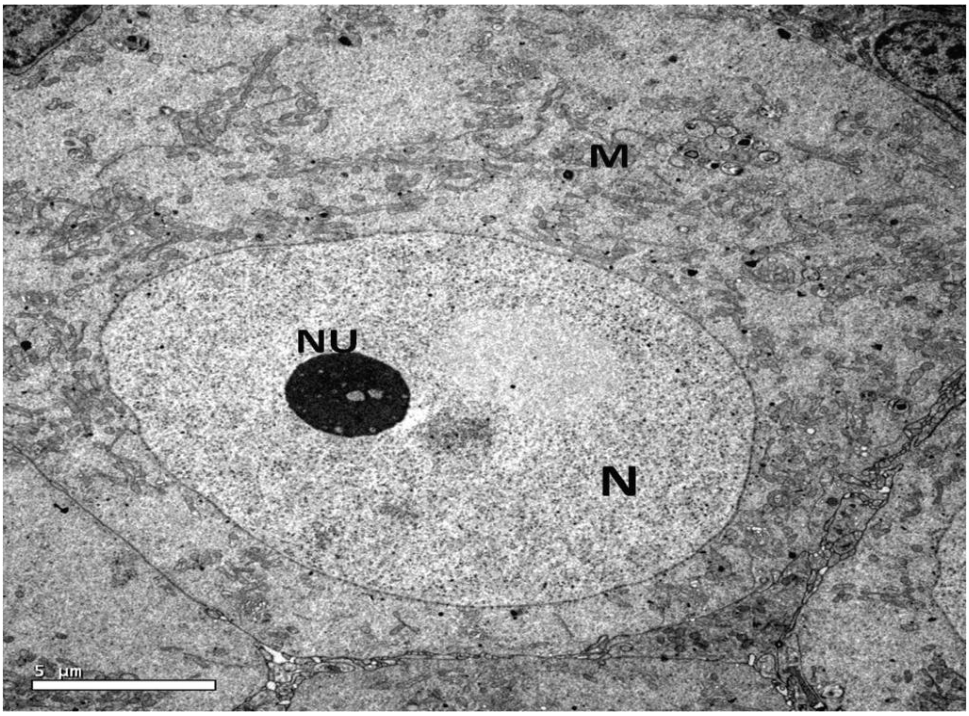

Figure 4.8M. TEM. Pyriform cell with large nucleus (N) and prominent nucleolus (NU). Large number of mitochondria (M) in the cytoplasm.

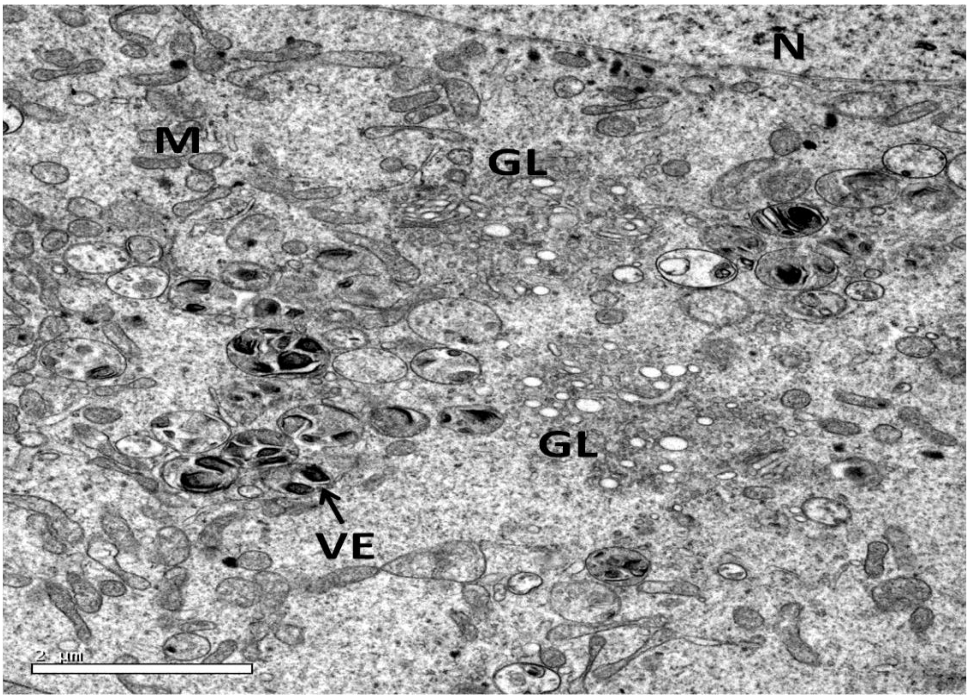

Figure 4.8N. TEM. Pyriform cytoplasm with numerous mitochondria (M), Golgi complexes (GL), vesicles (VE) with varying granular contents. Nucleus (N).

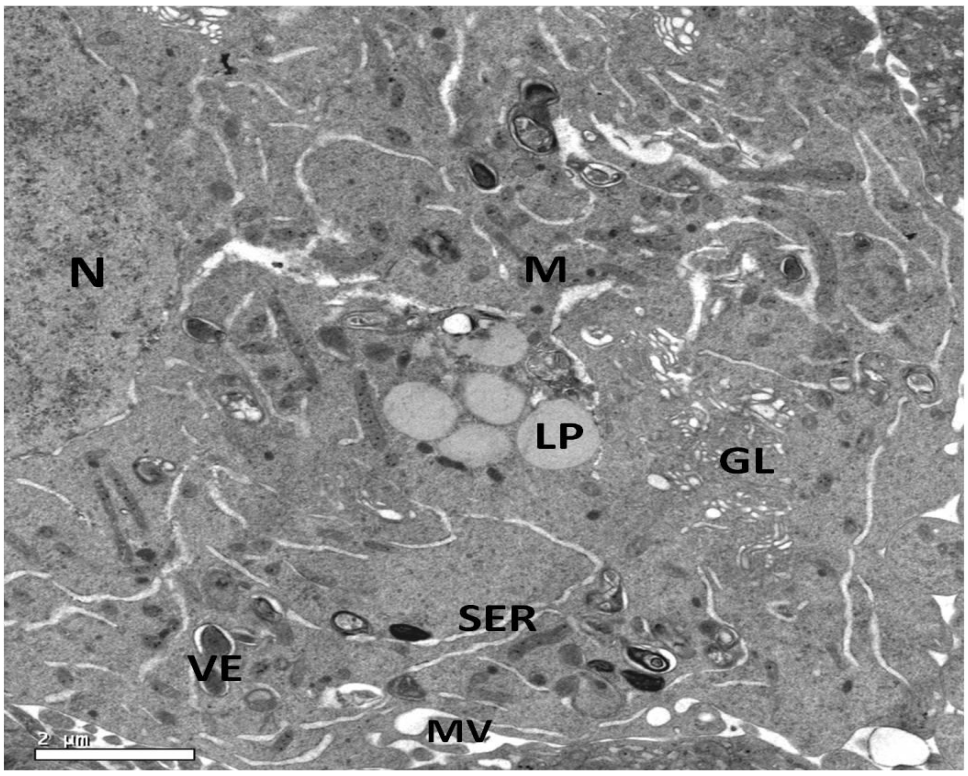

Figure 4.8O. TEM. Pyriform cell cytoplasm with mitochondria (M), Golgi complexes (GL), lipid droplets (LP), granular vesicles (VE). SER is loosely arranged. Nucleus (N), microvill (MV).

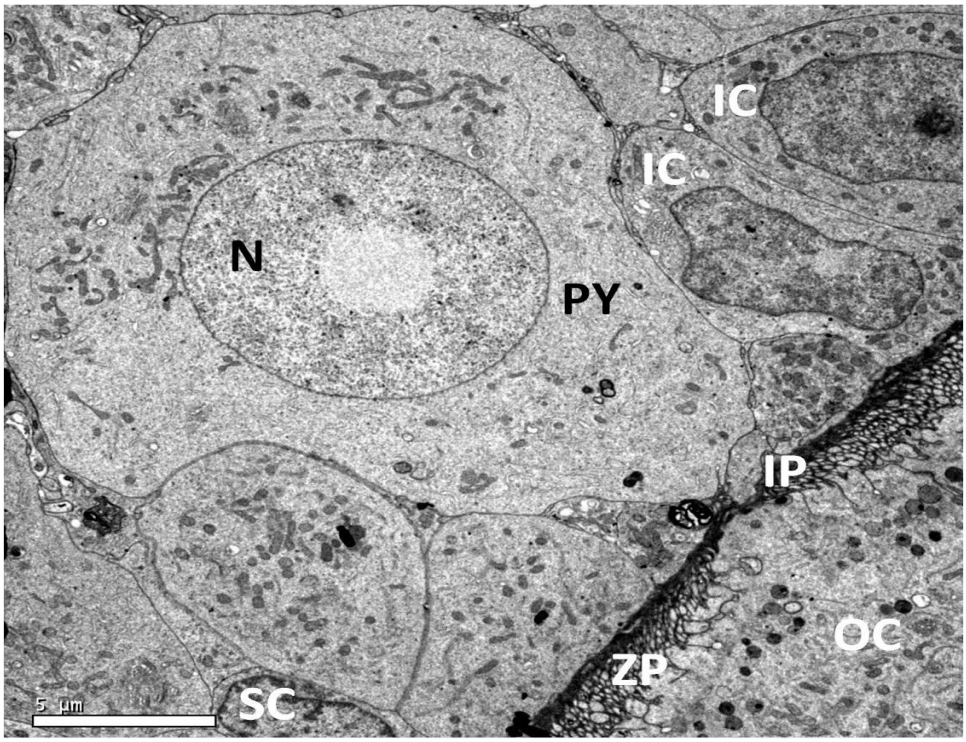

Figure 4.8P. TEM. Pyriform cell (PY) cytoplasmic extensions connect with oocyte (OC) via intercellular bridges (IP). Nucleus (N), intermediate cells (IC), small cells (SC), zona pellucida (ZP).

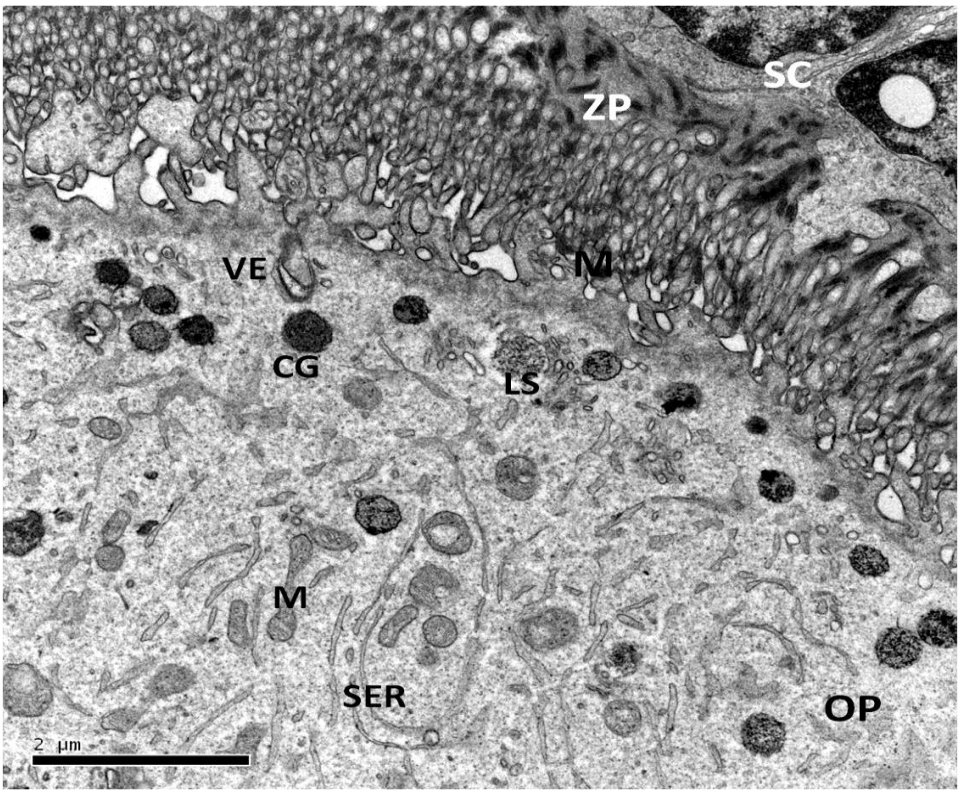

Figure 4.8Q. TEM. Ooplasm (OP) with vesicles (VE) of varying granular contents, mitochondria (M), SER, lysosomes (LS). Zona pellucida (ZP), small cells SC), cortical granules (CG).

4.3.9.4.3 Stage-III Vitellogenic follicles with late monolayered granulosa

During the active phase (vitellogenesis), the granulosa consisted of a single layer of small cells (Figure 4.8R). The cytoplasm of the small cells contained numerous lipid droplets and electron-dense vesicles or granules. Abundant RER and SER were present in granulosa cells (Figure 4.8S).

4.3.9.4.4 Thecal layer of previtellogenic and vitellogenic follicles

During late previtellogenesis the vascularity of the theca layer increased, and it differentiated into an outer theca externa and an inner theca interna (Figure 4.8T). The theca interna was more cellular than theca externa which was more fibrous and contained blood cells. The hypertrophied theca interna cells in late previtellogenesis and in vitellogenesis included ultrastructural changes in the cytoplasmic organelles such as an increase in SER, RER, lipid droplets and visculated mitochondria, and the close association between these organelles (Figure 4.8U). These ultrastructural changes are related to the increase in the steroidogenic activity of the theca interna.

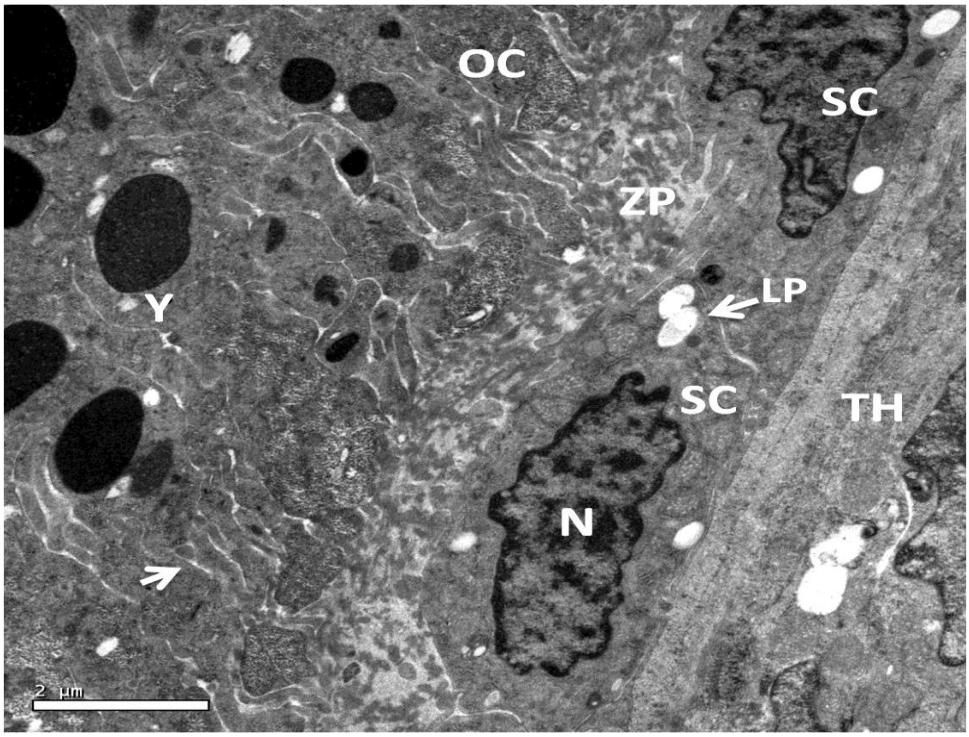

Figure 4.8R TEM. Granulosa of vitellogenic follicle with small cells (SC). Oocyte (OC) with yolk platelets (Y) adjacent to the granulosa layer. Zona pellucida (ZP) appeared extended (arrow) into the oocyte. Nucleus (N), lipids (LP), theca (TH).

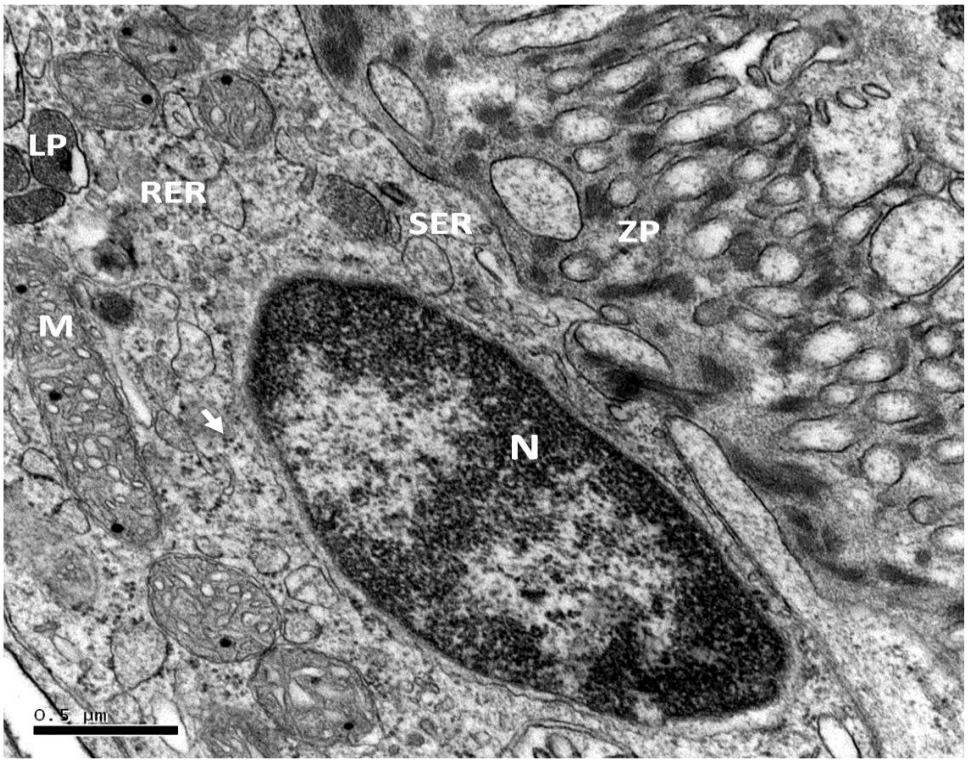

Figure 4.8S TEM. Preovulatory granulosa small cell showing cytoplasm with abundant RER and free ribosomes (arrowhead). Vesiculated SER, mitochondria (M) with tubular cristae and electron-dense material, and lipid droplets (LP). Zona pellucida (ZP) appears adjacent to granulosa cell. Nucleus (N).

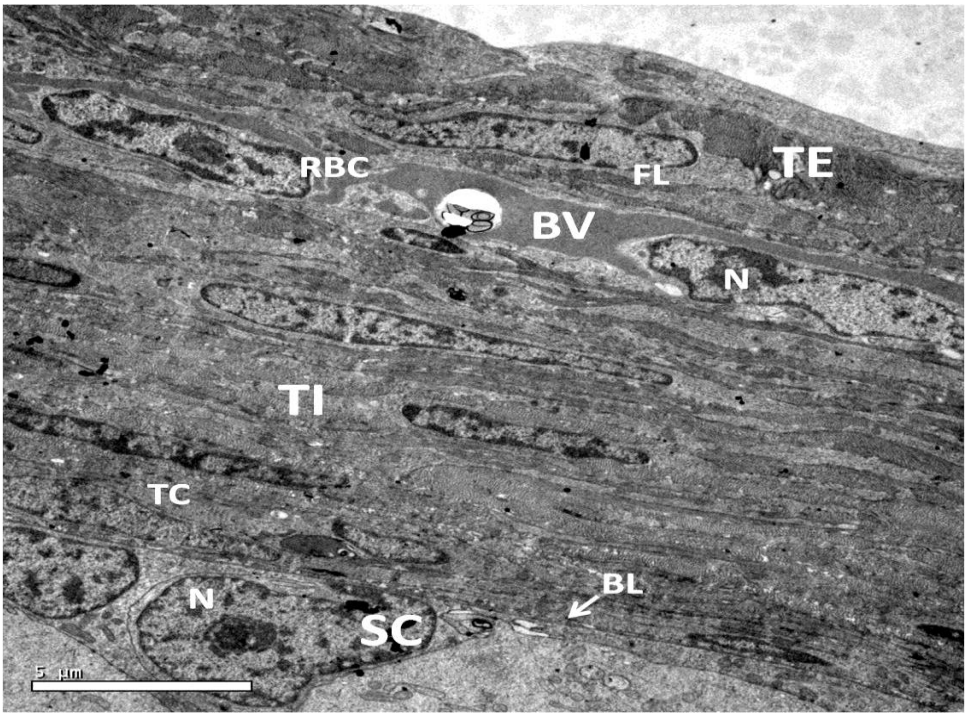

Figure 4.8T TEM. Late previtellogenesis. Theca interna (TI) separated from theca externa (TE) by blood vessels (BV). TI cells (TC), TE fibroblasts (FL), small cell (SC), basal lamina (BL), red blood cells (RBC), nucleus (N).

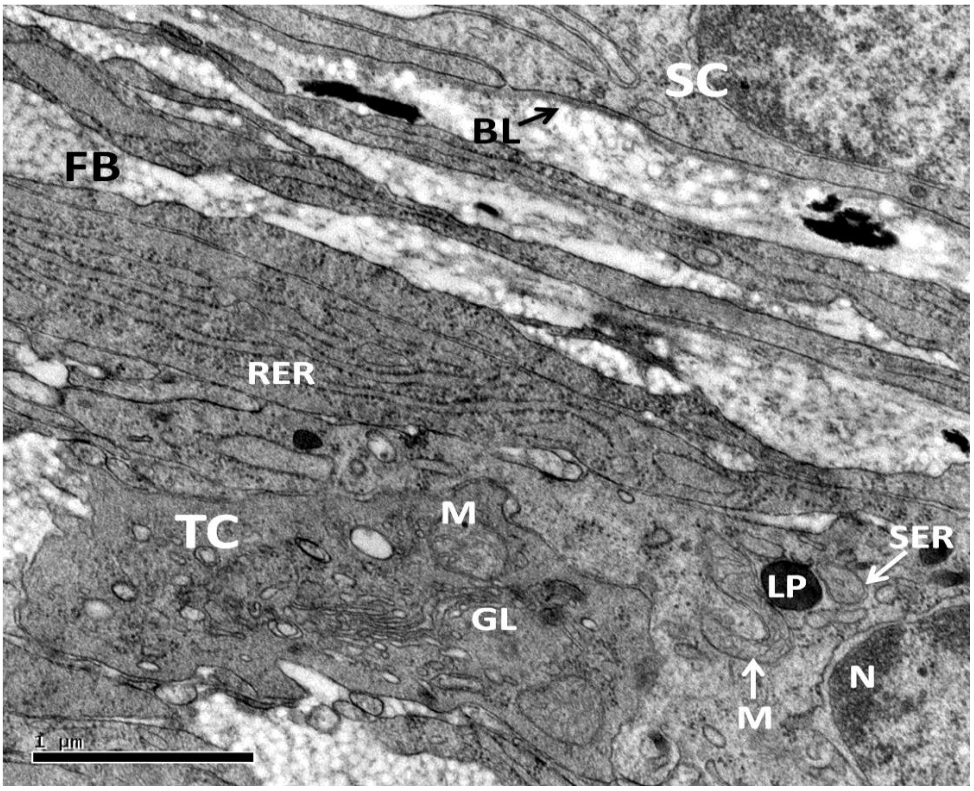

Figure 4.8U TEM. Late previtellogenesis. High magnification of theca interna cell (TC). Cytoplasm with SER, RER, vesiculated mitochondria with tubular cristae (M), lipid droplets (LP), Golgi (GL). Small cell (SC), basal lamina (BL), fibres (FB), nucleus (N).

4.3.9.5 Follicular atresia (Previtellogenic follicles)

Atresia can affect the previtellogenic follicles at any stage of their development during the reproductive cycle; however, it was more frequent in growing follicles with a polymorphic epithelium.

4.3.9.5.1 Stage-I Early atresia

Atretic follicles were similar in size to normal follicles. However, some features of atresia were initiated. Erosion of the zona pellucida, and distortion in the shape of the follicle which started losing its original spherical shape, were among the first signs of atresia (Figures 4.9A & 4.9B). The zona pellucida appeared folded inward toward the ooplasm (Figure 4.9B). The polymorphic nature of granulosa disappeared. The granulosa cells had many cytoplasmic and intercellular vacuoles and began invading

the ooplasm (Figures 4.9B & 4.9C). The theca did not differ from that of a normal follicle at this stage (Figures 4.9A & 4.9B).

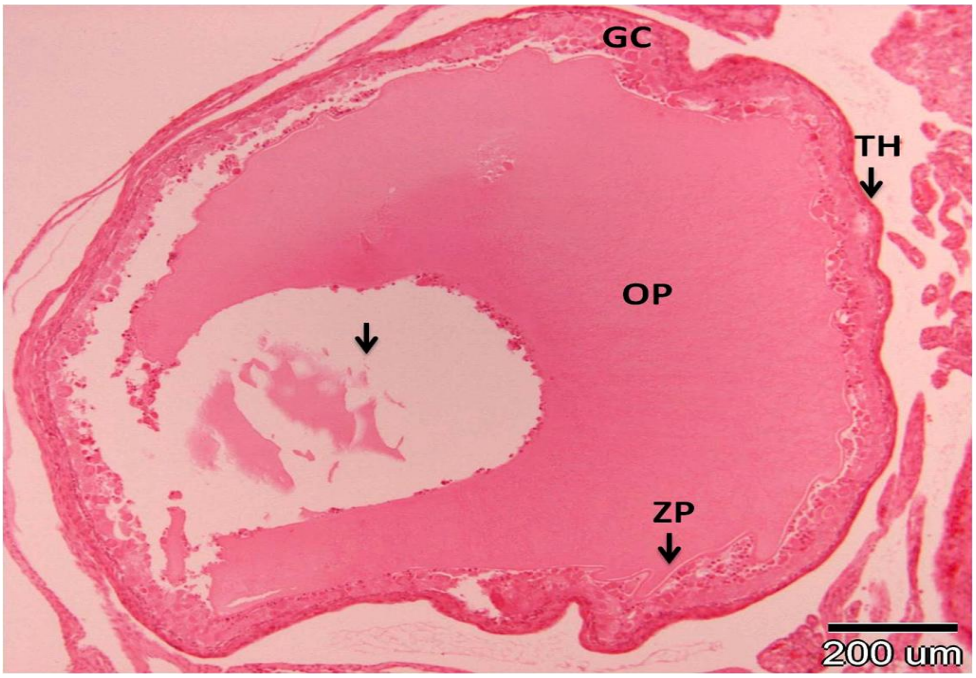

Figure 4.9A. H&E. Atretic follicle stage-I with disrupted granulosa cells (GC). Note the distorted shape of the follicle. Oocyte nucleus was lost during preparation (arrow). Ooplasm (OP), zona pellucida (ZP), thecal layer (TH).

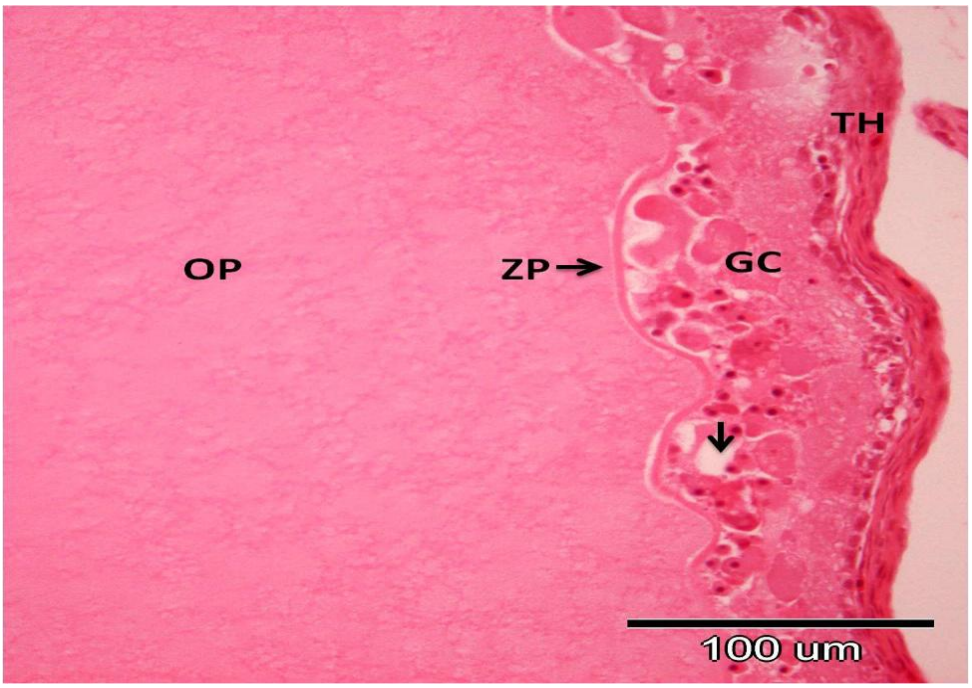

Figure 4.9B. H&E. Higher magnification of Figure 4.9A. Erosion of zona pellucida (ZP) which folded inward toward the ooplasm (OP). Granulosa cells (GC) with cytoplasmic and intercellular vacuoles (arrow). Theca (TH) appeared normal at this stage.

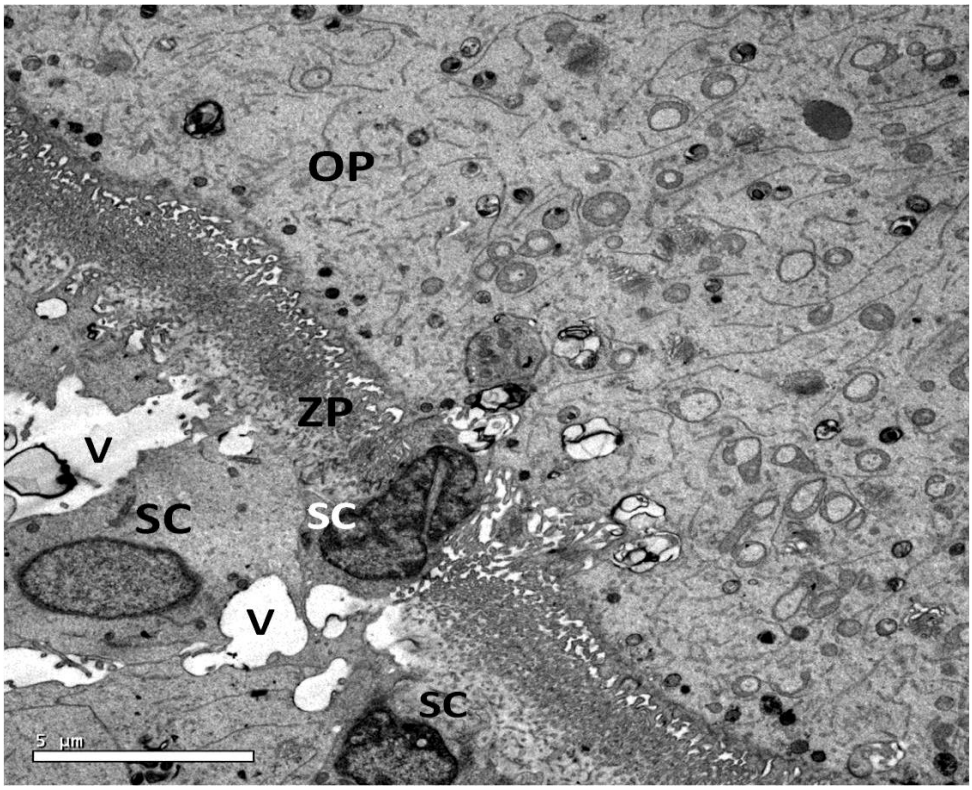

Figure 4.9C. TEM. Atretic follicle stage-I . Folding of zona pellucida (ZP) inward toward the ooplasm (OP). Granulosa small cells (SC) with cytoplasmic and intercellular vacuoles (V) and began invading the ooplasm.

4.3.9.5.2 Stage-II Atresia

The follicle became further wrinkled and collapsed. Proliferation of granulosa cells towards the ooplasm and the presence of large vacuoles in the ooplasm was clearly evident in this stage. The thecal layer was slightly thicker than in Stage-I (Figure 4.9D).

4.3.9.5.3 Stage-III Atresia

The ooplasm appeared to be completely vacuolated and disorganized (Figure 4.9E). The oolemma and zona pellucida were fragmented and lost homogeneity around the oocyte (Figure 4.9F). The follicular epithelium had abundant cytoplasmic and intercellular vacuoles. The granulosa became irregularly stratified, and contained only one cellular type (intermediate cells) (Figure 4.9F). Some granulosa cells penetrated the ooplasm at the cortical region. The basal lamina was fragmented and was progressively lost (Figure 4.9F).

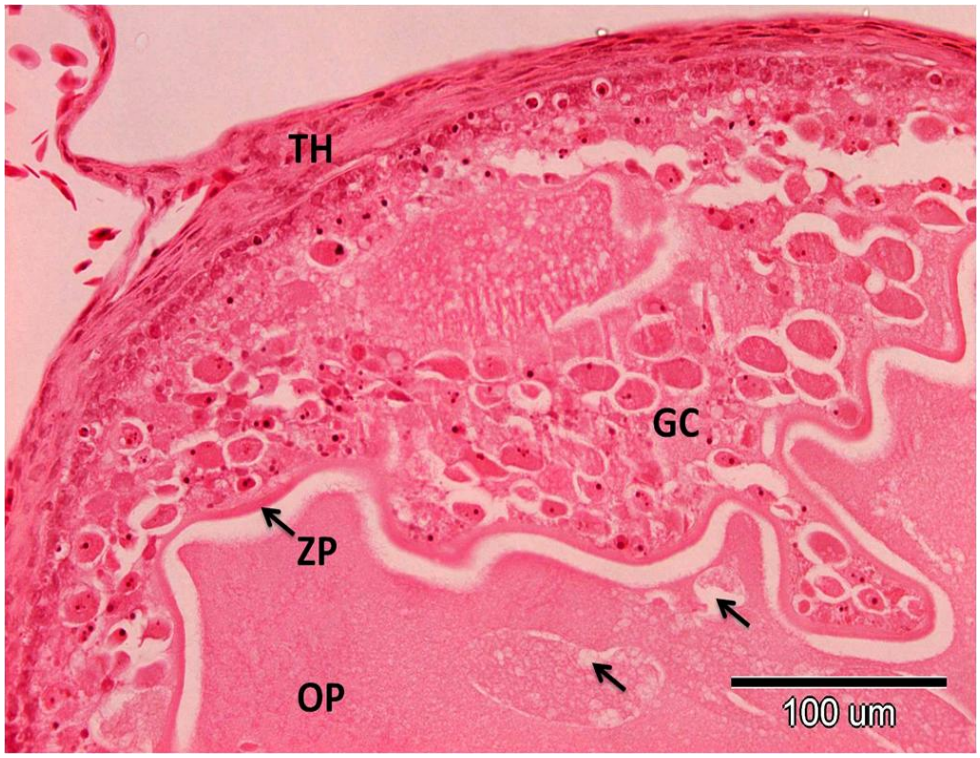

Figure 4.9D. H&E. Atretic follicle stage-II. Proliferation of granulosa cells (GC) towards the ooplasm (OP), and presence of vacuoles in the ooplasm (arrow). Zona pellucida (ZP) folded inward toward the ooplasm (OP). Theca (TH) is slightly thicker that in Stage I.

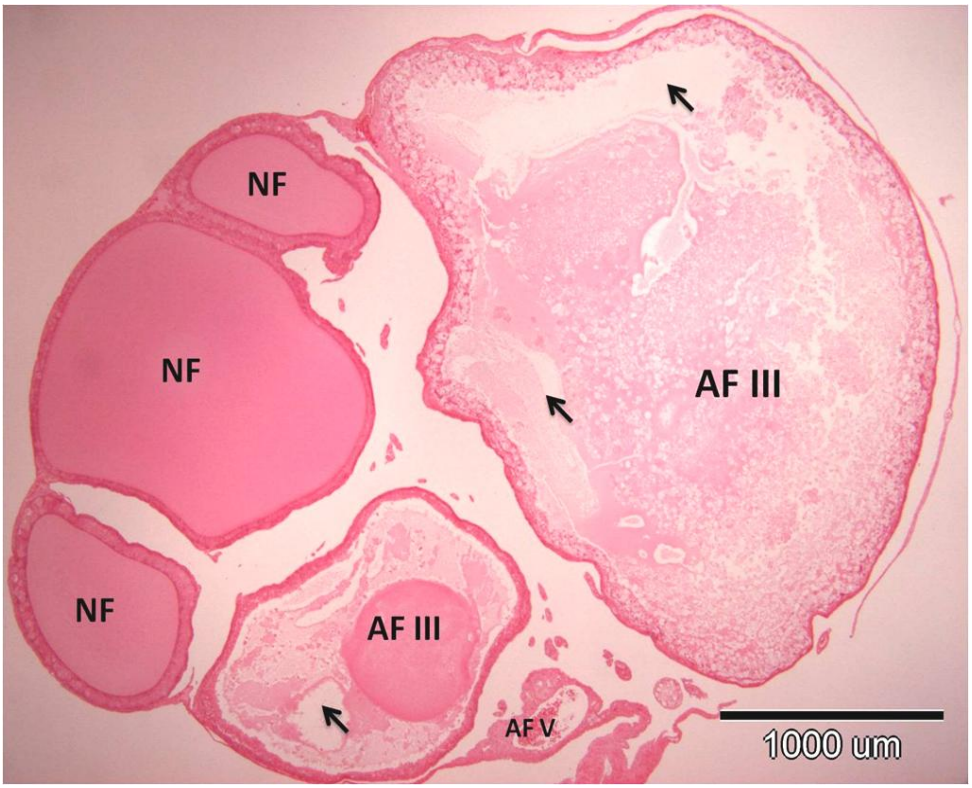

Figure 4.9E. H&E. Atretic follicles (AF) stage-III and stage-V. Ooplasm in stage III vacuolated and disorganised in shape (arrow). Normal follicles (NF).

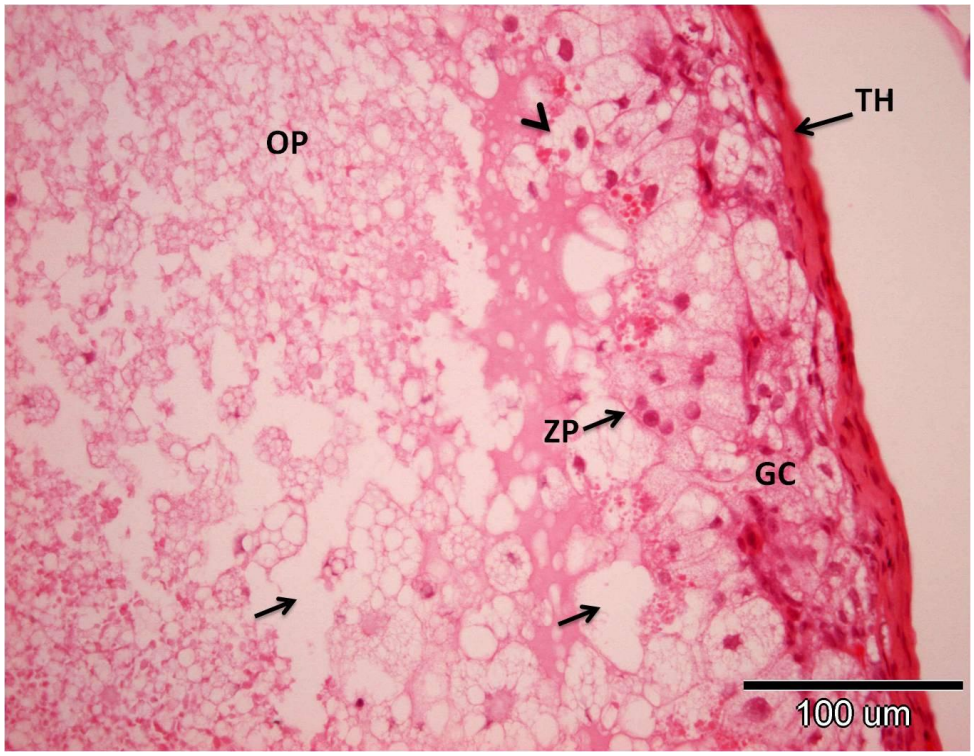

Figure 4.9F. H&E. Higher magnification of Figure 4.9E in stage-III. Vacuolated ooplasm (arrow) and fragmented zona pellucida (ZP). Granulosa cells (GC) with abundant vacuoles. Some granulosa cells penetrated ooplasm (arrowhead). The thecal layer (TH) appeared to be disrupted.

4.3.9.5.4 Stage-IV Atresia

During this stage the follicular size diminished and there was more hypertrophy of granulosa cells. The vacuolated and disorganized ooplasm decreased in amount and appeared coarse. It was gradually reabsorbed due to phagocytosis by the hypertrophied granulosa cells (Figure 4.9G). The latter were seen spreading everywhere in the ooplasm. The theca interna was thick and theca externa remained unchanged (Figure 4.9G).

4.3.9.5.5 Stage-V Atresia

At this stage most of the ooplasm had already been phagocytised by the hypertrophied granulosa cells (Figure 4.9H). The latter showed progressive degenerative changes evidenced by the presence of pycnotic nuclei (Figure 4.9I). The theca interna cells further hypertrophied, which formed a thick conspicuous zone in the wall of the degenerating follicle (Figures 4.9G & 4.9I). No change occurred in

the theca externa which consisted of fibroblasts and collagenous fibres. Large blood vessels were seen at this stage between the theca externa and theca interna (Figure 4.9I).

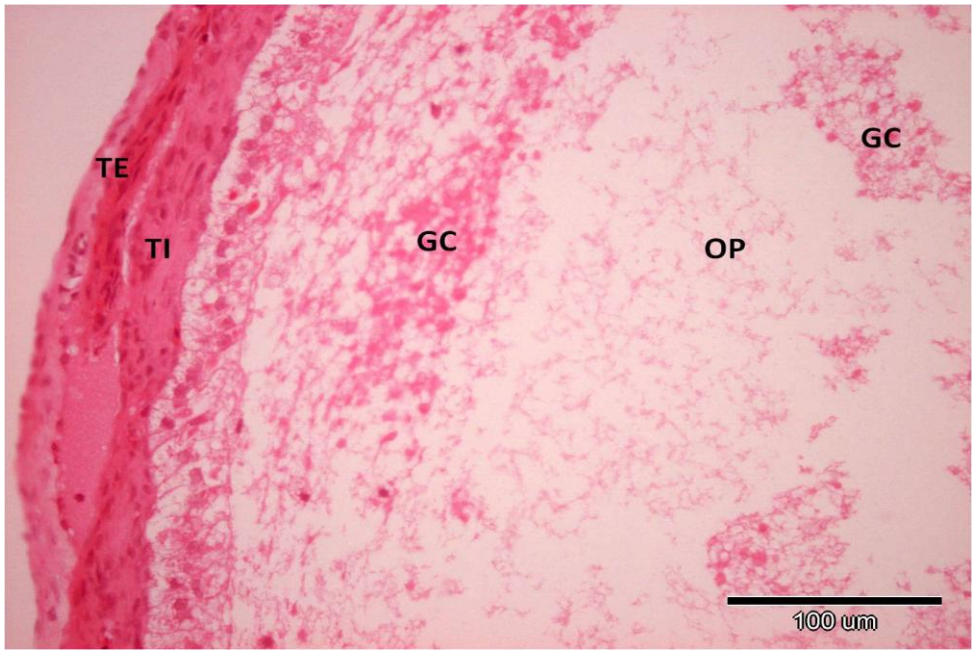

Figure 4.9G. H&E. Atretic follicles stage-IV. Ooplasm (OP) gradually resorbed due to phagocytosis by hypertrophied granulosa cells (GC). Theca interna (TI) was thick and theca externa (TE) was normal.

Figure 4.9H. H&E. Atretic follicles stage-V. Most ooplasm (OP) phagocytised by hypertrophied granulosa cells (GC). The theca interna cells (TI) further hypertrophied, whereas no change occurred in the theca externa (TE).

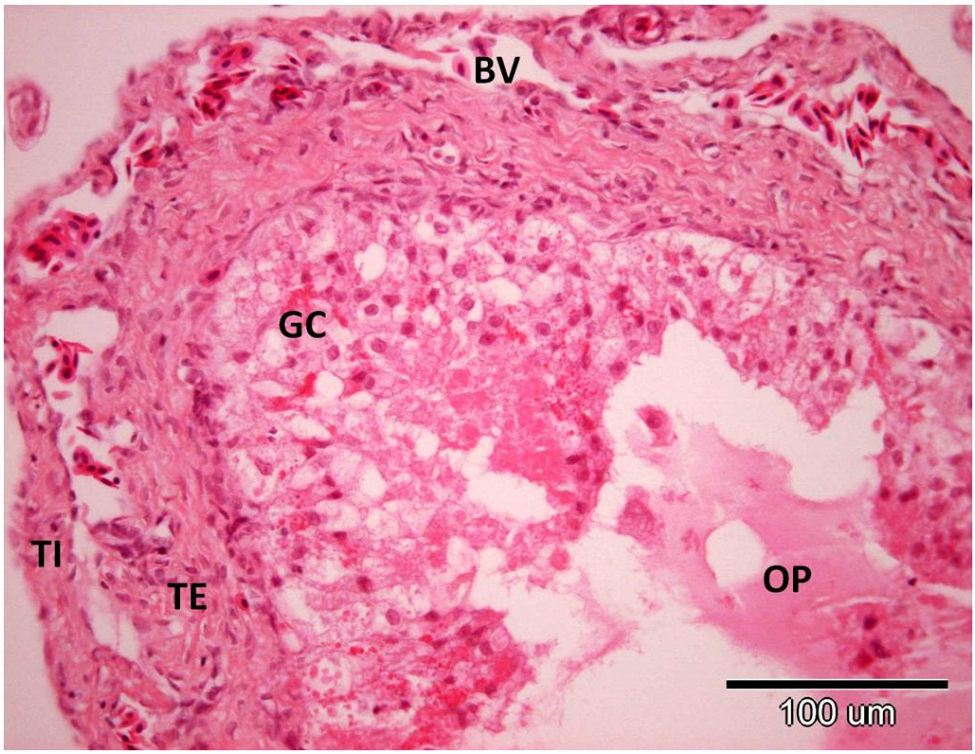

Figure 4.9I. H&E. Higher magnification of Figure 4.9H. Degenerative granulosa (GC) with presence of pycnotic nuclei. Theca interna cells (TI) further hypertrophied. No change occurred in the theca externa (TE). Large blood vessels (BV) appeared at this stage.

4.3.9.5.6 Stage-VI Late atresia

This stage was characterized, more or less, by complete disappearance of the ooplasm. The granulosa cells or phagocytes which filled the follicular cavity showed lightly stained cytoplasm and deeply stained pycnotic nuclei (Figure 4.9J). Large empty vacuoles were seen in the follicular cavity. The theca interna cells further hypertrophied in the wall of degenerated follicle (Figure 4.9J).

4.3.9.5.7 Stage-VII Final atresia

During the most advanced stage of follicular atresia, the interior of the degenerated follicle was filled completely with multiocular granulosa cells having empty vacuoles (Figure 4.9K). Their nuclei were shrunken and pycnotic. The elements of connective tissue derived from thecal layers penetrated into the mass of degenerating granulosa cells and formed septa. The remnants of these follicles were observed on the ovarian wall, making the wall thicker in older females ((Figure 4.9K).

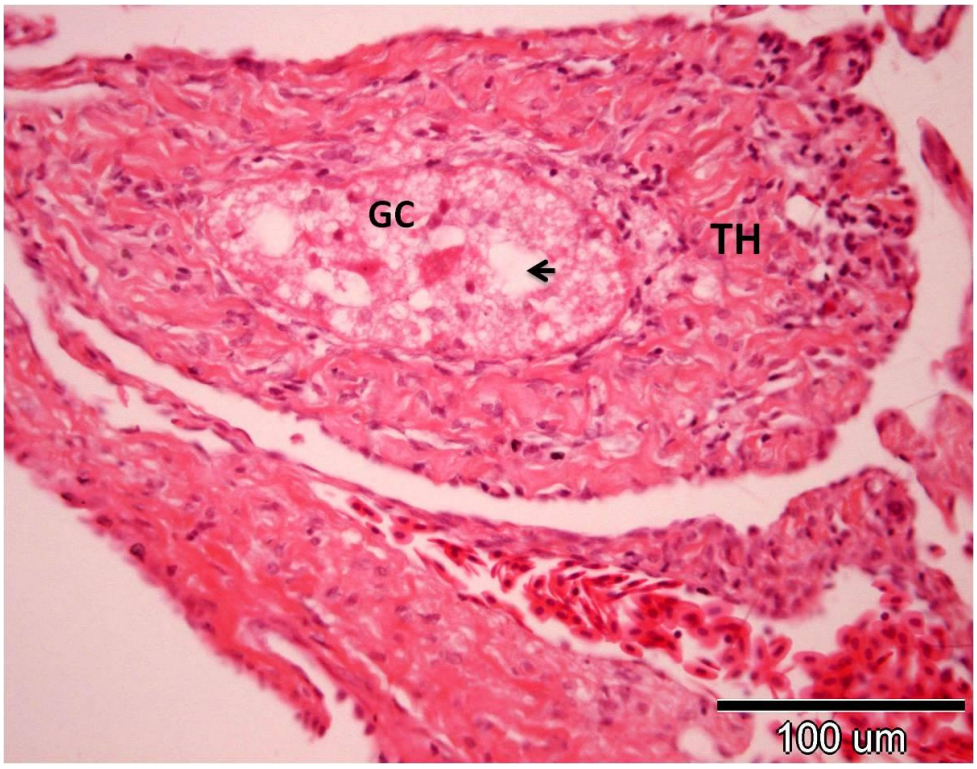

Figure 4.9J. H&E. Atretic follicles stage-VI. phagocytotic granulosa cells with pycnotic nuclei (GC). Vacuoles in follicular cavity (arrow). Theca (TH) was further hypertrophied.

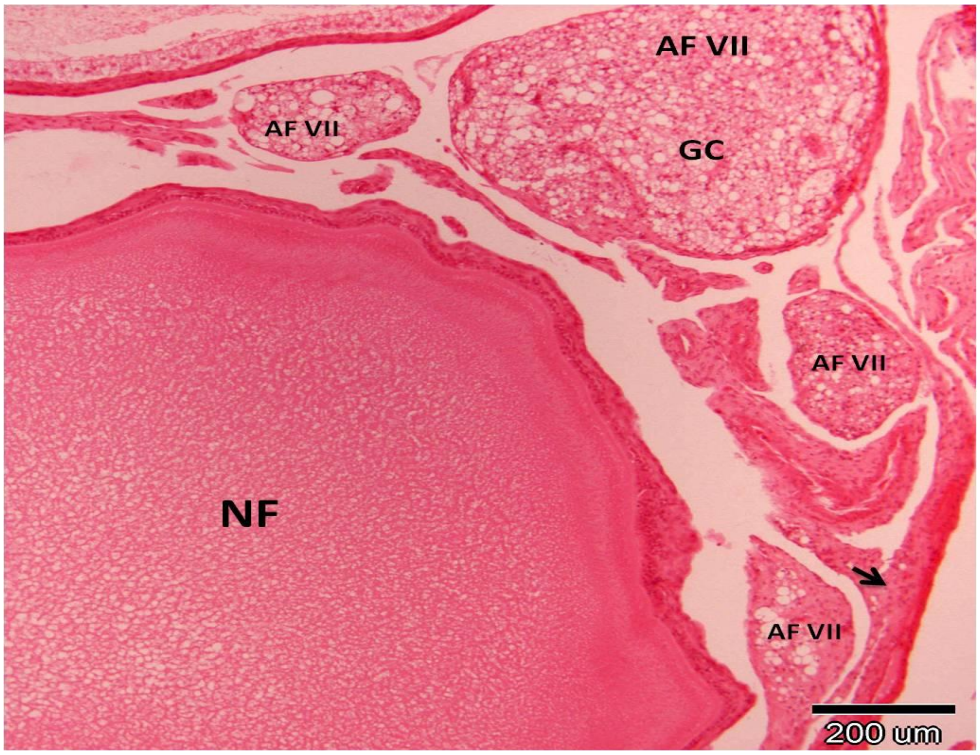

Figure 4.9K. H&E. Atretic follicles (AF) stage-VII. Multiocular granulosa cells (GC) with septa already formed. Remnants of atretic follicles causing ovarian wall thickening (arrow). Normal follicle (NF).

4.3.9.6 Vitellogenic follicles in atresia (Corpora atretica)

Vitellogenic follicles rarely underwent atresia. With the start of their atresia, the yolk bodies at the periphery of the ooplasm began to coalesce with each other (Figure 4.10A). The granulosa cells were separated from each other and began invading the yolk platelets. Simultaneously they were hypertrophied and developed many vacuoles and yolk fragments in their cytoplasm, indicating the phagocytosis of yolk bodies (Figure 4.10B). Coalescence of yolk bodies progressed at the peripheral portions of the follicle. Digestion and removal of yolk by the granulosa cells continued (Figures 4.10B & 4.10C). The theca layers showed no changes in the early stages of degeneration of vitellogenic follicles (Figure 4.10A). As the vitellogenic follicle in atresia progressed it diminished in size and most of the ooplasm had already been phagocytised by the hypertrophied granulosa cells (Figures 4.10D & 4.10E). Yolk platelets were seen in the follicular cavity in different sizes. The theca layer was thick with numerous blood vessels (Figures 4.10D & 4.10E). The subsequent stages of degeneration of vitellogenic follicles in atresia followed similar steps as were seen in the late and final stages of atresia of the previtellogenic follicles.

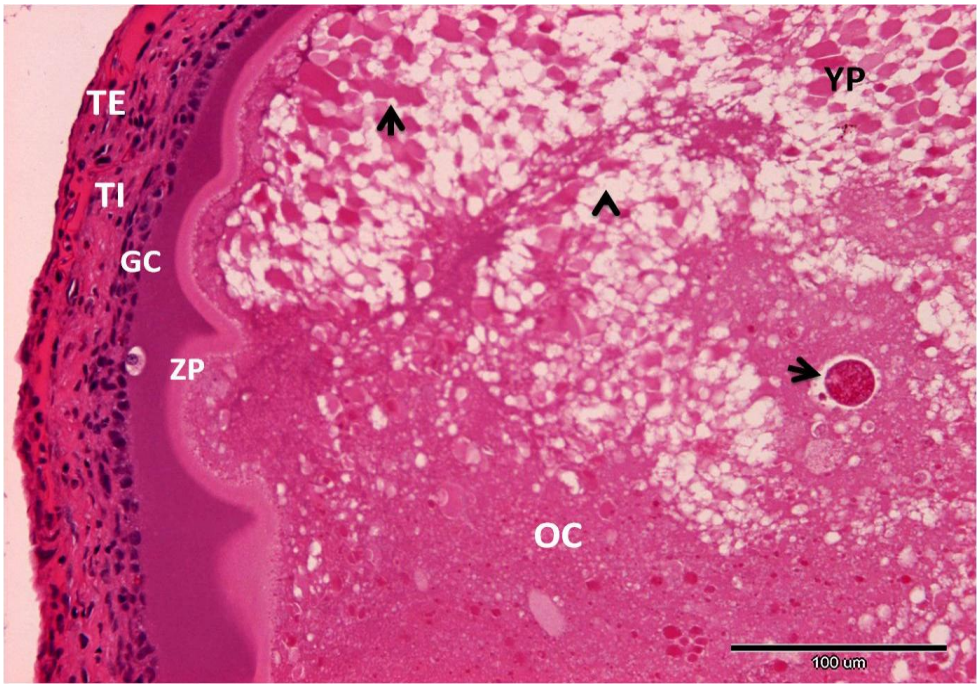

Figure 4.10A. H&E. Early corpora atretica. Yolk (YP) coalesce with each other (arrow) and vacuoles (arrowhead) appeared in oocyte (OC). Zona pellucida (ZP) folded. Granulosa cells (GC), theca externa (TE) and interna (TI) appeared normal.

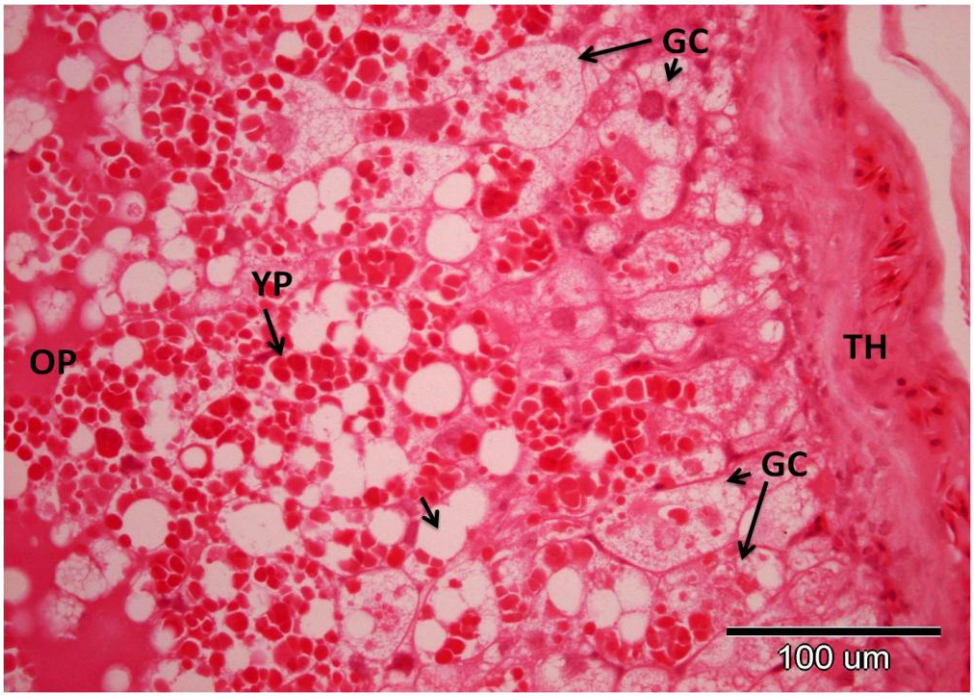

Figure 4.10B. H&E. Corpora atretica with numerous vacuoles (arrow) in ooplasm (OP). Phagocytosis of yolk (YP) by hypertrophied granulosa cells (GC). Zona pellucida already disappeared. Theca (TH) appeared thick.

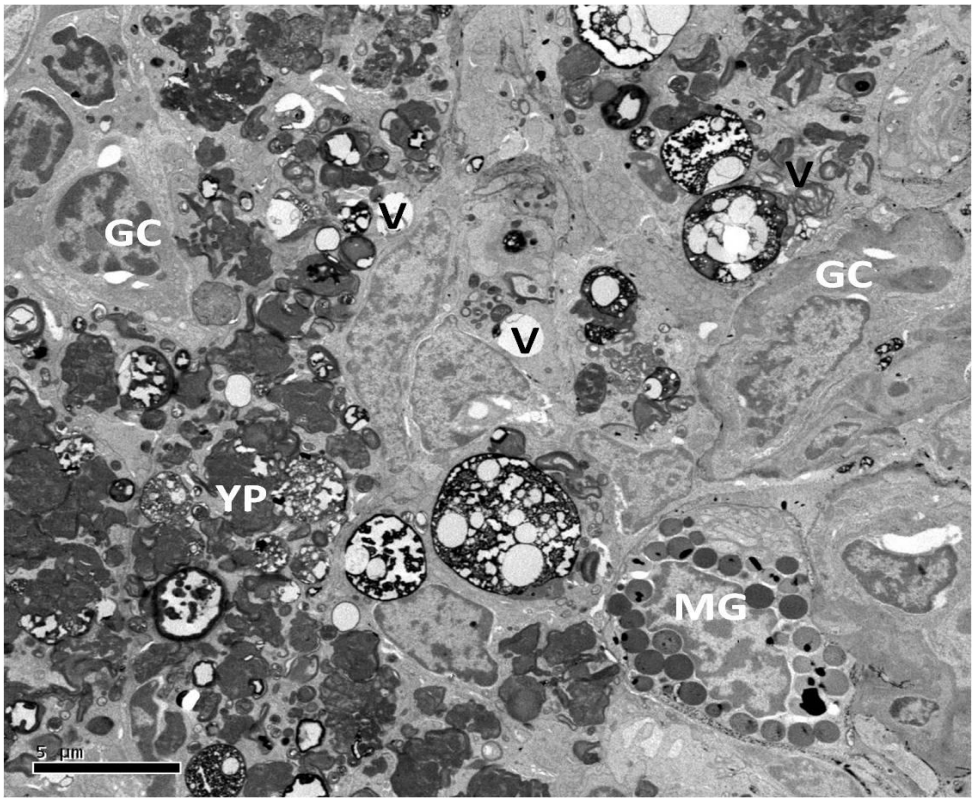

Figure 4.10C. TEM. Corpora atretica. Phagocytosis of yolk (YP) by hypertrophied granulosa cells (GC). Macrophage (MG) also appeared in ooplasm. Vacuoles (V).

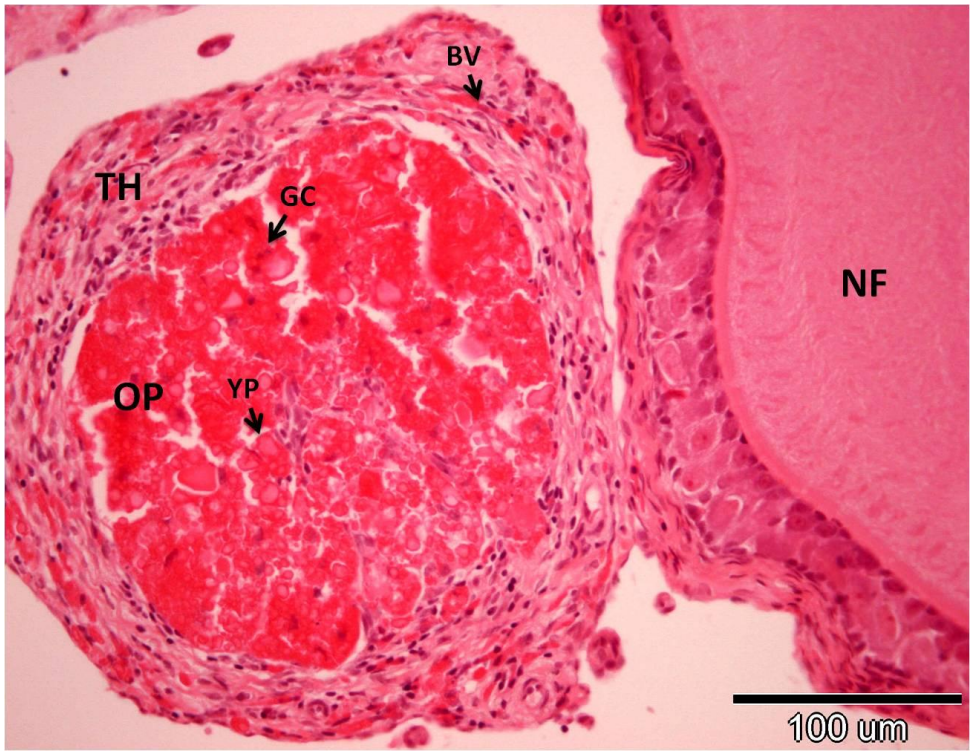

Figure 4.10D. H&E. Corpora atretica at advanced stage. Ooplasm (OP) and yolk platelets (YP) phagocytised by granulosa cells (GC). Thick theca layer (TH) with blood vessels (BV). Normal follicle (NF).

Figure 4.10E. H&E. Corpora atretica advanced stage. Most ooplasm phagocytised by granulosa cells (GC). Yolk (Y) in follicular cavity (CA). Thickening of thecal layer (TH) continued. Large blood vessels (BV) present at this stage.

4.3.9.7 Corpora lutea (CL)

The CL were observed in gravid females between March and May. The postovulatory follicles were collapsed sacs of connective tissue, epithelioid tissue and debris left behind in the ovary after ovulation. After discharge of eggs the various components of postovulatory follicles underwent a series of morphological and histological changes during evolution or development and involution or degeneration of CL.

Changes in the size of CL structures (follicular diameter, follicular epithelial height, and thickness of thecal layer) during the seasonal reproductive cycle of *H. flaviviridis* are summarised in Table 4.4. The size of CL structures (P <0.001) varied significantly during the stages of development and degeneration in the breeding season (Table 4.4). The size of CL structures increased significantly during luteogenesis and active CL (P <0.001) coinciding with the formation of CL, but decreased significantly during luteolysis (P <0.001) coinciding with the degeneration of CL.

4.3.9.7.1 Stage-I Luteogenesis

The CL consisted of an outer layer of connective tissue (theca externa and theca interna) and an inner thick band of granulosa lutein cells. Following ovulation, the postovulatory follicle presented a large irregular central cavity (aperture of rupture). The cavity did not contain yolk and zona pellucida (Figure 4.11A). The follicle shrunk in size due to the contraction of its various layers. This resulted in the thickening and folding of its wall. The folded follicular epithelium underwent rapid hypertrophy (luteinisation) and began its cellular proliferation toward the central cavity to form the granulosa lutein cells.

Table 4.4. Morphometry of corpus luteum (CL) of *H. flaviviridis* (N = Individual geckos).

Stage	Follicular diameter (μm)	Follicular epithelial height (μm)	Theca thickness (μm)
Luteogenesis / Active CL (N=6)	3150±554.2[b]	438.3±112.9[b]	300±75.3[a]
Range	1300 – 5000	100 – 850	150 – 650
Luteolysis (N=14)	375±70.6[a]	120.7±33.7[a]	175±28.4[a]
Range	100 – 1000	10 – 350	60 – 500
T-test			
T(18)	7.584	3.599	1.930
P-value	<0.001	0.035	0.146

Statistical differences between groups obtained by Duncan's multiple-comparisons test. Stages with significantly different values (mean ± S.E.M) in vertical column were assigned different letters. Stages with the same letter shows statistically no significant difference between them at the 0.05 level of significance.

4.3.9.7.2 Stage-II Active CL

The size of the CL was smaller; the multistratified granulosa lutein cells almost completely occupied the follicular cavity, forming an active and compact CL (Figure 4.11B). The layer of granulosa lutein cells lacked blood vessels. Granulosa lutein cells were rounded and contained an ovoid nucleus with one to two nucleoli and the eosinophilic cytoplasm was abundant (Figures 4.11C & 4.11D). The theca interna was thick and consisted of a few fibroblasts, hypertrophied cells (theca lutein cells), and dispersed macrophages (Figures 4.11C & 4.11D). The theca interna was separated from the theca externa by blood vessels that contained many macrophages. The theca externa was thinner and more fibrillar than the theca interna (Figure 4.11C). When the cavity was filled, the cytoplasm of some luteal cells was vacuolated, showing the firsts signs of luteolysis (Figure 4.11E). Some collagenous

fibres, blood vessels, and fibroblasts progressively invaded the granulosa luteal tissue from the theca interna, forming several thin septa that converge in the central region. The theca externa was thin and fibrous (Figure 4.11F).

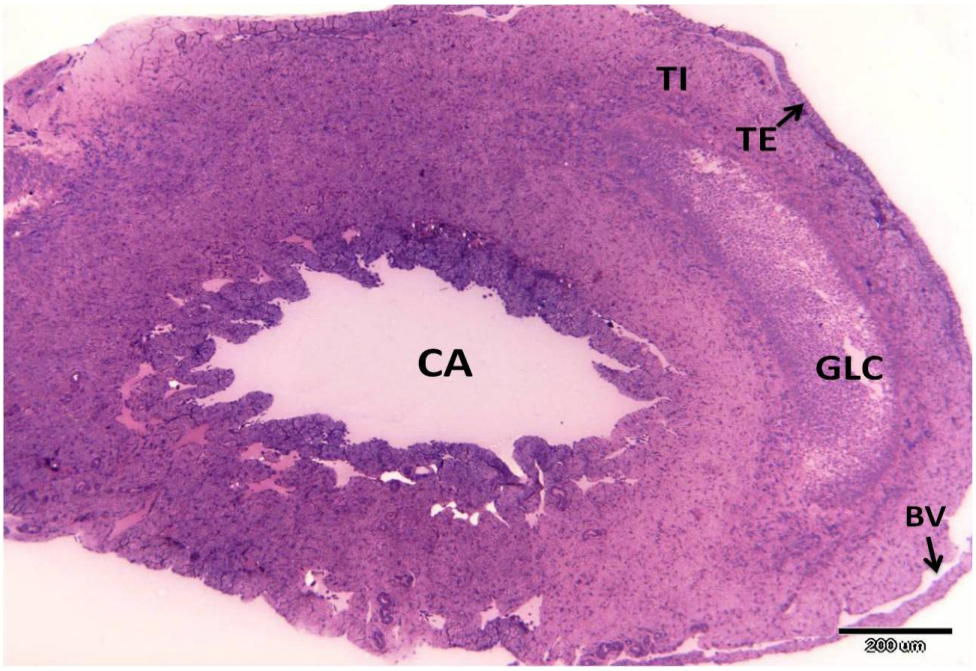

Figure 4.11A. TB. Postovulatory follicle (corpus luteum) of gravid female. During luteogenesis granulosa lutein cells (GLC) proliferating towards the cavity (CA) to form the luteal tissue. Thecal layer; thecal externa (TE) and theca interna (TI) separated by blood vessels (BV).

Figure 4.11B. H&E. Active corpus luteum with multistratified granulosa lutein cells (GLC) filling the cavity (CA). Theca layer (TH) becomes thick.

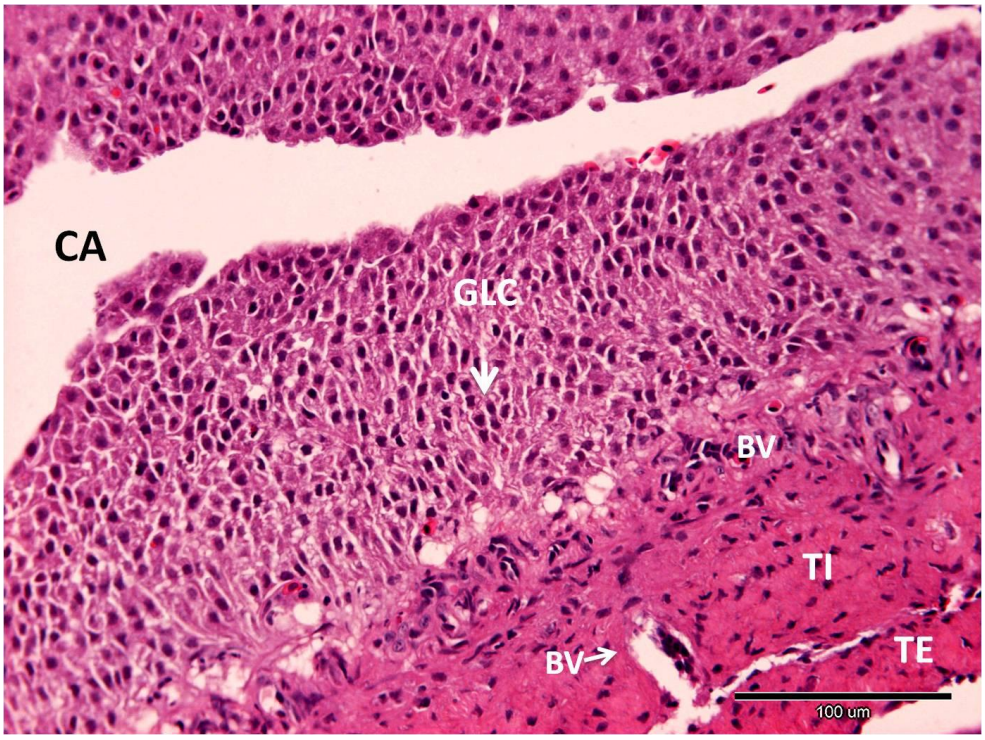

Figure 4.11C. H&E. Higher magnification of Figure 4.11B. Granulosa lutein cells (GLC) appeared with an ovoid nuclei (arrow). Theca interna (TI) separated from theca externa (TE) by numerous blood vessels (BV). Numerous blood vessels also seen between the granulosa and theca. Cavity (CA).

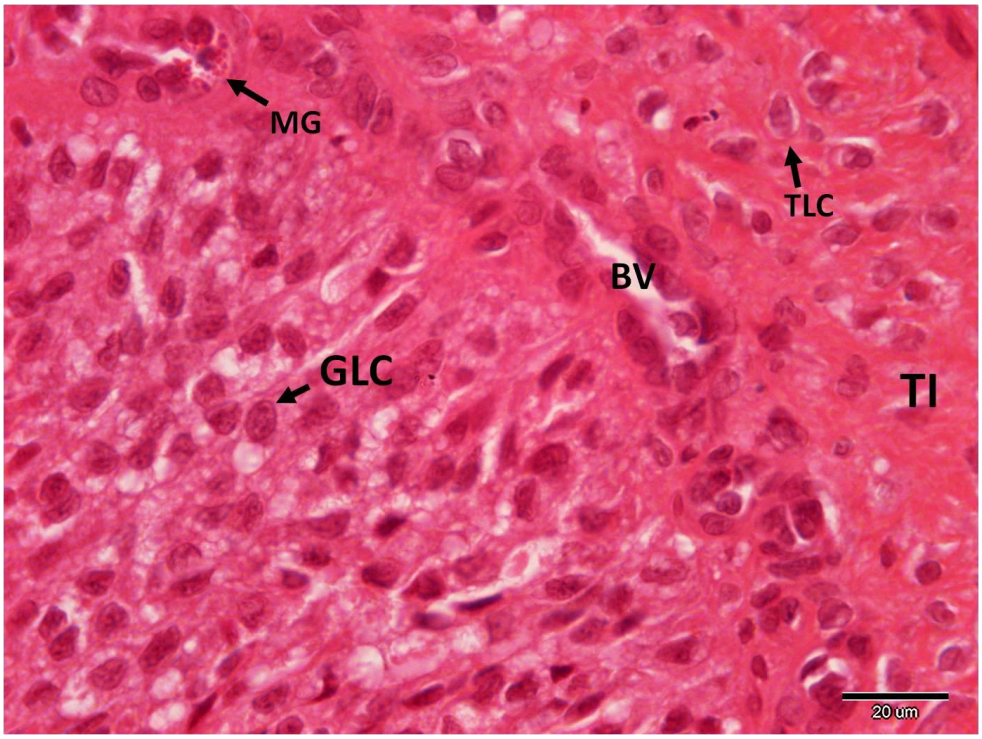

Figure 4.11D. H&E. Higher magnification of Figure 4.11C. Granulosa lutein cells (GLC) with ovoid nuclei. Theca interna (TI) with hypertrophied theca lutein cells (TLC). Macrophages (MG), blood vessels (BV).

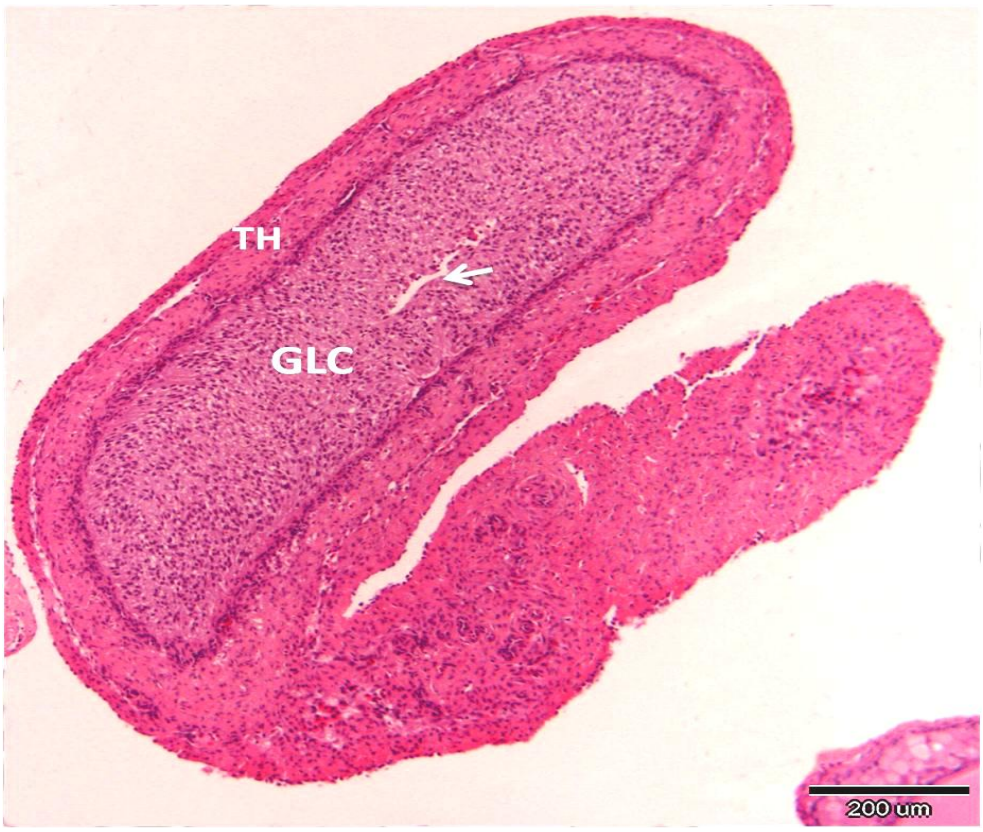

Figure 4.11E. H&E. Active CL. Multistratified granulosa lutein cells (GLC) almost completely occupied the follicular cavity (arrow). Thecal tissue. (TH).

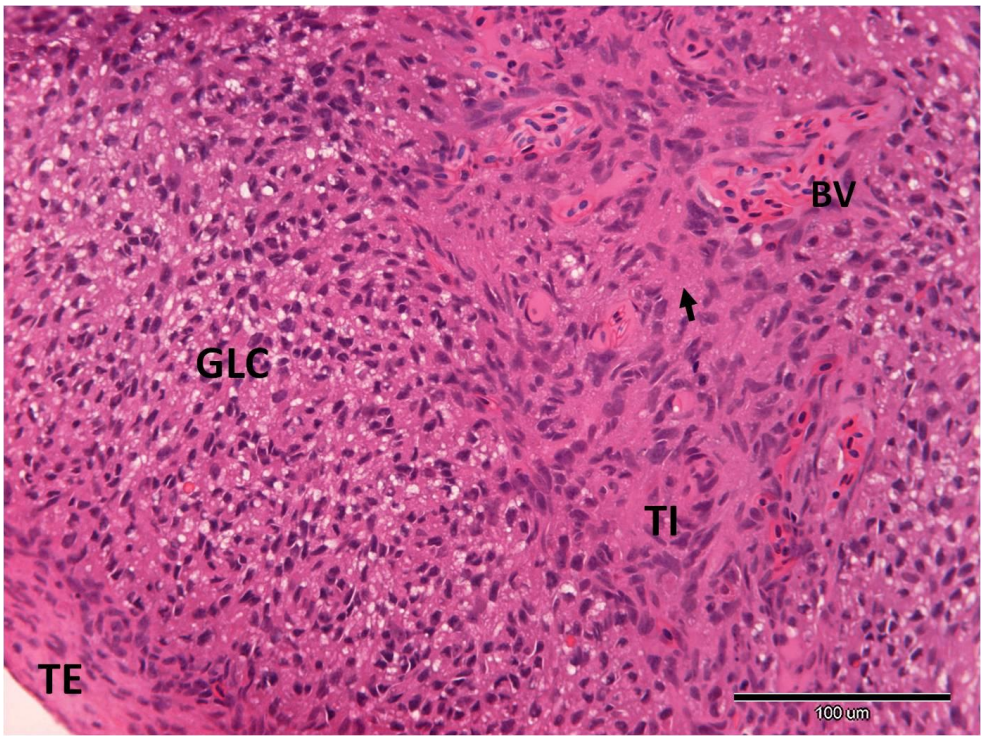

Figure 4.11F. H&E. Active corpora luteum showing the first sign of luteolysis. Blood vessels (BV), fibres and fibroblasts (arrow) invade the luteal tissue (GLC) from the theca interna (TI) forming septa. The theca externa (TE) is thin and fibrous.

4.3.9.7.3 Stage-III Luteolysis

The degeneration or involution of the luteal cell mass occurred in ovaries from females with embryos in late gravidity stages of development. The CL was smaller in size and was very vacuolated. The cytoplasm of the luteal cells had numerous vacuoles and their nuclei were irregular and flattened. The process advanced from the centre to the periphery. The amount of thecal tissue increased, forming thicker septa, and the granulosa luteal tissue appeared to diminish. As luteolysis progressed, there were many vacuoles in the theca interna and in the luteal tissue (Figure 4.11G). The latter almost disappeared and only dispersed wrinkled cells were present. These structures were immersed within the stromal tissue near the ovarian wall.

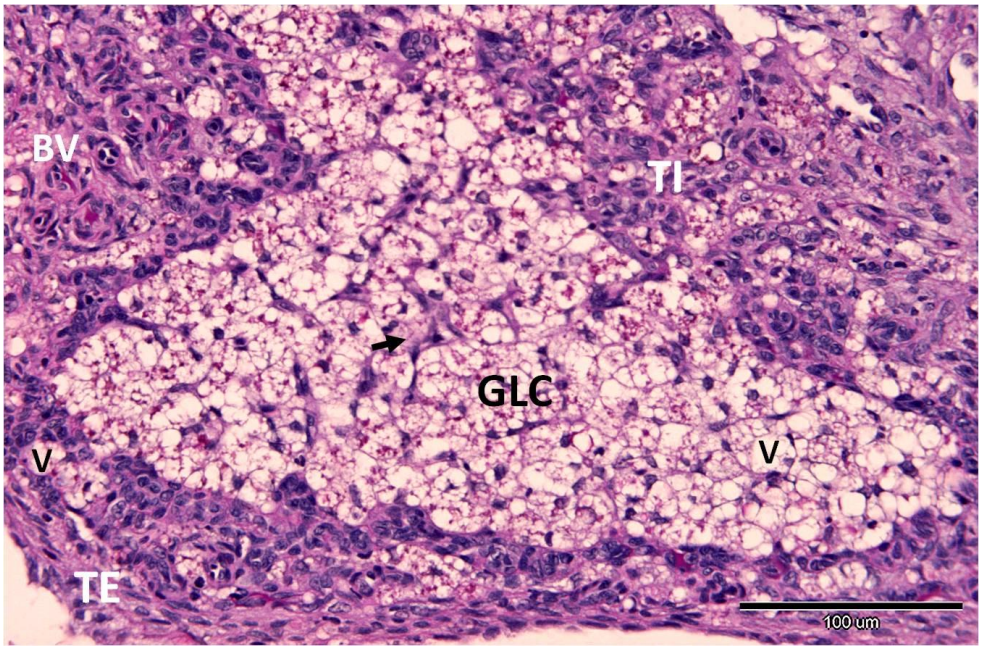

Figure 4.11G. PAS-Haem. Advanced stage of corpora luteum luteolysis. The granulosa luteal cells (GLC) replaced by numerous large vacuoles (V). Theca interna (TI) at this stage contain several large vacuoles (V) with numerous blood vessels (BV). Theca externa (TE) is thin and fibrous.

4.3.4.8 Ultrastructure of the granulosa lutein cells of the CL

Active granulosa lutein cells were polygonal with an eccentric nucleus containing one or two nucleoli. Vesiculated and cisternal SER were abundant in the cytoplasm of granulosa lutein cells (Figures 4.12A & 4.12B). Scattered regions of RER and free

ribosomes were also present. The cisternae of SER in some areas were organized into folded arrays and elaborate concentric whorls. The folded membrane arrays and cisternal whorls were often associated with lipid droplets or mitochondria (Figure 4.12A). In some areas there was a close association between mitochondria and lipid droplets. The mitochondrial cristae were vesiculated and swollen. Lipid droplets were abundant and numerous vesicles were produced by the Golgi complexes (Figure 4.12B). The cells also contained conspicuous bundles of microfilaments and scattered microtubules (Figure 4.12A). Degeneration of CL (luteolysis) occurred by the end of the active phase, which was associated with a sharp fall in plasma P concentrations and formation of septae which started to invade granulosa lutein cells and the central cavity (Figure 4.12C). As a result, most of the granulosa lutein cells were isolated into clusters. During the final stage of granulosa degeneration the cells disintegrated and were replaced by connective tissue.

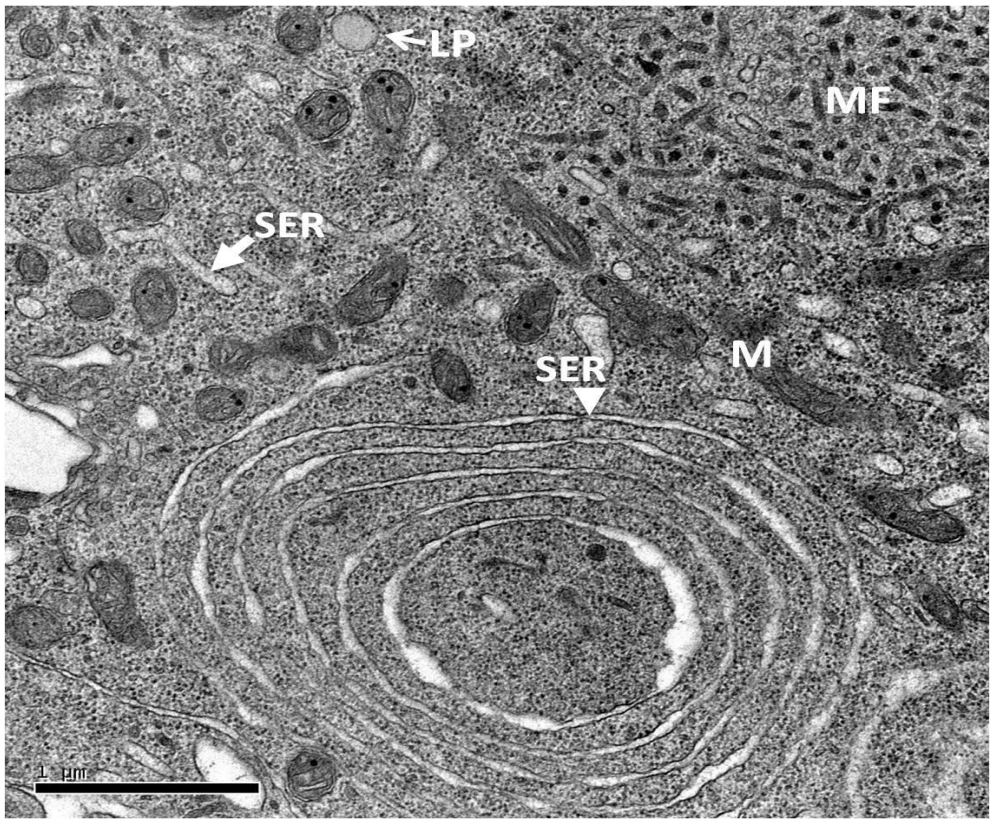

Figure 4.12A. TEM. Active corpus luteum with vesiculated (arrow) and cisternal (arrowhead) SER. The cisternae organised into folded arrays and elaborate cisternal whorls and closely associated with mitochondria (M). Bundles of microfilaments (MF) and lipid droplet (LP) were present.

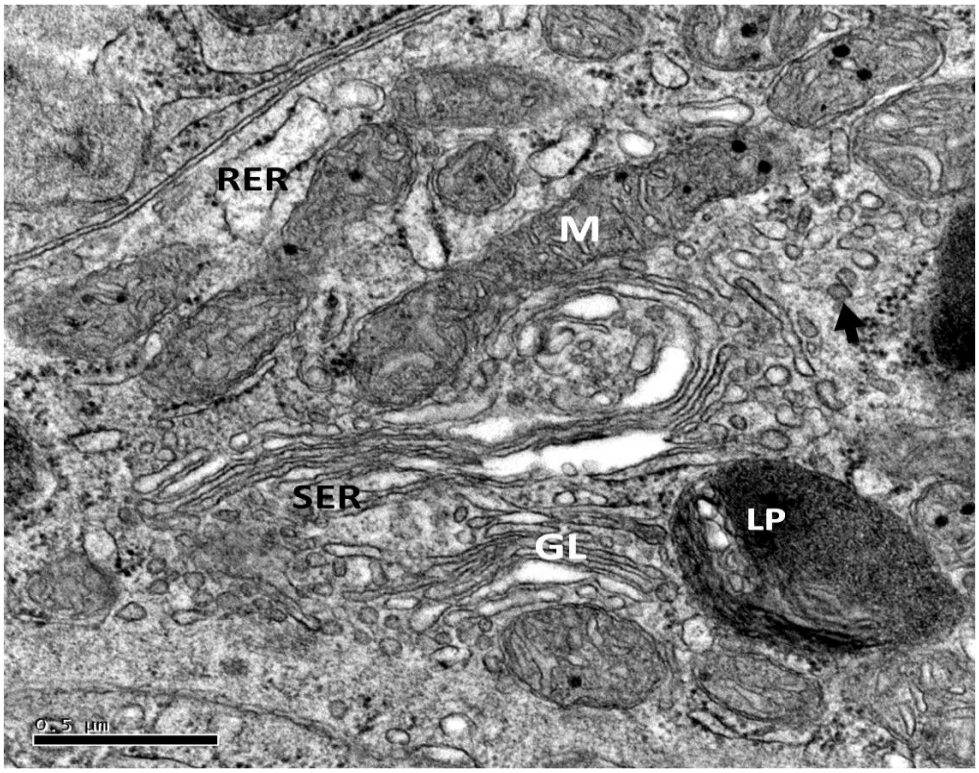

Figure 4.12B. TEM. Active corpus luteum with tubular SER and numerous vesiculated mitochondria (M) associated with lipid droplet (LP). Numerous vesicles (arrow) produced by Golgi apparatus (GL) and scattered RER were present.

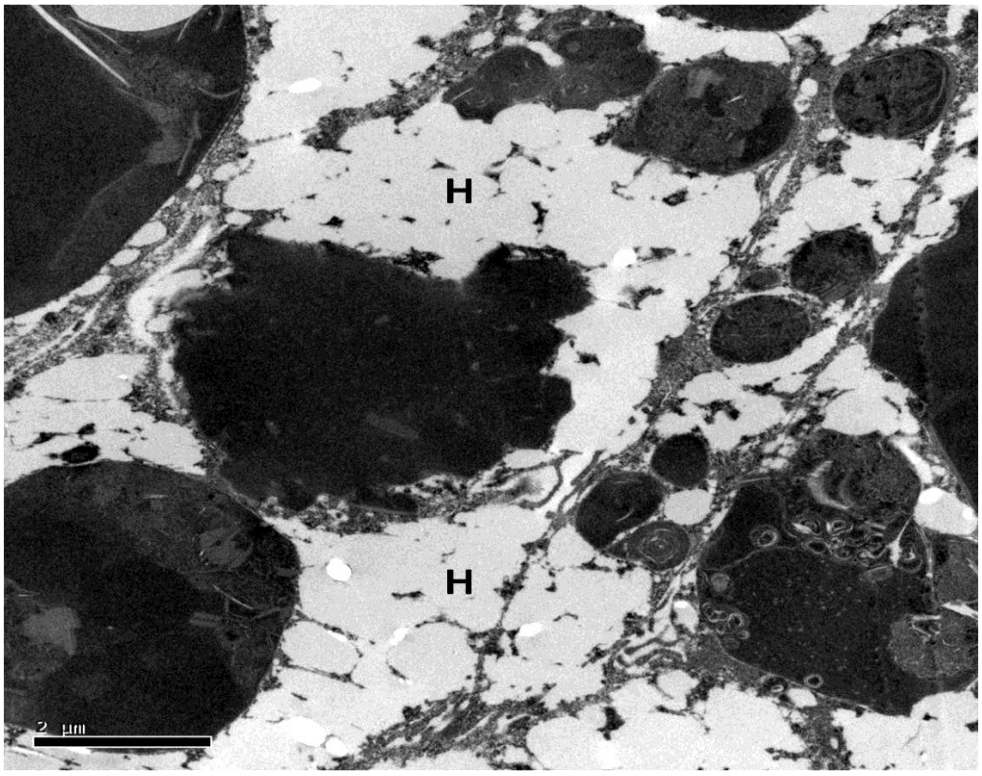

Figure 4.12C. TEM. Portion of degenerative corpora luteum. Note the contorted hyaline material (H) in white which surrounds the septum. Septae invaded granulosa lutein cells and central cavity.

4.3.10 Development of the oviduct during the reproductive cycle

The oviducts of *H. flaviviridis* are paired, thin-walled tubes extended length-wise along the body cavity on either side of the midline and supported by dorsal mesenteries that are continuous with the peritoneum. The paired ovaries, suspended from dorsal midline via their mesovaria, lie medial to the oviducts and caudal to their infundibular ostia.

The oviducts are composed of five different regions that differ in their structures and function in the different reproductive phases: the infundibulum, the uterine tube, the isthmus, the uterus, and the vagina (Figures 4.13A, 410B, 4.13C & 4.13D). Both oviducts laterally joined a single urogenital sinus which emptied into the cloaca. Oviducts differentiated into several tissue layers of varied thickness in the different regions; the luminal epithelial layer, the mucosal glandular layer (endometrium), the lamina propria (connective tissue) underlying the epithelium, the muscularis externa (myometrium), and externally, the oviduct lined by the serosal membrane (perimetrium) (Figure 4.13E). Three cell types composed the luminal epithelium of the oviduct: ciliated, nonciliated microvillous, and bleb cells.

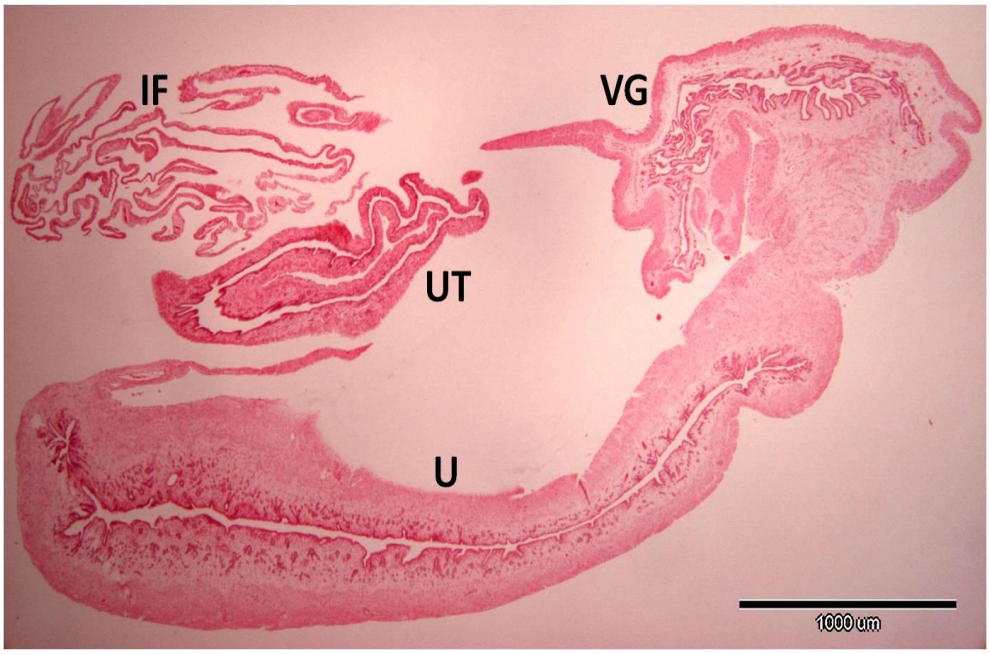

Figure 4.13A. H&E. Oviduct from the quiescent phase showing: infundibulum (IF), uterine tube (UT), uterus (U) and vagina (VG).

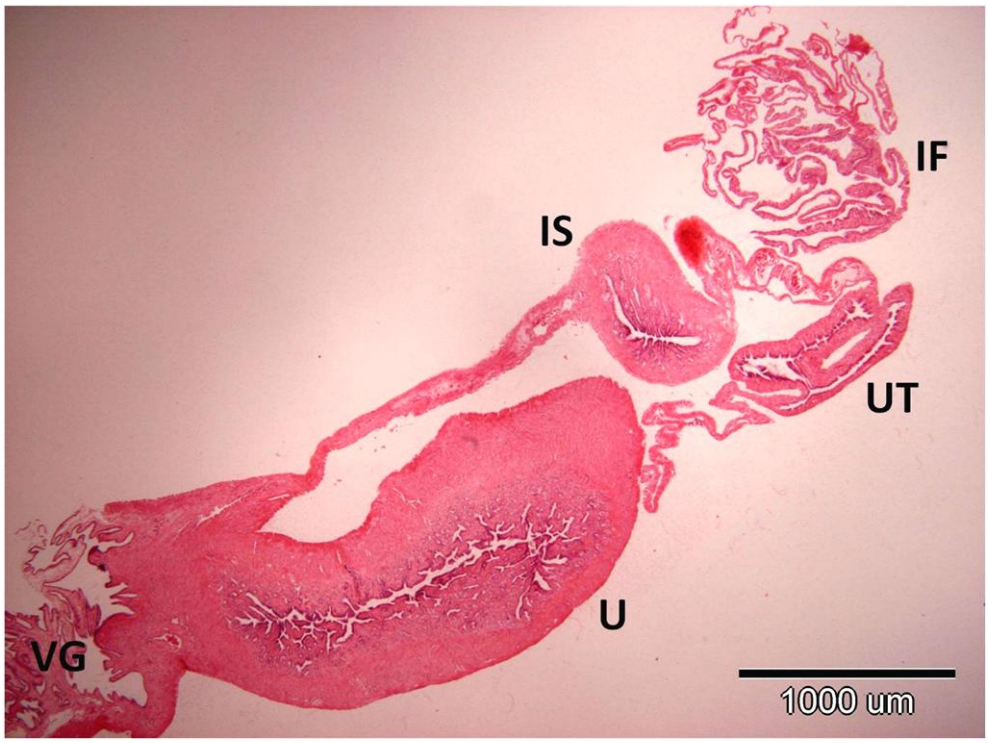

Figure 4.13B. H&E. Oviduct from the recrudescent phase: infundibulum (IF), uterine tube (UT), isthmus (IS), uterus (U) and vagina (VG).

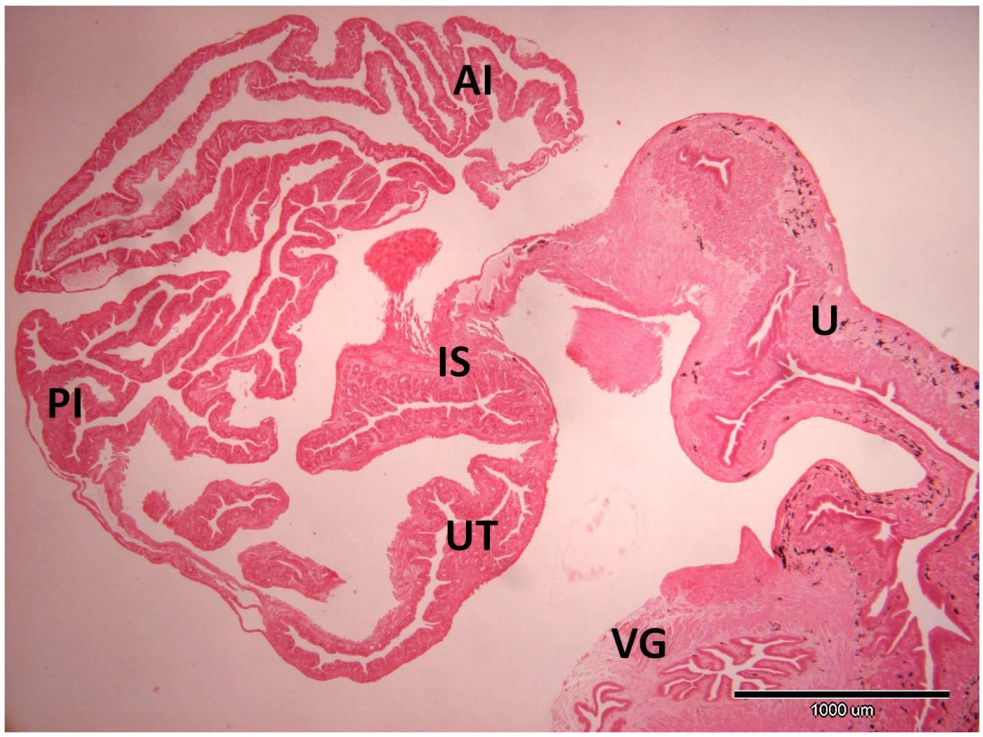

Figure 4.13C. H&E. Portion of the oviduct from the early active phase (early vitellogenesis) showing; anterior infundibulum (AI), posterior infundibulum (PI), uterine tube (UT), isthmus (IS), uterus (U) and vagina (VG).

Figure 4.13D. AB-PAS. Portion of the oviduct from the active phase (vitellogenesis/gravidity) showing; anterior infundibulum (AI), posterior infundibulum (PI), uterine tube (UT) and uterus (U).

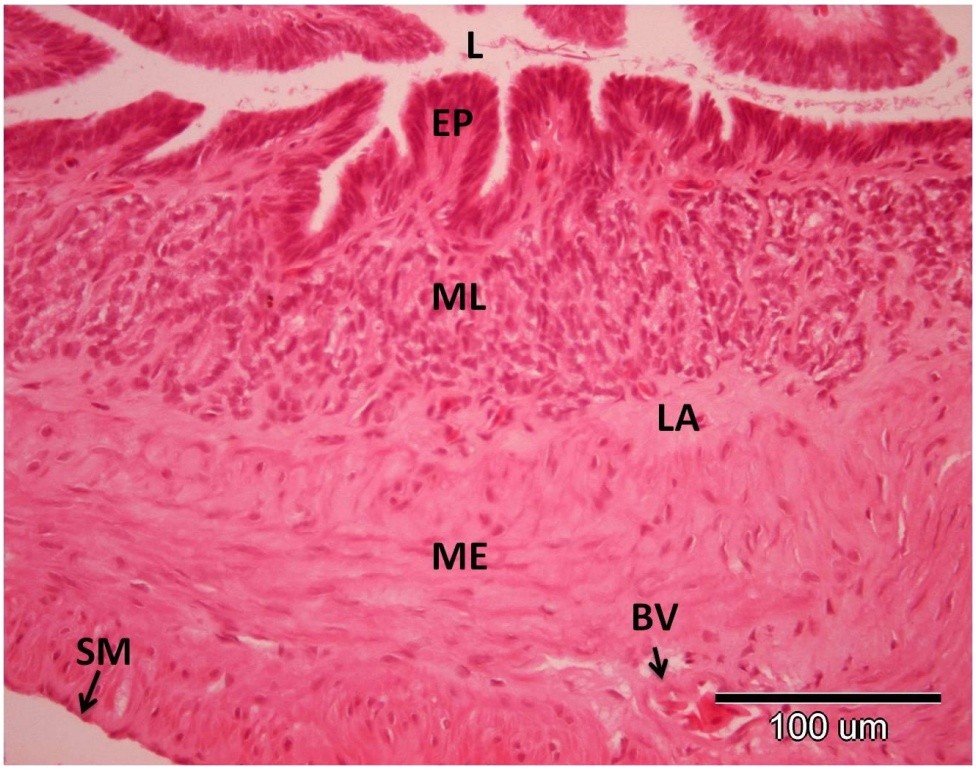

Figure 4.13E. H&E. Uterus from the active phase showing; luminal epithelial layer (EP), mucosal layer (ML), lamina propria (LA), muscularis externa (ME), serosal membrane (SM). Blood vessel (BV), lumen (L).

At the anterior end, the infundibulum received the ovulated eggs through an ostial opening. The fertilization of eggs took place within the infundibulum. The infundibulum led into the uterine tube for albumen secretion, and then into the uterus through the isthmus for eggshell formation. Eggs were retained in the uterus during gravidity until oviposition. Most posterior was the vagina, which led into a common urogenital sinus.

The histological changes in the oviducts were evident during the reproductive cycle of *H. flaviviridis*. During the early vitellogenic period, oviduct crypts were small, but epithelial cells began to hypertrophy. During gravidity, the oviduct was lined by a columnar epithelium which began to degenerate after gravidity. Oviductal hypertrophy was maximal during the active phase.

Changes in the oviductal weight during the reproductive cycle of *H. flaviviridis* are summarised in Table 4.1, and the changes in epithelial cell height in different oviductal regions during the different reproductive phases are summarised in Table 4.5.

The epithelial cell height ($P < 0.001$) varied significantly during the different phases of the reproductive cycle (Table 4.5). The epithelial cell height was low in the quiescent phase between June and August and in the recrudescent phase (September through to December) but increased during vitellogenesis and ovulation in March and increased significantly ($P < 0.001$) in April and May, coinciding with gravidity. After oviposition in May, the epithelial cell height began to regress during the quiescent phase, and remained low during the recrudescent phase until the next cycle.

Table 4.5. Changes (mean ± S.E.M) in epithelial cell height in different oviductal regions during the reproductive cycle of *H. flaviviridis* (N= Individual geckos).

Phase	N	Infundibulum (µm)	Uterine tube (µm)	Uterus (µm)	Vagina (µm)
Quiescent (June – Aug)	10	9.40 ± 0.27^{a}	12.20 ± 0.47^{a}	8.80 ± 0.42^{a}	7.70 ± 0.34^{a}
Recrudescent (Sept – Dec)	18	10.00 ± 0.28^{a}	14.11 ± 0.40^{a}	9.39 ± 0.29^{a}	8.00 ± 0.27^{a}
Active (vitellogenesis) (Jan)	10	18.90 ± 1.06^{b}	28.30 ± 1.14^{b}	17.60 ± 0.65^{b}	12.40 ± 0.75^{b}
Active Ovulation (March)	11	23.73 ± 0.94^{c}	33.91 ± 1.28^{c}	20.82 ± 0.40^{c}	15.45 ± 0.65^{c}
Active 1st Gravidity (March-April)	11	42.00 ± 1.62^{e}	54.36 ± 1.55^{e}	33.91 ± 0.85^{e}	22.82 ± 0.71^{e}
Active 2nd Gravidity (April- May)	9	32.22 ± 0.81^{d}	43.78 ± 1.09^{d}	29.89 ± 0.51^{d}	19.22 ± 0.32^{d}
Oviposition (Late April & Late May)	11	22.55 ± 1.32^{c}	33.55 ± 1.92^{c}	20.55 ± 0.79^{c}	12.45 ± 0.53^{b}
ANOVA					
	F(6,73)	155.13	177.03	289.69	119.77
	P-value	< 0.001	< 0.001	< 0.001	< 0.001

Statistical differences between groups obtained by Duncan's multiple-comparisons test. Months with significantly different values (mean ± S.E.M) in vertical column were assigned different letters. Phases with the same letter show statistically no significant difference between them at the 0.05 level of significance.

4.3.10.1 Infundibulum

The infundibulum can be subdivided into an expanded anterior portion forming an ostial opening and a constricted, posterior tubal portion. The infundibulum received the ovulated egg from the ovary via a funnel-shaped ostium opening to the coelomic

cavity. Prior to ovulation, the anterior infundibulum extended anteriorly to surround the mature ovarian follicle in the ovary. After ovulation, it retracted from the ovary as the size of the ovary was reduced. The ostium was a very thin-walled region with irregular mucosal folds (Figure 4.14A). The anterior segment of the infundibulum was slender and flaccid. At the ostial end, it was characterized by a thin muscularis externa and mucosa with a simple squamous epithelium (Figure 4.14A). The mucosa formed low folds, which gradually increased in height toward the posterior portion (Figures. 413C, 4.13D & 4.14B). The lumen was lined by ciliated and nonciliated cuboidal cells which became more columnar towards the posterior infundibulum, and were negatively stained with the PAS stain (Figures 4.14B, 414C & 4.14D). Ciliated cells contained SER and numerous mitochondria associated with basal bodies, which anchored the cilia. Nuclei of all the epithelium cells were euchromatic and located basally. Epithelial cells were connected apically by tight junctions and desmosomes, and intercellular canaliculi, which were convoluted (Figure 4.14E). Nonciliated cells contained euchromatic nuclei and prominent nucleoli. The cytoplasm consisted of mitochondria, SER and secretory granules which tended to be at the apical surface (Figure 4.14F). During the reproductive season (active phase), the vascularity in the anterior portion was high (Figures 413C, 4.13D, 4.14B & 4.14G).

Figure 4.14A. H&E. Oviduct from the quiescent phase showing anterior infundibulum at the ostial end with irregular mucosal folds (arrow).

Figure 4.14B. PAS-Haem. Cross section of the oviduct from the early active phase showing anterior infundibulum (AI), posterior infundibulum (PI) and uterine tube (UT).

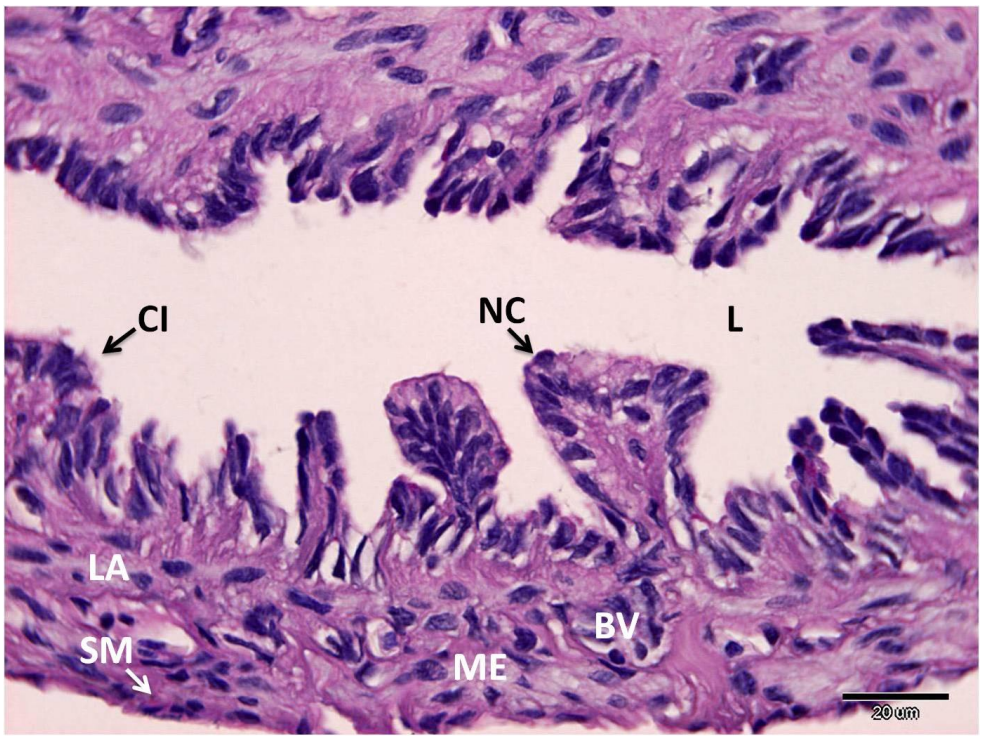

Figure 4.14C. PAS-Haem. Higher magnification of Figure 4.14B of anterior infundibulum with ciliated (CI) and nonciliated (NC) cells. The anterior infundibulum stained negative for PAS. Lamina propria (LA), muscularis externa (ME), serosal membrane (SM), blood vessel (BV), lumen (L).

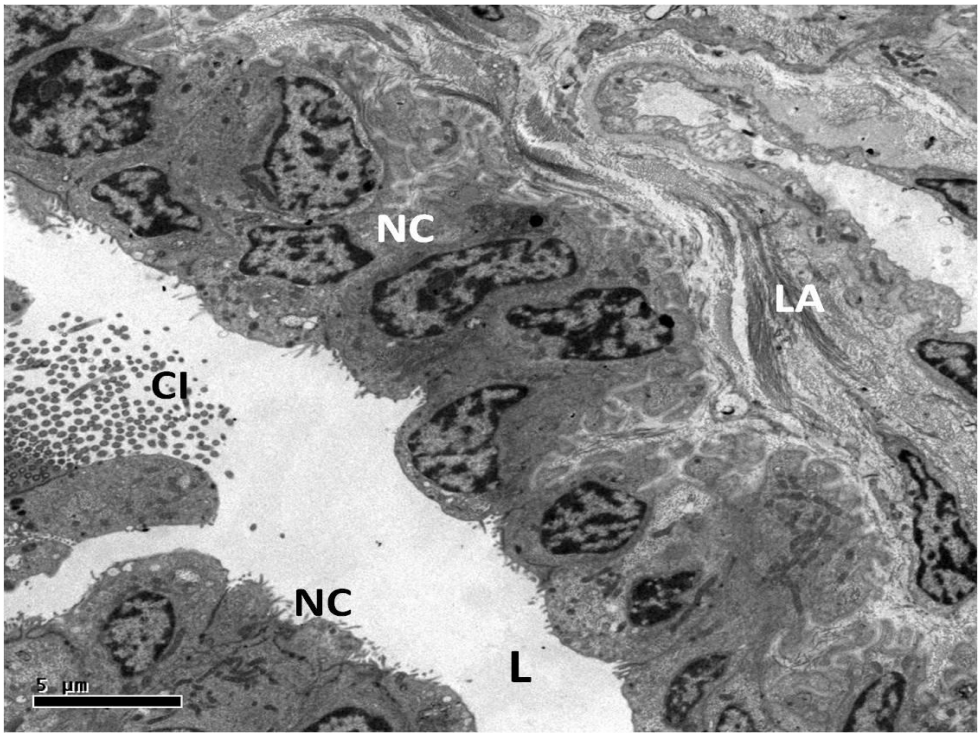

Figure 4.14D. TEM. Anterior infundibulum from the early active phase showing ciliated (CI) and nonciliated (NC) cells. Lamina propria (LA), lumen (L).

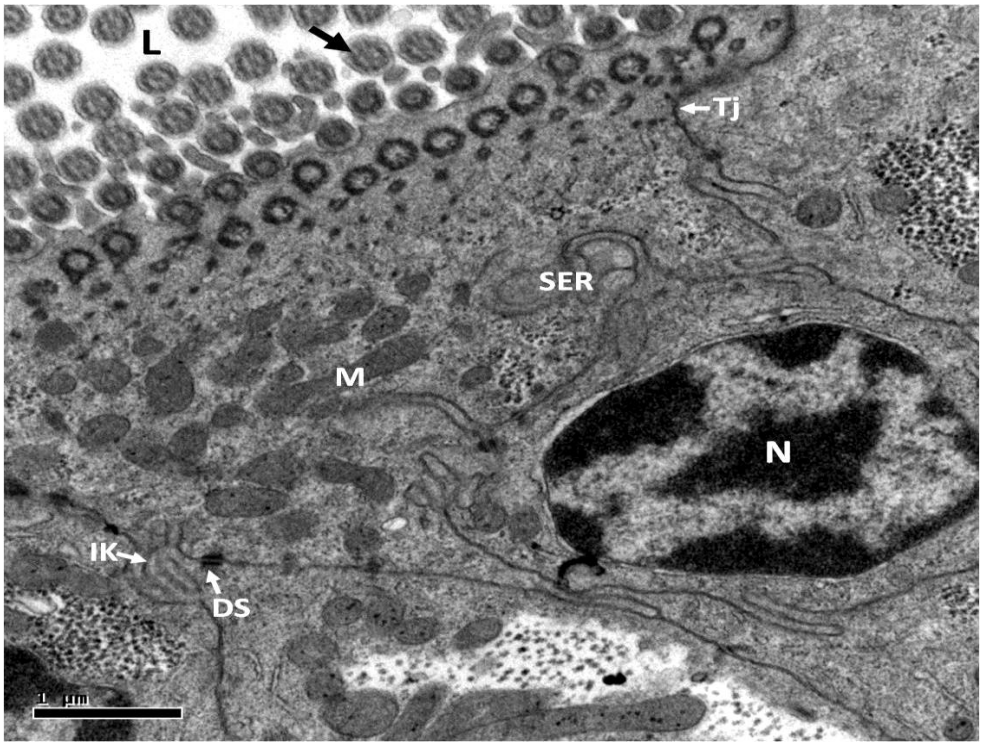

Figure 4.14E. TEM. Higher magnification of Figure 4.14D showing ciliated cell with euchromatic basal nucleus (N) numerous mitochondria (M), SER. The epithelial cells connected apically by tight junctions (Tj), desmosomes (DS) and intercellular canaliculi (IK). Cilia (thick arrow), lumen (L).

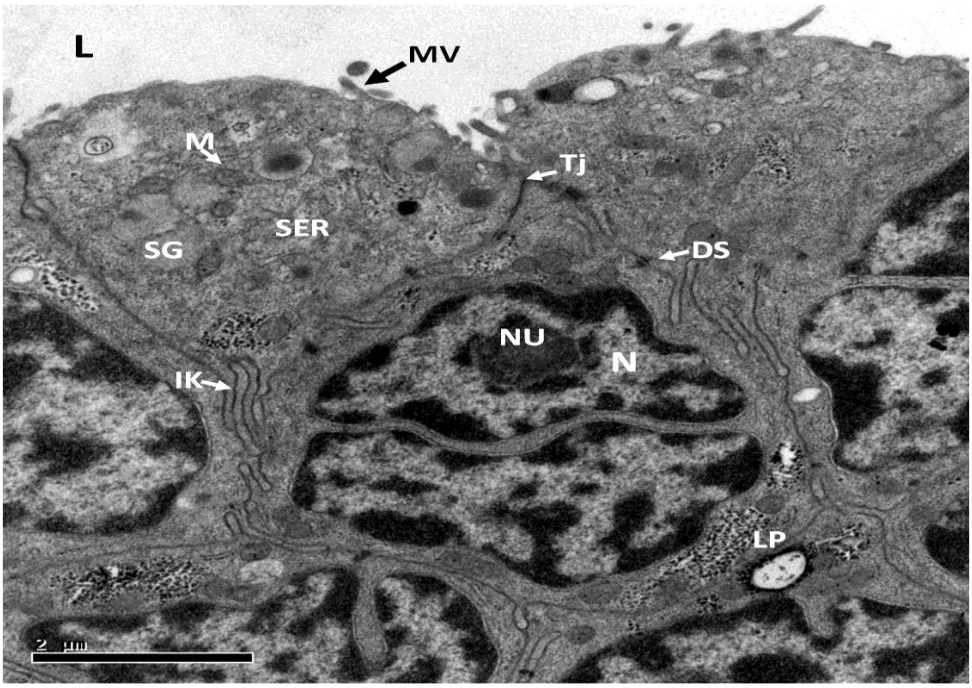

Figure 4.14F. TEM. Higher magnification of Figure 4.14D showing nonciliated cells with euchromatic basal nuclei (N) and prominent nucleoli (NU), mitochondria (M) associated with SER and lipids (LP). Few secretory granules (SG) appeared in the cytoplasm, and few microvilli (MV) at the cell surface. Tight junctions (Tj), desmosomes (DS) and intercellular canaliculi (IK), lumen (L).

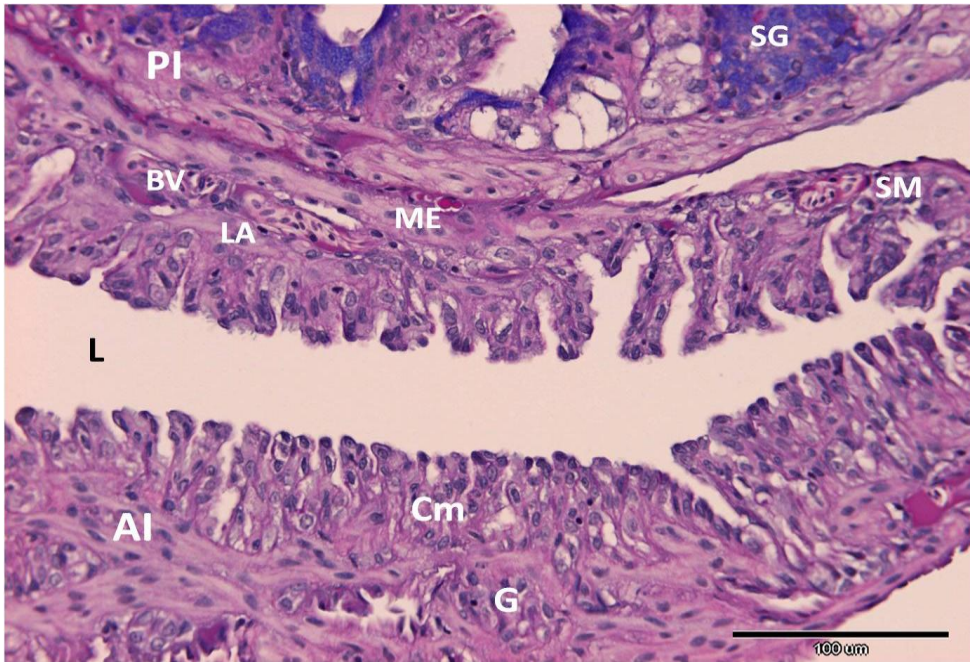

Figure 4.14G. AB-PAS. Higher magnification of Figure 4.13D showing hypertrophied columnar epithelium (Cm) of the anterior infundibulum (AI). Note that the anterior portion stained negative for PAS whereas posterior portion (PI) stained positive showing the presence of secretory granules (SG). Gland (G), lamina propria (LA), muscularis externa (ME), serosal membrane (SM), blood vessel (BV), lumen (L).

The posterior portion of the infundibulum was more constricted, characterized by the presence of a columnar epithelium and appeared similar to the uterine tube towards its posterior end (Figures 4.13C, 4.13D, 4.14B & 4.14H). The mucosa at the end of this portion had longitudinal folds and each fold had crypts extending at different directions that periodically extended into the lamina propria and made connection with the ducts of the endometrial glands. Throughout the posterior segment, the mucosa consisted of columnar ciliated, nonciliated microvillous and occasional bleb cells (Figure 4.14I). Ciliated cells contained euchromatic nuclei which were located basally. The cytoplasm contained SER and numerous mitochondria associated with basal bodies, which anchored the cilia (Figure 4.14J). The nonciliated cells contained euchromatic nuclei with large cytoplasmic secretory granules of varying densities which were located at the apical cell surface (Figure 4.14K). Numerous microvilli covered the nonciliated cell surfaces (Figure 4.14K). Bleb cells were occasionally seen and were characterized by apical protrusions with few microvilli and cytoplasmic secretory granules (Figure 4.14I).

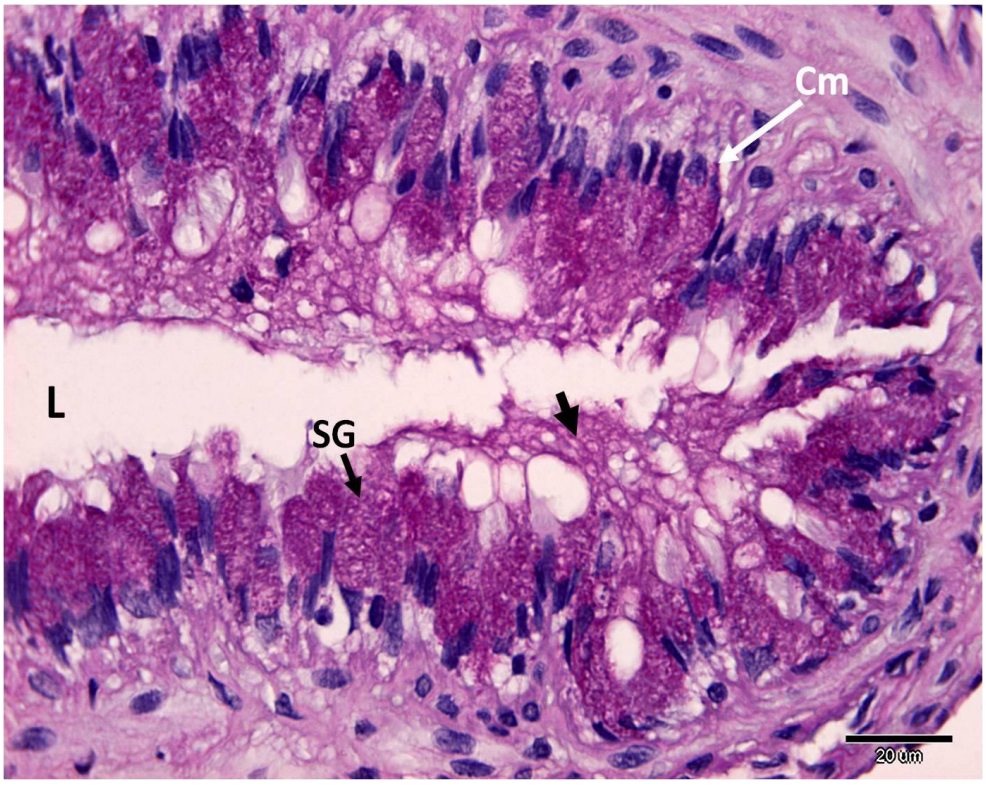

Figure 4.14H. PAS-Haem. Higher magnification of Figure 4.14B of posterior infundibulum showing columnar epithelia cells (Cm) filled with cytoplasmic secretory granules (SG) and their secretions (thick arrow) released into the lumen (L). The posterior infundibulum was strongly stained with PAS.

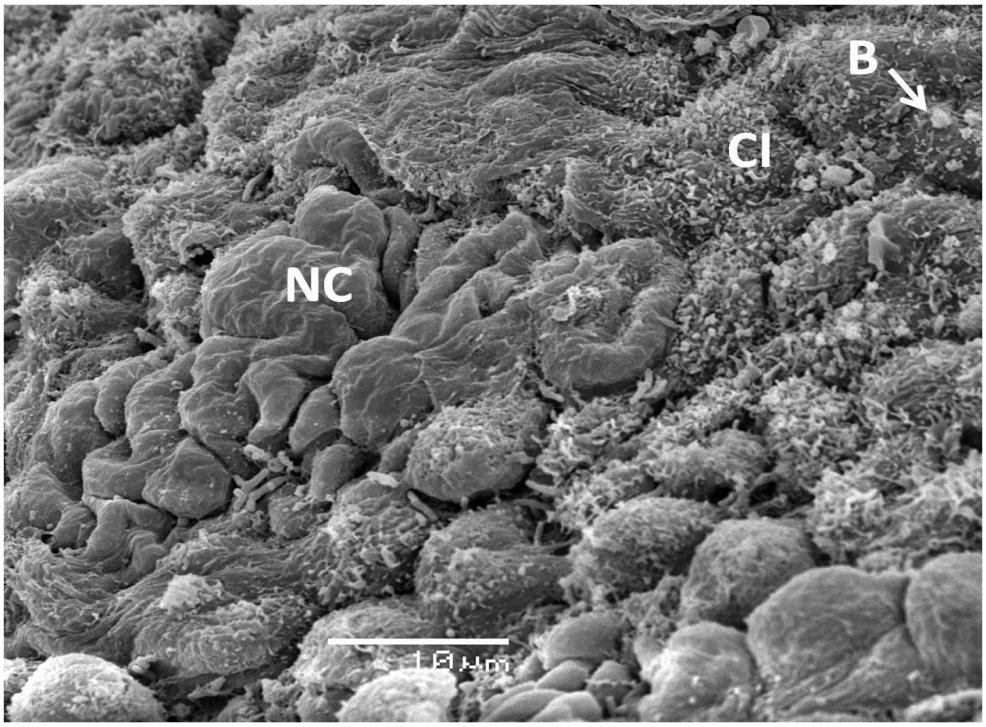

Figure 4.14I. SEM. Surface view of the posterior infundibulum from the quiescent / recrudescent phases showing epithelium with ciliated (CI), nonciliated (NC) and occasional bleb (B) cells.

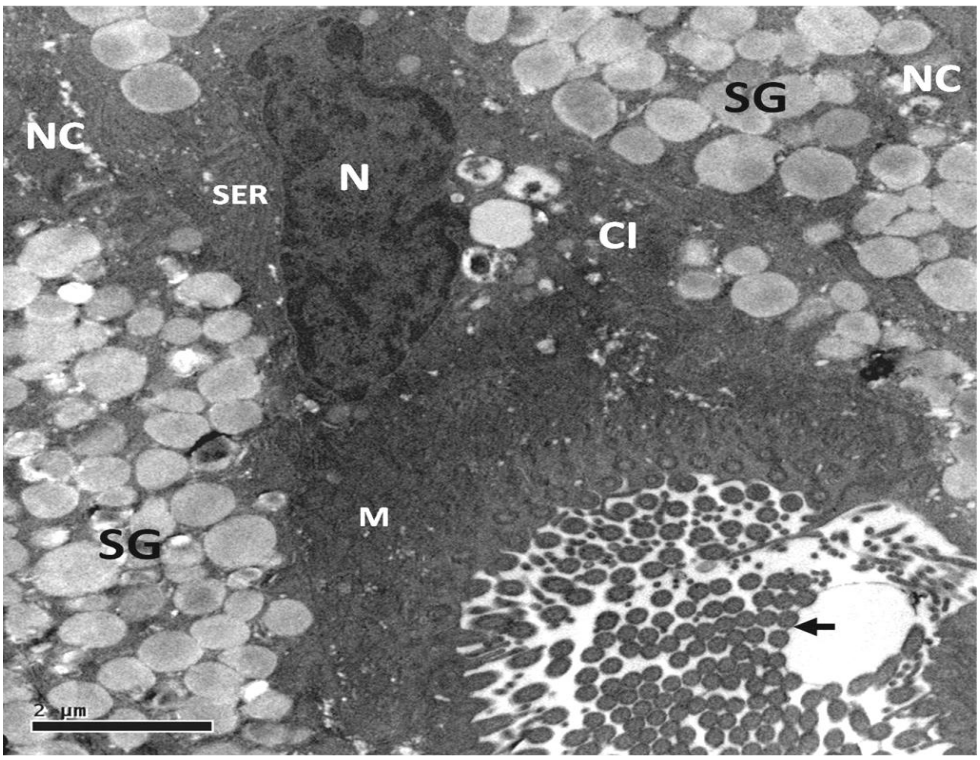

Figure 4.14J. TEM. Posterior infundibulum showing ciliated (arrow) columnar cell (CI) with euchromatic basal nucleus (N), mitochondria (M) associated with SER. Adjacent nonciliated cells (NC) filled with secretory granules (SG).

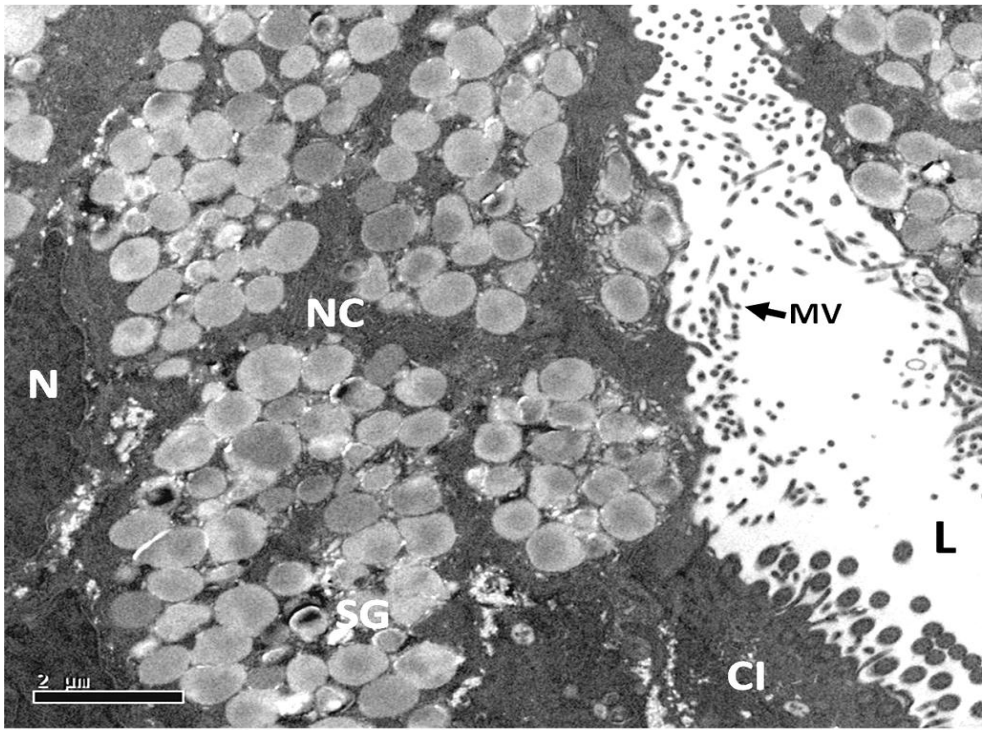

Figure 4.14K. TEM. Posterior infundibulum from the active phase showing epithelium with ciliated (CI) and nonciliated (NC) cells. NC appeared with numerous large cytoplasmic secretory granules (SG) of varying densities and numerous microvilli (MV). Nucleus (N), lumen (L).

The endometrial glands were found predominantly in the lamina propria of the posterior portion (Figures 4.14L & 4.14M). Only a few scattered endometrial glands were present in the anterior portion, especially near the junction with the posterior portion (Figure 4.14G). The epithelium of the posterior infundibulum was strongly stained with PAS (Figures 4.14H, 4.14L, 4.14M & 4.14N), suggesting the secretory granules contained some form of carbohydrate. The endometrial glands, however, reacted negatively with PAS stain. During vitellogenesis and early gravidity, the columnar epithelium became highly hypertrophied (Figures 4.13D & 4.14M), and in the non-reproductive season (quiescent and recrudescent phases) both folds and epithelial cells declined in height and the secretory activity in the epithelium and glands ceased after oviposition (Figures 4.13A & 4.13B).

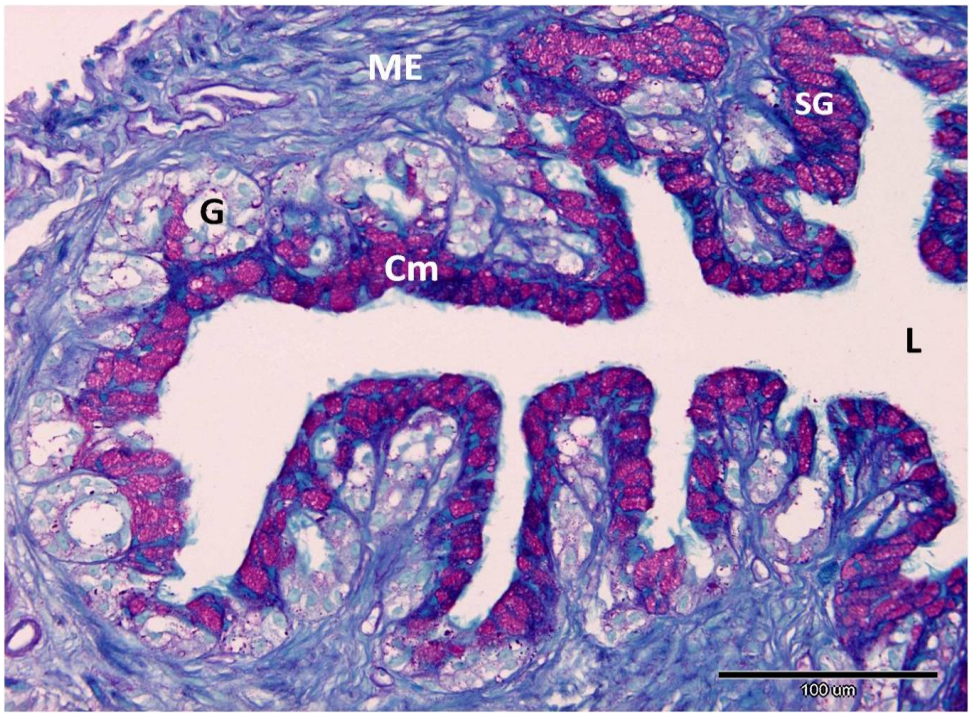

Figure 4.14L. PAS-FG. Posterior infundibulum from early active phase showing columnar epithelial cells (Cm) filled with cytoplasmic secretory granules (SG). Epithelium strongly stained with PAS. Glands (G) stained negatively with PAS. Muscularis externa (ME), lumen (L).

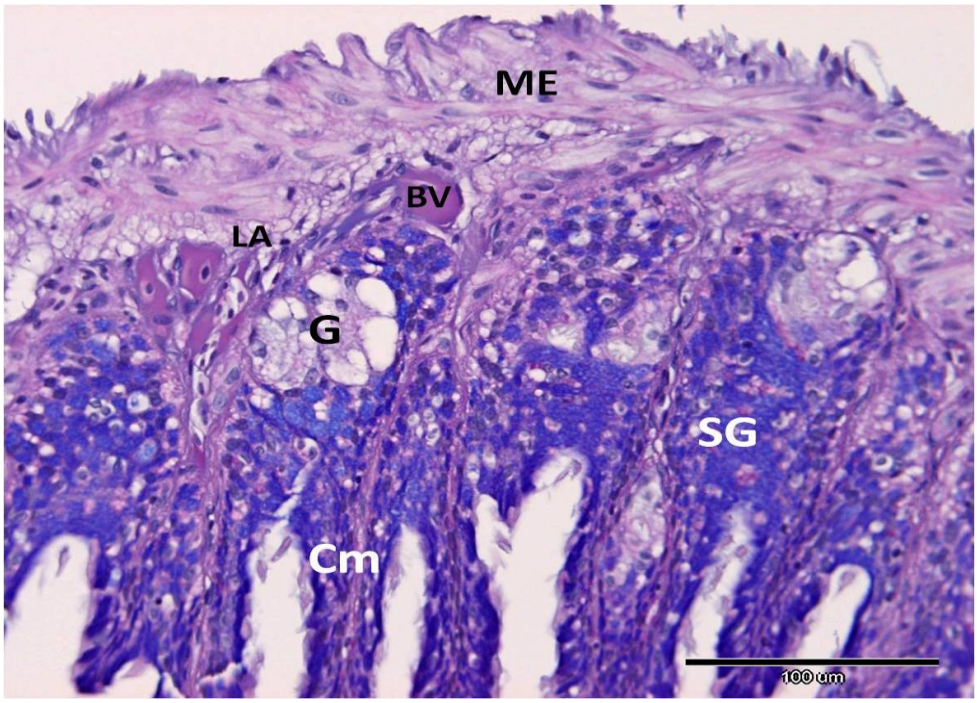

Figure 4.14M. AB-PAS. Higher magnification of Figure 4.13D. Posterior infundibulum from the active phase (vitellogenesis/gravidity) showing hypertrophied columnar epithelial cells (Cm) filled with cytoplasmic secretory granules (SG), and mucosa glands (G). The epithelium strongly stained with PAS. Lamina propria (LA), muscularis externa (ME), blood vessel (BV).

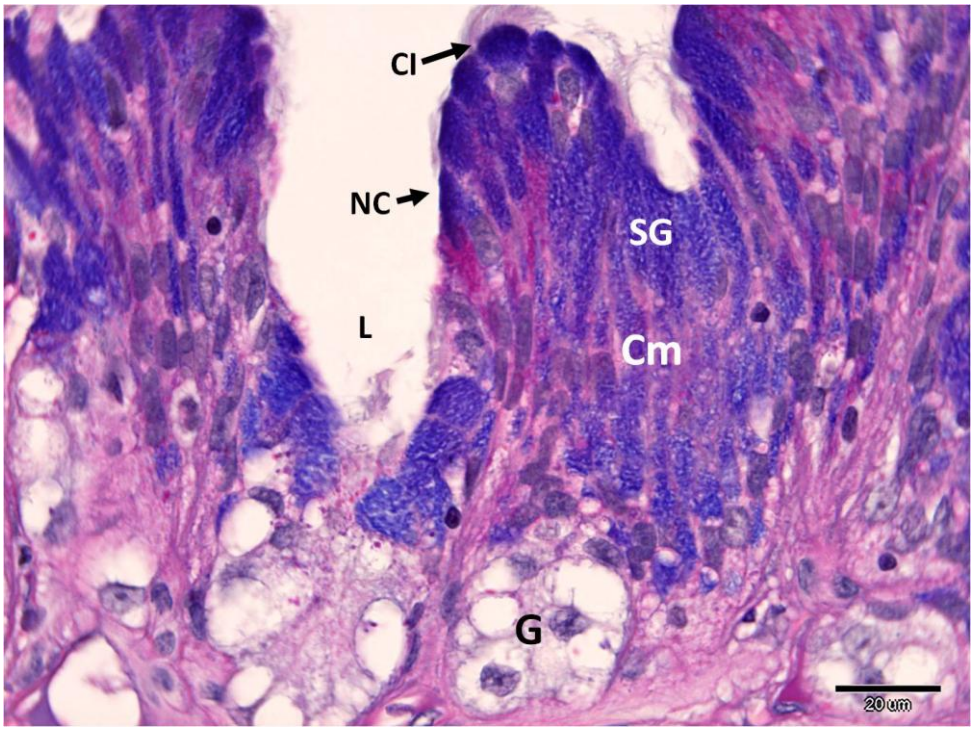

Figure 4.14N. AB-PAS. Higher magnification of Figure 4.14M. Columnar epithelial cells (EP) filled with cytoplasmic secretory granules (SG). The epithelium stained strongly for PAS, whereas the glands (G) stained negatively with PAS. Ciliated cell (CI), nonciliated cell (NC), lumen (L).

4.3.10.2 Uterine tube

The uterine tube is relatively thin-walled with high longitudinal elevations of mucosal folds of uneven height and intersected at random by deep crypts (Figures 4.13D, 4.15A & 4.15B). The epithelium lining these folds was folded and associated with the lamina propria establishing a connection with the ducts of the endometrial glands. The endometrial glands of the mucosa were numerous and occupied most of the lamina propria (Figures 4.15A, 4.15B & 4.15C). The luminal epithelium consisted of ciliated and nonciliated cells (Figure 4.15D). Ciliated cells were narrow and columnar in appearance, with nuclei generally basally situated. Nonciliated cells had few microvilli during early vitellogenesis. During vitellogenesis and early gravidity the epithelium became highly hypertrophied (Figure 4.15C). Nonciliated cells were covered in microvilli and their cytoplasm contained a large number of secretory materials (Figure 4.15E). Epithelial cells stained positively with PAS, however, the glands stained negatively for PAS (Figures 4.15A, 4.15C & 4.15E). The nonciliated cells contained euchromatic nuclei with large cytoplasmic secretory granules (Figures

4.15F & 4.15G). Occasional bleb cells, with cytoplasmic secretory granules and smooth apical surface protruding into the lumen, were also seen in this region. Sperm were seen in the uterine tube, singly or in bundles inside the endometrial glands (Figure 4.15H). Sperm were stored in elongated branched tubules that communicated with the lumen by ciliated ducts. In the non-reproductive season both folds and the epithelial cells which lined them declined in height and the secretory activity in the epithelium and glands ceased after oviposition (Figures 4.13A, 4.13B & 4.15D).

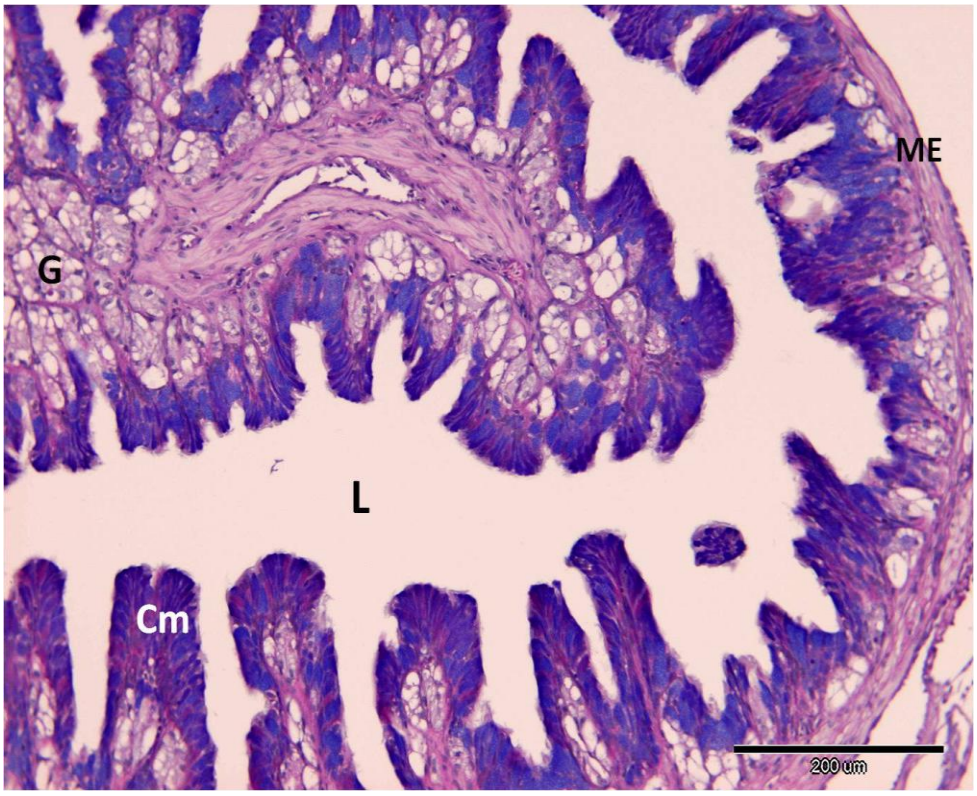

Figure 4.15A. AB-PAS. Higher magnification of Figure 4.13D. Uterine tube showing thin muscularis externa (ME) and columnar epithelial cells (Cm) lining the mucosal folds connected with the endometrial glands (G). Lumen (L).

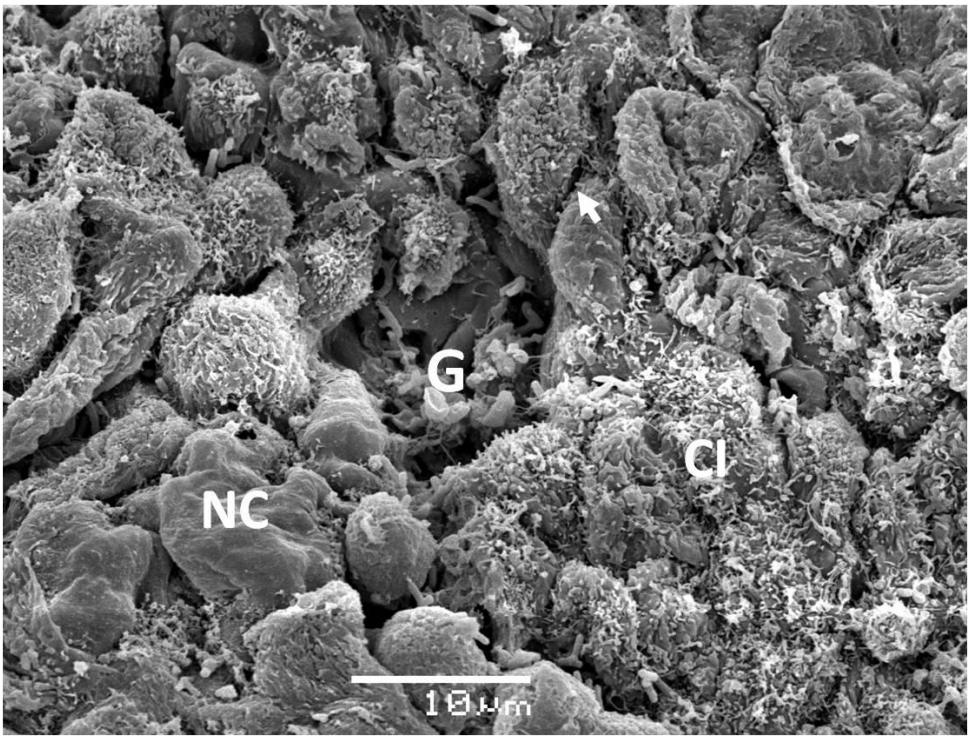

Figure 4.15B. SEM. Surface view of the uterine tube from the early active phase showing mucosal folds intersected at random by deep crypts (arrow). Ciliated (CI) and nonciliated (NC) cells appeared connected to endometrial gland (G).

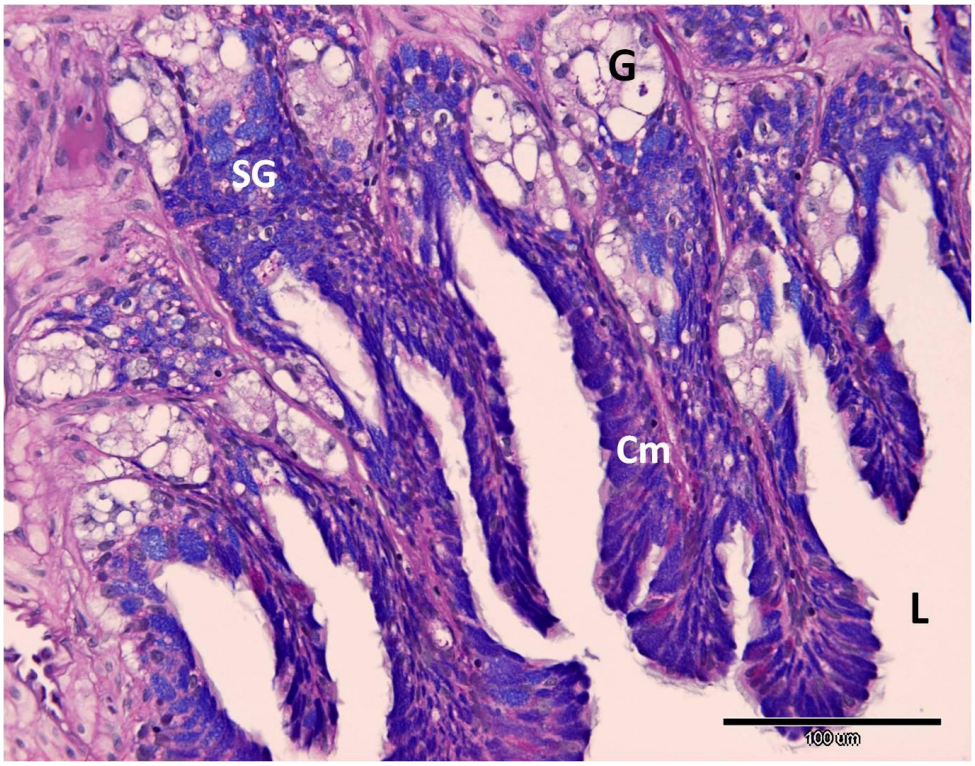

Figure 4.15C. AB-PAS. Higher magnification of Figure 4.13D. Uterine tube showing columnar epithelial cells (Cm) lining the mucosal folds connected with the endometrial glands (G). The epithelium filled with secretory material (SG) and stained strongly for PAS, whereas the glands (G) did not stain with PAS. Lumen (L).

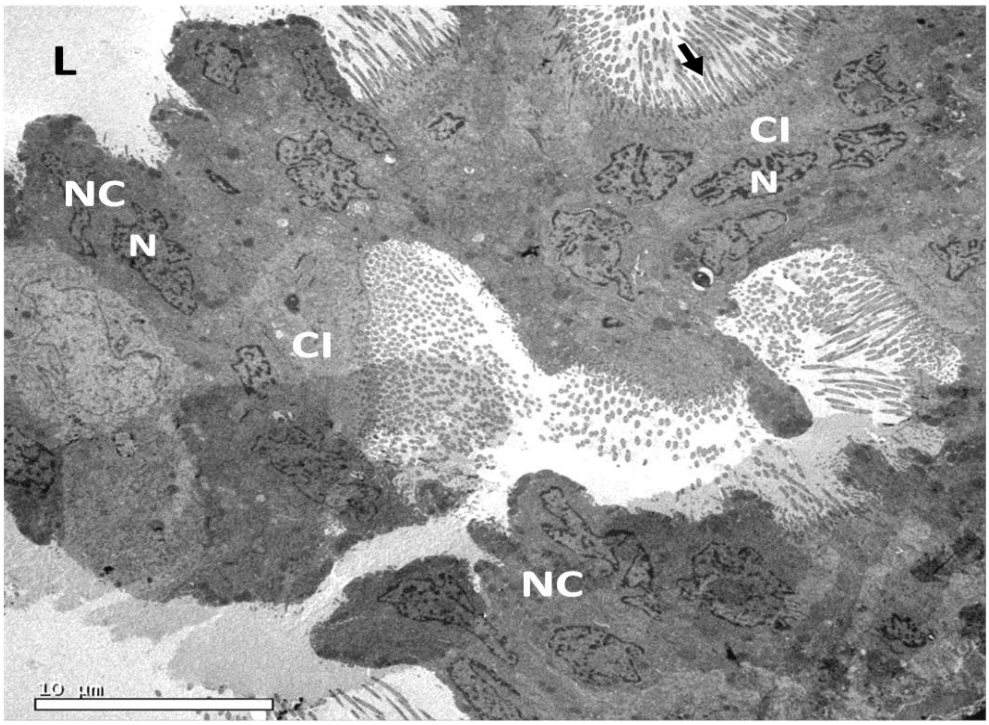

Figure 4.15D. TEM. Uterine tube from the quiescent phase showing luminal epithelium (L) with ciliated (CI) and nonciliated (NC) cells. Nonciliated cells devoid of any secretory granules. Cilia (arrow), nucleus (N), lumen (L).

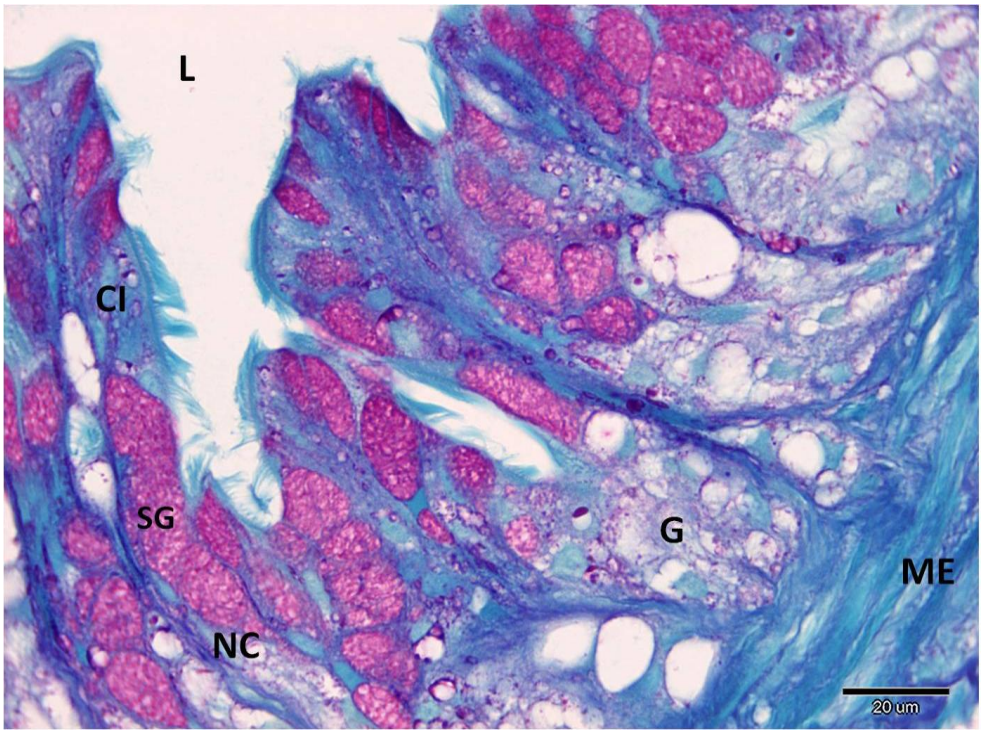

Figure 4.15E. PAS-FG. Uterine tube from the active phase. The cytoplasm of nonciliated cells (NC) contains numerous secretory material (SG). The epithelium stained strongly for PAS, whereas the glands (G) stained negatively with PAS. Ciliated cells (CI), muscularis externa (ME), lumen (L).

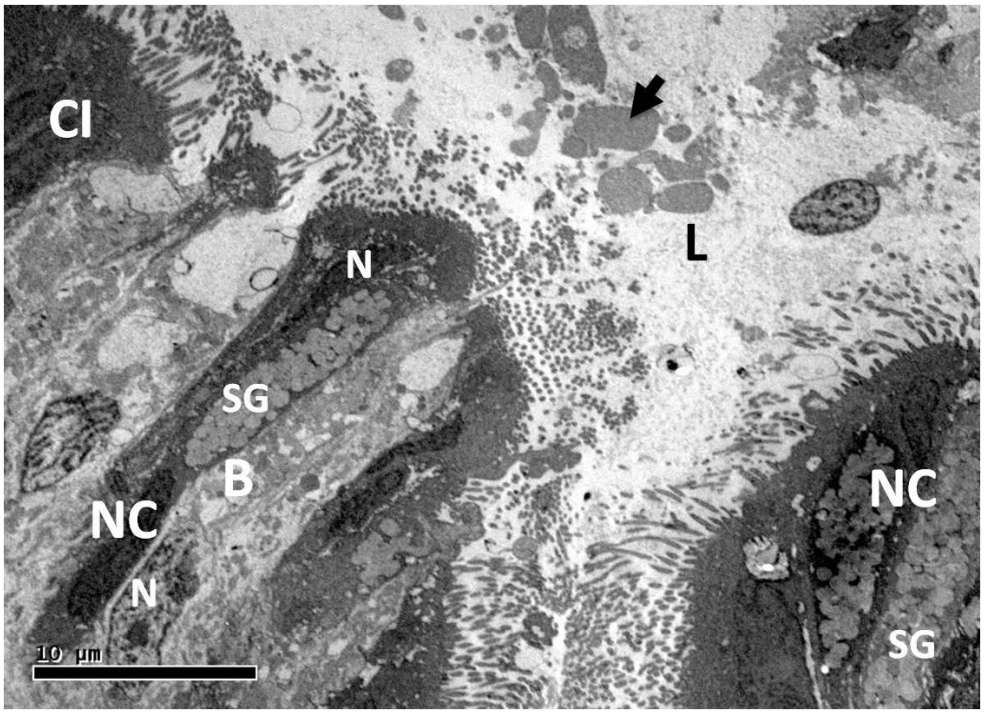

Figure 4.15F. TEM. Uterine tube from the active phase with luminal epithelium. Nonciliated (NC) and bleb (B) cells with numerous secretory granules (SG). Lumen (L) contains secretory material (arrow). Ciliatd cells (CI), nucleus (N).

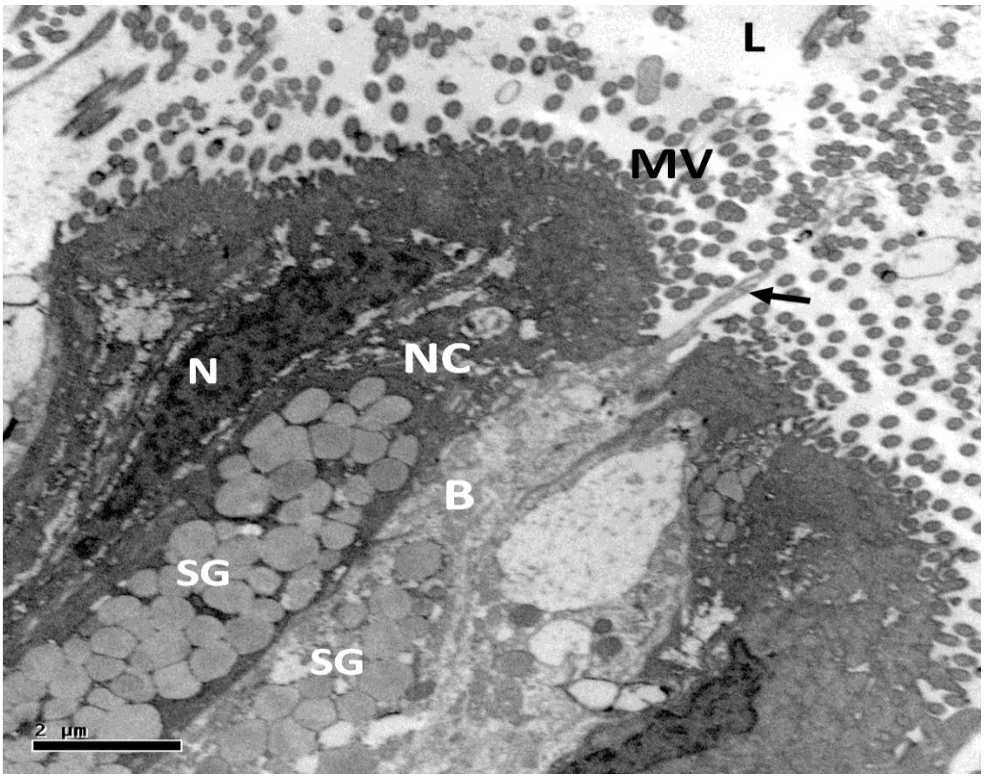

Figure 4.15G. TEM. Higher magnification of Figure 4.15F. Bleb cell (B) with secretory granules (SG) and smooth apical surface protruding into the lumen (arrow). Nonciliated (NC) cells with euchromatic nuclei (N) and numerous microvilli (MV). Lumen (L).

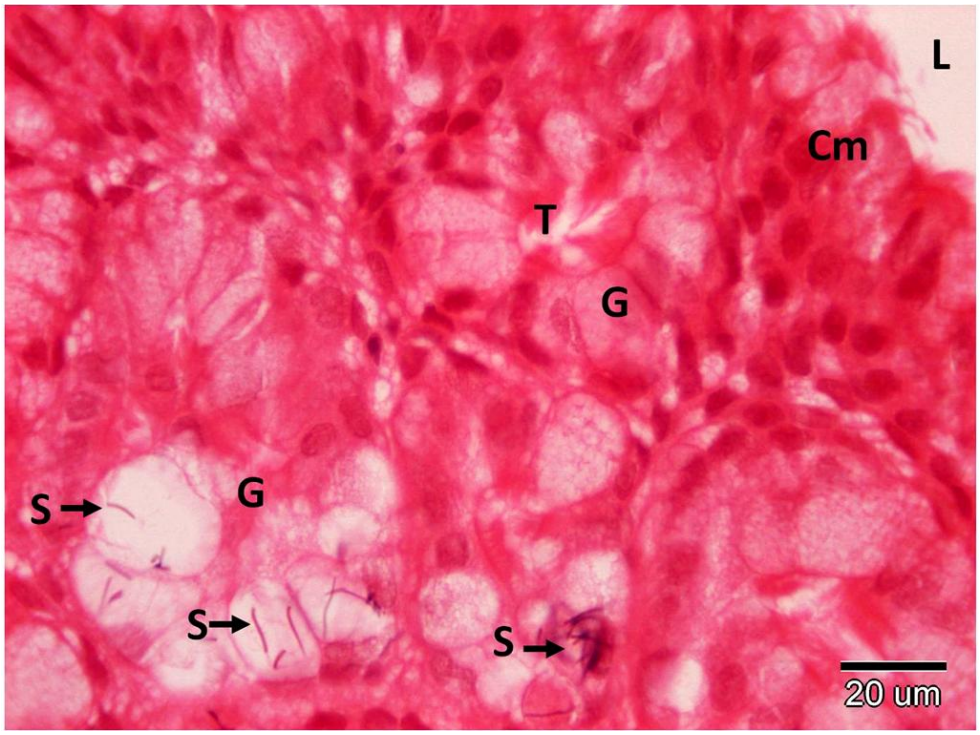

Figure 4.15H. H&E. Uterine tube from the active phase. Sperm (arrow) appeared at the endometrial glands (G). Columnar epithelium (Cm), gland tubule (T), lumen (L).

4.3.10.3 Isthmus

The isthmus or junction was a short connection between the uterine tube and the uterus, and appeared to have no function in eggshell formation. Several glands were found in the mucosa. However, near the ends, the mucosa showed similarity with the uterine tube on the upper side and with the uterus on the lower side (Figures 4.10B, 4.13C & 4.15I). Epithelial cells stained negatively with the carbohydrate stain, PAS (Figure 4.15J). The general appearance of the isthmus remained the same during gravidity.

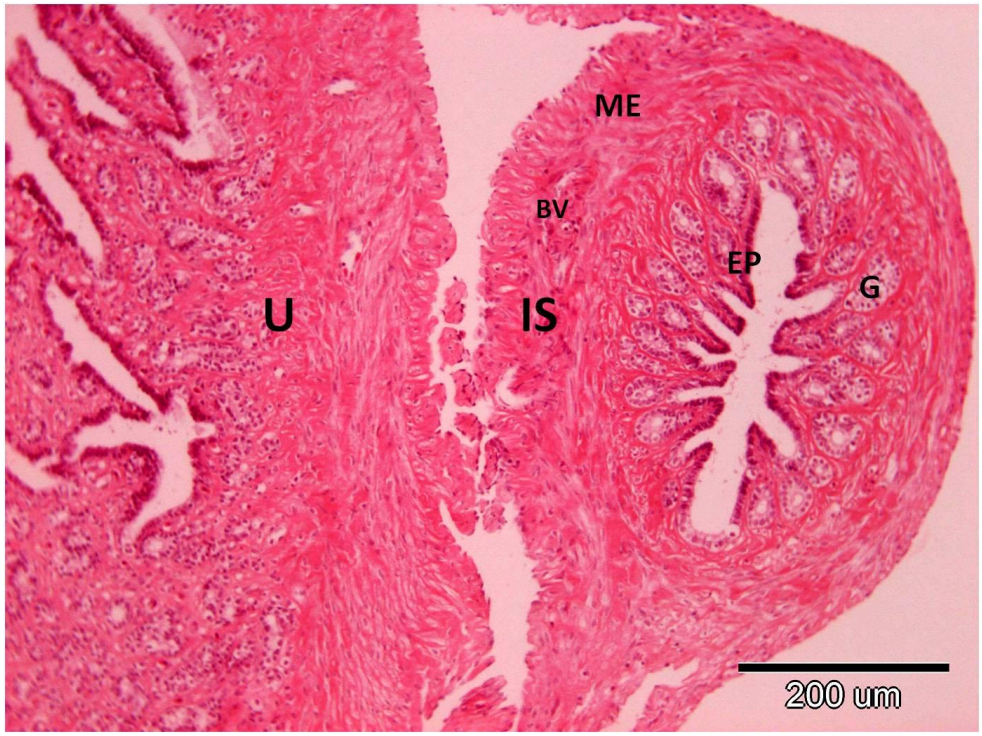

Figure 4.15I. H&E. isthmus from the early active phase. The isthmus (IS) closely resembles the uterus (U) at the uterus end with thick muscle and mucosal layers. Epithelium (EP). Gland (G), muscularis externa (ME), blood vessel (BV).

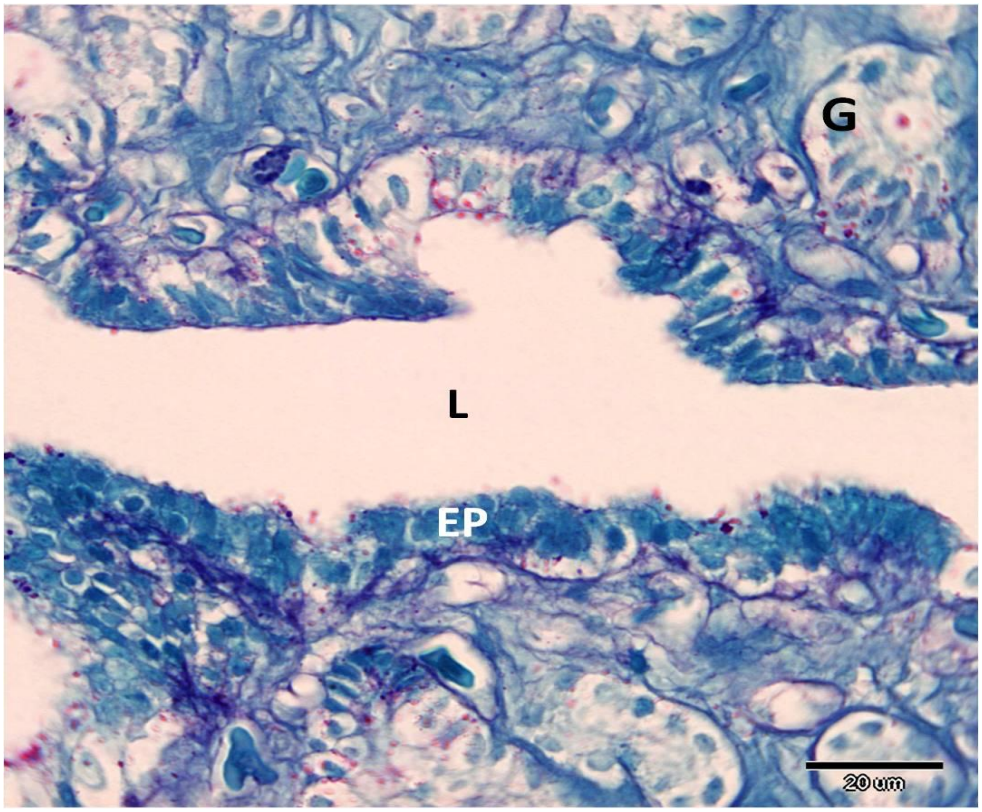

Figure 4.15J. PAS-FG. Isthmus from the active phase. The epithelium and glands stained negatively with PAS. Epithelium (EP). Gland (G), lumen (L).

4.3.10.4 Uterus

The uterus was glandular and had a thick muscular wall with an outer longitudinal and inner circular layer (Figure 4.13E). The uterine mucosa lacked the extensive folds found in the posterior infundibulum, uterine tubes and vagina. The mucosa was thick and folded in a generally longitudinal direction and intersected by deep crypts extending in different directions. These folds were supported by a thick layer of lamina propria with small blood vessels under the epithelial layer (Figures 4.13E, 4.16A, 4.16B & 4.16C). The mucosal endometrial glands dominated the lamina propria and were more abundant and more organized than the glands of the uterine tube (Figure 4.16B). The glands communicated with the lumen by their ducts (Figure 4.16C) and were composed of ciliated low columnar and microvillous cells (Figure 4.16D). These glands contained secretory granules of varying electron densities (Figure 4.16E) and stained negatively with PAS (Figure 4.16D). Like the condition observed in the posterior infundibulum and the uterine tube, the epithelium extended deeply into the lamina propria and periodically connected with the ducts of the endometrial glands (Figure 4.16C). The epithelium consisted of columnar ciliated and nonciliated cells with their nuclei basally situated (Figures 4.16C, 4.16F & 4.16G, 4.16H). The nonciliated cells stained strongly with PAS for carbohydrate (Figures 4.16C, 4.16F & 4.16G). This corresponded to the large numbers of secretory granules seen in the apical regions of the cells (Figure 4.16H).

The uterus changed dramatically over a reproductive season. During vitellogenesis the uterus was thick walled, the mucosa was well vascularised and the epithelium was hypertrophied and contained large numbers of secretory granules (Figures 4.13E, 4.16A, 4.16B, 4.16C, 4.16E, 4.16F, 4.16.G & 4.16H). During gravidity, the uterine region was highly stretched owing to the presence of a large yolky egg. After oviposition, both folds and epithelial cells lining them declined in height (Figures 4.13A & 4.13B). The secretory activity ceased in the epithelium and glands, and both stained negative for PAS (Figure 4.16I). Nonciliated cells of the epithelium lining the lumen contained no secretory granules (Figure 4.16J). The uterus remained in this state until the next reproductive season began.

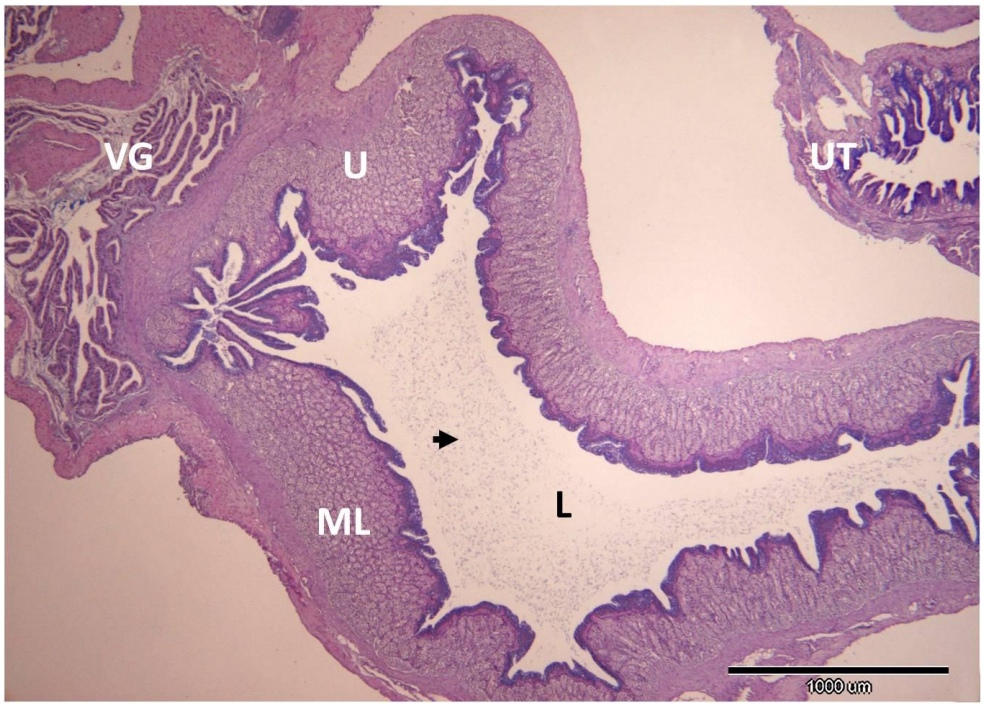

Figure 4.16A. AB-PAS. The second portion of the oviduct (see Figure 4.13D) from the active phase showing the uterus (U) with thick mucosal layer (ML). Note secretion (arrow) in the lumen (L). Vagina (VG), uterine tube (UT).

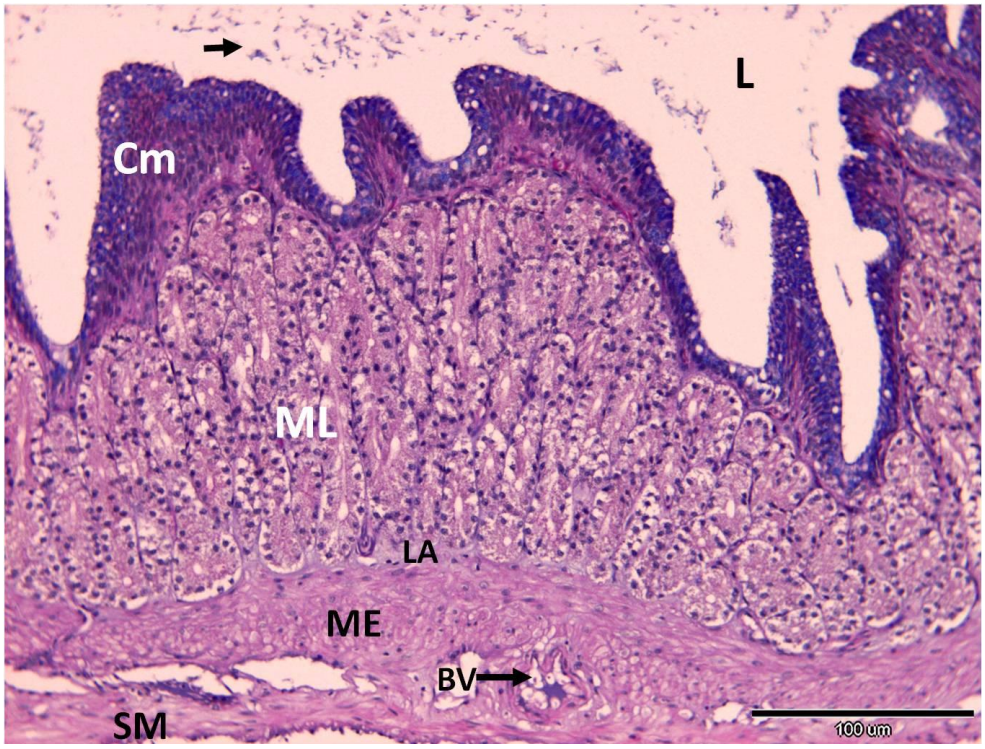

Figure 4.16B. AB-PAS. Higher magnification of Figure 4.16A. mucosa (ML) supported by lamina propria (LA) and dominated by glands. Secretory material (arrow) in the lumen (L). Columnar epithelium (Cm), muscularis externa (ME), serosal membrane (SM), blood vessel (BV).

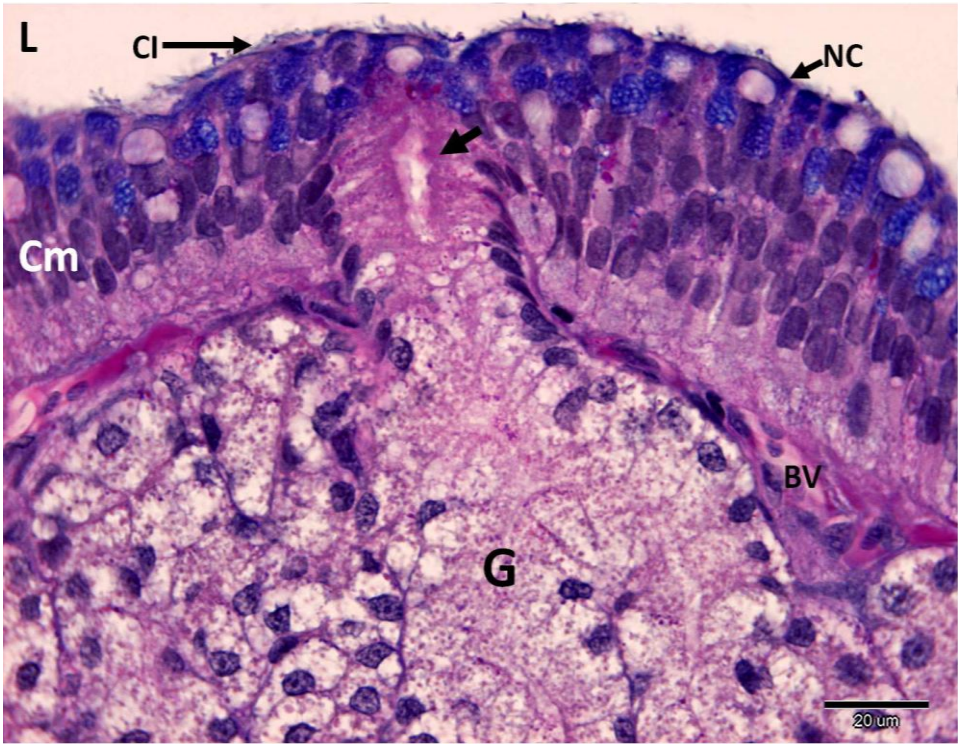

Figure 4.16C. AB-PAS. Higher magnification of Figure 4.16A. Mucosa glands (G) connect to the lumen (L) by their ducts (arrow). Luminal columnar epithelium (Cm) with ciliated (CI) and nonciliated (NC) cells. The epithelium stained strongly for PAS, whereas the glands (G) did not stain with PAS. Mucosal blood vessels (BV) present under the epithelial layer.

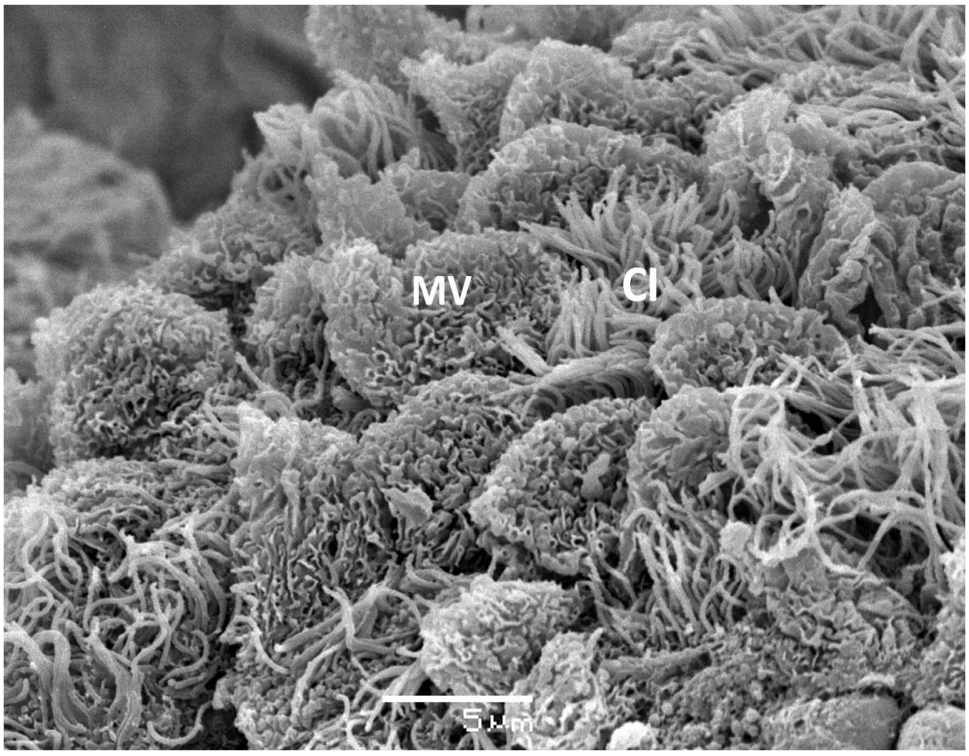

Figure 4.16D. SEM. Surface view of the uterus from the active phase showing ciliated (CI) and microvillous (MV) cells of the epithelium.

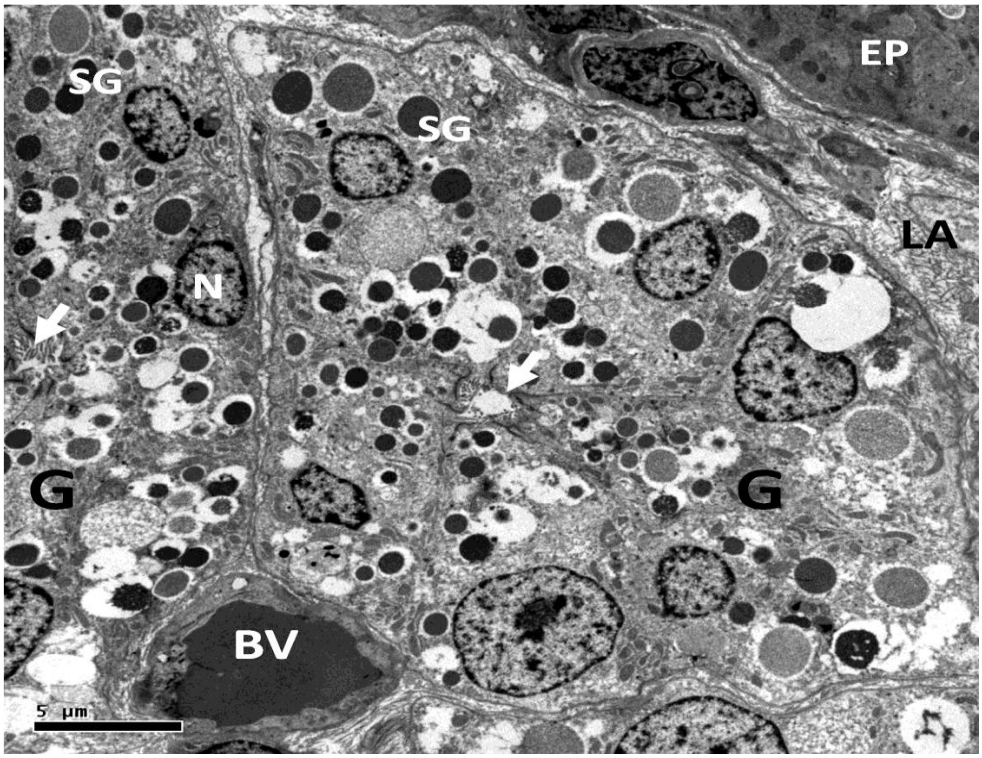

Figure 4.16E. TEM. Uterus from the active phase with mucosal glands (G) containing secretory granules (SG) of varying electron densities. Gland duct lumen (arrow), epithelium (EP), lamina propria (LA), blood vessel (BV).

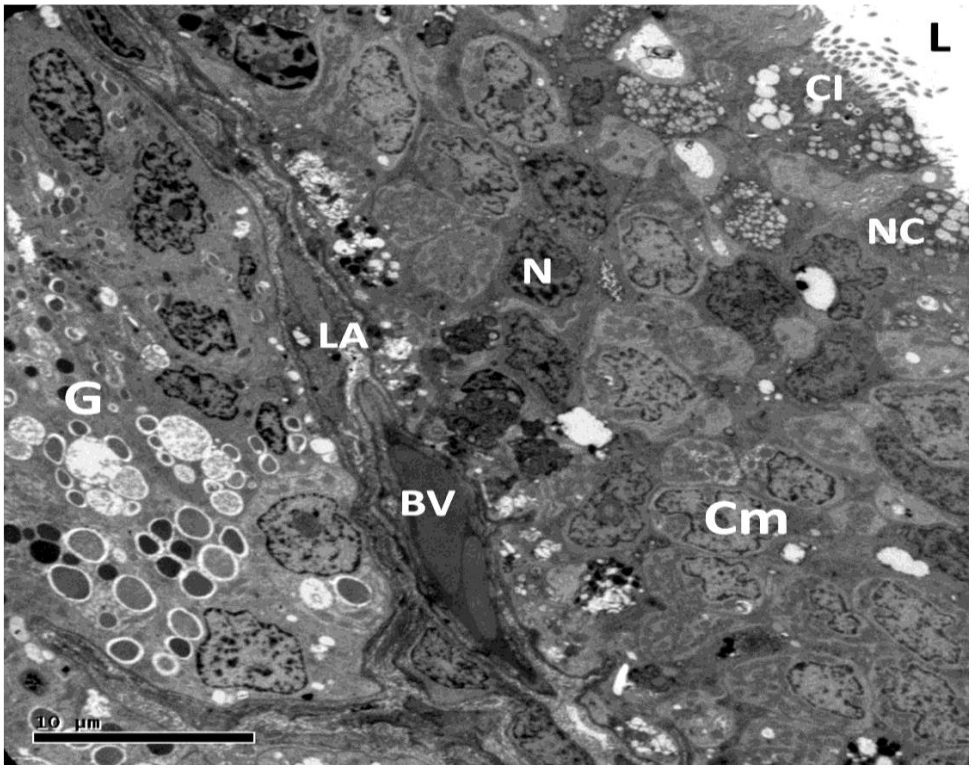

Figure 4.16F. TEM. Uterus from the early active phase showing luminal columnar epithelium (Cm) with ciliated (CI) and nonciliated (NC) cells. Nucleus (N), lamina propria (LA), blood vessel (BV), mucosal glands (G). lumen (L).

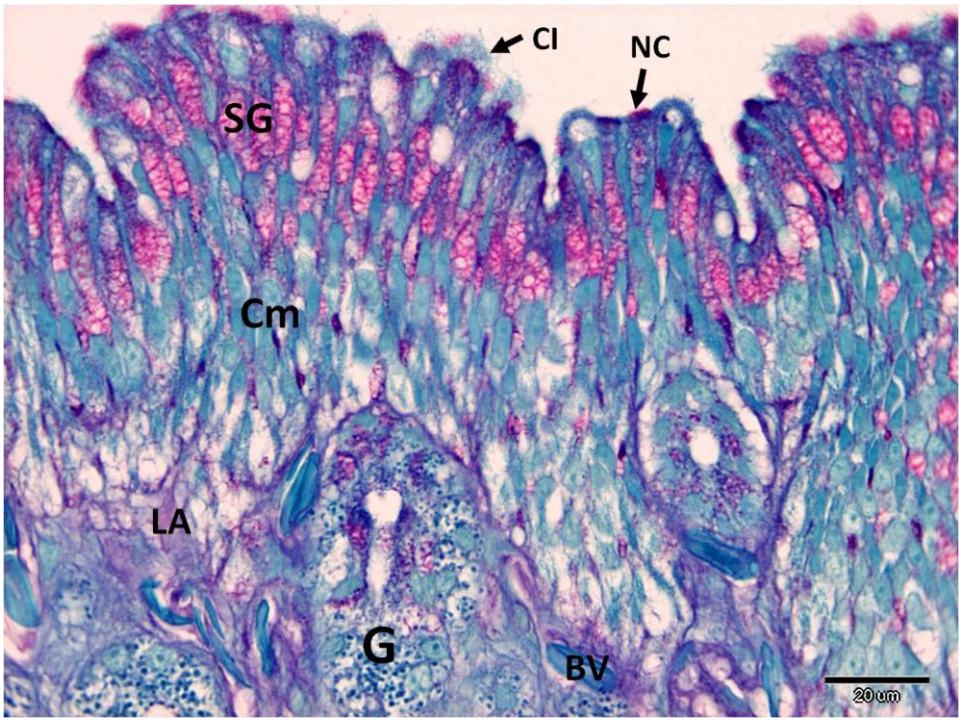

Figure 4.16G. PAS-FG. Uterus from the active phase showing columnar epithelial cells (Cm) with ciliated (CI) and nonciliated (NC) cells. The epithelium stained strongly for PAS, whereas the glands (G) stained negatively with PAS. Nonciliated (NC) cells contained secretory granules (SG). Lamina propria (LA), blood vessel (BV).

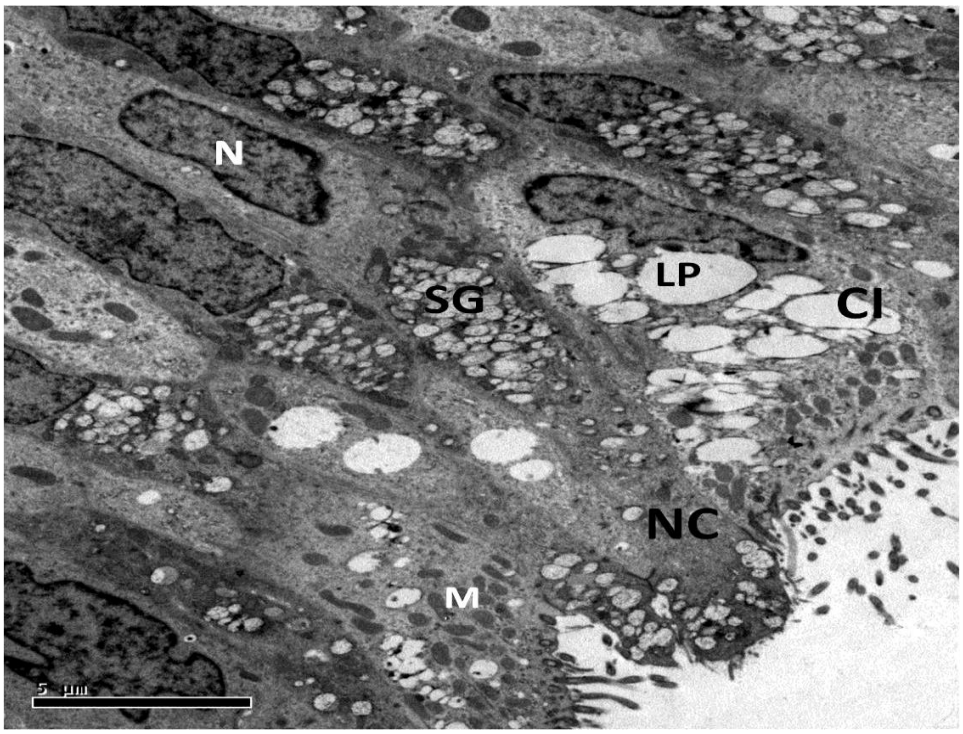

Figure 4.16H. TEM. Uterus from the active phase showing luminal epithelium with ciliated (CI) and nonciliated (NC) cells. Secretory granules seen in the apical regions of the NC cells. Nucleus (N), mitochondria (M), lipid droplets (LP).

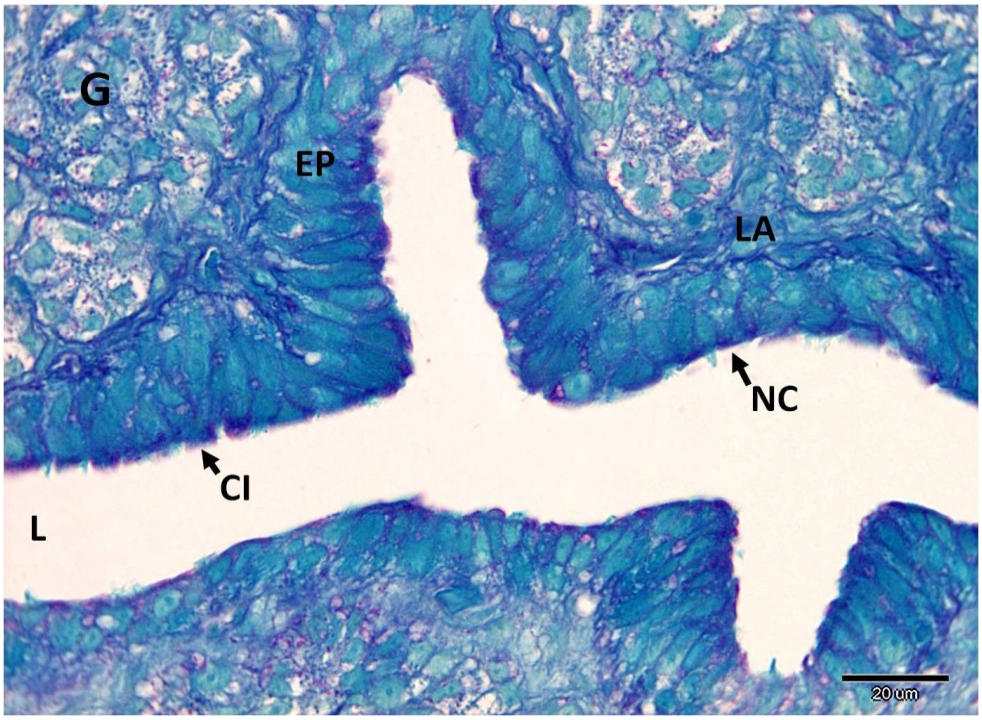

Figure 4.16I. PAS-FG. Uterus from the quiescent phase showing luminal (L) epithelium (EP) with ciliated (CI) and nonciliated (NC) cells, and mucosal glands (G). Both the epithelium and glands stained negatively with PAS. Lamina propria (LA).

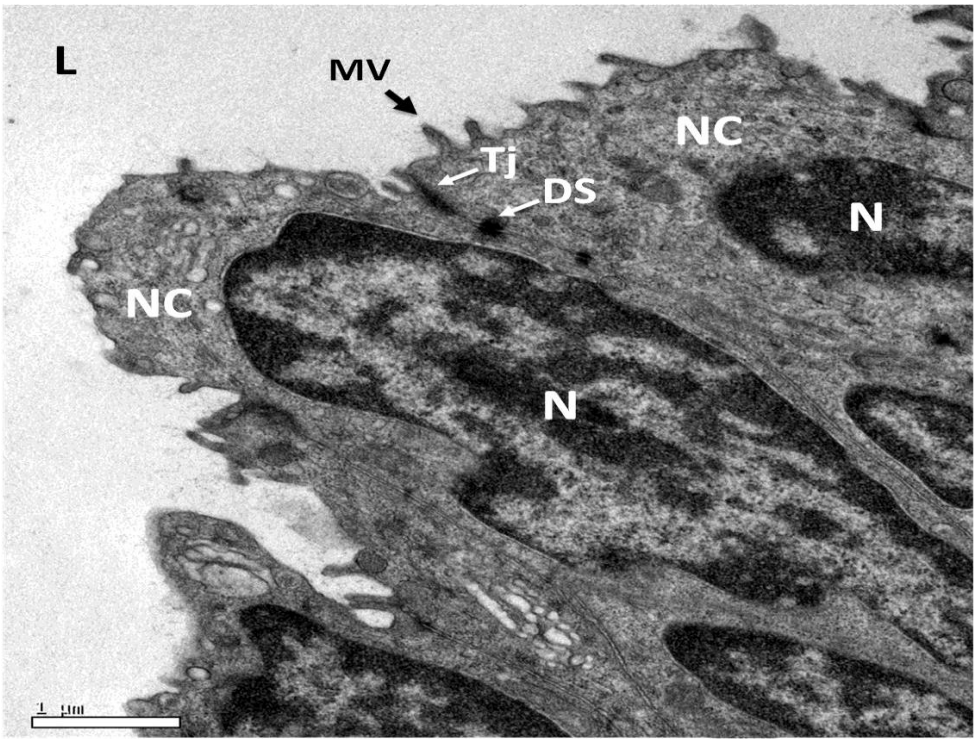

Figure 4.16J. TEM. Uterus from the recrudescent phase showing nonciliated (NC) cells of the luminal epithelium. Nonciliated cells contained no secretory granules in their cytoplasm with few microvilli (MV) on their surfaces. Nucleus (N), lumen (L), tight junctions (Tj), desmosomes (DS).

4.3.10.5 Vagina

The vagina was the most posterior region of the oviduct and is comparatively short (Figures 4.13A, 4.13B & 4.13C). It connects each uterine horn with the cloaca. The vaginal mucosa protruded into the urogenital sinus. The mucosa was surrounded by a thick layer of circular and longitudinal muscle. The mucosa of the vagina was characterized by extremely tall, thin longitudinal folds with secondary branching, which reduced the volume of the lumen. The folds were supported by an extensive nonglandular lamina propria (Figure 4.17A). The mucosa consisted predominantly of epithelial ciliated cells with few noncilliated cells (Figure 4.17B). Epithelial cells were cuboidal to columnar with nuclei situated basally or medially. Nonciliated cells contained secretory granules of varying electron densities, mainly at the apical surface (Figure 4.17C). The nonciliated secretory cells stained positively with PAS (Figure 4.17D). During the early active phase (breeding) a large number of sperm were seen in the lumen of the vagina (Figures 4.17E & 4.17F). Most were present between the folds of the mucosa and were associated with an extracellular matrix. No obvious change in structure was seen in the vagina between vitellogenesis and gravidity.

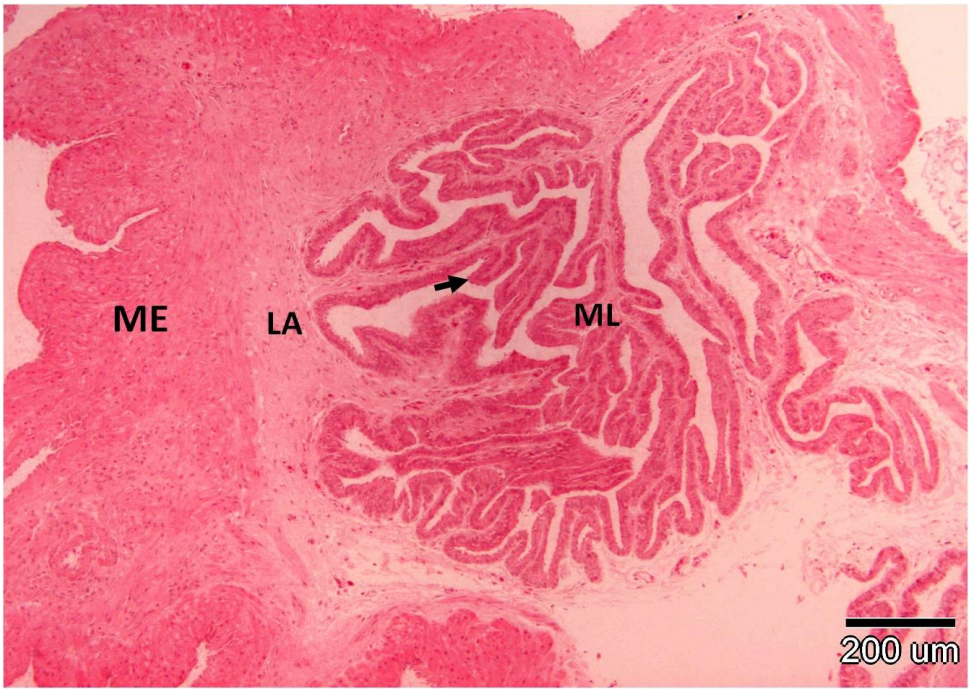

Figure 4.17A. H&E. Vagina from the active phase showing longitudinal mucosa folds (ML) with secondary branching (arrow), supported by lamina propria (LA) and surrounded by thick muscularis externa (ME).

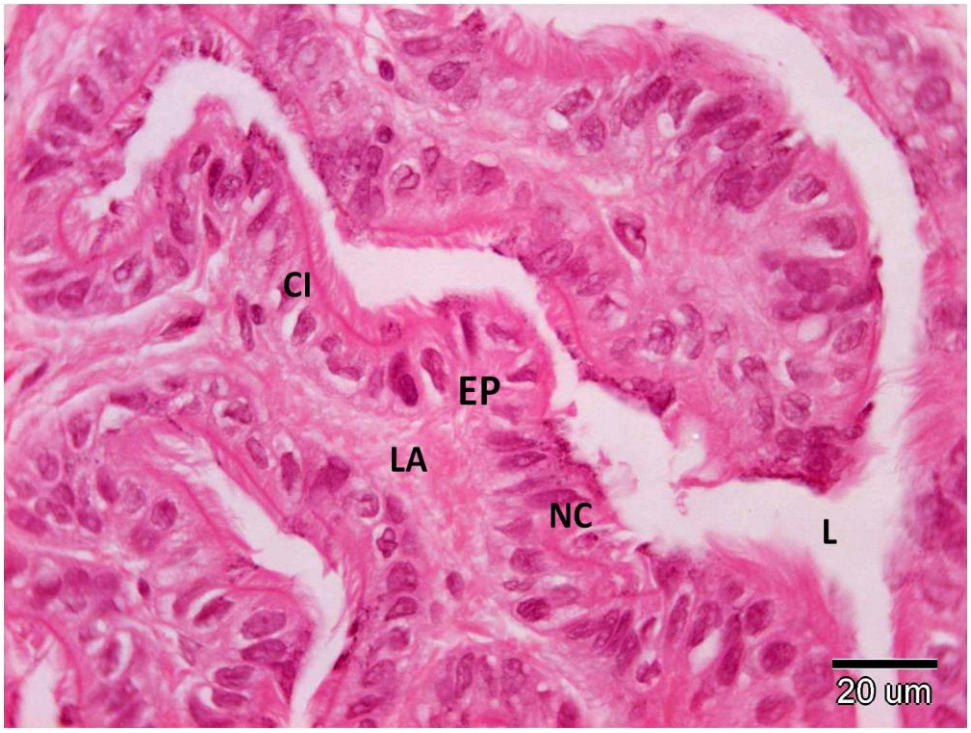

Figure 4.17B. H&E. Higher magnification of Figure 4.17A. Mucosa epithelium (EP) consists predominantly of ciliated (CI) and few nonciliated (NC) cells. Lamina propria (LA), lumen (L).

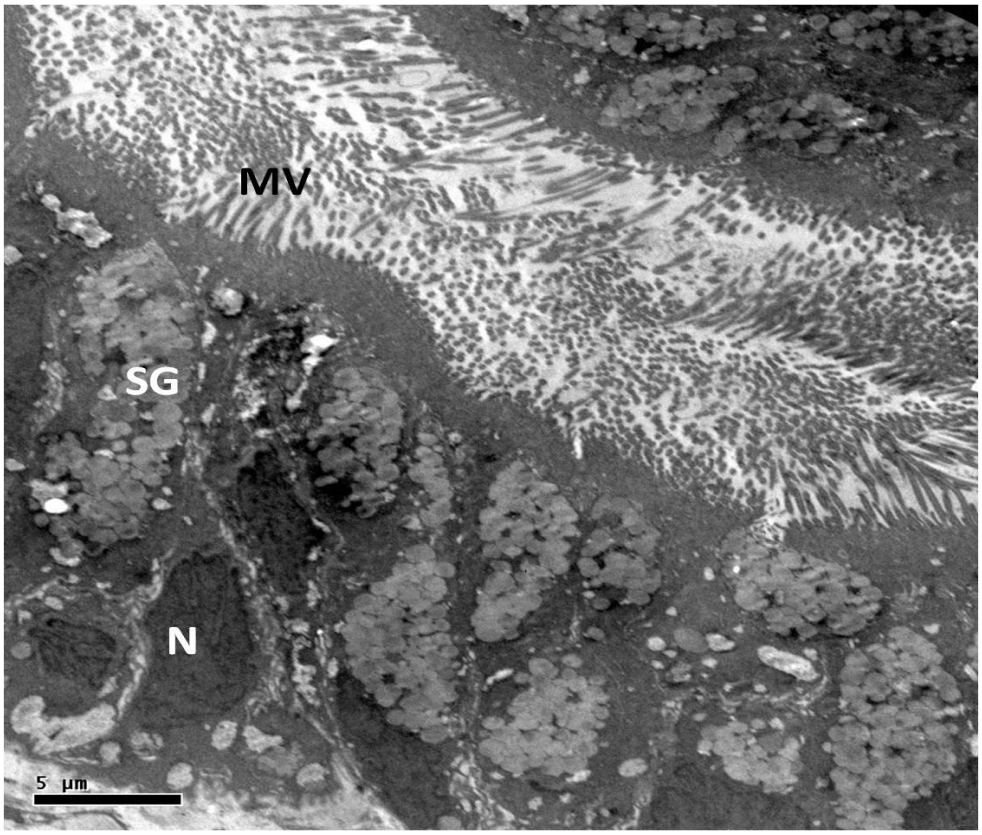

Figure 4.17C. TEM. Vagina from the active phase showing mucosa epithelium with numerous secretory granules (SG). Nucleus (N), microvilli (MV).

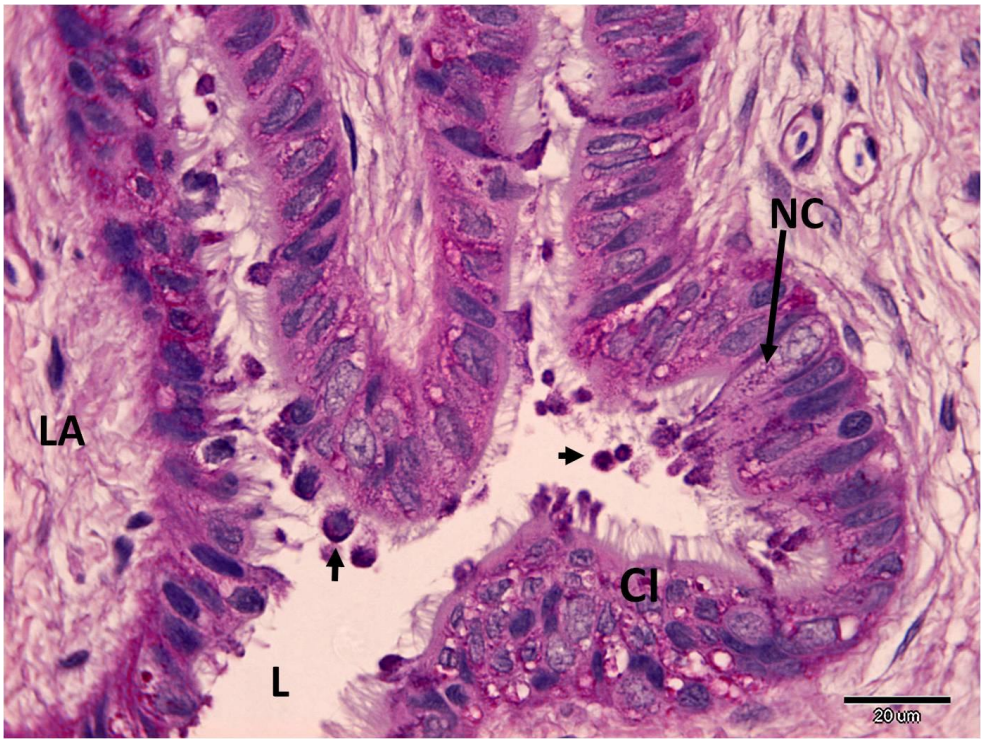

Figure 4.17D. PAS-Haem. Vagina from the active phase showing mucosa with ciliated (CI) and nonciliated (NC) cells. The nonciliated cells (NC) stained positively for PAS and actively producing mucin (arrow) into the lumen (L). Lamina propria (LA).

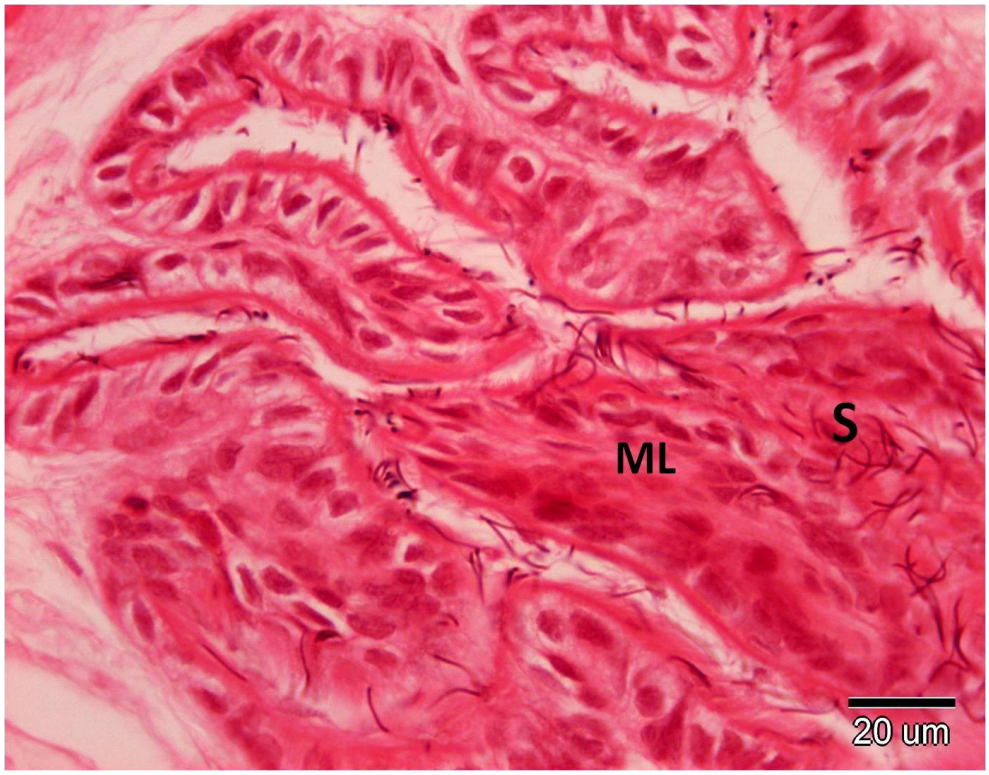

Figure 4.17E. H&E. Vagina from the early active phase showing mucosa folds (ML) with numerous sperm (S) associated with the extracellular matrix.

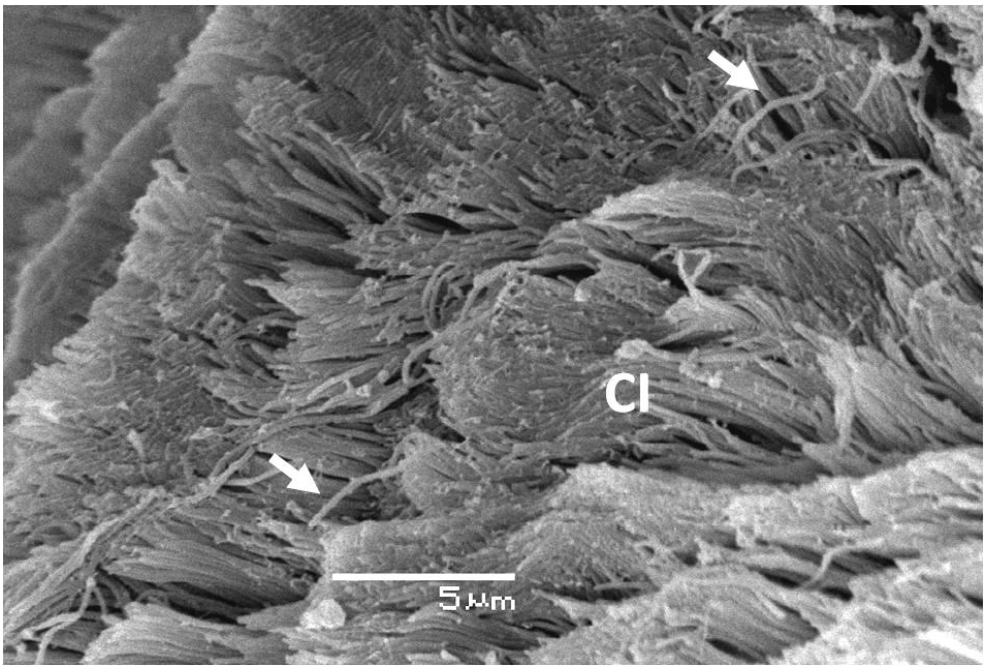

Figure 4.17F. SEM. Vagina from the active phase. Sperm (arrow) adhere to the epithelial cilia (CI).

4.4 Discussion

This investigation is based on a comprehensive study of the female house gecko (*H. flaviviridis*) from a natural population throughout different phases of the reproductive cycle. This study examined the plasma steroid concentrations in relation to the functional, ultrastructural, histological, histochemical, and immunohistochemical changes in the ovary and oviduct throughout the reproductive cycle. Mean sex steroids concentrations were related to the ovarian and oviductal growth and development. The data were based on freshly captured lizards to avoid stress and to ensure that the plasma hormone concentrations were closely related to the natural conditions (Owens and Ruiz, 1980).

The pattern of plasma E_2, P and T concentrations throughout the reproductive season of *H. flaviviridis* were typical of those observed in other lizard species (Jones *et al.*, 1997; Moore *et al.*, 1985; Fox and Guillette, 1987; Carnevali *et al.*, 1991; Diaz *et al.*, 1994; Radder *et al.*, 2001; Lovern, 2011). There was a significant increase in plasma E_2 concentrations during the active phase (January–May) which is essential to the vitellogenic process and follicular growth (Bona-Gallo *et al.*, 1980; Joss, 1985;

Owens and Morris, 1985; Moore and Crews, 1986; Ho, 1987; Nagahama, 1987; Jones *et al.*, 1997; Amey and Whittier, 2000). Plasma E_2 concentrations decreased significantly during the quiescent phase (June–August) coinciding with follicular regression and remained low during the recrudescent phase (September–December).

P appeared to play an important role for the maintenance of egg retention. Plasma P concentrations in *H. flaviviridis* were generally elevated after ovulation (March–May) when CL were active and may function to slow the rate of ovarian development, but activate the formation of eggshell and eggshell membrane and, consequently, delaying ovulation and gravidity (Callard *et al.*, 1972a,b; 1978; 1992; Lewis *et al.*, 1979; Xavier, 1987; Jones and Guillette, 1982; Moore and Crews, 1986; Fox and Guillette, 1987; Jones and Baxter, 1991; Sarkar *et al.*, 1996; Mahmoud and Licht, 1997; Edwards and Jones, 2001a; Shanbhag *et al.*, 2001). It may also influence the rate of development (Gemmell, 1995) or delay gravidity by reducing oviductal contractility (Guillette *et al.*, 1991). Moreover, P plays an important role in egg retention and inhibition of vitellogenesis (Ho *et al.*, 1982; Callard *et al.*, 1992) by inhibiting E_2-stimulated follicular growth.

Plasma P concentrations in *H. flaviviridis* increased during the breeding phase (March–May) and showed a significant rise during April, which coincided with elevated plasma E_2 concentrations. The decline in mean plasma P concentrations was associated with the degeneration of CL after oviposition in May.

T appears to be an important hormone in oviparous reptiles (Owens, 1997; Staub and De Beer, 1997). Elevated plasma T concentrations have been found to be coincident with follicular growth and elevated plasma E_2 concentrations in turtles (Mahmoud and Licht, 1997). In *H. flaviviridis* mean plasma T concentrations were significantly elevated during the breeding phase in April in relation to the elevated plasma E_2, follicular growth, courtship and mating. The presence of T in physiologically relevant concentrations implied a biological function for this hormone beyond its role as a precursor for the synthesis of E_2 (Staub and De Beer, 1997). The profile of plasma T concentrations in female *H. flaviviridis* provided circumstantial evidence that T may be involved in the regulation of vitellogenesis, courtship, and ovulation in this species.

The ultrastructural steroidogenic features in the granulosa cells of *H. flaviviridis* in previtellogenic follicles (June–Augest) were undeveloped and plasma sex hormones concentrations were low. An increase in the ultrastructural steroidogenic features coincided with the rise in plasma steroid concentrations. The increase in RER in the gecko suggests a potential role in hormone receptor synthesis and insertion into the cell membrane (Midgley, 1973). The increase in free ribosomes reflected an enhanced synthesis of proteins for intracellular use, presumably for steroidogenesis (Bjersing, 1967; Cyrus *et al.*, 1978). The appearance of mitochondria with swollen cristae and increased quantity of free ribosomes in the preovulatory follicles was an indication of an increase in the secretion of sex steroids, particularly E_2 and T (Mahmoud and Licht, 1997). These ultrastructural changes, therefore, suggested a direct correlation with steroidogenic activity.

Ultrastructural features of the active steroidogenic cell in CL (March–May), such as abundant SER often found arranged in cisternal whorls and active mitochondria closely associated with lipid droplets found in turtle granulosa lutein cell (Cyrus *et al.*, 1978), were also found in *H. flaviviridis*.

Klicka and Mahmoud (1973) reported that homogenates of active CL from the snapping turtles taken before and after oviposition were capable of converting exogenous cholesterol to P. Turtles with eggs had higher rates of conversion to P than turtles which had already laid their eggs. However, adding pituitary homogenate to the luteal homogenate from turtles that had already laid their eggs significantly increased the rate of conversion.

The luteal P conversion from cholesterol may be related to the presence of enzymatic activities which are necessary for the exogenous cholesterol conversion. Moreover, the addition of pituitary homogenate to the luteal homogenate is a clear indication of the gonadotropin effect on the ovarian steroidogenic stimulation.

Mahmoud *et al.*, (2006) intraperitoneally injected pituitary glands removed from sexually mature female painted turtles (*Chrysemys picta*) into steroidogenically inactive turtles with CL undergoing luteolysis. The luteal granulosa cells developed ultrastructural steroidogenic features 48 hours post-injection and the saline injected controls continued to undergo luteolysis. In addition, plasma P and E_2 concentrations

were significantly higher in the pituitary-injected turtles compared to the controls. These findings offer important information on the direct effect of gonadotropins on the activation of the ovarian ultrastructural steroidogenic tissues in relation to the rise in the ovarian steroid concentrations during the non-reproductive period.

In the oviducts of *H. flaviviridis*, there appeared to be a strong relationship between the high steroid concentrations and the luminal glandular secretion, which coincided with follicular growth. The oviductal secretory activity reached a peak just prior to ovulation and during the egg retention in the uterus. There was a large amount of secretory products on the luminal surface of the uterus, which coincided with the high plasma E_2, P and T concentrations. The steroid concentrations remained in this condition throughout the active phase of the reproductive cycle and dropped sharply in the quiescent phase. Thus, there was convincing evidence that the steroids had some influence on the secretory activity of the oviductal glands during the cycle.

In reptiles there is some evidence to suggest that E_2 may have an important role during vitellogenesis in influencing the development of oviduct in preparation for gravidity (Girling, 2002). In the gecko *H. flaviviridis*, only slight (but significant) oviductal hypertrophy was induced by E_2, but a greater increase in oviductal weight was noted after treatment with T propionate, methyl T, or 19-nortestosterone (Prasad and Sanyal, 1969). T also stimulated some oviductal hypertrophy in the spiny tailed lizard, *Uromastyx hardwickii* (Akhtar, 1988), but not to the same extent as E_2. Since T is a precursor for E_2 synthesis, it may be that localised conversion of plasma T to E_2 within the oviduct may stimulate oviductal development (Guillette *et al.*, 1997). In this study, there was a significant rise in plasma E_2 concentrations during the active phase which coincided with the development of the oviduct and an increase in the glandular secretory activity.

P may also act during oviductal growth. In the viviparous saurian lizard, *Xantusia vigilis*, there was no significant difference in oviductal weight between ovariectomised females treated with vehicle solution and those treated with P (Yaron, 1972). An increase in oviductal weight was seen in ovariectomised females treated with E_2, but this increase was less than in females treated with both E_2 and P. A similar pattern was seen in the garter snake *Thamnophis elegans*, except that P,

administered concurrently with E_2, produced effects no different from those of E_2 alone (Mead *et al.*, 1981). In the whiptail lizard *Sceloporus serrifer* (*cyanogenys*), P administered concurrently with PMSG, prevented the oviductal development seen in females treated with PMSG only (Callard *et al.*, 1972a). In *H. flaviviridis*, plasma P concentrations increased significantly during the active phase, which may be related to oviductal development. P may also have a role in activating the formation of eggshell and eggshell membrane and, consequently, delaying gravidity by reducing oviductal contractility.

Plasma concentrations of T have been measured during the reproductive cycle in females of a few reptilian species. A peak in plasma T concentrations was noted around the time of ovulation in some reptilian species (e.g., Whittier *et al.*, 1987; Guillette *et al.*, 1997; Edwards and Jones, 2001a), whereas, in others T was low or nondetectable over the entire reproductive cycle (Moore *et al.*, 1985; vanWyk, 1994). In this species, a peak in plasma T concentrations was observed during the active phase which may suggest a role in the oviductal development.

In this study, PRs were strongly expressed in the granulosa and theca cells of previtellogenic, vitellogenic follicles and hepatic cells when plasma E_2 concentrations were high. However, in CL P values were high, during luteinisation, where the opposite condition occurred, as PR were weakly expressed in the granulosa and the hepatic cells as with the uterine lining during gravidity.

PRs have been identified in several species of reptiles in association with reproductive organs (*Tracey's script*, Seller and Leavitt, 1991, Kleist-San Francisco and Callard, 1986; *Chelydra serpentina*, Mahmoud *et al.*, 1986; *Chrysemys picta*, Riley *et al.*, 1988; Custodia-Lora and Callard, 2002b ;Custodia-Lora *et al.*, 2004; *Alligator mississippiensis*, Vonier *et al.*, 1997); however, little data has been published on the lizard PR in association with reproductive organs (*Cnemidophorus uniparens*, Young *et al.*, 1994; *Podarcis sicula*, Paolucci and Di Cristo, 2002; *Uromastyx acanthinura*, Hammouche *et al.*, 2007).

PR expression in the theca and follicular cells of the previtellogenic follicles correlated with high plasma E_2 concentrations, but not P, which indicated a paracrine

regulation of P (Hammouche *et al.*, 2007). Furthermore, E_2 is essential for hepatic vitellogenin production. E_2 exerts an autocrine and paracrine action in the previtellogenic follicles.

PRs are necessary for ovulation, *in vitro* and *in vivo* studies showed that the expression of PRs in the granulosa is restricted to preovulatory follicles after the ovulatory discharge (Chandrasekher *et al.*, 1994; Svensson *et al*., 2000; Shao *et al.*, 2003). PR antagonist treatment reduced the level of both PRA and PRB (Shao *et al.*, 2003), activated caspase 3 activity (Svensson *et al*., 2000; Shao *et al.*, 2003) and decreased ovulations (Shao *et al.*, 2003). These results indicate the participation of the two isoforms in the control of ovulation by allowing survival of the granulosa cells. Hammouche *et al*. (2007) reported in the lizard *Uromastyx acanthinura* that PRs were strongly expressed in the follicular cells during previtellogenesis. The immunohistochemical staining for PR was expressed in both the nucleus and cytoplasm of follicular cells and theca cells. In contrast, PR was weakly expressed in vitellogenic follicles, whereas oestrogen receptors (ER) were not expressed. These findings suggested that the main action of E_2 in the ovary is not mediated by ER (Hammouche *et al*., 2007).

The hepatic PRs (PRB) appears to be controlled to some degree by E_2. This PR isoform fluctuates during the annual reproductive cycle in *C. picta*, being most abundantly expressed in the luteal phase, after the high E_2 follicular phase and in the autumn vitellogenic period (Giannoukos and Callard, 1995). Further, E_2 treatment of reproductively inactive turtles can induce PRB expression in the oviduct (Giannoukos and Callard, 1996). The increase in hepatic PRB in the postovulatory period, when P plasma concentrations are high (Giannoukos and Callard, 1995), may be supportive of a role for PRB in the inhibition of vitellogenesis. Paolucci and Di Cristo (2002) reported that PRs are expressed differently in the liver and the oviduct of the lizard, *Podarcis sicula*, throughout the reproductive cycle. PRs may fulfill different requirements in relation to the different physiological functions of tissue during the reproductive cycle. Custodia-Lora *et al*. (2004) found in *Chrysemys picta* that the hepatic PR (PRB:PRA) ratios are markedly changed by E_2 treatment due primarily to a decrease in PRA. The change in the PRB:PRA ratio after hormonal treatment confirmed that P and E_2 exposure will be a determinant in the regulation of

vitellogenesis, and, in turn, the regulation of vitellogenesis will be determined by the ratio of PR isoforms and the physiological concentrations of steroids.

Such fluctuation in PR expression during the reproductive cycle in *H. flaviviridis* is in agreement with previous investigations which concluded that E_2 is an important hormone that stimulates PR (Mahmoud *et al.*, 1986; Giannoukos and Callard, 1995; Custodia-Lora and Callard, 2002a,b).

The positive PR expression, in this study, coincided with the rise in plasma E_2 concentrations and well developed steroidogenic ultrastructural features and the activation of glandular secretion during gravidity.

Moreover, PRs were expressed in the oviduct of *H. flaviviridis* during the active phase, which indicated a role of P in oviductal development. Custodia-Lora and Callard, (2002b) reviewed PRs in liver and reproductive tissue of several reptilian species especially in the turtle *Chrysemys picta*. They reported that the distribution of receptor binding sites in the oviduct were associated with physiological activities such as glandular secretion and contraction during gravidity. In the ovariectomized turtles, ER decreased while PRs increased and ERs were not restored by any steroid regimen.

Several types of stress are known to induce increased corticosteroid secretion which appears to adversely affect gonadal functions, possibly through inhibition of GnRH secretion or by direct effect on gonads in reptiles (Greenberg and Wingfield, 1987; Tokarz and Summers, 2011). Correlative changes between the ovarian and adrenocortical cell activities during the annual reproductive cycle are reported in *C. versicolor* (Vankudre and Shanbhag, 1989). In *M. carinata*, C caused a decrease in the number of oogonia in the germinal bed and primordial follicles in a dose dependent manner (Nijagal and Yajurvedi, 1999). The captured female tuataras, *Sphenodon punctatus*, showed a significant rise in P and T (Cree *et al.*, 1990b). Woodley and Moore (2002) reported that stressed vitellogenic oviparous female tree lizards (*Urosaurus ornatus*) had high plasma C concentrations whereas gravid females did not. Other studies have shown a positive correlation between C and vitellogenesis (Wilson and Wingfield, 1992, 1994; Woodley and Moore, 2002), a negative correlation (Grassman and Crews, 1990), a seasonal change due to reproductive

condition (Whittier *et al.,* 1997), elevation during gravity (Tyrrell and Cree, 1998), or a seasonal change regardless of reproductive condition (Girling and Cree, 1995; Whittier *et al.,* 1987). The role of C in female reptilian reproduction is currently poorly understood but it is obviously complex and variable between species. In *P. barbata (*Amey and Whittier, 2000), the lack of correlation with any reproductive condition or month suggests a lack of involvement in the reproductive process.

In this study, the lizards were sacrificed immediately upon capture and there was only a brief period for the lizards to react to capture and handling. Thus there was no pattern in the plasma C concentrations except for the months of January–March where plasma C concentrations rose slightly. In the house gecko, *H. flaviviridis*, plasma C concentrations remained stable throughout the year and there were no significant variations throughout the year. The stable condition in plasma C concentrations may indicate that capturing the lizards did not cause a significant change in plasma C concentrations. On the other hand, C concentrations were not related to the plasma sex hormones concentrations at any time of the year. This possibly indicates that C may not have a direct effect on the other three hormone concentrations. Girling and Cree (1995) reported no significant relationship between plasma C concentrations and reproductive stages in female common geckos *Hoplodactylus maculates*. In the northern pacific rattlesnake (*Crotalus oreganus*), plasma C concentrations in both sexes were not related either to time of year or to plasma sex hormone concentrations (Lind *et al.,* 2010). In addition, plasma C concentrations remained stable throughout the year with small changes. In this study, there was no significant relation between the haematocrit and plasma C concentrations. Amey and Whittier (2000) reported that in the bearded dragon lizard (*Pogona barbata*), high haematocrit is an indicator of dehydration and may stimulate C secretion. Only three studies have been reported on the effects of C on reproduction within the Gekkonidae (Girling and Cree, 1995; Cree *et al.*, 2003; Preest *et al.*, 2005).

Temperature and other physical factors such as photoperiod (13 hours during the breeding period and 12 hours during the prebreeding period), rainfall and humidity appear not to be important factors in influencing the reproductive events in the female house gecko of Oman (Figures 3.1A, 3.1B, and 3.1C). However, between January and

February there was a decrease in the daily activities when the temperature reached below 20^{o}C.

In this study, females of the oviparous *H. flaviviridis* exhibited a reproductive cycle that was completed within a single active season (January–May). The ovarian follicular cycle began an active phase in late winter with the initiation of vitellogenesis and marked increase in the GSI and relative ovarian weight over the vitellogenic period, which was completed in spring (mid-March and mid-May). Gravidity took place during the active phase in March–April and oviposition occurred late in the active phase (April–May). This type of reproductive cycle followed a similar pattern to those reported in *H. flaviviridis* from different geographical populations in northern India (Sanyal and Prasad, 1967; Varma and Guraya, 1975). In the present study, ovulation occurred during the mating period. Thus, the female reproductive cycle of *H. flaviviridis* is classified as a typical prenuptial (associated) cycle, like other female lizards in temperate zones (Sanyal and Prasad, 1967; Varma and Guraya, 1975; Hikida, 1981; Goldberg and Lowe, 1997; Ikeuchi 2004). Moreover, *H. flaviviridis* ovulates two eggs at a time, one from each ovary. This is followed by a second clutch of two eggs, suggesting that this species laid two clutches of eggs annually, each clutch containing two eggs. In addition, histological and gross morphological examinations of the ovary during April–May showed that there were two sets of CL, a degenerated and freshly formed. This further indicates that the house gecko in Oman has two clutches during the reproductive season. This finding is similar to that reported for the same species in northern India (Varma and Guraya, 1975). The length of gravidity was not recorded in this study due to animals not being kept in captivity. However, *H. flaviviridis* laid eggs between April and May. Sanyal and Prasad (1967) reported that young *H. flaviviridis* hatched during May–June grew rapidly and attained adult length by August– September.

Histological examination of the ovaries revealed that the germinal beds in *H. flaviviridis* were found as a single patch of dorsal epithelium on each ovary. Similar arrangements have been reported in other lizard species (*Calotes versicolor*, Varma, 1970; *Hemidactylus flaviviridis*, Guraya and Varma, 1976; *Elgaria coerulea*, Klosterman, 1983; *Phenacosaurus heterodermus*, Ramírez-Pinilla *et al.*, 1989; *Mabuya brevicollis*, Al-Dokhi, 1998; *Anolis sagrei, A. porcatus*, Sanz-Ochotorena *et*

al., 2001). Jones *et al.* (1982) reported that although the number of germinal beds varies in some families, it may be fixed and species-specific. The number of germinal beds is also related to clutch size regulation. Jones *et al.* (1982) suggested that species with two germinal beds could have a higher instantaneous fecundity than species with only one germinal bed.

The number of germinal cells also varies with the reproductive stage and seasonally in those females with well defined reproductive cycles. Sica *et al.* (2001) found that a seasonal recruitment of oocytes occurs in *Podarcis sicula* and that the control of this recruitment is a diffusible factor (low molecular weight protein) released by the pyriform cells of previtellogenic follicles, whereas FSH has an indirect effect in oogonial proliferation. However, for most squamates the numbers of germinal cells in the germinal beds is not known, nor are the dynamics of oogonial proliferation and oocyte recruitment (Gómez and Ramírez-Pinilla, 2004). Other factors also must be considered in relation to the control of clutch size, e.g., follicular atresia (Andreuccetti *et al.*, 1990). Seasonal mitosis by the oogonia of the germinal bed produces groups of naked oocytes that enter meiotic prophase, thereby giving rise to oocytes needed for folliculogenesis (Jones, 1978; Guraya, 1989). The origin of the follicular cells in reptiles is unknown, but they might possibly arise from the surface epithelium overlying the germinal beds (Guraya, 1989).

Ovarian follicles in *H. flaviviridis* exhibited a sequence of follicular development correlated with the timing of mating, gravidity, and oviposition. The sequence of events is similar in most respects to those previously described for other squamates (Guraya and Varma, 1976; Shine, 1985; Diaz *et al.*, 1994; Ota, 1994; Motta *et al.*, 1995; Uribe *et al.*, 1995; 1996; Huang, 1997; Shanbhag, 2002; Ikeuchi, 2004). The ovarian cycle of *H. flaviviridis* can be divided into early follicular (previtellogenic), vitellogenic, and luteal phases, as reported in other squamates (Graya and Varma, 1976; Fox and Guillette, 1987; Shanbhag and Prasad, 1993; Uribe *et al.*, 1996; Shanbhag *et al.*, 1998; Gómez and Ramírez-Pinilla, 2004; Hernández-Franyutti *et al.*, 2005; Vieira *et al.*, 2010). In *H. flaviviridis* ovaries, the granulosa layer surrounding the oocyte of previtellogenic follicles passes through several morphological changes during successive stages of development. In early previtellogenesis, ovaries contain

small follicles in the earliest stage of development. The oocyte of these follicles is surrounded by a granulosa composed of a monolayered cells and a thin theca layer.

As the follicle grows, the single granulosa layer differentiated into a polymorphic epithelium with three cellular types described as: small, intermediate, and large pyriform cells (Uribe *et al.,* 1995; 1996; Motta *et al.,* 1996; Sanz-Ochotorena *et al.*, 2001; Andreuccetti *et al.,* 2001; Gómez and Ramírez-Pinilla, 2004; Vieira *et al.*, 2010). These cells are in constant communication with each other from the time of formation of the follicle. Thus, the relation of the oocyte to its granulosa cells is considered to be a mutualistic (obligatory) symbiosis (Rothchild, 2003). Small cells differentiated, via intermediate cells, into pyriform cells (Motta *et al.*, 1995). The latter extended from the theca to the zona pellucida (ZP). Small basal cells of the granulosa are suggested to be germinative cells of the follicular epithelium (Filosa *et al.*, 1979; Laughran *et al.,* 1981) from which intermediate and large cells differentiate. Apical small cells that enter lysis losing parts of their apical membrane could be destined to provide material for the zona pellucida and, subsequently, for the ooplasm.

Many of the pyriform cells contain PAS-positive secretory granules similar to those seen in the cortical region of the ooplasm just prior to the onset of vitellogenesis. Several authors have suggested that these cells are related to previtellogenic oocyte growth (Varma, 1970; van Wyk, 1984). Pyriform cells produce cytoplasmic intercellular extensions or bridges by fusing their plasma membrane with that of the oocyte. These bridges are thought to be a pathway through which the pyriform cell provides macromolecules and organelles such as vesicles, Golgi, ribosomal bodies, RNA, and mitochondria to the oocyte of previtellogenic follicle (Motta *et al.*, 1995; 2001). The cytoplasmic components derived from the pyriform and intermediate cells allow the growth of the oocyte at the end of previtellogenesis, just before the dramatic increase of follicular size associated with vitellogenesis. Thus, these cells serve as nurse cells to the developing previtellogenic squamate oocyte. Motta *et al*. (1995) found that intermediate and pyriform cells of the oviparous lizard *Podarcis sicula* are fundamental in the synthesis and transfer of RNA and probably also a great variety of subcellular components through these intercellular bridges. At the onset of vitellogenesis, the cytoplasmic bridges disappear (Etches and Petitte, 1990) and the intermediate and pyriform cells degenerate (Motta *et al.*, 1996), leaving the maturing

follicle with a monomorphic granulosa (Etches and Petitte, 1990; Motta *et al.*, 1995). Motta *et al.* (1996) found that in *Podarcis sicula* intermediate and pyriform cells regress by apoptosis, and that the different cytoplasmic constituents are transferred into the oocyte, while the nuclear remnants are recycled by the small cells that become the only constituents of the follicular epithelium during vitellogenesis.

As in pyriform cells of other lizards (e.g., Klosterman, 1987), the pyriform and intermediate cells of the granulosa layer of *H. flaviviridis* displayed ultrastructural features indicative of synthetic activity, including abundant Golgi complexes, ER, mitochondria, vacuoles, lipid droplets and large euchromatic nuclei. This type of nucleus is associated with a high production of cytoplasmatic materials which could eventually be transferred to the zona pellucida and the oocyte.

Ultrastructural steroidogenic features in the granulosa cells are reported for the first time in this species. The ultrastructural changes in the three types of granulosa cells of the ovarian follicles were related to the increase in the steroidogenic activity of the ovarian follicles. These included ultrastructural steroidogenic characteristics such as an increase in SER, lipid droplets, and the presence of swollen vesiculated mitochondria with tubular cristae. In some cells, SER were formed as a tubular and cisternal SER organized into folded arrays and elaborate concentric whorls which were associated with lipid droplets or mitochondria. Steroidogenic activity in the granulosa was also reported in other lizards, including *H. flaviviridis*, using enzyme histochemical techniques (Gouder and Nadkarni, 1976).

The nucleus of early previtellogenic oocytes of *H. flaviviridis*, similar to other reptiles, displayed morphological changes at the chromosomal level. Diplotene chromosomes were transformed into lampbrush chromosomes, characteristic of the successive stages of growing oocytes. In a wide variety of reptiles, early previtellogenic oocytes show a juxtanuclear aggregation of organelles called Balbiani's vitelline body (Guraya, 1989; Uribe and Guillette, 2000; Calderón *et al.*, 2004; Vieira *et al.*, 2010). This structure was not observed in the early oocytes of *H. flaviviridis*. Balbiani's vitelline body has been described as an ooplasmic region of high metabolic activity involved in the initial accumulation of various molecules and organelles (e.g., RNA, mitochondria, Golgi, endoplasmic reticulum cisternae,

ribosomes and lipid bodies) (Guraya,1989; De Smedt *et al.*, 2000; Jaglarz *et al.*, 2003). These organelles are related to biosynthetic pathways in the cell. Specifically in oocytes, abundance of Golgi complexes and ER cisternae have been associated with the synthesis of macromolecules including acid phosphatases, the main hydrolytic enzymes found in lysosomes, multivesicular bodies and lamellar bodies (Guimaráes and Quagio-Grassiotto, 2005; 2008). This aggregate of organelles disperses to the peripheral cytoplasm of the oocyte in mid and late previtellogenesis. Little is known of the precise function of this structure in reptiles.

Clumps of fibrillar material were observed in the previtellogenic follicles of *H. flaviviridis* which dispersed prior to the onset of vitellogenesis. Similar structures have been reported in the lizard *Ctenosaura pectinata* (Uribe *et al.*, 1996). These might be actin microfilaments accumulated in the cytoplasm that plays a role in the cytokinetic process during cleavage and normal mitosis (Schroeder, 1973). Future studies are required to examine the fibrillar distribution in more details.

In late previtellogenesis, the zona pellucida in *H. flaviviridis* was formed by an outer homogeneous layer and an inner striated layer. This morphology was similar to that reported for other lizards (e.g., *Calotes versicolor,* Varma, 1970; *Sceloporus torquatus,* Uribe *et al.*, 1995; *Ctenosaura pectinata,* Uribe *et al.*, 1996; *Mabuya mabouya,* Gómez and Ramírez-Pinilla, 2004). The striations of the zona radiata correspond to microvilli that originate on the surface of the oocyte and to cytoplasmic extensions of the follicular cells that interdigitate, increasing the absorptive surface of the oocyte and facilitating the transport of nutritive substances from the follicular epithelium to the ooplasm (Guraya, 1978; Laughran *et al.*, 1981). The remarkable increase of the absorptive surface in the oolemma during vitellogenesis was related to the transport of yolk precursors.

Thickening of the theca interna during late previttelogenesis and in vitellogenesis in *H. flaviviridis* might be related to the production of steroid hormones, which is essential for stimulating follicular and oviductal development before ovulation take place. Guraya (1971) reported that the hypertrophied theca interna cells of mammalian preovulatory follicles have been designated as the thecal gland cells which apparently produced E_2. Varma (1970) has also made a similar suggestion

about their function in the lizard *Calotes versicolor*. Gouder and Nadkarni (1976) reported steroidogenic activity in the theca interna of three lizards (*Calotes versicolor, H. flaviviridis, Chamaeleon calcaratus*) using enzyme histochemical techniques. A recent study by Hammouche *et al.* (2007) on the lizard *Uromastyx acanthinura* reported that theca interna cells are involved in steroid hormone production during vitellogenesis.

The ooplasm of previtellogenic follicles of *H. flaviviridis* acquired several small vacuoles that grew and coalesced during vitellogenesis. This ooplasmic vacuolization has been recorded in other reptiles (Hubert, 1985; Uribe *et al.*, 1995; Gómez and Ramírez-Pinilla, 2004). Previous studies have reported that during early vitellogenesis, the first primordial or small yolk spheres developed in these vacuoles consisted of proteid yolk bodies that contained proteins, lipoproteins, triglycerides, and some carbohydrates (Guraya, 1989). Formation of yolk platelets, which marks the onset of vitellogenesis, began during early spring in this species. The proteinaceous component of the yolk was derived primarily from the yolk precursor protein, vitellogenin. Vitellogenin is synthesised in the liver in response to the stimulation of E_2 derived from the growing follicles of the ovary (Ho, 1987). Furthermore, small granular vesicles observed in the periphery of vitellogenic follicles may be associated with vitellogenin uptake. The presence of coated vesicles in the periphery and along the inner surface of the vitellogenic oocyte microvilli is associated with the uptake of vitellogenin from the blood through pinocytocis (Guraya, 1989). Fusion between these vesicles and lysosomes at the microvilli constitute the mechanism by which vitellogenin is hydrolysed to produce yolk platelets, the main source of energy for embryo development (Guraya, 1989). Gómez and Ramírez-Pinilla (2004) reported that in early vitellogenesis of *Mabuya mabouya,* small peripheral granules appeared consisting of mucosubstances that remain in the cortical region until ovulation, which were alos seen in this study. These granules could correspond to the cortical granules found in other squamates (Guraya, 1989). They have been related to the cortical reaction or zone reaction during fertilization in teleosts, amphibians, and mammals (Gilbert, 1997).

The differences in the morphology of yolk platelets during vitellogenesis in *H. flaviviridis* was similar to that reported for other chelonians and squamates, which

corresponds to the role of pinocytotic accumulation of yolk droplets (Guraya and Varma, 1976; van Wyk, 1984; Guraya, 1989; Uribe *et al.*, 1995, 1996, Uribe and Guillette, 2000). At the onset of vitellogenesis, the yolk platelets at the ooplasm periphery were small and spherical. As vitellogenesis progressed, the vacuoles and spherical yolk increased in size and number, and migrated toward the central region of the ooplasm. A region of small platelets remained at the periphery, separated from the central cavity containing enlarged platelets by a homogeneous yolk-free cytoplasmic band. During late vitellogenesis, the yolk platelets showed great diversity in size and in shape. The variation in yolk platelet shape and size suggests that the platelets are formed by different sequestration methods and this diversity may also correspond to vesicles containing different contents (Uribe *et al.*, 1996).

Follicular atresia in *H. flaviviridis* occurred during the processes of follicular organisation in previtellogenic follicles. It also has been reported in other lizards (e.g. *H. flaviviridis*, Guraya and Varma, 1976; *Calotes Versicolor*, Gouder and Rao, 1979, *Gallus domesticus*, Guraya, 1989; Gómez and Ramírez-Pinilla, 2004). Factors related to the formation of follicular atresia and their role in the control of clutch size is still poorly understood. In mammals they have been related to hormonal stimulation (e.g., high concentrations of oestrogens or sharp decreases of gonadotropins; Peters, 1978).

The histological features observed in follicular atresia in *H. flaviviridis* were similar to those described by Guraya (1989) for reptiles, and to those observed in other species of squamates (Guraya and Varma, 1976; Gouder and Rao, 1979; Hubert, 1985; Uribe *et al.*, 1995; Gómez and Ramírez-Pinilla, 2004). The remnants of the atretic follicles are located in the ovarian wall; however, it is difficult to distinguish them from CL during advanced degeneration. Saidapur (1982) also suggested that the two structures could share morphological features.

Follicular atresia was very high in growing follicles and minimal in preovulatory follicles in *H. flaviviridis.* Although atresia occurs in all follicular stages, it is more common in the growing follicles with polymorphic granulosa. It has been noted that atresia also occurs in all follicular types but more frequently in previtellogenic follicles in squamates (Guraya, 1989). In preovulatory ovaries, atresia provides a mechanism for controlling the final number of follicles that ovulate during the process

of follicular selection (Jones *et al.*, 1982; Andreuccetti *et al.*, 1990). Jones and Swain (2000) suggested that there are two possible mechanisms regulating clutch size in squamates, either recruitment (Sinervo and Licht, 1991) or a subsequent atresia (Mèndez de la Cruz *et al.*, 1993). Low rates of atresia at the vitellogenic stages (corpora atretica) also have been documented in other lizard species (Guraya and Varma, 1976; Jones and Swain, 1996; Jones *et al.*, 1997; Gómez and Ramírez-Pinilla, 2004). Thus, as suggested by Jones and Swain (2000) for *Niveoscincus* spp., clutch size is determined early in follicular development. In this study, atresia was mostly constant in all reproductive stages from immature females to gravid females. However, in females with late gravidity, follicular atresia seemed to diminish. These facts could be related with the decline in plasma P concentrations at the end of gravidity, when oviposition occurs. Gouder and Rao (1979) reported that corpora atretica may be an active site of steroidogenesis. The granulosa and theca interna cells in corpora atretica exhibited a brief steroidogenic activity before degeneration. Further studies must be conducted to understand the factors underlying the formation of atretic follicles and their role in the control of clutch size or whether they correspond to an environmentally induced pathology in females of *H. flaviviridis.*

The luteal tissue of the CL in the *H. flaviviridis* ovary is formed only from granulosa cells, similar to those reported in other squamates (Arslan *et al.*, 1978a; Guraya and Varma, 1976; Guillette *et al.*, 1981; van Wyk, 1984; Moore *et al.*, 1985; Fox and Guillette, 1987; Guraya, 1989; Guarino *et al.*, 1998: Shanbhag *et al.*, 2001; Gómez and Ramírez-Pinilla, 2004). The structure of the CL is similar to those of other lizard species (Guraya and Varma, 1976; Guillette *et al.*, 1981; Fox and Guillette, 1987; Xavier, 1987; Guraya, 1989; Gómez and Ramírez-Pinilla, 2004). The changes in the morphology of the CL through gravidity in *H. flaviviridis* were similar to those described in other lizard species (Guraya and Varma, 1976; Guarino *et al.*, 1998). The thecal layers remain distinct and are not hypertrophied to form paraluteal cells. However, the septa of the theca interna along with the blood vessels invade the luteal cell mass which was formed by the luteinisation of granulosa cells.

In addition, the ultrastructural changes in the active granulosa lutein cells of *H. flaviviridis* were related to the increase in the steroidogenic activity of the CL for the production of P during gravidity. These ultrastructural features include abundant SER

often arranged in cisternal whorls and active mitochondria closely associated with lipid droplets. These findings were reported in turtles (*Chelydra serpentina* (Cyrus *et al.*, 1978), *Sternotherus odoratus* (Ba-Omar *et al.*, 2002) and *Chrysemys Picta* (Mahmoud *et al.*, 2006) but have not been previously described in the CL of lizard species.

In different species of squamates, it has been determined that the maximum activity of P secretion is associated with the duration and maintenance of gestation and gravidity (Saidapur, 1982; Xavier, 1987). The lifespan of the CL is variable and depends on the species and on the reproductive mode (Saidapur, 1982; Xavier, 1987; Villagrán-Santa Cruz and Mèndez de la Cruz, 1999). In oviparous and viviparous species, the CL may be active throughout gravidity and gestation or for a variable period after ovulation (Fox, 1977; Saidapur, 1982; Xavier, 1987; Guraya, 1989; Villagrán-Santa Cruz and Mèndez de la Cruz, 1999). In some viviparous species like *Chalcides ocellatus* (Badir, 1968) and *Sceloporus jarrovi* (Guillette *et al.*, 1981), plasma P concentrations remain high or even increase further when the CL degenerate during late gravidity. Thus, it has been suggested that the CL is not the only source of P for maintaining gravidity or gestation, implicating other structures such as the adrenal gland (Guillette and Fox, 1985), atretic follicles (Guraya, 1989), and chorioallantoic placenta (Guillette *et al.*, 1981; Jones *et al.*, 1997; Villagrán-Santa Cruz and Mèndez de la Cruz, 1999).

In this study, the CL appeared to be the major source of P and remained steroidogenically active during the period of egg retention. P was essential for triggering secretory activity as well as keeping the uterus in a quiescent state while the shelling process took place. Just prior to oviposition and around the time the shelling process was completed, the CL underwent degeneration (Mahmoud *et al.*, 1980 in turtle; Guillette and Fox, 1985 in lizards). P is also known to inhibit vitellogenesis (Klicka and Mahmoud, 1977 in turtles). However, soon after the degeneration of the CL, the process of vitellogenesis begins as plasma P concentrations decline. Cuellar (1979) reported that deluteinisation disrupted the shelling process in lizard, *Cnemidopherus uniparens*, which indicates that P may have the same role in the shelling process.

In this study, the oviducts of *H. flaviviridis* exhibited seasonal changes and their enlargement coincided with a gradual increase in the size of the ovaries. During the breeding season (active phase) the oviductal wall was lined by a tall, columnar epithelium which consisted of ciliated and nonciliated cells. The epithelium reacted strongly with PAS indicating that the oviducts of this lizard might be involved in steroid metabolism. In the non-breeding lizards (quiescent and recrudescent phases) the oviduct showed degeneration marked by the reduction in the size and height of the epithelium which reacted negatively with PAS stain.

The oviduct of *H. flaviviridis* can be divided into five regions according to its histological characteristics: infundibulum, uterine tube, isthmus, uterus, and vagina. This is consistent with other studies reported in oviparous geckos (*Hemidactylus flaviviridis* Haider, 1985b; *Tarentola mauritanica*, Picariello *et al.*, 1989; *Hemidactylus turcicus, Saltuarius wyberba*, Girling *et al.*, 1998) and the viviparous geckos (*Hoplodactylus maculates,* Girling *et al.*, 1997; *Hoplodactylus maculatus, Hoplodactylus duvauvelii,* Girling *et al*., 1998). Other gecko species have been reported to have three or four regions (Boyed, 1942; Nogueira *et al.*, 2011).

The lumenal epithelium of the oviduct of *H. flaviviridis*, presented three types of cells: ciliated cells, microvillous nonciliated secretory cells, and occasional bleb-like secretory cells. Bleb cells were found in the infundibulum and uterine tube of *H. flaviviridis*, and have been reported in other reptiles (Palmer and Guillette, 1988, Girling *et al.*, 1997; 1998; AlKindi *et al.*, 2006).

The infundibulum is considered here as a single region of the oviduct, in which anterior and posterior subdivisions can be recognised (following Palmer and Guillette, 1988), rather than two separate oviductal regions. The infundibulum and its ostial opening become greatly enlarged during late vitellogenesis and gravidity. The ostial opening of the anterior infundibulum may envelop the ovaries prior to ovulation, as shown by Cuellar (1970) in the lizard *Cnemidophorus uniparens.* The epithelium of the ostial opening in the infundibulum is predominantly ciliated, presumably to aid transport of the egg into the oviduct (Girling *et al.*, 1997; 1998). The anterior infundibulum of *H. flaviviridis* was non-glandular. This condition was also reported in other reptiles (Palmer *et al.*, 1993, AlKindi *et al.*, 2006). The epithelial cells stained

negatively for PAS and lacked secretory granules as was observed at the ultrastructural level, which may indicate low secretory activity in this portion.

The nonciliated cells in the posterior infundibulum stained positively for PAS and at the ultrastructural level revealed the presence of numerous secretory granules which confirmed secretory activity in these cells. This was also observed in other lizard species (Guillette *et al.*, 1989; Picariello *et al.*, 1989; Girling *et al.*, 1997; 1998). Nonciliated microvillous secretory cells are thought to produce mucus, which is necessary for the lubrication of the oviduct (Aitken and Solomon, 1976) and may be involved in sperm survival (Leese, 1988). In oviparous lizards, deposition of secretory material begins immediately upon entry of the egg into the oviduct (Palmer *et al.*, 1993). It was hypothesised that the secretions may include albumen proteins (Palmer *et al.*, 1993). It may simply be that the secretions may be mucus to aid in transport of the egg down the oviduct (Girling *et al.*, 1997; 1998). Very little is known of the nature of secretions produced by the infundibulum (Girling 2002). The ciliated cells presumably help maintain movement of mucus and cellular debris down the oviduct. They may also act in sperm transport and movement of the ova (Palmer and Guillette, 1988). Endometrial glands were observed at the posterior end in *H. flaviviridis*, and stained negatively for PAS. The function of this region is unclear, but similar to those in birds, it may be involved in the formation of the perivitelline membrane (Aitken, 1971). The function of bleb cells is unknown, but they may be involved in apocrine or merocrine secretory processes (Palmer and Guillette, 1988). The site of fertilization in the reptilian oviduct was suggested to be in the infundibulum, as fertilization should occur before any significant amount of albumen or shell membrane to cover the oocyte plasma membrane (Girling *et al.*, 1997; 1998).

The histological and ultrastructural features of the endometrium in the uterine tube of *H. flaviviridis* resemble those of other reptiles and the avian magnum in being the site for albumen production (Aitken and Solomon, 1976; Palmer and Guillette, 1988, 1990; Perkins and Palmer, 1996; Girling, 2002; AlKindi *et al.*, 2006). In this study, the endometrial glands of the uterine tube increased in size and in secretory activity just before and after ovulation. The secretions made their way into the lumen through the ducts of the endometrial glands. These conditions coincided with elevated plasma steroid concentrations during the onset of the ovarian cycle in the spring. The

longitudinal folds of the mucosa allow for expansion of the tube as the eggs pass through (Palmer and Guillette, 1988). The mucosa was packed with numerous glands that were presumably responsible for albumen production. These glands were branched and tubular in appearance, as reported in other reptiles (Palmer and Guillette, 1988; Girling *et al.*, 2002). The bases of mucosal folds in the posterior uterine tube form glandular crypts (in both oviparous and viviparous species, Girling *et al.*, 2002). Although epithelial cells which line the crypts stain negatively with PAS, gland cells do contain numerous secretory granules (Girling *et al.*, 1998). The glands of the uterine tube are the site for sperm storage for this species.

Nonciliated cells in the uterine tube region reacted strongly to the carbohydrate PAS stain and are therefore probably involved in the synthesis of secretory granules. This was also reported in the wall lizard *Podarcis* (*Lacerta*) *sicula* (Botte, 1973) and the gecko species studied by Girling *et al.* (1998). Most components of albumen were derived from the endometrial glands, but the avidin (a major fraction of the albumen in reptiles and birds) appeared to be secreted by the luminal epithelia (Aitken, 1971; Palmer and Guillette, 1988). The specific role of the bleb cells was unclear, but changes in size and number of these cells during preovulatory and postovulatory period suggested a secretory role. Girling *et al.* (1997) suggested that the bleb cells in the gecko *Hoplodactylus maculatus* might be involved in secretory activity during the egg shelling process. Albumen proteins were produced and secreted by the uterine tube *in vitro* in the turtle *Pseudemys s. scripta* (Palmer and Guillette, 1991). However, the composition, production and function of albumen in reptiles are poorly understood (Palmer and Guillette, 1988), and the function of the uterine tube in squamate reptiles is unknown (Girling *et al.*, 2002). Further studies are needed in these areas.

The isthmus or junction is a short region between the uterine tube and the uterus, and often appears to share similarities with both its neighbouring regions. This region was also noted in other gecko species (Girling *et al.*, 1998). The mucosal glands of the isthmus resembled those near the end, i.e. the uterine tube and uterus. The epithelium of the isthmus stained negatively for PAS, as is the case for the gecko species reported by Girling *et al.* (1998). This may suggest that the isthmus has no function in eggshell formation.

The uterus is the region where eggs are retained until oviposition. The uterus of *H. flaviviridis* undergoes dramatic seasonal changes in epithelial height as well as size and state of activity of the uterine glands, and the thickness of the lamina propria and myometrium. The presence of the yolky egg during gravidity causes the uterus to be highly stretched, in contrast to its thick-walled condition during vitellogenesis. The uterine epithelium of *H. flaviviridis* is lined by columnar ciliated and nonciliated cells, as it is in other oviparous lizards (Guillette *et al.*, 1989; Picariello *et al.*, 1989; Palmer *et al.*, 1993; Perkins and Palmer, 1996; Girling *et al.*, 1997, 1998, 2000; Girling, 2002; Adams *et al.*, 2004; Nogueira *et al.*, 2011). During vitellogenesis, the nonciliated cells stained positively with PAS, and contained numerous secretory granules at the ultrastructural level, suggesting secretory activity in these cells. This is consistent with reports concerning other lizard species (Girling *et al.*, 1997; 1998).

The vitellogenic uterus was greatly thickened by numerous uterine mucosal glands, as observed in other oviparous lizards of the family Gekkonidae (Guillette *et al.*, 1989; Palmer *et al.*, 1993; Girling *et al.*, 1998; Nogueira *et al.*, 2011). The glands reacted negatively to PAS in the vitellogenic period of *H. flaviviridis*, as observed in other gecko species (Girling *et al.*, 1997; 1998; Nogueira *et al.*, 2011). However, in *H. flaviviridis* these glands contained numerous secretory granules. Neutral lipids were found in glands of the oviparous gecko *H. mabouia* (Nogueira *et al.*, 2011) and the snake S. *pygaea* (Sever *et al.*, 2000). The secretory nature of these glands is probably modified in function by small hormonal alterations during the sexual cycle (Nogueira *et al.*, 2011). In oviparous species, the uterus is the region from which the eggshell membranes and calcium for the eggshell are secreted (Aitken and Solomon, 1976). The eggshell fibres are secreted by the uterine mucosal glands (Palmer *et al.*, 1993), and it is hypothesised that the calcium is secreted by the uterine luminal epithelium (Palmer and Guillette, 1988; Guillette *et al.*, 1989; Palmer *et al.*, 1993; Sarker *et al.*, 1995).

The function of the vaginal canal is related to the extensive myometrium which forms a sphincter, as reported for other reptiles (Girling, 2002). This sphincter probably functions in retaining the eggs during gravidity until the time of oviposition. According to Sánchez-Martínez *et al.* (2007), the vagina in squamates does not show consistent differences in its morphology that justify its division into regions, and the

differences are only present in response to sexual cycle phases. The vagina of *H. flaviviridis* had deep longitudinal folds that reduced the luminal volume during vitellogenesis but allowed for expansion during oviposition. It had a thick muscle layer that may act both as a sphincter and, during oviposition help expel the egg. Similar observations were reported in other oviparous lizards of the family Gekkonidae (e.g., Guillette *et al.*, 1989; Girling *et al.*, 1998). The epithelium had numerous cilia, which presumably aided transport of sperm up the oviduct and mucus and cellular debris downward during oviposition. The nonciliated cells stained positively with PAS, and numerous secretory granules presumably produced mucus for lubrication, as well as substances needed to maintain sperm while it was stored, as reported in other gecko species (Girling *et al*., 1998). Large numbers of sperm were seen in the lumen of the vagina of *H. flaviviridis*, which indicated that the vagina is another sperm storage site in this species.

In *H. flaviviridis*, sperm storage sites were found in the vagina and the uterine tube. Sperm storage is a common phenomenon in reptiles and has been reported in many species of lizard (e.g. Adams and Cooper, 1988; Picariello *et al.*, 1989; Murphy-Walker and Haley, 1996; Girling *et al.*, 1997; 1998; Blackburn, 1998; Girling, 2002; Sarkar *et al.*, 2003; Eckstut *et al.*, 2009; Nogueira *et al.*, 2011). Sperm storage may be advantageous because it allows copulation to be separated from fertilization, may reduce the risk of predation by reducing copulation frequency, or act as insurance against not finding a mate due to low densities or slow movement (Girling 2002). The mechanism by which sperm are released from storage sites in the vagina or anterior oviductal regions, along with mechanism and site of fertilization are poorly understood in reptiles (Girling 2002).

In conclusion, this chapter reports the general histology, histochemistry, immunohistochemistry, ultrastucture and hormonal control of the reproductive system in *H. flaviviridis*. The general histology and ultrastructure of the ovary and oviduct of *H. flaviviridis* is similar to that reported for other squamates. *H. flaviviridis* shares a common characteristic with other oviparous squamates in that changes are seen in the ovary and oviduct over the reproductive season with development occurring during vitellogenesis in preparation for gravidity. This study presents the first detailed ultrastructural description of folliculogenesis, steroidogenic ultrastructural features of

the granulosa cells and CL, and ultrastructual decription of the oviduct in *H. flaviviridis*. The relationship between sex hormones, their receptors, and the localization of PRs in the ovary, oviduct and liver have not been studied before in this species. The influence of steroid action on oviductal morphology, protein synthesis, and protein secretion in reptiles is poorly understood and more studies are needed. The present study represents a preliminary step in our understanding of these processes. Expanding our understanding of the regulatory mechanism which controls the timing of protein secretion during the ovarian cycle may help elucidate our understanding of the reproductive potential and the evolution of these processes among oviparous amniotic vertebrates.

Ultrastructural steroidogenic features, such as in granulosa cells and CL, reported in this study highlight the lack of understanding still surrounding the functions and method of action in the combination of tissues that make up the lizard ovary and oviduct. Further studies are needed to address many unknown functions and mechanisms, as mentioned above, related to the development and secretory activity and mode of actions in the different regions, and of the ovary and oviduct.

Chapter Five:

General Discussion

The house gecko *H. flaviviridis* is common in Oman and widely distributed across the country and the Arabian Peninsula. The house gecko was chosen because of its abundance and ease of collection which allowed undertaking a comprehensive experimental programme on freshly captured geckos from a natural population. To my knowledge, to date in Oman or the Arabian Peninsula, there has been no work carried out on this species relative to reproductive physiology and endocrinology.

The objective of this study was to employ a multifaceted approach to examine the hormonal control of reproduction in the oviparous *H. flaviviridis* in relation to physiological and morphological changes. Both male and female reproductive cycles have been characterised with respect to the timing of physiological events. This information was correlated with changes in plasma concentrations of the steroid hormones: E_2, P, and T, and the histological and ultrastructural changes in reproductive tissues. In addition, PRs localisation was investigated to determine the primary targets in these organs. The effect of stress on the circulating steroid hormones and corticosteroids was also addressed in this study (data are summarised in Table 5.1 and Table 5.2). The results are discussed in the context of present knowledge of the morphological and ultrastructural changes and steroid hormone control of reproduction in reptiles.

Male *H. flaviviridis* exhibited an annual reproductive cycle typical of many lizards inhabiting the temperate and subtropical regions. Prenuptial (associated) spermatogenesis commenced in late summer (September) and was completed by early winter (November). Males had a brief quasidormancy period between December–January, before mating which occurred in the breeding season (active phase) in spring (March–April). Plasma T concentrations peaked in the active phase and coincided with the final stages of spermatogenesis, courtship and mating, but started to decline in the second half of the mating period with a drop in the quiescent phase (early summer). This pattern resembles that which was reported in *H. flaviviridis* from different geographical populations in northern India (Sanyal and Prasad, 1967; Varma and Guraya, 1975) and species of lizards with a prenuptial type of spermatogenesis (e.g., Phillips and Millar, 1998; Tokarz *et al.*, 1998; Radder *et al.*, 2001; Hu *et al.*, 2004; Kumar *et al.*, 2011). In addition, *H. flaviviridis* exhibited a typical pattern of plasma T concentrations associated with the development of RSS and the epididymis,

as reported in other lizard species (e.g., Akbarsha and Balasuhramanian, 1983; Haider and Rai, 1987; Nirmal and Rai, 2000; Krohmer, 2004, Sever and Hopkins, 2005). The patterns of plasma T concentrations in *H. flaviviridis* may suggest a role in spermatogenesis and the development of accessory organs in this species. Bhaktaraj *et al.*, (2000) reported that administration of T alone initiated mitotic proliferation of spermatogonial cells in the lizard *Calotes versicolor* during the non-breeding phase. In mice, Johnston *et al.* (2004) reported that T is essential for the proliferation and maturation of Sertoli cells.

Annual plasma E_2 and P concentrations showed similar pattern to that of T. This has also been reported in a few lizard species (e.g. Edwards and Jones, 2001b). Several studies reported that high plasma E_2 concentrations may have a negative effect on spermatogenic activity (Cardone *et al.*, 2002; Bharti *et al.*, 2011). Other studies reported that E_2 induces spermatogonial proliferations via protein kinase in lizard species (Chieffi *et al.*, 2002). In this study, a gradual rise in plasma E_2 concentrations during the recrudescent phase (September-October) may suggest a role in spermatogenesis. However, a significant rise in plasma E_2 concentrations during late active phase (March–April) may have had some effect on the gradual degeneration of spermatogenic activity and the associated significant decrease in plasma T concentrations. The changes observed in plasma P concentrations, in this study, may be related to the conversion of P to other steroids. P may also have a primary role in stimulating reproductive behaviours in males, as P has been shown to stimulate male reproductive behaviour in some lizards (e.g., *Tiliqua nigrolutea*, Edwards and Jones, 2001b).

Immunohistochemical examinations revealed the presence of PR in Sertoli and Leydig cells during the reproductive cycle of *H. flaviviridis*. PRs expressed strongly in Leydig and Sertoli cells throughout the active cycle, but were weak during the quiescent phase. This may suggest hormonal control of the regulation of spermatogenesis in this species. In sperm, P was thought to induce AR expression to initiate the acrosome reaction (Sirivaidyapong *et al.*, 1999). In *H. flaviviridis*, PRs also were strongly expressed in the epididymis during the active phase, but was negatively expressed in the RSS. Expression of PRs in the epididymis of *H. flaviviridis* during the active phase may also suggest a hormonal role in sperm

maturation in the epididymis. Pietrobon *et al*., (2003) reported PR expression in mouse sperm during maturation and capacitation in the epididymis. A recent study by Otsuka *et al.* (2008) also reported PR expression in both testes and epididymis of the turtle *Chelonia mydas*. In these tissues, PRs were expressed in Sertoli, Leydig and germ cells, and in the epithelial cells of the excurrent ducts. These findings suggest that P may play a role in spermatogenesis, sperm transportation, and epithelial cell secretions through PR binding. Prasad and Sanyal (1969) demonstrated that anabolic and androgenic steroids stimulated the development of the RSS in male and female geckos and that E_2 and P had no stimulatory effect.

The findings related to PR expression in male *H. flaviviridis* are the first reported in this species and may provide further information to understanding the role of sex steroid hormones in the control and regulation of reproductive organs in reptiles. In general, few published studies have detailed comprehensively the correlation between plasma steroid hormone concentrations and the timing of reproductive events in male squamate reptiles, thus the information presented in this study may be useful for future research.

In male *H. flaviviridis*, plasma C concentrations remained stable throughout the year and there were no significant variations throughout the year. The stable condition in plasma C concentrations may indicate that capturing the lizards did not cause a significant change in plasma C concentrations. On the other hand, plasma C concentrations were not related to the plasma sex hormones concentrations at any time of the year. This may indicate that C may not have a direct effect on the plasma sex hormone concentrations. This condition was also similar for the female *H. flaviviridis* in this study.

Leydig and Sertoli cells of *H. flaviviridis* showed steroidogenic ultrastructural features characteristic of steroidogenic activity at different phases of the testicular cycle similar to those reported in other reptiles (e.g., Mahmoud *et al.*, 1985a; Dubois *et al.*, 1988; Mahmoud and Licht, 1997; Khan and Rai, 2004; Boretto *et al.*, 2010). These specialised steroid synthesising cell organelles or features include; extensively developed arrays or concentrations of SER, large mitochondria with tubular cristae, and lipid droplets. Evidence of temporal separation of function in the two cells was

also based on the asynchronous changes in the ultrastructure steroidogenic feature. The present study indicated that Leydig cells were partially active during the non-reproductive period (June–August) prior to spermatogenesis, associated with partial development of ultrastructural steroidogenic features, low plasma steroid concentrations and weak PR expression. In addition, accumulations of sudanophilic lipid droplets were observed in seminiferous tubules as well as in Leydig cells which indicated low steroidogenic activity in the Leydig cells during the non-reproductive period (quiescent phase).

The Leydig cells began to increase their steroidogenic activities at the onset of spermatogenesis, in September, in synchrony with the increase in the ultrastructural steroidogenic features, rise in plasma steroid concentrations, presence of sudanophilic lipids material, and strong expression for PR. Leydig cells remained active for the rest of the reproductive cycle. The ultrastructural steroidogenic features and the presence of sudanophilic lipids material in Sertoli cells began to develop in October and, like the Leydig cells, they remained active for the rest of the cycle. This is consistent with the concept of a temporal separation of androgen secretion and spermatogenesis (reviewed by Licht, 1982). The rise in plasma steroid concentrations associated with the steroidogenic activity of both cells also coincided with courtship, mating and the migration of sperm from seminiferous tubules to the epididymis for maturation.

Very few published studies have comprehensively detailed the correlations between plasma steroid hormone concentrations, steroidogenic ultrastructural changes and localisation of PRs in reproductive organs of male squamate reptiles. Thus, the changes in ultrastructural steroidogenic features in Sertoli and Leydig cells during the different phases of the reproductive cycle of *H. flaviviridis* provided further evidence for the role of these cells in regulating spermatogenesis and production of sex steroid hormones. Typically, the changes in these features were in synchrony with changes in plasma hormonal concentrations and PR expression during this study, suggesting that both cell types played major roles in hormone secretions and proliferation of spermatogonial cells.

The testicular organisation and germ cell development strategies in *H. flaviviridis* were similar to that reported in other lizard species (e.g., Gribbins and Gist, 2003; Rheubert *et al.*, 2009) in which a temporal germ cell development strategy is employed during spermatogenesis. Squamate reptiles including *H. flaviviridis* have a more temporal germ cell development, where germ cell generations move and complete the stages of spermatogenesis as a single cohort during the reproductively active months. In the house gecko, *H. flaviviridis*, spermatogonia were present throughout the entire year in close association with basally located Sertoli cell nuclei. Spermatogenesis occurred once every year with similar mitotic and meiotic activity for every cycle. Spermiogenesis climaxed during the active phase and major spermiation events occurred during this phase, leading to a single burst of spermatozoa release.

The ultrastructure of the spermatozoa of *H. flaviviridis* corresponded well to that of other gekkonidae species and in main parts to that of other squamate lizards (e.g., Teixeira *et al.*, 2002; Vieira *et al.*, 2004; Gribbins *et al.*, 2007; Rheubert *et al.*, 2010a; 2011a). The spermatozoa of *H. flaviviridis* exhibited the following ultrastructural characteristics: acrosomal complex consisting of acrosome and subacrosomal cone, acrosome vesicle divided into medulla and cortex, apical portion of acrosome was depressed; single prenuclear perforatorium positioned at the centre of the flattened acrosome, proximal centrioles, short distal centrioles, peripheral fibres of the distal centrioles and axoneme, short nuclear rostrum, nucleus narrow basally, midpiece short and fibrous sheath extending into midpiece, annulus, mitochondria columnar, dense bodies solid, in regular and complete rings, juxtaposed to the fibrous sheath, ring structures of dense bodies separated by mitochondrial tiers; and thick zone of cytoplasm between plasma membrane; fibrous sheath in the anterior portion of principal piece, and axoneme extending throughout the flagellum. This study has revealed for the first time detailed ultrastructural description of *H. flaviviridis* spermatogenesis. This work may contribute toward the confirmation of a close phylogenetic relationship between the species of this genus.

Histologically, the ductus epididymidis of *H. flaviviridis* can be divided into anterior, middle, and posterior regions. This is consistent with other studies reported in male *H. flaviviridis* from India (Haider and Rai, 1987; Nirmal and Rai, 2000). During the

active phase the epithelial cell height and lumen diameter of all the regions of the ductus epididymis were significantly increased and the cells of the anterior and middle regions were filled with PAS-positive secretory granules. In this study, the anterior and middle regions of the ductus epididymis were involved in the maturation and preparation of spermatozoa for storage, and protein secretion as PR were strongly expressed during the spermiation process. The posterior region of the ductus epididymis was involved in sperm storage where sperm transit was slowed by the occlusion of the end of the collapsed ductus deferens as is the case in other lizards (e.g., Haider and Rai, 1987; Akbarsha *et al.*, 2006). The anterior and middle regions secrete glycoproteins as discrete biphasic granules which contribute to the physiological maturation of spermatozoa (e.g., Morel *et al.*, 2000; Nirmal and Rai, 2000) Moreover, the epithelium of the ductus epididymis of *H. flaviviridis* is lined by only two types of cells, principal/secretory and basal/nonsecretory, as reported in several lizard species (e.g., Mesure *et al*. 1991; Desantis *et al*. 2002). Some lizard species were reported to have up to six types of cells (Akbarsha *et al.*, 2006).

The secretory cells of the epididymis undergo an annual cycle, in which numerous organelles such as vesiculated mitochondria, RER and Golgi complexes contribute to the secretory granules synthesis of various densities before being discharged into the lumen which contributes to the maturation of spermatozoa in the active phase. The epididymal secretion of proteins in the form of discrete and structured granules is already known in several lizard species (e.g., Akbarsha and Manimekalai 1999; Desantis *et al*. 2002; Akbarsha *et al.*, 2006). The present study confirms epididymal secretion in the form of discrete granules similar to these lizard species. This study describes in detail for the first time the ultrastructure of epididymal epithelial cells during the male active reproductive cycle.

Hypertrophy and recrudescence of *H. flaviviridis* RSS were in synchrony with androgen secretion and spermatogenic activity, similar to those reported in other squamates (e.g., Weil, 1984; Krohmer, 2004, Sever and Hopkins, 2005). Hypertrophied RSS have often been used as indicators of breeding because they have been implicated in seminal fluid production (Prasad and Reddy, 1972). Furthermore, the secretions from the RSS were PAS-positive and contained phospholipids, proteins and amino acids which are known to be androgen dependent and may serve as a

source of energy for survival of spermatozoa in the oviduct (e.g., Sarkar and Shivanandappa, 1989; Sever *et al.*, 2002; Sever and Hopkins, 2005). This study describes in detail the seasonal ultrastructural changes in the RSS during the reproductive cycle, which have not been reported before in this species. Similar studies on ultrastructural details have also been reported in the gecko, *H. turcicus* (Rheubert *et al.*, 2011b) and other squamates (Sever *et al.*, 2008; Siegel *et al.*, 2009a). The function of the RSS is still not clearly understood. Very few studies have been published on the ultrastructure of RSS. According to Rheubert *et al.* (2011b) only five ultrastructural studies on the RSS have been reported on lizard species. The present study reported seasonal variation at the light and electron microscopy level and the potential effect of steroid hormones on the secretory activity of the RSS in *H. flaviviridis*. This study provides comparative data that expands our knowledge of the ultrastructural variation of the RSS in relation to hormonal control in male squamates, and is the first study to examine this relationship in natural population of lizards collected throughout the entire reproductive cycle.

Females of the oviparous *H. flaviviridis* exhibited a reproductive cycle that was completed within a single active season (January–May). The ovarian follicular cycle began an early active phase in early spring with the initiation of vitellogenesis and marked increase in the GSI and relative ovarian weight over the vitellogenic period, which was completed in spring (mid-March – mid-May). Gravidity took place during the active phase in March–April and oviposition occurred late in the active phase (April–May). This type of reproductive cycle followed a pattern similar to *H. flaviviridis* in northern India (Sanyal and Prasad, 1967; Varma and Guraya, 1975). In the present study, ovulation occurred during the mating period. Thus, the female reproductive cycle of *H. flaviviridis* is classified as a typical prenuptial (associated) cycle, like other female lizards in temperate zones (e.g., Goldberg and Lowe, 1997; Ikeuchi 2004). Moreover, *H. flaviviridis* ovulates two eggs at a time, one from each ovary. This is followed by a second clutch of two eggs, suggesting that this species laid two clutches of eggs annually, each clutch containing two eggs. In addition, histological and gross morphological examinations of the ovary during April–May showed that there were two sets of CL, degenerated and freshly formed. This further indicated that *H. flaviviridis* in Oman had two clutches during the reproductive

season. The length of gravidity was not recorded in this study due to animals not being kept in captivity. However, *H. flaviviridis* laid eggs between April and May.

The pattern of plasma E_2, P and T concentrations throughout the reproductive season of *H. flaviviridis* were typical of those observed in other lizard species (e.g., Carnevali *et al.*, 1991; Diaz *et al.*, 1994; Radder *et al.*, 2001; Lovern, 2011). Increasing plasma E_2 concentrations were detected during the vitellogenic period in the active phase, but started to decline after ovulation and mating, as was also reported in other lizard species (e.g., Nagahama, 1987; Jones *et al.*, 1997; Amey and Whittier, 2000). Plasma E_2 concentrations decreased significantly during the quiescent phase (June–August), coinciding with follicular regression and remaining low during the recrudescent phase (September–December). In *H. flaviviridis* mean plasma T concentrations were significantly elevated during the breeding season in April in relation to the elevated plasma E_2 concentrations, follicular growth, courtship and mating. The profile of plasma T concentrations provided circumstantial evidence that T may be involved in the regulation of vitellogenesis, courtship, and ovulation in this species. Similar findings were also reported in other reptiles (e.g., Owens, 1997; Staub and De Beer, 1997; Mahmoud and Licht, 1997).

Mean plasma P concentrations in *H. flaviviridis* increased during the breeding season (March–May) and showed a significant rise during April, which coincided with elevated plasma E_2 concentrations, and when CL were active. P may function to slow the rate of ovarian development, but activate the formation of eggshell and eggshell membrane and, consequently, delay the ovulation (e.g., Callard *et al.*, 1992; Sarkar *et al.*, 1996; Mahmoud and Licht, 1997; Shanbhag *et al.*, 2001). It may also influence the rate of development (Gemmell, 1995) or delay gravidity by reducing oviductal contractility (Guillette *et al.*, 1991). Moreover, P plays an important role in egg retention and inhibition of vitellogenesis (Ho *et al.*, 1982; Callard *et al.*, 1992) by inhibiting E_2-stimulated follicular growth. The decline in mean plasma P concentrations in this study was associated with the degeneration of CL after oviposition in May.

In the oviducts of *H. flaviviridis*, there appeared to be a strong relationship between the high plasma sex steroid concentrations and luminal glandular secretion, which

coincided with follicular growth, similar to that reported in other reptiles (e.g., Blackburn, 1998; Girling; 2002; AlKindi *et al.*, 2006). The oviductal secretory activity peaked just prior to ovulation and during the egg retention in the uterus. There was a large amount of secretory products on the luminal surface of the uterus, which coincided with the high plasma E_2, P and T concentrations. The plasma sex steroid concentrations remained elevated throughout the active phase of the reproductive cycle and dropped sharply in the quiescent phase. Thus, there was convincing evidence that the steroids had some influence on the secretory activity of the oviductal glands during the cycle.

In this study, PRs were strongly expressed in the granulosa and theca cells of pre-vitellogenic, vitellogenic follicles and hepatic cells when plasma E_2 concentrations were high. However, plasma P concentrations were high, during luteinisation, where the opposite condition occurred, as PR were weakly expressed in the granulosa and the hepatic cells as with the uterine lining during gravidity. Such fluctuation in PR expression during the reproductive cycle in *H. flaviviridis* is in agreement with previous investigations which concluded that E_2 is an important hormone that stimulates PR (Mahmoud *et al.*, 1986; Giannoukos and Callard, 1995; Custodia-Lora and Callard, 2002a). Moreover, PRs were expressed in the oviduct during the active phase. Custodia-Lora and Callard, (2002a) reported that the distribution of receptor binding sites in the oviduct were associated with physiological activities such as glandular secretion and contraction during gravidity. The relationship between PR expression and sex steroid hormone regulation during the reproductive cycle of *H. flaviviridis* was first reported for this species in this study, which may provide further evidence for the hormonal control of follicular and oviductal development.

The ultrastructural steroidogenic features in the granulosa cells of *H. flaviviridis* in previtellogenic follicles (June–August), such as an increase in SER, lipid droplets, the presence of swollen vesiculated mitochondria with tubular cristae, and numerous free ribosomes, were undeveloped and the plasma sex hormone concentrations were low. Increase in the ultrastructural steroidogenic features coincided with the rise in plasma steroid concentrations. The increase in RER suggests a potential role in hormone receptor synthesis and insertion into the cell membrane (Midgley, 1973). The increase in free ribosomes reflected an enhanced synthesis of proteins for intracellular use,

presumably for steroidogenesis (Bjersing, 1967; Cyrus *et al.*, 1978). The appearance of mitochondria with swollen cristae and increased quantity of free ribosomes in the preovulatory follicles was an indication of an increase in the secretion of sex steroids, particularly E_2 and T (Mahmoud and Licht, 1997). These ultrastructural changes, therefore, suggested a direct correlation with steroidogenic activity. These findings are reported for the first time in *H. flaviviridis* and in lizard species, and may contribute to understating the modes of hormone secretions.

Ultrastructural features of the active steroidogenic lutein cell in CL found in *H. flaviviridis* (March–May), such as abundant SER often found arranged in cisternal whorls and active mitochondria closely associated with lipid droplets were similar to those reported in turtle granulosa lutein cells (Cyrus *et al.*, 1978). Active CLs are known to produce P under the control of gonadotropins which stimulated ovarian steroidogenesis (Klicka and Mahmoud, 1973; Mahmoud *et al.*, 2006). In this study, mean plasma P concentrations were elevated during the breeding season coinciding with the developed ultrastructural steroidogenic features in the lutein granulosa cells of the CL. These findings offer important information on the relationship between ultrastructural changes and hormone secretion, and provide further evidence on the direct effect of gonadotropins of the activation of the ovarian ultrastructural steroidogenic tissues. These findings have not been previously described in the CL of lizard species.

Histological examination of the ovaries revealed that the germinal beds in *H. flaviviridis* were found as a single patch of dorsal epithelium on each ovary. Similar arrangements have been reported in other squamate species (e.g., Klosterman, 1983; Ramírez-Pinilla *et al.*, 1989; Sanz-Ochotorena *et al.*, 2001). Jones *et al.* (1982) reported that although the number of germinal beds varies in some families, it may be fixed and species-specific. The number of germinal beds is also related to clutch size regulation. Jones *et al.* (1982) suggested that species with two germinal beds could have a higher instantaneous fecundity than species with only one germinal bed. The number of germinal cells also varies with the reproductive stage and seasonally in those females with well defined reproductive cycles. However, for most squamates the numbers of germinal cells in the germinal beds is not known, nor are the dynamics of oogonial proliferation and oocyte recruitment (Gómez and Ramírez-Pinilla, 2004).

Seasonal mitosis by the oogonia of the germinal bed produces groups of naked oocytes that enter meiotic prophase, thereby giving rise to oocytes needed for folliculogenesis (Jones, 1978; Guraya, 1989). The origin of the follicular cells in reptiles is unknown, but they might arise from the surface epithelium overlying the germinal beds (Guraya, 1989).

Ovarian follicles in *H. flaviviridis* exhibited a sequence of follicular development correlated with the timing of mating, gravidity, and oviposition. The sequence of events is similar in most respects to those previously described for other squamates (e.g., Motta *et al.*, 1995; Uribe *et al*., 1996; Shanbhag, 2002; Ikeuchi, 2004). The ovarian cycle of *H. flaviviridis* can be divided into early follicular (previtellogenic), vitellogenic, and luteal phases, as reported in other squamates (e.g., Shanbhag *et al*., 1998; Gómez and Ramírez-Pinilla, 2004; Vieira *et al.*, 2010).

During previtellogenesis in *H. flaviviridis*, the single granulosa layer differentiated into a polymorphic epithelium with three cellular types described as: small, intermediate, and large pyriform cells, as reported in other lizard species (e.g., Uribe *et al.*, 1996; Motta *et al.*, 1996; Andreuccetti *et al.*, 2001; Gómez and Ramírez-Pinilla, 2004; Vieira *et al.*, 2010). Many of the pyriform cells in the follicles of *H. flaviviridis* contained PAS-positive secretory granules similar to those seen in the cortical region of the ooplasm just prior to the onset of vitellogenesis. Several authors have suggested that these cells are related to previtellogenic oocyte growth (e.g., van Wyk, 1984). Pyriform cells produce cytoplasmic intercellular extensions which are thought to be a pathway through which the pyriform cell provides macromolecules and organelles such as vesicles, Golgi, ribosomal bodies, RNA, and mitochondria to the oocyte of previtellogenic follicles (e.g., Motta *et al.*, 1995; 2001). As in pyriform cells of other lizards (e.g., Klosterman, 1987), the pyriform and intermediate cells of the granulosa layer of *H. flaviviridis* displayed ultrastructural features indicative of synthetic activity, including abundant Golgi complexes, ER, mitochondria, vacuoles, lipid droplets and large euchromatic nuclei.

Furthermore, ultrastructural changes in the three types of granulosa cells (small, intermediate, and pyriform) of the ovarian follicles found in *H. flaviviridis* were related to the increase in the steroidogenic activity of the ovarian follicles. These

included ultrastructural steroidogenic characteristics such as an increase in SER, lipid droplets, and the presence of swollen vesiculated mitochondria with tubular cristae. In some cells, SER were formed as a tubular and cisternal SER organized into folded arrays and elaborate concentric whorls which were associated with lipid droplets or mitochondria. Steroidogenic activity in the granulosa was also reported in *H. flaviviridis*, using enzyme histochemical techniques (Gouder and Nadkarni, 1976). However, ultrastructural steroidogenic features in the granulosa cells of *H. flaviviridis* are reported for the first time in this study for this species, and may provide further information on the hormonal control of folliculogenesis.

Clumps of fibrillar material were observed in the previtellogenic follicles of *H. flaviviridis* which dispersed prior to the onset of vitellogenesis. These might be actin microfilaments accumulated in the cytoplasm that play a role in the cytokinetic process during cleavage and normal mitosis (Schroeder, 1973). Future studies are required to examine the fibrillar distribution in more detail.

At the onset of vitellogenesis, the intermediate and pyriform cells in *H. flaviviridis* follicles degenerated, as reported in other lizard species (Motta *et al.*, 1996), leaving the maturing follicle with a monomorphic granulosa (e.g., Etches and Petitte, 1990; Motta *et al.*, 1995). Formation of yolk platelets which marks the onset of vitellogenesis began during early spring in *H. flaviviridis*. The differences in the morphology of yolk platelets during vitellogenesis in *H. flaviviridis* was similar to that reported for chelonians and other squamates, which corresponds to the role of pinocytotic accumulation of yolk droplets (e.g., Guraya, 1989; Uribe *et al.*, 1996, Uribe and Guillette, 2000). The variation in yolk platelet shape and size suggests that the platelets are formed by different sequestration methods and this diversity may also correspond to vesicles containing different contents.

In this study, small peripheral granular vesicles were observed in the periphery of vitellogenic follicles of *H. flaviviridis* which may be associated with vitellogenin uptake. The presence of granular vesicles in the periphery and along the inner surface of the vitellogenic oocyte microvilli is reportedly associated with the uptake of vitellogenin from the blood through pinocytocis (Guraya, 1989). Small peripheral granules appeared in the cortical region. These granules could correspond to the

cortical granules found in other squamates (e.g., *H. flaviviridis*, Guraya, 1989). They have been related to the cortical reaction or zone reaction during fertilization in teleosts, amphibians, and mammals (Gilbert, 1997).

Follicular atresia in *H. flaviviridis* occurred during the processes of follicular organisation in previtellogenic follicles in early follicular development. It also has been reported in other lizards (e.g., Guraya, 1989; Gómez and Ramírez-Pinilla, 2004). The histological features observed in follicular atresia in *H. flaviviridis* were similar to those reported in other species of squamates (e.g., Guraya and Varma, 1976; Hubert, 1985; Uribe *et al.*, 1995; Gómez and Ramírez-Pinilla, 2004). Factors related to the formation of follicular atresia and their role in the control of clutch size is still poorly understood. In mammals they have been related to hormonal stimulation (e.g., high concentrations of oestrogens or sharp decreases of gonadotropins; Peters, 1978). It has been noted that atresia occurs in all follicular stages but is more frequent in the previtellogenic follicles of squamates (Saidapur, 1978; Guraya, 1989).

In this study, follicular atresia was very common in growing follicles and minimal in preovulatory follicles of *H. flaviviridis.* In preovulatory ovaries, atresia provides a mechanism for controlling the final number of follicles that ovulate during the process of follicular selection (Jones *et al.*, 1982; Andreuccetti *et al.*, 1990). Jones and Swain (2000) suggested that there are two possible mechanisms regulating clutch size in squamates, either recruitment (Sinervo and Licht, 1991) or a subsequent atresia (Mèndez de la Cruz *et al.*, 1993). In this study, atresia was more or less constant in all reproductive stages from immature females to gravid females. However, in females with late gravidity, follicular atresia appeared to diminish. These facts could be related to the decline of plasma P concentrations at the end of gravidity, when oviposition occurs. Further studies are needed to understand the factors underlying the formation of atretic follicles and their role in the control of clutch size or whether they correspond to an environmentally induced pathology in females of *H. flaviviridis.*

The luteal tissue of the CL in *H. flaviviridis* ovary was formed only from granulosa cells, similar to those reported in other squamates (e.g., Masson and Guillette, 1987; Guarino *et al.*, 1998: Shanbhag *et al.*, 2001; Gómez and Ramírez-Pinilla, 2004). The structure of the CL is similar to those of other lizard species (e.g., Fox and Guillette,

1987; Xavier, 1987; Gómez and Ramírez-Pinilla, 2004). The changes in the morphology of the CL through gravidity in *H. flaviviridis* were similar to those described in other lizard species (Guraya and Varma, 1976; Guarino *et al.*, 1998). In addition, the ultrastructural changes in the active granulosa lutein cells of *H. flaviviridis* were related to the increase in the steroidogenic activity of the CL for the production of P during gravidity, as discussed earlier in this chapter.

In this study, the CL appeared to be the major source of P and it remained steroidogenically active during the period of egg retention. P was essential for triggering secretory activity as well as keeping the uterus in a quiescent state while the shelling process took place in the uterus. Just prior to oviposition and around the time the shelling process is completed the CL undergoes degeneration (Mahmoud *et al.*, 1980; Jones *et al.*, 1979; Guillette and Fox, 1985). P is also known to inhibit vitellogenesis (Klicka and Mahmoud, 1977). However, soon after the degeneration of the CL, the process of vitellogenesis begins as plasma P concentrations decline. Cuellar (1979) reported that deluteinization disrupted the shelling process in the lizard, *Cnemidopherus uniparens,* which indicates that P may have the same role in the shelling process.

The oviducts of *H. flaviviridis* exhibited seasonal changes and their enlargement coincided with a gradual increase in the size of the ovaries. During the breeding season (active phase) the oviductal wall was lined by a tall, columnar epithelium which consisted of ciliated and nonciliated cells. The epithelium reacted strongly with PAS indicating that the oviducts of this lizard might be involved in steroid metabolism. In the nonbreeding lizards (quiescent-recrudescent phases) the oviduct showed degeneration marked by the reduction in the size and height of the epithelium which reacted negatively with PAS stain.

The oviduct of the house gecko *H. flaviviridis* can be divided into five regions according to its histological characteristics: infundibulum, uterine tube, isthmus, uterus, and vagina. This is consistent with other studies reported in oviparous geckos (Haider, 1985b; Picariello *et al.*, 1989; Girling *et al.*, 1998). The lumenal epithelium of the oviduct of *H. flaviviridis,* presented three types of cells: ciliated cells, microvillous nonciliated secretory cells, and occasional bleb-like secretory cells as

reported in other reptiles (Palmer and Guillette, 1988, Girling *et al.*, 1997; 1998; AlKindi *et al.*, 2006).

The infundibulum was greatly enlarged in *H. flaviviridis* during late vitellogenesis and gravidity. The ostial opening of the anterior infundibulum may envelop the ovaries prior to ovulation, as reported in other lizards (Cuellar, 1970). The posterior infundibulum stained positively for PAS, and at the ultrastructural level revealed the presence of numerous secretory granules which confirmed secretory activity in those cells. This was also observed in other lizard species (e.g., Guillette *et al.*, 1989; Girling *et al.*, 1998). Very little is known of the nature of secretions produced by the infundibulum (Girling, 2002). The function of bleb cells in the infundibulum is unknown, but they may be involved in apocrine or merocrine secretory processes (Palmer and Guillette, 1988).

The histological and ultrastructural features of the endometrium in the uterine tube of *H. flaviviridis* resemble those of other reptiles in being the site for albumen production (e.g., Perkins and Palmer, 1996; Girling, 2002; AlKindi *et al.*, 2006). In this study, the endometrial glands of the uterine tube increased in size and in secretory activity just before and after ovulation. The secretions made their way into the lumen through the ducts of the endometrial glands. These conditions coincided with elevated plasma steroid concentrations during the onset of the ovarian cycle in the spring. The glands of the uterine tube were the site for sperm storage of this species. The composition, production and function of albumen in reptiles are poorly understood (Palmer and Guillette, 1988), and the function of the uterine tube in squamate reptiles is unknown (Girling *et al.*, 2002). Further studies are needed in these areas.

The isthmus or junction is a short region between the uterine tube and the uterus, and often appears to share similarities with both its neighbouring regions. This region was also noted in other gecko species (Girling *et al.*, 1998). The epithelium of the isthmus stained negative for PAS, as is the case for the gecko species reported by Girling *et al.* (1998). This may suggest that the isthmus has no function in eggshell formation.

The uterus is the region where eggs are retained until oviposition. The uterus of *H. flaviviridis* underwent dramatic seasonal changes in epithelial height as well as size

and state of activity of the uterine glands, and the thickness of the lamina propria and myometrium. The presence of the yolky egg during gravidity causes the uterus to be highly stretched, in contrast to its thick-walled condition during vitellogenesis. The vitellogenic uterus was greatly thickened by numerous uterine mucosal glands, as observed in other oviparous lizards of the family Gekkonidae (e.g., Guillette *et al.*, 1989; Palmer *et al.*, 1993; Girling *et al.*, 1998; Nogueira *et al.*, 2011). The glands reacted negatively to PAS in the vitellogenic period of *H. flaviviridis*, as observed in other gecko species (Girling *et al.*, 1997; 1998; Nogueira *et al.*, 2011). However, in *H. flaviviridis* these glands contained numerous secretory granules at the ultrastructural level. The secretory nature of these glands is probably modified in function by small hormonal alterations during the sexual cycle (Nogueira *et al.*, 2011). In oviparous species, the uterus is the region from which the eggshell membranes and calcium for the eggshell are secreted (Aitken and Solomon, 1976).

The vagina of *H. flaviviridis* had deep longitudinal folds that reduced the luminal volume during vitellogenesis but allowed for expansion during ovipostion. It had a thick muscle layer that may act both as a sphincter and, during oviposition help to expel the egg. Similar observations were reported in other oviparous lizards (e.g., Guillette *et al.*, 1989; Girling *et al.*, 1998). The sphincter probably functions in retaining the eggs during gravidity until the time of oviposition as reported for other reptiles (Girling, 2002). The epithelium had numerous cilia, which presumably aided transport of sperm up the oviduct. The nonciliated cells stained positive with PAS, and numerous secretory granules presumably produced mucus for lubrication, as well as substances needed to maintain sperm while it was stored, as reported in other gecko species (Girling *et al*., 1998). Large numbers of sperm were seen in the lumen of the vagina of *H. flaviviridis*, which indicated that the vagina is another sperm storage site for this species.

In *H. flaviviridis*, sperm storage sites were found in the vagina and the uterine tube. Sperm storage is a common phenomenon in reptiles and has been reported in many species of lizard (e.g. Blackburn, 1998; Girling, 2002; Eckstut *et al.*, 2009; Nogueira *et al.*, 2011). Sperm storage may be advantageous because it allows copulation to be separated from fertilization, or may reduce the risk of predation by reducing copulation frequency, or act as insurance against not finding a mate because of low

densities or slow movement (Girling 2002). The mechanism by which sperm are released from storage sites in the vagina or anterior oviductal regions, and the mechanism of fertilization, and the site of fertilization are poorly understood in reptiles (Girling 2002).

In conclusion, based on the temporal relationships between gamete maturation and mating periods, both the male and female reproductive cycles of *H. flaviviridis* are classified as prenuptial (associated) cycles, and the oogenetic and spermatogenic patterns are typical of prenuptial reproductive cycles.

This study reports the general histology, histochemistry, immunohistochemistry, ultrastucture and hormonal control of the reproductive system in both the male and female house gecko *H. flaviviridis* during the annual reproductive cycle. The general histology and ultrastructure of the reproductive organs of *H. flaviviridis* were similar to that reported for other squamates. *H. flaviviridis* shares a common characteristic with other squamates, in that changes were seen in the reproductive organs over the reproductive season, with full development of these organs occurring during the active phase (breeding season). The epithelial organisation of these organs in relation to plasma hormone concentrations and environment reflects a role in the maintenance of the reproductive cycle.

This study presents the first detailed ultrastructural description of spermatogenesis, Leydig cells, Sertoli cells, epididymis and RSS in natural populations of male *H. flaviviridis*. This study also reports the first detailed ultrastructural description of folliculogenesis, granulosa cells and CL, and oviduct in female *H. flaviviridis*. The relationship between sex hormones and their receptors, and the localisation of PRs in the reproductive organs have not been studied before in this species. The influence of steroid action on reproductive morphology, protein synthesis, and protein secretion in reptiles is poorly understood and more investigation is needed. Ultrastructural steroidogenic features reported in this study highlight the lack of understanding still surrounding the functions and methods of action in the combination of tissues that make up the lizard reproductive organs. Our understanding of the evolution of germ cell development strategy and the process of reproductive organ development in relation to hormonal control within vertebrates may become clearer by investigating

the reproductive biology, patterns and strategies in other reptilian species. The present study represents a preliminary step in our understanding of these processes. Expanding our understanding of the regulatory mechanism which controls the timing of protein secretion during gamete cycles may help elucidate our understanding of the reproductive potential and the evolution of these processes among squamates.

Further studies are needed to address many unknown functions and mechanisms, as mentioned above, related to the development and secretory activity and mode of action in the different regions of the reproductive systems. Further studies are required to elucidate the hormonal control of reproductive biology in males and females of *H. flaviviridis* and other squamates due to a lack of published work in which data on reproductive physiology and coincident steroid hormone profiles are available. Further studies are also needed to examine the functional morphology of the female oviduct of *H. flaviviridis* to understand the role of this complex structure in reproductive events.

Table 5.1. Data summary for the male house gecko *H. flaviviridis* during a reproductive cycle

Season	**Early Summer (June–Aug)**	**Late Summer (Sept–Oct)**	**Winter (Nov–Jan)**	**Late winter & Spring (Late Jan–May)**
Phase	Postbreeding (Quiescent)	Prebreeding (Recrudescent)	Prebreeding (Active)	Breeding (Active)
Temp. range in Barka, Oman	33–47 °C	30–35 °C	13–23 °C	23–35 °C
Plasma T conc.	Low	Slightly increased	Increased	High
Plasma E_2 conc.	Low	Slightly increased	Increased	High
Plasma P conc.	Low	Slightly increased	Increased	High
Plasma C conc.	Unchanged	Unchanged	Unchanged	Slightly increased
PR expression in reproductive organs	Weakly expressed/-ve in RSS	Weakly expressed/-ve in RSS	Strongly expressed/-ve in RSS	Strongly expressed/-ve in RSS
Development of spermatog-enesis	Regressed/ Spermatogonia A & B	Spermatocytes ($1^{st}/2^{nd}$), Spermatids (1–7)	Spermatids (1–7) , Spermatozoa	Mature sperm in epididymis
Development of Steroidogenic features in gonad	Undeveloped SER and Mitochondira, abundance of lipids	developed SER and Mitochondira, presence of lipids	Highly developed SER and Mitochondira , some lipids	Highly developed SER and Mitochondira , some lipids
Development of Epididymis & vas deferens	Regressed/ no secretory granules	Increase in epithelial cell height/ no secretory granules	Enlarged ducts filled with secretory granules	Enlarged ducts filled with secretory granules
Development of RSS	Regressed/ no secretory granules in the lumen	Increase in epithelial cell height/ no secretory granules	Enlarged RSS filled with secretory granules	Enlarged RSS filled with secretory granules

Table 5.2. Data summary for the female house gecko *H. flaviviridis* during a reproductive cycle

Season	**Early Summer (June–Aug)**	**Late Summer (Sept–Oct)**	**Winter (Nov–Jan)**	**Late winter & Spring (Late Jan–May)**
Phase	Postbreeding (Quiescent)	Prebreeding (Recrudescent)	Prebreeding (Recrudescent)	Breeding (Active)
Photoperiod in Barka, Oman	13 hours	12 hours	12 hours	13 hours
Plasma E_2 conc.	Low	Slightly increased	Increased	High
Plasma P conc.	Low	Low	Low	High
Plasma T conc.	Low	Low	Low	High
Plasma C conc.	Unchanged	Unchanged	Unchanged	Slightly increased
PR expression in reproductive organs	Weakly expressed	Weakly expressed	Strongly expressed	Strongly expressed
Development of folliculoge-nesis	Oogonia, pre-vitellogenesis (II)	1^{st} oocytes, pre-vitellogenesis (III)	Pre-vitellogenesis (IV–V)	Vitellogenesi-s (VI –IX), preovulatroy follicles
Development of steroidogenic features in gonad	Undeveloped SER and Mitochondira, abundance of lipids	developed SER and Mitochondira, presence of lipids	Highly developed SER and Mitochondira, some lipids	Highly developed SER and Mitochondira, some lipids
Presence of atretic follicle	Degenerated	Present	Present	Present
Development of CL	Degenerated	Absent	Absent	Developed
Development of oviduct	Slight increase in epithelial cell height/ no secretory granules	Oviduct/ regressed/ no secretory granules in the lumen	Oviduct/ regressed/ no secretory granules in the lumen	Oviduct enlarged filled with secretory granules

Chapter Six:

References

Abe, K., and Takano, H. (1989) Early degeneration of the epithelial cells in the initial segment of the epididymal duct in mice after efferent duct cutting. *Archives of Histology and Cytology* **52**, 299-310.

Abrams Motz, V., and Callard, I.P. (1991) Seasonal variations in oviductal morphology of the painted turtle, *Chrysemys picta*. *Journal of Morphology* **207**, 59-71.

Adams, C.S., and Cooper, W.E., Jr. (1988) Oviductal morphology and sperm storage in the keeled earless lizard, *Holbrookia propinqua*. *Herpetologica* **44**, 190-197.

Adams, S.M., Hosie, M.J., Murphy, C.R., and Thompson, M.B. (2004) Changes in oviductal morphology of the skink, *Lampropholis guichenoti*, associated with egg production. *Journal of Morphology* **262**, 536-544.

Adkins-Regan, E. (1981) Hormone specificity, androgen metabolism and social behaviour. *American Zoologist* **21**, 257-271.

Aitken, R.N.C. (1971) The oviduct. In 'Physiology and Biochemistry of the Domestic Fowl. Vol. JII.' (Eds. DJ Bell and BM Freeman) pp. 1237-1289. (Academic Press: New York).

Aitken, R.N.C., and Solomon, S.E. (1976) Observations on the ultrastructure of the oviduct of the Costa Rican green turtle (*Chelonia mydas* L.). *Journal of Experimental Marine Biology and Ecology* **21**, 75-90.

Akbarsha, M.A., and Balasuhramanian, K. (1983) Seasonal differences in the effects of castration and testosterone administration on the accessory male reproductive organs of *Culotes versicolor*. *Biological Bulletin. India* **4**, 172-176.

Akbarsha, M.A., Kadalmani, B., and Tamilarasan, V. (2006) Histological variation along and ultrastructural organization of the epithelium of the ductus epididymidis of the fan-throated lizard *Sitana ponticeriana* Cuvier. *Acta Zoologica (Stockholm)* **87**, 181-196.

Akbarsha, M.A., Kadalmani, B., and Tamilarasan, V. (2007) Efferent ductules of the fan-throated lizard *Sitana ponticeriana* Cuvier. *Journal of Morphology* **267**, 713-729.

Akbarsha, M.A., and Manimekalai, M. (1999) Histological differentiation along the turtle ductus epididymis, with a note on secretion of seminal proteins as discrete granules. *Journal of Endocrinology and Reproduction* **3**, 36-46.

Akbarsha, M.A., and Meeran, M.M. (1995) Occurrence of ampulla in the ductus deferens of *Calotes versicolor* (Daudin). *Journal of Morphology* **225**, 261-268.

Akbarsha, M.A., Tamilarasan, V., Kadalmani, B., and Daisy, P. (2005) Ultrastructural evidence for secretion from the epithelium of ampulla ductus deferentis of the fan-throated lizard *Sitana ponticeriana* Cuvier. *Journal of Morphology* **266**, 94-111.

Akhtar, P. (1988) Effects of steroids on the oviduct of female spiny tailed lizard. *Pakistan Journal of Agricultural Research* **9**, 120-124.

Al-Dokhi, O.A. (1996) Ultrastructural studies on the differentiation of the sperm head in the Sand Skink *Scincus mitranus* (Anderson, 1871) (Squamata, Reptilia). *Arab Gulf Journal of Scientific Research* **14**, 471-482.

Al-Dokhi, O.A. (1998) Ovarian structure and follicle development in the lizard *Mabuya brevicollis*. *Saudi Journal of Biological Sciences* **5**, 12-23.

Al-Dokhi, O.A., Al-Onazee, Y.Z., and Mubarak, M. (2004) Light and electron microscopy of the testicular tissue of the snake *Eryx jayakari* (Squamata, Reptilia) with a reference to the dividing germ cells. *Journal of Biological Sciences* **4**, 345-351.

Al-Habsi, A.A., AlKindi, A.Y.A., Mahmoud, I.Y., Owens, D.W., Khan, T., and Al-Abri, A. (2006) Plasma hormone levels in the green turtles *Chelonia mydas* during peak period of nesting at Ras Al-Hadd-Oman. *Journal of Endocrinology* **191**, 9-14.

Al-Hajj, H., Janakat, S., and Mahmoud, F. (1987) Electron microscopic study of sperm head differentiation in the lizard *Agama stellio*. *Canadian Journal of Zoology* **65**, 2959-2968.

Al-Kindi, A.Y., Mahmoud, Y., and Woller, M.J. (2001) Ultrastructural changes in granulosa cells and plasma steroid levels after administration of luteinizing hormone-releasing hormone in the western painted turtle, *Chrysemys Picta*. *Tissue & Cell* **33**, 361-367.

Aldridge, R.D. (1979) Female reproductive cycles of the snakes *Arizona elegans* and *Crotalus viridis*. *Herpetologica* **35**, 256-261.

Aldridge, R.D. (1992) Oviductal anatomy and seasonal sperm storage in the southeastern crowned snake (*Tantilla coronata*). *Copeia* **1992**, 1103-1106.

Aldridge, R.D., and Brown, W.S. (1995) Male reproductive cycle, age and maturity, and cost of reproduction in the timber rattlesnake (*Crotalus horridus*). *Journal of Herpetology* **29**, 399-407.

AlKindi, A.Y.A., Mahmoud, I.Y., Woller, M.J., and Plude, J.L. (2006) Oviductal morphology in relation to hormonal levels in the snapping turtle, *Chelydra serpentina*. *Tissue and Cell* **38**, 19-33.

Amey, A.P., and Whittier, J.M. (2000) Seasonal patterns of plasma steroid hormones in males and females of the bearded dragon lizard, *Pogona barbata*. *General and Comparative Endocrinology* **117**, 335-342.

Ananjeva, N.B., Orlov, N.L., Khalikov, R.G., Darevsky, I.S., and Barabanov, A. (2004) 'The reptiles of northern Eurasia: taxonomic diversity, distribution, conservation status. Family *Geckkonidae*, Gray 1825.' (Pensoft: Saint-Petersburg) 510.

Andersen, M.L., and Tufik, S. (2006) Does male sexual behavior require progesterone? *Brain Research Reviews* **51**, 136-143.

Anderson, W.A., and Personne, P. (1969) Structure and histochemistry of basal body derivative, neck and axoneme of spermatozoa of *Helix aspersa*. *Journal of Microscopy* **8**, 87-96.

Ando, S., Ciarcia, G., Panno, M.L., Imbrogno, E., Tarantino, G., Buffone, M., Beraldi, E., Angelini, F., and Botte, V. (1992) Sex steroids levels in the plasma and testis during the reproductive cycle of lizard *Podarcis s. sicula* Raf. *General and Comparative Endocrinology* **172**, 225-233.

Ando, S., Panno, M.L., Ciarcia, G., Imbrogno, E., Buffone, M., Beraldi, E., Sisci, D., Angelini, F., and Botte, V. (1990) Plasma sex hormone concentrations during the reproductive cycle in the male lizard, *Podarcis s. sicula*. *Journal of Reproduction and Fertility* **90**, 353–360.

Andreuccetti, O., Motta, C.M., and Filosa, S. (1990) Regulation of oocyte number during oocyte differentiation in the lizard *Podarcis sicula*. *Cell Differentiation and Development* **29** 129-141.

Andreuccetti, P. (1992) An ultrastructural study of differentiation of pyriform cells and their contribution to oocyte growth in representative squamata. *Journal of Morphology* **212**, 1-11.

Andreuccetti, P., Famularo, C., Gualtieri, R., and Prisco, M. (2001) Pyriform cell differentiation in *Podarcis sicula* is accompanied by the appearance of surface glycoproteins bearing alpha-galNAc terminated chains. *Anatomical Record* **263**, 1-9.

Andrews, R.M., and Mathies, T. (2000) Natural history of reptilian development: constraints on the evolution of viviparity. *Bioscience* **50**, 227-238.

Aranda, A., and Pascual, A. (2001) Nuclear hormone receptors and gene expression. *Physiological Reviews*, **81**, 1269-1304.

Arslan, M., Zaidi, P., Bint akhtar, F., and Qazi, M.H. (1981) Effect of intratesticular administration of gonadotropins on plasma androgen concentration in the lizard, *Uromastix hardwickii*. *General and Comparative Endocrinology* **43**, 422-426.

Arslan, M., Zaidi, P., Lobo, J., Zaidi, A.A., and Qazi, M.H. (1978a) Steroid levels in preovulatory and gravid lizards (*Uromastix hardwicki*). *General and Comparative Endocrinology* **34**, 300-303.

Arslan, M.J., Lobo, J., Zaidi, A.A., Jalali, S., and Qazi, M.H. (1978b) Annual androgen rhythm in the spiny-tailed lizard, *Uromastix hardwicki*. *General and Comparative Endocrinology* **36**, 16-22.

Austin, C.R. (1965) Fine structure of the snake sperm tail. *Journal of Ultrastructure Research* **12**, 452-462.

Averal, H.I., Manimekalai, M., and Akbarsha, M.A. (1992) Differentiation along the ductus epididymis of the Indian garden lizard *Calotes versicolor* (Daudin). *Biological Structures and Morphogenesis* **4**, 53-57.

Ba-Omar, T., AlKindi, A.Y., and Mahmoud, I.Y. (2002) Changes in steroidogenic ultrastructural features of corpus luteum in the turtle, *Sternotherus odoratus*, relative to hormonal levels under natural conditions. *Microscopy and Microanalysis (Supplement 2)* **8**, 888-889.

Baccetti, B., and Afzelius, B.A. (1976) The biology of the sperm cell. *Monographs in Developmental Biology* **10**, 1-124.

Baccetti, B., Bigliardi, E., Vegni Talluri, M., and Burrini, A.G. (1983) The Sertoli cell in lizards. *Journal of Ultrastructure Research* **85**, 11-23.

Badir, N. (1968) Structure and function of the corpus luteum during gestation in the viviparous lizard *Chalcides ocellatus*. *Anatomischer Anzeiger* **122**, 1-10.

Baig, K.J., Masroor, R., and Arshad, M. (2008) Biodiversity and ecology of the herpetofauna of Cholistan Desert, Pakistan. *Russian Journal of Herpetology* **15**, 193-205.

Ballinger, R.E. (1978) Variation in and evolution of clutch and litter size. In 'The Vertebrate Ovary: Comparative Biology and Evolution.' (Ed. RE Jones) pp. 789-825. (Plenum Press: New York).

Bardin, C.W., Cheng, C.Y., Mustow, N.A., and Gunsulus, G.L. (1994) The Sertoli cells. In 'The Physiology of Reproduction. Vol. 1.' (Eds. E Knobil and JD Neill) pp. 1291-1334. (Raven Press: New York).

Bartlett, J.M.S., Weinbauer, G.F., and Nieschlag, E. (1989) Differential effects of FSH and testosterone on the maintenance of spermatogenesis in the adult hypophysectomised rat. *Journal of Endocrinology* **121**, 49-58.

Bauer, A.M. (2002) Lizards. In 'Encyclopedia of amphibians and reptiles.' (Eds. T Halliday and K Adler) pp. 138-175. (Andromeda Oxford Ltd: Abingdon).

Bellve, A.R., and Zheng, W. (1989) Growth factors as autocrine and paracrine modulators of male gonadal functions. *Journal of Reproduction and Fertility* **85**, 771-793.

Benahmed, M., Grenot, C., Tabone, E., Sanchez, P., and Morera, A.M. (1985) FSH regulates cultured Leydig cell function via Sertoli cell proteins: an in vitro study. *Biochemical and Biophysical Research Communications* **132**, 729-734.

Benner, S.L., and Woodley, S.K. (2007) The reproductive pattern of male dusky salamanders (genus *Desmognathus*) is neither associated nor dissociated. *Hormones and Behavior* **51**, 542-547.

Bergeron, J.M., Gahr, M., Horan, K., Wibbels, T., and Crews, D. (1998) Cloning and in situ hybridization analysis of estrogen receptor in the developing gonad of the red-eared slider turtle, a species with temperature-dependent sex determination. *Development, Growth and Differentiation* **40**, 243-254.

Bhaktaraj, B., Patil, S., and Patil, S.B. (2000) GnRH and/or testosterone induced changes in reproductive activities during non breeding season in *Calotes versicolor* (Daud.). *Indian Journal of Experimental Biology* **38**, 873-876.

Bharti, S., Misro, M.M., Mathur, A., and Rai, U. (2011) Role of estrogen in the regulation of spermatogenesis in the Indian wall lizard *Hemidactylus flaviviridis*. *General and Comparative Endocrinology* **172**, 225-233.

Billy, A.J., and Crews, D. (1986) The effects of sex steroid treatments on sexual differentiation in a unisexual lizard, *Cnemidophorus uniparens* (Teiidae). *Journal of Morphology* **187**, 129-142.

Bishop, J.E. (1959) A histological and histochemical study of the kidney tubules of the common garter snake, *Thamnophis sirtalis*, with special reference to the sexual segment in the male. *Journal of Morphology* **104**, 307-357.

Bjersing, L. (1967) On the ultrastructure of granulosa lutein cells in porcine corpus luteum. With special reference to endoplasmic reticulum and steroid hormone synthesis. *Zeitschrift für Zellforschung und Mikroskopische Anatomie* **82**, 187-211.

Blackburn, D.G. (1982) Evolutionary origins of viviparity in the Reptilia. I. Sauria. *Amphibia-Reptilia* **3**, 185-205.

Blackburn, D.G. (1998) Structure, function, and evolution of the oviducts of squamate reptiles, with special reference to viviparity and placentation. *Journal of Experimental Zoology* **282**, 560-617.

Bona-Gallo, A., Licht, P., MacKenzie, D.S., and Lofts, B. (1980) Annual cycles in levels of pituitary and plasma gonadotropin, gonadal steroid, and thyroid activity in the Chinese cobra (*Naja naja*). *General and Comparative Endocrinology* **42**, 477-493.

Bonnet, X., and Naulleau, G. (1996) Are body reserves important for reproduction in male dark green snakes (Colubridae: *Coluber viridiflavus*)? *Herpetologica* **52**, 137-146.

Boretto , J.M., Ibargüengoytía, N.R., Jahn, G.A., Acosta, J.C., Vincenti, A.E., and Fornés, M.W. (2010) Asynchronic steroid activity of Leydig and Sertoli cells related to spermatogenic and testosterone cycle in *Phymaturus antofagastensis*. *General and Comparative Endocrinology* **166**, 556-564.

Botte, V. (1973) Some aspects of oviduct development in the lizard *Lacerta sicula* in relation to the annual cycle. *Bollettino di Zoologia* **40**, 315-321.

Botte, V., Angelini, F., Picariello, O., and Molino, R. (1976) The regulation of the reproductive cycle of the female lizard *Lacerta sicula sicula* Raf. *Monitore Zoologico Italiano* **10**, 119-133.

Botte, V., and Delrio, G. (1964) Ricerche istochimiche sulla distribuzinone dei 3- e 17 cheto-steroidi e di alcuni enzimi della steroidogenase nell' ovario di *Lacerta sicula*. *Bollettino di Zoologia* **32**, 191-195.

Botte, V., and Granata, G. (1977) Induction of avidin synthesis by RNA obtained from lizard oviducts. *Journal of Endocrinology* **73**, 535-536.

Boulenger, G.A. (1890) 'Reptilia and batrachia.' (Taylor and Francis: London).

Bourne, A.R., Stewart, B.J., and Watson, T. (1986a) Changes in blood progesterone concentration during pregnancy in the lizard *Tilliqua* (*Trachydosaurus*) *rugosa*. *Comparative Biochemistry and Physiology* **84A**, 581-583.

Bourne, A.R., Taylor, J.L., and Watson, T.G. (1986b) Annual cycles of plasma and testicular androgens in the lizard *Tiliqua* (*Trachydosaurus*) *rugosa*. *General and Comparative Endocrinology* **61**, 278-286.

Boyd, M.M.M. (1942) The oviduct, foetal membranes, and placentation in *Hoplodactylus maculatus* Gray. *Proceedings of the Zoological Society of London* **112**, 65-104.

Brandt, Y., and Allen, J. (2004) Persistence of individually distinctive display patterns in fatigued side-blotched lizards (*Uta stansburiana*). *Behavioral Ecology and Sociobiology* **55**, 257-265.

Brueggemeier, R. W. (2005) Sex Hormones (Male): Analogs and Antagonists. In *Encyclopedia of Molecular Cell Biology and Molecular Medicine* (Ed. by R. A. Meyers). Wiley-VCH Verlag GmbH & Co., KGaA, Weinheim.

Bull, C.M., Bedford, G.S., and Schulz, B.A. (1993) How do sleepy lizards find each other? *Herpetologica* **49**, 294-300.

Butler, R.D., and Gabri, M.S. (1984) Structure and development of the sperm head in the lizard *Podarcis* (=*Lacerta*) *taurica*. *Journal of Ultrastructure Research* **88**, 261-274.

Calderón, M.L., De Pérez, G.R., and Ramírez-Pinilla, M.P. (2004) Morphology of the ovary of *Caiman crocodilus* (Crocodylia: Alligatoridae). *Annals of Anatomy* **186**, 13-24.

Callard, G. (1991) Spermatogenesis. In 'Vertebrate Endocrinology: Fundamentals and Biomedical Implications. Vol. 4.' (Eds. PKT Pang and MP Scriebman) pp. 303-341. (Academic Press: New York).

Callard, G.V., Petro, Z., and Ryan, K.J. (1977) Identification of aromatase in the reptilian brain. *Endocrinology* **100**, 1214-1218.

Callard, I.P., Bayne, C.G., and McConnell, W.F. (1972a) Hormones and reproduction in the female lizard, *Sceloporus cyanogenys*. *General and Comparative Endocrinology* **18**, 175-195.

Callard, I.P., Callard, G.V., Lance, V., and Eccles, S. (1976) Seasonal changes in testicular structure and function and the effects of gonadotropins in the freshwater turtle, *Chrysemys picta*. *General and Comparative Endocrinology* **30**, 347-356.

Callard, I.P., Doolittle, J., Banks, W.I., and Chan, W.C. (1972b) Recent studies on the control of the reptilian ovarian cycle. *General and Comparative Endocrinology Supplement* **3**, 65-75.

Callard, I.P., Fileti, L.A., Perez, L.E., Sorbera, L.A., Giannoukos, G., Klosterman, L.L., Tsang, P., and McCraken, J.A. (1992) Role of the corpus luteum and progesterone in the evolution of vertebrate viviparity. *American Zoologist* **32**, 264-275.

Callard, I.P., and Ho, S.-M. (1987) Vitellogenesis and viviparity. In 'Fundamentals of Comparative Vertebrate Endocrinology.' (Eds. I Chester-Jones, PM Ingelton and JG Phillips) pp. 257-282. (Plenum Press: New York).

Callard, I.P., and Ho, S.M. (1980) Seasonal reproductive cycles in reptiles. In 'Progress in Reproductive Biology: Seasonal Reproduction in Higher Vertebrates. Vol. 5.' (Eds. RJ Reiter and BK Follett) pp. 5-38. (Karger: Basel).

Callard, I.P., Lance, V., Salhanick, A.R., and Barad, D. (1978) The annual ovarian cycle of *Chrysemys picta*: Correlated changes in plasma steroids and parameters of vitellogenesis. *General and Comparative Endocrinology* **35**, 245-257.

Callard, I.P., Riley, D., and Perez, L. (1990) Vitellogenesis in reptiles as a model for mammalian sex-differentiated hepatic protein synthesis. *Journal of Experimental Zoology* Supplement, **4**, 106-111.

Carcupino, M., Corso, G., and Pala, M. (1989) Spermiogenesis in *Chalcides ocellatus tiligugu* (Gmelin) (Squamata, Scincidae): An electron microscope study. *Bollettino di Zoologia* **56**, 119-124.

Cardone, A., Angelini, F., and Varriale, B. (1998) Autoregulation of estrogen receptor mRNA and downregulation of androgen receptor mRNA by estrogen in primary cultures of lizard testis cells. *General and Comparative Endocrinology* **110**, 227-233.

Cardone, A., Comitato, R., and Angelini, F. (2002) Effect of aromatase inhibitor fadrozole on plasma sex steroid secretion, spermatogenesis and epididymis morphology in the lizard, *Podarcis sicula*. *Molecular Reproduction and Development* **63**, 63-70.

Carnevali, O., Mosconi, G., Angelini, F., Limatola, E., Ciarcia, G., and Polzonetti-Magni, A. (1991) Plasma vitellogenin and 17β estradiol levels during the annual reproductive cycle of *Podarcis s. sicula* Raf. *General and Comparative Endocrinology* **84**, 337-343.

Carranza, S., and Arnold, E.N. (2006) Systematics, biogeography, and evolution of *Hemidactylus* geckos (Reptilia: Gekkonidae) elucidated using mitochondrial DNA sequences. *Molecular Phylogenetics and Evolution* **38**, 531-545.

Carreau, S., Genissel, C., Belinska, B., and Levallet, J. (1999) Sources of oestrogens in the testis and reproductive tract of the male. *International Journal of Andrology* **22**, 211-223.

Castilla, A.M., and Bauwens, D. (1990) Reproductive and fat body cycles of the lizard, *Lacerta lepida*, in central Spain. *Journal of Herpetology* **24**, 261-266.

Castilla, A.M., and Swallow, J.G. (1996) Thermal dependence of incubation duration under a cycling temperature regime in the lizard, *Podarcis hispanica atrata*. *Journal of Herpetology* **30**, 247-253.

Censky, E.J. (1995) Reproduction in two lesser antillean populations of *Ameiva plei* (Teiidae). *Journal of Herpetology* **29**, 553-560.

Chan, S., Ziegel, S., and Callard, I.P. (1973) Plasma progesterone in snakes. *Comparative Biochemistry and Physiology* **44A**, 631-637.

Chandrasekher, Y.A., Melner, M.H., Nagalla, S.R., and Stouffer, R.L. (1994) Progesterone receptor, but not estradiol receptor, messenger ribonucleic acid is expressed in luteinizing granulosa cells and the corpus luteum in *Rhesus* monkeys. *Endocrinology* **135**, 307-314.

Cheung, J., and Smith, D. F. (2000) Molecular chaparone interactions with steroid receptors: an update. *Molecular Endocrinology*, **14**, 939-946.

Chieffi, G., and Botte, V. (1970) The problem of luteogenesis in nonmammalian vertebrates. *Bollettino di Zoologia* **37**, 85-102.

Chieffi, G., and Pierantoni, R. (1987) Regulation of ovarian steroidogenesis. In 'Hormones and Reproduction in Fishes, Amphibians and Reptiles.' (Eds. DO Norris and RE Jones) pp. 117-144. (Plenum Press: New York).

Chieffi, P., Colucci D'Amato, L., Guarino, F., Salvatore, G., and Angelini, F. (2002) 17 beta-estradiol induces spermatogonial proliferation through mitogen-activated protein kinase (extracellular signal-regulated kinase 1/2) activity in the lizard (*Podarcis s. sicula*). *Molecular Reproduction and Development* **61**, 218-225.

Ciarcia, G., Lancieri, M., Suzuki, H., Manzo, C., Vitale, L., Tornese Buonamassa, D., and Botte, V. (1986) A specific nuclear protein and poly (ADPribose) transferase activity in lizard oviduct during the reproductive cycle. *Molecular and Cellular Endocrinology* **47**, 235-241.

Cliffsnotes.com (2012) http://www.cliffsnotes.com/study_guide/The-Male-Reproductive-System.topicArticleId-277792,articleId-277788.html.

Cogger, H.G. (2003) Reptiles, in Biological Systematics. In 'Encyclopedia of Life Support Systems.' (Eds. G Contrafatto and A Minelli). (Eolss Publishers: Oxford, UK).

Colli, G.R., and Pinho, A.A. (1997) Interstitial cell cycle of *Ameiva ameiva* (Sauria, Teiidae) in the Cerrado region of central Brazil. *Journal of Morphology* **233**, 99-104.

Colli, G.R., Teixeira, R.D., Scheltinga, D.M., Mesquita, D.O., Wiederhecker, H.C., and Báo, S.N. (2007) Comparative study of sperm ultrastructure of five species of teiid lizards (Teiidae, Squamata), and *Cercosaura ocellata* (Gymnophthalmidae, Squamata). *Tissue & Cell* **39**, 59-78.

Cooper, W.E., and Perez-Mellado, V. (2002) Pheromonal discriminations of sex, reproductive condition, and species by the lacertid lizard *Podarcis hispanica*. *Journal of Experimental Zoology* **292**, 523-527.

Corso, G., Delitala, G.M., and Carcupino, M. (2000) Uterine morphology during the annual cycle in *Chalcides ocellatus tiligugu* (Gmelin)(Squamata: Scincidae). *Journal of Morphology* **243**, 153-165.

Courtens, J.L., and Depeiges, A. (1985) Spermiogenesis of *Lacerta vivipara*. *Journal of Ultrastructure Research* **90**, 203-220.

Courty, Y., and Dufaure, J.P. (1979) Levels of testosterone in the plasma and testis of the viviparous lizard (*Lacerta vivipara Jaquin*) during the annual cycle. *General and Comparative Endocrinology* **39**, 336-342.

Courty, Y., and Dufaure, J.P. (1980) Levels of testosterone, dihydrotestosterone, and androstenedione in the plasma and testis of a lizard (*Lacerta vivipara Jacquin*) during the annual cycle. *General and Comparative Endocrinology* **42**, 325-333.

Craig, M. A., Beppler, G. A., Santos, C., and Raffa, R. B. (2005) A second (non-genomic) steroid mechanism of action: possible opportunity for novel pharmacotherapy? *Journal of Clinical Pharmacy and Therapeutics,* **30**, 305-312.

Cree, A., Cockrem, J.F., and Guillette, L.J., Jr. (1992) Reproductive cycles of male and female tuatara (*Sphenodon punctatus*) on Stephens Island, New Zealand. *Journal of Zoology (London)* **226**, 199-217.

Cree, A., Guillette, L.J., Jr., Cockrem, J.F., Brown, M.A., and Chambers, G.K. (1990b) Absence of daily cycles in plasma sex steroids in male and female tuatara (*Sphenodon punctatus*), and the effects of acute capture stress on females. *General and Comparative Endocrinology* **79**, 103-113.

Cree, A., Guillette, L.J., Jr., Cockrem, J.R., and Joss, J.M.P. (1990a) Effects of capture and temperature stresses on plasma steroid concentrations in male tuatara (*Sphenodon punctatus*). *Journal of Experimental Zoology* **253**, 38-46.

Cree, A., Tyrrell, C.L., Preest, M.R., Thorburn, D., and Guillette, L.J., Jr. (2003) Protecting embryos from stress: corticosterone effects and the corticosterone response to capture and confinement during pregnancy in a live-bearing lizard (*Hoplodactylus maculatus*). *General and Comparative Endocrinology* **134**, 316-329.

Crews, D. (1984) Gamete production, sex hormone secretion, and mating behavior uncoupled. *Hormones and Bcrehavior* **18**, 22-28.

Crews, D., and Gans, C. (1992) The interaction of hormones, brain, emerging discipline in herpetology. In 'Biology of the Reptilia. Vol. 18.' (Eds. C Gans and D Crews) pp. 1-23. (The University of Chicago Press: Chicago and London).

Crews, D., Godwin, J., Hartman, V., Grammer, M., Prediger, E.A., and Sheppherd, R. (1996) Intrahypothalamic Implantation of Progesterone in Castrated Male Whiptail Lizards (*Cnemidophorus inornatus*) Elicits Courtship and Copulatory Behavior and Affects Androgen Receptor- and Progesterone Receptor-mRNA Expression in the Brain. *Journal of Neuroscience* **16**, 7347-7352.

Crews, D., and Sakata, J. (2000) Evolution of brain mechanisms, controlling sexual behavior. In 'Sexual Differentiation of the Brain.' (Ed. A Matsumoto) pp. 113-130. (CRC Press: Boca Raton, FL).

Crews, D., Traina, V., Wetzel, F.T., and Muller, C. (1978) Hormonal control of male reproductive behavior in the lizard, *Anolis carolinensis*: role of testosterone, dihydrotestosterone, and estradiol. *Endocrinology* **103**, 1814-1820.

Cuellar, H.S. (1979) Disruption of gestation and egg shelling in deluteinized oviparous whiptail lizards *Cnemidophorus uniparens* (Reptilia: Teiidae). *General and Comparative Endocrinology* **39**, 150-157.

Cuellar, O. (1966) Oviducal anatomy and sperm storage structures in lizards. *Journal of Morphology* **119**, 7-20.

Cuellar, O. (1970) Egg transport in lizards. *Journal of Morphology* **130**, 129-136.

Cuevas, M.E., and Callard, G. (1992) Androgen and progesterone receptors in shark (*Squalus*) testis: characteristics and stage-related distribution. *Endocrinology* **130**, 2173-2182.

Cunha, L.D., Tavares-Bastos, L., and Báo, S.N. (2008) Ultrastructural description and cytochemical study of the.spermatozoon of *Crotalus durissus* (Squamata, Serpentes). *Micron* **39**, 915-925.

Custodia-Lora, N., and Callard, I.P. (2002a) Progesterone and progesterone receptors in reptiles. *General and Comparative Endocrinology* **127**, 1-7.

Custodia-Lora, N., and Callard, I.P. (2002b) Seasonal changes in hepatic progesterone receptor mRNA, estrogen receptor mRNA, and vitellogenin mRNA in the painted turtle, *Chrysemys picta*. *General and Comparative Endocrinology* **128**, 193-204.

Custodia-Lora, N., Novillo, A., and Callard, I.P. (2004) Regulation of hepatic progesterone and estrogen receptors in the female turtle, *Chrysemys picta*: relationship to vitellogenesis. *General and Comparative Endocrinology* **136**, 232-240.

Cyrus, R.V., Mahmoud, I.Y., and Klicka, J. (1978) Fine structure of the corpus luteum of the snapping turtle *Chelydra serpentina*. *Copeia* **4**, 622-627.

De Smedt, V., Szöllösi, D., and Kloc, M. (2000) The Balbiani body: Asymmetry in the mammalian oocyte. *Genesis* **26**, 208-212.

DehIawi, G.Y., and Ismail, M.F. (1990) Studies on the Ultrastructure of the spermiogenesis of Saudian reptiles 1. The sperm head differentiation in *Uromastyx philbyi*. *Proceedings of the Zoological Society of Egypt* **21**, 75-85.

Dehlawi, G.Y., Ismail, M., and Sarhan, O.M. (1993) Ultrastructure of the spermiogenesis of Saudian reptiles. 8: sperm head differentiation in *Agama blandfordi*. *Molecular Andrology* **5**, 105-114.

Dehlawi, G.Y., Ismail, M.F., Hamdi, S.A., and Jamjoom, M.B. (1992) Ultrastructure of the spermiogenesis of Saudian reptiles. 6 :The sperm head differentiation in *Agama adrimatana*. *Archives of Andrology* **28**, 223-234.

Depeiges, A., and Dufaure, J.P. (1977) Secretory activity of the lizard epididymis and its control by testosterone. *General and Comparative Endocrinology* **33**, 473-479.

Depeiges, A., and Dufaure, J.P. (1981) Major proteins secreted by the epididymis of *Lacerta vivipara*. Identification by electrophoresis of soluble proteins. *Biochemica Biophysica Acta* **667**, 206- 266.

Depeiges, A., and Dufaure, J.P. (1983) Binding to spermatozoa of a major soluble protein secreted by the epididymis of the lizard *Lucerta uzuzparu*. *Gamete Research* **4**, 401-406.

Depeiges, A., Morel, F., and Dufaure, J.P. (1988) Identification of an epididymal immunorelated protein family, sequential appearance under testosterone stimulation. *Biochimica et Biophysica Acta* **964**, 383-387.

Desantis, S., Labote, M., Labote, G.M., and Cirillo, F. (2002) Evidence of regional differences in the lectin histochemistry along the ductus epididymis of the lizard, *Podarcis sicula* Raf. *Histochemical Journal* **34**, 123-130.

Devine, M.C. (1975) Copulatory plugs: Enforced chastity. *Science* **187**, 844-845.

DeWolfe, B.B., and Telford, S.R. (1966) Lipid-positive cells in the testis of the lizard, *Cnemidophorus tigris*. *Copeia* **1966**, 590-592.

Di Prisco, C.L., Delrio, G., and Chieffi, G. (1968) Sex hormones in the ovaries of the lizard *Lacerta sicula*. *General and Comparative Endocrinology* **1**, 292-295.
Diaz, J.A., Alonso-Gómez, A.L., and Delgado, M.J. (1994) Seasonal variation of gonadal development, sexual steroids, and lipid reserves in a population of the lizard *Psammodromus algirus*. *Journal of Herpetology* **28**, 199-205.

Dubois, W., Pudney, J., and Callard, I.P. (1988) The annual testicular cycle in the turtle *Chrysemys picta*: A histochemical and electron microscopic study. *General and Comparative Endocrinology* **71**, 191-204.

Duda, P.L. (1980) The effect of testesterone on female gecko *Hemidactylus flaviviridis*. *Current Science* **49**, 638-639.

Duda, P.L., and Annalakshmi, M. (1982) Size relationship between growing oocytes and their nuclei in two gekkonine lizards. *Amphibia-Reptilia* **3**, 231-236.

Dufaure, J.P. (1971) L'ultrastructure du testicule de lézard vivipare (Reptile, Lacertilien). II. Les cellules de Sertoli. Etude du glycogène. *Zeitschrift für Zellforschung und Mikroskopische Anatomie* **115**, 565-578.

Dufaure, J.P., and Hubert, J. (1961) Table de développment du lézard vivipare: *Lacerta* (*Zootoca*) *vivipara* Jaquin. *Archives d'Anatomie Microscopique et de Morphologie Expérimentale* **50**, 309-328.

Dufaure, J.P., and Saint-Girons, H. (1984) Histologie comparée de l'epididyme et de ses secretions cheztles reptiles (lézards et serpentes). *Archives d'Anatomisches Microskopische* **73**, 15-26.

Dunham, A.E., and Miles, D.B. (1985) Patterns of covariation in life history traits of squamate reptiles: the effects of size and phylogeny reconsidered. *American Naturalist* **126**, 231-257.

Dunlap, K.D., and Wingfield, J.C. (1995) External and internal influences on indices of physiological stress. 1. Seasonal and population variation in adrenocortical secretion of free-living lizards, *Sceloporus occidentalis*. *Journal of Experimental Zoology* **271**(36-46).

Duvall, D., Guillette, L.J., Jr., and Jones, R.E. (1982) Environmental control of reptilian reproductive cycles. In 'Biology of the Reptilia. Vol. 13. Physiology D.' (Eds. C Gans and FH Pough) pp. 201-231. (Academic Press: London).

Eckstut, M.E., Lemons, E.R., and Sever, D.M. (2009) Annual dynamics of sperm production and storage in the Mediterranean gecko, *Hemidactylus turcicus*, in the southeastern United States. *Amphibia-Reptilia* **30**, 45-56.

Edwards, A., and Jones, S.M. (2001a) Changes in Plasma Progesterone, Estrogen, and Testosterone Concentrations throughout the Reproductive Cycle in Female Viviparous Blue-Tongued Skinks, *Tiliqua nigrolutea* (Scincidae), in Tasmania. *General and Comparative Endocrinology* **122**, 260-269.

Edwards, A., and Jones, S.M. (2001b) Changes in plasma testosterone, estrogen and progesterone concentrations throughout the annual reproductive cycle in male viviparous blue-tongued skinks, *Tiliqua nigrolutea*, (Scincidae), in Tasmania. *Journal of Herpetology* **35**, 293-299.

Edwards, A., and Jones, S.M. (2003) Mating behaviour in the blotched blue-tongued lizard, *Tiliqua nigrolutea*, in captivity. *Herpetofauna* **33**, 60-64.

Edwards, A., Jones, S.M., and Wapstra, E. (2002) Multiennial reproduction in females of a viviparous skink, *Tiliqua nigrolutea*. *Herpetologica* **58**, 407-414.

Ellmann, S., Sticht, H., Thiel, F., Beckmann, M. W., Strick, R., and Strissel, P. L. (2009) Estrogen and progesterone receptors: from molecular structures to clinical targets. *Cellular and Molecular Life Sciences,* **66**, 2405-2426.

Elsevierdirect.com (2012) http://www.elsevierdirect.com/companions/ 9780123743466/images/04~Chapter%2004.ppt.

Endriss, D.A., Hellgren, E.C., Fox, S.F., and Moody, R.W. (2007) Demography of an urban population of the Texas horned lizard (*Phrynosoma cornutum*) in central Oklahoma. *Herpetologica* **63**, 320-331.

Ergün, S., Ungefroren, H., Holstein, A.F., and Davidoff, M.S. (1997) Estrogen and progesterone receptors and estrogen receptorrelated antigen (ER-D5) in human epididymis. *Molecular Reproduction and Development* **47**, 448-455.

Etches, R.J., and Petitte, J.N. (1990) Reptilian and avian follicular hierarchies: models for the study of ovarian development. *Journal of experimental Zoology Supplement* **4**, 112-122.

Everett, J.W. (1988) Pituitary and hypothalamus: perspectives and overview. In 'The Physiology of Reproduction.' (Eds. E Knobil and JD Neill) pp. 1143-1159. (Raven Press: New York).

Eyeson, K.N. (1971) The role of the pituitary gland in testicular function in the lizard *Agumu aguma*. *General and Comparative Endocrinology* **16**, 342-355.

Fawcett, D.W. (1970) A comparative view of sperm ultrastructure. *Biology of Reproduction (Supplement)* **2**, 90-127.

Fawcett, D.W., Anderson, W.A., and Phillips, D.M. (1971) Morphogenetic factors influencing the shape of the sperm head. *Developmental Biology*. **26**, 220-251.

Ferreira, A., and Dolder, H. (2003a) Cytochemical study of spermiogenesis and mature spermatozoa in the lizard *Tropidurus itambere* (Reptilia, Squamata). *Acta Histochemica* **105**, 339–352.

Ferreira, A., and Dolder, H. (2003b) Sperm ultrastructure and spermatogenesis in the lizard, *Tropidurus itambere*. *Biocell* **27**, 353-362.

Ferreira, A., Laura, I.A., and Dolder, H. (2002) Reproductive cycle of male green iguanas, *Iguana Iguana* (Reptilia: Sauria: Iguanidae), In the Pantanal Region of Brazil. *Brazilian Journal of Morphological Sciences* **19**, 23-28.

Ferreira, A., Silva, D.N., van Sluys, M., and Dolder, H. (2009) Seasonal changes in testicular and epididymal histology of the tropical lizard, *Tropidurus itambere* (Rodrigues, 1987), during its reproductive cycle. *Brazilian Journal of Biology* **69**, 429-435.

Filosa, S., Taddei, C., and Andreuccetti, P. (1979) The differentiation and proliferation of the follicle cells during oocyte growth in *Lacerta sicula*. *Journal of Embryology & Experimental Morphology* **5**, 5-15.

Fitch, H.S. (1970) Reproductive cycles in lizards and snakes. *Miscellaneous publication - University of Kansas, Museum of Natural History* **52**, 1-247.

Flemming, A.F. (1993) The male reproductive cycle of the lizard *Pseudocordylus. m. melanotus* (Sauria: Cordylidae). *Journal of herpetology* **27**, 473-478.

Flemming, A.F. (1994) Male and female reproductive cycles of the viviparous lizard, *Mabuya capensis* (Sauria: Scincidae) from South Africa. *Journal of Herpetology* **28**, 334-341.

Foreman, D. (1997) Seminiferous tubule stages in the prairie dog (*Cynomys ludovicianus*) during the annual breeding cycle. *Anatomical Record*. **247**, 355-367.

Fox, H. (1977) The urogenital system of reptiles. In 'Biology of Reptilia. Vol. 6.' (Eds. C Gans and TS Parson) pp. 1-158. (Academic Press: New York).

Fox, S.L., and Guillette, L.J., Jr. (1987) Luteal morphology, atresia, and plasma progesterone concentrations during reproductive cycle of two oviparous lizards, *Crotaphytus collaris* and *Eumeces obsoletus*. *American Journal of Anatomy* **179**, 324-332.

Frieden, E., and Lippner, H. (1971) 'Biochemical endocrinology of the vertebrates.' (Prentice-Hall: New Jersey, USA).

Furieri, P. (1970) Sperm morphology in some reptiles: Squamata and Chelonia. In 'Comparative Spermatology. Vol. 115-132.' (Ed. B accetti). (Academic Press Inc. : New York).

Gabri, M.S. (1983) Seasonal changes in the ultrastructure of the kidney collecting tubules in the lizard *Podacris (=Lacerta) taurica*. *Journal of Morphology* **175**, 143-151.

Gaitonde, S.G., and Gouder, B.Y.M. (1981) Effect of hypophysectomy on spermatogenesis, interstitial Leydig cells and male accessory organs in the garden lizard, *Calotes versicolor*. *Indian Journal of Experimental Biology* **19**, 314-318.

Gaitonde, S.G., and Gouder, B.Y.M. (1985) Spermatogenetic and steroidogenic activity in the testis of the lizard, *Calotes versicolor*, treated with mammalian gonadotropins and testosterone. *Bollettino di Zoologia* **52**, 393-405.

Ganesh, C.B., and Yajurvedi, H.N. (2002) Stress inhibits seasonal and FSH-induced ovarian recrudescence in the lizard *Mabuya carinata*. *Journal of Experimental Zoology* **292**, 640-648.

Gavaud, J. (1986) Vitellogenesis in the lizard *Lacerta vivipara* Jacquin. II. Vitellogenin synthesis during the reproductive cycle and its control by ovarian steroids. *General and Comparative Endocrinology* **63**, 11-23.

Gemmell, R.T. (1995) A comparative study of the corpus luteum. *Reproduction, Fertility and Development* **7**, 303-312.

Giannoukos, G., and Callard, I.P. (1996) Radioligand and immunochemical studies of turtle oviduct progesterone and estrogen receptors: correlations with hormone treatment and oviduct contractility. *General and Comparative Endocrinology* **101**, 63-75.

Giannoukos, G., Coho, D.W., and Callard, I.P. (1995) Turtle oviduct progesterone receptor: Radioligand and immunocytochemical studies of changes during the seasonal cycle. *Endocrine* **3**, 429-437.

Gilbert, S.F. (1997) 'Developmental biology.' 5 edn. (MA: Sinauer: Sunderland).

Girling, J.E. (2002) The reptilian oviduct: A review of structure and function and directions for future research. *Journal of Experimental Zoology* **293**, 141-170.

Girling, J.E., and Cree, A. (1995) Plasma corticosterone levels are not significantly related to reproductive stage in female common geckos (*Hoplodactylus maculatus*). *General and Comparative Endocrinology* **100,**, 273-281.

Girling, J.E., Cree, A., and Guillette, L.J., Jr. (1997) Oviductal structure in a viviparous New Zealand gecko, *Hoplodactylus maculate*. *Journal of Morphology* **234**, 51-68.

Girling, J.E., Cree, A., and Guillette, L.J., Jr. (1998) Oviducal structure in four species of gekkonid lizard differing in parity mode and eggshell structure. *Reproduction Fertility and Development* **10**, 139-154.

Girling, J.E., Guillette, L.J., Jr., and Cree, A. (2000) Ultrastructure of the uterus in an ovariectomized gecko (*Hemidactylus turcicus*) after administration of exogenous estradiol. *Journal of Experimental Zoology* **286**, 76-89.

Gist, D.H. (1998) Male reproductive system, reptiles. In 'Encyclopedia of Reproduction.' (Eds. E Knobil and J Neill) pp. 60-70. (Academic Press: New York).

Gist, D.H., Bradshaw, S., Morrow, C.M.K., Congdon, J.D., and Hess, R.A. (2007) Estrogen response system in the reproductive tract of the male turtle: An immunocytochemical study. *General and Comparative Endocrinology* **151**, 27-33.

Gist, D.H., Dawes, S.M., Turner, T.W., Sheldon, S., and Congdon, J.D. (2001) Sperm storage in turtles: a male perspective. *Journal of Experimental Zoology* **292**, 180-186.

Giugliano, L.G., Teixeira, R.D., Colli, G.R., and Báo, S.N. (2002) Ultrastructure of spermatozoa of the lizard *Ameiva ameiva*, with considerations on polymorphism within the family Teiidae (Squamata). *Journal of Morphology* **253**, 264-271.

Gobbetti, A., Zerani, M., Di Fiore, M.M., and Botte, V. (1994) Relationships among GnRH, substance P, prostaglandins, sex steroids and aromatase activity in the brain of the male lizard *Podarcis sicula sicula* during reproduction. *Journal of Reproduction and Fertility* **101**, 523-529.

Godwin, J., and Crews, D. (2002) Hormones, brain, and behavior in reptiles. In 'Hormones, Brain and Behavior. Vol. 2.' (Eds. DW Pfaff, AP Arnold, AM Etgen, SE Fahrbach and RT Rubin) pp. 545-585. (Academic Press: New York).

Godwin, J., Hartman, V.M., Grammer, M., and Crews, D. (1996) Progesterone inhibits female-typical receptive behaviour and decreases hypothalamic estrogen and progesterone receptor messenger ribonucleic acid levels in whiptail lizards (Genus *Cnemidophorus*). *Hormones and Behavior* **30**, 138-144.

Goldberg, S.R. (1972) Reproduction in the southern Alligator Lizard, *Gerrhonatus multicarinatus*. *Herpetologica* **28**, 267-73.

Goldberg, S.R., and Lowe, C.R. (1966) The reproductive cycle of the western whiptail lizard (*Cnemidophorus tigris*) in southern Arizona. *Journal of Morphology* **118**, 543-548.

Goldbergs, R., and Lowe, C.H. (1997) Reproductive cycle of the gila monster, *Heloderma suspectum*, in Southern Arizona. *Journal of Herpetology* **31**, 161-166.

Gómez, D., and Ramírez-Pinilla, M.P. (2004) Ovarian histology of the placentotrophic *Mabuya mabouya* (Squamata. Scincidae). *Journal of Morphology* **259**, 90-105.

Googleearth.com (2012) http://www.google.com/earth/index.html.

Gouder, B.Y.M., and Nadkarni, V.B. (1976) Steroid synthesizing cellular sites in the ovaries of *Calotes vesicolor* (Daud.), *Hemidactylus flaviviridis* (Ruppel) and *Chamaeleon calcaratus* (Boulenger): Histochemical study. *Indian Journal of Experimental Biology* **14**, 647-651.

Gouder, B.Y.M., and Rao, M.A. (1979) Histological and histochemical studies on follicular atresia in the ovary of the lizard *Calotes versicolor*. *Journal of Herpetology* **13**, 451-456.

Grassman, M., and Crews, D. (1990) Ovarian and adrenal function in the parthenogenetic whiptail lizard *Cnemidophorus uniparens* in the field and laboratory. *General and Comparative Endocrinology* **76**, 444-450.

Gray, J.E. (1825) A synopsis of the species of the class Reptilia. In 'The animal kingdom arranged in conformity with its organization by the Baron Cuvier. Vol. 9.' (Eds. E Griffith and E Pidgeon) pp. 1-110. (Treacher and Co: London).

Greenberg, N., Chen, T., and Crews, D. (1984) Social status, gonadal state, and the adrenal stress response in the lizard, *Anolis carolinensis*. *Hormones and behavior* **18**, 1-11.

Greenberg, N., and Wingfield, J. (1987) Stress and reproduction: reciprocal relationships. In 'Hormones and Reproduction in Fishes, Amphibians and Reptiles.' (Eds. DO Norris and RE Jones) pp. 461-503. (Plenum Press: New York).

Gribbins, K.M., Rheubert, J.L., Collier, M.H., Siegel, D.S., and Sever, D.M. (2008) Histological analysis of spermatogenesis and the germ cell development strategy within the testis of the male Western Cottonmouth Snake, *Agkristrodon piscivorous leucostoma*. *Annals of Anatomy* **190**, 461-476.

Gribbins, K.M., Elsey, R.M., and Gist, D.H. (2006) Cytological evaluation of the germ cell development strategy within the testes of the American Alligator, *Alligator mississippiensis*. *Acta Zoologica* **87**, 59-69.

Gribbins, K.M., and Gist, D.H. (2003) Cytological evaluation of spermatogenesis within the germinal epithelium of the male European Wall Lizard, *Podarcis muralis*. *Journal of Morphology* **258**, 296–306.

Gribbins, K.M., Gist, D.H., and Congdon, J.D. (2003) The cytological evaluation of spermatogenesis and organization of the germinal epithelium in the male slider turtle, *Trachemys scripta*. *Journal of Morphology* **255**, 337-346.

Gribbins, K.M., Happ, C.S., and Sever, D.M. (2005) Ultrastructure of the reproductive system of the Black Swamp Snake (*Seminatrix pygaea*). V. The temporal germ cell development strategy of the testis. *Acta Zoologica* **86**, 223-230.

Gribbins, K.M., Mills, E.M., and Sever, D.M. (2007) Ultrastructural examination of spermiogenesis within the testis of the Ground Skink, *Scincella laterale* (Squamata, Sauria, Scincidae). *Journal of Morphology* **268**, 181-192.

Griswold, M.D. (1988) Protein secretions of Sertoli cells. *International Review of Cytology* **110**, 133-156.

Guarino, F.M., Paulesu, L., Cardone, A., Bellini, L., Ghiara, G., and Angelini, F. (1998) Endocrine activity of the corpus luteum and placenta during pregnancy in *Chalcides chalcides* (Reptilia, Squamata). *General and Comparative Endocrinology* **111**, 261-270.

Guerrero, S.M., Calderón, M.L., De Pérez, G.R., and Ramirez- Pinilla, M.P. (2004) Morphology of male reproductive duct system of *Caiman crocodilus* (Crocodilia, Alligatoridae). *Annals of Anatomy* **186**, 235-245.

Guillette, L.J., Jr., and Casas-Andreu, G. (1987) The reproductive biology of the high elevation Mexican lizard, *Barisiaim bricata*. *Herpetologica* **43**, 29-38.

Guillette, L.J., Jr., Cree, A., and Rooney, A.A. (1995) Biology of stress: Interaction with reproduction, immunology and intermediary metabolism. In 'Health and welfare of captive reptiles.' (Eds. C Warwick, FL Frye and JB Murphy) pp. 33-81. (Chapman & Hall: London).

Guillette, L.J., Jr., Demarco, V., and Palmer, B.D. (1991) Exogenous progesterone or indo-methacin delays parturition in the viviparous lizard *Sceloporus jarrovi*. *General and Comparative Endocrinology* **81**, 105-112.

Guillette, L.J., Jr., and Fox, S.L. (1985) Effect of deluteinization on plasma progesterone concentration and gestation in the lizard, *Anolis carolinensis*. *Comparative Biochemistry and Physiology* **80A**, 303-306.

Guillette, L.J., Jr., Fox, S.L., and Palmer, B.D. (1989) Oviductal morphology and egg shelling in the oviparous lizards *Crotaphytus collaris* and *Eumeces obsoletus*. *Journal of Morphology* **201**, 145-159.

Guillette, L.J., Jr., Speilvogel, S.S., and Moore, F.L. (1981) Luteal development, placentation and plasma progesterone concentration in the viviparous lizard *Sceloporus jarrovi*. *General and Comparative Endocrinology* **43**, 20-29.

Guillette, L.J., Jr., Woodward, A.R., Crain, D.A., Masson, G.R., Palmer, B.D., Cox, M.C., You-Xiang, Q., and Orlando, E. (1997) The reproductive cycle of the female American alligator (*Alligator mississippiensis*). *General and Comparative Endocrinology* **108**, 87-101.

Guimaráes, A.C.D., and Quagio-Grassiotto, I. (2005) Cytochemical characterization of the endomembranous system during the oocyte primary growth in *Serrasalmus spilopleura* (Teleostei. Characiformes, Characidae). *Tissue Cell* **37**, 413-422.

Guimaráes, A.C.D., and Quagio-Grassiotto, I. (2008) Cytochemical characterization of the endomembranous system during oocyte secondary growth in *Serrasalmus spilopleura* (Teleostei. Characiformes, Characidae). *Acta Zoologica (Stockholm)* **89**, 37-46.

Guraya, S.S. (1968) A histochemical study of lipids in goat testis. *Acta morphologica Neerlando-Scandinavica* **7**, 15-27.

Guraya, S.S. (1971) Morphology, histochemistry and biochemistry of human ovarian compartments and steroid hormone synthesis. *Physiological Reviews* **51**, 785-807.

Guraya, S.S. (1978) Maturation of the follicular wall of nonmammalian vertebrates. In 'The Vertebrate Ovary: Comparative Biology and Evolution.' (Ed. RE Jones) pp. 261-329. (Plenum Press: New York).

Guraya, S.S. (1989) 'Ovarian follicles in reptiles and birds.' (Springer: Berlin).

Guraya, S.S., and Varma, S.K. (1976) Morphology of Ovarian Changes during the Reproductive Cycle of the House Lizard, *Hemidactylus flaviviridis*. *Acta Morphologica Neerlando-Scandinavica* **14**, 165-192.

Gutierrez, L.S., and Yapur, L.B. (1983) Spermiogenesis of the lizard *Liolaemus darwini*: an ultrastructural and cytochemical study. *Microscopia Electronica Y Biologia Celular* **7**, 57-71.

Haider, S. (1985a) The effect of castration and testosterone replacement on the histology and histochemistry of the epididymis in the Indian wall lizard *Hemidactylus flaviviridis* (Ruppell). *Monitore Zoologico Italiano (N.S.)* **19**, 189-195.

Haider, S. (1985b) Effect of season, ovariectomy and mammalian gonadotropins on the oviduct of Indian wall lizard *Hemidactylus flaviviridis* (Rüppell). *Archives d'Anatomie, d'Histologie et d'Embryologie Normales et Expérimentales* **68**, 119-126.

Haider, S., and Rai, U. (1986) Effect of cyproterone acetate and flutamide on the testis and epididymis of the Indian wall lizard, *Hemidactylus flaviviridis* (Ruppell). *General and Comparative Endocrinology* **64**, 321-329.

Haider, S., and Rai, U. (1987) Epididymis of the Indian wall lizard (*Hemidactylus flaviviridis*) during the sexual cycle and in response to mammalian pituitary gonadotropins and testosterone. *Journal of Morphology* **191**, 151-160.

Haider, S.G. (2004) Cell biology of Leydig cells in the testis. *International Review of Cytology* **233**, 181-241.

Haider, S.G. (2004) Cell biology of Leydig cells in the testis. *International Review of Cytology* **233**, 181-241.

Haimenoonline.com (2012) http://www.haimenonline.com/countries/oman-map.html/attachment/oman.

Hamilton, D.W., and Fawcett, D.W. (1968) Unusual features of the neck and middle-piece of snake spermatozoa. *Journal of Ultrastructure Research* **23**, 81-97.

Hammouche, S., Gernigon, T., and Exbrayat, J.M. (2007) Immunolocalization of estrogens and progesterone receptors within the ovary of the lizard *Uromastyx acanthinura* from vitellogenesis to rest season. *Folia Histochemica et Cytobiologica* **45**(Supp. 1), 23-27.

Han, D., Zhou, K., and Bauer, A.M. (2004) Phylogenetic relationships among gekkotan lizards inferred from c-mos nuclear DNA sequences and a new classification of the Gekkota. *Biological Journal of the Linnean Society* **83**, 353-368.

Healy, J.M., and Jamieson, B.G.M. (1992) Ultrastructure of spermatozoon of the tuatara (*Sphenodon punctatus*) and is relevance to the relationships of the Sphenodontida. *Philosophical Transactions of the Royal Society of London* **335B**, 193-205.

Heatwole, H., and Taylor, J. (1987) Reproductive ecology. In 'Ecology of Reptiles.' (Ed. H Heatwole) pp. 147-166. (Surrey Beatty and Sons Pty Ltd: N.S.W. Australia).

Henkel, F.-W. (2003) Herpetological expedition through Oman. *Reptilia (GB)* **27**, 50-55.

Herbert, J. (1995) Stress and reproduction: The role of peptides and other chemical messengers in the brain. *Current Science* **68**, 391-400.

Herkules.oulu.fi (2012) (http://herkules.oulu.fi/isbn951426844X/html/i232204.html.

Hermo, L., and Robaire, B. (2002) Epididymal cell types and their functions. In 'The epididymis: from molecules to clinical practice '. (Eds. B Robaire and BT Hinton) pp. 81-102. (Kluwer Academic/Plenum Publishers: New York).

Hernández-Franyutti, A., Uribe, A.M.C., and Guillette, L.J., Jr. (2005) Oogenesis in the viviparous matrotrophic lizard *Mabuya brachypoda*. *Journal of Morphology* **265**, 152-164.

Hernández-Gallegos, O., Méndez-De La Cruz, F.R., Villagrán-Santa Cruz, M., and Andrews, R.M. (2002) Continuous Spermatogenesis in the Lizard *Sceloporus bicanthalis* (Sauria: Phrynosomatidae) from High Elevation Habitat of Central Mexico. *Herpetologica* **58**, 415-421.

Highfill, D.R., and Mead, R.A. (1975) Sources and levels of progesterone during pregnancy in the garter snake, *Thamnophis elegans*. *General and Comparative Endocrinology* **27**, 389-400.

Hikida, T. (1981) Reproduction of the Japanese Skink (*Eumeces latiscutatus*) in Kyoto. *Zoological Magazine* **90**, 85-92.

Ho, S.-M. (1987) Endocrinology of vitellogenesis. In 'Hormones and Reproduction in Fishes, Amphibians, and Reptiles'. (Eds. DO Norris and RE Jones) pp. 145-169. (Plenum Press: New York).

Ho, S.-M., Kleis, S., McPherson, R., Heisermann, G.J., and Callard, I.P. (1982) Regulation of vitellogenesis in reptiles. *Herpetologica* **38**, 40-50.

Holmes, H.J., and Gist, D.H. (2004) Excurrent duct system of the male turtle *Chrysemys picta*. *Journal of Morphology* **261**, 312-322.

Holmes, K.M., and Cree, A. (2006) Annual reproduction in females of a viviparous skink (*Oligosoma maccanni*) in a subalpine environment. *Journal of Herpetology* **40**, 141-151.

Http://www.thepepproject.net. (2003) Pharmacology Education Partnership: Steroids and athletes: Genes work overtime. 6, 9-10.

Hu, J.R., Du, J.Z., and Ji, X. (2004) Pattern of plasma sex steroid hormone levels during the breeding season of male and female skink: *Eumeces chinensis*. *Shi Yan Sheng Wu Xue Bao* **37**, 443-448.

Huang, H.F.S., Pogach, L.M., Nathan, E., Giglio, W., and Seebode, J. (1991) Synergistic effects of follicle-stimulating hormone and testosterone on the maintenance of spermatogenesis in hypophysectomised rats: relationship with the androgen-binding protein status. *Endocrinology* **128**, 3152-3161.

Huang, W.S. (1996) Reproductive cycles and sexual dimorphism in the viviparous skink, *Sphenmorphis indicus* (Suaria: Scincidae), from Wushe, Central Taiwan. *Zoological Studies* **35**, 55-61.

Huang, W.S. (1997) Reproductive cycle of the oviparious lizard *Japalura brevipes* (Agamidae: Reptilia) in Taiwan, Republic of China. *Journal of Herpetology* **31**, 22-29.

Hubert, J. (1985) Origin and development of oocytes. In 'Biology of the Reptilia. Vol. 14.' (Ed. C Gans) pp. 41-74. (John Wiley & Sons: New York).

Huey, R.B., Deutsch, C.A., Tewksbury, J.J., Vitt, L.J., Hertz, P.E., Álvarez Pérez, H.J., and Garland, T., Jr. (2009) Why tropical forest lizards are vulnerable to climate warming. *Proceedings of the Royal Society B* **276**, 1939-1948.

Hughes, I. A. (1984) Steroid hormone receptors. *Archives of disease in childhood*, **59**, 498-500.

Ibrahim, A.A. (2000) Geographic distribution. *Hemidactylus flaviviridis*. *Herpetological Review* **31**, 185.

Ikeuchi, I. (2004) Male and female reproductive cycles of the Japanese gecko, *Gekko japonicus*, in Kyoto, Japan. *Journal of Herpetology* **38**, 269-274.

Jaglarz, M.K., Nowak, Z., and Bilinski, S.M. (2003) The Balbiani body and generation of early asymmetry in the oocyte of a tiger beetle. *Differentiation* **71**, 142-151.

James, C., and Shine, R. (1985) The seasonal timing of reproduction: a tropical-temperate comparison in Australian lizards. *Oecologia* **67**, 464-474.

Jamieson, B.G.M. (1995) The ultrastructure of spermatozoa of the Squamata (Reptilia) with phylogenetic considerations. In 'Advances in Spermatozoal Phylogeny and Taxonomy. Vol. 166.' (Eds. BGM Jamieson, J Ausio and J-L Justine) pp. 359-383. (Mémoires du Muséum national d'Histoire Naturelle,: Paris).

Jamieson, B.G.M. (1999) Spermatozoal phylogeny of the Vertebrata. In 'The Male Gamete: From Basic Science to Clinical Applications.' (Ed. C Gagnon) pp. 303-331. (Cache River Press: Vienna, USA).

Jamieson, B.G.M., and Healy, J.M. (1992) The phylogenetic position of the Tuatara, Sphenodon (Sphenodontida, Amniota), as indicated by cladistic analysis of the ultrastructure of spermatozoa. *Philosophical Transactions of the Royal Society of London* **335B**, 207-219.

Jamieson, B.G.M., Oliver, S.C., and Scheltinga, D.M. (1996) The ultrastructure of the spermatozoa of squamata. I. Scincidae, Gekkonidae, and Pygopodidae (Reptilia). *Acta Zoologica (Stockholm)* **77**, 85-100.

Jamieson, B.G.M., and Scheltinga, D.M. (1993) The ultrastructure of spermatozoa of *Nangura spinosa* (Scincidae, Reptilia). *Memoirs of the Queensland Museum* **34**, 169-179.

Jamieson, B.G.M., Scheltinga, D.M., and Tucker, A.D. (1997) The ultrastructure of spermatozoa of the Australian freshwater crocodile, *Crocodylus johnstoni* Krefft, 1873 (Crocodylidae, Reptilia). *Journal of Submicroscopic Cytology and Pathology* **29**, 265-274.

JCVI/TIGRl, R.D. (2012) http://www.reptile-database.org/ db-info/SpeciesStat.html. Accessed 24 December 2011).

Jenssen, T.A., and Nunez, S.C. (1994) Male and female reproductive cycles of the Jamaican lizard, *Anolis opalinus*. *Copeia*, 767-780.

Jimènez-Cruz, E., Ramírez-Bautista, A., Marshall, J.C., Lizana-Avia, M., and Nieto-Montes De Oca, A. (2005) Reproductive cycle of *Sceloporus grammicus* (Squamata: Phrynosomatidae) from Teotihuacán, México. *Southwestern Naturalist* **50**, 178-187.

Johnson, L.F., Jacob, J.S., and Torrance, P. (1982) Annual testicular and androgenic cycles of the cottonmouth (Agkistrodon piscivorus) in Alabama. *Herpetologica* **38**, 16-25.

Johnson, M.A., Cohen, R.E., Vandecar, J.R., and Wade, J. (2011) Relationships among reproductive morphology, behavior, and testosterone in a natural population of green anole lizards. *Physiology & Behavior* **104**, 437-45.

Johnston, H., Baker, P.J., Abel, M., Charlton, H.M., Jackson, G., Fleming, L., Kumar, T.R., and O'Shaughnessy, P.J. (2004) Regulation of Sertoli cell number and activity by follicle-stimulating hormone and androgen during postnatal development in the mouse. *Endocrinology* **145**, 318-329.

Jones, R.C. (1998) Evolution of the vertebrate epididymis. *Journal of Reproduction and Fertility (Supplement)* **53**, 163-181.

Jones, R.C. (2002) Evolution of the vertebrate epididymis. In 'The Epididymis: From Molecules to Clinical Practice.' (Eds. B Robaire and BT Hinton) pp. 11-33. (Kluwer Academic/ Plenum Publishers: New York).

Jones, R.E. (1978) Control of follicular selection. In 'The Vertebrate Ovary-Comparative Biology and Evolution.' (Ed. RE Jones) pp. 763-787. (Plenum Press: New York).

Jones, R.E., and Baxter, D.C. (1991) Gestation with emphasis on Corpus luteum biology, placentation and parturition. In 'Vertebrate Endocrinology: Fundamentals and Biomedical Implications Vol. 4.' (Eds. PKT Pang and MP Schreibman) pp. 238–244. (Academic Press: New York).

Jones, R.E., and Guillette, L.J., Jr. (1982) Hormonal control of oviposition and parturition in Lizards. *Herpetologica* **38**, 80-93.

Jones, R.E., Swain, T., Guillette, L.J., Jr., and Fitzgerald, K.T. (1982) The comparative anatomy of lizard ovaries, with emphasis on the number of germinal beds. *Journal of Herpetology* **16**, 248-252.

Jones, S.M. (2011) Hormonal Regulation of Ovarian Function in Reptiles. In 'Hormones and Reproduction of Vertebrates. Vol. 3.' (Eds. DO Norris and KH Lopez) pp. 89-115. (Academic Press: San Diego).

Jones, S.M., and Swain, R. (1996) Annual reproductive cycle and annual cycles of reproductive hormones in plasma of female *Niveoscincus metallicus* from Tasmania. *Journal of herpetology* **30**, 140-146.

Jones, S.M., and Swain, R. (2000) Effects of exogenous FSH on follicular recruitment in a viviparous lizard *Niveoscincus metallicus* (Scincidae). *Comparative Biochemistry and Physiology* **127A**, 487-493.

Jones, S.M., Wapstra, E., and Swain, R. (1997) Asynchronous male and female gonadal cycles and plasma steroid concentrations in a viviparous lizard, *Niveoscincus ocellatus* (Scincidae), from Tasmania. *General and Comparative Endocrinology* **108**, 271–281.

Joss, J.M.P. (1985) Ovarian steroid production in oviparous lizards of the genus *Lampropholis* (Scincidae). In 'Biology of Australasian Frogs and Reptiles.' (Eds. G Grigg, R Shine and H Ehmann) pp. 319-326. (Royal zoological society of New South Wales).

Katsu, Y., Ichikawa, R., Ikeuchi, T., Kohno, S., Guillette, L. J., Jr., and Iguchi, T. (2008) Molecular cloning and characterization of estrogen, androgen, and progesterone nuclear receptors from a freshwater turtle (*Pseudemys nelsoni*). *Endocrinology* **149**, 161-173.

Katsu, Y., Matsubara, K., Kohno, S., Matsuda, Y., Toriba, M., Oka, K., et al. (2010) Molecular cloning, characterization, and chromosome mapping of reptilian estrogen receptors. *Endocrinology*, **151**, 5710-5720.

Kearney, M., Shine, R., and Porter, W.P. (2009) The potential for behavioral thermoregulation to buffer ‘‘cold-blooded’’ animals against climate warming. *Proceedings of the National Academy of Sciences of USA* **106**, 3835-3840.

Khan, U.W., and Rai, U. (2004) In Vitro Effect of FSH and Testosterone on Sertoli Cell Nursing Function In Wall Lizard *Hemidactylus flaviviridis* (Ruppell). *General and Comparative Endocrinology* **136**, 225-231.

Khan, U.W., and Rai , U. (2005) Endocrine and Paracrine Control of Leydig Cell Steroidogenesis and Proliferation in the Wall Lizard: An In Vitro Study. *General and Comparative Endocrinology* **140**, 109-115.

Khan, U.W., and Rai, U. (2008) Paracrine role of testicular macrophages in control of leydig cell activities in the wall lizard, *Hemidactylus flaviviridis*. *General and Comparative Endocrinology* **156**, 44-50.

Kime, D.E. (1987) The steroids. In 'Fundamentals of Comparative Vertebrate Endocrinology.' (Eds. I Chester-Jones, PM Ingleton and JG Philips) pp. 3-56. (Plenum Press: New York).

Kleis-San Francisco, S.K., and Callard, I.P. (1986) Progesterone receptors in the oviduct of a viviparous snake (*Nerodia*): Correlations with ovarian function and plasma steroid levels. *General and Comparative Endocrinology* **63**, 220-229.

Klicka, J., and Mahmoud, I.Y. (1973) Conversion of cholesterol to progesterone by turtle corpus luteum. *Steroids* **21**, 483–495.

Klicka, J., and Mahmoud, I.Y. (1977) The effects of hormones on the reproductive physiology of the painted turtle, *Chrysemys picta*. *General and Comparative Endocrinology* **31**, 407-413.

Klosterman, L.L. (1983) The ultrastructure of germinal beds in the ovary of *Gerrhonotus coeruleus* (Reptilia: Anguidae). *Journal of Morphology* **178**, 247-266.

Klosterman, L.L. (1987) Ultrastructural and quantitative dynamics of the granulosa of ovarian follicles of the lizard *Gerrhonotus coeruleus* (family Anguidae). *Journal of Morphology* **192**, 125-144.

Kluge, A.G. (2001) Gekkotan lizard taxonomy. *Hamadryad* **26**, 1-209.

Klukowski, M. (2011) Effects of breeding season, testosterone and ACTH on the corticosterone response of free-ranging male fence lizards (*Sceloporus undulatus*). *General and Comparative Endocrinology* **173**, 295-302.

Kousteni, S., Bellido, T., Plotkin, L. I., O'Brien, C. A., Bodenner, D. L., Han, L., et al. (2001) Nongenotropic, sex-nonspecific signaling through the estrogen or androgen receptors: dissociation from transcriptional activity. *Cell*, **104**, 719-730.

Krause, W.J. (1996) Meiosis and male reproductive organs. In 'Essentials of Human Histology.' (Ed. W Krause). (Brown and Company: Little)

Kreger, M.D., and Mencsh, J.A. (1993) Physiological and behavioral effects of handling and restraint in the ball python (*Python regius*) and the blue-tongued skink (*Tiliqua scincoides*). *Applied Animal Behaviour Science* **38**, 323-336.

Krohmer, R.W. (1986) Effects of mammalian gonadotropins (oFSH and oLH) on testicular development in the immature water snake, *Nerodia sipedon*. *General and Comparative Endocrinology* **64**, 330-338.

Krohmer, R.W. (2004) Variation in seasonal ultrastructure of sexual granules in the renal sexual segment of the northern water snake, *Nerodia sipedon sipedon*. *Journal of Morphology* **261**, 70–80.

Kuchling, G.R., Skolek-Winnishch, R., and Bamber, E. (1981) Histochemical and biochemical investigation on the annual cycle of testis, epididymis, and plasma testosterone of the tortoise, *Testudo hermanni hermanni* Gmelin. *General and Comparative Endocrinology* **44**, 194-201.

Kumar, M. (1995) Spermatogenesis in the house sparrow, *Passar domesticus*: histological observations. *Pavo* **33**, 1-4.

Kumar , S., Roy, B., and Rai, U. (2011) Hormonal Regulation of Testicular Functions in Reptiles. In 'Hormones and Reproduction of Vertebrates. Vol. 3 '. (Eds. DO Norris and KH Lopez) pp. 63-88. (Academic Press: San Diego).

Kumari, T.R.S., Sarkar, H.B.D., and Shivandappa, T. (1990) Histology and histochemistry of the oviductal sperm storage pockets of the agamid lizard *Calotes versicolor*. *Journal of Morphology* **203**, 97-106.

LaDage, L.D., Gutzke, W.H.N., Simmons, R.A., II, and Ferkin, M.H. (2008) Multiple mating increases fecundity, fertility and relative clutch mass in the female leopard gecko (*Eublepharis macularius*). *Ethology* **114**, 512-520.

Lance, V. (1984) Endocrinology of reproduction in male reptiles. *Symposia of the Zoological Society of London.* **52**, 357-383.

Lance, V.A. (1998) Reptilian reproductive cycles. In 'Encyclopedia of Reproduction.' (Eds. E Knobil and J Neill) pp. 260-265. (Academic Press: New York).

Lance, V.A., and Elsey, R.M. (1986) Stress-induced suppression of testosterone secretion in male alligators. *Journal of Experimental Zoology* **239**, 241-246.

Lassurguere, J., Livera, G., Habert, R., and Jegou, B. (2003) Time and dose-related effects of estradiol and diethylstilbestrol on the morphology and function of the fetal rat testis in culture. *Toxicological Sciences* **73**, 160-169.

Laughran, L.J., Larsen, J.H., and Schroeder, P.C. (1981) Ultrastructure of developing ovarian follicles and ovulation in the lizard *Anolis carolinensis* (reptilia). *Zoomorphology* **98**, 191-208.

LeBas, N.R., and Marshall, N.J. (2000) The role of colour in signalling and male choice in the agamid lizard *Ctenophorus ornatus*. *Proceedings of the Royal Society B* **267**, 445-452.

Leese, H.J. (1988) The formation and function of oviduct fluid. *Journal of Reproduction and Fertility* **82**, 843-856.

Lejeune, H., Chuzel, F., Thomas, T., Avallet, O., Habert, R., Durand, P., and Saez, J. (1996) Paracrine regulation of Leydig cells. *Annales d'Endocrinologie* **57**, 55-63.

Leonhardt, S. A., Boonyaratanakornkit, V., and Edwards, D. P. (2003) Progesterone receptor transcription and non-transcription signaling mechanisms. *Steroids,* **68**, 761-770.

Lerchl, A., Sotiriadou, S., Behre, H.M., Pierce, H., Weinbauer, G.F., Eliesch, S., and Nieshlag, E. (1993) Restoration of spermatogenesis by follicle-stimulating hormone despite low intratesticular testosterone in photoinhibited hypogonadotropic Djungarian hamsters (*Phodopus sungorus*). *Biology of Reproduction* **49**, 1108-1116.

Lewis, J., Mahmoud, I.Y., and Klicka, J. (1979) Seasonal fluctuations in the plasma concentrations of progesterone and oestradiol-17β in the female snapping turtle (*Chelydra serpentina*). *Journal of Endocrinology* **80**, 127-131.

Licht, P. (1967) Environmental control of annual testicular cycles in the lizard *Anolis carolinensis* I. Interaction of light and temperature in the initiation of testicular recrudescence. *Journal of Experimental Zoology* **165**, 505-516.

Licht, P. (1972) Actions of mammalian pituitary gonadotropins (FSH and LH) in reptiles. I. Male snakes. *General and Comparative Endocrinology* **19**, 273-281.

Licht, P. (1979) Reproductive endocrinology of reptiles and amphibians: Gonadotrophins. *Annual Review of Physiology* **41**, 337-51.

Licht, P. (1982) Endocrine patterns in the reproductive cycle of turtles. *Herpetologica* **38**, 376-385.

Licht, P. (1984) Reptiles. In 'Marshall's physiology of reproduction. Vol. 1.' (Ed. GE Lamming) pp. 206-282. (Churchill Livingstone, Inc.: New York).

Licht, P., Breitenbach, G.L., and Congdon, J.D. (1985) Seasonal cycles in testicular activity, gonadotropin, and thyroxine in the painted turtle. *Chrysemys picta*, under natural conditions. *General and Comparative Endocrinology* **59**, 130-139.

Licht, P., and Gorman, G.C. (1975) Altitudinal effects on the seasonal testis cycles of tropical *Anolis* lizards. *Copeia* **1975**, 496-504.

Licht, P., Rainey, W., and Cliffton, K. (1980) Serum gonadotropin and steroids associated with breeding activities in the green sea turtle, *Chelonia mydas*. II. Mating and nesting in natural populations. *General and Comparative Endocrinology* **40**, 116-122.

Lind, C.M., Husak, J.F., Eikenaar, C., Moore, I., T. b., and Taylor, E.N. (2010) The relationship between plasma steroid hormone concentrations and the reproductive cycle in the Northern Pacific rattlesnake, *Crotalus oreganus*. *General and Comparative Endocrinology* **166**, 590-599.

Lindzey, J., and Crews, D. (1986) Hormonal control of courtship and copulatory behaviour in male *Cnemidophorous inornatus*, a direct sexual ancestor of a unisexual, parthenogenetic lizard. *General and Comparative Endocrinology* **64**, 411-418.

Lindzey, J., and Crews, D. (1988) Effects of progestins on sexual behaviour in castrated lizards (*Cnemidophorus inornatus*). *Journal of Endocrinology* **119**, 265-273.

Lindzey, J., and Crews, D. (1992) Interactions between progesterons and androgens in the stimulation of sex behaviours in male little striped whiptail lizards, *Cnemidophorus inornatus*. *General and Comparative Endocrinology* **86**, 52-58.

Lindzey, J., and Crews, D. (1993) Effects of progesterone and dihydrotestosterone on stimulation of androgen-dependent sex behavior, accessory sex structures, and in nitro binding characteristics of cytosolic androgen receptors in male whiptail lizards (*Cnemidophorus inornatus*). *Hormones and Behavior* **27**, 269-281.

Lofts, B. (1987) Testicular function. In 'Hormones and Reproduction in Fishes, Amphibians, and Reptiles.' (Eds. DO Norris and RE Jones) pp. 283-325. (Plenum Press: New York).

Lofts, B., and Tsui, H.W. (1977) Histological and histochemical changes in the gonads and epididymides of the male Soft-shelled turtle, *Trionyx sinensis*. *Journal of Zoology (London)* **181**, 57-68.

Lovern, M.B. (2011) Hormones and Reproductive Cycles in Lizards. In 'Hormones and Reproduction of Vertebrates. Vol. 3 Reptiles.' (Eds. DO Norris and KH Lopez) pp. 321-353. (Academic Press: San Diego).

Lupo Di Prisco, C., Delrio, G., and Chieffi, G. (1968) Sex hormones in the ovaries of the lizard *Lacerta sicula*. *General and Comparative Endocrinology* **10**, 292-295.

Mahmoud, I.Y., Ba-Omar, T.A., and AlKindi, A. (2006) Partial development of the steroidogenic ultrastructural features in degenerative corpora lutea after a single injection of pituitary extract in the Western painted turtle, (*Chrysemys picta*). *Tissue and Cell* **38**, 171-176.

Mahmoud, I.Y., Colas, A.E., Woller, M.J., and Cyrus, R.V. (1986) Cytoplasmic progesterone receptors in uterine tissue of the snapping turtle (*Chelydra serpentina*). *Endocrinology* **109**, 385-392.

Mahmoud, I.Y., Cyrus, R.V., Bennett, T.M., Woller, M.J., and Montag, D.M. (1985a) Ultrastructural changes in testes of the snapping turtle, *Chelydra serpentina*, in relation to plasma testosterone, Δ^5-3β-hydroxysteroid dehydrogenase, and cholesterol. *General and Comparative Endocrinology* **57**, 454-464.

Mahmoud, I.Y., Cyrus, R.V., Woller, M.J., and Bieber, A. (1985b) Development of the ovarian follicles in relation to changes in plasma parameters and Δ^5-3-β-HSD in snapping turtle, Chelydra serpentina. *Comparative Biochemistry and Physiology* **82A**, 131-136.

Mahmoud, I.Y., Guillette, L.J., Jr., McAsey, M.E., and Cady, C. (1989) Stress-induced changes in serum testosterone, estradiol-17β and progesterone in the turtle, *Chelydra serpentine*. *Comparative Biochemistry and Physiology* **93A**, 423-427.

Mahmoud, I.Y., Klicka, J., Cyrus, R., and Colás, A.E. (1980) The rate of conversion of (4-14C) progesterone by corpora lutea of the snapping turtle, *Chelydra serpentina*. *General and Comparative Endocrinology* **41**, 274- 277.

Mahmoud, I.Y., and Licht, P. (1997) Seasonal changes in gonadal activity and the effects of stress on reproductive hormones in the common snapping turtle, *Chelydra serpentine*. *General and Comparative Endocrinology* **107**, 359-372.

Marion, K.R. (1982) Reproductive cues for gonadal development in temperate reptiles: temperature and photoperiod effects on the testicular cycle of the lizard *Sceloporus undulatus*. *Herpetologica* **38**, 26-39.

Marion, K.R., and Sexton, C.J. (1971) The reproductive cycle of the lizard *Sceloporus malachiticus* in Costa Rica. *Copeia* **1971**, 517-526.

Martin Saint-Ange, G.J. (1854) 'Étude de l'appareil reproducteur dan les cinq d'animaux vertébrés, au point de vue anatomique, physiologique et zoologique.' (Imprimeri Impériale: Paris, France).

Masson, G.R., and Guillette, L. J., Jr. (1987) Changes in oviductal vascularity during the reproductive cycle of three oviparous lizards (*Eumeces obsoletus, Sceloporus undulatus* and *Crotaphytus collaris*). *Journal of Reproduction and Fertility* **80**, 361-371.

Mattison, C. (2004) 'Lizards of the World.' (Facts on File: New York).

McKinney, R.B., and Marion, K.R. (1985) Plasma androgens and their association with the reproductive cycle of the male fence lizard, *Scleroporus undulatus*. *Comparative Biochemistry and Physiology* **82A**, 515-519.

Mead, R.A., Eroschenko, V.P., and Highfill, D.R. (1981) E¡ects of progesterone and estrogen on the histology of the oviduct of the garter snake, *Thamnophis elegans*. *General and Comparative Endocrinology* **45**, 345-354.

Meehan, K. L., and Sadar, M. D. (2003) Androgens and androgen receptor in prostate and ovarian malignancies. *Frontiers in Bioscience,* **8**, 780-800.

Méndez de la Cruz, F., Guillette, L.J., Jr., and Villagrán-Santa Cruz, M. (1993) Differential atresia of ovarian follicles and its effect on the clutch size of two populations of the viviparous lizard *Sceloporus mucronatus*. *Functional Ecology* **7**, 535-540.

Méndez De La Cruz, F.R., Guillette, L.J., Jr., Villagrán Santa Cruz, M., and Casas-Andreu, G. (1988) Reproductive and fat body cycles of the viviparous lizard, *Sceloporus mucronatus* (Sauria: Iguanidae). *Journal of Herpetology* **22**, 1-12.

Mendonça, M.T., and Licht, P. (1986) Seasonal cycles in gonadal activity and plasma gonadotropin in the musk turtle, *Sternotherus odoratus*. *General and Comparative Endocrinology* **62**, 459-469.

Menezes, V.A., Rocha, C.F.D., and Dutra, G.F. (2004) Reproductive ecology of the parthenogenetic whiptail lizard *Cnemidophorus nativo* in a Brazilian restinga habitat. *Journal of Herpetology* **38**, 280-282.

Mesner, P.W., Mahmoud, I.Y., and V., C.R. (1993) Seasonal testesterone levels in Leydig and Sertoli cells of the Snapping turtle (*Chelydra serpentine*) in natural populations. *Journal of Experimental Zoology* **266**, 266-276.

Mesure, M., Chevalier, M., Depeiges, A., Faure, J., and Dufaure, J.P. (1991) Structure and ultrastructure of the epididymis of the viviparous lizard during the annual hormonal cycle: changes of the epithelium related to secretory activity. *Journal of Morphology* **210**, 133-145.

Midgley, A.R. (1973) Autoradiographic analysis of gonadotrophin binding to rat ovarian tissue sections. *Advances in Experimental Medicine and Biology*. **36**, 365.

Misra, U.K., Sanyal, M.K., and Prasad, M.R.N. (1965) Phospholipids of the sexual segment of the kidney of the Indian House Lizard, *Hemidactylus flaviviridis* Ruppell. *Life Sciences* **4**, 159-166.

Moberg, G.P. (1985) Influence of stress on reproduction, measure of well-being. In 'Animal Stress.' (Ed. GP Moberg) pp. 246-267. (American Physiological Society: Bethesda, MD).

Moore, I.T., and Jessop, T.S. (2003) Stress, reproduction, and adrenocortical modulation in amphibians and reptiles. *Hormones and behavior* **43**, 39-47.

Moore, M.C. (1986) Elevated testerone levels during non-breeding season territorially in a fall-breeding lizard, *Sceloporus jarrovi*. *Journal of Comparative Physiology* **158A**, 159-163.

Moore, M.C. (1987) Circulating steroid hormones during rapid aggressive responses of territorial male mountain spiny lizards, *Sceloporus jarrovi*. *Hormones and behavior* **21**, 511-521.

Moore, M.C., and Crews, D. (1986) Sex steroid hormones in natural populations of a sexual whiptail lizard *Cnemidophorus inornatus*, a direct evolutionary ancestor of unisexual parthenogen. *General and Comparative Endocrinology* **63**, 424-430.

Moore, M.C., and Lindzey, J. (1992) The physiological basis of sexual behavior in male reptiles. In 'Biology of the Reptilia. Physiology E. Vol. 18.' (Eds. C Gans and D Crews) pp. 70-113. (The University of Chicago Press: Chicago and London).

Moore, M.C., Thompson, C.W., and Marler, C.A. (1991) Reciprocal changes in corticosterone and testosterone levels following acute and chronic handling stress in the tree lizard, *Urosaurus ornatus*. *General and Comparative Endocrinology* **81**, 217-226.

Moore, M.C., Whittier, J.M., and Crews, D. (1985) Sex steroid hormones during the ovarian cycle of an all female, parthenogenetic lizard and their correlation with psedosexual behavior. *General and Comparative Endocrinology* **60**, 144-153.

Morel, L., Depeiges, A., and Dufaure, J.P. (1991) Molecular cloning and characterization of a cDNA encoding for the mature form of a specific androgen-dependent epididymal protein. *Cellular and Molecular Biology* **37**, 757-764.

Morel, L., Dufaure, J.P., and Depeiges, A. (1993) LESP, an androgenregulated lizard epididymal secretory protein family identified as a new member of the lipocalin superfamily. *Journal of Biological Chemistry* **268**, 10274-10281.

Morel, L., Dufaure, J.P., and Depeiges, A. (2000) The lipocalin sperm coating lizard epididymal secretory protein family: mRNA structural analysis and sequential expression during the annual cycle of the lizard, *Lacerta vivipara*. *Journal of Molecular Endocrinology* **24**, 127-133.

Mori, H. (1984) Ultrastructural and stereological analysis of Leydig cells. In 'Ultrastructural of Endocrine Cells and Tissues.' (Ed. PM Motta) pp. 225-237. (Martinus Nijhoff Publishers: Boston).

Motta, C.M., Filosa, S., and Andreuccetti, P. (1996) Regression of the epithelium in the late previtellogenic follicles of *Podarcis sicula*: a case of apoptosis. *Journal of Experimental Zoology* **276**, 233-241.

Motta, C.M., Scanderberg, M.C., Filosa, S., and Andreuccetti, P. (1995) Role of pyriform cells during the growth of oocytes in the lizard *Podarcis sicula*. *Journal of Experimental Zoology* **273**, 247-256.

Motta, C.M., Tammaro, S., Cicale, A., Indolfi, P., Iodice, C., Spagnuolo, M.S., and Filosa, S. (2001) Storage in the yolk platelets of Low MW DNA produced by the regressing follicle cells. *Molecular Reproduction and Development* **59**, 422-430.

Mubarak, M. (2004) Ultrastructure of Sperm Head, and its Differentiation in the Lizard, *Bunopus tuberculatus* (Squamata, Reptilia). *Saudi Journal of Biological Sciences* **11**, 143-152.

Muller, J., and Reisz, R.R. (2006) The phylogeny of early eureptiles: Comparing parsimony and Bayesian approaches in the investigation of a basal fossil clade. *Systematic Biology* **55**, 503-511.

Murphy-Walker, S., and Haley, S.R. (1996) Functional sperm storage duration in female *Hemidactylus frenatus* (family Gekkonidae). *Herpetologica* **52**, 365-373.

Nagahama, Y. (1987) Endocrine control of oocyte maturation. In 'Hormones and Reproduction in Fishes, Amphibians, and Reptiles.' (Eds. DO Norris and RE Jones) pp. 171-202. (Plenum Press: New York).

Newton, W.D., and Trauth, S.E. (1992) Ultrastructure of the spermatozoon of the lizard *Cnemidophorus sexlineatus* (Sauria: Teiidae). *Herpetologica* **48**, 330-343.

Nijagal, B.S., and Yajurvedi, H.N. (1999) Corticosterone interferes with seasonal recrudescence of germinal bed activity in lizard *Mayuba carinata*. *Indian Journal of Experimental Biology* **37**, 300-301.

Nilson, G. (1980) Male reproductive cycle of the European adder, *Vipera berus*, and its relation to annual activity periods. *Copeia* **1980**, 729-737.

Nirmal, B.K., and Rai, U. (1997) Epididymal influence on acquisition of sperm motility in the gekkonid lizard *Hemidactylus flaviviridis*. *Archives of Andrology* **39**, 105-110.

Nirmal, B.K., and Rai, U. (2000) Epididymal protein secretion and its androgenic control in wall lizard *Hemidactylus flaviviridis* (Rüppell). *Indian Journal of Experimental Biology* **38**, 720-726.

Nogueira, K.O.P.C., Rodrigues, S.S., Araújo, V.A., and Neves, C.A. (2011) Oviductal structure and ultrastructure of the oviparous gecko, *Hemidactylus mabouia* (Moreau De Jonnés, 1818). *The Anatomical Record* **294**, 883-892.

Noriega, T., Ibáñez, M.A., Bru, E., and Manes, M.E. (2002) The testicular cycle of the captive *Tupimabis merianae* lizards in temperate environment. *Cuadernos de Herpetología* **16**, 119-127.

Norris, D.O. (2007) 'Vertebrate Endocrinology.' 4th edn. (Elsevier Academic Press: Burlington, MA).

O'Reilly, K.M., and Wingfield, J.C. (2001) Ecological factors underlying the adrenocortical response to capture stress in arctic-breeding shorebirds. *General and Comparative Endocrinology* **124**, 1-11.

Okada, S., Izawa, M., and Ota, H. (2002) Growth and reproduction of *Gekko hokouensis* (Reptilia: Squamata) on Okinawajima Island of the Ryukyu Archipelago, Japan. *Journal of Herpetology* **36**, 473-479.

Oliver, S.C., Jamieson, B.G.M., and Scheltinga, D.M. (1996) The ultrastructure of spermatozoa of Squamata. II. Agamidae, Varanidae, Colubridae, Elapidae and Boidae (Reptilia). *Herpetologica* **52**, 216-241.

Olsson, M., Madsen, T., and Shine, R. (1997) Is sperm really so cheap? Costs of reproduction in male adders, *Vipera berus*. *Proceedings of the Royal Society B* **264**, 455-459.

Ota, H. (1994) Female reproductive cycles in the northernmost populations of the two gekkonid lizards, *Hemidactylus frenatus* and *Lepidodactylus lugubris*. *Ecological Research* **9**, 121-130.

Otsuka, S., Suzuki, M., Kamezaki, N., Shima, T., Wakatsuki, M., Kon, Y., and Ohtaishi, N. (2008) Growth-related changes in histology and immunolocalization of steroid hormone receptors in gonads of the immature male green turtle (*Chelonia mydas*). *Journal of Experimental Zoology* **309A**, 166-174.

Owens, D., and Ruiz, G.J. (1980) Obtaining blood and cerebrospinal fluid from marine turtles. *Herpetologica* **36**, 17-20.

Owens, D.W. (1997) Hormones in the life-history of sea turtles. In 'Biology of Sea-Turtles.' (Eds. PL Lutz and JA Musick) pp. 315-341. (CRC Press: Boca Raton, FL.).

Owens, D.W., and Morris, Y.A. (1985) The comparative endocrinology of sea turtles. *Copeia* 723-735.

Pak, T.R., Lynch, G.R., and Tsai, P.S. (2002) Estrogen accelerates gonadal recrudescence in photo-regressed male Siberian hamsters. *Endocrinology* **143**, 4131-4134.

Palmer, B.D., DeMarco, V.G., and Guillette, L.J., Jr. (1993) Oviductal morphology and eggshell formation in the lizard, *Sceloporus woodi*. *Journal of Morphology* **217**, 205-217.

Palmer, B.D., and Guillette, L.J., Jr. (1988) Histology and functional morphology of the female reproductive tract of the tortoise *Gopherus polyphemus*. *American Journal of Anatomy* **183**, 200-211.

Palmer, B.D., and Guillette, L.J., Jr. (1990) Morphological changes in the oviductal endometrium during the reproductive cycle of the tortoise, *Gopherus polyphemus*. *Journal of Morphology* **204**, 323-333.

Panchbudhe, A. (2011) http://www.indianaturewatch.net/displayimage.php?id= 220451. *Indianaturewatch.net*, 220451.

Paolucci, M., and Di Cristo, C. (2002) Progesterone receptor in the liver and oviduct of the lizard *Podarcis sicula*. *Life Sciences* **71**, 1417-1427.

Paolucci, M., and Di Fiore, M.M. (1992) Putative steroid-binding receptors and nonreceptors components and testicular activity in the lizard *Podarcis sicula sicula*. *Journal of Reproduction and Fertility* **96**, 471-481.

Paolucci, M., and Di Fiore, M.M. (1994) Estrogen and progesterone receptors in lizard *Podarcis s. sicula* oviduct: seasonal distribution and hormonal dependence. *Journal of Experimental Zoology* **269** 432-441.

Perkins, M.J., and Palmer, B.D. (1996) Histology and functional morphology of the oviduct of an oviparous snake, *Diadophis punctatus*. *Journal of Morphology* **227**, 67-79.

Perrard-Sapori, M.H., Chatelian, P.C., Rogemond, N., and Saez, J.M. (1987) Modulation of Leydig cell functions by culture Sertoli cells or with Sertoli cell-conditioned medium: effect of insulin, somatomedin- C and FSH. *Molecular and Cellular Endocrinology* **50**, 193-201.

Peters, H. (1978) Folliculogenesis in Mammalia. In 'The vertebrate ovary. Comparative biology and evolution. Vol. 121-144.' (Ed. J RE). (Plenum Press: New York).

Phillips, D.M., and Asa, C.S. (1993) Strategies for formation of the midpiece. In 'Comparative spermatology 20 years after.' (Ed. B Baccetti) pp. 997-1000. (Raven Press: New York).

Phillips, J.A., and Millar, R.P. (1998) Reproductive biology of the white-throated Savanna monitor, *Varanus albigularis*. *Journal of herpetology* **32**, 366-377.

Pianka, E.R., and Vitt, L.J. (2003) ' Lizards. Windows to the Evolution of Diversity.' (University of California Press: Berkeley).

Picariello, O., Ciarcia, G., and Angelini, F. (1989) The annual cycle of oviduct in *Tarentola m. mauritanica* L. (Reptilia, Gekkonidae). *Amphibia-Reptilia* **10**, 371-386.

Pietrobon, E.O., Monclus Mde, L., Alberdi, A.J. , Fornés, M.W. (2003) Progesterone receptor availability in mouse spermatozoa during epididymal transit and capacitation: ligand blot detection of progesterone-binding protein. *Journal of Andrology* **24**, 612-620.

Pough, F.H., Andrews, R.M., Cadle, J.E., Crump, J.L., Savitzky, A.H., and Wells, K.D. (2004) 'Herpetology.' (3rd ed.) edn. (Prentice-Hall, Inc.: Upper Saddle River).

Prasad, M.R.N., and Reddy, P.R.K. (1972) Physiology of the sexual segment of the kidney in reptiles. *General and Comparative Endocrinology Supplements* **3**, 649-662.

Prasad, M.R.N., and Sanyal, M.K. (1969) Effect of sex hormones on the sexual segment of kidney and other accessory reproductive organs of the Indian house lizard *Hemidactylus flaviviridis* Ruppell. *General and Comparative Endocrinology* **12**, 110-118.

Preest, M.R., Cree, A., and Tyrrell, C.L. (2005) ACTH-Induced stress response during pregnancy in a viviparous gecko: no observed effect on offspring quality. *Journal of Experimental Zoology* **303A**, 823-835.

Pudney, J. (1995) Spermatogenesis in Nonmammalian Vertebrates. *Microscopy Research and Technique* **32**, 459-497.

Radder, R.S., Shanbhag, B.A., and Saidapur, S.K. (2001) Pattern of plasma sex steroid hormone levels during reproductive cycles of male and female tropical lizard, *Calotes versicolor*. *General and Comparative Endocrinology* **124**, 285-292.

Rai, U., and Haider, S. (1986) Effects of mammalian pituitary gonadotropins and testosterone on the testes of sexually quiescent Indian wall lizard, *Hemidactylus flaviviridis* (Rüppell). *Journal of Zoology* **210**, 251-259.

Rai, U., and Haider, S. (1989) Effects of mammalian pituitary gonadotropins on the seasonally quiescent ovary of the Indian wall lizard, *Hemidactylus flaviviridis*. *Journal of Zoology* **217**, 341-348.

Rai, U., and Haider, S. (1991) Testis and epididymis of the Indian wall lizard (*Hemidactylus flaviviridis*): Effects of flutamide on FSH and Testosterone influenced spermatogenesis, Leydig cell, and epididymis. *Journal of Morphology* **209**, 133-142.

Rai, U., and Haider, S. (1995) Effects of cyproterone acetate on FSH and testosterone influenced spermatogenesis, steroidogenesis and epididymis in the Indian wall lizard, *Hemidactylus flaviviridis* (Ruppell). *European Journal of Morphology* **33**, 443-455.

Rai, U., and Nirmal, B.K. (2003) Significance of regional differences in ion concentrations in lizard *Hemidactylus flaviviridis* Rüppell: association of ionic influence on sperm motility in vitro. *Indian Journal of Experimental Biology* **41**, 1431-1435.

Ramaswami, L.S., and Jacob, D. (1963) Effect of testosterone on the male genital tract of the adult spiny-tailed lizard, *Uromastix hardwickii* Gray. *Naturwissenschaften* **50**, 453-454.

Ramírez-Bautista, A., Guillette, J., L., Gutierrez-Mayén, J.G., and Uribe-Peña, Z. (1996) Reproductive biology of the lizard *Eumeces copei* (Lacertilia: Scincidae) from the Eje Neovolcánico, Mèxico. *Southwestern Naturalist* **41**, 103-110.

Ramirez-Pinilla, M.P. (1995) Reproductive and fat body cycles of the oviparous lizard, *Liolaemus bitaeniatus* (Sauria: Tropiduridae). *Journal of Herpetology* **29**, 256-260.

Ramírez-Pinilla, M.P., De Pérez, G., and Ramírez-Perilla, J. (1989) Histología del tracto reproductivo de la hembra del lagarto *Phenacosaurus heterodermus* (Reptilia: Sauria: Iguanidae). *Trianea*, 3:93-103.

Reddy, P.R., Prasad, M.R.N., and Misra, N.K. (1972) Seasonal variation in the pattern of lipids in the sexual segment, kidney and liver of the Indian house lizard, *Hemidactylus flaviviridis* Rüppell. *Comparative Biochemistry and Physiology* **41**, 63-76.

Reddy, P.R.K., and Prasad, M.R.N. (1970a) Effect of gonadotropins and testosterone on the initiation of spermatogenesis in the hypophysectomised Indian house lizard, *Hemidactylus flaviviridis* (Rüppell). *Journal of Experimental Zoology* **174**, 205-214.

Reddy, P.R.K., and Prasad, M.R.N. (1970b) Hormonal control of the maintenance of spermatogenesis and sexual segment in the Indian house lizard *Hemidactylus flaviviridis* (Rüppell). *General and Comparative Endocrinology* **14**, 15-24.

Rheubert, J.L., McHugh, H.H., Collier, M.H., Sever, D.M., and Gribbins, K.M. (2009) Temporal germ cell development strategy during spermatogenesis within the testis of the Ground Skink, *Scincella lateralis* (Sauria: Scincidae). *Theriogenology* **72**, 54-61.

Rheubert, J.L., McMahan, C.D., Sever, D.M., Bundy, M.R., Siegel, D.S., and Gribbins, K.M. (2010a) Ultrastructure of the reproductive system of the Black Swamp Snake (*Seminatrix pygaea*). VII. Spermatozoon morphology and evolutionary trends of sperm characters in snakes. *Journal of Zoological Systematics and Evolutionary Research* **48**, 366-375.

Rheubert, J.L., Murray, C.M., Siegel, D.S., Babin, J., and Sever, D.M. (2011b) The Sexual Segment of *Hemidactylus turcicus* and the Evolution of Sexual Segment Location in Squamata. *Journal of Morphology* **272**, 802-813.

Rheubert, J.L., Sever, D.M., Geheber, A.D., and Siegel, D.S. (2010b) Proximal testicular ducts of the mediterranean gecko (*Hemidactylus turcicus*). *The Anatomical Record* **293**, 2176-2192.

Rheubert, J.L., Siegel, D.S., Venable, K.J., Sever, D.M., and Gribbins, K.M. (2011a) Ultrastructural description of spermiogenesis within the Mediterranean Gecko, *Hemidactylus turcicus* (Squamata: Gekkonidae). *Micron* **42**, 680-690.

Rhoades, R., and Pflanzer, R. (1992) 'Human Physiology.' 2nd edn. (Saunders College Publishing: USA)

Riley, D., and Callard, I.P. (1988) An estrogen receptor in the liver of the viviparous watersnake *Nerodia*; characterization and seasonal changes in binding capacity. *Endocrinology* **123**, 753-761.

Riley, D., Reese, J.C., and Callard, I.P. (1988) Hepatic progesterone receptors: Characterization in the turtle *Chrysemys picta*. *Endocrinology* **123**, 1195-1201.

Röll, B., and von Düring, M.U. (2008) Sexual characteristics and spermatogenesis in males of the parthenogenetic gecko *Lepidodactylus lugubris* (Reptilia, Gekkonidae). *Zoology* **111**, 385-400.

Romer, A.S., and Parsons, T. (1978) Excretory and reproductive systems. In 'The Vertibrate Body'. 5th edn. (Eds. AS Romer and T Parsons). (Saunders College: Philadelphia).

Romero, L.M. (2002) Seasonal changes in plasma glucocorticoid concentrations in free-living vertebrates. *General and Comparative Endocrinology* **128**, 1-24.

Romero, L.M., and Remage-Healey, L. (2000) Daily and seasonal variation in response to stress in captive starlings (*Sturnus vulgaris*): corticosterone. *General and Comparative Endocrinology* **119**, 52-59.

Rossen-Runge , E.C. (1977) 'The Process of Spermatogenesis in animals.' (Cambridge University Press: UK).

Rostal, D.C., Grumbles, J.S., Palmer, K.S., Lance, V.A., Spotila, J.R., and Paladino, F.V. (2001) Changes in gonadal and adrenal steroid levels in the leatherback sea turtle (*Dermochelys coriacea*) during the nesting cycle. *General and Comparative Endocrinology* **122**, 139-47.

Rostal, D.C., Owens, D.W., Grumbles, J.S., MacKenzie, D.S., and Amoss, M.S., Jr. (1998) Seasonal reproductive cycle of the Kemp's ridley sea turtle (*Lepidochelys kempi*). *General and Comparative Endocrinology* **109**, 232-243.

Rothchild, I. (1981) The regulation of the mammalian corpus luteum. *Recent Progress in Hormone Research* **37**, 183-298.

Rothchild, I. (2003) The yolkless egg and the evolution of eutherian viviparity. *Biology of Reproduction (Supplement)* **68**, 337-357.

Rubenstein, D.R., and Wikelski, M. (2003) Seasonal changes in food quality: a proximate cue for reproductive timing in marine iguanas. *Ecology* **84**, 3013-3023.

Ruiz, M., Davis, E., and P., M.E. (2008) Courtship attention in sagebrush lizards varies with male identity and female reproductive state. *Behavioral Ecology* **19**, 1326-1332.

Rüppell, E. (1835) Neue Wirbelthiere zu der Fauna von Abyssinien gehörig, entdeckt und beschrieben. In 'Amphibien.' (Ed. S Schmerber). (Frankfurt a. M.)

Russell, L.D., Hikim, S.A.P., Ettlin, R.A., and Legg, E.D. (1990) 'Histological and histopathological evaluation of the testis.' (Cache River Press: Clearwater, FL).

Saez, J.M., Perrard-Sapori, M.H., Chatelain, P.G., Tabone, E., and Rivarola, M.A. (1987) Paracrine regulation of testicular function. *Journal of Steroid Biochemistry* **27**, 317-329.

Saidapur, S.K. (1982) Structure and function of postovulatory follicles (corpora lutea) in the ovaries of nonmammalian vertebrates. *International Review of Cytology* **75**, 243-285.

Saint Girons, H. (1972) Morphologie compare du segment sexuel du rein des squamates (Reptilia). *Archives d'Anatomie Microscopique et de Morphologie Expérimentale* **61**, 243-266.

Saint Girons, H. (1985) Comparative data on lepidosaurian reproduction and some time tables. In 'Biology of the Reptilia. Development B.' (Eds. C Gans and F Billet) pp. 35-58. (Wiley: New York).

Saint Girons, H., Bradshaw, S.D., and Bradshaw, F.J. (1993) Sexual activity and plasma levels of sex steroids in the aspic viper *Vipera aspis* L. (Reptilia, Viperidae). *General and Comparative Endocrinology* **91**, 287-297.

Saita, A., Comazzi, M., and Perrotta, E. (1988) New data at the E.M. on the spermiogenesi s of *Iguana delicatissima* (Laurent) involving comparative signi. cance. *Acta Embryologiae et Morphologiae Experimentalis* **9**, 105-114.

Sánchez-Martínez, P.M., Ramírez-Pinilla, M.P., and Miranda-Esquivel, D.R. (2007) Comparative histology of the vaginal-cloacal region in Squamata and its phylogenetic implications. *Acta Zoologica (Stockholm)* **88**, 289-307.

Sanyal, M.K., and Prasad, M.R. (1966) Sexual segment of the kidney of the Indian house lizard, *Hemidactylus flaviviridis* Riippell. *Journal of Morphology* **118**, 511-528.

Sanyal, M.K., and Prasad, M.R.N. (1967) Reproductive cycle of the Indian house lizard, *Hemidactylus flaviviridis* Rüppell. *Copeia*, 627-633.

Sanz-Ochotorena, A., Moncada, F., and Uribe, M.C. (2001) Definición de los ciclos gonádicos de tres especies de Reptilia mediante el análisis de sus características histológicas. In 'Nuevos Retos de la Docencia y la Investigación en Histología.' (Eds. MC Uribe and ML García) pp. 161-170. (Soc Mex Hist. AC: México, DF).

Sapolsky, R.M. (1992) Neuroendocrinology of the stress-response. In 'Behavioral Endocrinology.' (Eds. JB Becker, SM Breedlove and D Crews) pp. 287-323. (MIT Press: Cambridge, MA).

Sarkar, H.B.D., and Shivanandappa, T. (1984) Androgen control of the accessory reproductive organs in the skink, *Mabuya carinata* (Schn.). In 'Recent Trends in Life Sciences.' (Ed. AGaAK Saxena) pp. 217-246. (Manu Publ.: Kanpur India).

Sarkar, H.B.D., and Shivanandappa, T. (1989) Reproductive cycles of reptiles. In 'Reproductive cycles of Indian vertebrates.' (Ed. SK Saidapur) pp. 225-272. (Allied Press: New Delhi).

Sarkar, S., Sarkar, N.K., and Maiti, B.R. (2003) Oviductal sperm storage structure and their changes during the seasonal (Dissociated) reproductive cycle in the soft-shelled turtle *Lissemys punctata punctata*. *Journal of Experimental Zoology* **295A**, 83-91.

Sarker, S., Sarker, N.K., and Maitia, B.R. (1995) Histological and functional changes of oviductal endometrium during seasonal reproductive cycle of the soft-shelled turtle, *Lissemys punctata punctata*. *Journal of Morphology* **224**, 1-14.

Sarker, S., Sarker, N.K., and Maiti, B.R. (1996) Seasonal pattern of ovarian growth and inter related changes in plasma steroid levels, vitellogenesis, and oviductal function in adult female the soft-shelled turtle, *Lissemys punctuata punctuata*. *Canadian Journal of Zoology*. **74**, 303-311.

Savouret, J.F., Misrahi, M., and Milgrom, E. (1988) Molecular action of progesterone. *Oxford Reviews of Reproductive Biology* **10**, 293-347.

Scheltinga, D.M., Jameison, B.G.M., Espinoza, R.E., and Orrel, K.S. (2001) Descriptions of the mature spermatozoa of the lizards *Crotaphytus bicinctores*, *Gambelia wislizenii* (Crotaphytidae), and *Anolis carolinensis* (Polychrotidae) (Reptilia, Squamata, Iguania). *Journal of Morphology* **247**, 160-171.

Scheltinga, D.M., Jamieson, B.G.M., Trauth, S.E., and McAllister, C.T. (2000) Morphology of the spermatozoa of the iguanian lizards *Uta stansburiana* and *Urosaurus ornatus* (Squamata, Phrynosomatidae). *Journal of Submicroscopic Cytology and Pathology* **32**(261-271).

Schroeder, T.E. (1973) Cell constriction: Contractile role of microfilaments in division and development. *American Zoologist* **13**, 687-696.

Schuett, G.W., Harlow, H.J., Rose, J.D., Van Kirk, E.A., and Murdoch, W.J. (1997) Annual cycle of plasma testosterone in male copperheads, *Agkistrodon contortrix* (Serpentes, Viperidae): relationship to timing of spermatogenesis, mating, and agonistic behaviour. *General and Comparative Endocrinology* **105**, 417-424.

Schwarzkopf, L., and Shine, R. (1991) Thermal biology of reproduction in viviparous skinks, Eulamprus tympanum: why do gravid females bask more? *Oecologia* **88**, 562-569.

Seiki, K., Fujii, H., Kawamura, N., Enomoto, T., Haruki, Y., and Nakano, M. (1981) Progestin receptors in testes from various animal species. *Tokai Journal of Experimental and Clinical Medicine* **6**, 343-351.

Seiler, P., Wenzel, I., Wagenfeld, A., Yeung, C.H., Nieschlag, E., and Cooper, T.G. (1998) The appearance of basal cells in the developing murine epididymis and their temporal expression of macrophage antigens. *International Journal of Andrology* **21**, 217-226.

Selcer, K.W., and Leavitt, W.W. (1991) Progesterone downregulates progesterone receptor but not estrogen receptor in the estrogenprimed oviduct of a turtle (*Trachemys scripta*). *General and Comparative Endocrinology* **83**, 316-323.

Sever, D.M. (2010) Ultrastructure of the reproductive system of the black swamp snake (*Seminatrix pygaea*). VI. Anterior testicular ducts and their nomenclature. *Journal of Morphology* **271**, 104-115.

Sever, D.M., and Hopkins, W.A. (2004) Oviductal sperm storage in the ground skink *Scincella laterale* Holbrook (Reptilia: Scincidae). *Journal of Experimental Zoology* **301A**, 599-611.

Sever, D.M., and Hopkins, W.A. (2005) Renal Sexual Segment of the Ground Skink, *Scincella laterale* (Reptilia, Squamata, Scincidae). *Journal of Morphology* **266**, 46-59.

Sever, D.M., Ryan, T.J., Morris, T., Patton, D., and Swafford, S. (2000) Ultrastructure of the reproductive system of the black swamp snake (*Seminatrix pygaea*). II. Annual oviductal cycle. *Journal of Morphology* **245**, 146-160.

Sever, D.M., Siegel, D.S., Bagwill, A., Eckstut, M.E., Alexander, L., Camus, A., and Morgan, C. (2008) Renal sexual segment of the Cottonmouth snake, *Agkistrodon piscivorous* (Reptilia, Squamata, Viperidae). *Journal of Morphology* **269**, 640-53.

Sever, D.M., Stevens, R.A., Ryan, T.J., and Hamlett, W.C. (2002) Ultrastructure of the reproductive system of the Black Swamp Snake (*Seminatrix pygaea*). III. Sexual segment of the male kidney. *Journal of Morphology* **252**, 238-254.

Shanbhag, B.A. (2002) Reproductive biology of Indian reptiles. *Proceedings of the Indian National Science Academy* **6**, 497-528.

Shanbhag, B.A. (2003) Reproductive strategies in the lizard, *Calotes versicolor*. *Current Science* **84**, 646-652.

Shanbhag, B.A., Karegouder, V.S., and Saidapur, S.K. (2000b) The Pattern of Testicular Activity in the Gecko *Hemidactylus brooki* from India. *Journal of Herpetology* **34**, 601-604.

Shanbhag, B.A., and Prasad, B.S.K. (1993) Follicular dynamics and germinal bed activity during the annual ovarian cycle in the lizard, *Calotes versicolor* (Daud.). *Journal of Morphology* **215**, 1-7.

Shanbhag, B.A., Radder, R.S., and Saidapur, S.K. (2000a) GnRH but not warm temperature induces recrudescence of quiescent testes in the tropical lizard *Calotes versicolor* (Daud.) during postbreeding phase. *General and Comparative Endocrinology* **119**, 232-238.

Shanbhag, B.A., Radder, R.S., and Saidapur, S.K. (2001) Plasma progesterone level and luteal activity during gestation and prolonged egg retention in the tropical lizard, *Calotes versicolor*. *General and Comparative Endocrinology.* **123**, 73-79.

Shanbhag, B.A., Subraya, L., and Saidapur, S.K. (1998) Pattern of recruitment, growth of developing follicles, and germinal bed activity in the tropical gecko, *Hemidactylus brooki*. *Journal of Herpetology* **32**, 566-572.

Shao, R., Markström, E., Friberg, P.A., Johansson, M., and Billig, H. (2003) Expression of progesterone receptor (PR) A and B isoforms in mouse granulosa cells: stage-dependent PR-mediated regulation of apoptosis and cell proliferation. *Biology of reproduction* **68**, 914-921.

Sherbrooke, W.C. (1975) Reproductive cycle of a tropical lizard, *Neusticurus ecpleopus* Cope, in Peru. *Biotropica* **7**, 194-207.

Sherwood, N.M., Lovejoy, D.A., and Coe, I.R. (1993) Origin of mammalian gonadotropin-releasing hormone. *Endocrine Reviews* **14**, 241-254.

Shine, R. (1983) Reptilian reproductive modes: The oviparity-viviparity continuum. *Herpetologica* **39**, 1-8.

Shine, R. (1985) The reproductive biology of Australian reptiles: a search for general patterns. In 'Biology of Australasian Frogs and Reptiles.' (Eds. G Grigg, R Shine and H Ehmann) pp. 297-303. (Surrey Beaty and Sons Pty, Ltd: Australia).

Shine, R., Harlow, P.S., Branch, W.R., and Webb, J.K. (1996) Life on the lowest branch: sexual dimorphism, diet, and reproductive biology of an African twig snake, *Thelotornis capensis* (Serpentes: Colubridae). *Copeia* **1996**, 290-299.

Shivanandappa, T., and Sarker, H.B.D. (1987) Androgenic regulation of epididymal function in the skink, *Mabuya carinata* (Sch.). *Journal of Experimental Zoology* **241**, 369-376.

Shivkumar, G.R., and Sarkar, H.B.D. (1980) Effect of cyproterone acetate on the testis and epididymis of the lizard, *Psammophilus dorsalis* (Gray). *Experintia* **36**, 616-618.

Sica, S., Fierro, D., Iodice, C., Muoio, R., Filosa, S., and Motta, C.M. (2001) Control of oocyte recruitment: regulative role of follicle cells through the release of a diffusible factor. *Molecular Reproduction and Development* **58**, 444-450.

Siegel, D.S., Aldridge, R.D., Clark, C.S., Poldemann, E.H., and Gribbins, K.M. (2009a) Stress and reproduction in *Boiga irregularis* with notes on the ultrastructure of the sexual segment of the kidney in squamates. *Canadian Journal of Zoology* **87**, 1138-1149.

Siegel, D.S., and Sever, D.M. (2008) Seasonal variation in the oviduct of female *Agkistrodon piscivorus* (Reptilia:Squamata): An ultrastructural investigation. *Journal of Morphology* **269**, 980-997.

Siegel, D.S., Sever, D.M., Rheubert, J.L., and Gribbins, K.M. (2009b) Reproductive biology of *Agkistrodon piscivorus* Lacépède (Squamata, Serpentes, Viperidae, Crotalinae). *Herpetological Monographs* **23**, 74-107.

Sinervo, B., and Licht, P. (1991) Hormonal and physiological control of clutch size, egg size, and egg shape in side-blotched lizards (*Uta stansburiana*): constraints on the evolution of lizard life histories. *Journal of Experimental Zoology* **257**, 252-264.

Sirivaidyapong, S., Bevers, M.M., and Colenbrander, B. (1999) Acrosome reaction in dog sperm is induced by a membranelocalized progesterone receptor. *Journal of Andrology* **20**, 537-544.

Sivaperuman, C., Baqri, Q.H., Ramaswamy, G., and Naseema, M. (2008) 'Faunal Ecology and Conservation: The Great Indian Desert.' (Springer-Verlag: Berlin).

Skinner, M.K., Norton, J.N., Mullaney, B.P., Rosselli, M., Whaley, P.D., and Anthony, C.T. (1991) Cell-cell interactions and the regulation of testis function. *Annals of the New York Academy of Sciences* **637**, 354-363.

Smith, C.F., Schuett, G.W., and Schwenk, K. (2010) Relationship of plasma sex steroids to the mating season of copperheads at the north-eastern extreme of their range. *Journal of Zoology* **280** 362-370.

Smith, H.M., Sinelnik, G., Fawcett, J.D., and Jones, R.E. (1973) A survey of the chronology of ovulation in anoline lizard genera. *Transactions of the Kansas Academy of Science* **75**, 107-120.

Smith, S.J., Palmer, B.D., and Selcer, K.W. (1995) Androgen receptor and aromatase in the turtle oviduct. *American Zoologist* **6A**(40), .

Soley, J.T. (1994) Centriole development and formation of the flagellum during spermiogenesis in the ostrich (*Struthio camelus*). *Journal of Anatomy* **185**, 301-313.

Somma, C.A., and Brooks, G.R. (1976) Reproduction in *Anolis oculatus*, *Ameiva fuscata*, and *Mabuya mabouya* from Dominica. *Copeia* **1976**, 249-256.

Staub, N.L., and De Beer, M. (1997) The role of androgen in female vertebrates. *General and Comparative Endocrinology* **108**, 1-24.

Summers, C.H. (1988) Chronic low humidity stress in the lizard, *Anolis carolinensis*: Effects on ovarian and oviductal recrudescence. *Journal of Experimental Zoology* **248**, 192-198.

Summers, C.H., Suedkamp, D.A., and Grant, T.L. (1995) Regulation of ovarian recrudescence; Effects of social interaction and size on female lizards, *Anolis carolinensis*. *Journal of Experimental Zoology* **271**, 235-241.

Svensson, E.C., Markström, E., Andersson, M., and Billig, H. (2000) Progesterone receptor-mediated inhibition of apoptosis in granulosa cells isolated from rats treated with human chorionic gonadotropin. *Biology of Reproduction* **63**, 1457-1464.

Swain, R., and Jones, S.M. (1994) Annual cycle of plasma testosterone and other reproductive parameters in the Tasmanian skink, *Niveoscincus metallicus*. *Herpetologica* **54**, 502-509.

Tanaka, S., Sakai, M., Hattori, M.A., Kikuyama, S., Wakabayashi, K., and Honoka, Y. (2004) Effect of bullfrog LH and FSH on newt testes under different temperature. *General and Comparative Endocrinology* **138**, 1-7.

Taylor, E.N., DeNardo, D.F., and Jennings, D.H. (2004) Seasonal steroid hormone levels and their relation to reproduction in the Western Diamond-backed Rattlesnake, *Crotalus atrox* (Serpentes: Viperidae). *General and Comparative Endocrinology* **136** 328-337.

Taylor, J.A. (1985) Reproductive biology of the Australian lizard *Ctenotus taeniolatus*. *Herpetologica* **41**, 408-418.

Teixeira, R.D., Colli, G.R., and Báo, S.N. (1999a) The ultrastructure of spermatozoa of the lizard *Polychrus acutirostris* (Squamata, Polychrotidae). *Journal of Submicroscopic Cytology and Pathology* **31**, 387-395.

Teixeira, R.D., Colli, G.R., and Báo, S.N. (1999b) The ultrastructure of the spermatozoa of the lizard *Micrablepharus maximiliani* (Squamata, Gymnophthalmidae), with considerations on the use of sperm ultrastructure characters in phylogenetic reconstruction. *Acta Zoologica (Stockholm)* **80**, 47-59.

Teixeira, R.D., Scheltinga, D.M., Trauth, S.E., Colli, G.R., and Báo, S.N. (2002) A comparative ultrastructural study of spermatozoa of the teiid lizards *Cnemidophorus gularis gularis*, *Cnemidophorus ocellifer*, and *Kentropyx altamazonica* (Reptilia, Squamata, Teiidae). *Tissue & Cell* **34**(3), 135-142.

Tienhoven, A. (1968) 'Reproductive Physiology of Vertebrates.' (W.B. Saunders Company: Philadelphia).

Tilbrook, A.J., Turner, A.I., and Clarke, I.J. (2000) Effects of stress on reproduction in non-rodent mammals: The role of glucocorticoids and sex differences *Reviews of Reproduction* **5**, 105-113.

Tokarz, R.R. (1986) Hormonal regulation of male reproductive behavior in the lizard *Anolis sagrei*: A test of the aromatization hypothesis. *Hormones and Behavior* **20**, 364-372.

Tokarz, R.R. (2006) Importance of prior physical contact with familiar females in the development of a male courtship and mating preference for unfamiliar females in the lizard *Anolis sagrei*. *Herpetologica* **62**, 115-124.

Tokarz, R.R., Crews, D., and McEwen, B.S. (1981) Estrogen-sensitive progestin binding sites in the brain of the lizard, *Anolis carolinensis*. *Brain Res* **220**, 95-105.

Tokarz, R.R., McMann, S., Seitz, L., and John-Alder, H. (1998) Plasma corticosterone and testosterone levels during the annual reproductive cycle of male brown anoles (*Anolis sagrei*). *Physiological Zoology* **71**, 139-146.

Tokarz, R.R., and Summers, C.H. (2011) Stress and Reproduction in Reptiles. In 'Hormones and Reproduction of Vertebrates. Vol. 3.' (Eds. DO Norris and KH Lopez) pp. 169-213. (Academic Press: San Diego).

Townsend, T.M., Larson, A., Louis, E., and Macey, J.R. (2004) Molecular phylogenetics of Squamata: the position of snakes, amphisbaenians, and dibamids, and the root of the squamate tree. *Systematic biology* **53**, 735-757.

Trauth, S.E. (1994) Reproductive cycles in two Arkansas skinks in the genus *Eumeces* (Sauria: Scincidae). *Proceedings of the Arkansas Academy of Science*. **48**, 210-218.
Tyrrell, C.L., and Cree, A. (1998) Relationships between corticosterone concentration and season, time of day and confinement in a wild reptile (tuatara, *Sphenodon punctatus*). *General and Comparative Endocrinology* **110**, 97-108.

Tsai, M., and O'Malley, B. (1994) Molecular mechanisms of action of steroid/thyroid receptor superfamily members. *Annual Review of Biochemistry,* **63**, 451-486.

Universe-Review.ca (2012) (http://universe-review.ca/R10-33-anatomy.htm).

Upadhyay, S.N., and Guraya, S.S. (1972) Histochemical observations on the interstitial gland (or Leydig) cells of the lizard testis. *General and Comparative Endocrinology* **19**, 88-95.

Uribe, M.C.A., and Guillette, L.J., Jr. (2000) Oogenesis and ovarian histology of the American alligator *Alligator mississippiensis*. *Journal of Morphology* **245**, 225-240.

Uribe, M.C.A., Omaña, M.E.M., Quintero, J.E.G., and Guillette, L.J., Jr. (1995) Seasonal variation in ovarian histology of the viviparous lizard *Sceloporus torquatus torquatus*. *Journal of Morphology* **226**, 103-119.

Uribe, M.C.A., Portales, B., Gloria, L., and Guillette, L.J., Jr. (1996) Ovarian folliculogenesis in the oviparous Mexican lizard *Ctenosaura pectinata*. *Journal of Morphology* **230**, 99-112.

Uribe, M.C.A., Velasco, S.R., Guillette, L.J., Jr., and Estrada, E.F. (1988) Oviduct histology of the lizard, *Ctenosaura pectinata*. *Copeia* **1988**, 1035-1042.

van Wyk, J.H. (1984) Ovarian morphological changes during the annual breeding cycle of the rock lizard *Agama atra* (Sauria: Agamidae). . *Navors nas. Mus. Bloemfontein* **4**, 237-275.

van Wyk, J.H. (1994) Physiological changes during the ovarian cycle of the female rock lizard *Cordylus giganteus* (Sauria: Cordyliae). *Herpetologica* **50**, 480-493.

van Wyk, J.H. (1995) The male reproductive cycle of the lizard, *Cordylus giganteus* (Sauria: Cordylidae). *Journal of Herpetology* **29**, 522-535.

Vanakudre, S.B., and Shanbhag, B.A. (1989) Histological and histochemical studies on the adrenal gland of female garden lizard *Calotes versicolor* during different phases of reproductive cycle. *Journal of Karnataka University* **XXXIV**, 13-19.

Varma, S.K. (1970) Morphology of ovarian changes in the garden lizard *Calotes versicolor*. *Journal of Morphology* **131**, 195- 210.

Varma, S.K., and Guraya, S.S. (1973) Histochemical observations on granulose (follicular) cells in the preovulatory and postovulatory follicles of garden lizard. *Acta Anatomica* **85**, 563-579.

Varma, S.K., and Guraya, S.S. (1975) Gross morphology of ovarian changes during the reproductive cycle of Indian lizard (*Calotes versicolor* and *Hemidactylus flaviviridis*). *Acta morphologica Neerlando-Scandinavica* **13**, 201-212.

Veri, J.P., Hermo, L., and Robaire, B. (1993) Immunocytochemical localization of the Yf subunit of glutathione S-transferase P shows regional variation in the staining of epithelial cells of the testis, efferent ducts and epididymis of the male rat. *Journal of Andrology* **14**, 23-44.

Vidal, N., and Hedges, S.B. (2005) The phylogeny of squamate reptiles (lizards, snakes, and amphisbaenians) inferred from nine nuclear protein-coding genes. *Comptes Rendus Biologies* **328**, 1000-1008.

Vidal, N., and Hedges, S.B. (2009) The molecular evolutionary tree of lizards, snakes, and amphisbaenians. *Comptes Rendus Biologies* **332**, 129-139.

Vieira, G.H.C., Colli, G.R., and Báo, S.N. (2004) The ultrastructure of the spermatozoon of the lizard *Iguana iguana* (Reptilia, Squamata, Iguanidae) and the variability of sperm morphology among iguanian lizards. *Journal of Anatomy* **204**, 451-464.

Vieira, G.H.C., Colli, G.R., and Báo, S.N. (2005) Phylogenetic relationships of corytophanid lizards (Iguania, Squamata, Reptilia) based on partitioned and total evidence analyses of sperm morphology, gross morphology, and DNA data. *Zoologica Scripta* **34**, 605-625.

Vieira, G.H.C., Cunha, L.D., Scheltinga, D.M., Glaw, F., Colli, G.R., and Báo, S.N. (2007) Sperm ultrastructure of hoplocercid and oplurid lizards (Sauropsida, Squamata, Iguania) and the phylogeny of Iguania. *Journal of Zoological Systematics and Evolutionary Research* **10**, 439-469.

Vieira, G.H.C., Wiederhecker, H.C., Colli, G.R., and Báo, S.N. (2001) Spermiogenesis and testicular cycle of the lizard *Tropidurus torquatus* (Squamata, Tropiduridae) in the Cerrado of central Brazil. *Amphibia-Reptilia* **22**, 217-233.

Vieira, S., De Pérez, G.R., and Ramírez-Pinilla, M.P. (2010) Ultrastructure of the ovarian follicles in the placentotrophic andean lizard of the genus *Mabuya* (Squamata: Scincidae). *Journal of Morphology* **271**, 738-749.

Villagrán-Santa Cruz, M., and Méndez de la Cruz, F.R. (1999) Corpus luteum through the gestation of *Sceloporus palaciosi* (Sauria: Phrynosomatidae). *Copeia* **1999**, 214-218.

Vitt, L.J. (1992) Diversity of reproductive strategies among Brazilian lizards and snakes: the significance of lineage and adaptation. In 'Repro-ductive Biology of South American Vertebrates.' (Ed. WC Hamlett) pp. 135-149. (Springer Verlag: New York).

Vitt, L.J., and Blackburn, D.G. (1991) Ecology and life history of the viviparous lizard, *Mabuya striata* (Scincidae) in the Brazilian Amazon. *Copeia* **1991**, 916-927.

Volsøe, H. (1944) Structure and seasonal variation of the male reproductive organs of Vipera berus (L.). In 'Spolia Zoologica Musei Hauniensis.' (Ed. V Skrifter). (Universitetets Zoologiske Museum: København).

Vonier, P.M., Guillette, L.J., Jr., McLachlan, J.A., and Arnold, S.F. (1997) Identification and characterization of estrogen and progesterone receptors from the oviduct of the American alligator (*Alligator mississippiensis*). *Biochemical and Biophysical Research Communications* **232**, 308-312.

Wack, C.L., Fox, S.F., Hellgren, E.C., and Lovern, M.B. (2008) Effects of sex, age, and season on plasma steroids in free-ranging Texas horned lizards (*Phrynosoma cornutum*). *General and Comparative Endocrinology* **155**, 589-596.

Wake, M.H. (1985) Oviduct structure and function in non-mammalian vertebrates. *Fortschritte der Zoologie* **30**, 427-435.

Weber, M.A., Groos, S., Aumuller, G., and Konrad, L. (2002) Post-natal development of the rat testis: steroid hormone receptor distribution and extracellular matrix deposition. *Andrologia* **34**, 41-54.

Weil, M.R. (1984) Seasonal histochemistry of the Rss in male common water snakes, *Nerodia sipedon* (L.). *Canadian Journal of Zoology* **62**, 1737-1740.

Whittier, J.M., Corrie, F., and Limpus, C. (1997) Plasma steroid profiles in nesting loggerhead turtles (*Caretta caretta*) in Queensland, Australia: Relationship to nesting episode and season. *General and Comparative Endocrinology* **106**, 39-47.

Whittier, J.M., and Crews, D. (1987) Seasonal reproduction; patterns and control. In 'Hormones and Reproduction in Fishes, Amphibians, and Reptiles.' (Eds. DO Norris and RE Jones) pp. 385-409. (Plenum Press: New York).

Whittier, J.M., Stewart, D., and Tolley, L. (1994) Ovarian and oviductal morphology of sexual and parthenogenetic geckos of the *Heteronotia Binoei complex*. *Copeia* **1994**, 484-492.

Wiebe, J.B. (1985) Steroidogenesis: what happens in the vertebrate testis at the onset of puberty? In 'Current Trends in Comparative Endocrinology.' (Eds. B Lofts and WN Holmes) pp. 273-276. (Hong Kong University Press: Hong Kong).

Wierman, M. E. (2007) Sex steroid effects at target tissues: mechanisms of action. *Advances in Physiology Education*, **31**, 26-33.

Wilhoft, D.C. (1963) Gonadal histology and seasonal changes in the tropical Australian lizard *Leiolopisma rhomboidalis*. *Journal of Morphology* **113**, 185-204.

Wilhoft, D.C., and Quay, W.B. (1961) Testicular histology and seasonal changes in the lizard, *Sceloporus occidentalis*. *Journal of Morphology* **108**, 95-106.

Wilhoft, D.C., and Reiter, E.O. (1965) Sexual cycle of the lizard, *Leiolopisma fuscum*, a tropical Australian skink. *Journal of Morphology* **116**, 379-388.

Williams, T.D. (1992) Reproductive endocrinology of macaroni (*Eudyptes chrysolopus*) and gentoo (*Pygoscelis papua*) penguins. II. Plasma levels of gonadal steroids and LH in immature birds in relation to deferred sexual maturity. *General and Comparative Endocrinology* **85**, 241-247.

Willson, R.J., and Brooks, R.J. (2006) Thermal biology of reproduction in female eastern Foxsnakes (*Elaphe gloydi*). *Journal of Herpetology* **40**, 285-289.

Wilson, B.S., and Wingfield, J.C. (1992) Correlation between female reproductive condition and plasma corticosterone in the lizard *Uta stansburiana*. *Copeia* **1992**, 691-697.

Wilson, B.S., and Wingfield, J.C. (1994) Seasonal and interpopulational variation in plasma levels of corticosterone in the sideblotched lizard (*Uta stansburiana*). *Physiological Zoology* **67**, 1025-1049.

Witt, D.M., Young, L.J., and Crews, D. (1994) Progesterone and sexual behavior in males. *Psychoneuroendocrinology* **19**, 553-562.

Woodley, S.K., and Moore, M.C. (2002) Plasma corticosterone response to an acute stressor varies according to reproductive condition in female tree lizards (*Urosaurus ornatus*). *General and Comparative Endocrinology* **128**, 143-148.

Xavier, F. (1982) Progesterone in the viviparous lizard *Lacerta vivipara*: Ovarian biosynthesis, plasma levels, and binding to transcortin-type protein during the sexual cycle. *Herpetologica* **38**, 62-70.

Xavier, F. (1987) Functional morphology and regulation of the corpus luteum. In 'Hormones and Reproduction in Fishes, Amphibians and Reptilia.' (Eds. OO Norris and RE Jones) pp. 246-256. (Plenum Press: New York).

Yajurvedi, H.N., and Menon, S. (2005) Influence of stress on gonadotrophin induced testicular recrudescence in the lizard *Mabuya carinata*. *Journal of Experimental Zoology* **303A**, 534-540.

Yaron, Z. (1972) Effects of ovariectomy and steroid replacement on the genital tract of the viviparous lizard, *Xantusia vigilis*. *Journal of Morphology* **136**, 313-326.

Yokoyama, F., and Yoshida, H. (1994) The reproductive cycle of the female habu, *Trimeresurus flavoviridis*. *Journal of Herpetology* **28**, 54-59.

Young, L.J., Greenberg, N., and Crews, D. (1991) The effects of progesterone on sexual behavior in male green anole lizard (*Anolis carolinensis*). *Hormones and Behavior* **25**, 477-488.

Young, L.J., Lopreato, G.F., Horan, K., and Crews, D. (1994) Cloning and in situ hybridization analysis of estrogen receptor, progesterone receptor, and androgen receptor expression in the brain of whiptail lizards (*Cnemidophorus uniparens* and *C. inornatus*). *Journal of Comparative Neurology* **347**, 288-300.

Yu, M.S., and Ho, S.-M. (1989) Nuclear acceptor sites for estrogen-receptor complexes in the liver of the turtle, *Chrysemys picta*. I. Sexual differences, species specificity and hormonal dependency. *Molecular and Cellular Endocrinology* **61**, 37-48.

Zug, G.R., Vitt, L.J., and Caldwell, J.P. (2001) 'Herpetology: An introductory biology of amphibians and reptiles.' (Academic Press: New York)

Appendix 1: Staining protocols

Harris's haematoxylin and eosin Y (H&E):

1- The slides were removed from the oven (60^{o}C) and sections deparaffinised in 2 changes of xylene for 3 minutes in each change.
2- The sections then hydrated through graded alcohol concentration (100%, 90%, 80% &70%) for 10 dips in each change.
3- The slides were washed in running tap water for 3 minutes.
4- The slides were taken into Harris's haematoxylin for 12 minutes, and then washed well in running tap water for 5 minutes or until slides became blue.
5- The slides were then differentiated in 1% acid alcohol (1% HCL in 70% alcohol) for 5–10 seconds, and then rinsed in running tap water.
6- The slides were taken into the blueing solution (weak ammonia) for 30–45 seconds, and then rinsed in running tap water.
7- The slides then stained in 1% aqueous eosin Y for 6 minutes and then rinsed in tap water.
8- The slides were dehydrated through graded alcohol concentration (90%, 100%, 100%, & 100%) with 10 dips in each change, and cleared through a series of xylene changes with 10 dips in each change.
9- The slides were then mounted in D.P.X.

Periodic acid-Schiff and fast green (PAS-FG):

1- The slides were taken through steps 1–3 following the H&E procedure.
2- The slides were then put into 1% periodic acid for 5 minutes, and then rinsed in running tap water.
3- The slides were then stained in Schiff's reagent for 10 minutes, and washed in running tap water for 5–10 minutes.
4- The slides were then stained in acetic fast green for 5 minutes, and then washed in running tap water for 5 minutes.
5- The slides were taken through steps 8 and 9 following the H&E procedure.

Periodic acid-Schiff and Mayer's haematoxylin (PAS-Haem):

1- The slides were taken through steps 1–3 following the H&E procedure.
2- The slides were put into 1% periodic acid for 5 minutes, and then rinsed in running tap water.
3- The slides were then stained in Schiff's reagent for 10 minutes, and washed in running tap water for 5–10 minutes.
4- The slides were then stained in Mayer's haematoxylin for 2 minutes, and washed in running tap water for 5 minutes.
5- The slides were taken through steps 8 and 9 following the H&E procedure.

Alcian blue and periodic acid-Schiff (AB-PAS):

1- The slides were taken through steps 1–3 following the H&E procedure.
2- The slides were put into filtered Alcian blue solution for 20 minutes, and washed in running tap water for 5 minutes.
3- The slides were then rinsed in distilled water, and washed in running tap water for 5 minutes.
4- The slides were put into 1% periodic acid for 5 minutes, and rinsed in running tap water.
5- The slides were then stained in Schiff's reagent for 10 minutes, and washed in running tap water for 5–10 minutes.
6- The slides were then stained in Mayer's haematoxylin for 2 minutes, and washed in running tap water for 5 minutes.
7- The slides were taken through steps 8 and 9 following the H&E procedure.

Alcian blue pH 2.5 and nuclear fast red (AB-NF):

1- The slides were taken through steps 1–3 following the H&E procedure.
2- The slides were put into filtered Alcian blue solution for 20 minutes, and washed in running tap water for 5 minutes.
3- The slides were then rinsed in distilled water, and washed in running tap water for 5 minutes.

4- The slides were then stained in nuclear fast red solution for 5 minutes, and rinsed in tap water.
5- The slides were taken through steps 8 and 9 following the H&E procedure.

Sudan black-B (SB)

1- The paraffin slides were put into 70% ethyl alcohol for 3 minutes.
2- The slides were then placed in a Coplin jar and stained overnight in filtered saturated Sudan black B solution in 70% ethyl alcohol at room temperature.
3- The slides were then rinsed well in 70% ethyl alcohol to differentiate excess dye in the background.
8- The slides were washed in running tap water for 5 minutes.
9- The slides were taken through steps 8 and 9 following the H&E procedure.

Masson's trichrome (MT)

1- The slides were mordent in Bouin's solution, and then put into water bath for 30 minutes.
2- The slides then washed in running tap water for 5minutes, to remove the picric acid.
3- The slides were taken into Celestin blue solution for 10 minutes.
4- The slides were then stained in Harris's haematoxylin for 10 minutes, and washed in running tap water for 5 minutes or until slides became blue.
5- The slides were then differentiated in 1% acid alcohol (1% HCL in 70% alcohol) for 5–10 seconds, and rinsed in running tap water.
6- The slides then rinsed in distilled water.
7- The slides were then put into Biebrich scarlet solution for 10 minutes, and rinsed in distilled water.
8- The slides were then taken into 1% phosphomolybdic acid for 5 minutes, and the solution was then discarded.
9- The slides were then transferred directly into 1% acidic fast green for 5 minutes, and rinsed in distilled water.

10- The slides were taken through steps 8 and 9 following the H&E procedure.

Toluidine blue (TB)

1- The slides were placed on a hot plate (70–80 ^{o}C) for 5 minutes.
2- The slides were then stained with filtered 1% toluidene blue solution for 15–30 seconds until a golden ring appears at the periphery of the stain drop.
3- The stain was rinsed from the slides with distilled water.
4- The slides were then mounted in D.P.X.

Uranyl acetate and lead citrate

1- A piece of dental wax was placed in a glass Petri dish.
2- Drops of filtered aqueous super saturated uranyl acetate (4–6 drops depending on the number of grids) were placed on the dental wax using a 5 ml filtering syringe.
3- Using fine forceps, copper grids, with the ultrathin sections facing down, were placed on top of the uranyl acetate drops for 30 minutes, then the Petri dish was covered with a dark lid to prevent oxidation of uranyl acetate.
4- The grids were then rinsed with 5–10 drops of 50% alcohol followed by 20–30 drops of double distilled water, and then plot dried in a filter paper.
5- A fresh piece of dental wax was placed on a clean Petri dish containing sodium hydroxide (NaOH) pellets to prevent contamination with CO_2.
6- Drops of filtered lead citrate were placed on the dental wax using a glass pipette.
7- The plotted grids were then placed on top of the lead citrate drops for 20 minutes and covered with Petri dish glass cover.
8- The grids were then rinsed with 20–30 drops of double distilled water, plot dried in a filter paper, and stored in a grid box until screening.

Immunohistochemistry

Thin paraffin sections (3 µm) from male and female house gecko reproductive organs were placed on polysin slides. Sections were then heated in citrate buffer (pH 9) using a microwave for 25 minutes. The slides were left to cool for 15 minutes and then placed in Tris buffer saline/tween 20 for 5 minutes.

Step 1: Peroxidase block: excess buffer was taped off, then using a lintels tissue the remaining liquid around the specimen was wiped off. A line was then drawn around the specimen section using Dako pen. Peroxidase block was the applied on the section and incubated for 5 minutes. Excess block was rinsed off gently with distilled water and section slides were then placed in fresh buffer bath.

Step 2: Primary antibody: excess buffer was tapped off, and optimal primary antibody was applied (PR with the dilution of 1:50) on the section area and Incubated for 30 minutes. Excess antibody was rinsed off gently with buffer solution and section slides were then placed in fresh buffer bath.

Step 3: Peroxidase labeled polymer: excess buffer was taped off and labeled Polymer was applied on the section area and incubated for 30 minutes. Excess polymer was rinsed and slides were then placed in fresh buffer bath.

Step 4: Substrate chromogen: excess buffer was tapped off and solution mixture was applied (1 ml of buffer substrate and one drop of DAB + chromogen) and incubated for 10 minutes. Excess solution was then rinsed with distilled water.

Step 5: Haematoxyline counter-stain: slides were then immersed in a bath of Mayer's Haematoxyline stain and incubated for 3 minutes. Slides then kept in running tap water for 3 minutes and were then dehydrated in graded alcohol concentrations and were then placed in Xyelen and then mounted with DPX.